Investigating neuronal calcium homeostasis in murine models of Alzheimer's disease

PhD Thesis presented by

Aidan Kaar *BSc (Hons)*

orcid.org/0000-0001-5025-6600

January 2019

National University of Ireland, Cork

Department of Physiology, School of Medicine

Supervisor: *Dr Mark G. Rae*

Head of Department: *Professor Ken D. O'Halloran*

Contents

Declaration

This thesis is my own work and has not been submitted for another degree, either at University College Cork or elsewhere. All external references and sources are clearly acknowledged and identified within the contents. I have read and understood the regulations of University College Cork concerning plagiarism.

Signed,

Aidan Kaar

Acknowledgements

The road to completing my PhD and thesis is not one which I found easy. It tested the limits of my memory, discipline, determination, patience and motivation. I started with the hope that my work could contribute in some small way to our knowledge of Alzheimer's disease and I am proud to say that I feel that this has been achieved. This would not have been possible without the help, belief and support of my supervisor Dr Mark Rae. Dr Rae encouraged my curiosity and allowed me to direct the path of my PhD based on my own goals and interests. I would like to thank him sincerely for his patience and for making himself available at any time of the day, regardless of circumstances, if I needed it. Under his guidance, we have asked some interesting questions and in the process of trying to answer them have reviewed and queried current literature, presented novel data and posed relevant future questions for the field.

My career as a researcher was sparked with personal motivation. I had seen Alzheimer's disease debilitate a beloved family member and observed a greater network of people I loved and people who loved him go through the trauma associated with the disease. I dedicate this work to Niall "Fuss" Finn who was a remarkable role model and whose dedication and devotion I hope to someday emulate. I also dedicate this work to Frances "Misus" Finn, Deirdre Kaar, Valerie O'Sullivan and Stephen O'Sullivan who loved, supported, guided and cared for Fuss throughout his illness in a manner which represents the pinnacle of human kindness.

I would like to thank my family and friends who checked-in, listened, empathised, encouraged and supported me. I am incredibly lucky to have such supportive parents who would have done anything to help me get this project over the line. I am eternally grateful for the hours my father put in to read draft documents throughout my PhD and to help me improve my writing. One paragraph cannot do these people justice. I am so grateful and love you all. I also feel incredibly lucky to have felt the support of colleagues within the entire scope of the Physiology department and its associated support staff. My interactions with these people were incredibly positive and critical to my success. Moreover, I have made fond personal connections which I will continue to value for the rest of my life. I would also like to sincerely thank Chris, Rory, Luigi and Colm who recognised the value I placed on my studies and allowed me to accommodate my part-time work around my PhD.

Finally, I am eternally grateful for everything you do Louise. Without you, I would not be here. You supported me in every conceivable way. The value of your guidance is incalculable. You gave me belief and encouragement when I needed it the most. I love you from the bottom of my heart. I cannot wait to overcome our future challenges together.

Abbreviations

$[Ca^{2+}]_i$	intracellular calcium concentration
AA	arachidonic acid
ABC	ATP-binding cassette
AC	adenylyl cyclase
ACM	astrocyte-conditioned medium
AD	Alzheimer's disease
ADDLs	Aβ–derived diffusible ligands (synonym for Aβo)
ADPR	ADP-ribose
AICD	APP carboxy-terminal intracellular domain
AMPAR	α-amino-hydroxy-5-methyl-4-isoxazolepropionic receptor
Ang II	angiotensin II
APLP	APP-like protein
ApoE4	ε4 allele of the polymorphic apolipoprotein E
ApoER	ApoE receptor 2
APP	amyloid precursor protein
APPsα	soluble APP fragment-α
APPsβ	N-terminal soluble APP fragment-β
ARC	ADP-ribosyl cyclase
ART	ADP-ribosyltransferases
ASPs	artificial signalling platforms
Aβ	amyloid β
Aβo	amyloid beta oligomers
B-27	B-27® serum-free supplement
BACE	beta-site APP cleaving enzyme
Bax	Bcl-2-associated X protein
Bcl-2	B-cell lymphoma 2
BDNF	brain-derived neurotrophic factor
bFGF	basic fibroblast growth factor
BH	Bcl-2 homology (domain)
BSA	bovine serum albumin
cADPR	cyclic adenosine 5'-diphosphoribose
CALHM1	calcium homeostasis modulator 1
CaM	calmodulin
CaMKII	calcium calmodulin-dependent protein kinase II
CaR	Ca^{2+}-sensitive receptor
CB	calbindin
CCh	carbachol
CCK	cholecystokinin
CCLs	continuous cell lines
Cdk5	cyclin-dependent kinase 5
cGMP	cyclic GMP
CICR	Ca^{2+}-induced calcium release
CLU/APoJ	clusterin
CN	calcineurin
CNS	central nervous system
CO	cytochrome c oxidase
CRAC	Ca^{2+} release-activated Ca^{+}
CRD	cysteine rich domains
CSF	cerebrospinal fluid
CTFα/C83	carboxy-terminal fragment-α
CTFβ/C99	carboxy-terminal fragment-β
Ctx	cortex
Cx	connexin
DAG	diacylglycerol
DG	dentate gyrus
dH_2O	deionised water
DHPG	(S)-3, 5-dihydroxyphenylglyccine
DIV	days *in vitro*

DKO	double knock-out
DMEM	Dulbecco's modified Eagle's medium
DR6	death receptor 6
DRG	dorsal root ganglion
DS	Down's syndrome
E	embryonic day
EC	entorhinal cortex
eEF2	eukaryotic elongation factor 2
EOAD	early-onset AD
EOFAD	early-onset familial AD
ER	endoplasmic reticulum
ERK	extracellular signal-regulated kinases 1 and 2
FBS	foetal bovine serum
FKBP	FK506 binding protein
FOV	field of view
GABA	gamma aminobutyric acid
GC	growth cone
GDP	guanosine 5′-diphosphate
GFAP	glial fibrillary acidic protein
GPCR	G-protein-coupled receptor
GPI	glycosylphosphatidylinositol
G-proteins	guanine nucleotide-binding regulatory proteins
GRK	G-protein coupled receptor kinase
GSH	glutathione
GSK3β	glycogen synthase kinase-3β;
GTP	guanosine 5′-triphosphate
HA	Hibernate® A
HCN	human cortical neurons
HD	heptahelical domain
HD	Huntington's disease
HFS	high frequency stimulation
HMW	high molecular weight
HNE	aldehyde 4-hydroxynonenal
I_{CRAC}	Ca^{2+} release activated Ca^{2+} current
IDE	insulin-degrading enzyme
iGluRs	ionotropic glutamate receptors
IL-1	interleukin-1
I-mGluR	group 1 metabotropic glutamate receptor
IP_3R	inositol-1, 4, 5-trisphosphate receptor
JNK	c-Jun N-terminal kinase
KD	knockdown
KO	knockout
LDLR	low-density lipoprotein receptor
LEC	lateral entorhinal cortex
L-Gln	L-glutamine
LMO4	lim only domain protein 4
LMW	low molecular weight
LOAD	sporadic/late onset AD
LPS	lipopolysaccharide
LRP1	low density lipoprotein receptor-related protein 1
LTD	long-term depression
LTP	long-term potentiation
mAChR	muscarinic acetylcholine receptors
MAP	microtubule associated protein
MAPK	mitogen activated protein kinases
MCI	mild cognitive impairment
MCU	mitochondrial Ca^{2+} uniporter
MEC	medial entorhinal cortex
MEF	mouse embryonic fibroblasts
mGluR	metabotropic glutamate receptor

mPTP	mitochondrial permeability transition pore
MTL	medial temporal lobe
NAADP	nicotinate adenine dinucleotide phosphate
nAChR	nicotinic acetylcholine receptors
NAD	nicotinamide adenine dinucleotide
NB-A	Neurobasal®-A
NCX	Na^+/Ca^{2+} exchanger
NFTs	intracellular neurofibrillary tangles
NG108-15	neuroblastoma *x* glioma hybrid cells
NGD^+	nicotinamide guanine dinucleotide
NICD	notch intracellular domain
NMDAR	N-methyl-D-aspartic acid receptor
NO	nitric oxide
NT	neurotransmitter
NTRs	nucleotide transporters
OT	oxytocin
P	Postnatal
P2X7R	purinergic receptor P2X, ligand-gated ion channel, 7
P2XCs	ATP gated purinergic channels
ParaSb	parasubiculum
PARP	poly-ADP-ribose polymerases
PBS	phosphate buffered saline
PD	Parkinson's disease
PET	polyethylene terephthalate
PI	phosphatidyl inositol
PI3K	phosphatidyl inositol 3-kin
PICALM	phosphatidylinositol binding clathrin assembly protein
PIP2	phosphatidylinositol-4, 5-bisphosphate
PKC	Ca^{2+} dependent kinase C
PKG	cGMP- dependent protein kinase
PLC	phospholipase C
PLD	phospholipase D
PM	plasma membrane
PMCA	plasma membrane Ca^{2+}-ATPases
PP	polypropylene
PP1	protein phosphatase 1
PreSb	presubiculum
PrP^{C-}	cellular prion protein
P-S	penicillin-streptomycin
PS	presenilin
PSD	post-synaptic density
P-tau	cytosolic abnormally hyperphosphorylated tau
PtdS	phosphatidylserine
PTx	pertussis-toxin
RAGE	advanced glycosylation end-product specific receptor
RGS4	regulator of G protein signalling
ROI	regions of interest
ROS	reactive oxygen species
RyR	ryanodine receptor
sAHP	slow after-hyperpolarising potential
sAPPα	soluble APP metabolite α
SIRT	sirtuins
SK	small conductance calcium-activated potassium channels
SOCCs	store operated calcium channels
SOCE	store operated calcium entry
SOICR	store-overload-induced Ca^{2+} release
SORL1	sortilin-related receptor 1
SR2	serum replacement 2
STIM1	stromal interaction molecule 1
Sub	subiculum

TGN	trans-Golgi-network
TM	transmembrane
TNF	tumour necrosis factor
TPN	thapsigargin
TREM2	triggering receptor expressed in myeloid cells 2
TRP	transient receptor potential cation channel
TRPC	transient receptor potential canonical (TRPC)
TTx	tetrodotoxin
UPR	unfolded protein responses
VDAC	voltage-dependent anion channel
VFD	Venus flytrap domain
VGCC	voltage-gated calcium channels
VGSC	voltage-gated sodium channel
VILIP	visinin-like protein

Abstract

This thesis is primarily concerned with the pathological remodelling of calcium homeostasis and signalling in murine Alzheimer's disease (AD) models, namely the 3xTg-AD (APP_{SWE}/$PS1_{M146V}$/Tau_{P301L}) mouse and TgF344-AD (APP_{SWE}/$PS1_{\Delta E9}$) rat models.

The majority of data contained herein was amassed from calcium imaging of primary neuronal hippocampal cultures. The development of a new protocol for the primary culture of *mouse* hippocampal neurons also represents a major research output of this thesis (Kaar et al., 2017). In addition to simplifying and optimising each facet of the culturing process, we identified the mechanical dissociation of hippocampal tissue (trituration) as the critical factor in determining the success or otherwise of culture preparations. Furthermore, we demonstrated that successful primary mouse hippocampal cultures could be prepared without the need for specialised and expensive proprietary supplements which many researchers in the field propose as being essential for this purpose. As such, this method fills a niche in the current published literature where efficient, cost-effective and succinct methods for postnatal mouse cultures are lacking.

Calcium imaging experiments were predominately conducted using cultures produced from three to 6-day-old mice and rats. In using animals at such a young age it is thought that any observed calcium dysregulation may reflect early pathological or perhaps even initiating AD events. In line with the "Calcium hypothesis of Alzheimer's disease" (Berridge, 2010), this research points to cellular Ca^{2+} remodelling in terms of both basal Ca^{2+} levels and Ca^{2+} signalling as an early pathogenic event in AD. In particular, we have studied how the main neuronal calcium store, the endoplasmic reticulum (ER), functions in both maintaining calcium homeostasis and mediating intracellular signalling processes, and how these functions might be disrupted in AD. Using calcium imaging, group 1 metabotropic glutamate receptor (I-mGluR)-mediated somatic responses were measured under basal conditions and also under conditions where the ER was 'preloaded' with calcium (using a depolarising stimulus (15mM K^+) which, we propose, mimics a 'learning event' in the hippocampus). In non-transgenic neurons from both murine models, I-mGluR activation combined with the loading stimulus-evoked enhanced Ca^{2+} signals relative to I-mGluR activation alone. In contrast, enhanced calcium responses were not observed in 3xTg-AD mouse hippocampal neurons, suggesting a loss of this signalling function. Notably however, under basal conditions, we did observe significantly larger responses to I-mGluR activation as well as attenuated SOCE in 3xTg-AD neurons suggesting a pathological increase in resting ER calcium levels in these neurons relative to controls. Furthermore, in TgF344-AD neurons, there were also subtle differences in I-mGluR response parameters when

compared with non-Tg controls. The fact that such stark alterations in calcium homeostasis and signalling were observed in neurons from 3xTg-AD mice at such a young age (≤6 days), suggests that calcium dysregulation may occur at a much earlier stage in the disease progression than previously thought and appear to greatly precede the appearance of Aβ or tau pathology.

The third major theme of this thesis involved identifying the downstream signalling cascade(s) involved in I-mGluR activation. The classical understanding of I-mGluR activation involves phospholipase C β (PLCβ)-mediated production of IP_3 and Ca^{2+} release from the ER *via* the IP_3 receptors (IP_3R). However, we show here that a significant contribution (approximately 10 - 40%) of I-mGluR mediated Ca^{2+} mobilisation from the ER is in fact mediated by the second messenger, cyclic ADP-ribose (cADPR), which culminates in RyR-mediated Ca^{2+} release. Furthermore, the relative contribution of both PLCβ/IP_3R and cADPR/RyR pathways to overall I-mGluR elicited signals is altered in transgenic neurons of both murine models.

Finally, the expression of key calcium toolkit components including relative IP_3R and RyR isoform expression, as well as the expression of Bcl-2 and Bcl-X_L, which modulate ER Ca^{2+} release channel function, was determined in hippocampal tissue from 5-, 15- and 21-day-old 3xTg-AD mice. It was found that there was a trend towards decreased expression of Bcl-2 and Bcl-$_{XL}$ and a trend towards increased expression of RyR and IP_3R1 with development (P5 *vs* P15 and P5 *vs* P21) regardless of transgenic status, however, this was significant solely in 3xTg-AD tissue and only in the case of Bcl-2, Bcl-$_{XL}$ and RyR (2) expression (and generally, solely at the latest stage of development tested, P21).

In summary, the work set out in this thesis investigates neuronal Ca^{2+} homeostasis and I-mGluR/ER signalling as well as relevant protein expression with a particular focus on possible AD-mediated dysregulation of these processes. Lastly, the method of primary hippocampal culture, the sources of experimental units from which this data has been accrued has been extensively optimised.

1. General introduction

1.1. Alzheimer's disease

According to the 'World Alzheimer Report 2015' by Alzheimer's Disease International the number of individuals worldwide aged 60 years and older will increase from the current figure of approximately 895 million to 2022 million by 2050, a trend that is mainly fuelled by increases in average life expectancy in the developing world. Unfortunately, as average life expectancy increases so too does the prevalence of age-related diseases such as dementia. There were an estimated 47 million people worldwide with dementia in 2015, with an associated cost of US$ 818 billion (1.09% of global GDP). Worryingly, the number of individuals affected by dementia is projected to increase to 131.5 million individuals by 2050. As an indication of the situation in the developed world, conservative estimates predict that 5.4 million people suffer from the most prevalent form of dementia, Alzheimer's disease (AD), in the US alone, where it is currently the sixth leading cause of death. These figures are projected to increase to 13.8 million by 2050, fuelled in large part by the ageing baby boom generation (Alzheimer's Association, 2016). As such, AD, is set to become one of the major public health concerns facing mankind in the 21st century and therefore the need for research into the underlying causes of the condition is more imperative than ever.

AD is an inexorably progressive neurodegenerative disorder characterised phenotypically by progressive memory and behavioural impairments, and histopathologically by both the progressive deposition of extracellular amyloid β (Aβ) protein plaques, formed from the polymerization of Aβ proteins and the formation of intracellular neurofibrillary tangles (NFTs), consisting of hyperphosphorylated, proteolysis-resistant, aggregates of tau protein (Buée et al., 2000; Gendron and Petrucelli, 2009). Chronic neuroinflammation and frank neuronal loss, particularly in the hippocampus and neocortical regions of the brain, complete the disease profile (Querfurth and LaFerla, 2010).

The first neuropathological changes of AD present in regions of the brain primarily associated with the acquisition of new memories, namely, the hippocampus and entorhinal cortex, and subsequently, the medial temporal lobe (Belleville et al., 2008; Reitz et al., 2009; Small et al., 2011). This likely explains the corresponding early effects of the disease, which primarily impair anterograde episodic memory (Ally et al., 2013; Collie and Maruff, 2000; Selkoe, 2002). The condition spreads out to affect the neocortex in later stages of the disease, whilst initially affected regions worsen and massive neuronal cell death becomes evident, with a concurrent deterioration in cognition, leading to fully developed AD (Braak et al., 2006).

AD is somewhat arbitrarily divided into two subtypes: sporadic/late-onset AD (LOAD) and early-onset AD (EOAD), based upon the respective ages of their clinically diagnosed onset. However, both types are positively associated with a family history of AD. The majority of cases (~ 95%) are classified as LOAD, which presents after 60 - 65 years (Bertram and Tanzi, 2004a). As the name implies, EOAD is diagnosed earlier than LOAD, at 30 - 60 years of age, and accounts for 1 – 6% of all cases. Of these, early onset familial AD (EOFAD), where there are multiple cases of AD within families, accounts for approximately 60% of cases, whilst 13% of EOFAD cases are inherited in an autosomal dominant manner, with at least three generations affected. This autosomal dominant inheritance pattern is due to mutations in either amyloid precursor protein (APP; on chromosome 21), presenilin 1 (PS1; on chromosome 14) or presenilin 2 (PS2; on chromosome 1; Campion et al., 1999). Complicating matters further, EOAD can also occur in families with a history of LOAD (Brickell et al., 2006).

Aside from these autosomal dominant cases which I will return to later in this Introduction, AD is generally thought to be due to the complex interaction of environmental and lifestyle factors combined with multiple susceptibility genes (Bekris et al., 2010; Bertram and Tanzi, 2004b; Kamboh, 2004; Roses, 2006; Serretti et al., 2005). Furthermore, it has been proposed that approximately 60 – 80% of 'sporadic' AD cases may, in fact, be genetically determined (Gatz et al., 2006), with each of the following three genetic 'risk factors' thought to contribute significantly to this genetic component of LOAD (Harold et al., 2009; Lambert et al., 2009): a) inheritance of the ε4 allele of the polymorphic apolipoprotein E (ApoE4) gene (chromosome 19; Coon et al., 2007; Roses et al., 1995) which results in less efficient breakdown and clearance of Aβ proteins (Liu et al., 2013), b) mutations in Triggering Receptor Expressed on Myeloid cells 2 (TREM2), which regulates microglial removal of Aβ (Colonna and Wang, 2016; Guerreiro et al., 2013; Neumann and Daly, 2013; Yaghmoor et al., 2014)), and c) mutations in Clusterin (CLU/APoJ), which affects Aβ processing, inflammation and apoptosis (Woody and Zhao, 2016).

The various hypotheses outlined in this general introduction to AD all attempt to explain the onset and progression of AD in the context of either Aβ proteins, Ca^{2+} dysregulation, tau pathology, mitochondrial impairment, oxidative stress and/or neuroinflammation. In reality, although establishing earlier versus later events in disease pathology is important for treatment development, focussing on any single one of these hypotheses fails to acknowledge the full breadth of the disease pathology. As such, it is likely that single or multiple components described by each of these hypotheses interact in a highly complex and feed forward manner to propagate the spread of the disease.

1.2 APP and the amyloid β cascade hypothesis

1.2.1 APP

APP is a type 1 transmembrane (TM) glycoprotein, with three isoforms: APP_{695} (neuron-specific isoform), APP_{751} and APP_{770} encoded for by an *APP* gene on chromosome 21 (Sandbrink et al., 1996). It consists of a long N-terminal ectodomain, a TM domain (within which an Aβ sequence is partly embedded) and a short C-terminal domain (Muller et al., 2017). APP expression is detectable from embryonic day 7.5 in mice (Ott and Bullock, 2001) and expression of APP mRNA and proteins in adult rodents is ubiquitous (Lorent et al., 1995; Slunt et al., 1994). In the CNS, APP is abundantly expressed in neurons (Guo et al., 2012) which predominantly express the APP_{695} isoform (Gralle and Ferreira, 2007). APP is expressed particularly strongly in cortical and hippocampal excitatory neurons and in inhibitory gamma-aminobutyric acid (GABA)ergic interneurons (Hick et al., 2015; Wang et al., 2014). The mammalian APP family consists of APP (ubiquitously expressed), the APP-like proteins (APLP) 1 (nervous system-specific expression) and APLP 2 (ubiquitously expressed; Lorent et al., 1995; Slunt et al., 1994), which are all enriched at the pre-synaptic active zones (Laßek et al., 2013). Aside from neuronal cells, i*n vitro* experiments indicate that all three APP isoforms are also expressed in microglia and astrocytes (LeBlanc et al., 1991). However*, in vivo* glial APP expression has not been detected (Guo et al., 2012).

APP is synthesised in the endoplasmic reticulum (ER) and transported by the Golgi secretory apparatus to the trans-Golgi-network (TGN) and on to the plasma membrane (PM; Jiang et al., 2014). The canonical pathway of APP processing is carried out by α-, β- and ɣ-secretases. However, the cellular localisation of APP metabolism is not definite, although it appears to occur primarily within the ER/Golgi/TGN (Greenfield et al., 1999), the endolysosomal system (Haass et al., 1993a, 1993b), as well as at the PM (Sisodia, 1992; Fig 1.2).

APP has wide-ranging physiological functions and numerous modes of action. It is beyond the scope of this thesis to describe these in detail (for reviews see Dawkins and Small, 2014; Müller and Zheng, 2012). Briefly, however, APP is known to function as both a cell surface receptor and as a ligand which can mediate its effects either by activating downstream signalling cascades or *via* active proteolytic fragments such as soluble APP fragment-α (APPsα; see below for APPsα production in the non-amyloidogenic pathway; Muller et al., 2017).

APP knockout (KO) mice are viable but exhibit abnormalities including: reactive gliosis (Burda and Sofroniew, 2014; Pekny and Pekna, 2016), impairment in a molecular model of memory formation- long-term

potentiation (LTP) as well as impaired cognitive function and locomotion (Dawson et al., 1999; Zheng et al., 1995). Interestingly, solely expressing the APP metabolite APPsα in these mice can rescue these abnormalities, suggesting it is the primary APP effector under normal physiological circumstances (Ring et al., 2007).

1.2.2 Amyloid β cascade hypothesis

The central tenet of the Aβ hypothesis is that alterations in the processing of APP, leading to the abnormal accumulation of Aβ into Aβ oligomers (Aβo), insoluble fibrils and plaques and/or alterations in its degradation and clearance, are responsible for the onset of AD (Selkoe and Hardy, 2016). In addition to the deposition of Aβ plaques in AD patients' brains, the strongest argument in support of the Aβ hypothesis of AD remains the correlation between AD susceptibility genes and Aβ production (Tanzi and Bertram, 2005). In this regard, there are currently 24 known associated pathogenic mutations of APP, which have been identified in several families across the world. These mutations include missense mutations which code for amino acid substitutions flanking, or within, the Aβ encoding region of APP. Most of these are near the γ-secretase cleavage site but there is one known double mutation which flanks the β-secretase site, known as the Swedish mutation (APP_{SWE}; cleavage at both sites are part of the amyloidogenic processing of Aβ, as explained in *Section 1.2.3 APP processing*) which is one cause of autosomal dominant EOFAD (Selkoe and Schenk, 2003). This APP_{SWE} mutation is expressed in both the 3xTg-AD (APP_{SWE}/$PS1_{M146V}$/Tau_{P301L}) mouse and TgF344-AD (APP_{SWE}/$PS1_{\Delta E9}$) rat model of AD, both of which have been examined for the work presented in this thesis. Generally, these mutations either increase the overall amount of Aβ production or the ratio of $Aβ_{42}$, the more toxic form of Aβ highly implicated in neuronal dysfunction, to $Aβ_{40}$ (Cacace et al., 2016). Notably, in Down syndrome (DS) where chromosome 21 is partially or fully triplicated (which is why it is also known as Trisomy 21), if this triplication includes the APP gene region it almost inevitably results in those individuals developing AD-like symptoms and pathology (Margallo-Lana et al., 2004; Rumble et al., 1989). This DS-related AD pathology occurs 20 to 30 years earlier than in the non-DS population (Wisniewski et al., 1985) and almost all adults over 40 with DS display AD neuropathology (Menéndez, 2005). The Aβ hypothesis of AD is further supported by the relatively recent discovery of the APP_{A673T} mutation in an Icelandic population. This mutation, rather than causing AD, actually seems to confer an 'immunity' against the development of the disease as well as age-related cognitive decline (Jonsson et al., 2012).

Although I have only provided a ‘snapshot’ here of the research implicating the role of APP in AD pathogenesis, this cascade has been the primary focus of AD research for the last 15 years (Hardy and Higgins, 1992; Selkoe and Hardy, 2016). As such, a large body of evidence on the pathological profile of APP metabolites has been generated from both human patients and animal models, a summary of which is provided in *Section 1.2.6 Molecular actions of Aβ.*

1.2.3 APP processing

APP undergoes extensive and complex proteolytic processing, resulting in numerous biologically active fragments with specific and even opposing functions. The so-called non-amyloidogenic and amyloidogenic pathways comprise the canonical APP processing pathway and involve the sequential activity of α- and β-secretase, respectively, followed by y-secretase activity. The δ- and η-pathways, meprin-β cleavage and caspase cleavage comprise non-canonical APP processing (Fig 1.1 Muller et al., 2017). It is important to note that all of these APP processing pathways exist in normal healthy individuals throughout life such that Aβ proteins are detectable in the plasma and cerebrospinal fluid (CSF) of healthy individuals as well as those with AD (Selkoe and Schenk, 2003).

APP is either cleaved at the PM by secretases or un-cleaved/partially cleaved APP (as well as secretases) are internalised within clathrin-coated vesicles where they are expressed throughout both early and late endosomes and the lysosome recycling system (Caporaso et al., 1994; Nordstedt et al., 1993). A fraction of the internalised APP is also recycled to the PM or retrieved back to the TGN. As such, the PM pool of APP reflects its secretion, internalisation and the efficiency of secretases (Jiang et al., 2014). In overexpression studies, APP is found targeted to the endosome (primarily) and TGN, as well as the plasma membrane (Huse et al., 2000; Vassar et al., 1999; Walter et al., 2001). The components required for APP processing, including secretases and APP as well as the products of processing, including Aβ, are expressed throughout these intracellular organelles (Fig 1.2; Jiang et al., 2014).

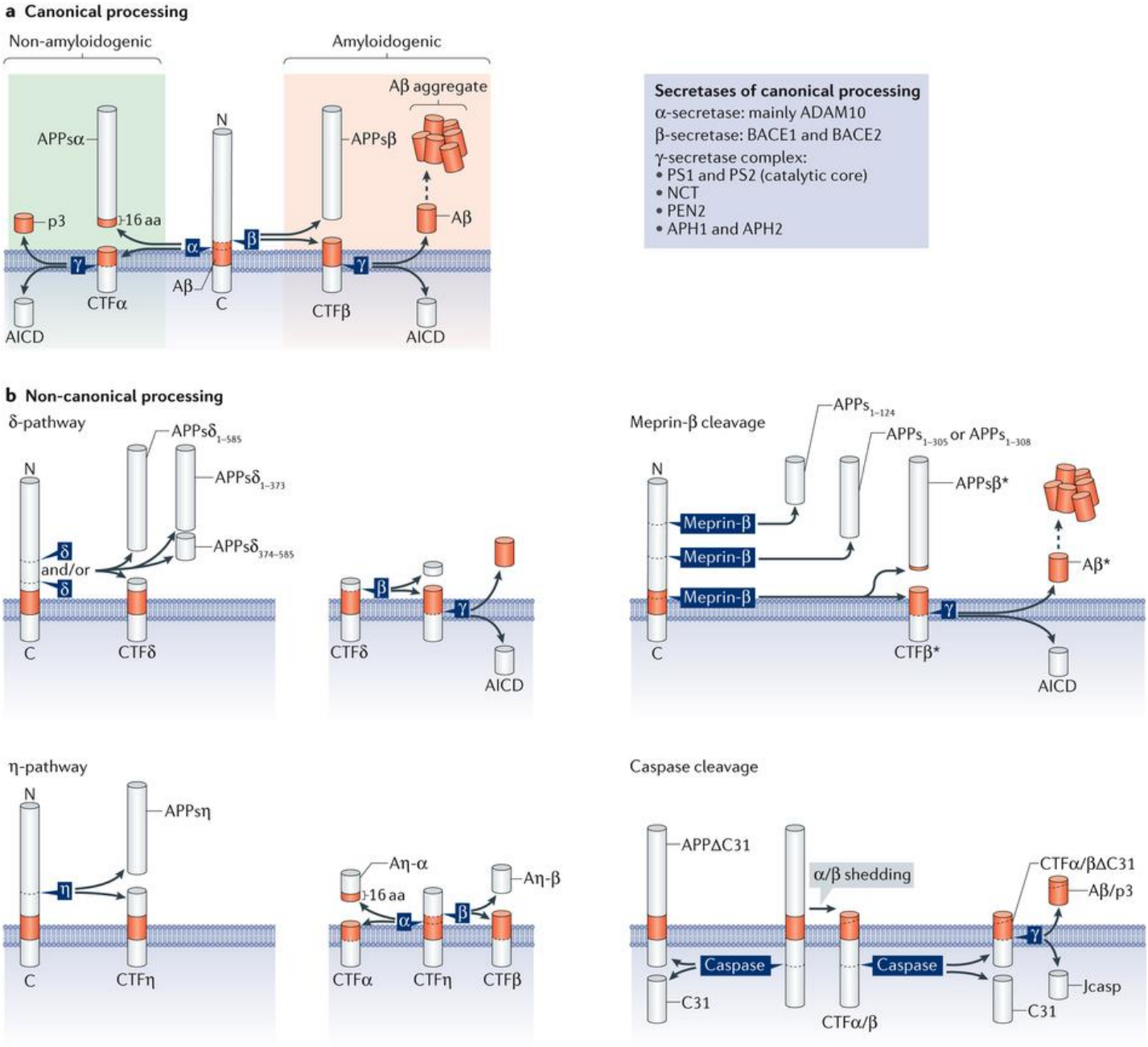

Figure 1.1. APP processing

APP can undergo canonical **(a)** and/or non-canonical **(b)** processing.

a) Canonical processing involves either the non-amyloidogenic or amyloidogenic pathway. In the non-amyloidogenic pathway APP is sequentially processed by *α*-secretase (cutting in the Aβ region of APP) and the γ-secretase complex to form what are generally considered non-toxic APPsα, p3 and AICD. In the amyloidogenic pathway APP is sequentially processed by β-secretase and the γ-secretase complex forming substances implicated in AD such as $Aβ_{40}$ and $Aβ_{42}$ monomers, sAPPβ and AICD.

b) Non-canonical processing. It is proposed that δ-, meprin-β and caspase cleavage also produce toxic Aβ monomers and oligomers. One identified function of non-canonical APP processing is the production of AICD *via* δ-, meprin-β and caspase-cleavage. Caspase cleavage can also, possibly in an isoform-specific manner, cleave within the AICD region of CTF to form the fragment C31 and leave a membrane bound fragment CTFα/βΔC31. This fragment is, in turn, cleaved by γ-secretase to form Jcasp and possibly toxic Aβ.

Reproduced with permission from Muller *et al.* (2017).

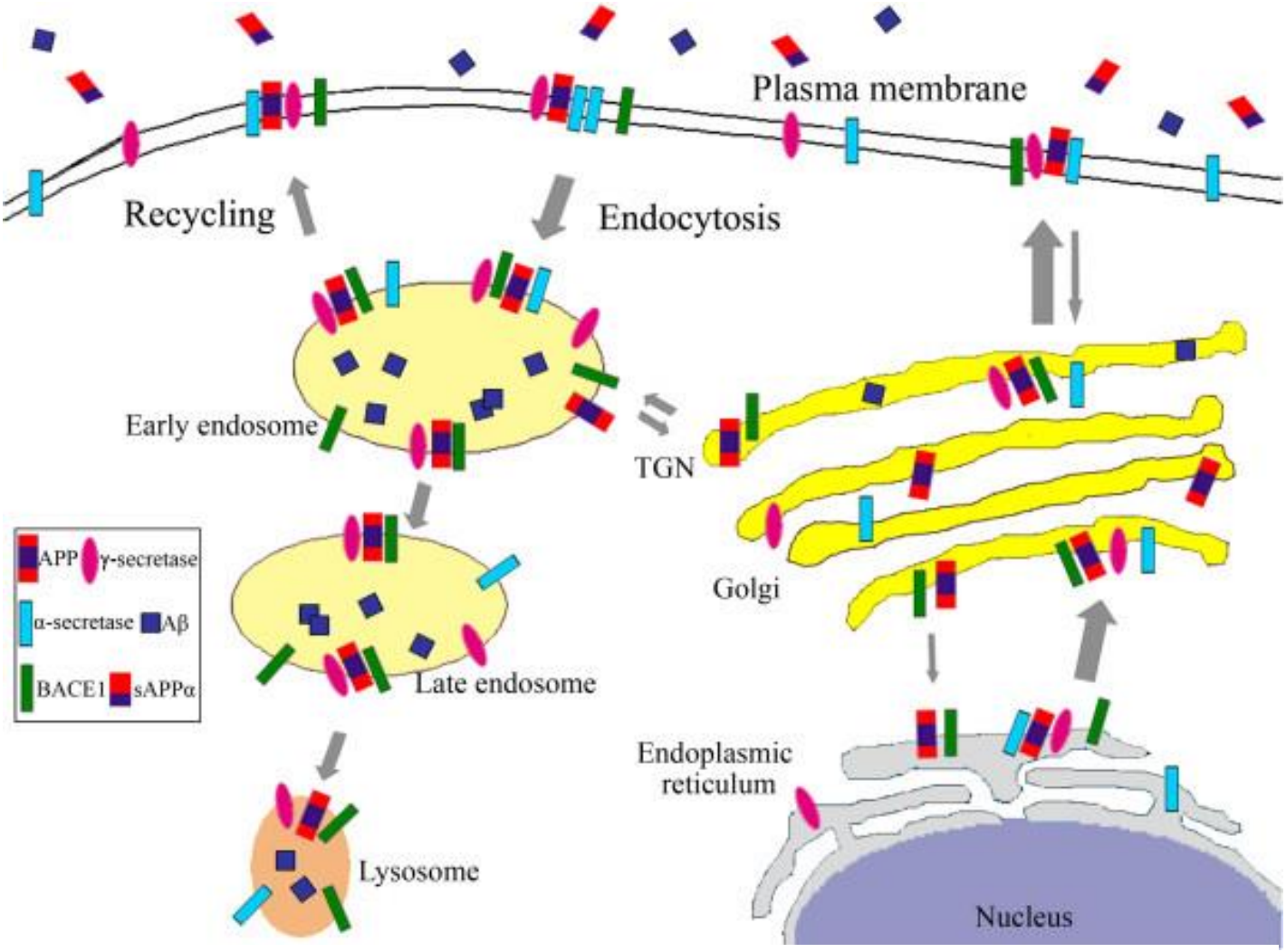

Figure 1.2. APP trafficking and flux

Newly synthesised APP, α-secretase, BACE1 (β-secretase) and γ-secretase are transported through the secretory pathway from the ER to the Golgi/TGN and from there to the plasma membrane (PM). This is counterbalanced by protein turnover and retrograde transport mechanisms directing proteins back to the PM or to the TGN. Non-amyloidogenic processing of APP (releasing soluble APP metabolite α (sAPPα/APPsα)) is thought to occur primarily at the PM. Conversely, un-cleaved/partially cleaved APP, as well as secretases, can undergo endocytosis and be expressed on early and late endosomes and lysosomes. Although toxic Aβ monomers can be produced in the majority of locations that APP flux occurs through, it is in these acidic endosomes/lysosomes where β-secretase activity is optimal and therefore amyloidogenic processing primarily occurs.

Reproduced with permission from Jiang et al. (2014).

Although toxic Aβ monomers can be produced in the majority of locations that APP flux occurs, including the PM, it is in acidic organelles of the endolysosomal system (particularly early endosomes (Das et al., 2015)) where β-secretase activity is optimal and therefore where amyloidogenic processing primarily takes place (Jiang et al., 2014; Tarassishin et al., 2004). Any AD-mediated redistribution of β- or γ-secretase which favours co-expression with APP in suitable organelles could increase Aβ generation (Zhang et al., 2011). The cleavage of APP by β-secretase is a critical rate-limiting step in Aβ production. Interestingly, the 'Icelandic' APP mutation mentioned earlier greatly attenuates APP-β-secretase interactions (Das et al., 2015). The endocytosis of APP and β-secretase to the early endosome is spatially segregated *via* targeted sorting. Manipulation of this process can decrease their interaction in early endosomes and therefore modulate APP processing and Aβ production (HeLa cells; (Sannerud et al., 2011). Neuronal activity is known to induce convergence of APP and β-secretase in recycling endosomes (Das et al., 2015, 2013) which may link the early-stage AD phenotypes of neuronal excitotoxicity and network hyperexcitability with Aβ production (Palop et al., 2007). That being said, neuronal and synaptic activity, including N-methyl-D-aspartate receptor (NMDAR) activation, which is critical for mediating forms of LTP and long-term depression (LTD; molecular models of learning), also stimulate the non-amyloidogenic pathway (Hoe et al., 2012; Hoey et al., 2009). It is possible that the latter occurs in a manner which is below the threshold for the induction of amyloidogenic processes.

Non-amyloidogenic APP processing

The non-amyloidogenic processing of APP occurs as a result of α-secretase cleavage of APP. These particular α-secretases appear to be primarily PM-bound endoproteases (Sisodia, 1992) which cleave APP at a point in the Aβ domain of the molecule, ensuring APP metabolism without the formation of β-amyloids. This proteolysis also releases the secreted ectodomain segment of APP, APPsα, whilst leaving a carboxy-terminal fragment-α (CTFα/C83; Zhang et al., 2011). It is notable that, amongst other activities, APPsα attenuates neuronal excitability by altering intracellular calcium ($[Ca^{2+}]_i$) responses to stimuli such as glutamate (see Section 1.2.6 Molecular Actions of APP metabolites; Barger et al., 1995; Furukawa et al., 1996a, 1996b; Hooper, 2005; Mattson, 1994). The other non-amyloidogenic pathway product, CTFα, is further hydrolysed in a series of cleavage events by the γ-secretase complex. Endoproteolytic ε-cleavage (near the cytoplasmic membrane boundary of APP) releases an APP intracellular domain metabolite (AICD/CTFγ), whilst sequential exoproteolytic cuts towards the N-terminus, termed γ-cleavage, produce metabolites including P3 (also called P83) produced by a cut in the middle of the membrane domain (Tomita, 2014; Weidemann et al., 2002). This P3 fragment is rapidly

degraded, has no established physiological function and does not assemble into stable oligomer formations which are synonymous with AD (Dulin et al., 2008).

The γ-secretase complex is composed of four integral membrane proteins; presenilins (PS1/PS2), nicastrin - a PS cofactor and scaffolding protein, which may have a role as an APP receptor for the complex (Luo et al., 2003), anterior pharynx defective 1 (APH-1) - implicated in γ-secretase complex assembly (Kimberly et al., 2003) and presenilin enhancer-2 (PEN-2) - which regulates PS endoproteolysis (Ahn et al., 2010) and genetic knockdown of which, is associated with increased ER calcium leak (therefore PEN-2 may have a role in regulating PS-mediated Ca^{2+} leak, discussed in Section 1.4 The Ca^{2+} hypothesis of AD; Bandara et al., 2013; Edbauer et al., 2003; Kimberly et al., 2003; Takasugi et al., 2003). Whilst this enzyme complex is located primarily within the ER/Golgi/TGN network as well as the endocytic and intermediate compartments, γ-secretase cleavage of APP occurs primarily within the TGN and early endosomal domains (Cupers et al., 2001; Kovacs et al., 1996).

Amyloidogenic APP processing

Processing of APP via the amyloidogenic pathway (Fig 1.1) involves its sequential cleavage by β- and γ-secretases, generating Aβ proteins which have become synonymous with AD pathology (Mattson, 2004, Shirwany et al., 2007).

APP is hydrolysed by β-secretase resulting in the shedding of the N-terminal soluble APP fragment-β (APPsβ), leaving a C-terminal fragment β (CTFβ/C99) on the endosomal membrane (Fig 1.1). The endogenous β-secretases are beta-site APP cleaving enzyme (BACE) 1 and BACE2, of which BACE1 is more widely implicated in this process (Cai et al., 2001; Luo et al., 2001). For example, in transgenic mouse models of AD involving APP-overexpressing APP_{SWE} mice (3 - 4-months-old) and 5xTg-AD mice $APP_{SWE/I716V/V717I}/PS1_{M146L/L286V}$ (15 -18-months-old), BACE1 KO rescues cholinergic dysfunction, neuronal loss and memory deficits with corresponding near removal of the β-secretase metabolites $Aβ_{40}$ and $Aβ_{42}$ (Luo et al., 2001; Ohno et al., 2007, 2004). Furthermore, BACE1 protein and activity were increased relative to healthy controls in the temporal and frontal cortex and hippocampal regions in human AD patients (Fukumoto et al., 2002; Tyler et al., 2002; Yang et al., 2003).

Following β-secretase cleavage, the γ-secretase complex further cleaves CTFβ in a sequential manner similar to the cleavage of CTFα. ε-cleavage again produces AICD, whilst γ-cleavage releases either monomeric $Aβ_{40}$ (majority) or $Aβ_{42}$ (minority; Suh and Checler, 2002).γ-secretase-mediated cleavage also produces Aβ monomers ranging from 39 to 49

residues (Nunan and Small, 2000) *via* ζ-site (Aβ46; G. Zhao et al., 2004) and ε-site (Aβ49) cleavage (Sastre et al., 2001). It is well known that APPsβ, AICD and Aβo (especially $Aβ_{42}$), as well as Aβ fibril and plaque formation, play significant roles in AD-associated neurodegeneration (Berridge, 2010). Indeed, these molecules are the primary focus of AD research in this area and will be discussed in more detail in subsequent sections.

The production of AICD, previously ascribed solely to γ-secretase activity, may also be generated through non-canonical APP processing (Fig 1.1), *via* δ-, meprin-β and/or caspase-cleavage (predominately caspase-3 (Gervais et al., 1999)). Furthermore, whilst research into the non-canonical pathway is still in its relative infancy, δ- and meprin-β cleavage have also been implicated in AD pathogenesis (Andrew et al., 2016; Jefferson et al., 2011) and can also produce toxic Aβ monomers and Aβos (Muller et al., 2017). Aside from Aη, which attenuates neuronal activity (Willem et al., 2015), the physiological roles of these cleavage mediators are currently unknown (Muller et al., 2017).

Caspase cleavage, the most well characterised non-canonical pathway cleavage enzyme, cleaves CTFα/β at Asp664 (within the AICD region) yielding a C31 fragment (Fig 1.1; (Lu et al., 2003), which is implicated in neuronal apoptosis (Nhan et al., 2015). However, caspase cleavage has been implicated in both AICD production (Gervais et al., 1999) and AICD proteolysis (Lu et al., 2003; Muller et al., 2017), possibly in a caspase subtype-specific manner (Harada and Sugimoto, 1999; Marín et al., 2000; Y. J. Park et al., 2014; Sáez-Valero et al., 2000). A Jcasp fragment composed of residues located between caspase- and γ-secretase cleavage sites on APP is also produced *via* this pathway (Park et al., 2009). Jcasp fragments may act to inhibit pre-synaptic transmitter release *via* interactions with, and sequestering of, molecules involved in vesicle release (Fanutza et al., 2015). Importantly, Aβ induces caspase cleavage of APP and production of C31, creating an apoptosis-promoting feed-forward cycle (Lu et al., 2003; Marín et al., 2000). Indeed, mutation of APP at the caspase cleavage site rescues electrophysiological impairments, synaptic loss, dentate gyrus atrophy and behavioural abnormalities in $APP_{SWE/V717F}$ mice, despite the presence of Aβos and plaques(Galvan et al., 2006). It is unknown, however, whether or not caspase cleavage ultimately affects the production of Aβo (Gervais et al., 1999; Soriano et al., 2001).

In healthy individuals, Aβ formation through the amyloidogenic pathway is usually balanced either by its subsequent degradation, primarily by the enzyme neprilysin and insulin-degrading enzyme (IDE; Hersh & Rodgers, 2008), and/or its extrusion from the brain, primarily *via* the efflux transporters LDLRs, particularly the low-density lipoprotein receptor-related protein 1 (LRP1) and the ATP-binding cassette (ABC) transporters. Conversely, the

main influx transporter is the advanced glycosylation end product-specific receptor (RAGE). Aβ accumulation and toxic insult, therefore, reflect an imbalance in the ratio of production to degradation and/or clearance mechanisms (Murphy and LeVine, 2010; Pearson and Peers, 2006). Interestingly, it is suggested that in LOAD, that impaired Aβ degradation, rather than increased production, underlies the disease (Saido et al., 2000). In support of this, neprilysin levels are decreased in AD brains, particularly in regions with high Aβ loads such as the hippocampus (Wang et al., 2003; Yasojima et al., 2001). This decreased degradation activity is likely exacerbated in AD by increased Aβ transport into the brain as there is a lower expression of LRP1 and ABC transporters and overexpression of RAGE (Tarasoff-Conway et al., 2015).

Whilst the majority of Aβ is secreted out of the cell where, in AD, it eventually forms Aβ plaques, Aβ molecules spend a significant portion of time in intracellular compartments following their production as well as when they are internalised and/or targeted for degradation. Under such circumstances, Aβ can impair mitochondrial (Zhao et al., 2010) and synaptic function (Takahashi et al., 2002) and thus contribute directly to AD pathology (Zheng et al., 2012).

Interestingly, alterations in the flux of APP itself may be involved in AD progression. It is thought that PM-localised APP is primarily processed *via* the non-amyloidogenic pathway. Therefore, upregulation of the endosomal/lysosomal recycling pathway may encourage amyloidogenic APP processing due to optimal β-secretase activity occurring within acidic organelles (Jiang et al., 2014; Muller et al., 2017). Two separate AD susceptibility genes illustrate the subtleties of subcellular localisations in AD pathology. Firstly, sortilin-related receptor 1 (SORL1), which regulates APP trafficking and processing, particularly anterograde and retrograde movement between TGN and early endosomes, is modulated by ApoE and tau (Yin et al., 2015). SORL1 normally functions in a neuroprotective manner through its targeting of APP to the recycling pathway. However, alterations in SORL1 expression or SORL1 mutation appear to direct APP towards amyloidogenic processing (Rogaeva et al., 2007). Secondly, internalisation of APP and Aβ can be enhanced by mutations in the gene coding for phosphatidylinositol binding, clathrin assembly protein (PICALM), which enhances $A\beta_{40}$ and $A\beta_{42}$ production (Kanatsu et al., 2014; Xiao et al., 2012). ApoE also removes Aβ molecules from the CNS by chaperoning them to insulin degrading enzyme (IDE) and/or by enhancing LDL receptor-related protein (*e.g.* SORL1)- mediated endosome recycling (Jiang et al., 2008). Increased expression of APP, partly due to the production of interleukin-1 (IL-1), a mediator in the inflammatory response to AD, may also accelerate the formation of ‘toxic’ Aβ metabolites (Griffin, 2006).

ApoE

Inheritance of the ε4 allele of the apolipoprotein *ApoE* gene is the strongest known genetic risk factor for the development of LOAD (Coon et al., 2007; Roses et al., 1995). The most likely mechanism for this increased risk is due to the fact that ApoE4 expression results in decreases in the efficiency of Aβ breakdown and clearance (Liu et al., 2013).

ApoE expression is highest in the liver, followed by the brain (Vance, 2012). The highest dynamic concentrations of ApoE are found in non-neuronal cells, primarily in astrocytes and, to some extent, in microglia (Grehan et al., 2001; Pitas et al., 1987). Neurons can also produce ApoE under certain conditions, such as in response to excitotoxicity, although it is present at much lower levels than in astrocytes (Grehan et al., 2001; Pitas et al., 1987; Xu et al., 2006).

Astrocytes produce and secrete ApoE which acquires cholesterol and phospholipids, generating ApoE-containing lipoproteins (Vance, 2012). ApoE then functions as a ligand in LDLR family-mediated endocytosis of lipoprotein particles (Boyles et al., 1989; Posse De Chaves et al., 2000). Following endocytosis, the majority of ApoE is recycled back to the cell surface by retro-endocytosis, whilst minor levels of ApoE degradation also occurs (Rensen et al., 2000). This process enables the transport of cholesterol between astrocytes and neurons (Michikawa et al., 2000; Vance, 2010), which is essential for normal neuronal function (Vance, 2012). ApoE containing lipoproteins are implicated in synaptogenesis (Mauch et al., 2001), maintenance of synaptic connections (Pfrieger, 2003) and axonal growth (Hayashi et al., 2004) and they prevent neuronal cell death (Hayashi et al., 2009). Outside of this specific cholesterol role, however, some ApoE receptors also function as signalling receptors (Beffert et al., 2004; Hayashi et al., 2007; Herz, 2001). ApoE synthesis is also increased 150-fold in response to nerve injury, suggesting a role for ApoE in nerve repair (Comley et al., 2011; Ignatius et al., 1986). Notably, ApoE also enhances the proteolytic breakdown of Aβ proteins, both within and between cells and thus regulates the clearance from and/or aggregation within the CNS of these proteins (Liu et al., 2013).

The human *ApoE* gene exists as three polymorphic alleles, ε2, ε3 and ε4, with a worldwide frequency of 4%, 77.9% and 13.7%, respectively. In the sporadic AD population, however, the frequency of the ε4 allele is approximately 40% (Farrer et al., 1997). These alleles give rise to ApoE isoforms, ApoE2, ApoE2 and ApoE4. These isoforms differ by only one or two AAs, but are profoundly different in terms of their structure and function (Mahley et al., 2006), including their ability to bind lipids, receptors and Aβ (J. Chen et al., 2011; Frieden and Garai, 2012; Zhong and Weisgraber, 2009). As mentioned previously, inheritance of the ε4 allele is the strongest known

genetic risk factor for the development of LOAD, whilst inheritance of the ε2 allele is neuroprotective (Bertram et al., 2007; Corder et al., 1993; Farrer et al., 1997; Huang and Mucke, 2012; Strittmatter et al., 1993). For example, people with a single or double copy of the ε4 allele have approximately four and twelve- times (conservative estimates) the likelihood of developing AD, respectively, when compared to those with ε3 allele inheritance (Bertram et al., 2007; Guojun Bu, 2009). Inheritance of the ε4 allele is also associated with an earlier age of AD onset (Gómez-Isla et al., 1996; Roses, 1996).

The reason why the ε4 form of ApoE leads to a decrease in the age of AD onset and speeds up its progression is likely due to the role that this lipoprotein plays in Aβ metabolism. Specifically, ApoE normally serves to facilitate Aβ clearance and/or degradation from/within the brain (Sanan et al., 1994). This is illustrated by the fact that ApoE KO mice exhibited impaired Aβ clearance, degenerating nerves (Fagan et al., 1998) and learning deficits (Masliah et al., 1995; Veinbergs et al., 1998). It has also been demonstrated that increasing ApoE-containing lipoprotein production in the hippocampus and cortex of a mouse model of AD (using the retinoid X receptor agonist bexarotene) enhanced Aβ degradation, reduced Aβ plaque area and improved memory and cognition (Cramer et al., 2012). Specifically, with regard to ε4 allele carriers, it is known that they have lower plasma and brain ApoE levels (Gupta et al., 2011). This is significant as low levels of ApoE in the brain also correlate with an increased risk of developing AD (Bales et al., 2009). Furthermore, in terms of ApoE4 function, it binds with less avidity to Aβ than ApoE3, thereby decreasing the efficiency of Aβ clearance (Castellano et al., 2011; Koistinaho et al., 2004; LaDu et al., 1994). Furthermore, ApoE2 and ApoE3, but not ApoE4, can form dimers which may enhance Aβ degradation (Xue et al., 2011). In support of this suggestion, there is increased Aβ deposition in mice expressing the ε4 allele compared with ε3 or ε2 (Bales et al., 2009; Castellano et al., 2011). In humans, inheritance of the ε4 allele acts to increase the generation and accumulation of Aβ proteins, particularly at early/pre-symptomatic AD stages in the cortex (Polvikoski et al., 1995), and decrease their removal from cerebrospinal fluid (Berridge, 2010).

Aside from Aβ degradation, the cholesterol-carrying, metabolism and homeostatic function of ApoE may also be implicated in AD, in the context of Aβ clearance. As mentioned previously, when the ε4 allele is expressed in transgenic mice, Aβ clearance mechanisms are inefficient, in comparison to those animals expressing ε3 allele (Bien-Ly et al., 2011). Cholesterol levels, can also modulate γ-secretase activity and increase Aβ production (Osenkowski et al., 2008).

Polymorphisms in the ApoE receptors, LRP and ApoER2, also appear to correlate with an increased risk of AD development (Elder et al., 2007;

Fryer et al., 2005; Kim et al., 2009b). These receptors function in both ApoE mediated endocytosis and signalling pathways (Beffert et al., 2004). Furthermore, LRP is involved in the uptake and clearance of Aβ (G. Bu, 2009).

ABC transporters, including ABCA1, ABCG1 and/or ABCG4 mediate the shuttling of cellular lipid to ApoE which contributes to the formation ApoE-containing lipoproteins (Vance, 2012). ABCA1 has been linked to AD and to the regulation of ApoE and cholesterol homeostasis in the brain (Hirsch-Reinshagen and Wellington, 2007; Vance, 2010). ABCA1 is required for the normal acquisition of lipids by ApoE during lipoprotein assembly (Hirsch-Reinshagen and Wellington, 2007; Wahrle et al., 2004). Furthermore, ABCA1 KO mice exhibited an 80% reduction in ApoE levels, illustrating its importance in ApoE homeostasis (Hirsch-Reinshagen and Wellington, 2007; Wahrle et al., 2004). Interestingly, when ABCA1 KO mice were crossed with mouse models of AD, there was no effect on Aβ production. However, poorly lipidated ApoE lipoproteins particles were responsible for an increased Aβ load, suggesting, once more, that reduced ApoE function/efficiency is involved in reduced brain Aβ clearance in AD (Hirsch-Reinshagen and Wellington, 2007; Wahrle et al., 2005). Furthermore, overexpression of ABCA1 in transgenic AD mice decreased Aβ deposition (Wahrle et al., 2008). Interestingly, the effect of ABCA1 may be ApoE isoform-dependent as the lack of one copy of ABCA1 resulted in decreased Aβ clearance, increased Aβ plaque deposition and memory deficits in mice carrying the ε4 allele, but not in those carrying the ε3 allele (Fitz et al., 2012). This evidence suggests that alterations in the machinery regulating lipid homeostasis are involved in the transport, processing and clearance of Aβ proteins.

More specific roles for ApoE in Aβ removal from the brain involve its transport to the systemic circulation across the BBB. ApoE4 impedes this process to a greater extent than both ApoE2 and ApoE3 (Deane et al., 2008). ApoE3 is also more efficient in stimulating microglial-mediated degradation of Aβ when compared with ApoE4 (Jiang et al., 2008). ApoE-lipoprotein particles may also sequester Aβ and promote its cellular uptake and degradation (Kim et al., 2009a). Conversely, ApoE4 enhances Aβ fibrillogenesis (Bales et al., 2009; Kim et al., 2009a; Liu et al., 2013).

Thus, it is clear that that isoform-specific expression of ApoE4 is strongly implicated in AD pathogenesis. The effects of ApoE4 appear to be multi-factorial, although the strongest link connecting it to AD pathology is *via* its involvement in the Aβ cascade. This has important implications for our understanding of the genetic component of AD, given that ApoE has such diverse effects and that inheritance of the ApoE ε4 allele is the main genetic determinant of AD risk.

1.2.4 Presenilins

Presenilins (PS) are integral membrane proteins containing nine transmembrane domains (Spasic et al., 2006), which are primarily localised to ER membranes (Annaert et al., 1999) and are ubiquitously expressed throughout the brain and most peripheral tissues. There are two PS mammalian homologs (with 80% sequence homology); PS1 (located on chromosome 14) and PS2 (located on chromosome 1), which are recognised as the catalytic subunit of the γ-secretase complex (De Strooper et al., 2012). PS undergo endoproteolytic cleavage to amino-terminal (NTF) and CTF fragments and it is this cleaved PS which forms a complex with nicastrin, aph-1, and pen-2 subunits. Together they function as the γ-secretase complex (Zhang et al., 2010) which directly processes APP to form Aβ (and related molecules), and indirectly processes Notch (Wolfe, 2010). Indeed, cells (SH-SY5Y, HEK293 and blastocyst cells) lacking in PS do not exhibit γ-secretase activity and produce no Aβ or AICD (Hass and Yankner, 2005; Zhang et al., 2000). That being said, $A\beta_{42}$ production remains after PS1 and PS2 KO in embryonic stem cells (Wilson et al., 2003), possibly due to the previously mentioned non-canonical APP processing pathway.

Mutations in human PS1, of which there have been 212 recorded to date, account for 2-3% of all AD cases and over half of EOFAD cases. The 3xTg-AD mouse model and TgF344-AD rat model studied for this thesis express human PS1 mutations associated with EOFAD ($PS1_{M146V}$ and $PS1\Delta E9$ respectively; Clark et al., 1995; Luo et al., 2014; Riudavets et al., 2013; Rogaeva et al., 2001). By contrast, mutations in PS2 only account for approximately 0.1% of AD cases (Tsai et al., 2002). Many of these known PS1 and PS2 mutations are implicated in Ca^{2+} signalling dysregulation, including mobilisation of calcium from the ER, ER-mitochondrial signalling and refilling of the ER through store-operated calcium entry (SOCE; Bezprozvanny and Mattson, 2008; Filadi et al., 2016; Stutzmann, 2007; Supnet and Bezprozvanny, 2010; Zampese et al., 2011; see Section 1.4 The Ca 2+ hypothesis of AD). Mutations in both PS homologs have been tangibly linked to altered APP processing resulting in increased Aβo and AICD production (Duff et al., 1996). It is likely that these roles are not independent as PS effects on Ca^{2+} dysregulation partially involves y-secretase activity (Akbari et al., 2004; Bojarski et al., 2009). Conversely, however, some PS1 FAD mutations can also reduce γ-secretase activity (Bentahir et al., 2006; Fernandez et al., 2014; Xia et al., 2015a).

In terms of effects on brain function, conditional PS1 and 2 KO in the postnatal mouse forebrain resulted in deficits in memory and hippocampal synaptic plasticity, as well as progressive neurodegeneration in the cerebral

cortex and an increased inflammatory response (Beglopoulos et al., 2004; Saura et al., 2004).

Aside from APP processing and modulation of intracellular calcium homeostasis however, it is worth noting that PS has numerous other biological substrates such as APoER2 lipoprotein receptor, the LDLR-related protein, ErbB4 receptor tyrosine kinase, CD44, p75 neurotrophin receptor, nectin-1α, syndecan-3, E- and N-cadherins and β subunits of voltage-gated sodium channels which are involved in functions like cell adhesion, cell signalling, neuronal structure and neuronal development (Koo and Kopan, 2004; Wong et al., 2005). Although it is beyond the scope of this thesis to detail in depth the function of these proteins, and the possible effects that PS activity has on them, it is clear that due to its potentially multiple effects on a host of biological activities, in addition to APP processing and calcium homeostasis, a clear and simple elucidation of the effects of PS mutations in conditions such as AD is challenging.

PS/γ-secretase mutations can also mediate cellular dysfunction *via* alterations in the processing of the integral membrane protein Notch (Pardossi-Piquard et al., 2005; Zhang et al., 2000). Notch functions as a receptor for ligands including Jagged and Delta, the binding of which results in Notch being proteolytically cleaved within its TM domain by PS1, resulting in the release of Notch Intracellular Domain (NICD). This, in turn, affects the expression of genes which are essential for a wide variety of development processes, including haematopoiesis, somitogenesis, vasculogenesis, and neurogenesis (for reviews see (Baron, 2003; Lasky and Wu, 2005)). In the brain, NICD-mediated gene expression also affects proteins involved in structural and functional plasticity processes of learning and memory, processes which also implicate Notch dysfunction in AD memory impairments (Lathia et al., 2008). In support of altered Notch function arising from PS mutation, PS1 KO mice die shortly after birth (Conlon et al., 1995; Swiatek et al., 1994) and exhibit skeletal and neurological development abnormalities, which would be expected due to altered Notch activity (Selkoe and Schenk, 2003). Furthermore, γ-secretase inhibition in adult mice alters lymphocyte development and intestinal morphology, again likely *via* Notch cleavage alterations (Wong et al., 2004).

1.2.5 Types & activities of Aβ molecules

As discussed above, the biochemical mechanisms underlying APP processing and the production of numerous APP fragments and Aβ molecules is reasonably well understood. However, how this accumulation might lead to the progressive development of AD remains unclear. To date, much research has been conducted on the role that Aβ plaques play in AD

pathology. Indeed, AD is only definitively diagnosed following the identification of Aβ plaques in the brain post-mortem (Braak and Braak, 1991; McKhann et al., 1984). However, to date, clinical trials aimed at targeting such plaques and/or inhibiting their formation have been unsuccessful as they failed to alleviate cognitive impairments or even slow the rate of progression of AD (Galimberti and Scarpini, 2011). Additionally, cognition does not correlate well with plaque density in that cognitively healthy people at the time of death can also have high plaque loads. For example, 69% of cognitively normal people at a mean age of 84 had neuritic plaques in the neocortex and hippocampus and at least 25% had sufficient numbers of plaques and NFTs to meet diagnostic criteria for a diagnosis of AD (Maarouf et al., 2011). Furthermore, Aβ plaques can form directly after brain trauma. For instance, 30% of cognitively normal people who die within days of severe head injury exhibit Aβ plaques (consisting of both $A\beta_{40}$ and $A\beta_{42}$) in one or more cortical areas (Roberts et al., 1994). These lines of evidence suggest that plaque load in and of itself does not correlate well with cogitation and/or with cognitive decline in AD (Berg et al., 1998; Perry et al., 2000; Snowdon, 1997). That being the case, amyloid plaques are now *generally* regarded as 'markers' of AD rather than actual initiators of the disease process, although this does not necessarily rule out a role for them as the disease progresses. For instance, Ca^{2+} dysregulation and neuronal hyperexcitability occur in neurons close to Aβ plaques (Busche et al., 2008; Kuchibhotla et al., 2008). Thus, it is also possible that the plaques are acting to localise and target Aβo to extracellular/synaptic sites of action *via* 'secondary nucleation' (i.e. the catalyses of Aβo formation from Aβ monomers; Fig 1.3; Verma et al., 2015). These shortcomings of Aβ plaques in fitting with AD pathology lead to the question of where Aβ proteins do they 'fit' into the pathogenesis of AD?

In attempting to answer this question, the general focus in Aβ research has shifted from the insoluble amyloid plaques to the shorter, soluble, oligomers of Aβ which are the precursors to plaque formation (Fig 1.3; Deshpande et al., 2006; Haass and Selkoe, 2007; Klein et al., 2001; Lesné et al., 2006; McGowan et al., 2005; Näslund et al., 2000; Shankar et al., 2008; Walsh et al., 2002; Walsh and Selkoe, 2004).

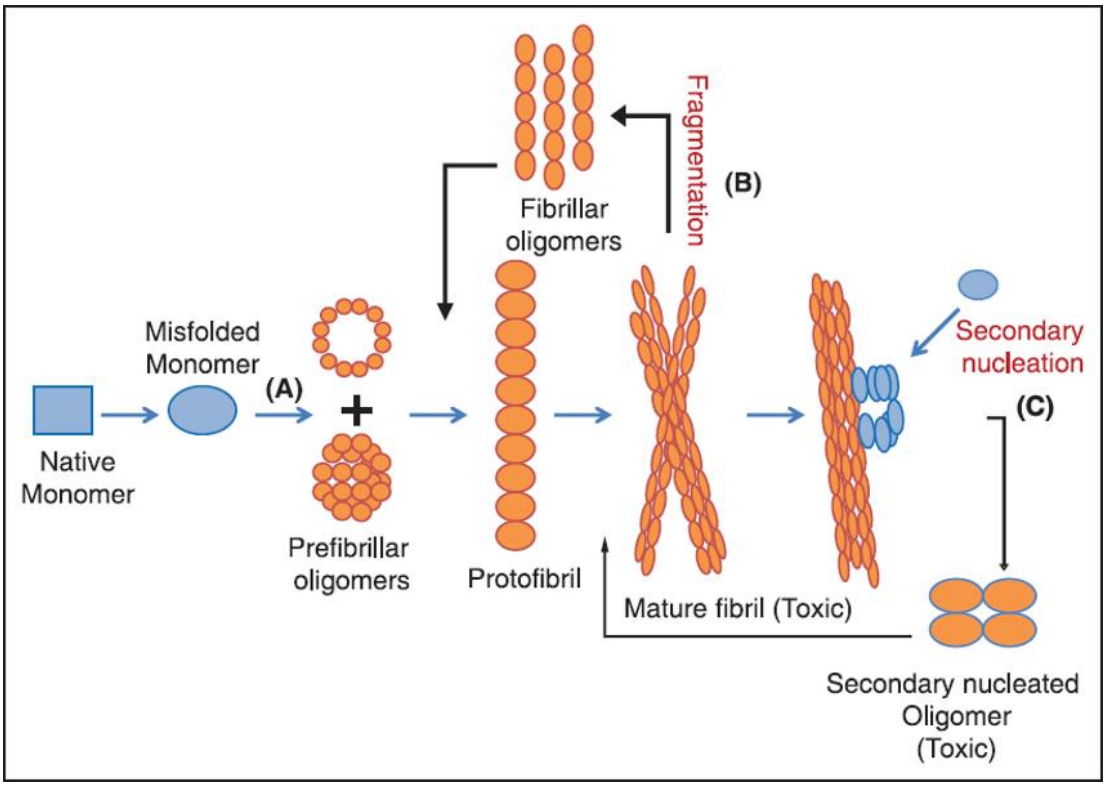

Figure 1.3. Amyloid aggregation

(A) Amyloid beta (Aβ) monomers form heterogeneous prefibrillar oligomers (Aβo) which aggregate to form insoluble protofibrils. These, in turn, form mature fibrils and, eventually, plaques.

(B) Mature fibrils undergo fragmentation to produce fibrillar oligomers (*i.e.* oligomers originating from fibrils) which can form protofibrils/mature fibrils again.

(C) Mature fibrils can also catalyse the formation of oligomers from monomers *via* 'secondary nucleation'. Such secondary nucleated oligomers are toxic, diffusible and can, in turn, contribute to fibril formation.

Adapted with permission from Verma et al. (2015)

Aβ dysregulation, as detected by alterations in CSF levels of $A\beta_{42}$ and/or PET imaging of fibrillar Aβ, occurs well before clinical diagnosis of AD and as such is one of the first detectable biomarkers for LOAD. This would suggest that these non-plaque Aβs play some role in the earlier stages of the disease or may even initiate the disease process (Holtzman et al., 2011). Non-toxic Aβ monomers can aggregate to form various toxic species (Fig 1.3) such as heterogeneous Aβo (also referred to as Aβ–derived diffusible ligands (ADDLs) and prefibrillar oligomers) which are composed of between approximately two to fifty Aβ monomers. These oligomers form protofibrils, insoluble mature fibrils and, eventually, plaques. Importantly, these Aβ molecules are likely to exist in dynamic equilibrium (Selkoe, 2002). Indeed, mature fibrils which undergo fragmentation to produce fibrillar oligomers (*i.e.* oligomers originating from fibrils) can re-form protofibrils/mature fibrils again (Fig 1.3, B; Kayed et al., 2009; Verma et al., 2015). Furthermore, mature fibrils can also catalyse the formation of oligomers from diffusing monomers *via* 'secondary nucleation' (Fig 1.3, C). These secondary nucleated oligomers are toxic, diffusible and can, in turn, contribute to fibril formation (S. I. A. Cohen et al., 2013).

It should be noted that although Aβo, particularly those composed of $A\beta_{42}$ (Sakono and Zako, 2010; which is more hydrophobic, and aggregates more readily, than Aβ40; Burdick et al., 1992; Gu and Guo, 2013; Nunan and Small, 2000), are widely recognised as the most toxic form of Aβ and believed to be most pertinent to AD onset and progression, the dynamic equilibrium of Aβ molecules is not well understood. Notably, FAD mutations increase the ratio of $A\beta_{42/40}$ (Borchelt et al., 1996; Scheuner et al., 1996), indicating that elevated $A\beta_{42}$ levels relative to $A\beta_{40}$ could be a factor in the disease pathogenesis. One hypothesis proposes that $A\beta_{42}$ provides the core for the assembly of oligomers, fibrils and plaques (Iwatsubo et al., 1994; Jarrett et al., 1993). Other studies have found that $A\beta_{40}$ maintains the solubility of $A\beta_{42}$ (J. Kim et al., 2007) and that an increase in $A\beta_{40}$ concentration results in 60 – 90% Aβ deposition decrease *in vivo* (Giuffrida et al., 2009).

Notably, the structure of Aβo is variously described as consisting of Aβo, $A\beta_{42}$o, $A\beta_{40}$o, ADDLs, low and high molecular weight Aβo (LMW- & HMW- Aβo), fibrillar oligomers, secondary nucleated oligomers, spherical oligomers and annular oligomers, among other components. These different descriptions may reflect either a difference in molecular structure, the specificity of the molecules for their related pathological roles and/or the formation of structures (such as protofibrils, fibrils, mature fibrils and plaque aggregates) into which these molecules tend to aggregate (Finder and Glockshuber, 2007; Kotler et al., 2014; Verma et al., 2015).

Importantly, as discussed above, APP undergoes extensive and complex processing into numerous bioactive molecules. A further level of complexity is added to this signalling system when one also takes into account that the effects of one group of these molecules, Aβ monomers, depends upon their structure, concentration and length of exposure, all of which results in great difficulties modelling the behaviour of these entities *in vivo* (Deshpande et al., 2006; Glabe, 2008; Renner et al., 2010). For instance, when investigating the synaptic binding of Aβo, LMW-Aβo applied at a low concentration, it initially diffused in the manner expected of regular proteins, then subsequently slowed with time. This did not result in any detectable synaptotoxicity over a 24hr time course. However, HMW-Aβo acted differently, demonstrating rapid and widespread synaptic binding which resulted in significant synaptotoxicity within 24 hrs (Lacor et al., 2007; Renner et al., 2010). Furthermore, the length of incubation time with Aβo also alters their effects, illustrated by the fact that acute application of Aβo induces calcium and mitochondrial dysregulation as well as widespread cell death, whilst chronic application of lower concentrations of Aβo induces more subtle mitochondrial alterations (human cortical neurons; HCNs; Deshpande et al., 2006).

The specific molecular actions of Aβ molecules, with a particular focus on Aβo and their Ca^{2+} dysregulating effects, will be described in the following section.

1.2.6 Molecular actions of Aβo and related metabolites

Several molecular mechanisms have been proposed to explain the varying and widespread effects of Aβo on neuronal physiology, including the formation of Ca^{2+} pores in the PM, modulation of membrane channel function and/or conductance (both PM and ER), synaptic impairment and mitochondrial dysfunction (Fig 1.4). A large proportion of these actions involve Ca^{2+} or act to destabilise intracellular calcium dynamics, which in turn can increase the amyloidogenic processing of APP (Mattson et al., 1992). It is this evidence that forms the basis of the Ca^{2+} hypothesis of AD (*Section 1.4)*. In the following section, I will outline some of the effects of Aβo on neuronal physiology.

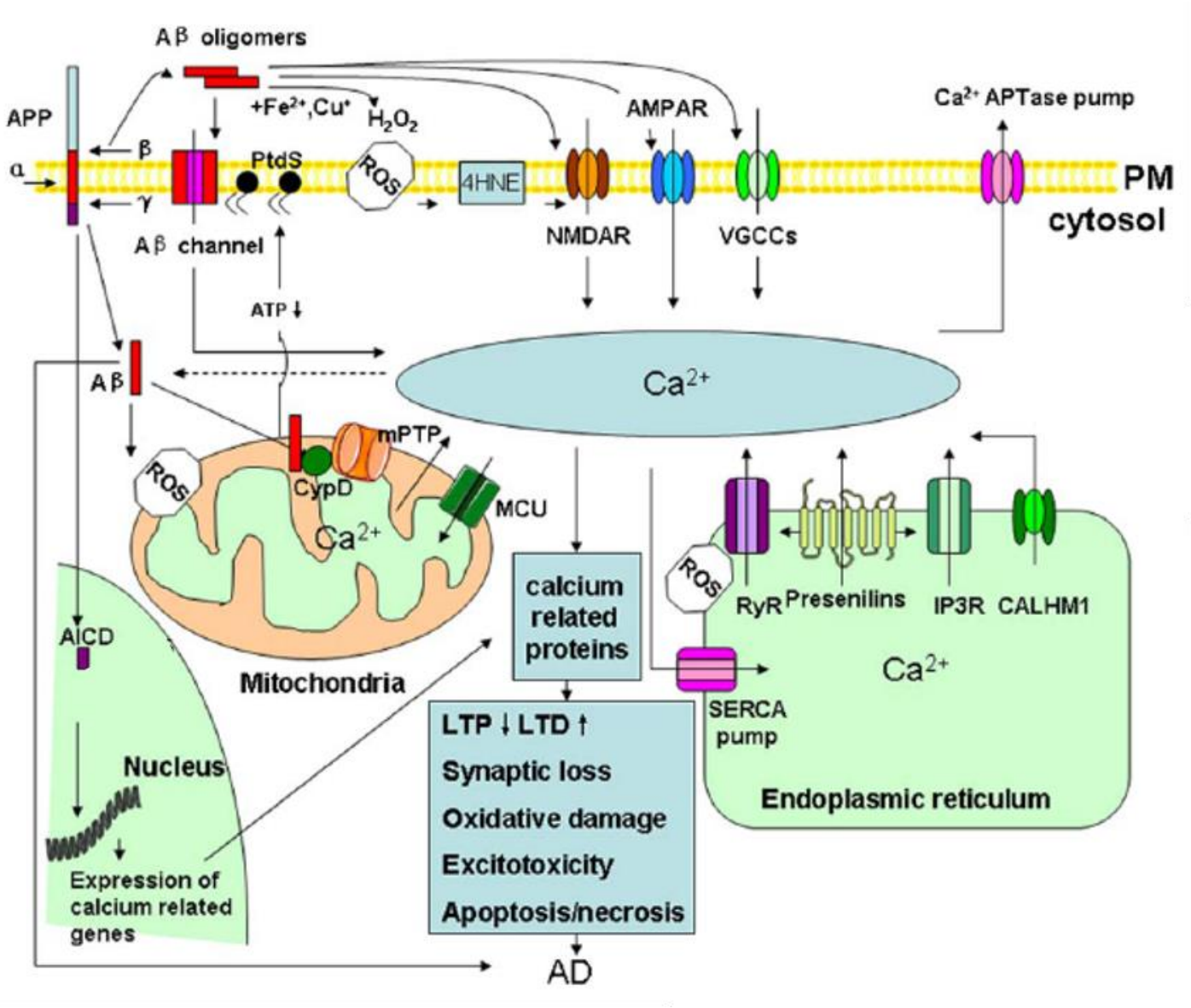

Figure 1.4. Molecular actions of APP metabolites

There are several molecular mechanisms for the varying and widespread effects of amyloid beta oligomers (Aβo; formed from sequential cleavage by β-secretase (β) and γ-secretase (γ)) on neuronal physiology including:

a) enhancing Ca^{2+} entry including through: i) the formation of Ca^{2+} specific channels/pores in the PM which is enhanced by phosphatidylserine (PtdS) positioning on the outer leaflet of the PM, which is in turn enhanced by mitochondrial impairment ii) alterations in membrane permeability *via* interactions with Fe^{2+} and Cu^{+} and subsequent generation of reactive oxygen species (ROS; including H_2O_2) at the PM. This results in lipid peroxidation, generating neurotoxic aldehyde 4-hydroxynonenal (HNE). HNE covalently modifies membrane transporters including PM Ca^{2+} ATPases (attenuating Ca^{2+} extrusion) and ion channels including VGCCs and NMDARs, iii) direct modulation of Ca^{2+} conductances through a plethora of PM channels including: NMDARs, α-amino-3-hydroxy-5-methyl-4-isoxazolepropanoic acid receptors (AMPARs) and VGCCs.

b) Aβ causes mitochondrial oxidative stress which is exacerbated by Ca^{2+} dysregulation. Cell-wide Ca^{2+} increases result in mitochondrial Ca^{2+} overload (via uptake the through mitochondrial Ca^{2+} uniporter (MCU) which results in impairment of the electron transport chain, increased ROS production and decreased ATP production. These effects eventually result in the opening the mitochondrial permeability-transition pore damaging the ultrastructure of the mitochondria and release Ca^{2+}

Cell-wide Ca^{2+} dysregulation also has causes stark disruption of ER Ca^{2+} dynamics, explained in *Section 1.4 Calcium hypothesis*. Furthermore, AICD migrates to the nucleus where it modifies expression of genes important for Ca^{2+} homeostasis. Ultimately, this Ca^{2+} dysregulation results in impaired synaptic plasticity (including long-term potentiation (LTP) and long-term depression (LTD), synaptic loss, oxidative damage, excitotoxicity and cell death.

Adapted with permission from Yu et al. (2009).

Membrane Alterations

Modulation of Receptor Activity

Ca^{2+} flux through the PM is controlled by three main transporters; the Na^+/K^+-ATPase, which serves to maintain the resting membrane potential and restores membrane potential following depolarisation (Stahl, 1984), the plasma membrane Ca^{2+}-ATPase (PMCA), which maintains basal $[Ca^{2+}]_i$, and the Na^+/Ca^{2+} exchanger (NCX) which rapidly removes Ca^{2+} following stimulation, but can reverse direction with membrane depolarization.

Acute Aβo exposure ($Aβ_{1-40}$ & $Aβ_{25-35}$) in cultured rat hippocampal neurons selectively impaired Na^+/K^+-ATPase activity and induced an elevation of $[Ca^{2+}]_i$ and apoptosis, effects which could be reversed by antioxidant treatment. The same acute Aβo exposure did not affect the activities of Mg^{2+}-dependent ATPases or NCX (Mark et al., 1995). Furthermore, exposure of synaptosomes derived from post-mortem human hippocampus (from neurologically normal individuals aged 79-85 years) to Aβ also impaired Na^+/K^+-ATPase and PMCA activity, without affecting other Mg^{2+}-dependent ATPase activities or NCX (Mark et al., 1995). Therefore, Aβ exposure has the potential to alter membrane potential and alter the flow of critical ions through the PM, all of which would have profound deleterious effects on neuronal activity/viability.

Aβo can also modulate the function and expression of several plasma membrane-, and ER-bound channels, including those involved in Ca^{2+} signalling. Consequently, there are a number of mechanisms by which they can affect neuronal function and stability. The receptors upon which Aβo exert modulatory effects include, a) voltage-gated calcium channels (VGCCs; N-, T-, L-, P- & Q- VGCCs (Dursun et al., 2011; Webster et al., 2006)), b) nicotinic acetylcholine receptors (nAChR; Dougherty et al., 2003; Liu et al., 2009), c) N-methyl-D-aspartic acid receptors (NMDARs; De Felice et al., 2007; Li et al., 2011), d) α-amino-3-hydroxy-5-methyl-4-isoxazolepropanoic acid receptors (AMPARs; Hsieh et al., 2006; Whitehead et al., 2017), e) metabotropic glutamate receptors (mGluRs; Haas et al., 2014; Renner et al., 2010; Sokol et al., 2011; Um et al., 2013), f) angiotensin II receptors (AbdAlla et al., 2009) and g) the ER calcium release channels, IP_3R (Demuro and Parker, 2013) and RyR (Supnet et al., 2006).

Aβ Pores

It is proposed that Aβo can form Ca^{2+}-specific channel-like structures which allow unregulated movement of Ca^{2+} into cells (Arispe et al., 1993a; Durell et al., 1994). These initial findings were supported by human studies in which electron microscopy was utilised to identified channel-like pores in post-mortem AD brains. Numerous Aβ oligomers, including $Aβ_{42}$, $Aβ_{40}$, as well as truncated Aβ fragments, $Aβ_{11-42}$ and $Aβ_{17-42}$ (generally considered

non-amyloidogenic but present in AD and DS plaques (Jang et al., 2010)), have been implicated in this ion channel forming ability (Bode et al., 2017; Huang et al., 2000; LIN et al., 2001; Sanderson et al., 1997; Sepulveda et al., 2010). Significantly, these types of Aβ pore were not found in healthy controls (Inoue, 2008).

Aβo-mediated Ca^{2+} entry into cells is enhanced by the presence of phosphatidylserine (PtdS) on the cell surface (Lee *et al.*, 2002). However, the movement of PtdS to the cell surface is usually indicative of cells undergoing apoptosis (van den Eijnde et al., 1998). Thus, it is proposed that AD-related mitochondrial impairment could cause PtdS to flip from the inner to the outer leaflet of the plasma membrane, allowing it to come in contact with Aβ which, in turn, appears to induce Ca^{2+} influx and cell death (Simakova & Arispe, 2006). Furthermore, neurons exhibiting increased surface PtdS are more vulnerable to Aβ toxicity (Simakova and Arispe, 2007).

There is also some evidence that Aβos (both $Aβ_{40}$ and $Aβ_{42}$) can disrupt membrane lipid integrity *via* interactions with phospholipids and modulation of membrane composition, with Aβo found to bind more avidly to phospholipids than fibrillar Aβ (Askarova et al., 2011; Williams and Serpell, 2011). Furthermore, Aβo may also cause an increase in membrane permeability in a receptor-independent fashion, through membrane thinning, thereby causing alterations in Ca^{2+}, Na^{2+} and K^{+} conductance/homeostasis. This, in turn, would impair transporter and ion channel activity (Sokolov et al., 2006), ultimately resulting in the induction of neurite and neuronal degeneration (Mattson, 2004). This disruption of membrane integrity may be mediated by interactions between Aβo (which is inserted in the PM) and Fe^{2+} and Cu^{+} to generate hydrogen peroxide and hydroxyl radicals (Morgan et al., 2000). Indeed, antioxidants which inhibit reactive oxygen species (ROS) formation such as vitamin E, oestrogen and uric acid, prevented impairment of membrane transporters, stabilised intracellular Ca^{2+} levels and prevented cell death in Aβ-treated neurons (Ba et al., 2004; Keller et al., 1997). However, as mitochondria are significant generators of cellular ROS (Murphy, 2009), this neuroprotective effect of antioxidants may also be due to their ability to ‘mop up’ mitochondrially-generated ROS (Birben et al., 2012), as opposed to that mediated by Aβo at the PM.

Synaptic Disruption

A key characteristic of Aβ-mediated pathology in AD is related to its ability to disrupt synaptic function, likely through factors such as altered Ca^{2+} homeostasis, dysregulation of PM and ER receptors, as well as more general cellular homeostatic and structural alterations. As an indication that synaptic dysfunction may be an early-stage disease event, cortical soluble Aβ levels correlate with the degree of synaptic loss, in mildly cognitively impaired (MCI) patients (Lue et al., 1999).

In this respect transgenic APP mice (APP_{695SWE} and APP_{V717F}) exhibit significant deficits in synaptic transmission and LTP compared with controls (hippocampal CA1 field; Aβ plaque independent; Hsiao et al., 1999; Larson et al., 1999). Failure to maintain LTP was also observed in 5-7-month-old APP(Val^{642} → Ile) mice (Moechars et al., 1999) and 15 – 17-month-old APP (Lys^{670} → Asn, Met^{671} → Leu double mutation) mice (Chapman et al., 1999). In the latter study, no alteration in basal synaptic transmission was observed. Conversely, in hippocampal slices taken from APP_{SWE} mice at 12 and 18 months, LTP was normal but there were significant alterations in basal synaptic transmission (Fitzjohn et al., 2001).

Discrepancies such as these may illustrate specific alterations in synaptic activity as the disease progresses. For example, in work utilising APP_{V717F} mice, at 1-4 months there was a 40% decrease in basal hippocampal SC-CA1 synaptic transmission, but no change in LTP. However, by 8 – 10 months, basal synaptic transmission had decreased by 80% and LTP was inhibited. This impairment appeared to be due to reduced synapse number rather than a decline in the function of individual synapses between 2 to 10 months. Interestingly, when these results are compared to those derived from a mouse cell line with lower APP expression, but higher Aβ production (APP_{695SWE}), impairment of synaptic transmission at 2-4 months was exacerbated, implying that Aβ-specific effects of APP are involved in mediating this effect (Hsia et al., 1999). Indeed, synaptic dysfunction appears to be specifically dependent upon $Aβ_{42}$ levels, and not on Aβ plaque burden or APP levels in APP transgenic mice (Hsia et al., 1999; Mucke et al., 2000).

The suggestion that the degenerative effects of Aβo are selectively targeted towards synapses, as opposed to being a generalised ‘attack’ across the entire neuronal surface, is supported by the fact that they accumulate extracellularly and selectively at hippocampal synapses (Renner et al., 2010). APP is also actively transported to pre-synaptic terminals and accumulates within synaptic regions, allowing a mechanism for mutated APP to cause a direct disruption of synaptic function (Bezprozvanny and Mattson, 2008). Receptors at the post-synaptic membrane are stabilised *via* interactions with scaffolding proteins (Renner et al., 2008). However, this stabilisation is transient, with receptors able to diffuse into and out of the post-synaptic membrane in a manner dependent upon synaptic activity (Renner et al., 2008; Triller and Choquet, 2008). Importantly, the population of synaptic receptors exists in equilibrium with extrasynaptic receptors, a fact which can leave synapses vulnerable to disruption if receptor diffusion is altered (Ehlers et al., 2007).

Such a vulnerability, specifically to the effects of Aβo, has clearly been demonstrated in experiments utilising single particle tracking of Aβo in living

synapses. These experiments showed that clusters of Aβo diffused laterally and accumulated at excitatory synapses. These clusters increased in number over time in mature cultured hippocampal neurons (21 – 27 days in vitro (DIV); Renner et al., 2010). Significantly, however, Aβo *decreased* (Renner et al., 2010) the ability of mGluR5 to diffuse laterally away from the synapses (Sergé et al., 2002). mGluR5 is primarily located on dendrites outside synapses, whilst any mGluR5 near the synapse is normally stabilised in a ring at the periphery of the post-synaptic density (Lujan et al., 1996; Luján et al., 1997). The decrease in mGluR5 mobility induced by Aβo is likely due to the formation of pathological extracellular stabilising matrices, resulting in their aggregation and the formation of 'artificial signalling platforms' which, in turn, results in aberrant Ca^{2+} signalling (neuronal Ca^{2+} signalling and that mediated by I-mGluRs is detailed in *Section 1.3 Ca^{2+} signalling)* that ultimately decreases synaptic NMDAR expression (Renner et al., 2010). The decrease in mobility induced by Aβo was specifically selective for mGluR5 as they had no effect on α-amino-hydroxy-5-methyl-4-isoxazolepropionic receptor (AMPAR) and GABAR mobility (Renner et al., 2010). These effects induced by Aβo were mimicked both by artificial clustering of mGluR5 (induced by crosslinking mGluR5s) and antagonists of mGluR5 (Renner et al., 2010). Furthermore, mGluR5 KO hippocampal cultures exhibited a large decrease in Aβo binding to the neuronal surface and a near halting of effects on synaptic NMDAR loss, revealing the mGluR5-dependent nature of the Aβo effects (Renner et al., 2010).

Aβo-mGluR mediated synaptic impairment is also supported by the following observations: a) membrane depolarisation is evoked by $Aβ_{42}$ and involves mGluR1 in differentiated human hNT neuronal cells and rat nerve growth factor-differentiated PC12 cells (Blanchard et al., 2002), b) Aβo suppresses hippocampal LTP and enhances LTD, actions which are reversed by mGluR5 agonists and antagonists, respectively (Rammes et al., 2011; Shankar et al., 2008; Q. Wang et al., 2004), c) mGluR5 antagonism or antibody intervention also reversed synapse loss in hippocampal neurons *in vitro* and *in vivo,* as well as memory deficits (Chung et al., 2010; Haas et al., 2014; Hu et al., 2014; Rammes et al., 2011; Renner et al., 2010; Um et al., 2013) and d) Aβo decreased the availability of phosphatidylinositol-4,5-bisphosphate (PIP2), the substrate for PLC which could decrease levels of the Ca^{2+} liberating second messenger IP_3 following I-mGluR stimulation (primary cortical neurons; Berman et al., 2008).

The evidence described in this section illustrates that mGluR5 is implicated in Aβo-mediated synaptic impairment. However, the nature of synaptic alterations, particularly with regard to NMDAR activity and expression, is variable across studies and may reflect differences in Aβo type

(natural or synthetic), concentration and length of exposure or may reflect a progression from one type of pathology to another (Renner et al., 2010).

Group I mGluRs (I-mGluRs) modulate NMDAR-dependent LTP and LTD in the hippocampus and are implicated in NMDAR-dependent learning (Benarroch, 2008). In agreement with the aforementioned study by Renner et al. (2010), research by Lacor's group found that Aβo (high concentrations of synthetic oligomers) induced increases in the immediate early gene *Arc*/Arg3.1 (Lacor et al., 2007, 2004a). mGluR5-LTD is dependent upon this memory-related immediate early gene (Waung et al., 2008) as *Arc* couples changes in neuronal activity patterns to alterations in synaptic plasticity (Bramham et al., 2010). Activation of *Arc* is enhanced above normal levels by Aβo binding to mGluR5 and may contribute to the pathological effects of Aβo at the synapse (Lüscher and Huber, 2010; Um et al., 2013). It also results in altered spine morphology, decreased spine number, depletion of surface NMDAR and dysregulation of NMDA signalling pathways (Lacor et al., 2007; Shankar et al., 2007; Snyder et al., 2005). Furthermore, mGluR5 antagonism or antibody intervention reverses synapse loss in hippocampal neurons *in vitro* and *in vivo,* as well as memory deficits (Chung et al., 2010; Haas et al., 2014; Hu et al., 2014; Rammes et al., 2011; Renner et al., 2010; Um et al., 2013). Interestingly, elevated Arc, mediated by mGluR5 activation, also stimulates Aβ production by redistributing APP and PS1 to endocytic vesicles (Wu et al., 2011), possibly leading to another deleterious AD feed-forward cycle.

An alternative mechanism of synaptic plasticity impairment by Aβo is proposed by Wang et al. (2004). This was adapted to include the recently discovered actions of Aβo mediated mGluR5 pathological signalling at the synapse (Renner et al., 2010). High-frequency stimulation (HFS) induces LTP *via* NMDAR activation and influx of Ca^{2+} *(see Section 1.7)*. mGluR5 is pathologically stimulated due to cellular prion protein (PrP^{C})-Aβo (see below) mediated activation and/or activation by the neurotransmitter glutamate released during HFS or by glia following their activation by Aβo. This combined activation then stimulates kinase-mediated inhibition of LTP. Specifically, the kinases proposed to be involved are c-Jun N-terminal kinase (JNK), cyclin-dependent kinase 5 (CdK5) and p38 mitogen-activated protein kinase (MAPK) which have been shown to be activated by Aβo (Bolshakov et al., 2000; Liu et al., 2001; Rush et al., 2002).

mGluR5 signalling can exacerbate NMDAR-induced excitotoxicity *via* activation of the Ca^{2+} dependent enzyme calcineurin (CN; Bruno et al., 2000, 1995). Furthermore, mGluR5 antagonism has been shown to protect neurons against Aβo-induced toxicity (cortical cultures; Bruno et al., 2000). This pathological mGluR5/NMDAR signalling may underlie the molecular

mechanism by which the NMDAR modulator memantine protects against Aβo-induced toxicity (De Felice et al., 2007; Lacor et al., 2007).

Notably, membrane fluidity and localisation of mGluR5 to the aforementioned artificial signalling platforms may also be influenced by PrP^C, which is known to localise with and form complexes together with group 1 mGluRs (comprised of mGluR1 and mGluR5) and NMDARs (Khosravani et al., 2008; Perroy et al., 2008a; Renner et al., 2010; Tu et al., 1999; Um et al., 2013).

Role of Cellular Prion Protein (PrP^C)

PrP^c is a glycosylphosphatidylinositol (GPI)-anchored protein, tethered to the extracellular surface of the cell membrane, which signals *via* complex formation with other TM receptors (Beraldo et al., 2016) such as mGluRs (Beraldo et al., 2016, 2011, Haas et al., 2016, 2014; Um et al., 2013) and NMDARs (Black et al., 2014).

PrP^c is of particular interest within AD research as a growing body of evidence suggests that it can function as a high affinity, Aβo-specific receptor which is essential for mediating the toxic effects of Aβo such as the suppression of synaptic activity (including hippocampal LTP), synapse loss, axonal degeneration and cell death as well as learning and memory deficits in transgenic APP/PS1 animals (Bate and Williams, 2011; Chen et al., 2010; Gimbel et al., 2010; Haas et al., 2014; Hu et al., 2014; Kudo et al., 2012; Larson et al., 2012; Laurén, 2014; Laurén et al., 2009; Ostapchenko et al., 2013; Um and Strittmatter, 2013). This is evidenced by the fact that anti-PrPc antibodies not only reduce the binding of Aβo to the PM but also rescue Aβo –induced impairments such as synaptic dysfunction in hippocampal slices (Barry et al., 2011; Chung et al., 2010; Freir et al., 2011; Laurén et al., 2009). Furthermore, in support of a disease-relevant role for PrP^C in AD, human AD brains contain PrPc- interacting Aβo and Aβ – PrP^c complexes (Barry et al., 2011; Freir et al., 2011; Laurén et al., 2009; Um et al., 2013; Zou et al., 2011).

At the post-synaptic density (PSD) these Aβ–PrP^c complexes interact with intracellular Fyn kinase (Larson et al., 2012; Um et al., 2012). Indeed, both PrP^C and Fyn are enriched in the PSD (Collins et al., 2006; Um et al., 2012). Fyn kinase functions are diverse and in the CNS include the regulation of synaptic function, plasticity and myelination (for review see (Resh, 1998). Under normal physiological conditions, Fyn kinase can regulate glutamate receptor trafficking and plasticity, in part, by phosphorylating NMDARs (Grant et al., 1992; Prybylowski et al., 2005).To this end, Aβo–PrP^C-Fyn complexes can evoke synaptic disruption *via* alterations in both mGluR5 (Beraldo et al., 2016) and NMDAR trafficking and activation (Larson et al., 2012; Um et al., 2012), as well as the

aforementioned effects on mGluR5 stabilisation at the PSD (Um et al., 2013). Although mGluR1 and mGluR5 can both form PrP^{c}-Fyn complexes, only mGluR5 mediates Aβo-induced calcium signalling in oocytes. These Aβo-PrP^{C}-mGluR5 complexes stimulate Fyn, which causes PLC-dependent increases in $[Ca^{2+}]_i$ (see *Section 1.3 Ca^{2+} signalling*) in both *Xenopus* oocytes and neurons (Um et al., 2013). Notably, Fyn can also interact with tau to mediate potentially mGluR5-independent neurotoxic effects (Ittner et al., 2010; Lee et al., 2004; Roberson et al., 2011).Aβo-PrP^{C}-mGluR5 complexes also appear responsible for eukaryotic elongation factor 2 (eEF2) phosphorylation, impairments in LTP, spine loss and spatial memory impairments (Um et al., 2013). eEF2 is a calcium/calmodulin (CaM) - dependent kinase which is activated physiologically by mGluR5 and mediates *Arc* translation (described previously).

Aside from mGluR5-specific effects, synaptic accumulation of Aβo and fibrils could also account for the synaptic breakdown observed in AD (Friedlich et al., 2004; Lee et al., 2002), which may also occur *via* increased *Arc* transcription (Lacor et al., 2004). Furthermore, application of Aβo at very low concentrations results in actin-depolymerizing factor/cofilin- (involved in cytoskeleton plasticity) and CN - dependent decreases in NMDAR activity and dendritic spine number after 5 -15 days. The number of cells expressing NMDAR subunits (NR1 and NR2A subunits) was also lower in transgenic mice (APP_{SWE} mice at 18 -22 months). Furthermore, this deficit could be reversed by the application of aducanumab (an anti-amyloid-β antibody; Sevigny et al., 2016, Shankar et al., 2007). These synaptic alterations could provide a mechanism for the synapse loss induced by Aβo application in culture (Lacor et al., 2007) and that is also observed in AD mouse models (Koffie et al., 2009).

Conversely, however, Aβo have also been shown to *increase* NMDAR responses and induce excitotoxicity (De Felice et al., 2007; Szegedi et al., 2005), effects which may mediate Aβo-stimulated oxidative stress and increased $[Ca^{2+}]_i$ (Bezprozvanny and Mattson, 2008; Cullen et al., 1996), Furthermore, the production of Aβ at nerve terminals is regulated by synaptic activity and downstream signalling pathways, likely involving the transport and processing of Aβ *in vivo* (Cirrito et al., 2005; Gandy et al., 1993). This overlap illustrates a continual trend therefore of molecular ‘opportunities’ for feedforward disease progression linking to the degenerative nature of the condition.

This summary provides a glimpse of the surfeit of mechanisms by which both APP processing and cleavage, as well as the relative concentrations of Aβ molecules and the assemblies that they form, can influence disease pathology. It is unsurprising therefore that any inherent neuroprotective mechanisms designed to clear or degrade such insults are

overwhelmed or that pharmacological intervention targeting Aβ plaques in the clinical setting is unsuccessful. Crucially, both Ca^{2+} dysregulation and Aβ converge on the majority of the AD-affected processes outlined above. Indeed, Ca^{2+} may often be the mediator of Aβo toxic effects and *vice versa*. As such, both the Aβ cascade and Ca^{2+} hypothesis of AD are inextricably linked. Before moving on to explain the Ca^{2+} hypothesis of AD, I will first endeavour to provide the reader with an insight into key aspects of neuronal calcium signalling, particularly as it pertains to hippocampal signalling. The hippocampus is one of the first regions to be affected in AD and was therefore chosen as the area from which the primary experimental unit utilised in the production of data for this thesis, the cultured hippocampal neuron, was harvested.

1.3 Calcium signalling

1.3.1 Overview

Calcium is the central signalling molecule of neurons and is intrinsically associated with their vital functions (Stutzmann, 2007). This versatile molecule and the cytostructural and homeostatic system pertaining to it allows for crucial physiological roles in cellular homeostasis, intracellular signalling, as well as mediating and transducing responses to a wide range of external stimuli. As such, it is implicated in cellular activities such as the regulation of gene transcription (Berridge, 1998; Mellstrom & Naranjo, 2001), modulation of membrane excitability (Davies *et al.*, 1996; Stutzmann *et al.*, 2003), enzyme/kinase activity and mitochondrial function (Supnet & Bezprozvanny, 2010). Ca^{2+} is also critical for determining synaptic activity such as basal synaptic transmission, synaptic plasticity (short and long-term forms) and dendritic spine morphology (Berridge, 2010; Chakroborty and Stutzmann, 2014; Fujii et al., 2000; Hayashi and Majewska, 2005; Nakamura et al., 1999).

The ability of calcium to regulate such diverse activities within the cell is facilitated by its strict cellular compartmentalization which, in turn, is mediated primarily *via* bi-directional interactions between the plasma membrane and the ER, the main calcium store in neurons. Together, these two structures form a continuous binary membrane within cells (Berridge, 2002). Structurally, the ER is relatively unorganised in neurons and whilst it spreads throughout the cell, there appears to be a division between rough ER in the soma, which is primarily involved in protein synthesis, but which transforms into smooth ER responsible for pre- and post-synaptic Ca^{2+} signalling events surrounding synaptic plasticity in the dendrites and spines (Berridge, 1998). The nuclear envelope, mitochondria, Golgi and lysosomes are also capable of Ca^{2+} storage and release and add a further level of complexity to cellular Ca^{2+} signalling and homeostasis which will be briefly touched upon in the following sections (Giorgi et al., 2009; Michelangeli et al., 2005; Rizzuto et al., 2009).

ER

The ER is implicitly involved in a number of signalling processes such as Ca^{2+} flux, apoptosis, arachidonic acid (AA) release and sterol biosynthesis (Berridge, 1998). Ca^{2+} homeostasis is critical for signaling-specific functions, but also for ER protein handling, including their synthesis, folding, trafficking, disaggregation and degradation. The ER, as a signalling organelle, is sensitive to numerous stimuli including Ca^{2+}, IP_3, cADPR, L-type channel inputs, ROS, sphingosine-1-phosphate S-1-P and sterols, to which the ER can respond through a variety of mechanisms including Ca^{2+} and arachidonic

acid (AA) release, as well as activation of store-operated calcium channels (SOCCs; see below), stress signals and numerous transcription factors with wide downstream implications (including NF-κB, CHOP, ATF-6 and SREBPs; Berridge 2002). Disturbances of these process result in the production of numerous pathological phenotypes, so-called 'calciumopathies' (Stutzmann, 2007). Indeed, dysregulation of calcium homeostasis at the level of the ER has the capacity to extensively disrupt Ca^{2+}-dependent signalling events in a global manner, given the concentration gradients involved, as well as the extensive ER network in the neuron (Berridge, 1998).

Resting cytosolic Ca^{2+} concentration ($[Ca^{2+}]_{cyt}$) is normally maintained between ~50-300nM (Verkhratsky *et al.*, 2004). Thus, a large electrochemical gradient exists between the cytosol and the ER (the concentration of Ca^{2+} in the ER ($[Ca^{2+}]_{ER}$) ranges from 100 to 500μM; LaFerla, 2002), and the extracellular space, with a $[Ca^{2+}]_o$ of 2.5mM. The differing Ca^{2+} concentrations within cells are maintained by four key components: 1) heterogeneous Ca^{2+} channels on the plasma membrane which allow Ca^{2+} entry into the cell, 2) transport to, from, and between organellar Ca^{2+} stores, including the ER, mitochondria and lysosomes, 3) Ca^{2+} release channels on the ER, including IP_3R and RyR and 4) ER and PM Ca^{2+} transporters, Ca^{2+} ATPases and $Na^{+/}Ca^{2+}$ exchangers, which establish baseline concentration gradients, with respect to both intracellular and extracellular compartmentalisation (Berridge et al., 2003). Indeed, it is the intricate interplay between these four components which enables Ca^{2+} microdomain maintenance and the production of complex spatiotemporal Ca^{2+} dynamics, which ultimately allow and control the disparate functions of Ca^{2+} in the cell (Berridge, 2006; Berridge et al., 2003).

Ca^{2+} ATPases and Na^{+}/Ca^{2+} exchangers on the plasma membrane (PMCA and NCX) control Ca^{2+} extrusion into the extracellular space. The concentration gradient between the ER and cytoplasm is maintained by the sarco/endoplasmic reticulum Ca^{2+} ATPases (SERCA), which sequester Ca^{2+} into the ER. These pumps are sensitive to both $[Ca^{2+}]_{ER}$ and $[Ca^{2+}]_{cyt}$, which affects the rate that Ca^{2+} is pumped into the ER (Berridge et al., 2003). However, once Ca^{2+} has been taken up by the ER, it does not remain there indefinitely. In the absence of further stimuli, Ca^{2+} leaks out into the cytosol over a finite time period in the order of seconds to minutes (Rae and Irving, 2003).

Several types of protein have been proposed to mediate this basal ER Ca^{2+} leak. These proteins include PS1 and 2 (Bezprozvanny and Mattson, 2008; Tu et al., 2006), Ca^{2+} homeostasis modulator 1 (CALHM1; Dreses-Werringloer et al., 2008), transient receptor potential (TRP) family-like polycystin-2 (TRPP2), members of anti-apoptotic proteins of the B-cell lymphoma 2 (Bcl-2 and Bcl-2-associated X protein (Bax)-inhibitor-1 (BI-1)

families and hemichannel-forming proteins such as pannexins (Sammels et al., 2010). Research concerning this ER leak function is in its infancy and there are numerous conflicting reports for the importance of most of the proteins listed above in the leak of Ca^{2+} from the ER. However, as described in *Section 1.4 Ca^{2+} hypothesis of AD*, the role of PS in ER Ca^{2+} leak and its AD-related impairment is generally accepted.

Mitochondria are localised close to the ER at specific contact sites, particularly at ER Ca^{2+} release sites (Rizzuto et al., 1993). This factor allows for a triad of communication with the ER, mitochondria and lysosomes (Burgoyne et al., 2015), possibly enabling a role for this triad in Ca^{2+} signalling and ER refilling (Arnaudeau et al., 2001). What is known is that the ER-mitochondrial network is critical in cell death regulation (Decuypere et al., 2011; Pinton et al., 2008). Ca^{2+} entry into the mitochondria occurs *via* the mitochondrial Ca^{2+} uniporter (MCU; Baughman et al., 2011) and voltage-dependent anion channel 1 (VDAC1; Giorgi et al., 2015). Mitochondria act as high-capacity, low-affinity transient calcium buffers in the cytoplasm, altering the dynamics of intracellular Ca^{2+} signalling such as limiting the peak of $[Ca^{2+}]_{cyt}$ following stimulation and broadening the time profile of the elevation (Nicholls, 2005). A strong driving force exists for mitochondrial Ca^{2+} accumulation due to the large negative membrane potential (approximately −180 mV) across the inner mitochondrial membranes (Rizzuto et al., 2012). This, combined with the existence of contact sites overcome the low-affinity Ca^{2+} transport characteristics of the mitochondrial uniporter (Baughman et al., 2011; De Stefani et al., 2011). Contact sites allow for significant localised Ca^{2+} increases (up to 20 μM) upon opening of IP_3Rs which can be taken up efficiently by mitochondria (Csordás et al., 2010). In the recovery phase of a calcium response, the mitochondrially-sequestered Ca^{2+} is released back into the cytoplasm *via* Na^+/Ca^{2+} and H^+/Ca^{2+} exchangers (Palty et al., 2012; Scanlon et al., 2000). It is then either returned to the ER by the SERCA pump or extruded from the cell. Faster mechanisms (ms timescale) of Ca^{2+} entry into mitochondria are also proposed, which may enable a more physiologically relevant continuity between ER and mitochondrial membranes (Beutner et al., 2005; Sparagna et al., 1995).

The calcium buffers BiP, calreticulin and calnexin stabilise free $[Ca^{2+}]$ in the ER, which influences the overall amount of Ca^{2+} that is available for stimulus-evoked release (Prins and Michalak, 2011). This obviously directly impacts upon ER-specific signalling processes, which are mediated by free $[Ca^{2+}]$ (Corbett & Michalak, 2000). The presence of ER calcium sensor proteins, including visinin-like protein (VILIP) and calcium-sensing processes such as store-operated calcium entry (see below) also allows the cell to react and adapt to different ER loading states (Mattson, 2007).

In addition to the relatively immediate regulatory and signalling roles described above, the ER itself is highly dynamic and can undergo longer-term (hours to days) regulatory adaptations. These adaptations can be in physical size, shape and composition in response to changing demands, such as that experienced during development, stress and/or disease and ageing (Federovitch et al., 2005; Sammels et al., 2010). Pathological ER adaptations will, in turn, have significant effects on cellular calcium dynamics, including mitochondrial dysfunction (Bergner and Huber, 2008; Deniaud et al., 2008; Roderick and Cook, 2008).

1.3.2 Extracellular calcium entry

Ca^{2+} ions can enter neurons from the extracellular space through a variety of ion channels, with varying selectivity and permeability for calcium. These channels include VGCCs and ligand-gated calcium channels such as NMDARs, AMPARs, nicotinic receptors, ATP gated purinergic channels (P2XCs), SOCCs and CALHM1 (Dreses-Werringloer et al., 2008; Habermacher et al., 2016; Supnet and Bezprozvanny, 2010).

Store-operated Ca^{2+} entry (SOCE, *a.k.a.* capacitative Ca^{2+} entry (CCE)) occurs through SOCCs of which the Ca^{2+} release-activated Ca^{+} (CRAC) channel and transient receptor potential canonical (TRPC) family of calcium-permeable channels have been characterised thus far (Cheng et al., 2013; Salido et al., 2009).

SOCE is thought to be triggered by ER Ca^{2+} depletion. This trigger threshold depletion is thought to be more likely to arise from a reduction in $[Ca^{2+}]_{ER}$ at specific microdomains within the ER because widespread depletion would activate stress signalling and disrupt cellular function (Berridge 2002). Stromal interaction molecule (STIM) 1 is a protein located on the ER membrane (Liou et al., 2005; Wu et al., 2006) which acts as a sensor of calcium depletion (Cahalan, 2009). When this occurs, STIM1 proteins oligomerise and migrate to the ER-PM junction (Liou et al., 2007; Roos et al., 2005). The oligomers then activate the PM channel Orai1 and induce Ca^{2+} influx through CRAC channels (measurable by the Ca^{2+} release-activated current, I_{CRAC} (Luik et al., 2008) and store replenishment *via* the ER SERCA pumps (LaFerla, 2002). The SOCE pathway is the principal Ca^{2+} entry pathway in non-excitable cells where it is implicated in motility, secretion and gene expression (Parekh and Putney, 2005). However, SOCE has also been observed in excitable cells of the nervous system (Putney, 2003; Verkhratsky and Toescu, 2003), including cultured hippocampal neurons (Baba et al., 2003; Berna-Erro et al., 2009).

There are two STIM homologs (STIM1 and STIM2) present in the ER of neurons (Moccia et al., 2015). Although a clear role for STIM 1 in neuronal SOCE has been identified, there is now considerable evidence to suggest that STIM2 also mediates neuronal SOCE (Gruszczynska-Biegala et al., 2011; Gruszczynska-Biegala and Kuznicki, 2013; Sun et al., 2014; Zhang et al., 2015b). Interestingly, although SOCE was originally thought to be activated in response to ER depletion, STIM2-activated Ca^{2+} influx can be activated by small decreases in $[Ca^{2+}]_{ER}$, and may thus play an important role in maintaining the tight regulation of $[Ca^{2+}]_{cyt}$ *vs* $[Ca^{2+}]_{ER}$ gradients (Brandman et al., 2007).

Briefly, TRPCs can be activated independently by the PLC-mediated production of diacylglycerol (DAG) and/or in a coordinated manner with CRAC channels following ER Ca^{2+} depletion, both of which can be mediated by I-mGluR stimulation (see below; Putney and Tomita, 2012).

1.3.3 Intracellular calcium release

Ca^{2+} release from the ER occurs primarily *via* activation of IP_3Rs and/or RyRs in a highly regulated manner that is controlled by Ca^{2+}, ATP, kinases and phosphatases (Ivanova et al., 2014). RyRs and IP_3Rs, of which there are three subtypes each, differ significantly from one another in terms of their expression, localisation, activation mechanisms and physiological roles. Numerous tissues express multiple IP_3R isoforms, although IP_3R1 is enriched in neurons, IP_3R2 in the heart and liver, and IP_3R3 in lymphocytes and multiple cell lines (Ivanova et al., 2014).

Neurons express all three subtypes of both RyRs and IP_3Rs, although IP_3R1 and RyR2 expression predominate (Berridge, 1998; Franzini-Armstrong and Protasi, 1997; Furuichi et al., 1994; Simpson et al., 1995). RyR2 is distributed widely in the brain, RyR3 expression is predominant in the CA1 hippocampal region and RyR1 is almost exclusively expressed in cerebellar Purkinje cells (Furuichi et al., 1994). Generally, IP_3R and RyRs co-localise on subsurface cisternae originating from the ER and are distributed throughout the compartments of the neuron (Fagni et al., 2000) including axonal endings and dendritic spines (Berridge, 1998; Sharp et al., 1993). Aside from this general pattern of co-localisation, RyRs are also distinctly localised to the soma of neurons (Kano et al., 1995; Kuwajima et al., 1992; Seymour-Laurent and Barish, 1995; Sharp et al., 1993). Furthermore, in the CA3 and hilar hippocampal regions as well as in the cerebral cortex, RyRs are more prominently expressed at dendritic spines than IP_3Rs (Augustine and Finch, 1998; Sharp et al., 1993; Takechi et al., 1998).

IP_3Rs are generally activated indirectly following agonist stimulation of PM-bound receptors, specifically G-protein (G_q subunit)-coupled receptors (GPCRs) such as I-mGluRs and M1 and M3 muscarinic acetylcholine receptors (mAChRs; Foskett et al., 2007; Wettschureck and Offermanns, 2005). When an agonist binds to these types of G_q-linked receptors it stimulates phospholipase C to cleave PIP2, forming diacylglycerol (DAG) and IP_3 (Niswender 2010). IP_3 then binds to IP_3Rs on the ER membrane, opening them to allow Ca^{2+} efflux from the ER, down its concentration gradient into the cytosol. IP_3Rs are sensitive to both cytosolic and ER Ca^{2+}, with maximal stimulation occurring when both Ca^{2+} and IP_3 are present in the cytosol (Missiaen et al., 1994). This relatively simplistic picture is complicated by the fact that I-mGluRs are part of a multi-molecular complex which contains NMDAR and possibly PrPc, suggesting that their signalling is inherently linked to these molecules and their downstream pathways and/or substrates (Khosravani et al., 2008; Perroy et al., 2008b; Renner et al., 2010; Tu et al., 1999). This is evidenced by the ability of I-mGluRs to modulate NMDAR-dependent LTP and LTD in the hippocampus (Benarroch, 2008).

RyRs on the other hand, are generally activated by Ca^{2+}-induced calcium release (CICR) *via* Ca^{2+} influx or ER calcium release. For example, CICR can be induced following membrane depolarisation and activation of VGCCs and following ER Ca^{2+} mobilisation through IP_3Rs and RyRs (Zalk et al., 2007). Therefore, cytosolic calcium serves to enhance IP_3R-and RyR-mediated signals. However, upon reaching a threshold concentration, cytosolic calcium then inhibits subsequent ER calcium release by negative feedback (Stutzmann, 2007). This prevents an increase in cytosolic Ca^{2+} levels above a threshold which could lead to neurotoxic effects (Friel & Tsien, 1992).

Although it is possible to activate IP_3Rs and RyRs independently of each another, as demonstrated in cultured hippocampal and sensory neurons where receptor-stimulated- and IP_3-mediated Ca^{2+} mobilisation was independent of caffeine -sensitive (*i.e.* RyR-mediated) Ca^{2+} release (Murphy and Miller, 1989; Thayer et al., 1988), there is evidence that both channels can indirectly regulate each other's activity. This is primarily due to the fact that both channels are sensitive to cytoplasmic and luminal (ER) Ca^{2+} (Burdakov et al., 2005; Györke and Terentyev, 2008; Missiaen et al., 1994). Thus, by altering ER and cytoplasmic Ca^{2+} levels it is possible to create an excitable system whereby signals can spread throughout a cell (Berridge, 2002)

In support of this, cerebellar granule neurons exhibit characteristics of a shared Ca^{2+} pool, as pre-application of RyR agonists significantly reduces carbachol- and IP_3R-mediated Ca^{2+} release and *vice versa* (Irving et al., 1992; Simpson et al., 1996). The question as to whether or not IP_3Rs and

RyRs access the same ER Ca^{2+} pool, however, is unclear, although the confluence *or* demarcation into microdomains of such Ca^{2+} pools could represent a mechanism of signal regulation in a cell type and/or intracellular localisation dependent manner (Berridge, 2006; Laude and Simpson, 2009). Notably, both of these channel types are thought to also contribute to Ca^{2+} leak currents from the ER in both health and disease (Suzuki et al., 2012; Szlufcik et al., 2006).

$[Ca^{2+}]_{cyt}$ can increase up to 1-5μM in response to agonist stimulation through the mechanisms outlined above. However, it is important to bear in mind that any evoked calcium increase triggers distinct spatiotemporal patterns of cytosolic Ca^{2+} release/accumulation depending on the initial source of Ca^{2+}. These patterns, in turn, can also result in different Ca^{2+}-dependent signalling cascades being activated (Supnet & Bezprozvanny, 2010). Due to the extensive and complex role of Ca^{2+} signalling in neurons, even minor alterations in the Ca^{2+} signalling apparatus could potentially have significant deleterious consequences at both a cellular and systems level over the lifetime of a cell or individual. Indeed, subtle intracellular calcium dysregulation has been linked to the pathogenesis of numerous proposed ‘calciumopathies’ including AD, Parkinson’s disease (PD) and Huntington’s disease (HD; Berridge, 2014a; Chakroborty and Stutzmann, 2014; Mattson, 2007).

1.4 The calcium hypothesis of Alzheimer's disease

The central tenet of the calcium hypothesis of AD is that remodelling of the Ca^{2+} signalling system, resulting in increased basal Ca^{2+} levels, is caused by, or precedes, excessive stimulation of the amyloidogenic APP processing pathway. This results in early-stage disease phenotypes including oxidative stress, mitochondrial impairment, synaptic dysfunction, cognitive deficits and, ultimately, widespread neuronal cell death which characterises the later stages of AD (Berridge, 2010; Bezprozvanny and Mattson, 2008; Deshpande et al., 2006; Glabe and Kayed, 2006; Kelly and Ferreira, 2006; Stutzmann, 2007; Townsend et al., 2006). Importantly, it is thought that these phenotypic changes can be induced by small fluctuations in normal intracellular and/or luminal Ca^{2+} levels over the lifetime of a neuron, as was postulated for ageing and neurodegeneration, in general, several years previously by Khachaturian (Khachaturian, 1989).

Ca^{2+} is a key factor in cytotoxicity (Kass and Orrenius, 1999) and Ca^{2+} dysregulation is seen in neurons from both human AD patients and AD animal models (LaFerla, 2002; Stutzmann and Mattson, 2011), as well as with ageing (Gant et al., 2014). The sheer number of components of the calcium signalling system altered in AD is staggering (Fig 1.4), as reviewed by Yu et al. (2009) with more recent findings reviewed by The Alzheimer's Association Calcium Hypothesis Workgroup (2017). The following section aims to provide the reader with an overview of some of these alterations, such as dysregulation of basal $[Ca^{2+}]_i$ as well as Ca^{2+} influx and intracellular mobilisation, which have particular relevance to the work conducted over the course of this project. Such changes impact severely upon several critical cellular systems including mitochondria and synapses (Berridge, 2010; Bezprozvanny and Mattson, 2008; Smith et al., 2005; Thibault et al., 2007).

Significantly, several studies in animal models of AD suggest that disruption of normal Ca^{2+} homeostasis occurs well in advance of any behavioural or synaptic deficits (Chakroborty et al., 2009; Jacobsen et al., 2006; Oddo et al., 2003a; Smith et al., 2005; Vale et al., 2010) and/or Aβ or tau aggregation (Chakroborty et al., 2009; Chakroborty and Stutzmann, 2014; Del Prete et al., 2014; Popugaeva et al., 2012; Stiller et al., 2014; Stutzmann et al., 2004; Zhang et al., 2010). The possibility exists therefore that the cognitive deficits seen in AD patients are, in fact, a result of early onset, chronic and insidious neurotoxic processes involving Ca^{2+} dyshomeostasis that occurs before any functional loss or amyloidogenic processes became apparent (Stutzmann, 2007). This calcium hypothesis is gaining credence within a field where scepticism continues to grow around the proposal that amyloid plaques are solely to blame for the pathological effects of AD (Castellani and Smith, 2011; Castello et al., 2014; Herrup, 2015).

1.4.1 Remodelling of basal calcium levels

It is known from ageing studies that decreased serum calcium levels correlate well with the level and rate of cognitive decline during ageing (Schram et al., 2007). Therefore, it is interesting to note that, AD patients also exhibit altered systemic calcium homeostasis in terms of decreased serum Ca^{2+} and increased urinary Ca^{2+} excretion, relative to age-matched controls (Landfield et al., 1992; Ogihara et al., 1990). Furthermore, alterations in the levels of proteins and genes which are directly involved in neuronal Ca^{2+} signalling are commonly observed in brain tissue samples from AD patients and animal models of AD (Bezprozvanny and Mattson, 2008; Chin et al., 2007; Emilsson et al., 2006; Iritani et al., 2001; Landfield et al., 1992; Ogihara et al., 1990; Stutzmann, 2007). For instance, overall levels of both IP_3 and PLC, as well as protein kinase C (PKC; important in synaptic plasticity and activated by calcium-dependent pathways) activation, are decreased relative to the degree of AD progression in the human brain (Kurumatani et al., 1998).

Although there have been relatively few studies examining Ca^{2+} homeostasis in tissues and fluids from human AD patients, one study has shown that lymphocytes from LOAD patients did exhibit higher basal $[Ca^{2+}]_i$ concentrations and an enhanced Ca^{2+} response to lymphocyte activation than controls (Sulger et al., 1999). Similarly, lymphocytes from $PS1_{M146L}$ mice also exhibited increased basal $[Ca^{2+}]_i$ and larger Ca^{2+} responses to lymphocyte activation, as well as increased sensitivity to Ca^{2+}- and ROS-mediated apoptosis (Eckert et al., 2001; Mattson, 2002). Furthermore, double PS KO (DKO) or PS2 KO mouse embryonic fibroblasts (MEF) displayed increased basal $[Ca^{2+}]_i$. Interestingly, however, MEFs from PS1 KO mice only displayed modest $[Ca^{2+}]_i$ changes relative to controls (Green et al., 2008). *In vivo* studies measuring Ca^{2+} levels in spines and dendrites of pyramidal neurons from the neocortex of mature APPswe/$PS1_{\Delta E9}$ and APP_{SWE} mice (4.5 – 5 and >17 months of age, respectively), found that approximately 22% of neurites located near amyloid plaques had increased resting $[Ca^{2+}]_i$ above a pathological threshold. This apparently resulted in structural and functional neuronal network dysfunction in these animals. However, only about 5% of neurites from either wild-type, single transgenic $PS1_{\Delta E9}$, $PS1_{M146V}$ and young (4.5 – 5 months of age) APP_{SWE} mice exhibited similar signs of Ca^{2+} overload (Kuchibhotla *et al.*, 2008), suggesting that this phenomenon in mice is dependent upon APP mutations and is a late, rather than early, stage disease effect, correlating with the appearance of plaques at this stage. In contrast, cultured cortical neurons from 3xTg-AD and APP_{SWE} mice (8 – 12 months of age), which did not exhibit Aβ plaques but did have chronically elevated intracellular Aβ levels (specifically, Aβ trimers and $Aβ_{56}$; Lesné et al., 2013), resting $[Ca^{2+}]_i$ was double that of age-matched

controls and was found to rely on both Ca^{2+} entry and ER mobilisation (Lopez *et al.*, 2008).

It is important to note that most of the evidence for increases in basal neuronal $[Ca^{2+}]_i$ in AD comes, in fact, from indirect observations of altered Ca^{2+} transients due to Ca^{2+} influx or ER Ca^{2+} mobilisation as exemplified by the following data. Firstly, the $PS1_{\Delta E9}$ mutation is associated with increased basal $[Ca^{2+}]_i$ and enhanced basal phosphoinositide (PI) hydrolysis in cultured human SH-SY5Y neuroblastoma cells. These effects can be reversed by the PLC inhibitor neomycin and the IP_3R inhibitor xestospongin C (Cedazo-Mínguez et al., 2002). Secondly, in PC12 neurosecretory cells, expression of the human $PS1_{L286V}$ mutation increased their susceptibility to apoptosis induced by trophic factor withdrawal and synthetic $A\beta_{25–35}$ (Guo et al., 1998). These apoptotic stimuli resulted in an oxidative stress response and increased $[Ca^{2+}]_i$ levels which were much greater in $PS1_{L286V}$ cells than controls. The authors proposed that this insult was superimposed upon already increased basal $[Ca^{2+}]_i$, a suggestion that was supported by the finding that the SERCA pump inhibitor, thapsigargin (TPN; Lytton et al., 1991), evoked larger elevations in $[Ca^{2+}]_i$ in $PS1_{L286V}$ PC12 cells relative to controls, indicating that they possessed higher $[Ca^{2+}]_{ER}$ (Guo et al., 1998). Thirdly, this Ca^{2+} perturbation in PC12 cells could be counteracted by blocking either Ca^{2+} influx (*e.g.* through VGCCs) or ER Ca^{2+} mobilisation (*e.g.* by blocking IP_3Rs and/or RyRs, or increasing the expression of the constitutive IP_3R modulator, Bcl-2; Guo et al., 1997, 1996). Lastly, cells from a neuronal cell line (CTb) derived from the cerebral cortex of APP-overexpressing mice exhibited increased $[Ca^{2+}]_i$, and decay kinetics of the Ca^{2+} responses to glutamatergic and nAChR agonists, and depolarization (Rojas et al., 2008). These cells also displayed increased responses to the calcium ionophore, ionomycin (Dedkova et al., 2000; Liu and Hermann, 1978), which causes the release of Ca^{2+} from most intracellular stores (into the cytosol) thereby indicating that the ER of these cells was overloaded relative to control cells (Green et al., 2008). Significantly, all of the effects listed previously were normalised by APP knockdown (KD) in these cTb cells (Rojas et al., 2008).

Aβo are thought to increase basal $[Ca^{2+}]_i$ *via* increased Ca^{2+} entry and ER mobilisation (as discussed in Section 1.3.3 Molecular actions of Aβo and related metabolites; Hartmann et al., 1993; Mattson et al., 1993a, 1993b, 1992). For example, human foetal cerebral cortical cell cultures exhibited increased $[Ca^{2+}]_i$ levels and an increased vulnerability to neurotoxicity following exposure to synthetic Aβ peptides. Conversely, chronic exposure of the cell to elevated $[Ca^{2+}]_i$ levels, in turn, enhances Aβ production (Buxbaum et al., 1994; Querfurth et al., 1997).

These increases in $[Ca^{2+}]_i$ likely reflect an AD-mediated enhancement of Ca^{2+} entry and impaired ER calcium release as well as the impaired buffering capacity of both the ER and mitochondria. The ER and mitochondria may either be directly impaired by Ca^{2+} overload or indirectly impaired by ROS and mitochondrial collapse, mediated by Ca^{2+} dysregulation and/or other AD-related processes (Yu et al., 2009).

1.4.2 Enhanced calcium entry

Role of Aβ oligomers

There is a large body of evidence suggesting that APP mutations, including $APP_{SWE,}$ in single as well as multi-transgenic animal models *(e.g.* 3xTg-AD mice; Lopez et al., 2008), APP_{SWE} overexpression (Lopez et al., 2008; Niu et al., 2009; Rojas et al., 2008), and $Aβ_{42}$ aggregates, can all induce calcium dysregulation by, generally, enhancing Ca^{2+} entry and increasing $[Ca^{2+}]_i$ (Arispe et al., 1993a, 1993b; Bezprozvanny and Mattson, 2008; Demuro et al., 2010, 2005; Deshpande et al., 2006; Green and LaFerla, 2008; Hirakura et al., 1999; Kuchibhotla et al., 2008; Mirzabekov et al., 1996; Shirwany et al., 2007; Simakova and Arispe, 2007; Walsh et al., 2002). However, the mechanism(s) underlying Aβ-mediated Ca^{2+} dysregulation remains unclear, although numerous potential mechanisms, including Ca^{2+} entry *via* PtdS and/or PrP^c-dependent pore formation, PM receptor modulation and impaired Ca^{2+} extrusion due to PM transporter impairment, are postulated. This evidence is discussed in more detail in *Section 1.3.3 Molecular actions of Aβo and related metabolites*).

CALHM1

CALHM1 is a Ca^{2+} selective pore subunit of a non-selective PM channel which can also localise to the ER (Gallego-Sandín et al., 2011). It is of interest here because mutations of this protein have been associated with EOAD (Rubio-Moscardo et al., 2013) and LOAD (Dreses-Werringloer et al., 2008; Lambert et al., 2010), although the latter finding is controversial (Beecham et al., 2009; Bertram et al., 2008; Minster et al., 2009). CALHM1 is expressed in neurons in all brain regions, with the highest concentrations being observed in the hippocampus and temporal lobes (Dreses-Werringloer et al., 2008; Rubio-Moscardo et al., 2013). In terms of its mechanism of action, CALHM1 is allosterically regulated by both membrane voltage and extracellular Ca^{2+} concentration (Dreses-Werringloer et al., 2008; Ma et al., 2012; Moreno-Ortega et al., 2015). Indeed, CALHM1 is essential for controlling extracellular Ca^{2+}-dependent excitability in primary cultured cortical neurons (E15) and may interact with IP_3Rs in so doing (Ma et al., 2012; Moreno-Ortega et al., 2011). Specifically, it is activated when extracellular $[Ca^{2+}]_i$ is decreased, as may happen during periods of high-

frequency synaptic activity (Benninger et al., 1980; Vassilev et al., 1997). In CALHM1-expressing N2A cells (mouse neuroblastoma cell line), SH-SY5Y and HeLa cells, as well as embryonic cortical neurons (Dreses-Werringloer et al., 2008; Ma et al., 2012; Moreno-Ortega et al., 2015), when Ca^{2+} was subsequently re-introduced, there was a significant Ca^{2+} influx through CALHM1. This so-called 'Ca^{2+} paradox' (MacDonald et al., 2006) is observed in cells of the heart and neurons of the hippocampus where decreased $[Ca^{2+}]_o$ leads to increased $[Ca^{2+}]_i$, particularly when $[Ca^{2+}]_o$ is returned to normal levels, which in turn often leads to toxic insult (Deshpande et al., 2007; Zimmerman and Hülsmann, 1966).

Notably, a single nucleotide polymorphism in CALHM1 ($CALHM1_{P86L}$), which has been associated with an increased risk of developing LOAD, decreased PM Ca^{2+} permeability in CHO cells and decreased $[Ca^{2+}]_i$ in HT-22 cells (Dreses-Werringloer *et al.*, 2008). Furthermore, CALHM knock-down and $CALHM1_{P86L}$ transfection triggered an increase in amyloidogenic APP metabolism and $A\beta_{40}$ and $A\beta_{42}$ secretion in SH-SY5Y cells and APP_{695} expressing N2a cells, respectively (Dreses-Werringloer *et al.*, 2008). Rubio-Moscardo *et al.* (2013) also found that Ca^{2+} entry was abolished by two CALHM1 mutations associated with EOAD ($CALHM1_{G330D}$ and $CALHM1_{R154H}$) and diminished in $CALHM1_{P86L}$ -transfected HEK 293 cells relative to WT CALHM1. However, they did not witness any alterations in APP metabolism resulting from the CALHM1 mutations (Rubio-Moscardo et al., 2013).

However, in spite of the evidence above implicating $CALHM1_{P86L}$ in various forms of calcium dysregulation, it remains a considerable point of debate as to whether (Boada et al., 2010; Dreses-Werringloer et al., 2008; Lambert et al., 2010; Li et al., 2008) or not $CALHM1_{P86L}$ on its own is a significant risk fact for LOAD (Beecham et al., 2009; Bertram et al., 2008; Lambert et al., 2010; Minster et al., 2009; Sleegers et al., 2009). Rather, it appears to reduce the age of LOAD onset by interacting with the effect of the ε4 allele of the ApoE gene on Aβ metabolism (Lambert et al., 2010).

Store-operated calcium entry (SOCE)

SOCE, the process of ER Ca^{2+} refilling, which is triggered by the intraluminal depletion of Ca^{2+} (Berridge 2002), is also significantly disrupted in AD and will be discussed in more detail in following sections related to ER calcium remodelling and synaptic dysfunction. However, given the fact that SOCE is not just involved in replenishing ER Ca^{2+} levels but may also play a role in the regulation of the ER/cytoplasmic Ca^{2+} gradient (Brandman et al., 2007), alterations in SOCE could have important implications for overall cellular Ca^{2+} homeostasis.

1.4.3 ER remodelling

AD-associated Ca^{2+} remodelling at the level of the ER has important effects on both neuronal/cellular Ca^{2+} homeostasis and associated Ca^{2+} signalling systems, disrupting physiological signalling cascades as well as hijacking others to upregulate a variety of pathogenic processes.

ER overload

The steady-state level of Ca^{2+} within the ER, which will also reflect $[Ca^{2+}]_{cyto}$, results from the balance between the passive leak of calcium through PS, IP_3Rs and RyRs (and potentially CALHM1), and the activity of SERCA pumps (Bandara et al., 2013; Das et al., 2012; Tu et al., 2006). However, enhanced $[Ca^{2+}]_{ER}$ (relative to controls) has been observed in several different cell types expressing PS mutations, such as T-lymphocytes (PS1M146L and 5xTg-PS1 - M146L, H163R, A246E, L286V, C410Y; Eckert et al., 2001), fibroblasts (PS1M146V; Leissring et al., 2000) oocytes (PS1M146L, PS2NI121I and PS2M239V; Leissring et al., 1999a, 1999b), HEK293 cells, neurosecretory PC12 cells (PS1M146L, PS1M146V & PS1L286V; Chan et al., 2000; Guo et al., 1996) and cultured hippocampal neurons ($PS1_{M146V}$; Chan et al., 2000). This increased $[Ca^{2+}]_{ER}$ also reflects the broader dyshomeostasis of the intracellular environment and increased $[Ca^{2+}]_{cyto}$ due to AD-dependent processes (Berridge, 2010; Mattson, 2002). The leading hypothesis concerning elevated $[Ca^{2+}]_{ER}$ posits that dysfunction in the ability of PS1 and 2 to act as Ca^{2+} leak channels, due to AD-associated mutations, causes an increase in luminal Ca^{2+} (Bezprozvanny and Mattson, 2008; Nelson et al., 2007; Tu et al., 2006; Zhang et al., 2010). However, the ability of PSs to form leak channels is still a contentious topic in the field (Bezprozvanny et al., 2012; Shilling et al., 2012). This is despite the fact that PSs (both PS1 and PS2) can function as low conductance, passive Ca^{2+} leak channels in planar lipid bilayers (Tu et al., 2006) and serve to counteract the activity of the SERCA pump (Green et al., 2008). This function is supported by channel structure studies, which suggest that a PS holoprotein structure, in particular, can allow for the movement of Ca^{2+} (Li et al., 2012; Nelson et al., 2011).

Functional evidence in favour PSs playing a role in ER leak includes the fact that HEK293 cells overexpressing non-mutated PS1 have decreased ER Ca^{2+} release in response to IP_3R activation relative to untreated cells (Honarnejad et al., 2013). Furthermore, PS2 overexpression in HEK293 cells decreased ER Ca^{2+} load relative to PS null cells (Bandara et al., 2013). Conversely, PS1 KO (hippocampal neurons; Herms et al., 2003), PS2 KD (HEK293 cells; Bandara et al., 2013) and PS DKO (cultured hippocampal neurons and MEFs; Zhang et al., 2010 and Nelson et al., 2006, 2010; Tu et al., 2006, respectively) increased $[Ca^{2+}]_{ER}$ and mobilisation. Furthermore, decreased or increased $[Ca^{2+}]_{ER}$ is evident in cells depending upon the type

of AD-associated PS mutation (*e.g.* 'gain-of-leak' *vs* 'loss-of-leak' function; Zhang et al., 2010). Notably, utilising PS DKO MEFs, Tu et al. (2006) revealed that PSs account for approximately 80% of the passive leak from the ER, which was independent of any γ-secretase activity (Tu et al., 2006).

The majority of evidence for the role of PSs in mediating an ER leak function has been determined by measuring ER calcium release in cells either transfected with various PS mutations or cells from transgenic animals which constitutively expressed selected PS mutations. Of particular relevance to this thesis, increased $[Ca^{2+}]_{ER}$ (as determined by robustly increased ionomycin responses) was measured in cultured hippocampal neurons from various genotypes of transgenic mice, including 3xTg-AD mice (which expresses the $PS1_{M146V}$ mutation) and $PS1_{L166P}$ - and $PS1_{D385A}$-transfected hippocampal neurons, relative to controls (Zhang et al., 2010). Importantly, in the context of the TgF344-AD rat model which was also used in the current study, the $PS1_{\Delta E9}$ mutation was associated with a 'gain of leak function' and decreased $[Ca^{2+}]_{ER}$ relative to WT (Zhang et al., 2010). In human lymphoblast cells from FAD patients, those cells which expressed either PS1-M139V (in agreement with Zhang et al., 2010), M146L, K239E, V261F, A431E or PS2-N141I, all displayed increased $[Ca^{2+}]_{ER}$ (Nelson et al., 2010). Conversely, in cells transfected with either PS1- ΔE9, P264L, R269G, C410Y or A426P mutations, no differences in $[Ca^{2+}]_{ER}$ relative to controls were observed (Nelson et al., 2010).

Although the calcium ionophore ionomycin is a commonly used tool to indirectly determine ER calcium levels, it should be borne in mind that it also initiates the release of Ca^{2+} from all other intracellular organelles, which is an effect that effectively 'contaminates' the desired measurement. However, experiments described in the previous section which utilised ionomycin to determine intracellular store content were confirmed by Zhang et al. (2010) using the ER-targeted Ca^{2+} indicator D1ER (for review see McCombs and Palmer, 2008). A 3-fold increase in the levels of $[Ca^{2+}]_{ER}$ in transgenic cultured hippocampal neurons, relative to controls, was determined using this method. Interestingly, in the same study (Zhang et al., 2010), when TPN was added to control and 3xTg-AD neurons (in Ca^{2+} free extracellular medium), following ER Ca^{2+} loading, the ER Ca^{2+} levels of both cell types fell to their respective basal levels (which were higher in 3xTg-AD mice). Significantly, however, it took over three times longer for the 3xTg-AD neurons to reach baseline compared to the control neurons, indicating the presence of an intact, but severely impaired, leak pathway in the transgenic neurons.

PEN-2, which is a key regulatory component of the γ-secretase complex (Haass, 2004), may have a role in regulating PS-mediated Ca^{2+} leak by altering the expression of PS 'holoprotein' at ER membranes

(Bandara et al., 2013; Edbauer et al., 2003; Kimberly et al., 2003; Takasugi et al., 2003). Specifically, PEN-2 KD resulted in decreased PS endoproteolysis leading to its stabilisation and the accumulation of a holoprotein form of PS (Honarnejad et al., 2013; Takasugi et al., 2003; Xie et al., 2005). This holoprotein form appears to be responsible for PS-attributed ER Ca^{2+} leak (Tu et al., 2006) and is upregulated in human AD brain samples (Honarnejad et al., 2013), possibly as a compensatory mechanism for increased $[Ca^{2+}]_{ER}$ (Popugaeva and Bezprozvanny, 2013). In support of this finding, PEN-2 KD increased ER Ca^{2+} leak rate and attenuated Ca^{2+} mobilisation following stimulation by bradykinin, TPN and carbachol in HEK293 cells (Bandara et al., 2013; Honarnejad et al., 2013).

The role of PSs as leak channels is also indirectly supported by the observation that SOCE is attenuated in fibroblasts, SH-SY5Y and CHO cells expressing $PS1_{M146V}$ and $PS1_{M146L}$, in embryonic cortical cultures expressing $PS2_{N131I}$ (Leissring et al., 2000; Yoo et al., 2000) and in 3xTg-AD and PS DKO mouse hippocampal neurons, in comparison to WT controls (Zhang et al., 2010). Such an effect makes intuitive sense as SOCE is normally stimulated by low ER calcium, but if the ER is overloaded with Ca^{2+}, as occurs in cells/neurons derived from transgenic animals with ER leak-inhibiting PS mutations (as described previously), relative to wild-type controls, then the stimulus for SOCE initiation will either be blocked or attenuated. This SOCE disruption also stimulates $A\beta_{42}$ generation, whereas SOCE disruption itself is not due to Aβ-mediated effects (Herms et al., 2003; Leissring et al., 2000; Yoo et al., 2000). Notably, the contribution of the PS-mediated leak to ER Ca^{2+} homeostasis appears to be a brain region-dependent phenomenon as, in contrast to hippocampal neurons, ER store levels were unaffected by AD-associated PS1 mutations in striatal neurons (Zhang et al., 2010).

Interestingly, although most researchers point to a loss of PS leak function as the primary factor underlying chronic increases in $[Ca^{2+}]_{ER}$ due to PS mutations, in *Xenopus* oocytes the $PS1_{M146V}$ mutation seems to mediate a similar $[Ca^{2+}]_{ER}$ increase *via* an enhancement of SERCA2b-mediated sequestration of cytosolic Ca^{2+} (Green et al., 2008). Specifically, PS1 and PS2 co-localise with SERCA in MEFs and PS1 or PS2 overexpression enhance cytosolic Ca^{2+} clearance (Green et al., 2008). Conversely, PS null fibroblasts and oocytes exhibit attenuated SERCA activity despite increased SERCA2b steady-state levels (SERCA2b is the SERCA isoform expressed in neurons; Green et al., 2008).

It is also important to note that in contrast to the studies outlined previously, other studies have shown that PS DKO (or PS-null MEF and B-cells; Leissring et al., 2002; Shilling et al., 2012; Kasri et al., 2006), PS1 KO (embryonic cortical neurons; Yang and Cook, 2004) and PS2 KO MEF cells

seem to have decreased ER store content, including decreased TPN- and ionomycin-induced Ca^{2+} signals (Green et al., 2008). This suggests that SERCA filling of the ER is impaired without the normal PS regulatory input, resulting in an increased $[Ca^{2+}]_{cyt}$ relative to controls (Green et al., 2008). Furthermore, FAD-PS mutations ($PS2_{M239I}$ - Zatti et al., 2004; $PS2_{T122R}$ – human FAD fibroblasts - Giacomello et al., 2005) also resulted in lower $[Ca^{2+}]_{ER}$. A noteworthy and extensive study in this regard by Zatti et al. (2006) utilised numerous cell models to determine the effect of PSs $[Ca^{2+}]_{ER}$ content in human fibroblasts from controls and FAD patients as well as cell lines (SH-SY5Y, HeLa, HEK293, MEFs) and rat primary neurons expressing a number of PS mutations, i.e. P117L, M146L, L286V, and A246E in PS1 and M239I, T122R, and N141I in PS2. Importantly, independent of the cell model used, agonist-stimulated Ca^{2+} mobilisation was either unchanged (in the case of $PS1_{L286V}$ solely), or reduced in cells expressing these PS mutations. ER Ca^{2+} content was also reduced in cells expressing PS2 (M239I, T122R, N141I, D366A) and modestly reduced or unchanged in cells expressing PS1 (P117L, M146L, L286V, A246E; Zatti et al., 2006).

Taken together then, these observations suggest that ER calcium dysregulation cannot be the sole explanation for the effects of *all* FAD PS1 mutations. Other possible mechanisms may include the modulation of γ-secretase and caspase activities which would have numerous important effects on intracellular homeostasis, including on APP metabolism and cell death pathway stimulation (Miyoshi et al., 2009; Shen et al., 2007; Xia et al., 2015b).

Alterations in receptor function

Enhanced ER-mediated Ca^{2+} release has been widely reported in cellular systems expressing mutant PS (Cedazo-Mínguez et al., 2002; Chan et al., 2000; Cheung et al., 2008; Guo et al., 1996; Johnston et al., 2006; Leissring et al., 2001, 1999a, 1999b), transgenic AD mouse models (Barrow et al., 2000; Guo et al., 1996; Leissring et al., 2000; Mattson et al., 2000; Schneider et al., 2001; Stutzmann et al., 2006, 2004; Supnet et al., 2006; Supnet and Bezprozvanny, 2010) and cells from human FAD patients (Etcheberrigaray et al., 1998; Hirashima et al., 1996; Ito et al., 1994), which I will discuss in more detail below.

IP_3Rs

There is significant evidence, from the utilisation of murine- and human-derived cells as well as *in vitro* brain slices, to support a connection between PS mutation and enhanced IP_3R activity. For example, fibroblasts from $PS1_{M146V}$ mice and from FAD patients, as well as *Xenopus* oocytes expressing PS1 and PS2 mutant constructs, all had upregulated IP_3R Ca^{2+} release (Ito et al., 1994; Leissring et al., 2000, 1999b, 1999a). Furthermore,

$PS1_{M146L}$ and $PS2_{N141I}$ mutations expressed in cultured non-neuronal DT-40 (chicken B cell line) and Sf9 (insect cell line) cells (Cheung et al., 2008; Müller et al., 2011), cultured FAD patient B cells and cortical neurons from 3xTg-AD and $PS1_{M146L}$ mice (Cheung et al., 2010, 2008) all exhibited increased IP_3R open-probability, resulting in the generation of ROS (Müller et al., 2011). *Ex vivo* cortical brain slices from $PS1_{M146V}$ and 3xTg-AD mice also exhibited increase IP_3R-stimulated Ca^{2+} mobilisation, accompanied by an increase in membrane Ca^{2+}-evoked K^+ conductance. This, in turn, decreased overall membrane excitability (Stutzmann et al., 2006, 2004). However, it is interesting to note that between 6 and 18 months of age, the enhanced transgenic IP_3R-mediated responses observed at 6 weeks, progressively decrease (Stutzmann et al., 2006), possibly due to as-yet-unknown compensatory mechanisms.

Somewhat surprisingly, the aforementioned increase in IP_3R activity observed in transgenic AD models does not seem to be mediated by a significant increase in IP_3R expression in either early or late stage transgenic AD animal models (Schneider et al., 2001; Stutzmann et al., 2006, 2004; Zhang et al., 2010). Furthermore, IP_3R-mediated responses elicited by GPCRs are enhanced by certain PS1 mutations (Müller et al., 2011; Shilling et al., 2014). This has been confirmed in *ex vivo* brain slice pyramidal neurons from several AD mouse models and in fibroblasts from AD patients (Leissring et al., 2000; Stutzmann et al., 2006). This may be due to a PS1-mediated increase in basal PLC (Abdul-Ghani et al., 1996; Hannan et al., 2001) and $[Ca^{2+}]_i$, as has been determined in human SH-SY5Y neuroblastoma cells expressing the $PS1_{\Delta E9}$ mutation (Cedazo-Mínguez et al., 2002).

IP_3R activation specifically represents a convergence point for the Ca^{2+} and Aβ hypotheses as well as cell death pathways. This is because not only can the Aβ cascade influence IP_3R-mediated ER Ca^{2+} mobilisation *via* $Aβ_{42}$ enhancement of IP_3 production, and subsequent Ca^{2+} liberation (Demuro and Parker, 2013), but apoptotic pathways which activate caspase-3 can also evoke CTF cleavage of PS2 to form PS2-“loop peptide”, which activates IP_3R and results in pathological ER Ca^{2+} mobilisation in NRP-154 cells (rat prostate adenocarcinoma; Cai et al., 2006). Furthermore, AD-mediated alterations in the Ca^{2+}-sensitive receptor (CaR) also appear to be mediated by IP_3Rs.

Role of the CaR

CaRs are G_q-protein coupled, transmembrane receptors which respond to, and regulate serum Ca^{2+} levels which may influence localised Ca^{2+} regulation in the brain (Conley et al., 2009; Kos et al., 2003). At a cellular level, CaRs are activated by high extracellular $[Ca^{2+}]$ and modulate several signalling pathways such as PLC-mediated signalling, in a tissue-

specific manner (D'Souza-Li, 2006). This G_q-mediated PLC activation can be inhibited by the regulator of G-protein signalling 4 (RGS4; Xu et al., 1999).

Interestingly, not only is there evidence for a mutation in the gene encoding CaR, being involved in human AD development (Conley et al., 2009) but *in vitro* receptor activation studies have also shown that Aβ and ApoE can both modulate CaR function (Conley et al., 2009). Specifically, Aβ directly stimulates CaR on HEK293 cells (Ye et al., 1997), Cos-1 cells (Conley et al. 2009), cultured hippocampal neurons (Ye et al., 1997) and cortical astrocytes (Armato et al., 2013), which resulted in increased IP_3 levels and Ca^{2+} mobilisation. Importantly, RGS4 levels are decreased in human AD brains, which may reveal a mechanism for exacerbated IP_3R signalling in the human condition (Emilsson et al., 2006).

RyRs

The RyR is also heavily implicated in mediating calcium dysregulation in AD, with several studies demonstrating enhanced activity and expression in transgenic models of AD, including 3xTg-AD and $PS1_{M146V}$ mice (Chakroborty et al., 2009; Chan et al., 2000; Guo et al., 1999; Smith et al., 2005; Stutzmann et al., 2006; Zhang et al., 2010). Specifically, RyR activity is increased 2-3-fold in the soma and 10-fold in the dendrites and spines of cortical pyramidal neurons from young (4 – 6 week-old) transgenic models, including pre-symptomatic $APP_{SWE}/PS1_{M146V}$ and 3xTg-AD mice (Goussakov et al., 2010). Moreover, RyR-mediated Ca^{2+} responses were increased approximately 4-fold in 3xTg-AD hippocampal cultures and PS DKO hippocampal cultures (P0 – P1, DIV12 – 13). This suggests that either the $PS1_{M146V}$ mutation is a loss-of-function mutation (at least in terms of its interaction with RyRs) or that this mutation enhances RyR-mediated ER Ca^{2+} release by a separate mechanism to that resulting from DKO/loss-of-function mutation. Notably, in DKO neurons, the enhanced RyR signalling could be rescued by transfection with PS1, only when its functioning leak ability was intact (*i.e.* not by 'loss-of-function' leak mutant PSs such as $PS1_{M146V}$) and the effect was not dependent on γ-secretase activity (Zhang et al., 2010). This study is of particular relevance to a major theme of this thesis investigating ER Ca^{2+} dynamics in young murine models of AD (*Chapter 3 and* 4; P2 – 6; 2 – 20 DIV).

RyR sensitivity to both caffeine and cytosolic Ca^{2+} (which can, under certain circumstances, induce CICR (Kong et al., 2008) is also enhanced in animal models expressing either single PS, APP and/or multiple AD-related mutations (Chakroborty et al., 2009; Chakroborty and Stutzmann, 2014; Del Prete et al., 2014; Hayrapetyan et al., 2008; Rybalchenko et al., 2008; Smith et al., 2005), possibly due to either increased ER Ca^{2+} loading (Koizumi et al., 1999; Shmigol et al., 1996) and/or PS or $Aβ_{42}$-mediated increases in RyR open probability (Supnet et al., 2006). In the case of the PSs, PS1 increases

RyR channel open probability and single-channel currents (Rybalchenko et al., 2008), whereas PS2 appears to reduce feedback inhibition of RyR2 (Hayrapetyan et al., 2008; Payne et al., 2015).

Increased RyR expression, particularly of the RyR2 and RyR3 isoforms, which has been demonstrated across various models and studies of AD, such as pre-symptomatic or early disease stage mice - where RyR2 was upregulated 2-5-fold (Chakroborty et al., 2009; Kelliher et al., 1999; Oules et al., 2012; Stutzmann et al., 2006; Zhang et al., 2010), late-stage murine models – where RyR3 was upregulated (Supnet et al., 2006), and in human AD patients and those with mild cognitive impairment (MCI), which displayed loss of synapses relative to age-matched controls (Bruno et al., 2011; Kelliher et al., 1999). Not surprisingly, increased RyR expression enhances overall RyR activity and evokes a concomitant increase in ER Ca^{2+} release (Chan et al., 2000; Smith et al., 2005; Supnet et al., 2006). Such RyR upregulation may be due to the amyloidogenic production of the transcription factor AICD, which both stimulates RyR expression and may be enhanced by PS mutation (LaFerla, 2002; Leissring et al., 2002; Oules et al., 2012). Furthermore, PS KO and/or inhibition of γ-secretase activity, which both inhibit AICD production (Alves da Costa et al., 2006; Zhang et al., 2007), decrease ER Ca^{2+} mobilisation.

Aβo may also play a role in RyR upregulation, as the application of $Aβ_{42}$ to wild-type cortical neuronal cultures (E16) resulted in a 3.5-fold increase in RyR3 mRNA levels, but with no effect on either RyR2 or IP_3R1 expression (Supnet et al., 2006). Notably, Aβos and fibrillar Aβ (synthetic; $Aβ_{42}$) promoted ER Ca^{2+} release through RyRs (and IP_3Rs) and promoted ER stress, which resulted in glycogen synthase kinase-3 (GSK-3β)-mediated tau phosphorylation (Liu et al., 2003), and caspase-9-dependent apoptosis (Brewster et al., 2006) in cultured rat embryonic cortical neurons (Ferreiro et al., 2008; Resende et al., 2008). Similarly, in cultured rat embryonic hippocampal neurons, Aβos stimulated RyR-mediated Ca^{2+} mobilisation. This generated prolonged Ca^{2+} signals which induced mitochondrial fragmentation and attenuated BDNF/RyR-mediated dendritic spine remodelling (Paula-Lima et al., 2011). Critically, increased RyR- and IP_3R-mediated Ca^{2+} mobilisation enhanced γ secretase-mediated formation of $Aβ_{40}$, $Aβ_{42}$, Aβo and increased $Aβ_{42}/Aβ_{40}$ ratio (Buxbaum et al., 1994; Cheung et al., 2008; Green et al., 2007; Pierrot et al., 2004; Querfurth et al., 1997; Querfurth and Selkoe, 1994; Zhang et al., 2010; Zhao et al., 2010). In contrast to the aforementioned effects of AICD on RyR expression and observations from animal models of AD, RyR2 and RyR3 mRNA and RyR2 protein expression were decreased 6 hours post-Aβo application, likely in a negative-feedback manner due to increased RyR-mediated signalling (Paula-Lima et al., 2011). Notably, although RyR-evoked Ca^{2+} release was

increased in hippocampal pyramidal neurons from $APP_{SWE}/PS1_{M146V}$ mice (3–14 months of age) relative to control, this was independent of proximity to Aβ plaques (Briggs et al., 2013), suggesting that at this relatively later disease late stage, Aβ-mediated RyR modulation has peaked.

It is also possible that the RyR upregulation, described above in response to 'amyloidogenic' stimuli and observed in animal models of AD may be an early compensatory mechanism to ER overload and synaptic deficits, including synaptic network depression (Chakroborty et al., 2012). Indeed, Zhang *et al.* (2010) showed that impaired PS-mediated ER Ca^{2+} leak resulted in increased $[Ca^{2+}]_{ER}$ and RyR expression. Support for this suggestion lies in the fact that in cultured 3xTg-AD hippocampal neurons (0 - 1-day-old; 12- 13 DIV), inhibition of RyRs for 6 days, either with dantrolene or receptor knockdown, prior to ER Ca^{2+} measurements, exacerbated the increase in $[Ca^{2+}]_{ER}$. Such an effect seems to illustrate that RyR upregulation and an increased RyR 'leak' current serves to compensate for increases in luminal Ca^{2+} (Zhang et al., 2010). A process known as store-overload-induced Ca^{2+} release (SOICR), which occurs when the ER becomes pathologically loaded with Ca^{2+}, may be responsible for this RyR leak ability. Thus, SOICR is proposed to hyper sensitise RyRs to release Ca^{2+} in response to resting levels of $[Ca^{2+}]_{cyt}$ (Zhang *et al.*, 2010). To date, however, SOICR has only been documented in cardiac cells (Jiang et al., 2004; MacLennan and Chen, 2009).

However, compensatory or otherwise, there remains conflicting evidence as to whether or not the type of RyR upregulation discussed above in response to increased luminal Ca^{2+} is neuroprotective or actually exacerbates Ca^{2+} dyshomeostasis. For example, in addition to the normalisation of ER Ca^{2+} levels perturbed by impaired leak function mentioned above, long-term feeding of dantrolene to $APP_{SWE}/PS1_{L166P}$ mice resulted in a 3-fold increase in amyloid load, loss of excitatory markers of synaptic transmission in the hippocampus and cortical and hippocampal neuronal atrophy, suggestive of a neuroprotective role for RyR currents (Zhang et al., 2010). Furthermore, the increased RyR expression exhibited in APP_{SWE}/APP_{V717F} cortical neurons was neuroprotective whereby despite increased Aβ deposition and RyR-mediated ER Ca^{2+} release, basal intracellular Ca^{2+} levels, depolarisation induced Ca^{2+} influx, SOCE and vulnerability to glutamate and H_2O_2-mediated stress were no different to control neurons. Significantly, these neuroprotective effects could be reversed by siRNA knockdown of RyR3 expression and culminated in the death of these neurons (Supnet et al., 2010). However, in complete contrast to the studies described above, glutamate-mediated toxicity in $PS1_{M146V}$ and 3xTg-AD mouse hippocampal neurons was actually *reduced* by dantrolene application (Guo et al., 1999; Zhang et al., 2010).

A primary function of RyRs in AD is to amplify IP_3-mediated ER Ca^{2+} release (Stutzmann *et al.*, 2006). IP_3-induced Ca^{2+} release in cortical neurons from non-transgenic mice was mediated predominantly through IP_3Rs, with only a modest contribution from RyRs (Stutzmann *et al.*, 2006). In cortical neurons from $PS1_{M146V}$ and 3xTg-AD mice, the relative contribution of the two channels seemed to be shifted such that RyRs (which were up-regulated in these transgenic mice) accounted for the exaggeration in IP_3-induced Ca^{2+} release. Notably, mice expressing APP_{SWE} and Tau_{P301L} mutations had no effect on the measured Ca^{2+} dynamics, suggesting that the $PS1_{M146V}$ mutation in the 3xTg-AD mice was the 'calciopathic' factor (Stutzmann *et al.*, 2006). Therefore, any upregulation of RyR expression, for example through AICD production, RyR will amplify IP_3-mediated signals, leading to globally enhanced ER Ca^{2+} mobilisation. In support of this idea, AICD can up-regulate IP_3-mediated Ca^{2+} signalling (Leissring *et al.*, 2002), whilst AICD itself is not associated with direct alterations in IP_3R expression (Hamid et al., 2007).

Taken together then, this evidence implies that the ER has the potential to be a devastating pathological environment, through a combination of Ca^{2+} overload and enhanced SERCA pump activity, disrupted leak function, increased IP_3R and RyR channel sensitivity and expression, and altered SOCE signalling. Together, these phenomena would result in markedly increased ER Ca^2 signals, calcium dyshomeostasis and increased Aβ production, providing an overwhelming feed-forward cycle. Increased basal cytosolic Ca^{2+} levels also enhance tau phosphorylation and aggregation (Hartigan & Johnson, 1999). This inhibits axonal transport and constitutes a significant toxic insult which contributes to AD-mediated neurodegeneration (Maccioni et al., 2010).

Furthermore, this hypersensitive and exaggerated ER release network would likely result in improper coupling to many associated calcium signalling mechanisms including PM channels and their associated cascades. For instance, Ca^{2+} activated K^+ channels and nitric oxide (NO) synthase are both activated *via* this type of ER remodelling (Bradley and Steinert, 2016; Chakroborty et al., 2015; Colton et al., 2006; Kakizawa et al., 2012; Nakamura and Lipton, 2011; Yuste et al., 2015). Under normal physiological conditions Ca^{2+} activated K^+ channels are activated by calcium entry through L-type VGCCs and reduce membrane excitability (Chakroborty et al., 2012, 2009; Stutzmann et al., 2006; Supnet and Bezprozvanny, 2010) whereas NO synthase is activated by NMDAR-mediated Ca^{2+} influx (Standaert, 1999) and modulates synaptic activity, excitotoxicity (Mehta et al., 2008; Moreno-López and González-Forero, 2006) and neuroprotection (Calabrese et al., 2007).

No less important in terms of neuronal survival, Ca^{2+}-dependent cysteine proteases called calpains, which regulate intracellular signalling

pathways, begin to induce neuronal cell death and modulate APP and tau function and metabolism in the presence of elevated neuronal Ca^{2+} (Lebart and Benyamin, 2006). They are also implicated in hippocampal and cerebral cortical impairments in AD (Yu et al., 2009). Numerous studies have illustrated the central role of calpain activation in mediating neuronal apoptosis (for review see Momeni, 2011; Vosler et al., 2008), all of which are supported by the finding that inhibition of calpains restores normal synaptic function in hippocampal cultures and slices from APP/PS1 mice (Trinchese et al., 2008).

1.5 Tau hypothesis of AD

Although not a focus of the current thesis, for completeness sake it is necessary to discuss one of the other main theories underlying AD pathogenesis, the tau hypothesis.

Neuronal microtubule-associated proteins (MAP) include tau (principally), MAP1 and MAP2. There are six tau isoforms, which exhibit expression profiles determined by their development in the human brain (Goedert et al., 1989) and which are coded for by a single gene on chromosome 17 (Himmler et al., 1989). Tau is a phosphoprotein which promotes tubulin assembly into microtubules and subsequently stabilises these structures (Weingarten et al., 1975). Microtubules are involved in the transport of nutrients, vesicles, mitochondria and chromosomes throughout the neuron and are necessary for the development and growth of stable neurites (Griffin, 2006).

In AD, and other related neurodegenerative conditions termed 'tauopathies', tau undergoes extensive post-translational modification processes such as hyperphosphorylation (Šimić et al., 2016) and acetylation (Tracy and Gan, 2017). This results in cytotoxic, self-assembling protein aggregates including oligomers and insoluble fibrils or NFTs. NFTs occur as paired helical filaments alone or combined with straight filaments which are, as mentioned previously, a principal neuropathological hallmark of AD (Iqbal et al., 2010; Noble et al., 2013). NFT formation and accumulation follow the predicted norms of brain regions affected in AD, *i.e*. formation occurs initially in layer II of the EC, from which emanates the performant pathway linking the hippocampus and cerebral cortex (Gómez-Isla et al., 1996). As the disease progresses, NFTs propagate throughout the limbic and associated cortices (Hyman and Trojanowski, 1997). Interestingly, a Tau_{P301L} mutation which was originally expressed in a fraction of layer II EC cells was transmitted along with tau pathology to other neuronal regions (de Calignon et al., 2012).

Hyperphosphorylated tau and its accumulation are particularly evident within the somatodendritic compartments of AD models. This results in morphological alterations of the rough ER and Golgi within these regions (Liazoghli et al., 2005; Lin et al., 2003). Furthermore, tau accumulation as misfolded protein in the ER could contribute to ER stress-mediated neurodegeneration (I. Kim et al., 2008). In terms of neuronal composition, decreased mitochondria and rough ER has also been observed in Tau_{P301S} mice (Yoshiyama et al., 2007).

Like the plaques which accumulate as part of the Aβ cascade, NFTs are largely considered the end stage of a tau cascade which starts with cytosolically-localised, abnormally hyperphosphorylated tau (P-tau). This P-tau seems to be oligomeric (Bancher et al., 1989; Iqbal et al., 1986) and

makes up ≥ 40% of abnormally hyperphosphorylated tau in AD brains (Iqbal et al., 2010). The total level of tau is four- to eight- times higher in AD brains relative to age-matched control brains (Khatoon et al., 1992), most likely due to its resistance to proteolysis (J. Z. Wang et al., 1996), decreased turnover (Poppek et al., 2006) and / or upregulation of tau translation *via* p70 s6 kinase activation in AD (An et al., 2003).

NFTs are inert and do not bind further tubulin or promote microtubule assembly (Alonso et al., 2006), whilst P-tau actively inhibits these processes (Alonso et al., 1994; B. Li et al., 2007) by sequestering functioning tau (Alonso et al., 1996) and MAP1 A/B and MAP2 (Alonso et al., 1997). Furthermore, the appearance of soluble P-tau correlates with cognitive deficiencies in mice expressing a repressible Tau_{P301L} mutation. Such mice also exhibit age-related NFT formation and neuronal loss (SantaCruz et al., 2005). Cognitive deficiencies could be reversed and neuronal number stabilised by suppressing tau expression. These changes were independent of NFT load, which continued to accumulate over this period. This suggests that NFTs, alone, are not sufficient to cause cognitive decline or neuronal death. (SantaCruz et al., 2005).

Tau phosphorylation is tightly regulated and Ca^{2+} dependent (Yu et al., 2009). For example, enzymes whose activity can be increased in the presence of Ca^{2+} and are implicated in tau phosphorylation (Ahlijanian et al., 2000; Flaherty et al., 2000), include cyclin-dependent kinase 5 (Cdk5; Cruz et al., 2003; Lee et al., 2000; Lew et al., 1994) and (GSK3β; Hartigan and Johnson, 1999).

Furthermore, tau phosphorylation/dephosphorylation is dependent upon Ca^{2+} influx and its rate of influx, at least in SH-SY5Y cells (Shea and Ekinci, 1999). In cultured neurons, membrane depolarisation results in Ca^{2+}-mediated transient tau phosphorylation by GSK3β and Cdk5 kinases, after which it is subsequently dephosphorylated by calcineurin (Pierrot et al., 2006). Such transient and reversible phosphorylation mechanisms are employed by healthy neurons during development (Schmitt et al., 1977). Therefore, Ca^{2+} dysregulation associated with AD has the potential to alter this balance to favour tau phosphorylation *via* a number of mechanisms including basal Ca^{2+} increases, enhanced NMDAR-mediated Ca^{2+} signals (Li et al., 2004), CN impairment (Fleming and Johnson, 1995; Pierrot et al., 2006), CAMKK2 activation/increased AMPK activity (Mairet-Coello et al., 2013; Yoshimura et al., 2003), calpain activation (X. Chen et al., 2008) and increased transglutaminase (Miller and Johnson, 1995). Conversely, tau mutation can also affect the Ca^{2+} signalling system, including promoting increased VGCC Ca^{2+} influx (Furukawa et al., 2003) and acute ER Ca^{2+} mobilisation through RyR and IP_3R as well as synaptotoxicity (Moreno et al., 2016), representing another AD mechanism for feed-forward degeneration.

In terms of where the tau cascade fits into the progression of AD, Tau_{P301S} mice displayed NFTs and profound neuronal loss at 9-12 months. However, microglial activation, which is proposed to connect the neuroinflammatory and tau hypotheses, as well as supposedly inducing synapse dysfunction and loss, was evident from 3 months of age (Yoshiyama et al., 2007). Tau pathology has been observed after Aβ deposition in animal studies, (Hardy et al., 1998; Jack et al., 2010) suggesting that tau pathology is secondary to Aβ proliferation (Lewis et al., 2001). That being said, tau deposition in the temporal lobe correlates more closely with dementia status in humans, and, indeed, deposition in any brain region correlates more closely with cognitive performance than Aβ deposition in early-stage AD (Brier et al., 2016). Moreover, as reviewed by (Bloom, 2014) “a steadily accumulating body of evidence has indicated that soluble forms of Aβ and tau work together, independently of their accumulation into plaques and tangles, to drive healthy neurons into the diseased state and that hallmark toxic properties of Aβ require tau.”

1.6 Impairment of hippocampal synaptic plasticity in AD

1.6.1 Hippocampal anatomy and function

Before discussing specific AD-induced alterations in synaptic plasticity, it is first necessary to provide the reader with a brief overview of the structure and function of this important brain area as all of the studies described within this thesis were conducted upon hippocampal tissue.

The hippocampal formation, also referred to as the medial temporal lobe (MTL), is an area of the brain that is essential for the acquisition (and possibly storage and recall) of declarative memories (*i.e*. memories which support fact and event recollection) and includes: the hippocampus proper (composed of CA1, 2 and 3 fields), dentate gyrus (DG), subiculum (Sb), parasubiculum (ParaSb), presubiculum (PreSb) and entorhinal cortex (EC; which in turn is divided into medial and lateral EC (MEC and LEC; Hartley et al., 2013; Squire et al., 2004; Squire and Zola-Morgan, 1991; Fig 1.5).

Interestingly, there are notable abnormalities with the myelination of SC-CA1 fibres in 3xTg-AD mice as young as 2-months-old (Desai et al., 2009). Significantly, this abnormality occurs prior to the appearance of any Aβ or tau pathology, despite the fact that the hippocampus is a principal and early target for Aβ pathology (Gouras et al., 2000). Furthermore, it is possible that synaptic impairment precedes even these early myelination abnormalities, as discussed below.

The CA1 region and Sub are the primary output structures of the hippocampal formation (Naber et al., 2000), whilst the EC acts as an interface for both incoming (*via* perirhinal and postrhinal cortices) and outgoing information from/to the surrounding cortical/subcortical association areas (van Groen et al., 2003). The perforant pathway (#1 in Fig 1.5) is the main entrance for information to the hippocampus proper and nerves projects from the EC to DG, CA3, CA1 and Sb. The mossy fibre projections from DG granule cells to CA3 pyramidal cells (#2 in Fig 1.5) and the Schaffer Collateral (SC) pathway from CA3 to CA1 pyramidal neurons (#3 in Fig 1.5) complete the hippocampal ‘tri-synaptic pathway’, with each pathway connected by excitatory/glutamatergic synapses (Hartley et al., 2013; Yeckel and Berger, 1990). The SC pathway and CA3/CA1 synapses have been extensively studied in terms of hippocampal LTP and are generally the sites from which the numerous LTP studies referred to throughout this introduction have garnered their data (Kumar, 2011).

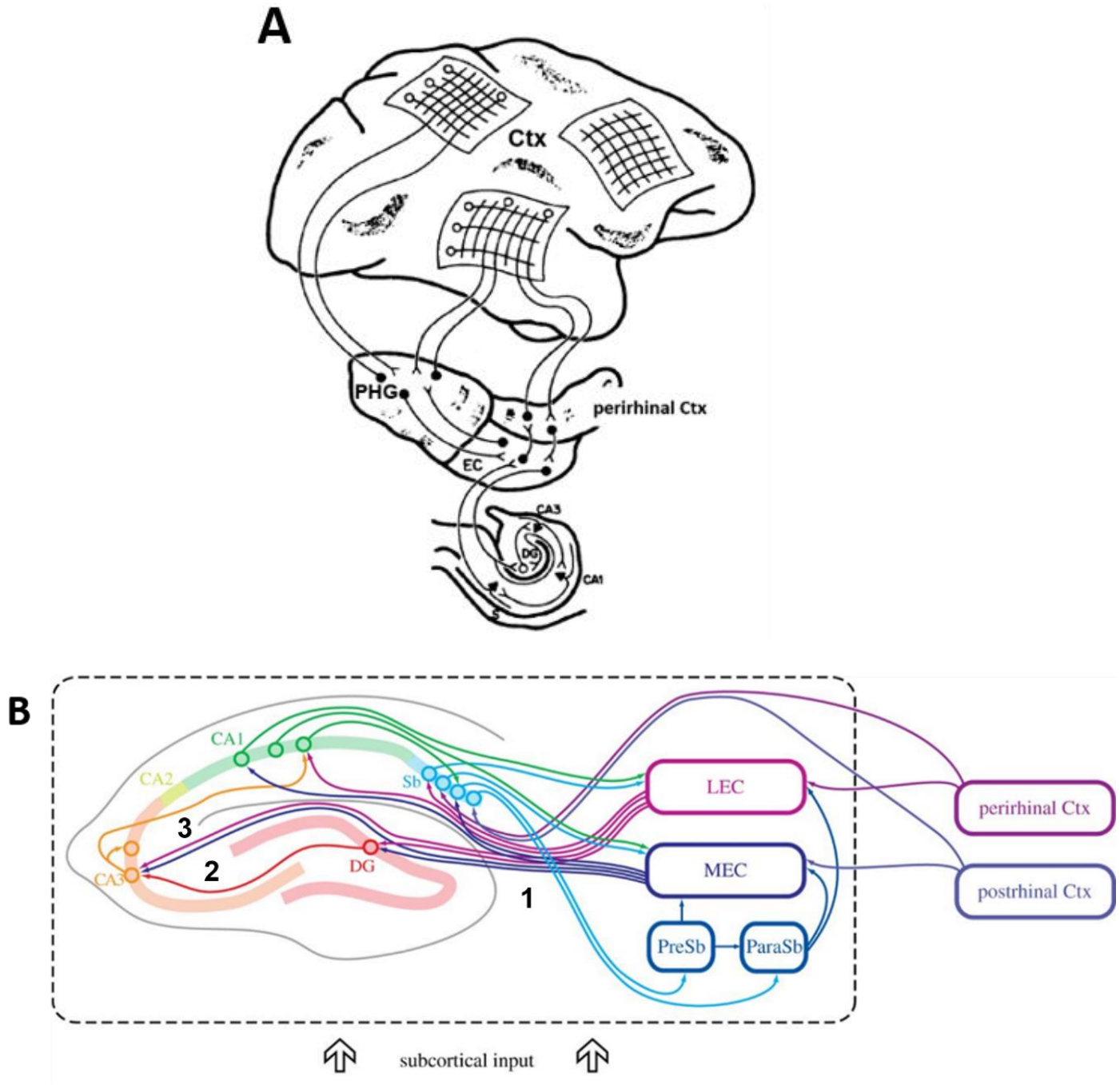

Figure 1.5. Hippocampal Formation Structure and Networks

A. Schematic drawing of the neocortex and its connections with components of the hippocampal formation in primates. These components and networks are critical in the translation from perception to memory. Cortical regions (Ctx) receive sensory information, which is transmitted to the hippocampal formation *via* projections to the parahippocampal gyrus (PHG) and perirhinal cortex and from there to the entorhinal cortex (EC). The inputs are then processed through regions of the hippocampus proper including the dentate gyrus (DG), CA3, CA2 and CA1 regions. The main output region of the circuit is the subiculum (Sb) where widespread efferents return to the neocortex.

Adapted with permission from Squire and Zola-Morgan (1991).

B. Schematic drawing of major anatomical pathways in the hippocampal formation of the rat. Arrows indicate the direction of projections, whilst circles indicate cell bodies. The left-hand side of the figure illustrates the gross morphology of cell layers in the hippocampus and DG and their unidirectional projections. Following input from the EC, which is divided into lateral entorhinal cortex (LEC) and medial entorhinal cortex (MEC) to the dentate gyrus (DG; perforant pathway), nerve fibers project from the DG to CA3 (mossy fiber projection) and from CA3 to CA1 (Schaffer collateral pathway), completing the classical tri-synaptic pathway. Entorhinal input to the hippocampus proper also consists of direct LEC and MEC projections to CA3, to CA1, and to Sb. Other circuits within the hippocampal formation, involve projections from subiculum to presubiculum (PreSb) and to parasubiculum (ParaSb), and projections from PreSb to MEC, and ParaSb to both LEC and MEC.

Adapted with permission from Hartley et al. (2013).

The output from the hippocampus can return to the surrounding neocortex v*ia* the deep layers of the EC and/or re-enter the formation *via* projections from the deep to superficial EC (Kloosterman et al., 2004, 2003). This 're-entrance' process is believed to be critical for memory formation and may act as a way to compare processed input with new information and/or be involved in memory consolidation during sleep (Egorov et al., 2002; Gerrard et al., 2008; Naber et al., 2000; Ribeiro et al., 2004).

The importance of the entire hippocampal formation in memory processes (including spatial learning and memory) is evident in the profound disruption of these regions within the MTL (Backman et al., 2001; Becker et al., 1980; Buckmaster et al., 2004; Gouras et al., 2000; Jarrard, 1993; Olton and Papas, 1979; Reed and Squire, 1997; Zola-Morgan et al., 1986). Furthermore, it is well documented that this region is targeted early in AD, which explains the characteristic concomitant learning and memory deficits associated with the disease (Golby et al., 2005).

The ventral hippocampus is directly connected to the medial prefrontal cortex (Ctx), both functionally and anatomically (Degenetais et al., 2003; Tripathi et al., 2016) and exhibits prominent early tissue loss in AD pathogenesis (Frisoni et al., 2008; Qiu et al., 2009). Aβ plaques and tau-containing dystrophic neurites appear primarily in the terminal zone of the perforant pathway (Hyman et al., 1988, 1986) which is responsible for the majority of cortico-hippocampal afferents (Van Hoesen and Pandya, 1975). Tau pathology affects areas of the hippocampal formation responsible for cortical and subcortical efferent projections, most notably in the Sb and CA1 regions and layer IV of the EC. Hippocampal input is also impaired by NFT formation, particularly in stellate cells of the EC layer II, causing a degenerative alteration in the perforant path (Van Hoesen and Hyman, 1990). Such changes disrupt the structural and/or functional circuitry of the hippocampus on many levels, impairing efferent and afferent connections with cortical and subcortical structures that are important for memory (Van Hoesen and Hyman, 1990) and which may play a role in early AD cognitive deficits (Davis et al., 2014).

1.6.2 Synaptic plasticity and its impairment in AD

Long-term potentiation (LTP) and long-term depression (LTD) are enduring changes in synaptic strength and efficacy that are induced by specific patterns of synaptic activity, (Bear and Malenka, 1994), and which are proposed to be cellular models of memory storage and erasure, respectively, that have been discovered to occur within the hippocampus and numerous other brain regions (for reviews see Bliss and Cooke, 2011; Malenka and Bear, 2004).

In the context of the work conducted for this thesis and its specific focus on neuronal calcium signalling, it is notable that the induction of almost all forms of LTP and LTD so far investigated (and indeed synaptic transmission itself; Malenka and Bear, 2004) are contingent on an initial increase in intracellular Ca^{2+} (Lynch et al., 1983; Mulkey and Malenka, 1992). However, it is the manner in which LTP or LTD is induced, in conjunction with the different magnitudes and locations of calcium elevations, as well as specific co-requirements of LTP/LTD for second messengers, which determines if one or the other is induced (Cummings et al., 1996; Malenka et al., 1988), *e.g.* high frequency, large amplitude Ca^{2+} influx generally evokes LTP, whereas low frequency, prolonged, low-level Ca^{2+} influx and/or mobilisation generally evokes LTD (Connor et al., 1999). Indeed, as described previously, the calcium signalling system is replete with subtleties and complexities which could allow for the selective, localised and magnitude-specific increases of both pre-synaptic and post-synaptic [Ca^{2+}] required for the induction of different forms of plasticity. Molecular entities specifically implicated in synaptic plasticity-induced Ca^{2+} signalling include; glutamate-gated receptors (*e.g.* NMDAR and I-mGluRs), depolarisation-activated channels (*e.g.* VGCCs), and ER Ca^{2+} release *via* IP_3Rs and RyRs (Reyes-Harde et al., 1999b). Each of these signalling components has been investigated in the context of an induced 'learning event' in control and AD-transgenic hippocampal neurons (*Chapters 3, 4 and 5*). Given the proposed chronic disruption of intracellular calcium homeostasis and signalling and its effects on synaptic function, it becomes clear how AD pathology may correlate with deficits in learning and memory.

As alluded to above, both LTP and LTD rely upon similar molecular mediators such as NMDARs and I-mGluRs in a manner that is not yet fully understood. Additionally, interpreting exactly how pathological signals mediated by such receptors equates to deficits in plasticity is difficult. However, what is clear is that Ca^{2+} remodelling, the Aβ cascade and altered CN levels may upset the normal delicate balance between the induction of LTP and LTD (Deshpande et al., 2008). Indeed, as will be discussed next, disruptions in plasticity that correlate with memory impairments and Aβ proteins have been observed across disease stages in several murine AD models (Jang and Chung, 2016; Marchetti and Marie, 2011; Oddo et al., 2003b).

Impairments in NMDAR-dependent LTP and spatial working memory have been noted in 3 and 8-month-old 3xTg-AD mice (Chakroborty et al., 2015; Clark et al., 2015). Notably, non-NMDAR LTP appears to be dominant at both 3 and 8 months of age in 3xTg-AD mice, possibly due to Aβ-mediated upregulation of this LTP pathway in order to compensate for the deficits in the NMDAR-dependent form (Clark et al., 2015). Indeed, reduced NMDAR-

LTP at CA1 synapses *in vitro* has also been reported in $APP_{SWE,}$ $APP_{INDIANA}$ (Tozzi et al., 2015) and $PS1_{M146V}$ (Y. Wang et al., 2009) mutant mice at 2 months and 9 – 12 month-old, respectively. However, $APP_{SWE}/PS1_{M146L}$) and Tg2576 mutant mice ($APP_{Lys670 \rightarrow Asn, Met671 \rightarrow Leu}$) at 10 months and 24 months of age, respectively, exhibited decreased Na^{2+} currents, proportional to Aβo load, which contributed to decreased VGCC activation (Brown et al., 2011). It is possible then, that a failure of this compensatory upregulation of non-NMDAR LTP (which is mediated by L-type VGCCs and/or I-mGluRs) in transgenic AD mice due to reduced VGCC activity, underpins a total impairment of LTP observed at 8 months in the 3xTg-AD mouse (Clark et al., 2015).

With regard to the Aβ cascade, intracellular Aβo and/or extracellular Aβ accumulation can disrupt neuronal plasticity *in vitro* and *in vivo* in both the hippocampus and dentate gyrus, as has been shown in numerous murine models of AD (Hsiao et al., 1999; Larson et al., 1999; Li et al., 2009; Moechars et al., 1999; Shankar et al., 2008; Tyszkiewicz and Yan, 2005; Q. Wang et al., 2004). Generally, the appearance (due to transgene expression) or acute administration of Aβo in various murine AD models results in a decline in LTP (Oddo et al., 2003a; Townsend et al., 2006; Walsh et al., 2002). Interestingly, at least in terms of adult rat hippocampal slices, application of 'natural' Aβo with abundant monomers, but not solely monomers or fibrils, mediated this effect on LTP (Walsh et al., 2002). Synthetic Aβ peptides can induce similar deficits in LTP, but greater, possibly non-physiological micromolar, as opposed to picomolar, concentrations are required for them to exert this effect (Hartley et al., 1999; Lambert et al., 1998). Furthermore, synthetic $Aβ_{40}$ and $Aβ_{43}$ application results in their *in vivo* aggregation into amyloid deposits, the formation of which was associated with impaired basal synaptic transmission and LTP maintenance in rat hippocampal slices and which correlated with short-term working memory deficits (Stéphan et al., 2001). Aβo-induced impairment of LTP may be due to an inhibition of AMPAR mediated signalling (Palop et al., 2003; Snyder et al., 2005) or *via* inhibition of calcium/calmodulin-dependent protein kinase II (CAMKII; D. Zhao et al., 2004).

Consistent with the theory of the deleterious effects of Aβo on synaptic plasticity being mediated by Ca^{2+} dysregulation, $Aβ_{25-35}$-induced depression of LTP could be reversed by applying an L-type VGCC antagonist *in vitro* and *in vivo* (Freir et al., 2003). Furthermore, Aβo-induced inhibition of LTP in the dentate gyrus is reversed by CN inhibition (Chen et al., 2002). Ca^{2+} dyshomeostasis itself also appears to favour LTD whilst increasing the threshold frequency required for LTP induction, at least in aged neurons (Foster, 2007). Interestingly, supporting the theory that subtle chronic alterations in Ca^{2+} regulation underlie AD, Briggs et al. (2017)

suggest that short-term plasticity deficits are a function of the emergent stage of the disease (where compensatory mechanisms can likely act) before widespread synaptic deficits take hold. Indeed, 3-month-old 3xTg-AD mice exhibit LTP characteristics which are very similar to age-matched controls. At this stage in the disease early pre- and post-synaptic Ca^{2+} signalling abnormalities, namely increases in pre-synaptic spontaneous vesicle release, altered probability of vesicle release, and upregulated post-synaptic small conductance calcium-activated potassium channels (SK) channel activity, are masked by increased RyR-mediated Ca^{2+} mobilisation in transgenic hippocampal neurons. However, progressive calcium dysregulation, manifesting as increased $[Ca^{2+}]_i$, in these AD mice produces a profound enhancement of LTD (Chakroborty et al., 2012; Chakroborty and Stutzmann, 2014). Furthermore, short-term LTP is impaired in young and old 3xTg-AD models which are proposed to be reflective of alterations in pre-synaptic Ca^{2+} signalling *via* RyR (Chakroborty et al., 2012, 2009; Clark et al., 2015; Unni et al., 2004). Aberrant RyR activation and subsequent excessive Ca^{2+} release via NMDAR (Goussakov et al., 2010; Y. Wang et al., 1996), AMPAR (Rossi et al., 2008) and VGCCs (Thibault et al., 2007) have all been recorded in AD models. Although this increased calcium would logically stimulate LTP, conversely, it will also activate small conductance calcium-activated potassium (SK) channels. This, in turn, will inhibit synaptic depolarisation, thereby limiting Ca^{2+} influx via NMDAR which may act to impede LTP and impair the post-excitation stabilisation of dendritic spines (Faber et al., 2005; Zhang et al., 2015a). Furthermore, the transcription factor Lim-only domain protein 4 (LMO4), a positive regulator of RyR2 expression, is upregulated by $A\beta_{42}$ (Barucker et al., 2015) in the entorhinal cortex and hippocampus in AD (Leuba et al., 2004). Knockout of LMO4 also reduced RyR-mediated Ca^{2+} signalling and, of particular relevance to this project, it also reduced the facilitation of glutamatergic synaptic transmission and LTP (Qin et al., 2012).

CN is upregulated in aged rats and APP Tg mice which display related defects in cognition (Dineley et al., 2007; Ferguson, 2001). The importance of this fact is illustrated by the finding that the CN inhibitor, FK506, improved memory function in APP transgenic mice as determined by fear conditioning tests (Dineley et al., 2007).

It is proposed then that the above effects, in particular, those driven by increases in basal Ca^{2+}, result in LTD being continuously enhanced, preventing memory consolidation which ultimately may lead to severe memory loss (Fig 1.6; Berridge, 2014a, 2014b).

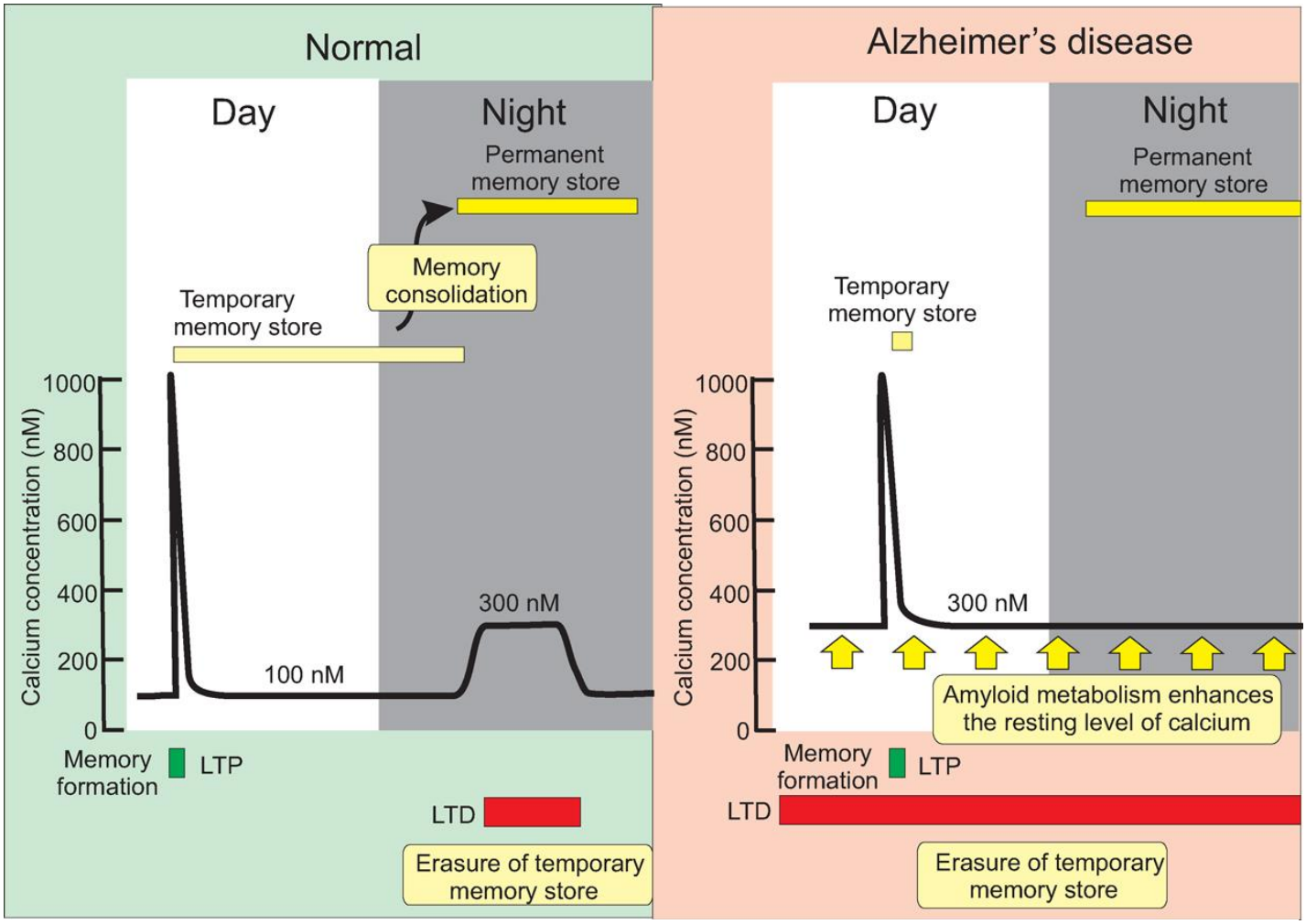

Figure 1.6. The LTD hypothesis of Alzheimer's disease

During the day, the formation of memories and their 'temporary' storage relies on brief high concentration (approximately 1000 nm) Ca^{2+} spikes which activate long-term potentiation (LTP). These memories are consolidated to a 'permanent memory store' at night. Also during sleep, relatively long and low concentration (approximately 300 nM) Ca^{2+} signals stimulate long-term depression (LTD) and erasure of the temporary store.

In Alzheimer's disease, LTD is chronically stimulated due to increased basal levels of intracellular Ca^{2+}. This causes deletion of new memories in the temporary store before consolidation during sleep can occur.

Functionally *and* Structurally intact synapses are absolutely essential for functioning memory systems (Harris and Weinberg, 2012; Mayford et al., 2012). It is perhaps no surprise then that synaptic loss is the best known correlate of cognitive impairment that we are aware of in human AD (as opposed to, for example, the accumulation of plaques or NFTs, neuronal cell death or cortical gliosis; Coleman and Yao, 2003; DeKosky and Scheff, 1990; Hamos et al., 1989; Robinson et al., 2014; Terry, 2000; Terry et al., 1991). Therefore, it is significant that both APP mutations and the Aβ cascade, as well as PS mutations, have all been implicated in disrupting synaptic function (for review see; Koffie et al., 2011; Sheng et al., 2012). For example, post-mortem cortical human AD brain samples exhibit a decrease in synaptic density and a compensatory increase in synapse size, relative to age-matched controls (Arnold et al., 2013; DeKosky and Scheff, 1990; Scheff et al., 1990). Furthermore, biopsies performed 2 - 4 years after AD diagnosis (mild to moderate AD patients) revealed a 25 – 35% decrease in synapse density and 15 – 35% decrease in the number of synapses per neuron (DeKosky and Scheff, 1990). Notably, a novel method which allows for the imaging of synaptic density in living human brain has the potential to extensively examine differences in synaptic density between control and AD brains *in situ* (Finnema et al., 2016)

In terms of which specific aspects of synaptic physiology may be affected by AD-related cognitive decline, studies have revealed a correlation with loss of the presynaptic vesicle protein, synaptophysin in the hippocampus and associated cortices (Dickson et al., 1995; Sze et al., 1997; Terry et al., 1991). This is supported by the fact that synaptophysin immunoreactivity was decreased by approximately 25% in the frontal cortex in MCI and early AD patients (Masliah et al., 2001). This decrease was mirrored by a 30% decrease in synaptophysin-containing pre-synaptic terminals as well as decreased microtubule-associated protein (MAP) 2 (which promotes assembly and stability of the microtubule network; for review see; Dehmelt and Halpain, 2005) positive neurons, in $APP_{717V-->F}$ and APP_{SWE} mice at 2-3 months of age, before any plaque formation (Hsia et al., 1999).

It is also worth noting that pre-synaptic nerve terminals are particularly vulnerable to Ca^{2+}-mediated degeneration as they experience repeated bouts of Ca^{2+} influx and have an unusually high energy demand to maintain ion homeostasis and signalling systems. As such, the Ca^{2+}- and/or ROS-mediated pathological effects of mitochondrial dysregulation have the potential to be particularly severe in these regions. Similarly, pre-synaptic nerve terminals and post-synaptic dendritic spines are both also particularly vulnerable to dysregulated Ca^{2+} signalling mediated by RyRs (Briggs et al., 2017). The activity of these receptors plays a role in modulating dendritic

structure, function and NT release, and in so doing influences both short- and long-term plasticity (Briggs et al., 2017).

There are also numerous lines of evidence implicating PS mutations in synaptic impairment. For instance, PS DKO in both hippocampal cultures and acute hippocampal slices results in synaptic deficits (Saura et al., 2004; Zhang et al., 2009). Hippocampal neurons from $PS1_{A246E}$ mice also exhibit a reduction in the amplitude of evoked AMPAR- and NMDAR-mediated excitatory currents and reduced frequency of spontaneous miniature synaptic currents suggesting a decrease in synaptic activity and a reduction in the number of functional synapses. These impairments could be rescued in transgenic neurons with the application of a γ-secretase blocker (suggesting involvement of PSs and/or APP processing) and could be replicated in WT neurons with the application of monomeric $A\beta_{42}$, suggesting APP processing mediates the actions of $PS1_{A246E}$ mutation (Priller et al., 2007).

It is also postulated that PS-mediated synaptic deficits in AD are mediated by dysregulated neuronal SOCE (Bezprozvanny et al., 2013; Popugaeva et al., 2012; Tong et al., 2016) and/or synaptic vesicle recycling (Zhang et al., 2009; D. Zhang et al., 2010). SOCE- mediated calcium entry can stabilise dendritic mushroom spine synapses of pyramidal neurons via CAMKII (Briggs et al., 2017). Conversely, STIM2 (ER Ca^{2+} sensor involved in SOCE (Moccia et al., 2015) upregulation and SOCE enhancement in a Huntington's disease model results in dendritic spine disruption (Wu et al., 2016). As such, SOCE- mediated effects on synaptic function appears to be circumstance specific, i.e. it is likely to be dependent upon disease state, cell type and a variety of other confounding factors.

Endogenous PS1 and STIM1 interact allowing γ-secretase cleavage of STIM1, reducing its activity in human neuroblastoma SH-SY5Y cells, human fibroblasts, and mouse primary cortical neurons (Tong et al., 2016). On the other hand, PS1KO in SH-SY5Y cells (Tong et al., 2016) or cultured cortical neurons as well as SH-SY5Y cells expressing loss-of-y-secretase-function PS mutations ($PS1_{D257A}$ and $PS1_{D385A}$; Yoo et al., 2000b) exhibit enhanced SOCE. Moreover, PS-deficient MEFs and human FAD patient B lymphocytes as well as $PS1_{M146V}$ mouse hippocampal neurons have significantly elevated STIM1 protein levels and decreased STIM2 levels (Bojarski et al., 2009; Sun et al., 2014). Conversely, SOCE is attenuated in SH-SY5Y cells expressing $PS1_{M146L}$ which, specifically, exhibited impaired STIM1 oligomerisation as well as impaired STIM1-ORAI1 interaction. Furthermore, cultured hippocampal neurons expressing the $PS1_{M146L}$ mutation exhibited destabilisation of dendritic spines which is rescued by overexpression of STIM1 or γ-secretase (Tong et al., 2016).

The study by Tong et al. (2016) proposes that PS-mediated SOCE impairment is γ-secretase dependent (Shideman et al., 2009; Yoo et al., 2000), a statement which is supported by studies utilising cells expressing PS mutations ($PS1_{M146L,\ V97L,\ A136G\ or\ A246E}$) which confer enhanced γ-secretase activity (Bentahir et al., 2006; Fang et al., 2006) and exhibit impaired SOCE (Bojarski et al., 2009; Tong et al., 2016). However, at least one of the y-secretase enhancing PS mutations utilised in the study by Tong et al. (2016) also confers impaired ER leak function (Nelson et al., 2010; Zhang et al., 2010). Therefore, PS-mediated SOCE impairment may also result from an indirect increase in $[Ca^{2+}]_{ER}$ due to impaired leak function (as discussed previously).

1.7 Transgenic murine models

The well characterised 3xTg-AD mouse model and the novel TgF344-AD rat model of AD were utilised for the completion of this study.

1.7.1. 3xTg-AD mouse model

The well characterised 'triple transgenic' model of AD expresses three human transgenes: $PS1_{M146V}$, APP_{SWE} (or $APP_{KM670/671NL}$) and Tau_{P301L} (Oddo et al., 2003b). Whilst in humans the presence of either PS1 or APP mutations results in EOFAD, in mice, knock-in of all three mutations is required in order to recapitulate the main hallmarks of the disease: Aβ oligomers and plaques, NFTs and calcium dysregulation. These primary hallmarks likely underlie the appearance of a larger number of AD-related phenotypes in this model including impairment of neuronal signalling, synaptic efficacy, synaptic plasticity and behaviour and memory (Oddo et al., 2003b; Selkoe, 2002; Sterniczuk et al., 2010a; Stover et al., 2015). Importantly, Aβ and tau pathology has a similar temporal and spatial pathological progression through the hippocampus and other MTL structures as that seen in human AD, with concomitant cognitive decline (Mastrangelo and Bowers, 2008; Oddo et al., 2003b).

Aβ is first detectable (in terms of immunoreactivity) in CA fields of the hippocampus by 3 weeks of age (Billings et al., 2005; Oh et al., 2010, Kazim 2017) and has been independently documented to be present at 2 months in the entorhinal cortex (both $Aβ_{40}$ and $Aβ_{42}$; Duffy et al., 2015) and at 3-5 months in the neocortex (Oddo et al., 2003b). Furthermore, soluble $Aβ_{42}$ levels remain constant from 2-6 months of age in 3xTg-AD mice (Brown et al., 2011), but increase by 8 months (Clark et al., 2015). Interestingly, there appears to be a correlation between $Aβ_{42}$ levels and spatial working memory performance deficits at 3 months. However, exaggerated $Aβ_{42}$ levels at 8 months of age do not correlate with exaggerated performance deficits, perhaps because of the fact that deficits due to soluble $Aβ_{42}$ have already reached a pathological 'threshold' by 3 months of age (Clark et al., 2015; Oddo et al., 2003a). In humans, elevated $Aβ_{42}$ levels in the cortex are correlated with mild clinical dementia prior to tau pathology (Näslund et al., 2000). Similarly, transgenic AD mice with high levels of $Aβ_{42}$ exhibited synaptic loss and behavioural impairments in the absence of plaques or tau pathology (Koistinaho et al., 2001; Mucke et al., 2000). Conversely, in $APP_{SWE}/PS1_{M146L}$ mice, $Aβ_{42}$ burden appeared to only correlate with spatial reference memory performance (tested using a Morris water maze (MWM)) when amyloid plaques were also present (Brown et al., 2011). Total Aβ load may also be important, as in a behavioural study analysing 4 different transgenic mouse lines with differing Aβ deposition profiles, it was concluded that impaired acquisition and memory retention in the MWM were correlated

with “diffuse” and “compact” Aβ deposition in the brain, respectively (Leighty et al., 2004).

Neurotransmission and synaptic plasticity at CA1 synapses, as well as spatial working memory, are impaired in 3xTg-AD mice from 3 months of age (Clark et al., 2015). *In vitro*, abnormalities in synaptic transmission and profound LTP deficits were also apparent in CA1 region*s* by 6 months of age (LaFerla and Oddo, 2005; Oddo et al., 2003b).

The earliest cognitive deficits in this model appear by 2-3 months (Davis et al., 2013b; Stevens and Brown, 2015). Specifically, there is a decline in episodic-like memory which progresses to a complete deficit by 6 months (Davis et al., 2013a, 2013b). By 4 months of age, performance in long-term retention, a hippocampal-dependent behavioural task Is impaired, coinciding with the appearance of intraneuronal Aβ (Billings et al., 2005). By 7.5 – 11 months of age, behavioural alterations, including increased fear, anxiety and restlessness, can also be observed (Sterniczuk et al., 2010b).

More subtle alterations are seen in the Ca^{2+} signalling toolkit well before these overt cognitive or synaptic deficits, in accordance with the proposal that AD may be a form of lifelong ‘calciumopathy’ (Stutzmann, 2007). Alterations in the Ca^{2+} signalling toolkit in the 3xTg-AD mouse are well documented throughout *Section 1.4 The Calcium Hypothesis of AD,* although of particular note are the following early-stage observations.

1) Reduced $K_V2.1$ potassium channel function, which likely contributes to synaptic disruption, as it increased excitability in cultured hippocampal neurons from embryonic 3xTg-AD mice (Frazzini et al., 2016).

2) 3xTg-AD primary neuronal hippocampal cultures exhibited impaired leak function and altered ER Ca^{2+} release (Zhang et al., 2010). Importantly, Zhang et al. (2010) concluded from reverse transcription PCR experiments that APP_{SWE} and tau_{P301L} transgenes were not expressed in hippocampal cultures from 3xTg-AD mice before DIV18 and therefore Ca^{2+} dysregulation was most likely due to the PS1 mutation alone.

3) Enhanced ER mobilisation at 6 weeks in *ex vivo* hippocampal slices, stimulated by IP_3R stimulation is primarily *via* increased CICR due to RyR expression upregulation (Stutzmann et al., 2006, 2004).

4) Increased coupling of $[Ca^{2+}]_{CYT}$ with K^+ channels to enhance hyperpolarisation mediated by ER Ca^{2+} release (Stutzmann et al., 2006).

5) An increase in RyR-mediated Ca^{2+} responses (by 2-3-fold in the soma and 10-fold in the dendrites and spines) in young (4 - 6-weeks-old), pre-symptomatic, 3xTg-AD mice (Goussakov et al., 2010).

6) Aberrant network activity, specifically CA3 network hyperexcitability and enhanced seizure susceptibility, likely due to intraneuronal Aβ, is evident at 3-weeks-old and is reversible with mGluR5 blockade (Kazim et al., 2017). This increased excitability appeared to be a chronic process as increased entorhinal cortex excitability was also observed in Tg2576 mice (APP_{SWE} mutation) at 2-4 months (Duffy et al., 2015) and has also been observed in the hippocampal formation at 3-6 months after the appearance of episodic memory deficits in the 3xTg-AD mouse (Davis et al., 2014).

7) Ca^{2+} dysregulation worsens with disease progression, as evidenced by the fact that in the 3xTg-AD mouse, basal $[Ca^{2+}]_i$ in cultured cortical neurons (produced from 8 – 12 month-old mice) was double that of age-matched controls and was found to rely on both Ca^{2+} entry and ER mobilisation (Lopez *et al.*, 2008).

Tau pathology was evident in 3xTg-AD mice by 9 to 12 months of age, which is significantly later than previously mentioned pathology (Billings et al., 2005; Oddo et al., 2003b, 2003a). Tau accumulates in an age-dependent manner starting in the hippocampus, progressing to the cortex (Oddo et al., 2003a). Taking these observations into account, this transgenic animal model would appear to follow the generally accepted pathological cascade of AD, namely calcium dysregulation and/or Aβ oligomer production followed by tauopathy (Karran et al., 2011; Oh et al., 2010; Selkoe and Hardy, 2016). However, an extensive immunohistochemical study investigating the presence of a plethora of tau isoforms found pathological tau formations from 3 weeks of age in the hippocampus and Sb (Oh et al., 2010).

1.7.2 TgF344-AD rat model

The TgF344-AD rat model used in this study, which expresses two human mutant genes, APP_{SWE} and $PS1_{\Delta E9}$, was recently developed and characterised by Cohen *et al*. (2013) and displays the full spectrum of AD hallmarks, including the sequential appearance of cerebral amyloidosis, tauopathy, gliosis and frank hippocampal and cortical neuronal loss. More specifically, this AD rat model displays the following characteristics:

1) Robust and progressive accumulation of intraneuronal Aβ, $Aβ_{40}$, $Aβ_{42}$, soluble Aβo and Aβ plaques. Interestingly, cerebral Aβ abundance was large enough in this model to be within the clinicopathological range of the human syndrome.

2) Intraneuronal $Aβ_{42}$ and Aβo, but not $Aβ_{40}$, appeared by 16 months of age. $Aβ_{40}$ is robustly increased by 6 months, which was well before plaque formation. Furthermore, with increasing age (but beginning at 16 months of age), $Aβ_{40}$ and $Aβ_{42}$ and the ratio of $Aβ_{42}/Aβ_{40}$ increases significantly. Soluble

Aβo (which first appeared at 6 months of age) and CTFβ levels, also increased in an age-dependent manner in the cerebral cortex and hippocampus.

3) Despite having no specific tau mutation, this model displays increased hyperphosphorylated tau (ptau) at 6 months of age, which is before Aβ deposition but coincides with increases in Aβo. Furthermore, NFT-like structures form by 16 months of age. A possible reason for this unique observation may lie in the fact that rats, unlike mice, but like humans, all express six tau isoforms, making rats more physiologically comparable to humans than mice (Breunig et al., 2013; R. M. Cohen et al., 2013).

4) Outside of these major AD hallmarks, this model is characterised by progressive microgliosis and astrogliosis in the cerebral cortex and hippocampus. Although activated astrocytes and microglia appeared in close proximity to Aβ plaques, activation also occurred by 6 months of age, which was before robust Aβ deposition and coincided with the appearance of Aβo.

5) Amyloidosis and tauopathy are accompanied by frank neuronal loss (ranging from 23 – 45%) in the cerebral cortex and hippocampus at 16 and 26 months.

6) Behaviourally, amyloidosis was associated with hyperactivity in open-field as well as age-related deficits in spatial learning and memory.

7) Finally, it is worth noting that although tauopathy and neuronal loss were observed in close proximity to Aβ plaques, this pathology was also evident in brain areas devoid of Aβ deposits but where Aβo were present. Indeed, Aβo and $A\beta_{42}$ levels were most strongly correlated with neuronal loss in the cerebral cortex and hippocampus. A correlation between Aβ deposition and neuronal loss was also evident.

2. Primary hippocampal neuronal culture

Abstract

This chapter centres on a publication by Kaar et al. (2017) entitled '*An efficient and cost-effective method of generating postnatal (P2–5) mouse primary hippocampal neuronal cultures*' in The Journal of Neuroscience Methods (Appendix 1).

Primary culture of postnatal central neurons is a widely used methodology for applications such as the investigation of neuronal development, protein trafficking/distribution and cellular signalling. However, successful production and maintenance of such cultures, particularly from postnatal animals, can be challenging. In attempting to surmount these difficulties, several disparate culturing methodologies have been developed. Such methodologies are centred upon the identification and optimisation of critical steps and, therefore, the techniques and reagents utilised can differ quite markedly from protocol to protocol. Often, it is suggested that the use of a proprietary reagent, lengthy substrate preparation and/or cell isolation techniques are necessary for successful culture preparation. These invariably lead to increased costs of research.

Herein, we present a simple and inexpensive protocol for the preparation of primary hippocampal neurons from postnatal (2 - 5-day-old) mice, which remain viable for experimental use for over one month. Neurons cultured using this method follow well-established developmental norms and display typical responses to standard physiological stimuli such as depolarisation and pharmacological agents.

By using a novel trituration technique, simplified methodology and non-proprietary reagents, we have developed a reliable protocol that enables the cost-effective and efficient production of high-quality postnatal mouse hippocampal cultures. This method, if required, can also be utilised to prepare neurons both from other regions of the brain and from other species such as the rat.

2.1. Introduction

2.1.1 Uses of primary neuronal culture

Primary neuronal culture enables the conversion of complex, three-dimensional brain tissue, which is difficult to study *in vivo,* into a two-dimensional monolayer of cells, thus allowing easy access to, and visualisation of, individual neurons and synapses (Nunez, 2008). Primary neuronal cultures are also advantageous over continuous cell lines (CCLs) as they exhibit important markers of physiologically-relevant neuronal networks such as well-defined axons and dendrites, dendritic spine formation and synapse formation, which are absent in CCLs (Kaech and Banker, 2006). Consequently, the technique is routinely utilised for a wide variety of applications in neuroscience including, *inter alia* pharmacological, electrophysiological, immunohistochemical, neurotoxicological, developmental and cell signalling studies (Beaudoin et al., 2012; Brewer and Torricelli, 2007; Nunez, 2008).

However, in addition to ease of access to, and visualisation of, neurons and synapses, this simplified monolayer system is also of use for several other purposes. For example, neuronal cell culture eliminates, or at least reduces, potential hormonal, vascular and/or inflammatory confounding influences that one might encounter when using intact or whole brain tissue systems (Brewer and Torricelli, 2007). Such a feature may be important when investigating phenomena such as the subcellular localisation and trafficking of neuronal proteins such as neurotransmitter receptors (Y. Chen et al., 2008). To further reduce intercellular interactions, so-called “low-density” cultures can also be prepared (Kaech and Banker, 2006). Conversely, one can easily and very specifically manipulate the cellular environment of cultured neurons/glia to determine the effect of a particular pharmacological or hormonal intervention in the absence of any other confounding factors. Thus, careful and selective manipulation of the cellular environment in this way provides more specific and reproducible information than could be achieved by using whole-tissue or *in vivo* animal studies in the same way (Zhang et al., 2006).

Neuronal culturing also enables the preparation of multiple, separate neuronal ‘populations’ which can be considered as identical experimental replicates (Brewer and Torricelli, 2007). As it is usually possible to seed a relatively large number of identical neuronal populations from a single piece of brain tissue, this technique represents a highly efficient method of increasing sample size, whilst reducing variability. Finally, but no less important, given the *relative* long-term viability of cultured cells compared to, for example, intact tissue such as brain slices, cell culture also allows for longer-term studies investigating toxicology and neuronal development (Y. Chen et al., 2008; Zhang et al., 2006).

2.1.2 Embryonic versus postnatal brain tissue

The possible advantages of using cultured neurons/glia over intact brain tissue notwithstanding, there can be significant practical limitations to producing viable neuronal cultures, as the technique itself is technically demanding and can be hampered by a lack of reproducibility.

Variation in the quality of neuronal cultures can be ameliorated to some extent by utilising embryonic, rather than postnatal, tissue. This is most likely due to the increased plasticity of embryonic, relative to postnatal, neurons. As such, they have fewer complex neurites, lower interneuronal connectivity and a decreased reliance on trophic support (Brewer and Torricelli, 2007; Kivell et al., 2000; Zhang et al., 2006). Taken together, these factors are likely to bestow upon embryonic cultures a higher resistance to, and higher survival rate following, chemical and mechanical tissue dissociation. This is evidenced by the fact that the use of brainstem tissue from postnatal (P) rat (P6) resulted in an increase in unattached cells and debris on the day of dissection in comparison to embryonic (E) tissue (E14 – 20). Furthermore, when the same protocol was applied utilising P15 tissue, few neurons survived after 1 day (Kivell et al., 2000). In a separate study, rat hippocampal cultures produced from E18 and E19 tissue were compared in terms of neurite length (multiple measurements during weeks in culture), an indicator of neuronal survival and active growth. Neurite length was more than twice as long in younger cultures, despite a difference of only one day in the age of animals (Kaneko and Sankai, 2014). This technical advantage has led to the widespread use of embryonic tissue, particularly that of mice, for the preparation of neuronal cultures.

Although, the use of embryonic neuronal culture may be relevant for studies concerned with, for example, neuronal/glial development, disease aetiology, or where, due to genetic mutation, animals die at, or soon after birth, it would often be more appropriate to use more physiologically-relevant postnatal tissue in other situations. The investigation of the function and role of developed neurons and studies of age-developed pathology such as Alzheimer's disease are two examples where it would be more appropriate to use such postnatal tissue.

The developmental stage of the animal used for culture preparation also influences the cellular composition of a given culture. For example, late-stage embryonic tissue has an abundance of pyramidal neurons, whilst dentate gyrus neuron production has not begun at this stage (Banker and Cowan, 1977; Kaech and Banker, 2006).

It is also recognised that embryonic neurons display a different phenotype to that of adult neurons in terms of their pharmacology, electrophysiology and degree of pathology (Brewer and Torricelli, 2007).

Importantly, in the context of the research that is described in this thesis, embryonic neurons display different calcium dynamics (Brewer et al., 2006), mitochondrial function (Parihar and Brewer, 2007) and responses to glutamate and Aβ (Brewer, 1998) when compared to postnatal neurons. Specifically, in terms of Ca^{2+} dynamics, inhibitory circuitry in the hippocampus and NMDAR-mediated signalling is not fully developed until 1 - 2 weeks after birth in rat hippocampal cultures (Corradetti et al., 1988; Swann et al., 1989; Wyss and van Groen, 1989).

Unfortunately, however, in contrast to embryonic tissue, postnatal brain tissue is relatively sensitive to the culturing process. This is thought to be due to the fact that as neurons develop, they become more susceptible to glutamate-mediated excitotoxicity (Brewer, 1998) and exhibit enhanced caspase activation and apoptosis (Brewer et al., 2005). Physical degradation of neurons also removes intra-neuronal trophic support, thereby decreasing cell viability still further (Brewer and Torricelli, 2007).

This susceptibility to culturing seems to be particularly true when one considers the culturing of hippocampal and other central neurons derived from postnatal *mice*, where there are limited documented successful culturing methodologies for either very early postnatal (P0 - 1; Ahlemeyer and Baumgart-Vogt, 2005; Beaudoin et al., 2012) or adult mice (Brewer and Torricelli, 2007; Eide and McMurray, 2005), relative to protocols published for producing postnatal rat neuronal cultures (*e.g.* (Brewer, 1997; Drysdale et al., 2006; Edwards et al., 2010; Hogins et al., 2011; Irving et al., 2000; Kivell et al., 2000; Nunez, 2008; Pozzi et al., 2017; Rae et al., 2000; Rao and Sikdar, 2004; Stoppelkamp et al., 2010; Ternaux and Portalier, 1993; Zhang et al., 2006). Given that the vast majority of transgenic animal models that have been developed to date are mice, this is a very significant issue. Thus, a reliable and cost-effective postnatal mouse primary hippocampal culturing protocol could have widespread applications, particularly in the fields of learning and memory, and neurodegeneration.

2.1.3 Limitations of the culturing method

Despite the numerous advantages of using primary neuronal cultures for experimental research, their limitations do also, however, need to be acknowledged. Firstly, the physiological relevance of a monolayer of dispersed cells is debatable. The removal of environmental, hormonal and ageing influences could result in an altered cellular phenotype, which may include factors such as a different epigenetic response to transgenes in culture. That being said, even so-called monolayer systems, in reality, have an elaborate three-dimensional distribution of neurites and synapses which

could be up to 18 µm thick, at least in high-density rat cortical cultures (3000 – 4500 neurons/mm^2; E18; 21 days *in vitro* (DIV); Cullen et al., 2010).

Secondly, it is standard practice to maintain neurons at 5% CO_2 and ambient O_2 (approximately 20%). At sea level, the partial pressure of O_2 is approximately 150 mmHg whilst the arterial partial pressure of O_2 is approximately 75 – 100 mmHg (Chernecky and Berger, 2013; Trulock, 1990; Weinberger et al., 2014). The partial pressure of O_2 in the brain, however, is low (24 – 33 ± 13 mmHg; human brain at a range of probe depths) and non-uniform (Dings et al., 1998; Erecińska and Silver, 2001). Ambient O_2 is unphysiological and inhibits neurite growth, resulting in processes which are half the length of those in 9% O_2 at 3 DIV. Indeed, 9% is considered to be an optimal O_2 tension, in terms of neuronal survival and neurofilament synthesis, in culture (Brewer and Cotman, 1989; Kaplan et al., 1986), which tallies with average *in vivo* oxygen levels of between 1 and 11% (Tiede et al., 2011). Importantly, neurons cultured under controlled O_2 conditions (at 9%) had higher anatomical polarisation, lower ROS production rates, larger mitochondrial networks, an increased number of mitochondria and an increased susceptibility to cell death induction, relative to those cultured in ambient O_2 (Tiede et al., 2011).

Thirdly, the culturing process, by its very nature, saturates neurons with supplements and growth factors. This nutritional state does not reflect the nutrient profile arising from normal animal/human behaviour and/or the physiological process of nutrient assimilation and distribution.

However, despite these limitations, neurons in primary culture develop in an anatomically relevant manner, exhibiting numerous dendrites with spines, branched and extended axons and synapses (Kaech and Banker, 2006). Furthermore, the physiological relevance of primary cultures has been verified by Ca^{2+} signalling studies (*e.g.* Chakroborty et al., 2012; Kaar et al., 2017; Kaar and Rae, 2014; Rae et al., 2000; Rae and Irving, 2004; Zhang et al., 2010).

In reality, results accrued from cultured cells are generally further investigated utilising more intact three-dimensional tissue environments, such as acute hippocampal slice and organotypic cell culture systems or *in vivo* studies. Previous work by this lab group suggested that results generated using cultured rat hippocampal cells were generally similar to those in rat hippocampal slices (Rae et al., 2000; Rae and Irving, 2004). Conversely, however, electrophysiological measurements have been shown to vary between *in vitro* slices and cultured cells and are also modulated depending on culture conditions (Mynlieff, 1997). Where this culture technique excels is in the ability to form inexpensive and high-quality

biological replicates where hypothesis testing can be carried out efficiently and on an extensive number of experimental units.

2.1.4 Characteristics of hippocampal cultures

The primary advantage of using hippocampal tissue for the work detailed within this thesis was its relevance to the aetiology of AD, in that it is one of the first regions to be targeted by the disease (Belleville et al., 2008; Reitz et al., 2009; Small et al., 2011). Furthermore, there is a large body of research which has utilised cultured hippocampal neurons and this both aids in directing hypotheses and forms a large data pool which novel data can be compared to. The neuronal population of the hippocampus is also comparatively simple with pyramidal neurons composing the majority of the tissue, with only a relatively small number of interneurons (Benson et al., 1994).

The development of neurons in hippocampal culture is well defined and appears to be relatively consistent across most research groups. Thus, neurons develop polarity during the first two days *in vitro* (DIV), during developmental stage one. This begins soon after cell plating onto coverslips, whereby hippocampal neurons extend a lamella around the cell body. In developmental stage two, this lamella then collects at distinct regions of the cell periphery and it is at these points that minor neurites, of approximately 20 – 30 μM in length, begin to extend. Growth cones (GC) and their filopodia at neurite tips show characteristic motility and the neurites intermittently extend and retract short distances (Craig and Banker, 1994; Dotti et al., 1988). Although little is known about *in vivo* GC morphology with which to compare the *in vitro* situation, there is evidence to suggest that they are elaborate structures with numerous filopodia, especially in the early stages of development (Hossain et al., 2012). However, there is little *net* growth at this stage and the cell maintains a symmetrical appearance (Craig and Banker, 1994; Dotti et al., 1988; Kaech and Banker, 2006). Notably, at this point in development, most axonal and dendritic markers will stain all neurites and, indeed, any neurite appears to be able to form either an axon or a dendrite (Jacobson et al., 2006; Kaech and Banker, 2006). Cells remain in developmental stage two for 12 – 36 hours, after which a rapid transformation to phase three occurs.

During phase three, a single neurite continues to elongate rapidly and continuously for 2 – 3 hours and acquires axonal characteristics (Dotti et al., 1988; Kaneko and Sankai, 2014). Such a neurite will eventually extend for many hundreds to thousands of micrometres (Dotti et al., 1988; Kaneko and Sankai, 2014). Notably, transitions from phase to phase do not occur synchronously. Indeed, under optimal conditions, approximately 50% of

neurons reach stage three by 1 DIV, with 80% reaching this stage by 1.5 – 2 DIV (Kaech and Banker, 2006). This is fuelled by specific and targeted signalling events which emphasise the growth of this single neurite (Arimura and Kaibuchi, 2005; Wiggin et al., 2005). The other neurites grow 5 – 10 times slower (Kaneko and Sankai, 2014) and form dendrites, normally between 3 - 4 DIV (Craig and Banker, 1994; Dotti et al., 1988). It is within this time frame that the first synapses also begin to form (Fletcher and Banker, 1989), which is known as developmental stage four.

Stage five is a relatively slowly progressing phase, normally observed between 1 and 4 weeks *in vitro,* and comprises the following events: dendrites become highly developed and branched, a synaptic network forms, spines form on the dendrites of pyramidal neurons and, finally, synaptic plasticity is evident (Kaech and Banker, 2006). As an example of cell appearance at this developmental stage, by 13 DIV nerve bodies have grown significantly larger and an extensive network of intertwined axons and dendrites forms in hippocampal cultures (E18; Kaech and Banker, 2006). Dendrites emerge gradually, and project radially, from and around the cell body, taper with distance and are between approximately 20 – 300 μM in length. Axons are thinner at their point of origin and are less tapered. In fact, an axonal diameter is generally uniform over long distances (Kaech and Banker, 2006). Axons also extend along a more meandering course, including several branches, for millimetres of distance. Often, axons will also loop back on themselves (Kaech and Banker, 2006).

2.1.5 Previous studies

To date, opting to use postnatal tissue to prepare primary neuronal cultures has often meant ‘accepting the fact that there will be some bad culture days’ (Banker et al., 2007). Such ‘bad cultures’ and lack of reproducibility are likely to arise from subtle variations in the reagents used (Beaudoin et al., 2012) and/or techniques employed between labs. This has resulted in the utilisation and publication of several distinct culturing protocols, with each containing highly specific, often very different, and sometimes even conflicting, advice for each facet of the culturing protocol.

However, differences in protocol notwithstanding, a review of recent literature reveals the widely held belief that the preparation of postnatal mouse cultures specifically necessitates the use of expensive, defined media and supplements, namely, Neurobasal®-A (NB-A) and the HEPES-based Hibernate® A, which are utilised in combination with a proprietary serum-free supplement solution, B-27® (see *inter alia,* Ahlemeyer and Baumgart-Vogt, 2005; Beaudoin et al., 2012; Brewer, 1997; Brewer and Torricelli, 2007; Drysdale et al., 2006; Eide and McMurray, 2005; Hui et al., 2015; Kivell et al.,

2000; Nunez, 2008; Rao and Sikdar, 2004; Stoppelkamp et al., 2010; Xie et al., 2000; Zhang et al., 2006). Indeed, their use is so prevalent that one would be forgiven for thinking that it is nigh on impossible to prepare postnatal cultures without using these proprietary reagents and supplements (as well as lengthy protocols such as gradient separation to further optimise the procedure; Brewer and Torricelli, 2007). However, not only are these proprietary media and supplements much more expensive than standard, non-proprietary, media preparations such as Dulbecco's modified Eagle's medium (DMEM), there is also a concern in some quarters about variable quality and uniformity between batches of B-27 (Y. Chen et al., 2008) and certain, possibly neurotoxic, ingredients contained within NB-A (Hogins et al., 2011).

Therefore, it was the aim of the present study to determine the possibility of producing consistent, successful postnatal primary mouse hippocampal neuronal cultures utilising non-proprietary solutions and supplements. Further, we also wanted to simplify the overall culturing protocol relative those published in recent times (*e.g.* Brewer and Torricelli, 2007, Beaudoin et al., 2012; Table 1 provides a comparison of the main components of previously published postnatal mouse hippocampal culture methods with our method).

Therefore, with these goals in mind, in this section, I will describe a simplified, technically straightforward and reliable method for the production of postnatal (P2 - P5) mouse hippocampal cultures of consistently high quality that remain viable and responsive to normal physiological stimuli for over one month post-culture.

Age of mouse	Maintenance Medium	Supplement	Plating Density (cells/cm²)	Recorded Upper-limit of Survival (days *in vitro* (DIV))	Measured Composition	Pre-culture Protocol			Dissection and Plating Protocol	Post-plating Protocol		Total Time	Reference
						Preparation of Coverslips	Coating of Coverslips	Washing of coverslips		Addition of maintenance medium	Inversion of Coverslips		
3 – 6 days*	DMEM	Serum replacement 2 (SR2)	1 – 1.5 x 10^4	29 DIV	5 DIV Neuronal/Glial ratio of 3:2 Culture composition from DIV 2 - 20 is presented in Fig. 5	≥ 1 h pre-plating (10 min)	≥ 1 h pre-plating (1 h)	≥ 1 h pre-plating (5 min)	≤ 2 h	1 h post plating (2 min)	3 h post plating (5 min)	≤ 6 h	(Kaar et al., 2017)
0 – 1 days	Neurobasal	B-27	6.5 x 10^3	28 DIV	5 DIV 6 – 8 % glia	5 d pre-culture (2 d)	2 d pre-culture (1 h)	1 d pre-culture (1 h)	3 – 4 h	4 h post plating (unknown)	N/A	≥ 8 h	(Beaudoin et al., 2012)
6 Months	Neurobasal A	B-27	3.2 x 10^4	60 DIV	8 – 12 DIV*** 80 % neurons 10 % oligodendrocytes 5 % astroglia 5 % microglia	Autoclaved pre-culture (unknown)	3 – 24 h pre-culture (1 ≤ h)	3 – 24 h pre-culture (1 ≤ h)	≤ 4 h	1 h post plating (unknown)	N/A	≥ 4 h	(Brewer & Torricelli, 2007)
0.5 days	Neurobasal	B-27	3 x 10^{5}**	No figure given. Published results show cultures up to 6 DIV	6 DIV 7 % astrocytes ≤ 1% oligodendrocytes	N/A	≥ 1 d pre-culture (overnight)	pre-culture (unknown)	≤ 1 h 50 min	N/A		≥ 1 h 50 min	(Ahlemeyer & Baumgart-Vogt, 2005)

Table 2.1. Comparison of current methods for the production of postnatal mouse hippocampal cultures.

All figures are approximate and gleaned as accurately as possible from the published methods. *3 - 6-day-old mice are used routinely. We have produced numerous cultures up to P14. **Assumed from publication to be 3 x 10^5 cells/cm^2. ***Expected results based on a previous publication (Brewer et al, 2006).

2.2 Materials and methods

2.2.1 Chemicals and reagents

- Mice (2 - 5-days-old)
- Serum replacement 2 (SR2; 50×; Sigma, cat. no. S9388).
- GlutaMAX™ supplement (ThermoFisher Scientific, cat. no. 35050038).
- L-glutamic acid (Sigma, cat. no. G1251).
- Penicillin-streptomycin (P-S; Sigma, cat. No. P4333).
- Foetal bovine serum (FBS; Sigma, cat. no. **F7524**).

  Optimisation: Storage limitations, as described by Beaudoin et al., 2012, were adhered to, namely storage at -80ºC and limit freeze-thaw cycles to one.
- Dulbecco's Modified Eagle's Medium-low glucose (Sigma, cat. no. D5546).
- Papain (Worthington, cat. no. 3119) **(see *Reagent Setup*).**
- Poly-D-lysine hydrobromide (Sigma, cat. no. P6407) **(see *Reagent Setup*).**
- Dissection, trituration, plating and culture solutions **(see *Reagent Setup*).**
- Trypan blue solution (Sigma, cat. no. T8154).
- 70% ethanol solution for sterilisation of surfaces and hands.
- Deionised water (dH_2O).
- Immunocytochemistry reagents: Triton™ X-100 (Sigma, cat. no. X100), paraformaldehyde (Sigma, cat. no. P6148), sucrose (Sigma, cat. no. S7903), glycine (*e.g.*, Sigma, cat. no. G7126), bovine serum albumin (BSA; Sigma, cat. no. 05470), mounting medium (Sigma, cat. no. F6182), microscope slides (25 x 75 mm; Sigma, cat. no. S8400). Primary antibodies: pan-neuronal marker (mouse monoclonal, Millipore, cat. no. MAB2300, Antibody Registry: AB_1587299), anti-glial fibrillary acidic protein (GFAP; rabbit monoclonal, Cell Signalling, cat. no. 12389, Antibody Registry: AB_2631098), anti-Synapsin I (rabbit polyclonal, Millipore, cat. no. AB1543, Antibody Registry: AB_2200400). Secondary antibodies: FITC goat anti-mouse (Jackson, cat. no. 115-095-003, Antibody Registry: AB_2338589), Cy5 goat anti-rabbit (Abcam, cat. no. ab97077, Antibody Registry: AB_10679461), TRITC donkey anti-rabbit (Jackson, cat. no. 711-025-152, Antibody Registry: AB_2340588).
- Compounds used for calcium imaging: (S)-3, 5-dihydroxyphenylglyccine (DHPG; Tocris, cat. no. 0805), caffeine (Sigma, cat. no. C0750), carbachol (CCh; Tocris, cat. no. 2810), NMDA (Sigma, cat. no. M3262)

2.2.2 Equipment

- 35 mm cell culture dish (untreated; Sigma, cat. no. CLS430588).

  Optimisation: Previous studies have suggested “cell culture treated” dishes (*i.e.* those pre-treated with a cell-adherent substrate) give rise to altered neuronal morphology (W. S. Chen et al., 2011). Implementing the use of untreated dishes ensured normal neuronal development with no negative effects on culture success.
- 145 mm cell culture dish (Sigma, cat. no. Z652539)
- 13 mm glass coverslips, other sizes can be used as desired (TAAB, cat. no. M160/1).

  Optimisation: A thickness measurement of both 0 and 1 (as defined by manufacturer) can be used, indicating that a relatively thin glass is conducive to cell development in an inverted culture system. There are recommended providers of coverslips with proven reliability, without which cells will initially grow but detach soon after, such as Type “D” glass from Schott Desag (Kaech and Banker, 2006). In our hands, coverslips provided by TAAB have also been conducive to long-term reliable culturing.
- 15- and 50-ml sterile polypropylene (PP) centrifuge tubes (Fisher Scientific, cat. no. 11849650 and 11512303 respectively).

  Optimisation: Previous studies have recommended the routine use of polystyrene or polyethylene terephthalate (PET) tubes given reports of toxicity from PP tubes (Brewer and Torricelli, 2007), but we did not find any adverse effects using PP tubes.
- 15 ml and 30 ml syringes (Fisher Scientific, cat. no. 12931031 and 10313015 respectively)
- Haemocytometer.
- Sterile syringe filter, 0.2 µm pore size (Sigma, cat. no. CLS431229).
- 150 mm Pasteur pipette (VWR, cat. no. 612-1701) **(see *Equipment Setup*).**
- 3.5 ml Plastic transfer pipette (Sarstedt, cat. no. 86.1171).

  Optimisation: Pipette material, shape and size were selected based upon numerous optimisation procedures using both glass and plastic pipettes of different shapes and end aperture sizes.
- Incubator, controlled 5% CO_2, humidified. Other studies have recommended the use of an O_2 regulated incubator (Brewer and Torricelli, 2007). However, in our experience, these costlier incubators are not necessary for producing successful cultures.
- Inverted microscope, phase contrast, with a long working distance objective.
- Sterile laminar flow hood, HEPA-filtered air.
- Sterile dissection hood, HEPA-filtered air.

- Swinging bucket centrifuge compatible with the use of 15 ml tubes, ambient room temperature, capable of speeds of 258 g.
- Water bath.
- Temperature-regulated orbital shaker, capable of incubating at 37ºC.
- Fine and course dissection tools.
- Osmometer.

2.2.3 Reagent setup

- **HEPES-buffered saline solution (HBSS)** of the following composition (in mM): NaCl 130, HEPES 10, KCl 5.4, $MgCl_2$ 2, D-glucose 2 and $CaCl_2$ 0.5, pH 7.4, 310 mOsm.
- **Dissection solution.** Prepare 8 ml of HBSS solution containing 0.5 mM GlutaMAX, 0.025 mM L-glutamic acid and 1% P-S.

  Optimisation: All solutions were supplemented with L-glutamic acid and GlutaMAX as detailed in the discussion section.
- **Trituration solution.** Prepare 15 ml of HBSS solution containing 10% FBS, 5 mM GlutaMAX, 0.025 mM L-glutamic acid and 1% P-S. Place in an incubator at 37ºC.

  Optimisation: Hibernate A and HBSS, with and without Ca^{2+} and Mg^{2+}, were compared for use in the dissection and trituration solutions, with Hibernate A providing no obvious advantage on culture quality. Therefore, due to its greater cost-effectiveness, lab-made HBSS was routinely used in preference to Hibernate A. Furthermore, no advantage was observed with the use of Ca^{2+}-and Mg^{2+} -free HBSS over normal HBSS in the trituration solution.
- **Plating solution.** Prepare 2 ml of DMEM solution containing 10% FBS, 5 mM GlutaMAX, 0.025 mM L-glutamic acid and 1% P-S. Place in the incubator and allow CO_2 to buffer solution.
- **Culture solution.** Prepare 35 ml of DMEM solution containing 2% SR2, 5 mM GlutaMAX, 0.025 mM L-glutamic acid and 1% P-S. Place in the incubator and allow CO_2 to buffer solution.

  Optimisation: As mentioned previously, almost all methodologies in this field utilise a combination of NB and B27 for maintenance media. We found that using non-proprietary DMEM and a basic SR2 was equally conducive to successful and cost-effective culture production. Subjectively, we found that using another alternative proprietary supplement, NeuroPlex™ (Gemini Bio-Products), provided no advantage over either SR2 or B27 on neuronal quality.

  Practical Use: Numerous published methods provide guidelines on the time culture solutions can be prepared in advance of the actual dissection, as well as the number of temperature changes which these solutions should undergo, whilst still maintaining reliability (Beaudoin

et al., 2012; Brewer and Torricelli, 2007; Eide and McMurray, 2005). However, we felt that it was more beneficial to negate such variables by making solutions fresh each day and to keep them at a stable temperature, dependent upon their temperature of use.

- **Poly-D-lysine solution**. Dissolve at 0.1 g/ml in dH_2O. Store as frozen 2 ml aliquots in 15 ml tubes.
- **Papain solution.** Immediately prior to beginning the dissection, dissolve 2.5 mg/ml papain in Dissection solution with a total volume of 2 ml (approximately 25 U $ml^{-}1$). To ensure full dissolution of papain, the solution should be placed in a water bath at 37˚C for approximately four minutes. Filter sterilise the solution into a 15 ml tube and store on ice.

  Note: Papain has been found to be the most suitable protease for cell culture (Brewer, 1997). The supplier, Worthington Scientific, is reported as being superior for papain than Sigma (Brewer and Torricelli, 2007). The merits of dissolving papain in Ca^{2+}- and Mg^{2+}- free solution, to aid tissue digestion (Copray and Liem, 1993; Harris et al., 2007; McDonough et al., 2012) are debated, due to the damage that an absence of these cations may have directly on cells. It is recommended that papain is stored on ice for no longer than three hours (Brewer and Torricelli, 2007).

  Optimisation: In our hands, papain from Worthington Scientific was superior to that purchased from Sigma, but the specific supplier does not appear to be crucial to culture success. No advantage was observed using Ca^{2+}- and Mg^{2+}- free HBSS over normal HBSS for the trituration solution. In contrast to Brewer and Torricelli (2007), who suggest that papain treatment of tissue is improved at 30ºC in comparison to 25ºC or 37ºC, in our hands, tissue breakup was optimal after incubation at 37ºC. We tried various tissue incubation periods of 30-60 minutes at 37ºC, with 45 minutes incubation, combined with light tissue agitation, proving to be optimal for tissue dissociation.
- **Phosphate buffered saline (PBS)** of the following composition (in mM): NaCl 137, KCl 2.7, Na_2HPO_4 10, KH_2PO_4 2, pH 7.4.
- **Mice (2 - 5-days-old).** The volumes provided in this protocol are designed for hippocampi from three to four mice aged between 2 - 5-days-old and would have to be adjusted accordingly if one wished to use older animals. Animals were euthanised in accordance with European Directive 2010/63/EU and experiments approved by the Animal Experimentation Ethics Committee of University College of Cork.

  Optimisation: The culture of rat hippocampal tissue results in a greater proportion of successful cultures. However, with care and significant optimisation, mouse hippocampal cultures could also be routinely and reliably produced. Although mice from 2 - 5-days-old were routinely used for preparing my hippocampal cultures, as a proof

of concept of the effectiveness of our culture protocol, mice up to 14-days-old (and rats up to 18-days-old) were also used.

2.2.4 Equipment setup

150 mm Pasteur pipette

Glass pipettes were flame polished briefly (approximately two seconds) to smooth off any sharp edges, but not to significantly reduce aperture size. These polished pipettes were used to transfer small volumes of the plating solution to coverslips and to transfer the enzyme-treated hippocampal tissue into the trituration solution.

> **Note:** The use of siliconised glass is recommended by some in the field for ease of trituration and transfer due to the viscous nature of the dissociated cell suspension (Brewer and Torricelli, 2007). However, in our hands, standard glass pipettes were sufficient.

Preparation of coverslips

In a laminar flow hood, coverslips were transferred to a 35 mm cell culture dish containing 2 ml of 70% ethanol for sterilisation. Two coverslips were then removed and placed upright in each of sixteen 35 mm cell culture dishes and allowed to air dry. Once dried, coverslips were placed flat on the base of each 35 mm dish.

> **Note:** Substrate cleaning and coating are key steps in the culture process as they ensure neuronal attachment and survival, as well as their standard development and maturation (Kaech and Banker, 2006). As such, neurons are highly sensitive to the cleaning methods and coatings which are utilised (Beaudoin et al., 2012). In terms of substrate material, adult neurons do not grow well on plastic (Brewer and Torricelli, 2007) and, therefore, glass coverslips are routinely used. ‘Etching’ of these substrates with nitric acid is discouraged by some (Brewer, 1997), but recommended by others, in combination with subsequent cleaning and heat and/or radiation sterilization (Beaudoin et al., 2012; Kaech and Banker, 2006).
>
> **Optimisation:** In our hands, brief prior sterilisation in 70% ethanol followed by air drying was sufficient to allow for poly-D-lysine attachment and subsequent cell adherence, without any adverse effects on neuronal survival, despite the assertion that solvents leave a ruinous toxic residue (Brewer and Torricelli, 2007). Although the use of nitric acid etching and heat sterilisation were both trialled, improvements in terms of poly-D-lysine coating, cell adherence or cell survival were not observed

Poly-D-lysine coating of coverslips

One drop of sterile filtered poly-D-lysine solution was added to the centre of each coverslip. The 35 mm cell culture dishes were then placed into two larger ‘holding’ culture dishes (145 mm) and left at ambient room

temperature. After one hour, the poly-D-lysine was aspirated and the coverslips rinsed twice with dH_2O.

Timing: This step can be conducted during the tissue incubation with papain.

Note: Poly-D-lysine is superior in terms of consistent cell attachment and neurite outgrowth when compared with poly-L-lysine (Kivell et al., 2000). Alternative substrates used in the field include the following: a) poly-ornithi-nylated coated substrates which are reported as being conducive to rapid cell adhesion (Eide and McMurray, 2005; it is unclear however how this adhesion compares to that facilitated by poly-D-lysine), b) Polyethyleneimine, which is reported to initially result in good neuron attachment, survival and process outgrowth but thereafter is “unstable”, giving rise to inconsistent cultures. However, the specific manner of this instability and inconsistency was not elaborated upon by the authors (Eide and McMurray, 2005). The benefit of subsequently treating substrates with laminin (10mg ml^{-1}) is debated and was found to have no benefit in hippocampal culture (Brewer and Torricelli, 2007). However, laminin does provide an extracellular matrix/scaffold and enhances cell growth in culture systems *in general* (Hall et al., 2008; Manthorpe et al., 1983).

Optimisation: Evidence for the superiority of poly-D-lysine over other substrates for cell attachment, its widespread use and its low cost resulted in its selection for use in this method. We did not use laminin to reduce any unnecessary procedures and increase the efficiency of the method. Although serum pre-treatment of coverslips is reported as being essential for cell attachment, presumably due to an initial stimulus for neurite growth that it provides, thereby facilitating neuronal attachment (Kivell et al., 2000), we opted to provide this stimulus through a serum-containing plating medium.

Storage: In the interest of efficiency, we opted not to prepare poly-D-lysine fresh for each dissection as recommended by Kaech and Banker (2006) and instead used frozen stocks, whilst limiting freeze-thaw cycles to no more than two (Brewer and Torricelli, 2007).

Practical use: Poly-D-lysine was generally reconstituted at 100mg ml^{-1} in sterile water (Brewer and Torricelli, 2007; Kaar et al., 2017) or borate buffer (Kaech and Banker, 2006). In terms of physically coating the coverslips, 0.1ml of poly-D-lysine per cm^2 of the glass substrate to be covered is recommended (Brewer and Torricelli, 2007). In our hands, an objective measurement of one drop per coverslip was sufficient, whereas other protocols recommend enough to coat the entire coverslip (Beaudoin et al., 2012; Kaech and Banker, 2006). Indeed, the ability of poly-D-lysine to spread over the area of the coverslip, without signs of visible aggregation, is regarded as a measure of correct cleaning of the substrate (Kaech and Banker,

2006). Once applied, poly-D-lysine is stable for between 3 d (Brewer and Torricelli, 2007) and 7 d at 4ºC (Beaudoin et al., 2012). To prevent any issues concerning poly-D-Lysine stability, our method recommends substrate treatment with poly-D-Lysine on the day of culture preparation.

Troubleshooting: In preparation and after thawing, it is recommended that poly-D-lysine is thoroughly dissolved. The appearance of bubbles, which stick to the side of holding tubes, is a sign of undissolved poly-D-lysine. Applied poly-D-lysine should not be allowed to dry out on the coverslip prior to washing. Although some authors identify this as a critical step, no reason is given for its importance (Kaech and Banker, 2006). As a precaution, this recommendation is adhered to for the protocol described here. If unbound poly-D-lysine is not rinsed away thoroughly, cell attachment is compromised and cell death occurs (Brewer and Torricelli, 2007). In our hands, two quick rinses with water were sufficient for effective neuron attachment.

2.2.5 Methods

Unless otherwise stated, all procedures were carried out in a sterile laminar flow hood, using equipment and reagents which, if not already contained in sterile packaging, were sterilised with 70% ethanol. Strict aseptic technique was adhered to at all times in order to avoid contamination of the culture.

Solution preparation

Approximately 3 ml of dissection solution was sterile filtered into each of two 35 mm dishes which were then placed on ice in a dissection hood.

Tissue isolation and treatment

Hippocampi were isolated as described previously (Beaudoin 2012) and placed in the 35 mm dish on ice. Any extraneous tissue was cleaned from the hippocampi before they were transferred to the second 35 mm dish on ice. The tissue was then chopped into smaller pieces with fine scissors and then transferred to a 15ml tube using a Pasteur pipette. This tube was placed in a water bath at 37ºC with the papain solution, separately, and both were allowed to equilibrate at this temperature for five minutes. The tissue was then carefully transferred into the papain solution and placed onto an orbital shaker at 100 rpm at 37ºC for 45 minutes. The tissue was then gently removed from the papain solution and placed into another 15 ml tube containing 2 ml HBSS. This step was repeated two more times (to remove any residual papain), each time being careful to avoid trituration of the tissue

at this stage. The tissue was then transferred into another 15 ml tube containing approximately 6 ml of trituration solution.

Trituration

The tissue was allowed to settle to the bottom of the 15 ml tube containing the trituration solution. The tip of a plastic transfer pipette, with the bulb fully depressed, was firmly pushed against the bottom of the 15 ml tube (Fig 2.1). The solution containing the tissue was then aspirated into the pipette such that the tissue experienced a certain degree of friction as it moved between the edges of the bottom of the tube and the pipette itself. This friction helped to dissociate individual hippocampal neurons from the larger pieces. When all the tissue had been aspirated into the pipette, the tip of the pipette was then placed under the meniscus of the trituration solution and forcefully expelled. Depending on the resulting tissue break up, this procedure was repeated up to an absolute maximum of four times, allowing the tissue to settle to the bottom of the tube between each aspiration. The supernatant was then placed into another 15 ml tube, leaving behind as much as possible of the un-triturated tissue. This whole procedure took no more than five minutes. The supernatant was then centrifuged at 258 xg for two minutes at room temperature. A video illustrating this trituration procedure is published at https://doi.org/10.1016/j.jneumeth.2017.05.020.

Practical use: A practical measure of the suitability of one's trituration technique can be garnered by observing the consistency of the trituration solution. A sticky accumulate of floating tissue pieces indicates DNA release due to cell rupture (Brewer and Torricelli, 2007).

Optimisation: See discussion section for trituration optimisation information. Centrifugation parameters were optimised to allow for the formation of a relatively cohesive pellet, without compromising cell viability due to sheer stress or compression of cells.

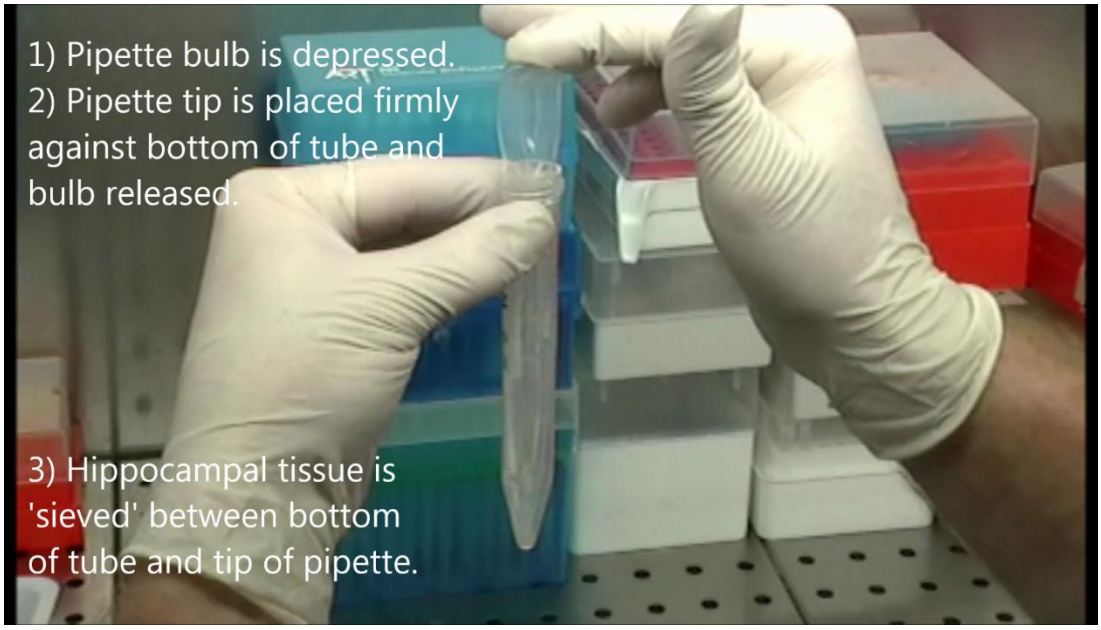

Figure 2.1. Trituration method

The trituration procedure is the most critical step in determining the success of a culture. The following procedure is considered optimal:

1) The pipette bulb is fully depressed. 2) The pipette tip is then pushed firmly against the bottom of the tube and the bulb is released whilst maintaining downward pressure. 3) This results in tissue being "sieved" between the bottom of the tube and pipette tip. 4) Firmly dispel contents of pipette into the tissue solution. The majority of tissue will be dissociated following 2 – 3 repetitions.

Video still, taken from a video illustrating the trituration method in full, is published by Kaar et al. (2017) and can be found at: https://doi.org/10.1016/j.jneumeth.2017.05.020#

Cell seeding and culture

After centrifugation, the supernatant was carefully poured out of the tube without disturbing the pellet of cells. Two drops of plating solution were then gently added and subsequently removed to dilute any residual supernatant. The volume of plating solution added (0.6 - 1 ml) is determined subjectively, depending on the size of the pellet which, in turn, is dependent upon the effectiveness of trituration. This resulted in a plating density of approximately 1 – 1.5 x 10^5 cells/cm^2, which was optimal for cell survival and our subsequent calcium imaging experiments. The pellet was carefully dislodged from the bottom of the 15 ml tube using a Pasteur pipette, and the cells re-suspended by firmly finger vortexing 2 - 3 times, depending upon the level of re-suspension. An indication of successful technique up to this point

was routinely determined by employing a trypan blue staining and cell counting protocol (see below).

> **Optimisation:** Cells undergo considerable mechanical stress during pellet re-suspension. Optimisation of this technique was achieved by observing the extent of cell dispersion by either mixing with a glass transfer pipette or “finger vortexing” using various forces and a number of repetitions. Whether these processes resulted in culture success or failure was noted. Careful dislodging of the pellet with a glass transfer pipette followed by relatively forceful finger vortexing (2 – 3 times) was determined to be optimal.

A drop (approximately 25 µl) of the final plating solution was then added to each coverslip using a Pasteur pipette. The coverslips were then placed in an incubator, where the cells were allowed to adhere to the coverslips for one hour. 2 ml of the culture solution was then very gently added to each 35 mm dish (to prevent damaging the cells through sheer stress), before returning the dishes to the incubator.

> **Note:** Limiting exposure of cells to ambient air during plating to 3 minutes is recommended (Brewer and Torricelli, 2007). In practical terms, this was achieved through competence and the speed at which the protocol is carried out. Furthermore, the splitting of culture dishes into larger “holding dishes” reduced the number of dishes which were exposed to ambient air at any given time and made this process logistically easier. Measurement of culture success at this point could subjectively be determined by noting neuronal morphology soon after plating. Cells tend to start as isolated spheres and quickly grow neurites and processes. Such processes are regarded as being important for neuronal attachment to the substrate (Eide and McMurray, 2005) and their appearance can be taken as initial markers of success from 1 hour to several days post-culture (Kivell et al., 2000; Zhang et al., 2006). Previous studies have shown that cell viability immediately before plating is approximately 65 – 80% (rat brainstem cultures between E14 and P6). Neuron maturity is inversely proportional to viability at this stage (Kivell et al., 2000).

Trypan blue exclusion

100 µl of the cell suspension solution was gently mixed with 200µl of trypan blue. Approximately 10 µl of this mixture was then added to each side of a haemocytometer. A 1 ml pipette was used for this purpose as a narrow-tip pipette excludes cell clusters and results in an underestimation of cell numbers (Brewer and Torricelli, 2007). The field of view was observed under a 10x phase contrast microscope. Phase-bright (dye-excluding) spherical cells were counted in four separate squares on both sides of the

haemocytometer. This count was averaged and multiplied by 10^4 to determine cell concentration per millilitre.

Coverslip inversion

Three hours after the culture medium was added to the 35mm dishes, the coverslips were inverted using sterile forceps. To prevent cross-contamination, forceps were flame sterilised between each dish**.**

> **Note:** It has been shown previously that neurite growth, neuron survival and long-term neuronal maintenance is improved by the sandwiching of cells between the substrate and a coverslip (Brewer and Cotman, 1989; W. S. Chen et al., 2011; Kaneko and Sankai, 2014; Lucius and Mentlein, 1995). The proposed mechanism underlying this improvement is thought to be the creation of a microenvironment where the diffusion of various growth factors and nutrients from neurons and glia into the surrounding media is limited, and extracellular [O_2] is also reduced to more physiological levels (Brewer and Cotman, 1989; Kaech and Banker, 2006).
>
> **Optimisation:** In agreement with the findings described above, by subjective observation, we determined that neuron morphology and survival was improved upon coverslip inversion. Previous studies have shown that maximum neurite length, an indicator of neuronal viability and active growth, is highest with coverslip sandwich at 1 or 3 hours when compared to 22 hours at 3 - 8 DIV. For longer-term maintenance (14 – 38 DIV), 3 or 22 hours inversion induced the greatest extent of neurite length. Therefore, 3 hours post-plating would appear to be a practical compromise for both short- and long-term viability (Kaneko and Sankai, 2014). In line with this study, in our protocol cells were generally left to adhere to coverslips for 3 hours prior to coverslip inversion. However, an incubation ranging from between 2 – 4 hours does not appear to alter culture success.

Immunocytochemistry

Wash steps consisted of three changes of PBS, each lasting five minutes. Cells were fixed with paraformaldehyde (4%) and sucrose (4%) prepared in PBS and warmed to 37ºC for ten minutes. All subsequent steps, unless otherwise stated, were carried out at room temperature. After washing, a permeabilisation solution (0.25% Triton™X-100 in PBS) was added to the cells for ten minutes. Cells were washed once more with PBS and a blocking buffer (BSA 5% and glycine 0.3 M in PBS) was added for one hour. Primary antibody incubation was carried out overnight at 4ºC, using the following antibodies: pan-neuronal marker (1: 100), GFAP (1: 500) and Synapsin I (1: 200). The pan-neuronal marker is an antibody cocktail containing NeuN, βii-tubulin, NF-H and microtubule-associated protein 2 (MAP-2). MAP-2 is only present on dendritic microtubules (Kaech and Banker, 2006). All antibodies were diluted in an antibody buffer containing

BSA (1%) in PBS. After washing, cells were incubated with the corresponding secondary antibody at 1: 200 dilution for one hour. Cells were again washed before being mounted on microscope slides.

Determining the neuron versus glial cell composition of cultures

The ratio of neurons to glia was determined by counting the number of pan-neuronal and GFAP-positive cells, respectively, under a confocal fluorescent microscope. As described previously, when cells were initially added to coverslips following their dispersal, a drop was placed in the centre of each coverslip. As a result, there is a non-uniform distribution and density of cells, with the highest density of cells appearing in the centre of the coverslip and receding outwards towards the perimeter of the initial cell droplet (Fig 2.2). Consequently, to obtain an accurate representation of overall cell numbers, a central point was chosen and three randomised points radiating from the middle to the edge of the immunostained region of each coverslip were selected for counting (such regions contained an average of 16 cells in an area of approximately 200 μm^2). Compositional analysis was conducted upon coverslips fixed at 2, 5, 8, 11, 14, 17 and 20 days *in vitro* and from three separate culture preparations (from three separate mouse litters), harvested from five-day-old mice.

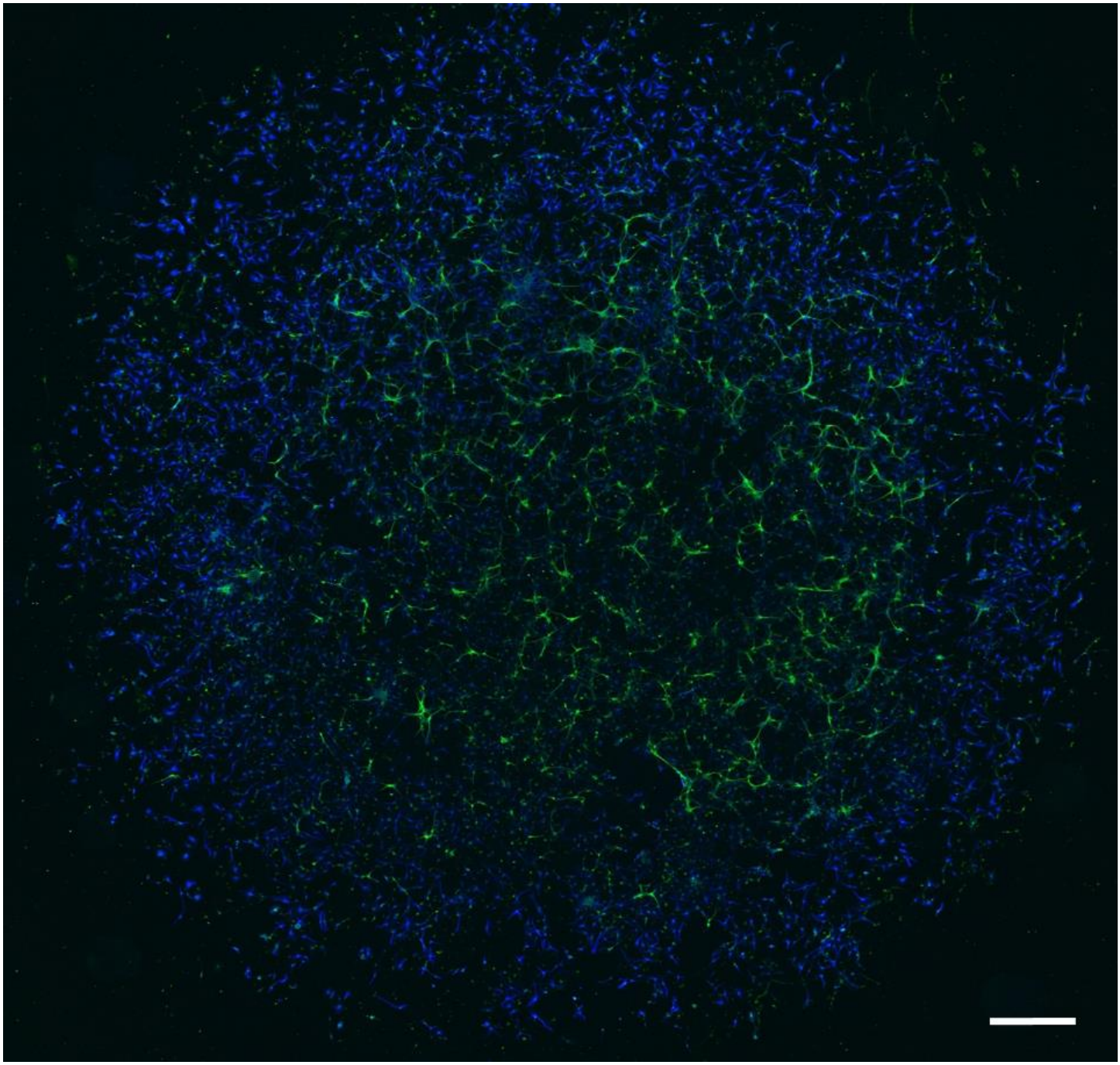

Figure 2.2. Global image of an immunostained coverslip

Representative image displaying the non - uniformity of cell density and distribution of mouse hippocampal cultures. Neuronal marker, pan-neuronal stain containing NeuN, βii-tubulin, NF-H and MAP-2 (green). Glial marker, GFAP (blue). Image captured at 5 days *in vitro*. Scale bar, 500 μM.

Calcium imaging

Intracellular calcium measurements from neuronal somata were conducted as previously described (Rae et al., 2000). Briefly, using a conventional fluorescence imaging system consisting of a bright light source (Olympus TH4-200), monochromator (Cairn Optoscan), integrating camera (Hamamatsu ORCA-ER), DAQ device (USB6229) and frame grabber, neurons that had been preloaded for one hour in an incubator with the single wavelength, intensity modulating calcium indicator, fluo-2 AM (4 μM dissolved in a solution of HBSS with 0.1% pluronic) were imaged (excitation at 488 nm, emission at 550 nm; no neutral density filters were used) under both 20x and 40x magnification, where appropriate. The intensity of excitation light was minimised using neutral density filters. Under these conditions, there was no discernible bleaching or phototoxicity.

Once loaded, washed and mounted on the microscope stage, neurons were continuously superfused with HBSS (2 ml/min) and all drugs were added to the superfusate. In so doing, we reduced the risk of inducing experimental artefacts which may have been caused by the pipetting of compounds directly onto cells within the field of view. However, this method of drug application also meant that it took a finite 'lag time' for the drug to reach the neurons (~30s).

To block indirect actions of I-mGluR activation *via* synaptically driven Ca^{2+} transients/action potential-mediated release of neurotransmitter, all experiments were performed in the presence of the voltage-gated sodium channel (VGSC) antagonist tetrodotoxin (TTx; 1 μM). Experiments involving NMDA were performed in Mg^{2+}-free HBSS supplemented with 10 μM glycine.

Images were acquired at one-second intervals using the open source imaging software, Winfluor (John Dempster, University of Strathclyde, Scotland) *via* an Olympus BX50 WI microscope. Pixel binning (2-times) was applied to images. Winfluor calculated fluorescence values for each pixel in the frame after subtraction of background fluorescence intensities. Data files with time (seconds) *vs* fluorescence values (arbitrary units) for each region of interest (ROI) were exported from Winfluor as standard text files. This information was then imported into GraphPad Prism where XY line graphs were produced and analysed for each ROI.

2.3 Results

2.3.1 Production and optimisation of postnatal primary mouse hippocampal cultures

We have consistently produced postnatal hippocampal mouse cultures from animals between 3 - 5-days-old, which are routinely used for calcium imaging experiments. The ability to produce such cultures reliably and in a cost-effective manner is a result of optimising almost all facets of the culturing procedure. These optimisation steps are described in the materials and methods section and are also displayed in *Table 2.2* Critical steps, including trituration, which we have identified as a primary determinant of culture success will be elaborated upon in *Section 2.4 Discussion.*

Aspect of methodology	Parameters investigated	Reason for optimisation	Currently used	Result
Species used	Mouse and rat	Although primary hippocampal culture using rat tissue is relatively easier, our research aims required the use of cultured control and transgenic mouse neurons.	Mouse and rat	The culture of rat hippocampal tissue results in a greater proportion of successful cultures. With care and optimisation, mouse hippocampal cultures could also be reliably produced.
Age of mice used	2 - 5-days-old	As a proof of concept of the effectiveness of our culture protocol and to enable investigations in older animals, mice up to 14-days-old have also been used.	2 - 5-days-old (routinely) 14-days-old	Cultures from 2 – 5-days-old mice are routinely used. Viable cultures from older animals can also be produced and maintained.
35 mm cell culture dish	Cell culture treated	Cell culture treated dishes give rise to altered neuronal morphology (W. S. Chen et al., 2011).	Untreated	Implementing the use of untreated dishes ensured normal neuronal development with no negative effects on culture success.
15 and 50 ml centrifuge tubes	Polypropylene (PP) and polyethylene terephthalate (PET) tubes	Routine use of polystyrene or PET tubes is recommended, given reports of toxicity from PP tubes	PP tubes	We found no adverse effects using PP tubes.

			(Brewer and Torricelli, 2007).		
Pipette used for plating		Glass pipettes	The use of siliconised glass is recommended for ease of trituration and transfer due to the viscous nature of the dissociated cell suspension (Brewer and Torricelli, 2007).	Standard 150 mm glass pipette	In our hands, standard glass pipettes were sufficient for transfer. Polished pipettes are used to accurately transfer small volumes of the plating solution to coverslips. They are not used for trituration.
Papain	**Papain supplier**	Sigma Aldrich Worthington Scientific	Papain from Worthington Scientific is superior to that supplied by Sigma-Aldrich (Brewer and Torricelli, 2007).	Worthington scientific	In our hands, papain from Worthington Scientific was superior to that supplied by Sigma in terms of tissue digestion. However, the specific supplier is not a determinant of culture success.
	Papain incubation solution	HBSS HBSS - Ca^{2+} and Mg^{2+} free	Ca^{2+} and Mg^{2+} free solution aid tissue digestion (Copray and Liem, 1993; Harris et al., 2007; Mcdonough et al., 2012). However, the absence of these cations may damage cells.	HBSS	No additional advantages were observed with the use of Ca^{2+}- and Mg^{2+}-free HBSS in the trituration solution.
	Tissue incubation in papain	Incubation time of 30,45 and 60 min Incubation temperature of 25, 30 and $37^{o}C$	Papain treatment of tissue is improved at $30^{o}C$ in comparison to $25^{o}C$ or $37^{o}C$ (Brewer and Torricelli, 2007).	45 minutes at $37^{o}C$	45 minutes incubation of tissue at $37^{o}C$, combined with light tissue agitation resulted in optimal tissue preparation.
Trituration	**Pipette used for trituration**	3.5 ml – 5 ml plastic transfer pipettes of various shapes.	The trituration procedure is the most critical step in determining the success of	3.5 ml plastic transfer pipette –specific shape and aperture size used	A plastic, wide tip diameter (drop size 35–55 µl) transfer pipette was optimal for

		150 mm glass pipettes, flame polished to various extents.	a culture (Kaar et al., 2017).	(Sarstedt, cat. No. 86.1171).	achieving tissue dissociation whilst maintaining neuronal viability.
	Trituration method	Glass and plastic pipettes used in combination with various trituration strengths, speeds and repetitions.	Large variability in techniques recommended in the literature.	Sieving trituration. Relatively forceful expelling of pipette contents. Absolute maximum of four triturations	See 3.2.5 methods
	Dissection and trituration Solution	Hibernate A HBSS	HA is a form of NB which maintains stable pH in ambient conditions. Has been used to successfully culture adult hippocampal neurons (Brewer and Torricelli, 2007).	HBSS	HA provided no advantage, objectively, on culture quality. Given the cost-effectiveness of lab-made HBSS, this was utilised routinely.
	Centrifugation of cell suspension	Various centrifugation speeds for 1 – 3 min	Large variation in recommended speeds (80 – 1000 g) and duration (2-15 min) in published literature.	258 xg for two minutes at room temperature.	These parameters allowed for a relatively cohesive pellet to form without compromising cell viability due to cell shear stress or compression.
L-glutamic acid/glutamate		Culture solutions with and without L-glutamic acid	Very low concentrations of glutamate (25 µM) promote a persistent enhancement of physiological neuronal activity (Edwards et al., 2010).	All solutions were supplemented with L-glutamic acid (25 µM).	We utilised this low glutamate concentration throughout our culture method in order to promote physiological cell signalling.
L-glutamine		Addition of L-Glutamine (L-Gln) or GlutaMAX	GlutaMAX, a stable form of L-Gln, is recommended due to decreased toxicity relative to L-Gln	All solutions were supplemented with GlutaMAX.	Subjectively, we found that there were more successful cultures when using GlutaMAX over L-Gln and so this

		(Seibenhener and Wooten, 2012).		supplement was used routinely.
Plating and culture solution	DMEM Neurobasal-A (NB-A)	NB is used routinely in the field but is an expensive proprietary formulation.	DMEM	DMEM produced cultures of similar quality to NB, determined subjectively. Such neurons also adhere to developmental and functional norms (as determined by immunocytochemistry and Ca^{2+} signalling).
Culture medium supplement	Serum-replacement-2 (SR2) B27 NeuroPlex™ (Gemini Bio Products)	B27 is the most commonly used supplement in the field. As with NB, it is an expensive proprietary formulation. NeuroPlex is an alternative proprietary supplement.	SR2	The inexpensive SR2 supplement was a cost-effective alternative which allowed for the production of high-quality cultures.
Plating density	Low, medium and high density.	Large range of densities used in the field depending on the application.	The volume of plating solution added (0.6 - 1 ml) is determined subjectively, depending on the size of the pellet of triturated tissue. This, in turn, is dependent on the effectiveness of trituration.	Plating density from 1 – 1.5 x 10^5 cells/cm^2, which we found optimal for cell survival and for the subsequent use of coverslips in calcium imaging experiments.
Pellet re-suspension	Dispersion of tissue with pipette use and finger vortexing, using various forces and number of repetitions.	Cells undergo considerable mechanical stress during pellet re-suspension.	Dislodging of pellet with pipette Finger vortexing to re-suspend (2 - 3 repetitions).	The pellet was carefully dislodged from the bottom of the 15 ml tube using a glass Pasteur pipette and the cells subsequently re-suspended by firmly finger vortexing 2 -3 times, depending on

				the level of re-suspension.
Coverslip inversion	Inverted (1 – 4 hours post plating) and non-inverted cultures.	Neurite growth, neuron survival and long-term maintenance can be improved by the sandwiching of cells between the substrate and a coverslip (Brewer and Cotman, 1989; Chen et al., 2011; Kaneko and Sankai, 2014).	Coverslip inversion after 3 hours in culture.	By observation, we determined that neuron morphology and survival improved upon coverslip inversion. An incubation ranging from between 1 – 4 hours does not appear to alter culture success.

Table 2.2. Optimisation of the culture protocol

2.3.2 Characterisation of Hippocampal Cultures

Hippocampal cultures produced using this new method contained healthy, functional cells which responded appropriately to physiological stimuli (see *2.3.3 Calcium imaging experiments*). Cultures displayed normal neuronal morphology, arborisation, synaptic connections and intercellular associations from 2 DIV onwards, as evidenced by both bright field images (Fig 2.3 and 2.4) and from immunocytochemical images of neurons that had been stained with both a pan-neuronal marker, GFAP, and synapsin I antibodies (Fig 2.5 and 2.6).

In order to characterise the development and composition of such cultures *in vitro,* we examined the neuron to glial cell ratio after fixing cultures at 2, 5, 8, 11, 14, 17 and 20 DIV (Fig 2.7). Although there is a steady decline in the numbers of both glia and neurons with increasing DIV, the neurons which do remain respond to standard physiological stimuli for up to one month after initial culturing (*e.g.* Fig 2.9).

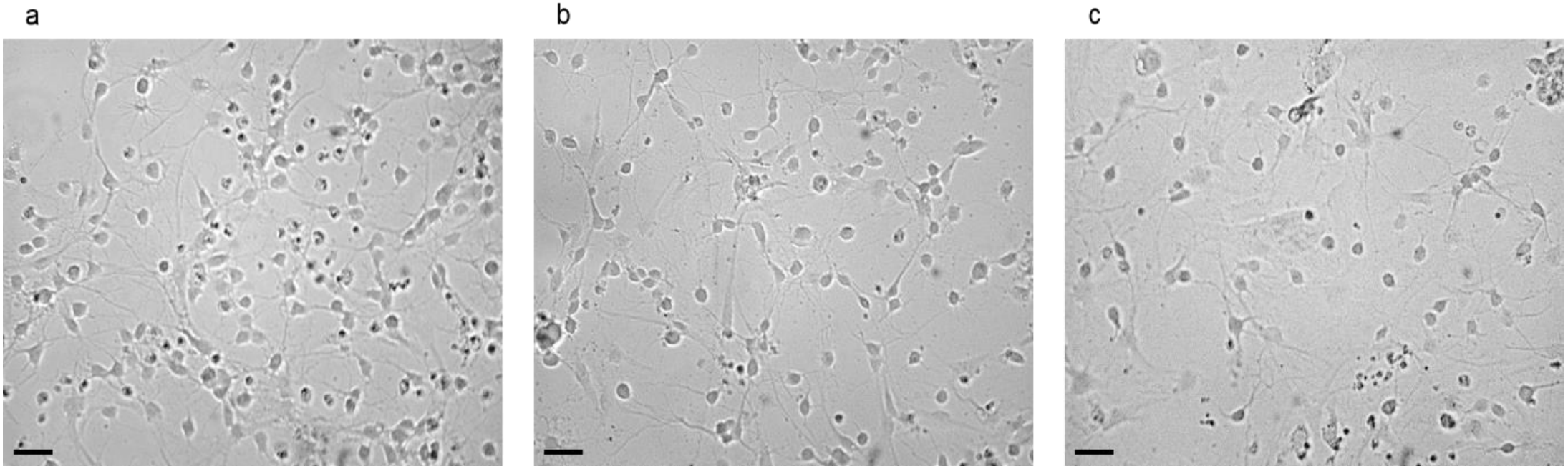

Figure 2.3. Hippocampal neurons obtained from progressively older animals at 2 days *in vitro*.

Bright field (DIC) images showing cultured postnatal mouse hippocampal neurons generated from 3- (a), 4- (b) and 5- (c) day-old mice. All images were captured at 2 days *in vitro*. Scale bar 30 µm.

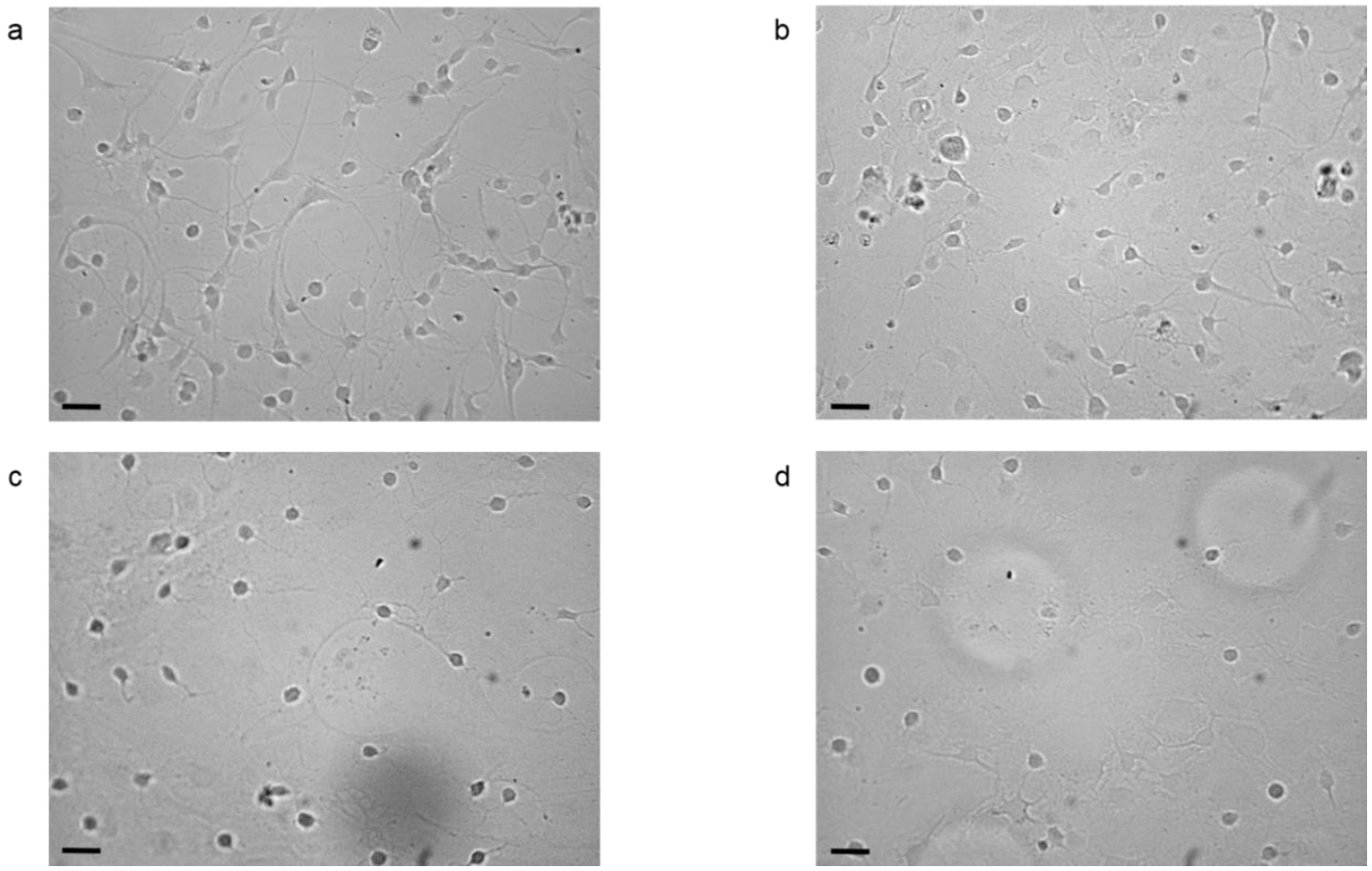

Figure 2.4. Development of neurons *in vitro*

Bright field (DIC) images of cultured mouse hippocampal neurons taken at progressively older days *in vitro*, 2 (a), 4 (b), 10 (c) and 13 (d). All cultures were generated from mice aged between 3 - 5 days of age. Scale bar 30 µm.

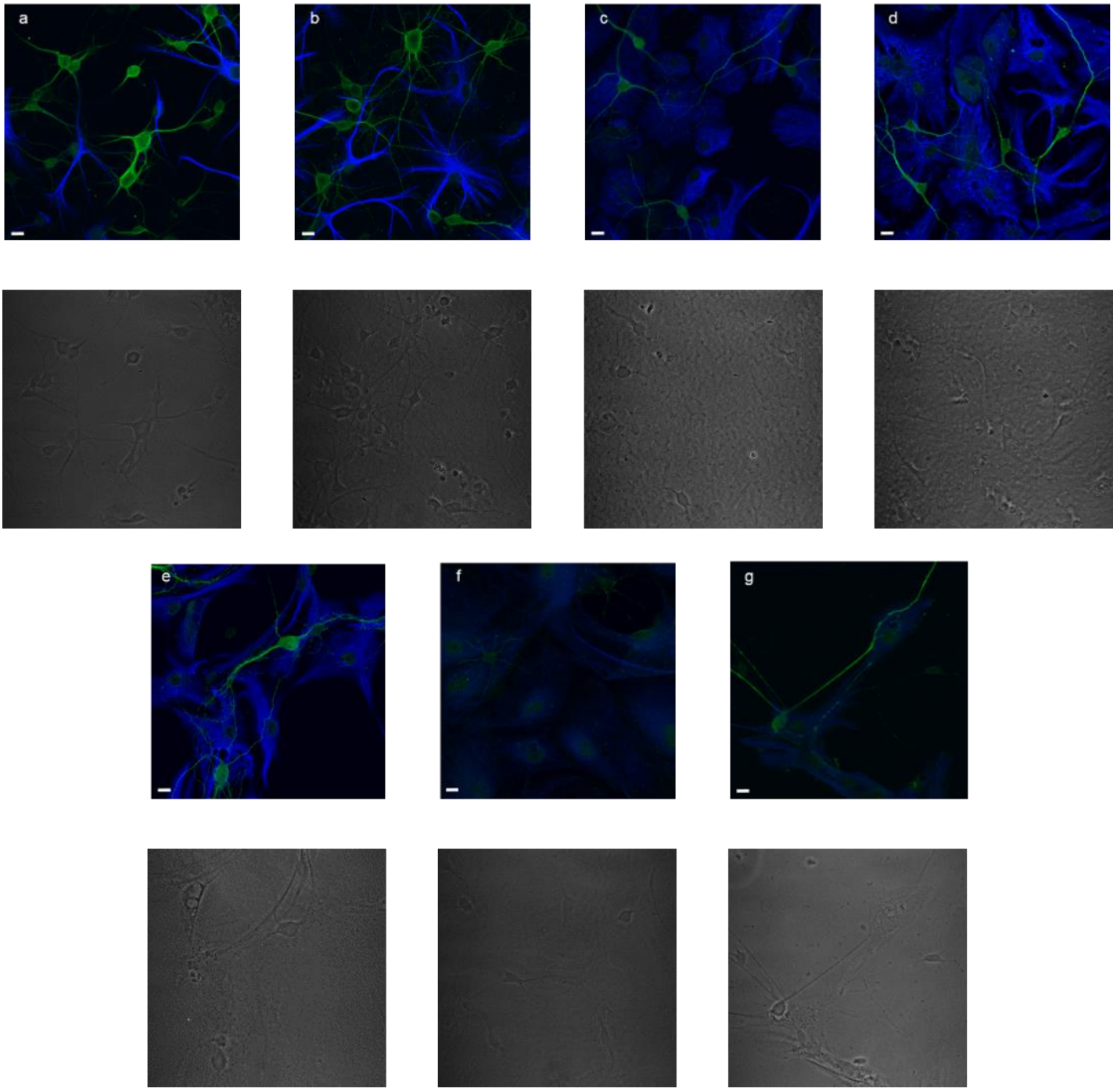

Figure 2.5. Immunocytochemical visualisation of culture composition with progressive time *in vitro*

Immunostaining of hippocampal cultures for neuronal and glial markers with corresponding phase - contrast images. Images were captured of cultures fixed at progressively older days *in vitro* 2 (a), 5 (b), 8 (c), 11 (d), 14 (e), 17 (f) and 20 (g). Neuronal marker, pan-neuronal stain containing NeuN, βii-tubulin, NF-H and MAP-2 (green). Glial marker, GFAP (blue). All cultures were generated from 5-day-old mice. Scale bars, 10 μM.

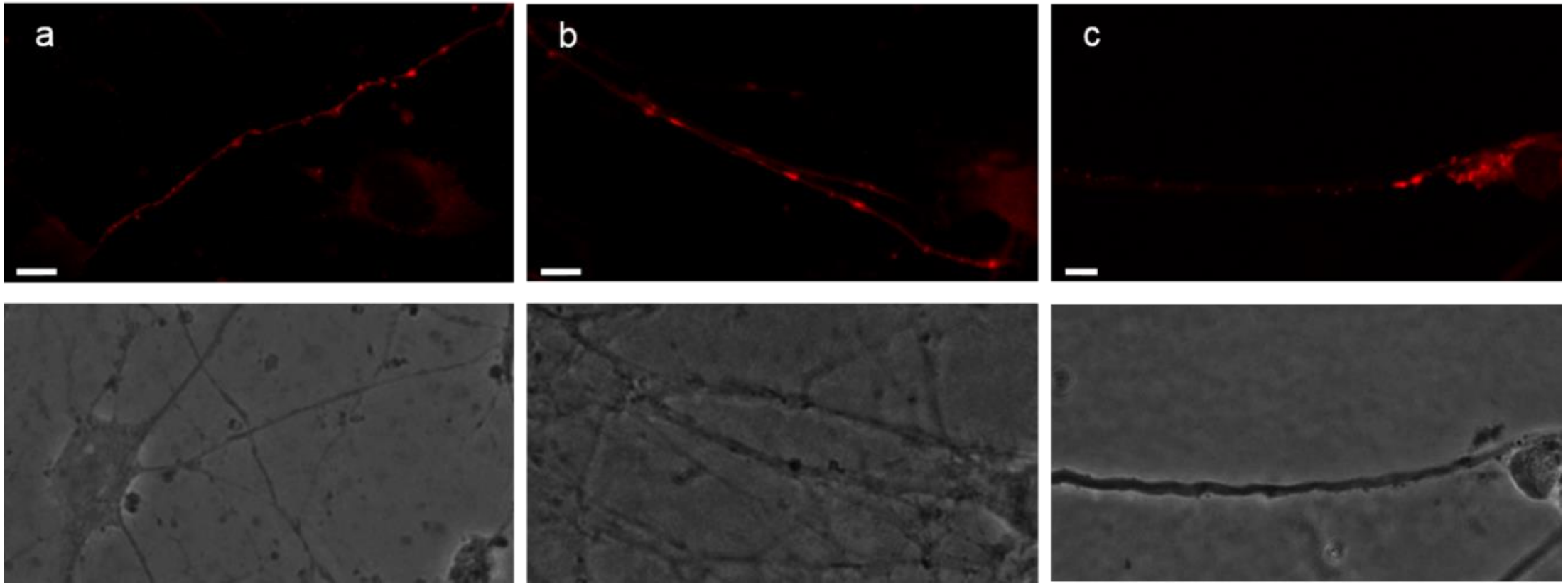

Figure 2.6. Evidence of synapse formation from two days *in vitro*

Immunostaining of hippocampal cultures for synaptic marker (synapsin I, red) with corresponding phase contrast images. Images were captured of cultures fixed at progressively older days *in vitro*, 2 (a), 10 (b) and 20 (c). All cultures were generated from 5-day-old mice. Scale bars, 5 μM.

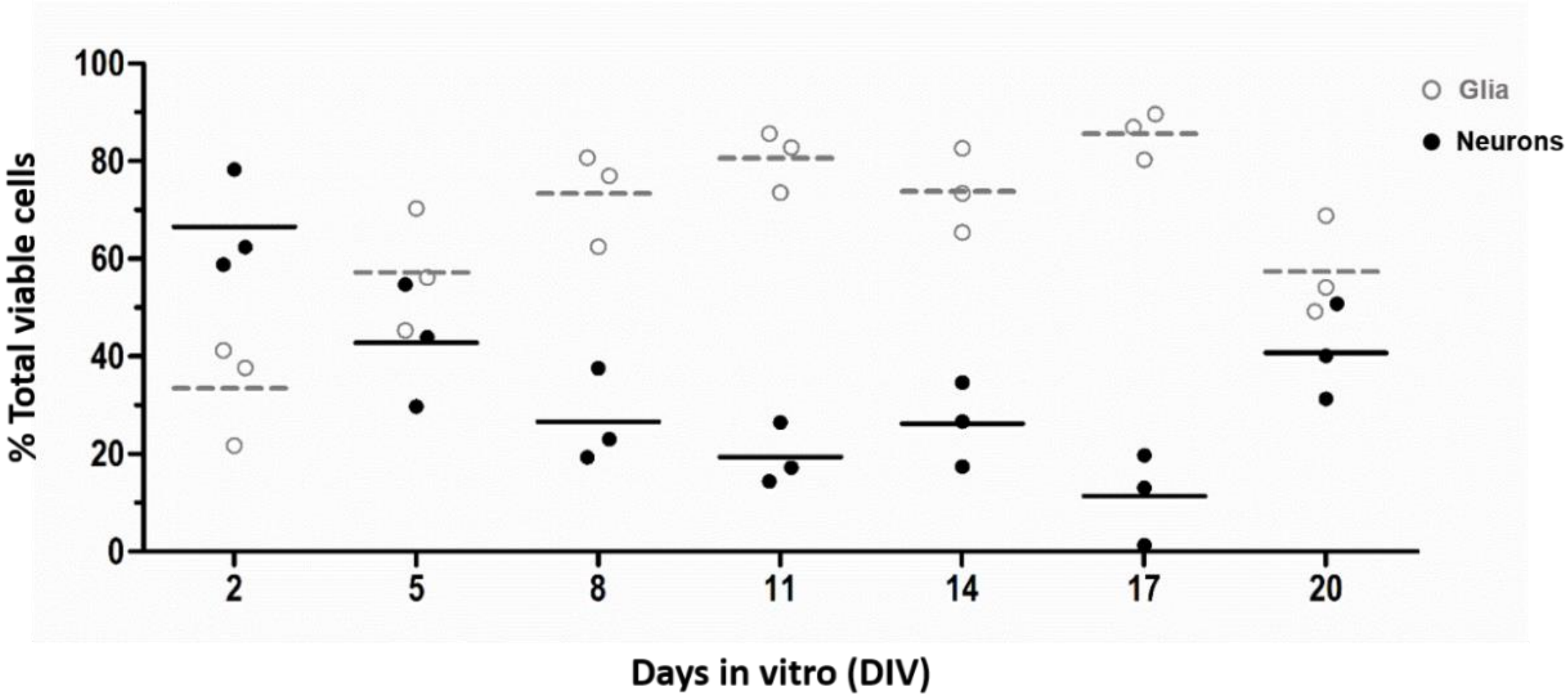

Figure 2.7. Graphical representation of the neuron versus glial cell composition of postnatal mouse hippocampal cultures at progressively older days in vitro (DIV)

The percentage of viable cells which are glia (grey, open circles) or neurons (black, closed circles) are presented at 2 – 20 DIV. All cultures were generated from 5-day-old mice.

2.3.3 Calcium imaging experiments

Cultured neurons harvested from 3 - 5-day-old mice were usually utilised for up to fourteen days *in vitro* for calcium imaging experiments (Kaar and Rae, 2016, 2014). However, some experiments were also carried out using neurons which had been cultured for approximately one month to test long-term cell function (*e.g.* Fig 2.9). In the course of our calcium imaging investigations, we have utilised various compounds which healthy and functional cultured hippocampal neurons would be expected to respond to. For example, we have conducted experiments in which these neurons have responded to physiologically relevant stimuli such as 15 mM and 50 mM K^+-containing HBSS (Fig 2.8 a and b; which depolarise neurons and thereby activate VGCCs on the neuronal plasma membrane); the specific I-mGluR agonist, (S)-DHPG (50 µM), the muscarinic acetylcholine receptor agonist, carbachol (10 µM) and the RyR agonist, caffeine (20 mM), which all evoke calcium release from the endoplasmic reticulum (ER; Fig 2.8 c, d and f, respectively); as well as the ionotropic glutamate receptor agonist, NMDA (1 µM; Fig 2.8 e). All compounds were added to the superfusate.

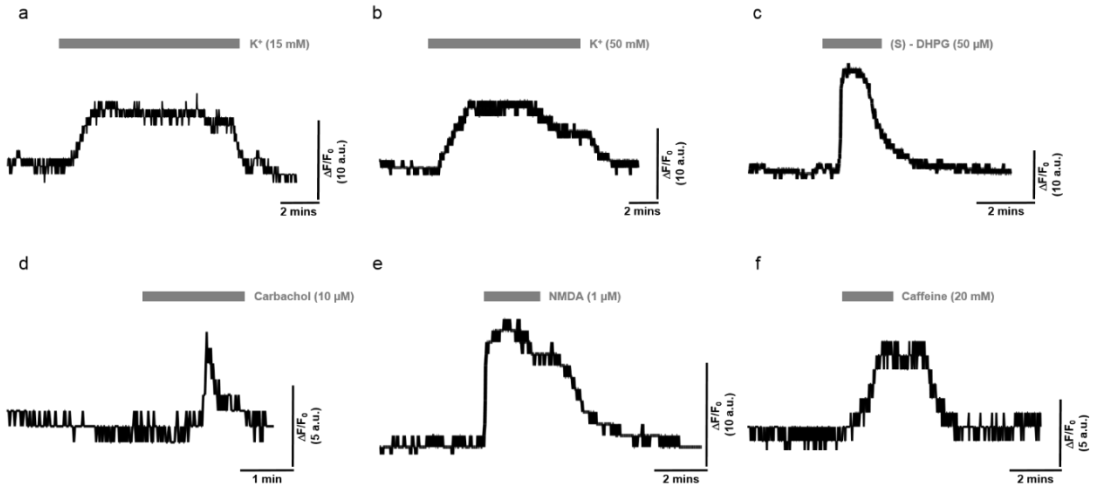

Figure 2.8. Representative traces showing changes in somatic [Ca^{2+}] levels within a cultured mouse hippocampal neuron in response to selected physiological stimuli

Representative traces display responses to the application of: K^+ (15 mM) (a), K^+ (50 mM) (b), (S)-DHPG (50 µM) (c), carbachol (10 µM) (d), NMDA (1 µM) (e) and Caffeine (20 mM) (f). All compounds were added to the superfusate. All neurons were generated from 3 - 5-day-old mice and imaged after 2 – 14 days *in vitro*.

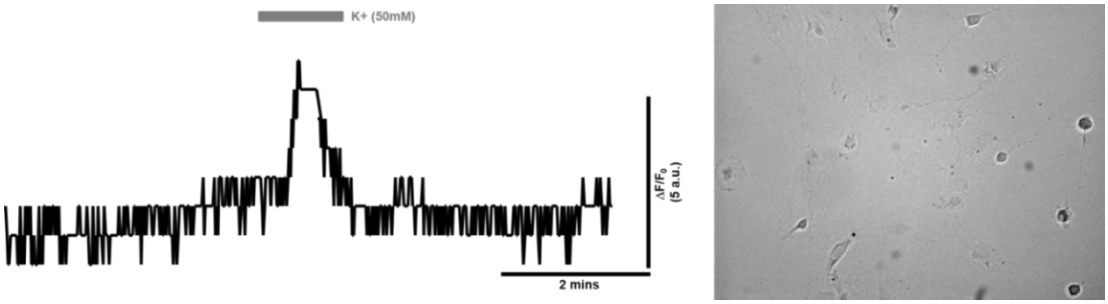

Figure 2.9. Aged cultured hippocampal neurons remain viable for up to 1 month

Representative trace showing changes in somatic $[Ca^{2+}]_i$ levels within an aged (29 days *in vitro*) cultured mouse hippocampal neuron in response to perfusion of a physiological solution (HBSS) containing 50 mM K^+ and corresponding bright field (DIC) image.

2.4 Discussion

The study and use of postnatal neurons and cultures are important for the investigation of chronic and/or age-dependent conditions such as neurodegeneration. Furthermore, as mentioned earlier, the importance and widespread use of transgenic *mouse* models, but the inherent difficulty in culturing postnatal mouse neurons relative to embryonic tissues (Brewer and Torricelli, 2007), or those of the rat (Beaudoin et al., 2012), underpins the need for an easily applicable and effective postnatal mouse culture protocol.

Herein, we have described a novel, simplified protocol for the cost-effective production of primary cultured neurons from postnatal mouse hippocampal tissue that remains viable for up to one-month post-culture. Hippocampal neurons within such cultures display normal development and arborisation, observable cellular interconnection (including synapses) and association with glial cells.

The optimisation of almost all facets of the culturing procedure is outlined in *Section 2.3 Results.* Decisions on optimisation were developed out of practical and objective measurements of neuronal survival and morphology. These results led to an incremental improvement of current practices and omission of unnecessary steps/procedures as discussed in the Methods and Results sections. Optimisation steps which warrant a more thorough discussion, as well as key considerations in the design of our culture system, are described in the following section.

2.4.1 Trituration

Contrary to previous studies such as that of Eide and McMurray (2005), we found that the manner in which the tissue is treated following incubation with tissue proteases, specifically the steps of trituration and subsequent resuspension after supernatant centrifugation, is absolutely critical to ensuring the production of consistent and successful cultures. In this respect, mouse neurons seem to be much more vulnerable and susceptible to mechanical stress than postnatal rat and embryonic neurons at this stage in the protocol.

Of these two phases of major mechanical stress, the trituration procedure is the most critical step in determining the success of a culture. Thus, a balance is required between reaching optimal cell yield by sufficient tissue dissociation, whilst minimising cell lysis. Such lysis and debris production can both directly and indirectly, by altering the pH of the trituration solution and releasing cytotoxic agents such as glutamate, hinder cell attachment, sprouting and viability (Brewer, 1997; Eide and McMurray, 2005).

Trituration pipette tip diameter is crucial in determining overall cell yield, with too small a tip diameter causing cell damage, but too large a diameter resulting in the insufficient tissue breakdown. We found that a plastic, wide tip diameter (drop size 35 – 55 µl) transfer pipette (see equipment) was optimal for reaching this compromise. Using such a plastic pipette allowed us to abandon using flame polished glass pipettes, which are routinely utilised for this purpose in the field. Thus, the requirement to create smooth tipped glass pipettes through flame polishing, which is inherently unreliable and can result in such a small a tip diameter that it damages cells, is circumvented (Beaudoin et al., 2012).

When the triturated cell suspension is expelled from the pipette and returned to the residual supernatant, it is done so *relatively* forcefully but with the pipette tip under the liquid surface (see video). This results in minimal bubble production. The production of such bubbles during trituration is actively discouraged by other research groups (Brewer and Torricelli, 2007). However, we have found that this relatively forceful expulsion from the pipette allows for improved tissue dissociation. Furthermore, it does not significantly affect the quality of our cultures in comparison to, say, over trituration which is much more damaging to the neurons.

Specific protocols can be utilised to reduce the production of cellular debris during trituration. These protocols include: the use of cell strainers (Beaudoin et al., 2012; Kaneko and Sankai, 2014), “washing” plated neurons after they adhere to the substrate (Brewer, 1997) and/or gradient enrichment

of neurons to remove both contaminating glia and debris (Brewer and Torricelli, 2007).

The process of washing adhered neurons (*i.e.* removing the cell suspension) increased cell sprouting by 7-fold at 5 DIV in adult rat hippocampal neurons (Brewer, 1997), suggesting that cellular debris contains factors which inhibit sprouting (Faissner and Steindler, 1995). However, it is proposed that because neurons depend upon their processes for adherence to the substrate, and because such processes are slow to develop, washing could remove healthy neurons which have not had sufficient time to attach (Eide and McMurray, 2005). This influences the period of time within which cells are allowed to adhere before the plating solution is washed off and/or culture medium is added. Experiments on cell attachment (using poly-L-ornithine substrates) by Eide et al. (2005) illustrated the importance of the length of plating incubation to culture success. Specifically, cell attachment to the substrate occurred within the first 10 minutes and a 15-minute incubation prior to washing was optimal whereas a 2-hour incubation resulted in *complete* culture failure (Eide and McMurray, 2005). We determined that a plating time of 1 hour was optimum for cell survival and for consistent culture success using poly-D-lysine-coated coverslips. This is within the time frame of 2 hours, which has previously been reported as allowing the majority of cells attach to poly-D-lysine (Brewer, 1997). A specific wash step was not employed in our method in an effort to reduce the time cells spend in unfavourable conditions outside of the incubator. Instead, any debris that was present was effectively diluted to apparently negligible amounts through the addition of a large volume of culture medium (~2.5 ml).

Debris removal using cell strainers (Chen et al., 2013) of various pore diameters or neuronal enrichment by gradient centrifugation (Brewer and Torricelli, 2007) did not yield significant improvements in culture quality to warrant their utilisation. Furthermore, these techniques increase the exposure of cells to ambient conditions, decrease the efficiency of protocol and add to the overall costs of the method.

By using the novel trituration technique described herein, combined with limiting the number of triturations to an absolute maximum of four, we effectively minimised the main mechanical stress experienced by neurons and also significantly reduced the amount of debris that would be produced under normal circumstances. The production of debris was further limited by implementing a gentle re-suspension of triturated cells by finger-vortexing rather than further trituration. In turn, this resulted not only in the production of very little potentially contaminating cellular debris but also, more importantly, a cell suspension containing a very high percentage of viable cells (85 - 90% viability as determined by trypan blue protocol). This

represents a significant improvement on previous studies, which have typically shown approximately 75-85% cell viability post-trituration in hippocampal prenatal mouse culture (E19; Seibenhener and Wooten, 2012) and 65–80% in rat brainstem culture (E14 – P6; Kivell et al., 2000).

2.4.2 Glial cells in culture

The utilisation of either “pure” neuronal cultures, mixed cultures (composed of neurons and glia) or removable glial feeder layers is dependent upon the suitability of these particular environments to specific experimental requirements. “Pure” neuronal cultures (*e.g.* Chen et al., 2011; Brewer 1995) exhibit minimal glial proliferation and represent a means of reducing the confounding factor of glial influence on neuronal physiology. However, this simplification in terms cellular environment must be balanced with physiological relevance.

Glia play a critical role in supporting neuronal function and development, including roles in signalling, synaptic plasticity and network formation (Allen and Barres, 2009; Araque and Navarrete, 2010; Auld and Robitaille, 2003; Banker, 1980; Barker and Ullian, 2008; Bazargani and Attwell, 2016; Nedergaard et al., 2003; Shaham, 2005). These functions are achieved, primarily, *via* the release of soluble factors, including growth factors, signalling molecules and lipids (Ebrahimi et al., 2016; Hassanpoor et al., 2013; Mauch et al., 2001). Therefore, the presence, or otherwise, of glial cells in neuronal cultures will almost certainly influence both culture development and phenotype.

With this evidence in mind, we opted not to use glial inhibitors such as β-D-cytosine arabinofuranoside (Beaudoin et al., 2012; Mao and Wang, 2001; Rae et al., 2000; Seibenhener and Wooten, 2012) and 5-fluro-2X-deoxyuridine (Oorschot, 1989). These inhibitors negatively impact upon culture viability and synaptic development and, indeed, can actually enhance neuronal cell death (Beaudoin et al., 2012; Kivell et al., 2000; Pfrieger and Barres, 1997; Seibenhener and Wooten, 2012; Ullian et al., 2001; Wallace and Johnson, 1989). Furthermore, we feel that the presence of glia is more reflective of the *in vivo* environment, which we are striving to model in these cultures as accurately as possible. Although some proponents of pure cultures point to cytotoxic factors which are produced and released during the lifespan of glia (Price and Brewer, 2001) as a reason not to include these cells (Seibenhener and Wooten, 2012), we believe that the benefits of glial-containing cultures far outweigh this negative aspect.

Numerous studies have characterised the interaction between neurons and glia in culture. Both multipolar and bipolar neurons, from rat

brainstem cultures (E14 – P6, 4 – 9 DIV) associated with glia (Kivell et al., 2000; Miller and Azmitia, 1999). Furthermore, rat hippocampal cultures (P2 - P3, 7 DIV) also contained glia which had complex shapes and several processes and which were also closely associated with neurons (Pozzi et al., 2017). Other types of cultured neurons (*e.g.* brainstem and cerebellum) can grow on top of a naturally occurring layer of type 1 astrocytes, although there were also viable neurons on the same coverslips which were not in proximity to glia (Kivell et al., 2000; Trenkner, 1992).

The positive effects of such interactions are evidenced by the following observations: i) glial proliferation in hippocampal cultures has been shown to be protective against excitatory amino acid-induced degeneration of hippocampal neurons (Mattson et al., 1995; Mattson and Rychlik, 1990), ii) the use of astroglial-conditioned media (ACM) increased long-term neuronal survival (up to 60 DIV) in rat embryonic hippocampal (P0 – 3) and hypothalamic (P21) cultures (Pozzi et al., 2017; Todd et al., 2013; Yamashita et al., 1992), and iii) we have observed (albeit unquantified) a positive association between neuron and glia interaction, where long-term viability and responsiveness of neurons in Ca^{2+} imaging experiments is increased in those cultures where neurons and glia are in proximity to each other.

The importance of neuron-glia interactions is also illustrated by the number of recently published primary culture methods which specifically seek to foster glial support through the utilisation of, a) astroglial monolayers which are used as a substrate on which to plate hippocampal neurons (Ivenshitz and Segal, 2010; Segal et al., 1998), b) glia feeder layers which, although time-consuming to implement, resulted in high-quality primary neurons (Beaudoin et al., 2012; Boraso and Viviani, 2011; Kaech and Banker, 2006; Shimizu et al., 2011) and, c) culturing neurons in ACM (Pozzi et al., 2017). However, the simplicity and effectiveness of our mixed culture method make the use of these technically demanding protocols redundant, at least for our particular application of subsequent Ca^{2+} imaging between 2 – 14 DIV. Depending upon the specific research question one wishes to investigate however, the components of the various media suggested herein could be fine-tuned to generate the particular final cellular composition that one desired.

2.4.3 Culture density

Paracrine support from glia and other neurons can also be fostered using a relatively high plating density. However, above a threshold density, cells and debris can clump into large aggregates. Although such aggregates are oftentimes viable it would be almost impossible to accurately visualise individual cells contained within them (*e.g.* during Ca^{2+} imaging experiments). Furthermore, in our experience at least, such high-density cultures are not amenable to long-term maintenance.

In line with previous reports (Kaneko and Sankai, 2014), in our hands, utilising a plating density which is below a certain threshold also resulted in the complete failure of our cultures. Specifically, rat hippocampal cultures at a density below 10^4 cells/cm^2 die within days (Banker and Cowan, 1979, 1977; Banker, 1980; Brewer et al., 1993; Brewer and Cotman, 1989; Lucius and Mentlein, 1995). This may be due to the relatively lower concentrations of trophic factors such as nerve growth factor, brain-derived neurotrophic factor and basic and acidic fibroblast growth factor (bFGF and aFGF), that are released from neurons and glia (Kaech and Banker, 2006), and which are important for neuronal survival (Barde, 1989; Kaech and Banker, 2006; Levi-Montalcini, 1966; Varon and Adler, 1980). Interestingly, mature neurons may be more dependent upon such trophic support, relative to embryonic tissue (Kivell et al., 2000). That there may be a so-called “sweet-spot” for culture density is illustrated in work by Kaneko et al. (2014), where rat hippocampal cultures (E18 – 19) were plated at the following concentrations: 3×10^3, $1 – 1.25 \times 10^4$, $2.5 – 3 \times 10^4$ and 10^5 cells ml^{-1}. Maximum neurite length was measured in these cultures as an indication of neuronal survival and active neurite growth, When this range of densities was investigated, it was determined that 3×10^4 cells ml^{-1} or 8.9×10^3 cells/cm^2 were the optimal plating density for survival of the culture (Kaneko and Sankai, 2014).

Plating density also has important implications for synapse formation and, therefore, the generation of neuronal networks in culture. In rat cortical cultures (E18), the mean number of synapses per neuron at 7 DIV was less than five and did not vary significantly between lower, medium and higher density cultures (ranging from 10 – 50,000 neurons/mm2; Cullen et al., 2010). Conversely, at 21 DIV, culture density was inversely proportional to synapse density (Cullen et al., 2010). Synapse-to-neuron ratio was greatest at lower neuronal densities (< 500 neurons/mm^2), with an average of 400 synapses per neuron, whereas mid to higher neuronal densities (500 - 4500 neurons/mm^2) had an average of approximately 150 synapses per neuron (Cullen et al., 2010). It is possible therefore, that if one wanted to investigate network activity using this culture method, plating density could be modified accordingly.

2.4.4 Choice of medium

Aside from the desired cell-type composition of one's culture, other factors which determine the choice of the medium one chooses to utilise include the age of the animal from which the culture is produced, evidence of the medium's reliability in fostering healthy cell growth, previous characterisation of cell development and phenotype in the medium and financial considerations. Each plating and culture medium has its own advantages and the composition of each can be altered depending upon the desired specific application. Investing time in researching optimum medium composition, to ensure that there are no pharmacological conflicts with one's experimental design, is suggested by Nunez et al. (2008). With respect to our subsequent calcium imaging experiments, DMEM/SR2 did not contain any compounds of concern. Related to this, the use of fully defined media and supplements, as opposed to undefined biological supplements such as FBS during culture maintenance, reduces confounding factors in experimental design (Kaneko and Sankai, 2014). Some common media and supplement combinations are listed below:

NB combined with B27. NB is widely used and is generally reported upon positively in the field (Kivell et al., 2000). It is a commercial formulation based upon DMEM, which is usually supplemented with B27. NB-A is formulated for postnatal use and has a higher osmolarity than media designed for foetal cultures. It is optimised for neuronal survival and growth, and when supplemented with B27 results in approximately 80% neuronal survival after 7 DIV for hippocampal cultures plated at 100 cells/mm^2 (Xie et al., 2000). NB/B27 also suppresses glial survival and growth (Zhang et al., 2006). Specifically, NB/B27 prevents the growth of astrocytes but not oligodendrocytes (Brewer et al., 1993; Svendsen et al., 1995).

The use of NB is however associated with the appearance of vacuoles and increased clumping, postulated to result from increased neuronal projections (Banker and Cowan, 1977; Brewer et al., 1993), when compared to an alternative medium, NM-2 (composed of 70% MEM and 30% NB; Xie et al., 2000). Furthermore, there is evidence that a component of NB, L-cysteine, causes NMDA receptor-mediated excitotoxicity in mature neuronal cultures (12 -14 DIV; Brewer, 1997). As a consequence of this feature, its use may be limited to maintaining neurons from 1-11 DIV (Hogins et al., 2011). Furthermore, NB may not be suitable for hippocampal neurons, which are particularly susceptible to NMDA receptor-mediated excitotoxicity (Hogins et al., 2011).

B27. In terms of supplementing the base media, serum or a "serum replacement" supplement is generally used. There are a wide variety of proprietary serum replacement additives available but B27 is by far the most

commonly used for a wide array culture protocols (Chen et al., 2008) probably because it contains a high proportion of antioxidants and promotes neuronal survival, whilst inhibiting glial growth (Brewer, 1997; Brewer et al., 1993; Kivell et al., 2000; Marriott et al., 1995). B27 supplementation has been used for culturing of embryonic neurons from multiple brain regions (Brewer, 1995) and for the culture of adult rat hippocampal neurons (24 - 36-months-old) which remained viable for several months without glial feeder layers (Brewer and Torricelli, 2007).

However, Chen et al. (2008), reported issues of reliability surrounding B27. The biological nature and differing procedures for the isolation of several components in this media, such as BSA and transferrin, results in variations in product quality. As a solution, this group altered 21 ingredients of an early published formula of B27, to produce **NS21** (Y. Chen et al., 2008). Key differences between it and NB which increased reliability were the use of specific product vendors for certain key ingredients and the use of holo-transferrin instead of apo-transferrin. This supplement enabled the production of high quality, reliable cultures, exhibiting normal neuronal morphology, synapse formation and post-synaptic responses. For instance, NS21 facilitated the growth of up to five times more filopodia-like structures during neuronal development than B27 (Y. Chen et al., 2008). We did not measure the effectiveness of this supplement using our protocol as we did not feel it was necessary given our success using less expensive SR2. However, again depending upon individual labs' requirements/preferences, this, or any other supplement, could be utilised instead of SR2.

NbActiv4 is described as a recent improvement on the NB/B27 combination, developed by the same group that formulated this classical medium (Brewer et al., 2008). Its use is associated with improved measurements of developed synapses in rat hippocampal neurons (E18), such as increased neuronal spike rates (4- to 8-fold) when compared with cultures prepared using NB/B27. However, this new proprietary medium combination is significantly more expensive than NB. Furthermore, aside from synaptic measurements, whether or not this formulation is a significant improvement, in terms of culture viability and cellular physiology, on classical formulations such as that presented herein, is unknown.

Hibernate A (Brewer and Price, 1996) is a form of NB (Brewer et al., 1993) which has the advantage of maintaining a stable pH out of the CO_2 buffering environment of the incubator. It has been used with B27 supplementation during the trituration and cell isolation procedures in numerous previously published hippocampal culture protocols (Brewer, 1997; Brewer and Torricelli, 2007; Todd et al., 2013). In our hands, Hibernate A did not provide any significant improvement in terms of culture success or

cell survival (determined subjectively) when compared with the use of standard lab-made HBSS during the trituration and cell isolation procedures.

DMEM and SR2. DMEM is referred to as a basal medium as it contains no proteins or growth promoting agents and therefore requires supplementation with specific additives. CO_2 regulation is essential to maintain a pH of 7.4 (Arora, 2013). In our hands, DMEM medium supplemented with a generic serum replacement supplement, SR-2, produced reliable and high-quality hippocampal cultures. Therefore, this combination was used as a replacement for the more expensive NB/B27 combination.

The choice of media becomes more complex when one studies protocols which utilise blends of currently available media. For example, Xie et al. (1999) compared the effectiveness of supplemented NB, MEM and various blends composed of different relative contributions of these two media such as “NM-2”. This study illustrated that one could tailor and balance culture solutions to suit one's desired outcomes, such as cell density and neuron-to-glial ratio.

Importantly, the preparation and long-term survival of our neuronal cultures was independent of any requirement for either proprietary media and/or supplements (Ahlemeyer and Baumgart-Vogt, 2005; Beaudoin et al., 2012; Brewer and Torricelli, 2007; Kivell et al., 2000; Nunez, 2008; Zhang et al., 2006). To the best of our knowledge, only three other papers have demonstrated viable mouse postnatal neuronal cultures from central nervous system tissue, but all utilised the aforementioned proprietary media and supplements. The method described by Eide and McMurray (2005), using striatal and cortical mouse tissue, is particularly impressive given the age of the animals involved, 1 – 1.5-years-old. Unfortunately, it is unclear how these researchers achieved this outcome as the paper in question lacks methodological detail about the protocol that was employed to prepare the neurons. Although the methods employed by both Beaudoin *et al.* (2012) and Brewer *et al.* (2007), using early postnatal (P0 – P1) and adult mouse hippocampal tissue, respectively, are well described and imply that good quality cultures can be produced, they are much more laborious and expensive than the protocol described here. Therefore, our technique would appear to offer several advantages over these aforementioned studies, in that the methodology is simple and efficient, cultures can be produced from older animals (routinely 3 - 6 day-old mice, but several cultures have been produced up to day 14) and the protocol has relatively lower costs of production (given the use of non-proprietary supplements).

2.4.5 Inclusion of glutamine and glutamate

The amino acid glutamine is essential for the survival and growth of cells in culture (Eagle et al., 1956). L-glutamine (L-Gln) and GlutaMAX / L-alanyl-L-glutamine, which is a stable form of L-Gln, are commonly used media supplements. The use of GlutaMAX is recommended over L-Gln as the latter degrades with time to produce ammonia and carboxylic acid, which are both toxic substances (Seibenhener and Wooten, 2012). According to the manufacturer's guidelines, the use of GlutaMAX increases cell viability and growth reduces or removes the need for medium change (due to the decreased build-up of ammonia in comparison to L-glutamine) and remains stable across a wide range of temperatures. Subjectively, we found that there were more successful cultures when using GlutaMAX over L-Gln and so this supplement was used routinely.

Another reason for the routine use in the field of GlutaMAX over L-Gln is that above 4ºC L-Gln deaminates to glutamate which builds up over time and is excitotoxic to neurons (Choi et al., 1987; Zhang and Bhavnani, 2005). That being said, when we replaced half the culture media every three days in an effort to prevent the cytotoxic build-up of glutamate and other toxic metabolites there were no observable benefits in terms of viability or development of the neurons. Furthermore, the *addition* of glutamate to neuronal cultures may actually be beneficial.

Glutamate plays a key role in CNS neurons where it acts as the principal fast excitatory transmitter (Verderio et al., 1999) and regulates neuronal differentiation, cell proliferation, CNS development, cell survival and synaptic plasticity (Balazs, 2006; Edwards et al., 2010; Verderio et al., 1999). Indeed, micromolar glutamate concentrations have been used to culture embryonic neurons, with the aim of facilitating glutamate-dependent developmental processes (Brewer et al., 1993). Similarly, in adult hippocampal neurons, glutamate was removed after 4 DIV, presumably after allowing for its positive developmental effects on plated neurons before glutamate toxicity occurred (Brewer, 1998, 1997; Brewer et al., 2005). Furthermore, incubation of adult hippocampal cultures (3 - 6-month-old; rat) with very low concentrations of glutamate (25 µM; 1 – 7 DIV), promoted a persistent enhancement of physiological neuronal activity and produced minimal excitotoxicity, relative to controls (Edwards et al., 2010). Therefore, we too utilised this low glutamate concentration in all our culture solutions to promote neuronal development and physiological cell signalling.

2.4.6 Maintenance

Kaech and Banker (2007) noted that “only the most resolute attempt to work with cultures beyond 4 weeks.” Indeed, typically with hippocampal cultures, widespread cell death occurs within 3 – 4 weeks *in vitro* (Kaech and Banker, 2006). “Replenishment”/replacement of the maintenance medium is routinely used in the field, with the aim of removing and diluting waste products of metabolism and supplying fresh nutrients, in order to maintain neuronal viability (see below).

However, medium changes are not without their disadvantages. For example, they risk infecting the culture medium and cell death through exposure of cells to ambient temperatures and CO_2. Furthermore, given the importance of trophic factors to mature neurons, if replacement is to be carried out it must be to an extent where these trophic factors are not diluted to the detriment of cell viability. Attempts to balance these advantages and disadvantages has resulted in quite varied recommended protocols for medium replacement, ranging from every 2 to 5 days (Beaudoin et al., 2012; Hilgenberg and Smith, 2007; Hogins et al., 2011; Lee et al., 2009; Srinivas et al., 2007), every week (Brewer and Torricelli, 2007; Chen et al., 2008; Kaech and Banker, 2006b; Kivell et al., 2000; Nunez, 2008; Potter and DeMarse, 2001; Zhang et al., 2006) or leaving it entirely unchanged (Ahlemeyer and Baumgart-Vogt, 2005; Eide and McMurray, 2005; Xie et al., 2000). Interestingly Potter et al. (2001) could maintain neuronal viability by replenishing evaporated water alone. Although in the early stages of the development of our protocol we did investigate the effects of replacing 50% of the culture medium every 3 days, we did not observe any significant difference in the quality or responsiveness of neurons relative to those in which the medium remained unchanged. Because of this and the fact that our cultures remain viable for up to one month without medium replacement (which is well within our needs for subsequent experimental use) we chose not to include this replacement step in the protocol described herein.

In terms of the upper limits of long-term maintenance in culture, we have observed sparse but viable cells in our cultures past 100 DIV. This is significant as the reported upper limit of survival in current mouse hippocampal culture protocols ranges from 6 – 60 DIV (Table 2.1; early postnatal and adult mice). As an indication of more long-term viability, Fig 2.9 displays a Ca^{2+} response from a neuron at approximately 1 month *in vitro*. In practice, and as previously mentioned, we generally utilised cultures within 2 – 14 DIV for Ca^{2+} imaging experiments.

2.4.7 Culture characterisation

Methodology

The determination of culture composition requires anatomical analysis of cell type as identification based on morphology alone is relatively unreliable (Raff et al., 1979). This is due, in part, to the morphological similarities between multipolar neurons and stellate-shaped type II astrocytes under phase contrast microscopy (Kivell et al., 2000). Therefore, immunocytochemistry-based identification, in tandem with morphological analysis (Kivell et al., 2000) is widely believed to be preferable. For instance, Kivell et al. (2000) utilised MAP-2 and GFAP positive immunoreactivity, for neuron and glia identification, respectively. Other cells were assumed to include fibroblasts, macrophages, oligodendrocytes, and endothelial cells (Magistretti et al., 1996). The protocol utilised herein adopts a similar identification protocol based on this method by utilising a pan-neuronal cocktail which contained MAP-2 and the glial marker, GFAP. Use of the pan-neuronal cocktail had the added advantage of illuminating, more comprehensively, the neuronal cytoarchitectural structure. This identification protocol allowed us to determine the composition, in terms of neuron and glial cells, of our cultures. In the next section, I will detail how this composition compares to that obtained using alternative methodologies to ours.

Culture composition of previous studies

Methods published by Kivell et al. (2000), utilising E14 – P6 rat brainstem tissue (B27/NB), contain the most extensive cell characterisation in the field. They presented the following findings:

1. Culture composition was dependent upon the age of the animal, with type I astrocytes constituting a greater proportion of total cells in older, (P6; 50 - 72%) relative to younger cultures (E14; 17 - 20%).

2. E14 cultures contained a higher proportion of glia than neurons (61% vs 35%) and most neurons were bipolar as opposed to multipolar (40% versus 21%).

3. Late embryonic (E16 and E20) and early postnatal (P3 and P6) cultures also contained a higher proportion of glia than neurons (67-73% versus 25-31%) and, as would be expected with a more developed nervous system, had an increased proportion of multipolar neurons (18-25%) compared with bipolar (5-9%) neurons with developmental age.

4. Type I astrocytes were more abundant than type II at all development ages (foetal and postnatal).

The majority of studies have displayed hippocampal culture composition as a percentage of neurons and glia present. These studies include, a) mouse hippocampal cultures (P0.5, 6 DIV, NB/B27) which contained 7% astrocytes and fewer than 1% oligodendrocytes (Ahlemeyer and Baumgart-Vogt, 2005), b) mouse hippocampal cultures (P0 - 1, DIV 5, NB/B27), which contained 6 – 8% glia (Beaudoin et al., 2012), and c) rat hippocampal cultures (P2 -P3, 7 DIV), which contained 23% glia, when cultures were maintained in NB/B27, and 32% when maintained in FBS (Pozzi et al., 2017).

These findings illustrate that before attempting to find correlations between our work and previous studies one must bear in mind the caveat that other studies may have utilised different animal species, brain regions, culture media and/or methods, which will undoubtedly affect the final culture composition. However, that said, such comparisons are still worthwhile in terms of identifying general trends in culture characterisation.

The majority of studies measured culture composition *in vitro* at one specific point in time or commented generally using subjective observational evidence. However, there are some exceptions, such as the work of Kivell et al. (2000), which showed that the proportion of glia in brainstem cultures (E14 – P6, rat) remained constant from 4 – 9 DIV. Although these cells did not proliferate and overgrow, they still remained viable. Serum-free culture conditions, such as the B27/NB medium used in the aforementioned study, are known to inhibit astrocytic cell division and proliferation in culture (Brewer et al., 1993; Kivell et al., 2000; Marriott et al., 1995).

Conversely, in our study we showed that by using our DMEM/SR2 medium combination without replacement, there was a steady increase in the percentage of glial cells (ranging from 25% to 60%), out of the total number of viable cells, from 2 – 20 DIV (Figs 2.5 and 2.7). Despite this increase, glial cells did not proliferate to an extent which hindered Ca^{2+} imaging experiments. The difference in glial composition between our protocol and that of Kivell et al. (2000) is likely due to the use of FBS to supplement plating media. Whilst FBS causes glial proliferation (and potentially enhances their trophic support of neurons), it also encourages neuronal attachment and survival during this critical plating period (Kivell et al., 2000; Pozzi et al., 2017). For instance, when rat hippocampal neurons (P2 – P3) were plated in serum-free NB/B27 media, neuronal death increased and there was an absence of electrical activity. When the same culturing procedure was repeated with ACM medium or plating medium supplemented with FBS, it produced viable hippocampal cultures with normal physiology which could be maintained for over one month (Pozzi et al., 2017). Therefore, the *dilution* of FBS after 1 hour of plating as opposed to the *removal* of FBS and the resulting glia growth was effective for culture

survival, maintenance and practical use of the experimental units. The ratio of glia to neurons in our cultures between 2 – 20 DIV could be altered, should a researcher desire a more neuron-enriched culture. This could be achieved, for example, by the removal of FBS after plating, instead of diluting it as we have done.

Measurement of Culture Quality

The immunocytochemical studies which allow culture composition to be determined also have the advantage of allowing us to study neuron morphology. A physiologically-relevant temporal change in neuron morphology is indicative of healthy and maturing neurons, as discussed in *Section 2.1.4 Characteristics of hippocampal cultures*. Such temporally determined observations include an increase in process length, the development of multiple well-arborised dendrites (Y. Chen et al., 2008) and increased neuron-neuron and neuron-glial (depending on the desired purity of culture) connections and synapses (Zhang et al., 2006).

With respect to glia, immature astrocytes have relatively simple and undifferentiated morphology with a low degree of arborisation. In contrast, mature astrocytes have highly branched and complex arborisation, observed after 2 months *in vitro* in rat hippocampal neurons (P2 - 3, NB/ACM; Pozzi et al., 2017), which is similar to their structure *in vivo* (Cerbai et al., 2012; Puschmann et al., 2013). If astrocytes have a fibroblast-like morphology, it is likely to be an artefact of serum being included in the culture medium (Foo et al., 2011; Landis et al., 1990). The fact that neurons and glia in our cultures clearly exhibit evidence of maturation (by 2 and 5 DIV, respectively), connectedness (Fig 2.5), and markers of functional synapses (Fig 2.6), is an indication of the usefulness of this protocol in modelling physiologically-relevant neurons, glia and neuronal networks. Notably, cultures produced by this method appear to mature much more rapidly than the relatively slow process outlined for previous methods in *Section 1.4.* Of particular note is the formation of mature axons, dendrites and synapses by 2 DIV, indicating stage five development, in comparison to previous cultures exhibiting such developmental markers at 3 – 4 DIV (Craig and Banker, 1994; Dotti et al., 1988; Fletcher and Banker, 1989).

Moreover, cultures produced using our method have been utilised routinely for hundreds of Ca^{2+} imaging experiments, including those presented in *Chapters 3 and 4*. These hippocampal cultures displayed physiological characteristics and responses which were similar to those previously presented using other hippocampal culture methods (*e.g.* Zhang et al., 2010). Examples of physiologically-relevant Ca^{2+} responses to stimuli

such as membrane depolarisation and stimulation of ACh, NMDA and glutamate receptors are presented in Fig 8.

Alteration of phenotype in vitro

Related to the anatomical changes of cells that occur during development *in vitro*, the question arises; does cellular physiology change in a similar temporal manner to development *in vitro* and, if so, what is the extent of these changes? Such physiological changes may be related to natural developmental and/or ageing processes and/or unnatural environmental influences generated by the particular culture methodology that was employed. Such unnatural influences include altered O_2 dependency, saturated nutritional state and/or the build-up of waste products, metabolites and signalling factors which may be processed and regulated differently *in vivo*. As an indication of how phenotype can be altered *in vitro*, to counterbalance the use of embryonic tissue as a proxy for 'mature' tissue, some methods recommend "maturing" cells *in vitro* before use. For example, *Xenopus* spinal neurons and rat superior cervical ganglia cells begin to exhibit "mature" action potentials after 14 DIV (Baccaglini and Spitzer, 1977; Nerbonne and Gurney, 1989). Conversely, when measuring Ca^{2+} currents in response to depolarising membrane potentials, no differences were detected in neurons between 1 - 7 DIV (Zhang et al., 2006). In our own Ca^{2+} imaging experiments, there is limited evidence that hippocampal neurons exhibit developmental differences, dependent on *in vitro* development (2 – 20 DIV), in depolarisation-induced Ca^{2+} influx (appendix figure 1 (Fig A.1), B, ii & iv; Fig A.2, B, ii; Fig A.7, F, ii) and I-mGluR-mediated signalling (Fig 3.6).

2.4.8 Improvement on methods

Increasing viability

The addition of neuroprotective mediators throughout the culture protocol may be one feasible means of increasing neuronal viability. Such neuroprotective strategies include using, a) the NMDAR antagonist ifenprodil (Graham et al., 1992), b) the caspase inhibitor carbobenzoxy-valyl-alanyl-aspartyl-[O-methyl]- fluoromethylketone (z-VAD-FMK; Han et al., 2002), c) 3-aminobenzamide to suppress oxidative stress-induced cell death (Zingarelli et al., 1997), d) deoxyribonuclease (DNase) inhibition of DNA-mediated neuron-debris clumping (Kaneko and Sankai, 2014), and e) cholesterol addition compensating for the lack of cholesterol released by glia (only relevant to pure cultures), a process which is essential for synaptogenesis (Mauch et al., 2001). However, Eide et al. (2005) found that no significant advantage was gained by exposing neurons to any of the factors mentioned above, as measured by cell attachment to a substrate or overall neuronal

survival. However, it should be noted that in this particular case, the hippocampal tissue was incubated with these compounds prior to cell dispersal (papain treatment and trituration), rather than the substances being added to the culture medium. It would be worthwhile repeating these experiments with compounds added during, or after, papain treatment, and/or trituration as they are the primary stress events that the neurons experience during the culturing process.

A role for bFGF in the development and viability of cultured neurons has been well established. bFGF is known to activate anti-apoptotic pathways (König et al., 1997; Miho et al., 1999) and promotes neurogenesis (Sun et al., 2009; Tao et al., 1996; Yoshimura et al., 2001). In culture, it facilitates the proliferation and differentiation of rat brainstem neurons (P3 – 5; Zhang et al., 2006). Furthermore, it can increase neuronal survival up to threefold, independent of age, in rat hippocampal (11 - 36-months-old) and brainstem cultures (Brewer, 1997; Zhang et al., 2006). Therefore, the inclusion of bFGF during plating and in the maintenance media could be investigated as further optimisation of the current method.

Use of an oxygen controlled incubator

The rationale behind the utilisation of controlled oxygen incubators has been outlined previously (Section *2.1.3 Limitations of the culturing method*). It would be of interest to investigate whether or not the use of such an incubator has similar positive effects on neurite growth in our cultures as that described previously (Brewer and Torricelli, 2007; Genetos et al., 2010). However, as mentioned previously, the inverted coverslip method and the resulting creation of a more physiological microenvironment may also reduce the partial pressure of O_2 which cultured cells are exposed to (Brewer and Cotman, 1989). Alternatively, a reducing agent, such as 2-mercaptoethanol (a thiol), which causes the chemical reduction of numerous substances, could also be used to replicate the low oxygen conditions *in vivo* (Grill and Pixley, 1993; Ishii et al., 1993; Kaneko and Sankai, 2014).

2.5. Conclusions

In summary, we present here a simplified, economical and reliable method for the consistent production of primary hippocampal cultures from postnatal mouse hippocampal tissue. Furthermore, the neurons within these cultures, in addition to displaying characteristics of normal, healthy neurons, also exhibit consistent and reproducible responses to physiological stimuli which have been investigated in *Chapters 3 and 4*. We propose that this method could also be utilised to produce cultures of other postnatal mouse neuronal tissues.

3. mGluR Signalling

3.1 Introduction

Glutamate is the primary excitatory neurotransmitter (NT) in the mammalian CNS and thus is essential for a wide range of neuronal and glial functions (Niswender and Conn, 2010). In the context of Ca^{2+} signalling, the primary pathways of glutamate signalling are: a) a rapid entry of Ca^{2+} through Ca^{2+} permeable PM bound ionotropic glutamate receptors (iGluRs), namely NMDARs (Sommer and Seeburg, 1992) and AMPARs (Wiltgen et al., 2010) which enables their modulation of cellular excitability (Niswender and Conn, 2010) and b) a relatively slower mobilisation of Ca^{2+} from intracellular stores following mGluR stimulation (specifically group I mGluRs; Morikawa et al., 2003) and activation of downstream signalling pathways, processes which are generally mediated by guanine nucleotide-binding regulatory proteins (G-proteins; Fagni et al., 2000). Stimulation of mGluRs, specifically I-mGluRs, and the subsequent downstream signalling pathways involved, comprise a central theme running through this PhD thesis.

The eight mGluR subtypes (mGluR1 - 8) are widely distributed throughout the CNS and are divided into three functional groups: group I (mGluR1 and 5), group II (mGluR2 and 3) and group III (mGluR4, 6, 7 and 8) mGluRs, based upon their sequence homology, structure, ligand selectivity, pharmacology, G-protein coupling and downstream signalling similarities (Conn and Pin, 1997; Nakanishi, 1992).

mGluR subtypes are differentially expressed in a cell type-dependent manner and display distinct distributions in particular brain regions, as well as at pre- and post-synaptic localisations in neurons (Nomura et al., 1994; Ottersen and Landsend, 1997; Shigemoto et al., 1997; Tamaru et al., 2001) and glia (Biber et al., 1999). I-mGluRs are expressed in both neurons and glia, including microglia and astrocytes (Bernstein et al., 1998; Biber et al., 1999). In the hippocampus, the tissue where the experimental unit of this study was produced from, I-mGluR immunostaining is dense in post-synaptic membranes and densities as well as in perisynaptic and extrasynaptic membranes (Baude et al., 1993; Lujan et al., 1996; Luján et al., 1997; Nusser et al., 1994; Petralia et al., 1997). Immunoreactivity of a splice variant of mGluR, $mGluR1_a$, is particularly strong in interneurons of the CA1 region and some CA3 pyramidal neurons. Conversely, $mGluR1_a$ staining is weak in hippocampal CA1 pyramidal cells and granule cells of the dentate gyrus (Baude et al., 1993; Chuang et al., 2002; Lu et al., 1997; Lujan et al., 1996; Petralia et al., 1997). mGluR5 staining is prominent in hippocampal CA1 pyramidal neurons (Chuang et al., 2002; Lu et al., 1997; Lujan et al., 1996; Luján et al., 1997). Such differential expression of I-mGluR splice variants may reflect a method of enhancing the specificity of I-mGluR coupling to

downstream signalling targets in different cell types and/or localisations (Fagni et al., 2000).

Indeed, often the role of specific mGluR sub-groups and subtypes is determined by their expression in a neuronal population and/or subcellular localisation (Niswender and Conn, 2010). For instance, I-mGluR mediated Ca^{2+} signalling can generate slow EPSPs in hippocampal pyramidal neurons (Congar et al., 1997) and cerebellar Purkinje cells (Batchelor and Garthwaite, 1997), whilst it generates IPSPs in dopaminergic neurons (of the ventral tegmental area; Williams and Fiorillo, 1998). Furthermore, I-mGluRs located pre-synaptically or post-synaptically can either increase or decrease NT release (Anwyl, 1999; Bellone et al., 2008; Pinheiro and Mulle, 2008). Importantly, there is also significant functional interaction between mGluRs at different localisations, evidenced by the fact that glutamate acting post-synaptically can exert positive feedback to increase NT release in the hippocampus (Hu and Storm, 1991), cerebral cortex (Herrero et al., 1992) and hypothalamus (Schrader and Tasker, 1997).

As mentioned previously, mGluRs are members of the G-protein-coupled receptor (GPCR) superfamily (Morikawa et al., 2003) and as such are membrane-bound and activated by a diverse range of extracellular ligands including hormones, peptides and NTs (Pierce et al., 2002). Ligand binding induces a conformational change in the GPCR which activates specific G-protein(s) associated with it (Niswender and Conn, 2010)

I-mGluRs canonically couple to G_q protein/PLC-mediated signalling resulting in Ca^{2+} mobilisation from intracellular stores (for reviews see Conn and Pin, 1997; Fagni et al., 2000; Krause et al., 2002; Valenti et al., 2002) such as those within hippocampal neurons (Rae et al., 2000; Rae and Irving, 2004; Sohn et al., 2011). More specifically, activated PLC catalyses the formation of inositol (1, 4, 5) trisphosphate (IP_3) and diacylglycerol (DAG; from phosphatidylinositol‑4, 5‑bisphosphate (PIP_2)). IP_3 activates IP_3-dependent receptor channels (IP_3Rs) on the endoplasmic reticulum (ER), resulting in Ca^{2+} release into the cytosol (Li et al., 2002; Niswender and Conn, 2010). This has critically important consequences for cellular signalling (described in more detail in section *1.7 Learning and Memory*). However, despite the widely accepted view that this type of I-mGluR signalling is PLC-dependent, it is well documented in both overexpression and recombinant systems, as well as more physiological cellular models, that these receptors are promiscuous, in that they appear to be capable of coupling to multiple intracellular signalling cascades (Hermans and Challiss, 2001). For example, several reports have suggested that certain downstream effects of I-mGluR activation on membrane currents and intracellular Ca^{2+} release can occur independently of either PLC (Chavis et al., 1998; del Río et al., 1999; Ireland et al., 2004, 2002; Sohn et al., 2007; Young et al., 2004)

and/or IP_3R activation (Chavis et al., 1996; Currie et al., 1995; del Río et al., 1999; Gafni et al., 1997). In this context, one possible explanation for these findings, and a key element to this thesis (discussed in *Chapter 4 mGluR-ARC Signalling*) is the coupling of I-mGluRs to the enzyme ADP-ribosyl cyclase (ARC; Sohn et al., 2011), which catalyses the production of cyclic ADP ribose (cADPR). cADPR, in turn, stimulates Ca^{2+} mobilisation through RyRs on the ER (Kaar and Rae, 2015).

Neuronal SOCE is considered essential to maintaining I-mGluR-driven Ca^{2+} signals, at least in cultured cortical neurons (González-Sánchez et al., 2017). Subsequently, this increased $[Ca^{2+}]_i$ combines with the actions of synthesised DAG to activate protein kinase C (PKC) which, in turn, determines the activation state of I-mGluRs and is intertwined with the activities of the downstream components of mGluR-stimulated signalling cascades (Conn and Pin, 1997; Hisatsune et al., 2005; Murphy and Miller, 1988; Sorrentino et al., 1996). It is also worth noting that $[Ca^{2+}]_i$ levels can also enhance the activity of PLC and thereby regulate intracellular Ca^{2+} mobilisation in a feedforward manner (Nakamura and Fukami, 2017; Suh et al., 2008).

Numerous downstream signalling cascades are modulated by the activity of G-proteins. For instance, depending upon cell type or neuronal population, Gq activates ion channels and protein kinase pathways including casein kinase 1, cyclin-dependent protein kinase 5 and c-Jun N-terminal kinase (JNK; Yin and Niswender, 2014). Two further kinase pathways, the mitogen-activated protein kinase/extracellular receptor kinase (MAPK/ERK) and the mammalian target of rapamycin (mTOR)/p70 S6 kinase pathway, are particularly important for the regulation of synaptic plasticity by mGluRs (Hou and Klann, 2004; Li et al., 2007; Page et al., 2006). I-mGluR activation also enhances the expression of the *c-fos* gene, an indicator of calcium-induced transcription of various genes (Mao and Wang, 2003).

Numerous roles specific for I-mGluRs have been revealed within the CNS, including the regulation of synaptic transmission and neuronal excitability, as well as the induction of long-lasting forms of synaptic plasticity including LTD and LTP (Anwyl, 1999; Bashir, 2003; Bellone et al., 2008; Bortolotto et al., 1999; Conquet et al., 1994; Ichise et al., 2000; Jia et al., 1998; Kullmann and Lamsa, 2008; Lu et al., 1997). This modulation of neuronal excitability is a function of an underlying modulation of a number of ion channel conductances and can result in robust excitation as well as more subtle effects, such as changes in the pattern of cell firing, synchronisation of network activity and cellular responses to excitatory input (Anwyl, 1999; Chuang et al., 2001; Cobb et al., 2000; Conn and Pin, 1997; Coutinho and Knöpfel, 2002; Valenti et al., 2002; Woodhall et al., 1999). This range of functions is also enabled by a repertoire of downstream effectors modulated

by I-mGluRs in both a G protein-dependent and - independent manner, as will be discussed in subsequent sections.

3.1.1 Downstream Signalling

Depolarisation

Stimulation of I-mGluRs depolarises hippocampal cells (Bianchi et al., 1999; Bortolotto and Collingridge, 1995; Davies et al., 1995). In this respect, within hippocampal neurons at least, mGluR1 is more effective at mediating depolarising responses than mGluR5. As such, the degree of depolarisation induced by I-mGluR activation will be dependent upon the expression of mGluR subtype which, in turn, differs according to cell type (Chuang et al., 2002). Mechanistically, I-mGluR mediated ion channel modulation can occur directly *via* G-proteins as well as downstream of second messenger formation. Furthermore, there are numerous conductance mechanisms proposed to underlie such I-mGluR mediated depolarisation (Chuang et al., 2002), as outlined below.

a) I-mGluRs decrease both voltage-dependent and -independent K^+ conductances (Chuang et al., 2001, 2000; Guérineau et al., 1994; Lüthi et al., 1996; Wu and Barish, 1999). Inhibition of this K^+ current results in an excitatory response manifesting as either a slowly developing depolarisation and inward current and/or an inhibition of action potential firing accommodation (Fagni et al., 2000).

b) I-mGluRs modulate Ca^{2+} -sensitive K^+ channel conductances (Bianchi et al., 1999; Charpak et al., 1990; Jaffe and Brown, 1997; Rae and Irving, 2004; Shirasaki et al., 1994). This modulation primarily results in decreased conductance, although variable results have been found, as discussed in greater detail below.

c) I-mGluRs activate the Na^+/Ca^{2+} exchanger resulting in depolarisation in neurons of the amygdala (Keele et al., 1997), striatum (Dumuis et al., 1993), melanin-concentrating hormone (MCH) neurons of the hypothalamus (Huang and van den Pol, 2007) and cerebellar Purkinje neurons; Linden et al., 1994; Staub et al., 1992).

d) I-mGluRs initiate a Ca^{2+} -activated non-selective cationic (CAN) current (I_{CAN}) through intracellular CAN channels (Partridge et al., 1994) in hippocampal CA1 pyramidal neurons. In CA3 neurons (rat; organotypic slice cultures) this excitatory current is characterised as a transient receptor potential (TRP)- like conductance which can be activated in a G-protein - independent (possibly by an *Src*-family protein tyrosine kinase, in a $[Ca^{2+}]_i$ dependent manner (Heuss et al., 1999)) and G-protein-dependent manner (Gee et al., 2003).Furthermore, the Ca^{2+} source of this current is likely to be

from intracellular stores (Congar et al., 1997; Crepel et al., 1994). These conductances can be activated synaptically and may be involved in regulating synaptic plasticity (Batchelor and Garthwaite, 1997).

e) I-mGluRs activate a PLCβ/ER-dependent, voltage-gated inward current ($I_{mGluR(V)}$) which may have a role in loading intracellular stores. This I-mGluR-mediated increase in $[Ca^{2+}]_{ER}$ could occur directly, *via* activation of VGCCs (Rae et al., 2000) or indirectly *via* an "intrinsic Ca^{2+} permeability" through linking I-mGluR signalling with TRP channels (Kim et al., 2003; Tozzi et al., 2003). Although this current has been investigated across numerous neuronal cell types it likely reflects a mixture of currents dependent upon differing underlying conductances in the cell being investigated (Anwyl, 1999). I_{mGluR} is activated in CA3 pyramidal cells (where it is critical in generating prolonged rhythmic bursts in these cells (Chuang et al., 2001, 2000; W. Zhao et al., 2001)) but not CA1 cells, and as such the overall I-mGluR mediated response is decreased in CA1 cells, due most likely to a functional deficit in mGluR1 expression (Bortolotto and Collingridge, 1995; Chuang et al., 2002; Lu et al., 1997). It is also worth noting that such a functional deficit in mGluR1-mediated signalling in CA1 cells is dependent upon murine species (*i.e.* mouse *vs* rat), developmental stage and/or differences in experimental protocols (Chuang et al., 2002; Ireland et al., 2002; Mannaioni et al., 2001). However, a role for mGluR1 in CA1 pyramidal neuronal signalling (both $[Ca^{2+}]_i$ and I_{mGluR}) has been observed in numerous studies (Ireland et al., 2002; Mannaioni et al., 2001; Nakamura et al., 2000). With regard to I_{mGluR} specifically, functional studies utilising hippocampal neurons show that either mGluR5 alone (Rae et al., 2000) or both mGluR1 and 5 are critical in mediating this current (Gee et al., 2003; Rae and Irving, 2004). In CA1 pyramidal neurons, I_{mGluR} is thought to reflect a mixture of inhibition of certain K^+ conductances, and activation of a I_{CAN} (Chuang et al., 2002; Congar et al., 1997; Crepel et al., 1994; Ireland et al., 2002; Mannaioni et al., 2001). Specifically, in CA1 pyramidal neurons this inward current exhibits the following characteristics; a) prolonged time course (ranging from 9 – 30 minutes), b) a decrease in membrane conductance, c) it is temporally distinct from the brief increase in $[Ca^{2+}]_i$ following I-mGluR activation (Rae and Irving, 2004) and, d) is facilitated by neuronal depolarisation (Chuang et al., 2000; Lüthi et al., 1996; Rae and Irving, 2004). This depolarisation results in an increase in ionic driving force for K^+ efflux which, along with removal of Mg^{2+} block from cationic NMDAR-mediated currents (Congar et al., 1997; Guerineau et al., 1995), or increased $[Ca^{2+}]_i$ (Gee et al., 2003), may further potentiate this I_{mGluR} (Rae and Irving, 2004).

However, the dependence of this I-mGluR-activated inward current on intracellular Ca^{2+}, possibly generated *via* ER Ca^{2+} mobilisation (Congar et al., 1997; Crepel et al., 1994; Gee et al., 2003; Kettunen et al., 2003; Woodhall

et al., 1999) is debatable (Bianchi et al., 1999; Guerineau et al., 1995; Ireland et al., 2002; Nakamura et al., 2000). Indeed, Rae and Irving (2004) demonstrated that although the I-mGluR activated inward current evoked in rat CA1 pyramidal neurons by DHPG (I-mGluR agonist) did display some dependence on Ca^{2+} (only being significantly reduced in amplitude with either prolonged, high intracellular concentrations of the Ca^{2+} buffer BAPTA or perfusion with Ca^{2+}-free/EGTA (calcium chelator; 1 mM) aCSF, it was much less sensitive to alterations in cytosolic Ca^{2+} than the release of Ca^{2+} from the ER.

Regulation of VGCCs and iGluRs

Aside from the mechanisms of ion channel modulation and depolarisation listed above, I-mGluRs also possess numerous means of modulating VGCC and iGluR activity.

Direct G-protein mediated modulation of P/Q- and N-type VGCC-mediated Ca^{2+} conductances by mGluR1 and 5 has been observed in both neurons and recombinant cell systems (Choi and Lovinger, 1996; Kammermeier and Ikeda, 1999; McCool et al., 1998). Glutamate-induced depolarisation by either mGluRs (as discussed in the previous section) or iGluRs can activate VGCCs and also evoke Ca^{2+} influx indirectly. This results in a significant degree of physiologically relevant cross-talk between these receptors and their related signalling pathways (Fagni et al., 2000). In acutely dissociated hippocampal neurons, for example, glutamate-mediated Ca^{2+} influx was due to both AMPAR-mediated depolarisation which subsequently activated L-type VGCCs, but did not involve NMDAR activation (Sohn et al., 2011). The fact that this was an NMDAR-independent effect may be due to where the NMDARs are localised. Thus, NMDAR-mediated Ca^{2+} entry occurs primarily in neuronal spines which tend to be more concentrated at oblique dendrites *in vivo* and in acute brain slices (Bannister and Larkman, 1995; Kovalchuk et al., 2000; Migliore et al., 2005; Nakamura et al., 2002). However, acutely dissociated neurons generally lack this type of ‘oblique’ dendrite which would therefore reduce, or eliminate, the role of NMDARs in glutamatergic signalling in these cells (Sohn et al., 2011). Interestingly, Sohn and colleagues (2011) also demonstrated that the contribution of the AMPAR/L-type VGCC -mediated calcium influx to glutamate-induced somatic Ca^{2+} signalling in acutely dissociated hippocampal neurons was larger than the contribution of Ca^{2+} release from intracellular stores mediated by I-mGluRs, illustrating the potential importance of this Ca^{2+} entry pathway to overall glutamatergic signalling (Sohn et al., 2011).

On the other hand, I-mGluRs modulate synaptic transmission by potentiating NMDAR-, but not AMPAR-, mediated currents in striatal and spinal cord neurons (Krieger et al., 2000; Pisani et al., 1997). The mechanism by which this occurs involves attenuation of the inhibitory actions

of CaM at NMDARs due to CaM buffering of I-mGluR/PLC-mediated increases in intracellular Ca^{2+} (Ehlers et al., 1996). Furthermore, I-mGluRs enhance NMDAR activity in rat hippocampal slices, in a manner independent of Ca^{2+} release from stores (Enokido et al., 1996; Harvey and Collingridge, 1993). This mechanism helps to explain the potentiating effect of mGluR agonists on NMDAR-mediated LTP induction in the hippocampus (McGuinness et al., 1991; Otani and Ben-Ari, 1991). Conversely however, one study has shown that NMDAR-mediated whole-cell currents were reversibly attenuated by I-mGluR stimulation in cultured mouse cortical neurons (Yu et al., 1997). The reason for these contradictory findings remains unclear, however.

Interestingly, NMDAR activation can also enhance I-mGluR activity. For example, NMDAR-mediated Ca^{2+} influx in cultured rat hippocampal neurons and hippocampal CA1 pyramidal neurons (Luthi et al., 1994, Rae et al., 2000), and L-type VGCCs in apical dendrites of hippocampal CA1 neurons; (Emptage 1999, Nakamura et al., 2000, 1999), cultured mouse and rat hippocampal neurons, and CA1 pyramidal neurons from rat hippocampal slices, potentiates I-mGluR mediated ER Ca^{2+} signals, to evoke enhanced or “supralinear” intracellular calcium responses (Rae et al., 2000; Rae and Irving, 2004). These findings are supported by similar results showing that ER-mediated Ca^{2+} release in hippocampal cultures, acutely dissociated adult mouse DRG neurons and PC12 cells (*via* muscarinic receptor or RyR activation) is potentiated by increased Ca^{2+} influx (via depolarisation and/or NMDAR activation; Friel and Tsien, 1992; Garaschuk et al., 1997; Irving and Collingridge, 1998; Koizumi et al., 1999; Shmigol et al., 1996).

So-called supralinear Ca^{2+} signals are a signalling paradigm of synaptic activation (Nakamura et al., 1999; Rae et al., 2000) and proposed to be a rough correlate of *in vivo* “learning events” (Magee and Johnston, 1997; Markram et al., 1997). Supralinear responses are proposed to arise from the Hebbian pairing of I-mGluR stimulation with a depolarisation stimulus to produce a Ca^{2+} response that is greater than that generated by the sum of each individual stimulus, *i.e.* the summation of the Ca^{2+} response due to depolarisation and that due to I-mGluR stimulation (Rae et al., 2000). Similar types of enhanced responses were also observed when NMDAR activation was paired with membrane depolarisation (Koester and Sakmann, 1998; Rae et al., 2000; Schiller et al., 1998; Yuste and Denk, 1995).

I-mGluR-mediated Ca^{2+} release also enhances action potential/L-type VGCC-mediated pre-synaptic Ca^{2+} transients, which can, in turn, enhance both NT release (Atlas, 2013) and synaptically-evoked EPSCs (Nakamura et al., 2015). These effects are blocked by ryanodine in the lamprey spinal cord, suggesting RyR involvement (Cochilla and Alford, 1998). mGluR5 stimulation also enhances L-type VGCC-mediated Ca^{2+} currents in GABAergic neurons

of the hippocampus, with L-type VGCC currents also being potentiated by RyR-mediated Ca^{2+} mobilisation and PKC in the same cells (Topolnik et al., 2009). Similarly, mGluR1 mediates a large, oscillatory increase in L-type VGCC conductance in cerebellar granule cells that is RyR-dependent, but IP_3-independent (Chavis et al., 1996). This particular study differs from those mentioned before it in that the proposed mechanism underlying the enhanced I-mGluR signalling is unaffected by calcium chelation (using BAPTA) or block of IP_3Rs (using heparin) and is not mimicked by intracellular IP_3 dialysis. Instead, this enhancement arises from the promotion of physical and functional coupling between I-mGluRs, RyRs and L-type VGCCs (Chavis et al., 1996; Fagni et al., 2000). Furthermore, it is proposed that I-mGluR coupling to L-type VGCCs occurs in the proximity of Ca^{2+} mobilisation sites. In so doing, this may allow for the replenishment of ER stores following I-mGluR stimulation (Irving et al., 1992a; Murphy and Miller, 1989). Lastly, cADPR may also play have a role in I-mGluR mediated L-type VGCC signal potentiation seen within NG108-15 cells (Hashii et al., 2000).

In contrast to the evidence listed above illustrating the numerous means of I-mGluR – mediated neuronal excitation, I-mGluR evoked Ca^{2+} elevations can also *inhibit* VGCC opening in numerous brain regions including the hippocampal formation (Anwyl, 1999; Ikeda et al., 1995; Shen and Slaughter, 1998) by activating/modulating Ca^{2+} -sensitive K^+ channel activity, as discussed next.

3.1.2 I-mGluR signalling and the Ca^{2+} hypothesis of AD

ER channels

As outlined in *Section 1.4 Ca^{2+} Hypothesis,* ER Ca^{2+} dyshomeostasis and signalling dysregulation are hallmarks of AD. However, at this point, it is worthwhile summarising the aspects of ER Ca^{2+} dysregulation which are of particular relevance to this thesis section.

- RyRs and IP_3Rs are heavily implicated in mediating neuronal calcium dysregulation in murine transgenic models of AD (including 3xTg-AD mice and PS1 mutant mice; Chakroborty et al., 2009; Chan et al., 2000; Guo et al., 1999b; Smith et al., 2005; Stutzmann et al., 2006; Supnet et al., 2006; Zhang et al., 2010).
- Significant differences are evident in Ca^{2+} signalling and electrophysiological parameters when 3xTg-AD neurons are compared with controls in response to direct activation of IP_3Rs and RyRs (Chakroborty et al., 2009; Kuchibhotla et al., 2008; Rae et al., 2000; Rae and Irving, 2004; Stutzmann et al., 2007). For instance, of particular relevance to the results contained herein, direct IP_3R stimulation with caged IP_3 results in somatic Ca^{2+} responses which were up to 300% larger in neurons of $PS1_{M146V}$ (same PS1 mutation

as that of 3xTg-AD mice) and 3xTg-AD mice than in control neurons (Stutzman et al. 2007). Similarly, RyR-mediated $[Ca^{2+}]_i$ responses were also much larger (approximately 400%) in cultured 3xTg-AD hippocampal neurons in comparison to non-Tg neurons (Zhang et al. 2010).

- Ca^{2+} responses mediated by SOCE are much larger in non-Tg neurons relative to 3xTg-AD and PS DKO neurons (2-fold increase; cultured hippocampal neurons; 0 - 1-days-old; 12 - 13 DIV) and *in vitro* in cells expressing PS FAD mutations, possibly reflecting PS mutation-dependent increases in $[Ca^{2+}]_{ER}$ (Akbari et al., 2004; Herms et al., 2003; Leissring et al., 2000; Yoo et al., 2000)

mGluRs

There are limited lines of evidence specifically implicating mGluR-mediated Ca^{2+} signalling, depolarisation-induced Ca^{2+} entry and/or ER Ca^{2+} mobilisation in AD, most of which are concerned with APP-related proteins. For example,

a) I-mGluR-mediated PLC activation is impaired in the cerebral cortex of AD patients (Albasanz et al., 2005).

b) Previous work from our lab group demonstrated that there are clear differences in hippocampal I-mGluR mediated Ca^{2+} signals from young 3xTg-AD mice (cultured hippocampal neurons; 3 - 5-days-old; 7-14 DIV) relative to age-matched control neurons (Morley et al., 2012, 2011).

c) mGluR5 inhibition suppressed early-stage (3-weeks-old) network hyperexcitability in 3xTg-AD mice (Kazim et al., 2017).

d) Depolarisation of cortical synaptoneurosomes (containing vesicularised elements of the pre-synapse and post-synapse which are used to study synaptic transmission, see Johnson et al., 1997; Westmark et al., 2011) from $APP_{SWE/V717F}$ mice (10 - 14-days-old; extracellular application of K^+ (40 mM)) resulted in Ca^{2+} influx *via* L-type VGCCs. This rapidly decreased levels of αCTF and βCTF, suggesting that γ-secretase was being rapidly activated (Kim et al., 2010). Depolarisation also activated α-, β- secretases and resulted in rapid $Aβ_{40}$ and $Aβ_{42}$ generation and release into the extracellular environment (Kim et al., 2010).

e) Stimulation of synaptoneurosomes with the I-mGluR agonist DHPG produced very different effects and resulted in αCTF and βCTF *accumulation* and $Aβ_{40}$ release, but not the release of $Aβ_{42}$. This suggests that activation of I-mGluRs and the subsequent profile of Ca^{2+} mobilisation, as opposed to that due to extracellular Ca^{2+} entry, results in activation of α- and β- secretases without significant activation of γ-secretase (Kim et al., 2010). Non-subtype-specific mGluR agonists can also stimulate the secretion of the

neuroprotective and Ca^{2+} stabilising APPsα in cultured hippocampal neurons (Lee et al., 1995) and cortical rat brain slices (Kirazov et al., 1997) likely *via* an enhancement of α-secretase activity (*i.e.* the non-amyloidogenic APP processing pathway). Furthermore, inhibition of either mGluRs or PKC prevented sAPP release, which suggests that PKC was the mediator of mGluR effects on α-secretase (Lee et al., 1995). Similarly, mGluR-mediated sAPP production was observed in HEK293 cells transfected with mGluR1α (Lee et al., 1995). In these cells, a more detailed mechanism of APP processing was proposed whereby protein kinases, phospholipase A2 (PLA2) and melittin (a peptide that stimulates PLA2; Nitsch et al., 2002) mediate mGluR1α-stimulated sAPP production. In rat cerebral cortical slices, APP cleavage and sAPPα formation are primarily mediated by mGluRs, whilst AMPAR activation suppressed the processing of APP to sAPP (Kirazov et al., 1997). Therefore, AD-dependent impairment of mGluR-mediated signalling (Albasanz et al., 2005) may reduce the overall levels of non-amyloidogenic APP processing within the CNS. Conversely, however, mGluR5 activation can also lead to rapid APP mRNA translation in the synapse, which has the potential to increase the levels of its toxic metabolites (Sokol et al., 2011; Westmark, 2013; Westmark and Malter, 2007).

f) As discussed in *Section 1.2.6 Molecular actions of APP metabolites,* clustered Aβo accumulate at excitatory hippocampal synapses where they interact with mGluR5 *via* PrP^C to prevent mGluR5 diffusion over the post-synaptic membrane (Um et al., 2013). This stabilises mGluR5 clusters at these sites and creates so-called 'artificial signalling platforms' (ASPs). These ASPs lead to aberrant neuronal Ca^{2+} signalling, increased $[Ca^{2+}]_i$ and *Arc* activation (Um et al., 2013). *Arc* activation ultimately results in altered spine morphology, decreased spine number, depletion of surface NMDAR and dysregulation of NMDAR-mediated signalling pathways (Lacor et al., 2007; Shankar et al., 2007; Snyder et al., 2005). Indeed, these synaptic deficits are observed in an Aβo-mGluR5 signalling dependent manner in models of AD (Haas et al., 2014; Renner et al., 2010; Sokol et al., 2011; Um et al., 2013).

g) Antagonists of mGluR5 prevent Aβo-mediated LTP disruption (Q. Wang et al., 2004) and genetic deletion of mGluR5 reduces circulating levels of Aβos, plaque deposition and cognitive decline in $APP_{swe}/PS1_{\Delta E9}$ mice (9-12 months of age; Hamilton et al., 2014). Chronic inhibition of mGluR5 using MTEP, which is a negative allosteric modulator of mGluR5 in 9-month-old $APP_{swe}/PS1_{\Delta E9}$ mice also rescued spatial memory deficits as well as deficits in episodic and recognition memory, the latter of which both developed earlier in the disease progression in this mouse model (Hamilton et al., 2016). Furthermore, mGluR5 antagonism (again using MTEP) improved

spatial memory and synapse density in $APP_{swe}/PS1_{\Delta E9}$ mice (9-10 months of age), as well as object recognition in 3xTg-AD mice (8-9 months of age; Um et al., 2013).

iGluRs

The function and expression of iGluRs also appear to be modified in AD (De Felice et al., 2007; Li et al., 2011). Examples of this include:

a) A reduction in the amplitude of evoked AMPAR- and NMDAR-mediated excitatory currents, in a γ-secretase dependent manner, in hippocampal neurons from $PS1_{A246E}$ mice relative to non-transgenic controls (Priller et al., 2007).

b) Evidence utilising prefrontal cortical brain slices from 4-6 week old 3xTg-AD and $APP_{SWE}/PS1_{M146V}$ mice suggest that although NMDAR-mediated currents are not measurably different amongst mouse strains (including when compared to non-Tg controls), dendritic spine Ca^{2+} transients are larger in both AD strains relative to age-matched controls. This effect was mediated by NMDAR-mediated activation of RyRs *via* CICR, which occurred in transgenic animals only. This abbarent NMDAR-mediated CICR activation is hypothesised to be due to increased intracellular calcium and therefore hypersensitisation of RyRs within spines and dendrites of transgenic neurons (Goussakov et al., 2010). Similarly, in experiments utilising hippocampal slices from 3-month-old $PS1_{M146V}$ mice, the magnitude of NMDAR-dependent field EPSPs was significantly increased relative to non-transgenic controls (Auffret et al., 2010).

c) As mentioned previously, Aβo-PrP^C mediates disruption of mGluR5 Ca^{2+} signalling at synapses and activates *Arc*. This leads to a decrease in NMDAR expression (Renner et al., 2010) and dysregulation of NMDAR-mediated signalling pathways (Lacor et al., 2007; Shankar et al., 2007; Snyder et al., 2005).

d) Aβo–PrP^C-Fyn complexes cause synaptic disruption mediated *via* alterations in NMDAR trafficking and activation (Larson et al., 2012; Um et al., 2012).

e) Application of very low concentrations of Aβo to organotypic hippocampal slices results in actin-depolymerizing factor/cofilin- (involved in cytoskeleton plasticity) and CN-dependent decreases in NMDAR activity and dendritic spine number after 5 -15 days (Shankar et al., 2007). The number of cells expressing NR1 and NR2A subunits of NMDAR were also lower in APP_{SWE} mice at 18 - 22 months relative to controls. Furthermore, this deficit could be reversed by administering the anti-amyloid-β antibody, aducanumab (Sevigny et al., 2016). These synaptic alterations may explain the synapse

loss induced by Aβo application *in vitro* in neuronal cultures (Lacor et al., 2007) and *in vivo* in AD mouse models (Koffie et al., 2009).

f) Conversely, however, Aβo have also been shown to increase NMDAR-mediated responses and induce excitotoxicity (De Felice et al., 2007; Szegedi et al., 2005), effects which may mediate Aβo-stimulated oxidative stress and increased $[Ca^{2+}]_i$ (Bezprozvanny and Mattson, 2008; Cullen et al., 1996).

3.2. Aims

The primary aim of the work covered in this chapter was to expand upon initial studies (including work I was involved with during my undergraduate project; Morley et al., 2012) within Dr M.G. Rae's lab group, investigating the molecular basis of the altered neuronal calcium handling observed in the 3xTg-AD mouse. The same experimental approaches were also applied to a novel model of AD, the TgF344-AD rat which was acquired part of the way through my PhD studies. The specific aims of this part of my project were:

1. To build upon initial findings of this lab group, which found that enhanced responses were observed in non-Tg cultured hippocampal neurons (3 - 6-days-old; ≥12 DIV) following I-mGluR stimulation under depolarisation conditions relative to basal conditions. These types of enhanced calcium signals were not observed in 3xTg-AD mouse neurons (Morley et al., 2011, 2012). Specifically, neurons in this study were utilised over a wider range of *in vitro* development (2 – 20 DIV) in order to determine how early this calcium dysregulation occurred and to determine the robustness of the previous findings during early-postnatal development.

2. Furthermore, this experimental approach was extended to Sprague Dawley (SD), non-Tg F344 and TgF344-AD rat hippocampal cultures. Not only would this allow us to determine whether this effect was replicated across species but also whether such calcium signalling alterations existed in an alternative AD model. We hypothesised that it was likely that neurons of this TgF344-AD rat might display ER-mediated calcium dysregulation but that it would occur through a different mechanism as these animals expressed a "gain-of leak" PS1 mutation rather than the "loss-of-leak" PS1 mutation expressed in 3xTg-AD mice (Zhang et al., 2010).

3. Aside from paired measurements comparing the magnitude of I-mGluR responses under depolarisation conditions relative to basal conditions within a single murine strain, we also wanted to determine whether responses to depolarisation and I-mGluR stimulation (under basal and depolarisation conditions) were different between 3xTg-AD and TgF344-AD neurons relative to non-Tg age-matched controls.

4. In addition to excitation-mediated Ca^{2+} entry, one of the primary means of loading the neuronal ER with Ca^{2+} is via SOCE. This process is initiated by the depletion of ER Ca^{2+} stores and involves the movement

of Ca^{2+} directly through plasma membrane-located channels into the ER. However, to date, little is known about how this Ca^{2+} entry pathway is affected by mutations which predispose to the development of AD. Therefore, we wished to a) determine if SOCE was present in mouse primary cultured hippocampal neurons and, if so, b) to investigate if it was altered in cultured 3xTg-AD hippocampal neurons relative to that in age-matched controls.

3.3. Materials and methods

3.3.1 Materials

- All materials and methods related to the production of hippocampal cultures are outlined in *Section 2 Primary Hippocampal Neuronal Culture* and the publication by Kaar et al. (2017).
- Fluo-2 High Affinity (AM; TEFLABS, cat. no. 0220)
- Fura-2 (AM; ThermoFisher scientific, cat no. F-1201)
- HEPES-buffered saline solution (HBSS) of the following composition (in mM): NaCl 130, HEPES 10, KCl 5.4, $MgCl_2$ 2, D-glucose 2 and $CaCl_2$ 2, pH 7.4, 310 – 340 mOsm. HBSS K^+ replaced NaCl with KCl to increase the concentration of K^+ to 10 – 15 mM.
- Pluronic F127 (TEFLABS, cat. no. 2510)
- (*S*)-3,5-dihydroxyphenylglycine (DHPG; Tocris, cat. no. 0805/5)
- Tetrodotoxin (TTx; Tocris, cat. no. 1078/1)
- Thapsigargin (TPN; Sigma, cat. no. T9033)
- Gadolinium (Gd^{3+}; Sigma, cat. no. 263087)

3.3.2 Methods

Data Analysis

Calcium imaging was carried out as described in *Section 2.2.5 Calcium imaging*. Where possible, data in studies presented were collated from at least 4 different experiments/coverslips and derived from at least four separate cultures. Throughout this results section, instead of solely using *n* numbers, collated data are presented as follows: (*x* number of cells – from *y* number of experiments/coverslips – from *z* separate cultures; *e.g.* (115 – 12 – 8) - Fig 3.5, B). Wild-type (WT) refers to neurons harvested from SD rat neurons. Non-transgenic (non-Tg) refers to neurons harvested from either the same background strain as the 3xTg-AD mice used (C57BL6/129sv) or non-Tg littermates of TgF344-AD rats (as determined by genotyping). “Transgenic” (Tg) is also used throughout this results section to describe neurons harvested from 3xTg-AD mice or TgF344-AD rats (as determined by genotyping).

“DHPG” refers to (S) 3, 5-dihydroxyphenylglycine and was always applied at a concentration of 50 µM and superfused for 120 s (See Fig 3.1 for a general timeline of experiments). The term “basal conditions” refers to the application of compounds in normal physiological solution (HBSS) as opposed to “depolarisation conditions” where a physiological solution with an elevated concentration of K^+ was used (HBSS K^+; 5.4 *vs* 15mM K^+). and applied for 120 s prior to DHPG application, for the period of DHPG application and for 120s following DHPG application in all experiments (Fig

3.1). These measures were taken in an effort to standardise experiments and reduce variability.

In order to determine the potential effects of tachyphylaxis in our experimental protocol across in each neuronal population we determined that utilisation of a 50-minute washout period between DHPG applications was optimal for the production of statistically reproducible responses in SD rat, non-Tg rat and 3xTg-AD mouse neurons (when compared to 15, 30 and 40 minutes; data not shown). However, in non-Tg mouse neurons a significantly decreased peak amplitude (38 ± 4 *vs* 31 ± 3 a.u.; first application *vs* second; $p = 0.002$; $n = 58$) but not duration or AUC of the second DHPG response was observed and this desensitisation effect should be factored into any results obtained from these neurons.

For SOCE experiments (completed under my co-supervision by M. P. Wier), an initial baseline was determined in normal (*i.e.* Ca^{2+}-containing) HBSS for 4 mins after which the SOCE process was "primed" by depleting the ER using the SERCA pump inhibitor TPN (1 μM) in Ca^{2+}-free HBSS for 20 mins. SOCE was then subsequently triggered by adding Ca^{2+} "back in" by perfusing the neurons with normal HBSS (5 - 10 mins; Chauvet et al., 2016). We also utilised the non-specific SOCE antagonist Gd^{3+} (50 μM; added 5 min after Ca^{2+} "add back", for 20 mins) (Yeromin et al., 2004) to determine the susceptibility of the SOCE process to this antagonist in the two mouse genotypes. As we were unable to use the time taken for the calcium response to return to baseline in the presence of Gd^{3+} (50 μM) as our measure of the antagonist's effectiveness against SOCE, simply because the calcium signal did not return to baseline following its application in the continued presence of normal HBSS (*e.g.* see Fig 3.12), we instead measured the percentage drop in calcium signal amplitude (from peak SOCE) after 4 minutes in the presence of Gd^{3+}.

Representative traces were generated offline using GraphPad Prism where amplitude, duration and area under the curve (A.U.C.) of responses were measured. Baselines for amplitude and A.U.C. measurements were chosen based on the average fluorescence of either 120 s before or after a given response, depending on which baseline was higher. Cells were utilised after 2 - 20 days in culture. Following segregation of data into groups based on *in vitro* development (0 – 5, 6 – 10, 11 – 15 and 16 – 20 DIV) there were no significant differences between such groups within non-Tg mouse and rat, TgF344-AD rat and SD rat populations used in this study (data not shown). Conversely, 3xTg-AD mouse populations appeared (based on a single experiment; 33 – 1 – 1; 4 DIV) not to express a transgenic phenotype and rather responded in the same manner as non-Tg mouse neurons between 0 - 5 DIV and as such data for 3xTg-AD neurons (Fig 3.5) are pooled from 6 – 18 DIV (data not shown). Numerical data were derived from the *total* somatic

region as drawn by the experimenter for each neuron individually. Regions of interest (ROIs) were manually traced around the somata of cells subjectively observed to be neurons. Such identification was aided by comparison to bright field (DIC) images which were acquired for each individual experiment. At this stage neurons which had obviously deteriorated and/or were dead (*e.g.* those that were granular, misshapen, extremely bright or dark under excitation light or were obviously non-vital in any other way) were removed from the analysis. Furthermore, at the analysis stage, certain neurons were removed due to artefacts arising from debris moving over the field of view (FOV) and/or due to spontaneous activity, where the frequency or magnitude of spontaneous activity impacted upon genuine agonist-specific responses.

All data are presented as mean ± SEM. As described in *3.4.1 General I-mGluR response characteristics*, there is generally (across the different murine populations utilised in this study) an increased proportion of neurons which exhibit detectable responses to DHPG under depolarisation conditions relative to basal conditions (control). This most likely due to the fact that cultured hippocampal neurons appear to have an ER which is "functionally empty" under basal conditions (see i*nter alia* Rae et al., 2000; Zhang et al., 2010). Cells which only displayed DHPG-evoked responses following depolarisation are included in data displayed in histograms (*i.e.* peak amplitude (arbitrary units (a.u.)), duration (s) and A.U.C (a.u.; *e.g.* Fig 3.5 – B – i, iii, iv)), where changes in intracellular calcium are displayed in absolute numbers (*i.e.* as opposed to data which have been normalised). For the subset of cells that displayed responses to DHPG under both basal and depolarised conditions, we were able to normalise the data to determine the percentage change in response amplitude and magnitude (*e.g.* Fig 3.5 – B - ii). Only these cells were included for such analysis as it was impossible to determine the magnitude of the DHPG-evoked calcium increase in cells where there had been no basal response as one would have to divide the numerator by 0 (*i.e.* the value would be infinity). Statistical analyses were performed using a paired Student's *t*-test or Wilcoxon matched paired signed rank test (for normalised data) for paired observations or repeated measures ANOVA with Tukey's multiple comparison test or Dunnett's multiple comparison test (normalised AUC data only) for group data on repeated measures. Unpaired *t*-tests and one-way analysis of variance with Tukey's multiple comparison test or Dunnett's multiple comparison test (for normalised AUC data only) were utilised for unpaired observations and grouped data, respectively. Unpaired t-test was utilised for comparing the frequency of observations between neuronal populations. *P value* (p) of < 0.05 was considered significant. Degree of significance was displayed as follows: $*p < 0.05$, $**p < 0.01$ and $***p < 0.001$. Pearson correlation (data assumed from Gaussian populations) was used to measure the correlation between A.U.C. of DHPG responses and depolarisation responses.

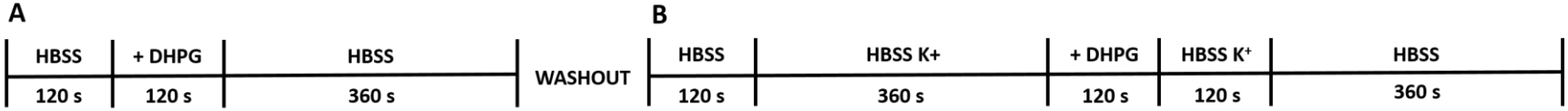

Figure 3.1 Experimental protocol and timeline

Experiments were standardised as follows:

Basal conditions **(A)** involved recording somatic $[Ca^{2+}]_i$ for 120 seconds (s) in basal Hanks' buffered salt solution (HBSS; K^+ 5.4 mM) to determine a baseline, DHPG (50 μM) was then added for 120 s before being washed out and somatic $[Ca^{2+}]_i$ allowed to return to baseline again. A drug washout period, where cells were superfused with HBSS for 15 – 50 mins (see results below), was then initiated.

Depolarisation conditions **(B**) involved recording $[Ca^{2+}]_i$ for 120 s in basal HBSS followed by depolarisation with HBSS K^+ (K^+ 15 mM) for 360 s, followed by DHPG application in HBSS K^+ for 120 s. DHPG responses are superimposed upon K^+ (15 mM) -mediated increases in somatic Ca^{2+} as shown in Fig 2.2. Cells were then allowed to return to baseline conditions by removing HBSS K^+ after 120 s and recording in basal HBSS for 360 s.

Neuron identification

During the analysis process, neuronal identification was carried out primarily based on the morphological characteristics of cultured cells. However, identification of cultured neurons based solely on morphology (as opposed to immunohistochemical identification) has been shown to be unreliable (Raff et al., 1979). This is, in part, due to the morphological similarities between multipolar neurons and stellate-shaped type II astrocytes (Kivell et al., 2000). With this in mind, functional Ca^{2+} imaging data can also aid in the categorisation of cells because neurons are selectively sensitive to depolarisation stimuli *via* application of elevated extracellular K^{+} (Rae et al., 2000). Aside from visual identification, glial and neuronal identification can also be clarified by examining their spontaneous activity as outlined by Pozzi et al. (2017). Briefly, according to their protocol, spontaneous calcium transients are defined as beginning when the fluorescence signal exceeds, by at least by three times, the standard deviation of the noise. When TTx was added, such transients disappear from the majority of cells in culture, which are considered to be neurons whilst the remaining cells are deduced to be astrocytes and can, therefore, be removed from the analysis (Pozzi et al., 2017). This exclusion is based upon the fact that astrocytes display Ca^{2+} signals even after TTx addition in the typical form of calcium waves (Scemes and Giaume, 2006). In practical terms, using our imaging and data analysis protocol, each ROI was individually screened by the user and, as such, cells which exhibited this glial-type oscillatory wave activity were removed from the analysis (Fig 3.2).

With this in mind, there were a small number of cells in the neuronal populations (outlined in Fig 3.3 & 3.4) which responded to DHPG under basal conditions but not in the presence of depolarisation (< 1%). As these cells did not display Ca^{2+} 'waves', they may reflect a sub-population of neurons which are relatively insensitive to these mechanisms of depolarisation, or they may be glial cells which were atypical in that they did not exhibit Ca^{2+} waves. Due to this ambiguity, these data were removed from the analysis.

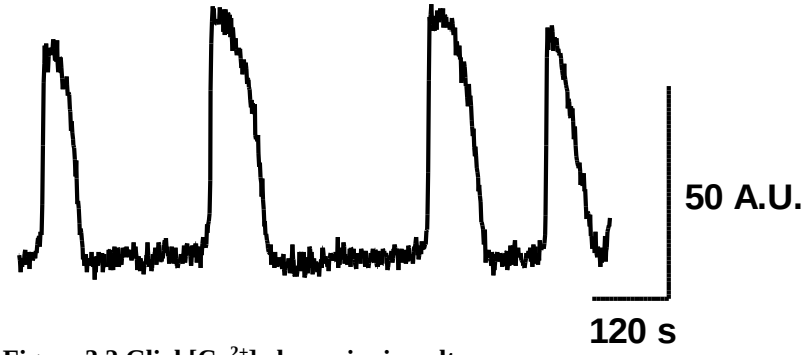

Figure 3.2 Glial $[Ca^{2+}]_i$ dynamics in culture

Representative somatic intracellular Ca^{2+} response (SD rat; 3-days-old; 13 DIV) illustrating distinctive Ca^{2+} oscillations associated with glia which facilitates their identification in culture.

3.4. Results

3.4.1 I–mGluR response characteristics

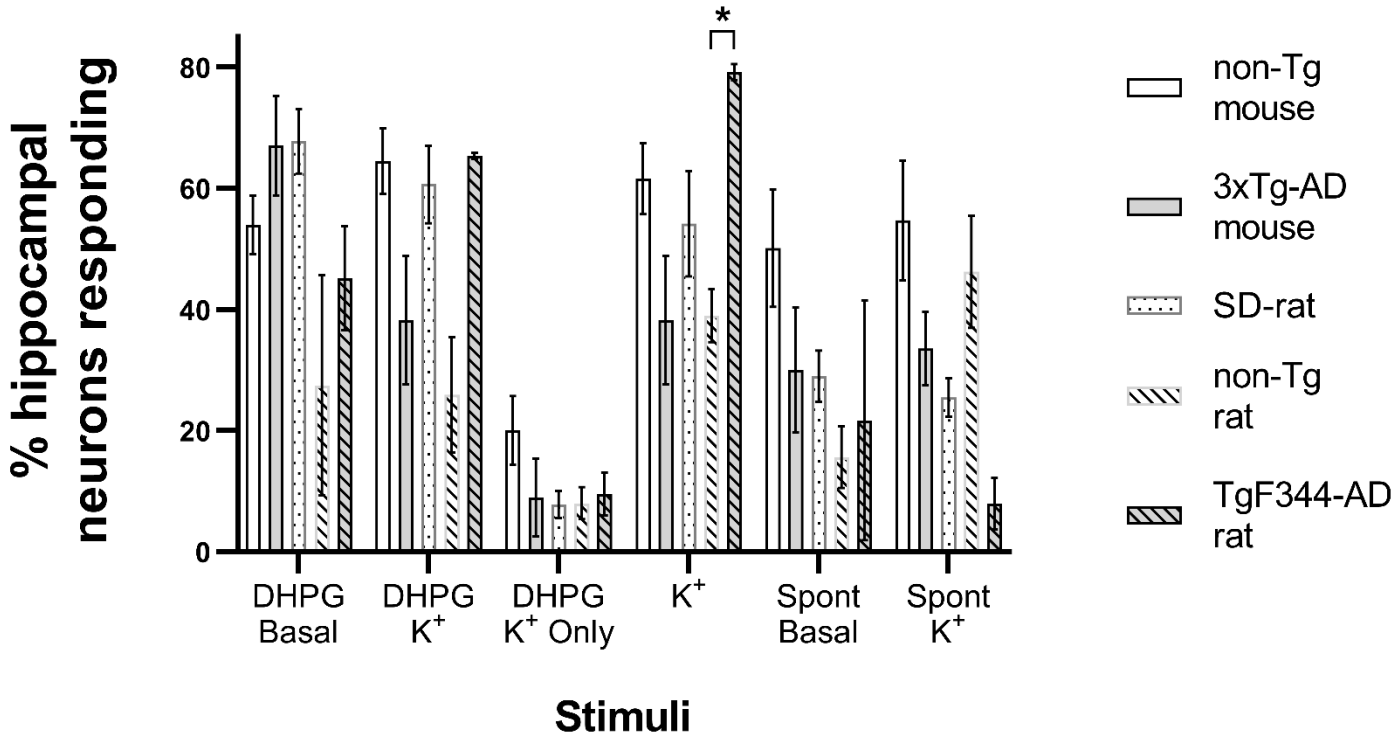

Figure 3.3 Response characteristics of neuronal populations

The percentage of cultured hippocampal neurons which exhibited detectable responses to I-mGluR stimulation (DHPG) under: basal (K^+ 5.4 mM), depolarisation conditions (K^+ 15 mM) and depolarisation conditions alone as well as to the depolarisation stimulus itself is shown for each population utilised in this study: non-transgenic (non-Tg; 3 – 20 DIV; 237 – 12 – 8; white boxes) and 3xTg-AD mouse (138 – 9 – 6; grey boxes), wild-type rat (SD rat; 406 – 14 – 7; white spotted boxes) and non-Tg (372 – 9 – 4; white dashed boxes) and TgF344-AD rat (95 – 2 – 1; grey dashed boxes). The percentage of neurons which exhibited spontaneous activity under basal and depolarisation conditions is also displayed.

Figure 3.3 displays the percentage of cultured hippocampal neurons harvested from non-Tg and Tg mouse (3xTg-AD model) and rat (TgF344-AD model) as well as WT rat (SD rat) populations which exhibited detectable responses to a) DHPG under basal and depolarisation conditions (including those which responded solely under depolarisation conditions) and b) the depolarisation stimulus itself. The percentage of neurons which exhibited spontaneous activity under basal and depolarisation conditions is also shown. There were no significant differences between proportions of responding neurons with respect to any parameter measured between non-Tg and 3xTg-AD mouse, WT rat and non-Tg rat or non-Tg rat and TgF344-AD rat with one exception, namely that a greater proportion of TgF344-AD neurons per experiment responded to the depolarisation stimulus (K^+; 15mM) than non-Tg age-matched controls ($p = 0.02$; 79% *vs* 39%; $n = 2$ *vs* $n = 4$ experiments; TgF344-AD *vs* non-Tg rat). The quantitative data accrued from

these responses (peak amplitude, normalised peak amplitude, duration and A.U.C.) across these populations are presented in Fig 3.5 – 3.10.

Once DHPG reached the tissue bath, all of the responding cells on the coverslip were activated in a synchronised manner. Regardless of species or strain (no significant differences between proportions of neuronal populations responding monophasically when comparing non-Tg and 3xTg-AD mouse, WT rat and non-Tg rat or non-Tg rat and TgF344-AD rat), DHPG-mediated responses were predominately monophasic under basal (Fig 3.4; 84 ± 3%; n = 41 experiments) and depolarisation conditions (Fig 3.2; 89 ± 2%; n = 41 experiments). Monophasic responses consisted of a rapid rising phase and a slower decay phase, as reported previously in rat hippocampal cultures (Rae et al., 2000). Multiphasic responses were observed in a manner typical of that illustrated in Fig 3.3 (ii). Ca^{2+} responses, generally, were variable both in amplitude and duration.

Application of a depolarisation stimulus of K^+ (15 mM) evoked a rapid increase in somatic $[Ca^{2+}]_i$, which we attributed to activation of VGCCs. When this depolarisation stimulus was applied prior to DHPG application, a small number of neurons (generally, across species and strains) responded to the depolarisation stimulus alone (and not DHPG; < 1%; Fig 3.2, iii; n = 41 experiments). This response consisted of a rapid rising phase, which plateaued and remained at a steady level until the depolarisation stimulus was removed. Those cells which responded to both the depolarisation stimulus and DHPG exhibited a DHPG response that was superimposed upon this depolarisation- mediated plateau (59 ± 3; Fig 3.2, iv; n = 41 experiments). 12 ± 2% (n = 41 experiments) of neurons which did not produce a measurable DHPG-evoked Ca^{2+} signal under basal conditions did, subsequently, under depolarisation conditions. There is a significant correlation between the increase in amplitude mediated by the depolarisation stimulus and the amplitude of DHPG responses exhibited by non-Tg mouse ($p = < 0.0001$; n = 92), 3xTg-AD mouse ($p = < 0.0001$; n = 14), SD rat ($p = < 0.0001$; n = 143) and non-Tg rat neurons ($p = < 0.0001$; n = 34). Conversely, TgF344-AD rat neurons do not exhibit a significant correlation ($p = 0.99$; n = 34) between these measurements.

Neurons frequently exhibited spontaneous activity across species, strains and experimental conditions (*i.e.* basal 35 ± 4% and depolarisation conditions 37 ± 4% of neurons in each experiment; n = 41 experiments) and these responses varied markedly in both their frequency, amplitude and duration. Numbers of spontaneously active cells increased with time in culture and as such we considered this a sign of cell deterioration as it coincided with the appearance of other Ca^{2+} signalling attributes that we felt were markers of cell deterioration such as steadily increasing or decreasing baselines (possibly due to a break down in the control of ion flow through a

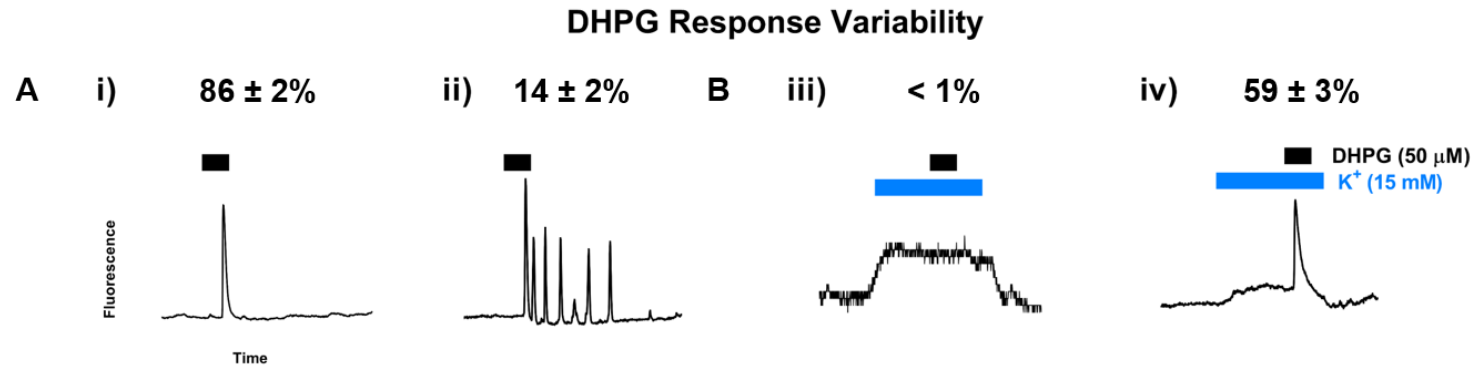

Figure 3.4 Variability of DHPG-mediated $[Ca^{2+}]_i$ responses in cultured hippocampal neurons

Representative somatic intracellular Ca^{2+} response traces illustrating inter-neuronal variability.

A) When a neuron exhibits a detectable response to DHPG application (50 μM; superfused for 120s; black bars) under basal (K^+ = 5.4 mM) or depolarisation conditions (K^+ = 15 mM; superfused for 360s, starting 120s prior to DHPG application; blue bars) the response is either monophasic (i) or multi-phasic (ii)

B) When DHPG was applied in the presence of the depolarisation stimulus, a small proportion of cells responded only to the depolarisation stimulus and exhibited an increase in somatic Ca^{2+} which plateaued thereafter and remained elevated until the depolarisation stimulus was removed (iii). The majority of cells responded to both depolarisation stimulus and DHPG (iv). Furthermore, a small proportion of cells did not exhibit a visible response to the depolarisation stimulus but did exhibit DHPG-mediated responses with the same profile as (i) under these depolarisation conditions.

% are displayed as ± SEM and are pooled from 41 experiments across all murine species and transgenic statuses utilised in this study.

membrane which is collapsing) and rapid drops in fluorescence (possibly due to cell lysis).

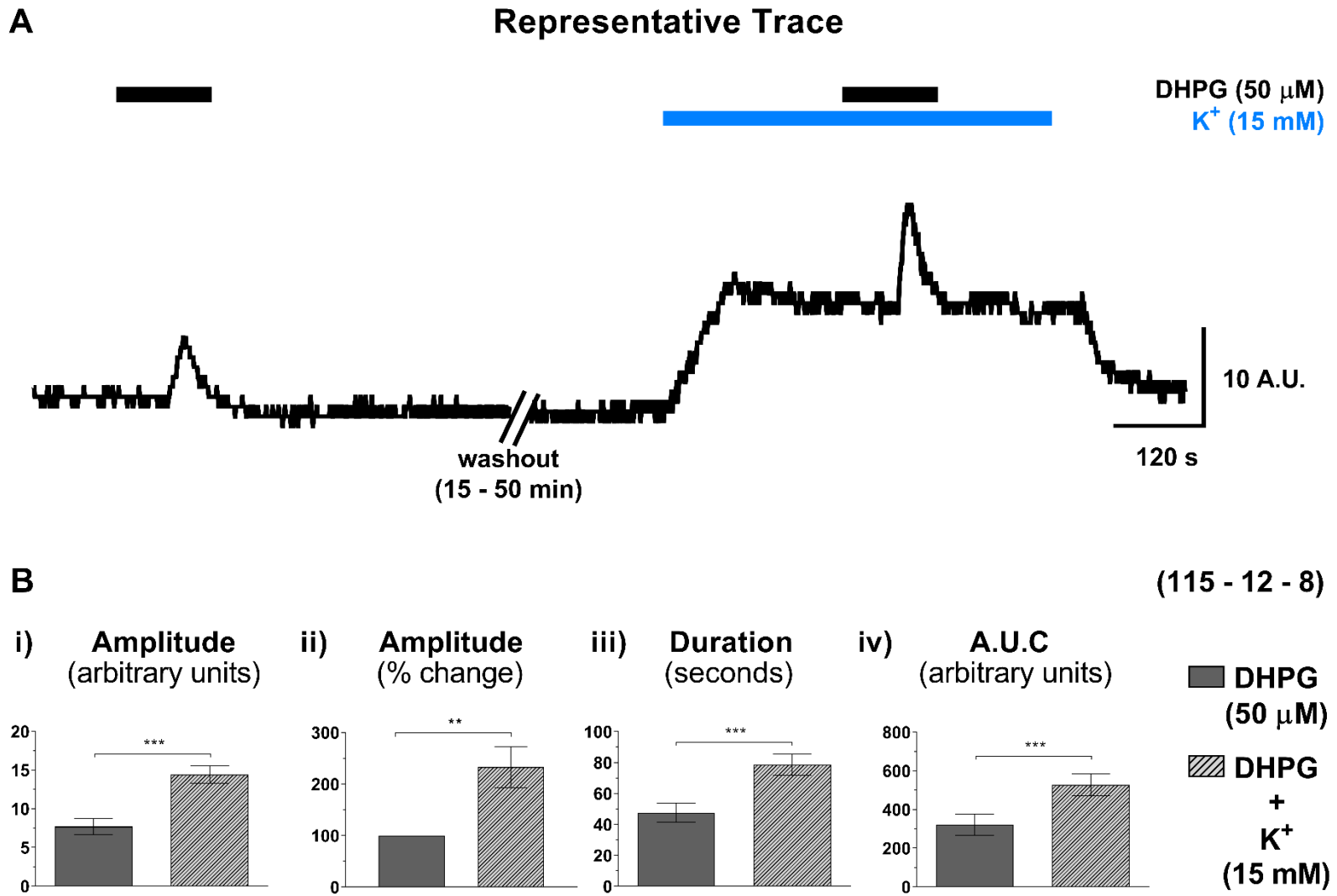

Figure 3.5. Somatic calcium dynamics of non-Tg mouse cultured hippocampal neurons (3 – 5-days-old) under basal conditions (DHPG (50 μM); 5.4 mM K^+) or depolarisation conditions (DHPG (50 μM); 15 mM K^+) from 3 – 20 days *in vitro*.

A Representative trace illustrating somatic intracellular Ca^{2+} response of a cultured non-Tg mouse hippocampal neuron (3-days-old; 20 days in vitro (DIV); strain: C57BL6/129sv) under basal conditions (DHPG application (black bar) in HBSS with 5.4 mM K^+), and depolarisation conditions (DHPG application subsequent to increasing the K^+ concentration of HBSS to 15 mM (grey bar) with a 15 minute agonist washout period separating both conditions.

B Histograms illustrating amplitude (arbitrary units (a.u.) **(i)**, normalised amplitude (% change) **(ii)**, duration (s) **(iii)** and area under the curve (A.U.C.) **(iv)** for pooled (3 - 5-day-old mice between 3 – 20 DIV) DHPG- mediated calcium responses under basal (solid dark grey bars) and

This series of experiments investigated neuronal DHPG-mediated $[Ca^{2+}]_i$ responses under basal and depolarisation conditions. Note: These data are pooled from experiments with washout times between DHPG applications ranging from 15 - 50 minutes (15, 30, 40 and 50 minutes). This reflects the fact that as the experimental protocol was optimised (see methods) the washout time between DHPG additions was increased from 15 mins to a standard 50 mins in order to minimise tachyphylaxis. Therefore, data pooled from experiments utilising a washout period of fewer than 50 minutes should be interpreted with the caveat that a slight temporal decrease in DHPG-mediated calcium response magnitude influences the displayed result and as such, any increased are likely under-emphasised in the data. Unlike all other murine species and strains utilised in this study, in the case of non-Tg mouse neurons a small but significant degree of tachyphylaxis was still evident when utilising a 50 minute washout (peak amplitude = 38 ± 4 *vs* 31 ± 3 a.u.; first application *vs* second; p = 0.002; n = 58).

Data resulting from DHPG-mediated calcium responses, in the absence and presence of depolarisation, in non-Tg mouse cells were pooled (3 - 5-days-old; 3 – 20 DIV; Fig 3.5; B) and were consistent with previous data from our lab (Morley et al., 2012, 2011; Rae et al., 2000), where significantly enhanced amplitude, normalised amplitude, duration and AUC of DHPG-mediated responses were observed under depolarisation conditions relative to basal conditions (Figs 3.5, B; amplitude = 8 ± 1 *vs* 14 ± 1 a.u., p = <0.0001, n = 115; normalised amplitude. = 100 *vs* 233 ± 40%, p = 0.0016, n = 62; duration = 47 ± 6 s *vs* 79 ± 7 s, p = <0.0001, n = 115; AUC = 322 ± 56 a.u. *vs* 528 ± 57 a.u., p = 0.0005, n = 115; basal *vs* depolarisation conditions).

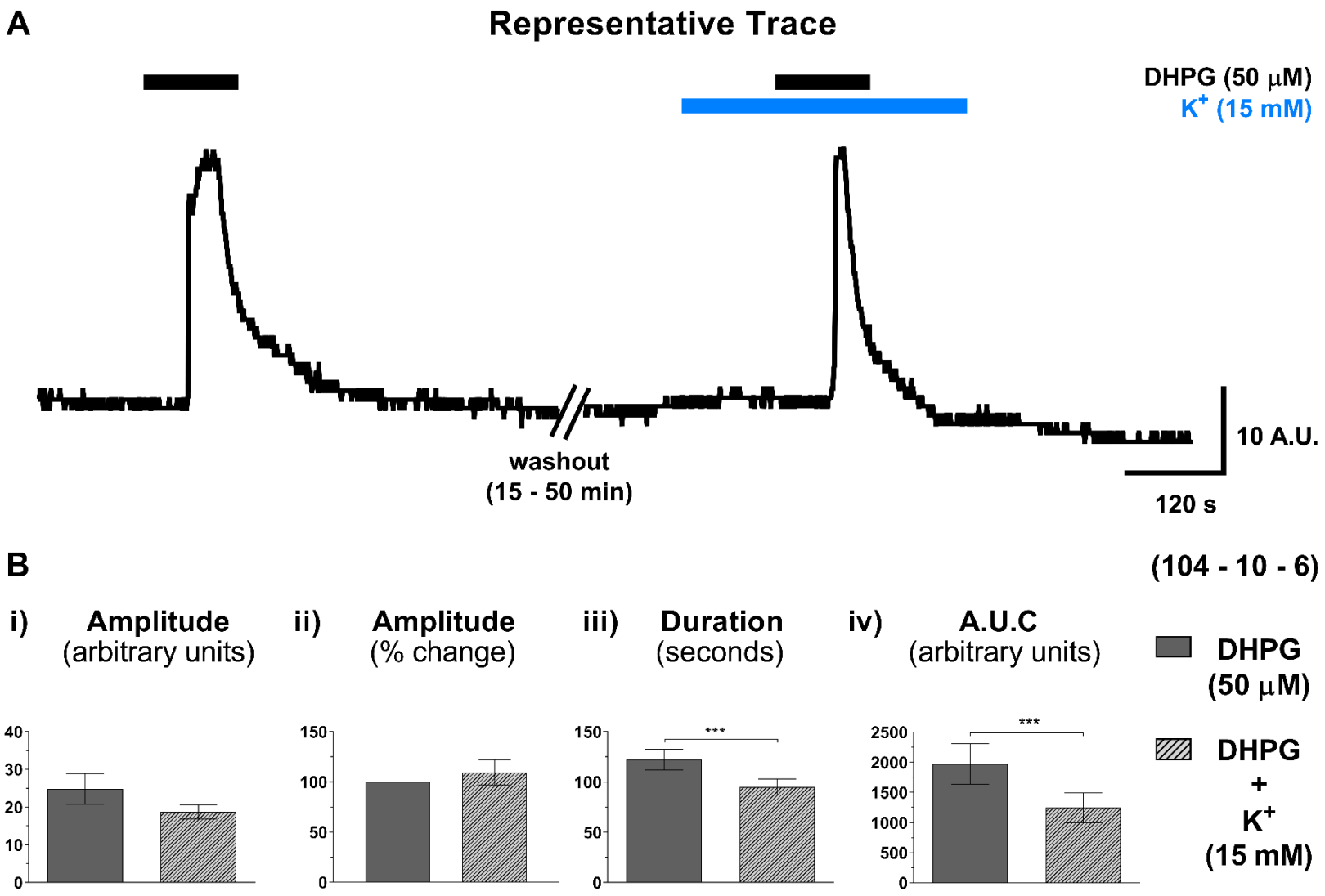

Figure 3.6. Somatic calcium dynamics of 3xTg-AD cultured hippocampal neurons (3 - 5 days old) under basal conditions (DHPG (50 μM); 5.4 mM K^+) or depolarisation conditions (DHPG (50 μM); 15 mM K^+) from 6 – 18 days in vitro.

A Representative trace illustrating a somatic intracellular Ca^{2+} response of a cultured 3xTg-AD mouse hippocampal neuron (3 days old; 18 days in vitro (DIV); strain: C57BL6/129sv) under basal conditions (DHPG application (black bar) in HBSS with 5.4 mM K^+) and depolarisation conditions (DHPG application subsequent to increasing the K^+ concentration of HBSS to 15 mM (grey bar).

B Histograms illustrating amplitude (arbitrary units (a.u.) **(i)**, normalised amplitude (% change) **(ii)**, duration (s) **(iii)** and area under the curve (A.U.C.) **(iv)** for pooled (3 – 5 day old mice between 6 – 18 DIV) DHPG- mediated calcium responses under basal (solid dark grey bars) and depolarisation (dashed light grey bars) conditions.

The experiments presented in Fig 3.5 which utilised cultured non-Tg hippocampal neurons were also conducted on cultured hippocampal neurons derived from 3xTg-AD mice (3 - 5-days-old; 6 - 18 DIV), the results of which are presented in Fig 3.6. As reported in previous studies undertaken by Dr Rae's lab group (Morley et al., 2011, 2012), but unlike findings obtained using cultured non-Tg hippocampal neurons (Fig 3.5), there was no enhancement in the any of the DHPG-mediated $[Ca^{2+}]_i$ signalling parameters (amplitude, normalised amplitude, duration and A.U.C.) under depolarisation conditions, relative to basal conditions, in these 3xTg-AD neurons (Fig 3.6; amplitude = 22 ± 3 a.u. *vs* 18 ± 2 a.u., p = 0.07, n = 104; normalised amplitude = 100% *vs* 109 ± 13%, p = 0.31, n = 79; basal *vs* depolarisation conditions). In fact, duration and AUC were significantly *decreased* in Tg neurons from 6 – 18 DIV under depolarisation conditions relative to basal conditions (duration = 122 ± 10 s *vs* 95 ± 8 s, p = 0.0004, n = 104; A.U.C. = 1973 ± 335 a.u. *vs* 1248 ± 247 a.u., p = 0.0002, n = 104; basal *vs* depolarisation conditions). Thus, the transgenic genotype has a particularly striking effect on attenuating the magnitude (AUC) of I-mGluR-mediated responses under depolarisation conditions relative to basal conditions when compared with the enhancement observed in non-Tg neurons.

Comparison of I-mGluR-evoked calcium signalling between non-Tg and 3xTg-AD mice

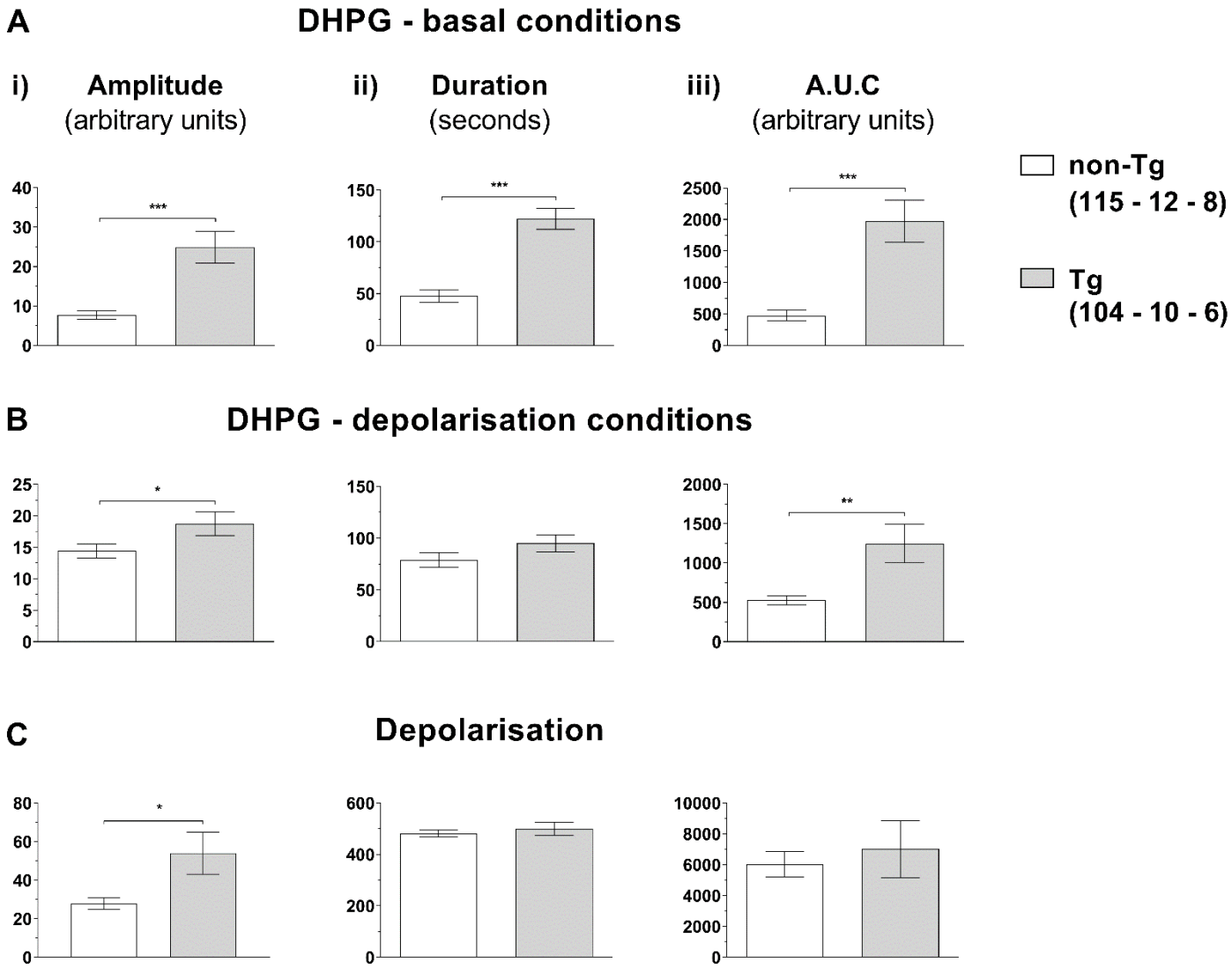

Figure 3.7. Somatic calcium dynamics of non-transgenic (non-Tg; 3 – 20 DIV) and 3xTg-AD (Tg; 6 - 18 DIV) cultured mouse hippocampal neurons (3 - 5-days-old) under basal conditions (DHPG (50 µM); 5.4 mM K^+) or depolarisation conditions (DHPG (50 µM); 15 mM K^+).

Histograms illustrating the amplitude (arbitrary units) **(i),** duration (s) **(ii)** and area under the curve of (A.U.C.; arbitrary units) **(iii)** of intracellular calcium responses from 3 – 5-day-old non-Tg (white bars) and Tg (grey bars) mouse neurons between 2 – 20 DIV. These responses were measured under basal conditions (A) or depolarisation conditions (B). The response due to depolarisation (K^+; 15 mM) alone (*i.e.* in the absence of DHPG-elicited responses or minus the superimposed DHPG-elicited component) is shown in section (C).

When DHPG-mediated calcium responses evoked under basal conditions in non-Tg and 3xTg-AD neurons were compared (non-Tg = 3 - 20 DIV, n = 115; 3xTg-AD = 6 - 18 DIV, n = 104 ; Fig 3.7; A) peak amplitude, duration and A.U.C. of responses were significantly increased in 3xTg-AD neurons relative to non-Tg neurons (amplitude = 25 ± 4 *vs* 8 ± 1 a.u., p = <0.0001; duration = 122 ± 10 s *vs* 48 ± 6s, p = < 0.0001; A.U.C. 1973 ± 335 a.u. *vs* 476 ± 88 a.u., p = 0.0001; Tg *vs* non-Tg).

Under depolarisation conditions (Fig 3.7; B), the amplitude (19 ± 2 *vs* 14 ± 1 a.u., p = 0.0492; Tg *vs* non-Tg) and AUC (1248 ± 247 *vs* 528 ± 57 a.u., p = 0.0054; Tg *vs* non-Tg) of DHPG responses were increased in Tg neurons relative to non-Tg controls, whereas duration was unchanged (95 ± 8 *vs* 79 ± 7 a.u., p = 0.13; Tg *vs* non-Tg)

When responses to depolarisation alone were analysed (Fig 3.7; C), the peak amplitude (54 ± 11 *vs* 28 ± 3 a.u., p = 0.0299; Tg *vs* non-Tg) was significantly increased in Tg neurons relative to non-Tg controls, whereas duration and AUC were unchanged (duration = 500 ± 26 s *vs* 482 ± 14s, p = 0.54; A.U.C. 7015 ± 1855 a.u. *vs* 6029 ± 837 a.u., p = 0.63; Tg *vs* non-Tg).

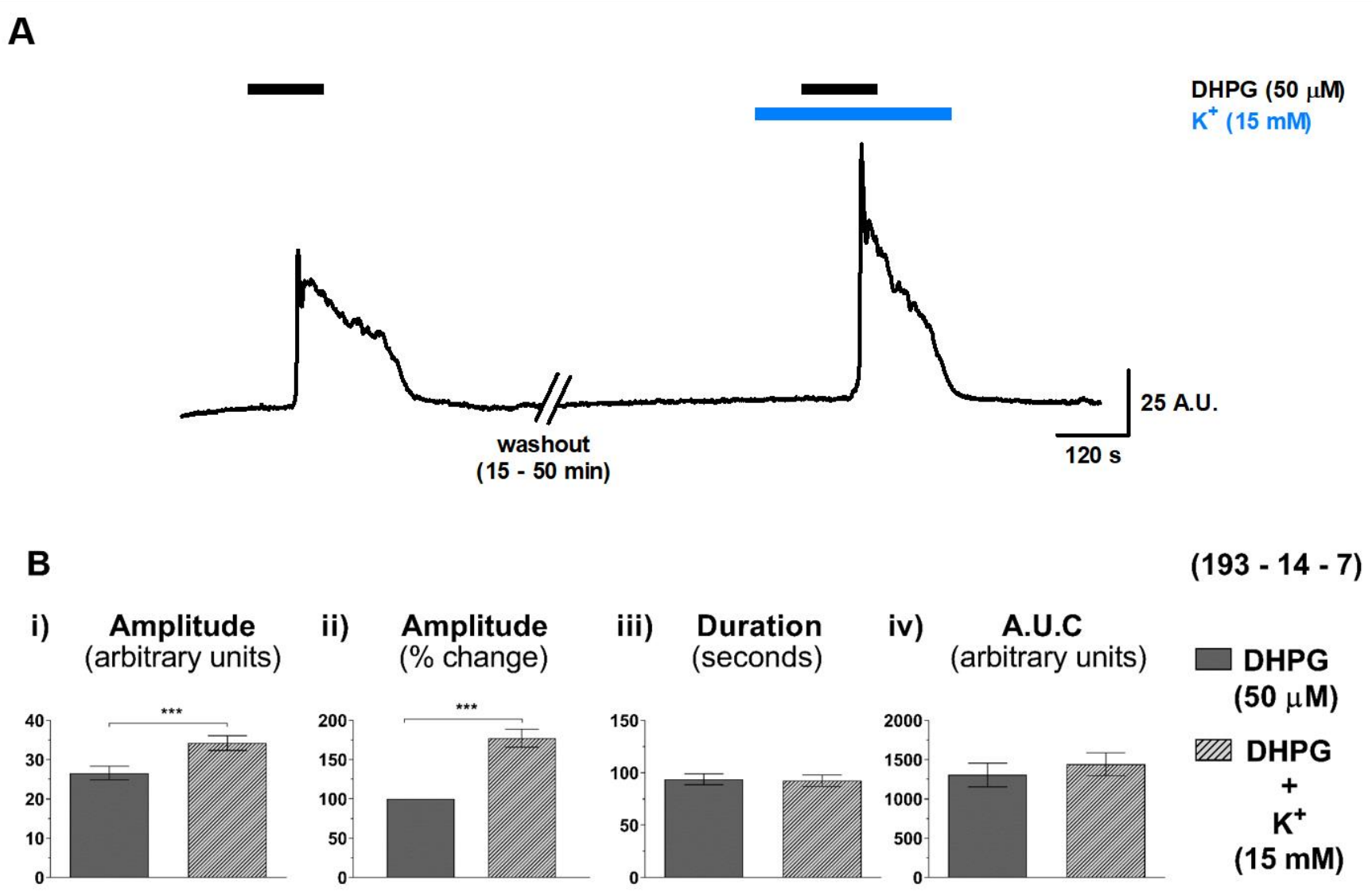

Figure 3.8. Somatic calcium dynamics of wild-type Sprague Dawley rat cultured hippocampal neurons (2 - 5 days old) under basal conditions (DHPG (50 μM); 5.4 mM K^+) or depolarisation conditions (DHPG (50 μM); 15 mM K^+) from 3 – 13 days *in vitro*.

A Representative trace illustrating a somatic intracellular Ca^{2+} response of a cultured wild type Sprague Dawley rat hippocampal neuron (3 days old; 4 days *in vitro* (DIV)) under basal conditions (DHPG application (black bar) in HBSS with 5.4 mM K^+) and depolarisation conditions (DHPG application subsequent to increasing the K^+ concentration of HBSS to 15 mM (grey bar).

B Histograms illustrating amplitude (arbitrary units (a.u.) **(i)**, normalised amplitude (% change) **(ii)**, duration (s) **(iii)** and area under the curve (A.U.C.) **(iv)** for pooled (2 – 5 day old rats between 3 – 13 DIV) DHPG- mediated calcium responses under basal (solid dark grey bars) and depolarisation (dashed light grey bars)

This study was next extended to the use of WT/SD rat neurons (2 - 5-days-old; 3 – 13 DIV) as a way of validating the data gathered from the utilisation of non-Tg mouse neurons (Fig 3.7), in an alternative species (Fig 3.8). Similar to data from non-Tg mouse neurons, in SD rat neurons, the amplitude and normalised amplitude of I-mGluR-mediated responses were significantly increased under depolarisation conditions relative to basal conditions (amplitude = 27 ± 2 a.u. *vs* 34 ± 2 a.u., p = < 0.0001, n = 193; normalised amplitude = 100% *vs* 177 ± 11%, p = < 0.0001, n = 169; basal *vs* depolarisation conditions).

In contrast to non-Tg mouse neurons where both duration and AUC were significantly increased under depolarisation conditions relative to basal conditions, in SD rat neurons there were no differences in these parameters (duration = 93.8 ± 5 s *vs* 92.6 ± 5 a.u., p = 0.80, n = 193, n = 193; A.U.C. = 1305 ± 150 a.u. *vs* 1442 ± 146 a.u., p = 0.14, n = 193; basal *vs* depolarisation conditions).

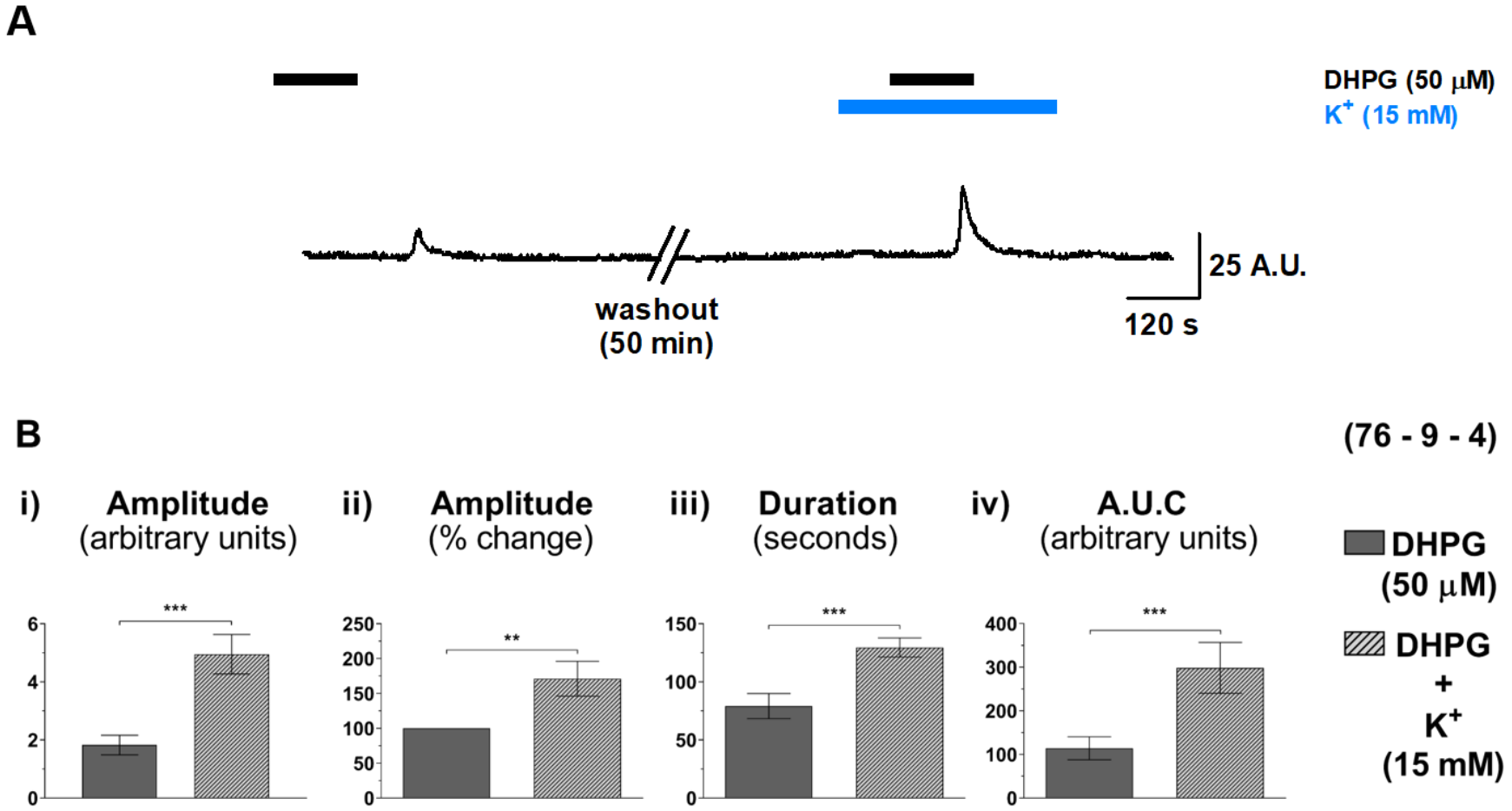

Figure 3.9. Somatic calcium dynamics of non-transgenic F344 rat cultured hippocampal neurons (3 - 9 days old) under basal conditions (DHPG (50 μM); 5.4 mM K^+) or depolarisation conditions (DHPG (50 μM); 15 mM K^+) from 3 – 12 days *in vitro*.

A Representative trace illustrating a somatic intracellular Ca^{2+} response of a cultured non-transgenic F344 rat hippocampal neuron (9 days old; 8 days in vitro (DIV)) under basal conditions (DHPG application (black bar) in HBSS with 5.4 mM K^+) and depolarisation conditions (DHPG application subsequent to increasing the K^+ concentration of HBSS to 15 mM (grey bar).

B Histograms illustrating amplitude (arbitrary units (a.u.) **(i)**, normalised amplitude (% change) **(ii)**, duration (s) **(iii)** and area under the curve (A.U.C.) **(iv)** for pooled (3 – 9 day old rats between 3 – 12 DIV) DHPG- mediated calcium responses under basal (solid dark grey bars) and depolarisation (dashed light grey bars) conditions.

Enhanced calcium signalling was also investigated in an alternative and novel AD model, the TgF344-AD rat. This work comprises the first Ca^{2+} signalling research in this animal model. Notably, whilst previous data was accrued from cultures produced from mice and rats from between two and five-days-old, cultures were produced from non-Tg and Tg F344 rats from three to nine-days-old. This difference reflects a practical limitation in that F344 litters had to be individually genotyped to allow for separation of pups into non-Tg or Tg sub-groups before a culture could be produced.

Pooled data from experiments between 3 and 12 DIV showed that the amplitude, normalised amplitude, duration and A.U.C. were all significantly increased under depolarisation conditions relative to control in non-Tg F344 neurons (amplitude = 1.8 ± 0.3 a.u. *vs* 4.6 ± 0.6 a.u., p = <0.0001, n = 76; normalised A.U.C. = 100% *vs* 171 ± 25%, p = 0.004, n = 42; duration = 79 ± 11 s *vs* 129 ± 8 s, p = <0.0001, n = 76; A.U.C. = 114 ± 26 a.u. *vs* 299 ± 58 a.u., p = 0.0007, n = 76; basal *vs* depolarisation conditions). Notably, the signalling phenotype expressed in non-Tg F344 rats is closer to the profile expressed in non-Tg mouse neurons (Fig 3.5) than that of SD rat neurons (Fig 3.6) where in the latter, duration and AUC of DHPG responses were not enhanced under depolarisation conditions relative to control.

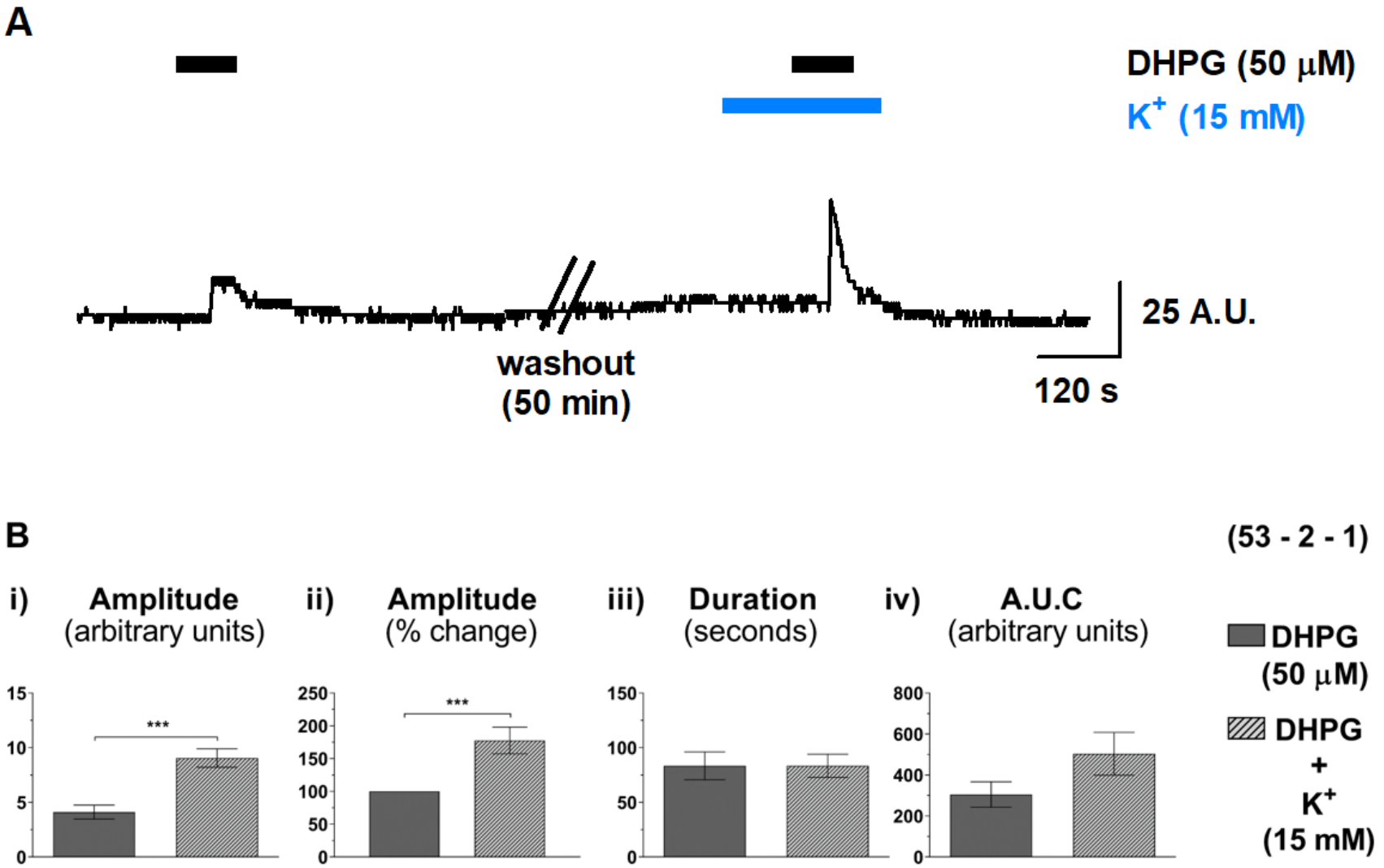

Figure 3.10. Somatic calcium dynamics of TgF344-AD rat cultured hippocampal neurons (7 days old) under basal conditions (DHPG (50 µM); 5.4 mM K^+) or depolarisation conditions (DHPG (50 µM); 15 mM K^+) from 3 – 7 days *in vitro*.

A Representative trace illustrating somatic intracellular Ca^{2+} measurements of a cultured TgF344-AD rat hippocampal neuron (7 days old; 7 days in vitro (DIV)) under basal conditions (DHPG application (black bar) in HBSS with 5.4 mM K^+) and depolarisation conditions (DHPG application subsequent to increasing the K^+ concentration of HBSS to 15 mM (grey bar) with a 15 minute agonist washout period separating both conditions.

B B Histograms illustrating amplitude (arbitrary units (a.u.) **(i)**, normalised amplitude (% change) **(ii)**, duration (s) **(iii)** and area under the curve (A.U.C.) **(iv)** for pooled (7 day old rats between 3 – 7 DIV) DHPG- mediated calcium responses under basal (solid dark grey bars) and depolarisation (dashed light grey bars) conditions.

TgF344-AD rat hippocampal neurons (7-days-old; 3 – 7 DIV) exhibit a significant enhancement in the amplitude and normalised amplitude of DHPG-mediated calcium responses under depolarisation conditions relative to basal conditions (amplitude= 4 ± 0.6 *vs* 9 ± 0.8 a.u.; p = <0.0001; n = 53; normalised amplitude = 100% *vs* 178 ± 20%, p = 0.0008, n = 31; basal *vs* depolarisation conditions). Therefore, in terms of these two parameters there is little difference between Tg and non-Tg F344 neurons with in both populations (both parameters approximately doubled under depolarisation conditions relative to basal conditions; for non-Tg see Fig 3.9).

Conversely, unlike in non-Tg F344 rat neurons where duration and AUC are significantly enhanced under depolarisation conditions, these parameters are unchanged in TgF344-AD neurons (Fig 3.10; A.U.C. = 305 ± 62 a.u. *vs* 503 ± 105 a.u., p = 0.09; duration = 83 ± 13 s *vs* 83 ± 11 s, p = 0.9; n = 53; basal *vs* depolarisation conditions).

3.4.3 Store-operated calcium entry (SOCE)

Comparison of SOCE between non-Tg and 3xTg-AD mice

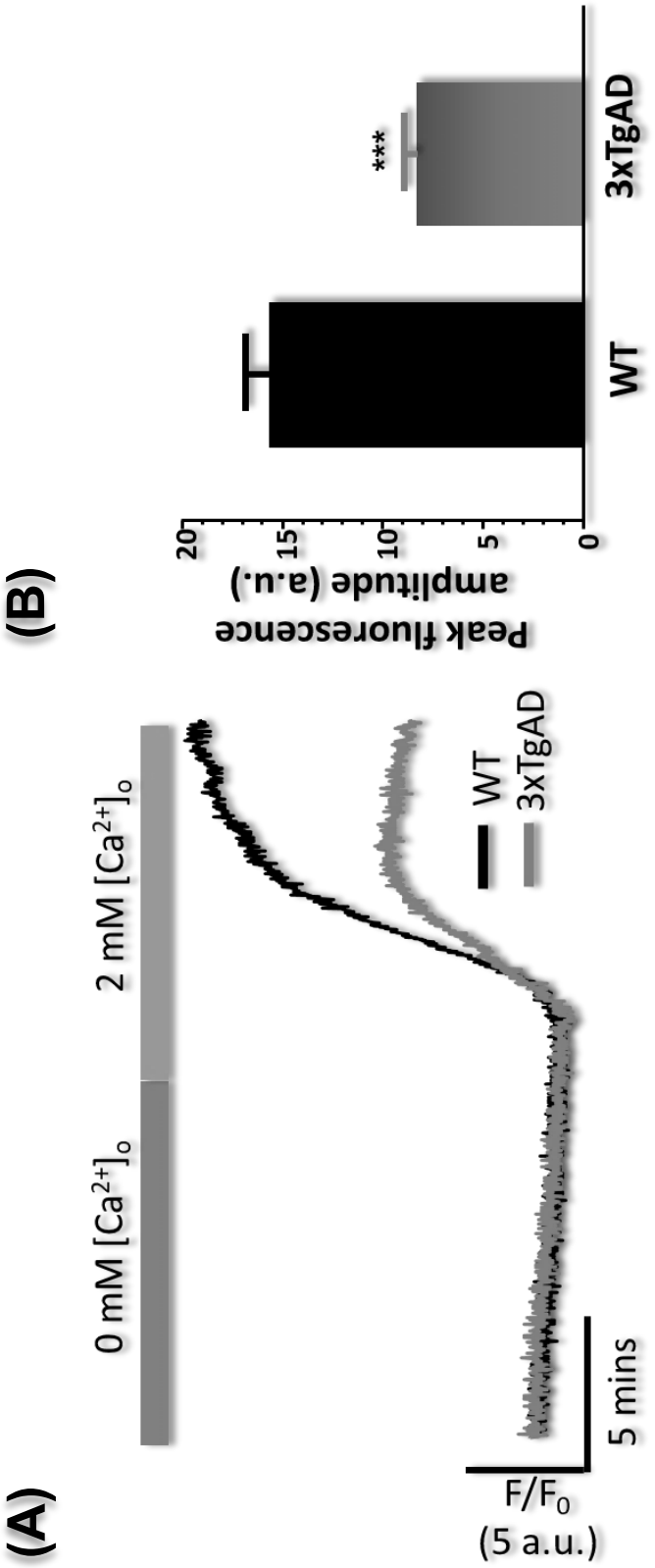

Figure 3.11. The peak amplitude of neuronal store operated Ca^{2+} entry (SOCE) is significantly reduced in 3xTg-AD hippocampal neurons relative to wild type (WT) age matched controls (3 – 5-days-old) from 5 – 14 days *in vitro*.

A. Superimposed calcium imaging traces obtained from WT (black) and 3xTg-AD (red) neurons.

B. Histogram illustrating that peak fluorescence induced following nSOCE is significantly greater in WT (n = 65; 5 separate experiments) than in 3xTgAD (n = 57; 7 separate experiments) hippocampal neurons.

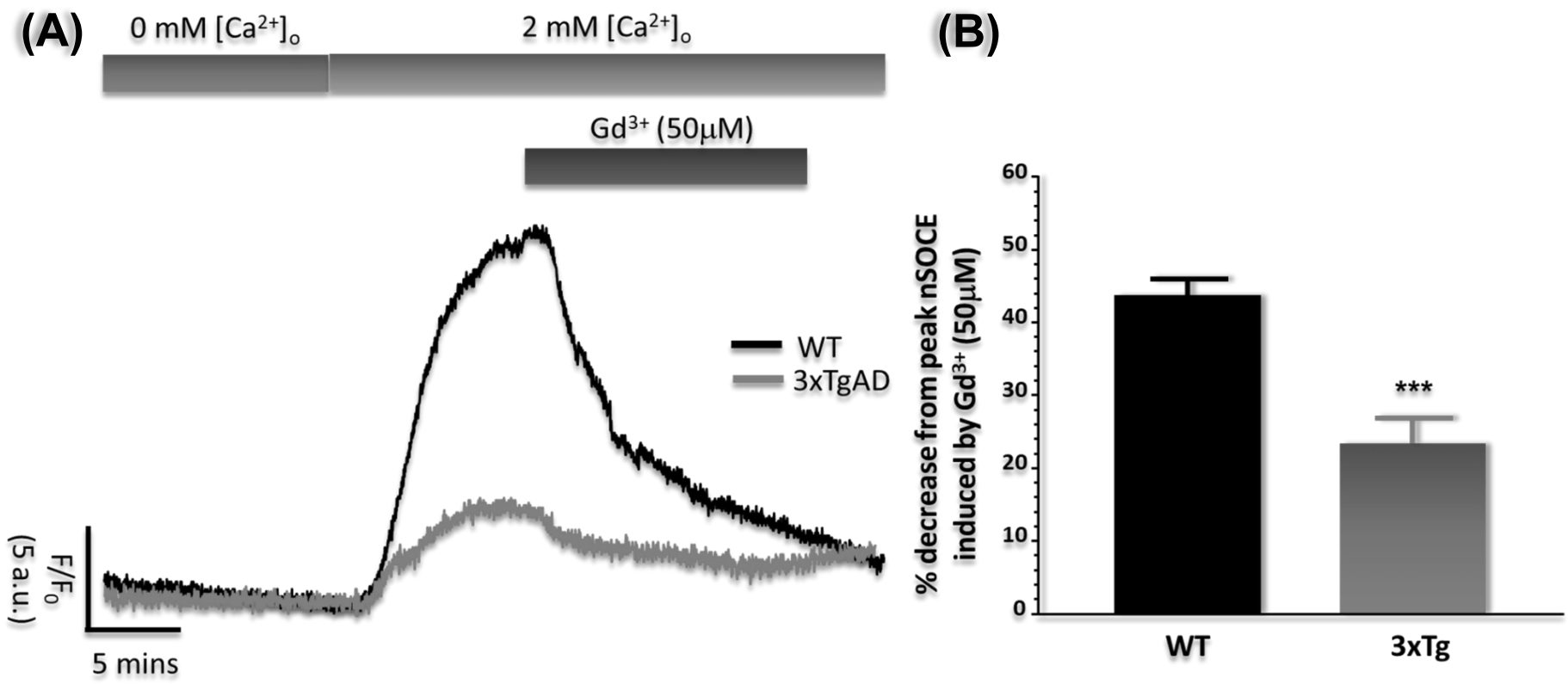

Figure 3.12. Gadolinium (Gd^{+3}; 50 mM) inhibits neuronal store operated Ca^{2+} entry (SOCE) in both 3xTg-AD hippocampal neurons and wild type (WT) age matched controls (3 – 5-days-old) from 5 – 14 days *in vitro.*

A. Superimposed calcium imaging traces obtained from WT (black) and 3xTg-AD (red) neurons.

B. Histogram illustrating that the percentage Gd^{+3} - evoked decrease in neuronal SOCE (determined 4 mins from peak fluorescence) is significantly smaller in 3xTg-AD (n = 29, 3 separate experiments) relative to WT (n = 35; 2 separate experiments) hippocampal neurons.

Comparison of ER Ca^{2+} levels using the SERCA inhibitor TPN between non-Tg and 3xTg-AD mice

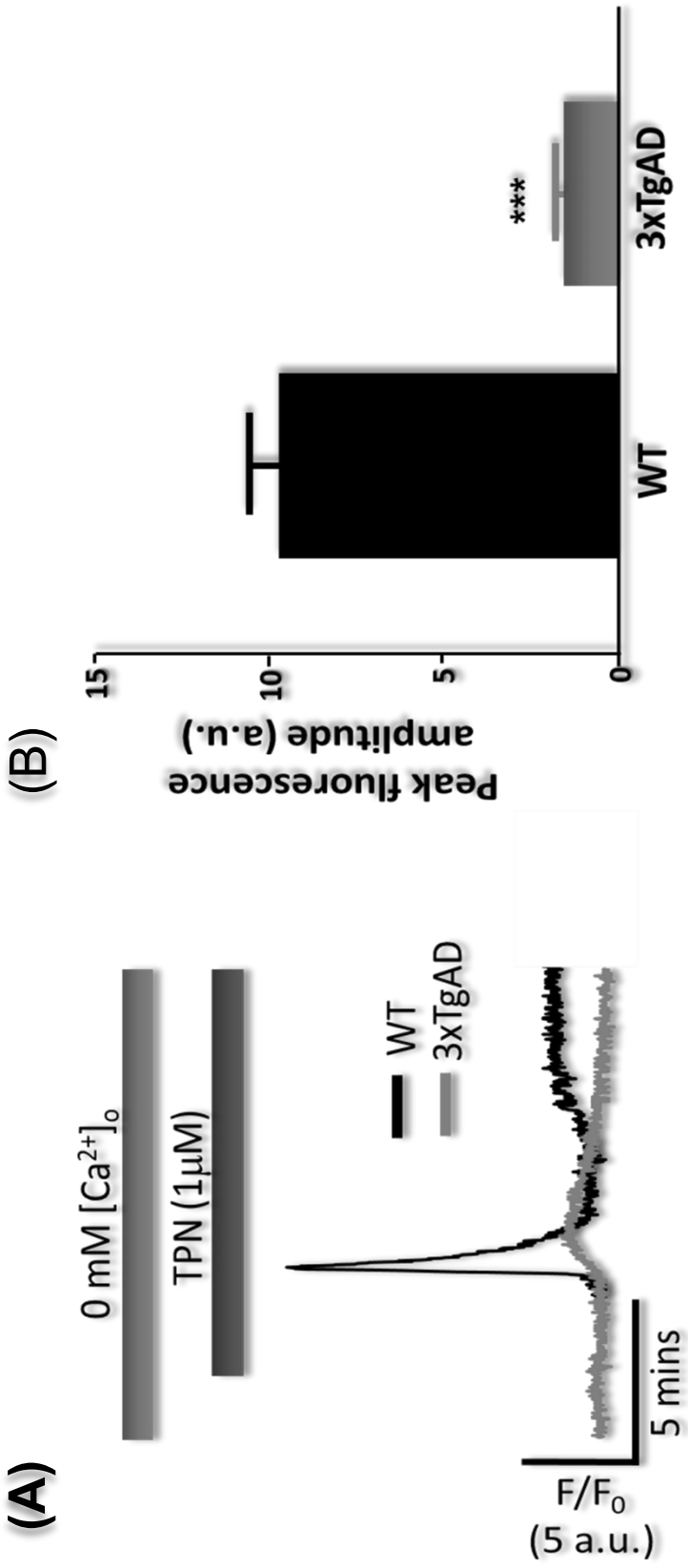

Figure 3.13. Thapsigargin (TPN; SERCA inhibitor; 1 mM)-evoked ER Ca^{2+} release is greater in wild type age matched controls (WT; 3 – 5-days-old) than 3xTg-AD hippocampal neurons from 5 – 14 days *in vitro*.

A. Superimposed calcium imaging traces obtained from WT (black) and 3xTg-AD (red) neurons.

B. Histogram illustrating that the peak fluorescence evoked by TPN (1mM; SERCA inhibitor) in Ca^{2+} free HBSS is significantly greater in WT (n = 35; 2 separate experiments) than 3xTgAD (n = 29; 3 separate experiments) hippocampal neurons.

The peak amplitude of SOCE-mediated Ca^{2+} influx (following Ca^{2+} “add back”) in 3xTg-AD neurons was significantly reduced compared to that evoked in non-Tg neurons (Fig 3.11; by 46 ± 10%, $p < 0.0001$; non-Tg, n=65; 3xTg-AD, n = 57). Gd^{3+} (50 μM) significantly inhibited SOCE in both non-Tg and 3xTg-AD hippocampal neurons but the degree of SOCE inhibition was significantly greater in non-Tg neurons (Fig 3.12; by 21 ± 5% (% decrease from peak SOCE-mediated amplitude); $p < 0.001$; non-Tg, n = 35; 3xTg-AD, n = 29). However, it should be noted that this effect may simply have been due to the fact that the peak amplitude of SOCE was significantly smaller in 3xTg-AD than in non-Tg neurons, and therefore there was already a reduced driving force for calcium entry in 3xTg-AD neurons relative to the non-Tg neurons. Additionally, the intracellular Ca^{2+} elevation evoked by TPN (1 μM) was significantly reduced in 3xTg-AD neurons relative to non-Tg neurons (Fig 3.13; by 85 ± 10%, $p < 0.001$; non-Tg, n = 25; 3xTg-AD, n = 11).

3.5 Discussion

3.5.1 General characteristics of I-mGluR responses

Previously established mechanism of depolarisation- and DHPG-mediated responses

This chapter centres on the intracellular Ca^{2+} responses of hippocampal neurons to I-mGluR stimulation under basal and depolarisation conditions. The mechanistic understanding of the intracellular processes occurring during these protocols has been extensively characterised in similar cells and as such was not a focus of investigation in the current study. Briefly, neuronal depolarisation results in the influx of Ca^{2+} through L-type VGCCs. This Ca^{2+} is then actively transported into the ER by SERCA such that it enhances I-mGluR-mediated Ca^{2+} mobilisation from this store, relative to basal conditions (*e.g.* Rae et al., 2000; Rae and Irving, 2004). As mentioned previously, L-type VGCC and I-mGluR co-activation produce supralinear/additive $[Ca^{2+}]_i$ responses (*e.g.* Rae and Irving, 2004). However, as the Ca^{2+} imaging technique used in the current study cannot accurately determine supralinearity, we will discuss similarly evoked responses in terms of whether they are simply “enhanced” under depolarisation conditions relative to control.

A notable difference between the current study and previous research was evident in the responses of hippocampal neurons to depolarisation. Rae and Irving (2004) showed that depolarisation of rat CA1 hippocampal pyramidal neurons in acute slices (by 30 mV from an initial holding potential of -60 mV) evoked only a ‘modest’ increase in $[Ca^{2+}]_i$. Rae et al. (2000) also showed, utilising cultured rat hippocampal neurons, that depolarisation (extracellular application of K^+ 10.8 mM (~18 mV depolarisation) *or* depolarisation of 10 ± 1 mV from a mean resting potential of −52 ± 2 mV) resulted in a ‘small’ increase in $[Ca^{2+}]_i$. In contrast to these studies, in the current experiments, application of the depolarisation stimulus (15 mM K^+ = ~28 mV depolarisation) caused a large intracellular calcium response and a characteristic plateau, in cultured hippocampal neurons (across species and strains; Fig 3.4; iii & iv). We had concerns that such a relatively large increase in $[Ca^{2+}]_i$ produced by the depolarisation stimulus may interfere in some way with the cells’ ability to handle Ca^{2+} and produce DHPG-mediated increases in $[Ca^{2+}]_i$. The degree of depolarisation will primarily alter Ca^{2+} influx but may also alter more subtle intracellular signalling dynamics. For instance, a difference in holding potential (-30 mV (Rae and Irving, 2004) *vs* -70 mV (Mannaioni et al. 2001) was proposed as a possible explanation as to why signs of both mGluR1- *and* mGluR5-mediated signalling could be detected at -30 mV (Rae and Irving, 2004), but only signs of mGluR1-mediated signalling could be detected at around resting potentials (Mannaioni et al. 2001) in rat CA1 pyramidal neurons. Notably, an increased

level of depolarisation may also allow for the activation of G protein-independent I-mGluR-mediated signalling pathways (Gee et al., 2003). In this context, we compared paired responses of neurons to I-mGluR stimulation following depolarisation with either 10 mM or 15 mM K^+ and found that although responses were increased with the utilisation of either depolarisation stimulus, relative to basal conditions, this was significant solely when utilising 15 mM K^+ (data not shown).

Rae et al. (2000) also utilised a 5 – 10 min equilibration period after depolarisation and prior to DHPG application. However, given the rapid increase and stable plateau of $[Ca^{2+}]_i$ (as long as the K^+ stimulus was present) following K^+ -mediated depolarisation (Fig 3.4, B, iii & iv; 3.5, A), we reduced this period to 2 minutes in our study. However, although time did not permit me to conduct such experiments, it would be interesting to determine how long the depolarisation-mediated enhancement of I-mGluR signalling persists for after removing the depolarisation stimulus, as depolarisation-mediated increases in $[Ca^{2+}]_{ER}$ have been proposed as a mechanism for recency detection of neuronal activity (Rae et al., 2000). In cultured rat hippocampal neurons and CA1 neurons from acute hippocampal slices, this facilitation persisted for up to 8 - 10 minutes following removal of the store loading stimulus (Rae and Irving, 2003; Rae et al., 2000). This supports the suggestion that the extent to which DHPG-mediated calcium responses are enhanced following depolarisation (relative to basal conditions) is a direct reflection of the state of loading of the Ca^{2+} stores and that leak from these stores occurs relatively slowly (Rae et al., 2000). The persistence of the ER-mediated calcium signals (and that seen by other groups; Garaschuk et al., 1997; Irving and Collingridge, 1998) also suggests that the enhancement of I–mGluR evoked $[Ca^{2+}]_i$ responses by depolarisation occurs independently of cytosolic Ca^{2+}, which returns to baseline within this persistence window, and thus may reflect $[Ca^{2+}]_{ER}$ solely.

We were also interested in how extracellular Ca^{2+} could modify I-mGluR signals in our cultured hippocampal neurons. Indeed, $[Ca^{2+}]_o$ modulates glutamate-stimulated mGluR1 responses in a variety of recombinant systems (Gabellini et al., 1993; Kubo et al., 1998; Kubokawa et al., 1996; Nash et al., 2001). In rat hippocampal CA1 neurons, the removal of Ca^{2+} from the external media (or removal of $[Ca^{2+}]_o$ combined with the inclusion of EGTA in the external media) for 20 mins prior to I-mGluR stimulation markedly decreased $[Ca^{2+}]_i$ responses (by 80.2 ± 6.9 and 95.6 ± 1.3% respectively; Rae and Irving, 2004). When we attempted to replicate this experiment utilising cultured non-Tg mouse neurons, albeit without the electrophysiological component, we also found that there was a trend towards decreased DHPG-evoked $[Ca^{2+}]_i$ signals under depolarisation conditions when external Ca^{2+} was removed, relative to control, although the

decrease was not statistically significant (67 ± 22% reduction; p = 0.17; n = 9; 3-days-old/13 DIV). Notably, several previous studies have suggested that calcium is required for receptor-ligand interactions in I-mGluR signalling (Mutel et al., 2008; Nash et al., 2001; Thomsen et al., 1993). Therefore, the fact we continued to observe DHPG-evoked $[Ca^{2+}]_i$ signals under "0" mM Ca^{2+} conditions could indicate that there was still sufficient residual Ca^{2+} in the perfusion system following the period of washout used (50 mins). On the other hand, the fact that Rae & Irving (2004) could still evoke I-mGluR-mediated $[Ca^{2+}]_i$ responses when removal of external Ca^{2+} from media was combined with EGTA calls this Ca^{2+} dependence suggestion into question.

Characterisation of I-mGluR responses in cultured mouse and rat hippocampal neurons

Previous research by Rae *et al.* (2000) found that under basal conditions DHPG (R, S-DHPG; 100μM) application to cultured SD rat hippocampal neurons evoked little or no increase in intracellular Ca^{2+} levels in the majority of neurons tested (45% and 23%, respectively). However, in acute hippocampal slices from the same group (Rae and Irving, 2004) found that the same concentration of DHPG (again under basal conditions) evoked a small increase in somatic Ca^{2+} in the majority (81%) of SD rat CA1 pyramidal neurons (Rae and Irving, 2004) which may reflect a fundamental difference in the nature of ER calcium signals between neurons that have been cultured compared to neurons *in situ* in a brain slice. In the current investigation, I conducted a similar but extended analysis of several genotypes of neurons, the results of which are presented in Figure 3.3. From this work, numerous notable differences in the nature of DHPG-elicited responses between the current study and previous research were identified.

Firstly, the aforementioned relatively small magnitude of DHPG-evoked $[Ca^{2+}]_i$ responses generated under basal conditions either in cultured neurons or in hippocampal slices suggests that in the majority of non-transgenic neurons, across numerous studies, species and cell types, ER Ca^{2+} stores are functionally depleted (Garaschuk et al., 1997; Irving and Collingridge, 1998; Koizumi et al., 1999; Rae et al., 2000; Rae and Irving, 2004; Shmigol et al., 1996). Although it is difficult make direct comparisons between the magnitude of calcium responses generated across studies (as they are not routinely quantified in terms of calcium concentration), DHPG-mediated responses of cultured SD rat hippocampal neurons under basal conditions were robust and not fundamentally dissimilar from responses under depolarisation conditions, in the current study (Fig 3.8). Such robust responses under basal conditions were also observed in neurons from non-Tg F344 rats (Fig 3.9) and non-Tg mice (Figs 3.5). One possible explanation for this finding is that the relatively small responses observed in previous studies are below the detection threshold of the equipment used in the

current study (personal communication comparing the nature of responses recorded in previous studies with those in the current study with one of the original authors, Dr M.G. Rae).

In terms of the proportion of neurons which responded under basal conditions, a response rate of 68 ± 5% for cultured SD rat neurons, (and indeed of 54 ± 5% and 27 ± 18% for non-Tg mouse and non-Tg rat neurons, respectively; Figure 3.3), is considerably lower than that seen by Rae et al. (2004) in SD rat intact slices (81%). This may reflect advantages in the function and/or health of the overall cell population utilising intact tissues as opposed to cultured cells. That being said, the total number of responding neurons under basal conditions was also slightly lower in our study relative to that of Rae et al. (2000) in similarly cultured SD rat hippocampal cells (68 ± 5% in this study *vs* 77%). However, this observation may simply reflect the aforementioned potential difference in the detection threshold of our equipment. Differences between these studies may also reflect the fact that "SD rats" are an outbred, genetically diverse group of animals which would likely lead to significant phenotypic variability in the rats held by different lab groups and possibly even between different litters (Brower et al., 2015; Jensen et al., 2016). Aside from phenotypic differences arising from the utilisation of acute hippocampal slices compared with cultured hippocampal neurons, differences in culturing techniques between groups may also increase phenotypic variability. For example, in contrast to the current study which utilised 2% SR2 to supplement culture media (in order to inhibit glial cell growth Kaar et al., 2017), Rae et al. (2000) supplemented their media with 10% FBS, which would almost certainly increase glial growth which, in turn, could alter the excitability and/or survival of cultured neurons (Igelhorst et al., 2015; Vezzani et al., 2008), as discussed previously (*Chapter 2*).

In agreement with Rae et al. (2004), DHPG-mediated calcium responses were monophasic (across species and under both depolarisation (89 ± 2%) and basal conditions (84 ± 3%) in this study *vs* 81% under basal conditions in the Rae et al. (2004) study) and consisted of a rapid rising phase and slower decay. Multi-phasic and/or oscillatory responses to DHPG were also observed across species and under both depolarisation and basal conditions in this study and, as noted by Rae et al. (2004), may reflect the initiation of CICR (Berridge et al., 2000).

The duration of DHPG-mediated calcium responses in SD rat hippocampal cultures observed in the current study was significantly longer than that observed in SD rat hippocampal slices (101 - 108 ± 6 s (basal and depolarisation conditions) *vs* 21 ± 4 s; current study *vs* Rae et al. (2004)). Moreover, the duration of DHPG-elicited calcium responses was in the range of 82 - 162 ± 11 s across the species and models utilised in this study and under basal and depolarisation conditions. Why the length of response to

DHPG is dramatically longer in the current study with respect to previous work is unknown but a possible explanation may be that the specific culturing method used in the current study in some way confers a phenotype which is less efficient at cytoplasmic Ca^{2+} clearance. Alternatively, and perhaps less likely, the equipment used in the current study may have been more sensitive to calcium elevations than earlier studies and so may have captured a greater duration of responses.

In contrast to our results with non-Tg mouse, non-Tg rat and SD rat neurons for which there was no significant difference in the temporal profile of I-mGluR responses, previous studies demonstrated that this parameter was increased under depolarisation conditions relative to basal conditions in SD rat hippocampal cultures and pyramidal neurons in intact tissue (unspecified and 72 ± 12 s increase, respectively; Rae et al., 2000, Rae and Irving, 2004). Why this aspect of I-mGluR responses was altered previously but not in the current study is unknown but may again reflect the genetic heterogeneity of "SD rats". Although not investigated in this study, the latency between agonist exposure and the subsequent response was also reduced under depolarisation conditions in SD rat neurons, suggesting that neurons are primed for activation in some manner, possibly due to depolarisation-mediated increases in IP_3 formation (Rae et al., 2000).

3.5.2 WT and non-Tg neurons

Enhanced neuronal calcium responses

The experiments carried out in this current study were largely guided by two previous studies which both utilised similar experimental protocols. In agreement with the first such study of Rae et al. (2000), the peak amplitude (370% *vs* approx. 126% (see Fig 3.8); Rae et al. (2000) *vs* current study) of DHPG-mediated calcium signals were significantly increased under depolarisation conditions relative to basal conditions (K^+ mM = 5.4 to 10.8 *vs* 5.4 to 15; Rae et al. (2000) *vs* current study) in cultured SD rat neurons (2-days-old, 6 – 21 DIV *vs* 2 - 5-days-old, 3 - 13 DIV; Rae et al. (2000) *vs* current study). Furthermore, in the sub-population of neurons which exhibited detectable responses under both basal and depolarisation conditions the normalised amplitude of the responses was increased by 77 ± 11% under depolarisation conditions in the current study (Fig 3.8).

The second guiding study by Rae and Irving (2004), using whole-cell patch-clamp recording, found that under depolarisation conditions (-70 mV to -30 mV), DHPG evoked enhanced $[Ca^{2+}]_i$ responses in SD rat CA1 hippocampal neurons in acute slices (743 ± 135% increase in normalised A.U.C.; increase in amplitude not quantified) relative to responses evoked

under basal conditions. (-70mV). In contrast to this study, we observed no statistically significant differences in the A.U.C. of responses when comparing depolarisation to basal conditions (Fig 3.8). Differences in the methodology used in each study, such as the use of cultured neurons over intact slices, the method utilised to produce cultured neurons, the age and/or development of neurons (previous studies utilised older/more developed cells *in vitro*), the degree of depolarisation used, as well as possible differences in analytical method, may explain these disparities. Furthermore, the aforementioned genetic diversity amongst SD rats may also play a role in the variable responses observed between studies.

The slightly less robust depolarisation-enhanced I-mGluR evoked calcium responses seen in the SD rats notwithstanding, the fact that these types of significantly enhanced calcium signals were also observed in non-Tg mouse neurons (Fig 3.5) and non-Tg F344 rat neurons (Fig 3.9), suggests that enhanced responses under depolarisation conditions may be a universal neuronal phenomenon, possibly acting a means of recency detection and/or triggering gene transcription (Rae et al. 2000).

3.5.3 Transgenic neurons

Neuronal calcium signalling under basal conditions

ER Ca^{2+} receptors are heavily implicated as mediators of neuronal calcium dysregulation in murine transgenic models of AD (including 3xTg-AD mice) and PS1 mutant mice (including $PS1_{M146V}$; cortical and hippocampal neurons; Chakroborty et al., 2009; Chan et al., 2000; Guo et al., 1999; Smith et al., 2005; Stutzmann et al., 2006; Supnet et al., 2006; Zhang et al., 2010).

The observation in the current study that DHPG-mediated $[Ca^{2+}]_i$ responses (amplitude, duration and A.U.C.) are dramatically and significantly larger in 3xTg-AD neurons when compared with non-Tg controls under basal conditions (Fig 3.7, A) is in agreement with preliminary observations by this group (which I was involved in) comparing non-Tg and 3xTg-AD cultured mouse hippocampal neurons (Morley et al., 2012). Furthermore, the findings are also in agreement with subsequent studies in my lab examining dentate gyrus neurons in *ex vivo* hippocampal slices (A.U.C. = 1558 ± 189 a.u. *vs* 700 ± 66 a.u.; $P < 0.05$, n = 20; 19 ± 10 days-old; Vaughan et al., 2018). These data were generated using similar experimental protocols, which have since been optimised with regard to the culture method employed (Kaar et al. 2017) and DHPG washout time (as previously described, see methods). Furthermore, it has been shown previously that direct stimulation of IP_3Rs (with caged IP_3) resulted in somatic $[Ca^{2+}]_i$ responses which were up to 300% larger in cortical neurons from 3xTg-AD and $PS1_{M146V}$ mice (same PS1

mutation as that of 3xTg-AD mice) relative to age-matched controls (Stutzman et al. 2007). Similarly, RyR-mediated $[Ca^{2+}]_i$ responses were also much larger (approximately 400%) in cultured 3xTg-AD hippocampal neurons in comparison to non-Tg neurons (Zhang et al. 2010).

As discussed in *Section 1.3 Ca^{2+} signalling* and investigated in *Chapter 4*, I-mGluR $[Ca^{2+}]_i$ responses are mediated primarily by Ca^{2+} release from the ER through IP_3Rs in hippocampal neurons. Thus, the enhanced ER Ca^{2+} mobilisation through IP_3Rs (and RyRs) is likely to be due to a pathological increase in $[Ca^{2+}]_i$ throughout the neuron, but particularly within the ER which is consistent with the Ca^{2+} hypothesis of AD (*Section 1.4*). In attempting to explain the elevated $[Ca^{2+}]_i$ caused by certain AD-linked mutations, Zhang *et al.* (2010) proposed that the $PS1_{M146V}$ mutation expressed in 3xTg-AD mice was the principal underlying cause of the enhanced $[Ca^{2+}]_{ER}$ as it impairs the normal constitutive calcium leak function of PS1. Specifically, ER Ca^{2+} leak was approximately 2.5 times less efficient in 3xTg-AD neurons relative to non-Tg neurons and, as a result, ER Ca^{2+} levels were 3-fold higher in 3xTg-AD neurons (Zhang et al. 2010). Interestingly, in these neurons, Ca^{2+} appeared to specifically accumulate in an ER pool which, in contrast to non-Tg neurons, was not depleted following TPN treatment. The authors suggested that the existence of this “TPN-insensitive” calcium pool was compensatory in nature and arose due to impaired PS1 leak function (Zhang et al., 2010). In agreement with this study and others (Leissring et al., 2000; Yoo et al., 2000), and with the proposal of increased ER Ca^{2+} levels in neurons from $PS1_{M146V}$ (specifically 3xTg-AD) mice, in the current study SOCE-mediated Ca^{2+} influx in 3xTg-AD neurons is significantly dampened (Fig 3.11) as is the effect of SOCE inhibition (Fig 3.12) relative to non-Tg neurons. Such an effect makes intuitive sense as SOCE is normally stimulated by low ER calcium, but if the ER is overloaded with Ca^{2+} then the stimulus for SOCE initiation may be blocked or attenuated. In further agreement with Zhang et al. (2010), the intracellular Ca^{2+} elevation evoked by TPN was significantly reduced in 3xTg-AD neurons relative to non-Tg neurons (Fig 3.13) suggesting a $PS1_{M146V}$-dependent impairment in the passive leak of Ca^{2+} from the ER leading to a hyper-loaded ER state.

Aside from utilising differences in SOCE-elicited signals as an indirect comparison of ER Ca^{2+} levels between non-Tg and 3xTg-AD neurons, the fact that SOCE is not just involved in replenishing ER Ca^{2+} levels but may also play a role in the regulation of the ER/cytoplasmic Ca^{2+} gradient (Brandman et al., 2007) could have important implications for differences in Ca^{2+} homeostasis and signalling between these two populations. Indeed, PS-mediated synaptic deficits in AD are thought to be mediated by dysregulated SOCE (Bezprozvanny et al., 2013; Popugaeva et al., 2012; Tong et al., 2016). Interestingly, specifically with regard to AD aetiology,

SOCE disruption stimulates $A\beta_{42}$ generation, whereas SOCE disruption itself is not due to Aβ-mediated effects (Herms et al., 2003; Leissring et al., 2000; Yoo et al., 2000).

Aside from the possibility of increased ER store content of Tg neurons being responsible for increased IP_3R- and/or RyR-mediated Ca^{2+} mobilisation, relative to non-Tg controls, it is also possible that increased RyR and IP_3R expression plays a role (Chakroborty et al., 2009; Chan et al., 2000; Smith et al., 2005; Stutzmann et al., 2007, 2006; Zhang et al., 2010). We investigated this possibility in 3xTg-AD, TgF344-AD hippocampal lysates and age-matched non-Tg controls in *Chapter* 5.

Unfortunately, it was not possible to carry out similar comparisons to those carried out utilising the 3xTg-AD model, between non-Tg and TgF344-AD rat neurons, due to the relatively low numbers of experiments that I was able to conduct using these animals. This was primarily due to the fact that, whilst conducting these experiments, and for reasons outside of my control, this animal model became unavailable.

Neuronal calcium signalling under depolarisation conditions

Unlike data obtained from non-Tg mouse neurons (Fig 3.5; and from non-Tg rat (Fig 3.9) and SD rat neurons (Fig 3.8)), the amplitude and normalised amplitude of DHPG-evoked responses were not enhanced under depolarisation conditions in 3xTg-AD neurons, relative to basal conditions (Fig 3.6). In fact, interestingly, duration and A.U.C. of DHPG-evoked responses were *decreased* in 3xTg-AD neurons under depolarisation relative to basal conditions (Fig 3.6) which is in stark contrast to non-Tg mouse and rat neurons (Fig 3.5 & Fig 3.9) which exhibited a significant increase in both parameters under depolarisation conditions relative to basal conditions, as well as in contrast to SD rat neurons where duration and A.U.C. were unchanged between the two experimental conditions (Fig 3.8). A similar significant decrease under depolarisation conditions, relative to basal conditions, has also been observed in subsequent studies utilising 3xTg-AD dentate gyrus neurons in *ex vivo* hippocampal slices (37 ± 7% a.u. decrease in A.U.C.; n = 20; 19 ± 10-days-old; Vaughan et al., 2018).In the context of our hypothesis of both an intracellular environment and ER which are overloaded with Ca^{2+} under basal conditions, it is logical that a depolarisation stimulus (which loads the ER with Ca^{2+}; Rae and Irving, 2003) does not facilitate a significant enhancement of subsequent DHPG-evoked calcium signals in 3xTg-AD neurons relative to basal conditions.

A decrease in the duration and A.U.C. of calcium responses upon depolarisation in 3xTg-AD neurons is more difficult to explain. It could be possible that the first exposure of cells to DHPG alleviates a *chronic* increase in ER Ca^{2+}, such that even with the Ca^{2+} influx and efficient uptake by the ER following depolarisation, this still results in an I-mGluR response which is

smaller than that observed under chronically elevated conditions. As this decrease is only evident in the parameters of duration and A.U.C. and not amplitude (unchanged), it may suggest that the initial response to DHPG is not enhanced in 3xTg-neurons, whereas the maintenance of the response is reduced. A potential mechanism underlying such a reduction in response persistence could be increased coupling between L-type VGCC-dependent Ca^{2+} entry (or the signal produced in combination with I-mGluR stimulation) and molecular mechanisms which return intracellular and ER Ca^{2+} levels to baseline in 3xTg-AD neurons, *i.e*. extrusion mediated by PMCA (Berrocal et al., 2015, 2012; Mata et al., 2011) and NCX (Kessete Afewerky, 2016; Magi et al., 2016) and ER sequestration mediated by SERCA (Green et al., 2008) which are impaired in AD, in a manner dependent on $[Ca^{2+}]_i$ and $A\beta_{42}$. Alternatively, depolarisation-mediated Ca^{2+} influxes into a cytosol which is already overburdened with Ca^{2+} could negatively regulate the production of subsequent I-mGluR/ER Ca^{2+} transients, possibly as a means of neuroprotection. A candidate mediator of such neuroprotective modulation would have to negatively regulate IP_3Rs and/or RyRs, be upregulated by chronic increases in $[Ca^{2+}]_i$, but also be activated by acute (possibly VGCC micro domain-dependent) increases in $[Ca^{2+}]_i$. Possible mediators of such an effect are outlined in *Chapter 5* and include proteins such as Bcl-2, which suppresses Ca^{2+} release through both IP_3Rs, RyRs (Vervliet et al., 2016) and calcineurin, which is activated by Ca^{2+} and suppresses IP_3R-mediated Ca^{2+} release *via* receptor dephosphorylation (Cameron et al., 1997, 1995a, 1995b). Conversely, it may simply indicate that there was a deterioration of cells as experiments progressed, although this suggestion seems to be contradicted by the finding that repeated DHPG application controls in the same cells evoked reproducible responses (50 minute washout; data not shown), and by the fact that there was no decrease in the proportion of 3xTg-AD neurons responding to DHPG nor was there an increase in spontaneously active neurons (which we used as an indirect measurement of deterioration in a given population of cultured cells) between experimental phases (Fig 3.3).

Furthermore, under depolarisation conditions, the amplitude and A.U.C. of DHPG-evoked calcium responses were significantly increased in 3xTg-AD neurons, relative to non-Tg (Fig 3.7, B). This suggested that although 3xTg-AD neurons were unable to produce *enhanced* responses under depolarisation conditions relative to basal conditions (Fig 3.6), the *magnitude* of their responses in K^+ HBSS was increased when compared to those produced by non-Tg neurons under identical conditions (Fig 3.7; B). This could simply be due to the previously described generally enhanced levels of $[Ca^{2+}]_i$ in 3xTg-AD/$PS1_{M146}$ neurons, which could negate the effect of the depolarisation stimulus, despite its amplitude being enhanced in 3xTg-AD neurons relative to non-Tg (Fig 3.7; C).

TgF344-AD rat neurons (Fig 3.10) exhibited a different phenotype to that observed for 3xTg-AD neurons (Fig 3.6) when compared with age-matched non-Tg controls. Specifically, the amplitude and normalised amplitude of I-mGluR responses were not different when TgF344-AD neurons were compared with non-Tg control (Fig 3.9), *i.e.* both parameters were enhanced under depolarisation relative conditions to basal regardless of transgenic status. This suggests that there is no overt dysregulation in I-mGluR-mediated signalling in TgF344-AD neurons relative to non-Tg control at this age (7-days-old) and this development *in vitro* (3 – 7 DIV). In contrast, in 3xTg-AD neurons, amplitude and normalised amplitude were not enhanced under depolarisation relative to basal conditions.

Where the TgF344-AD phenotype did differ from that of the non-Tg F344 neurons was with respect to duration and A.U.C. of DHPG-elicited responses which were not significantly different under depolarisation conditions relative to basal conditions in TgF344-AD neurons (Fig 3.10) but which were enhanced in non-Tg F344 neurons (Fig 3.9). Possible factors underlying such an observation are outlined above in the context of the significant decrease observed in both duration and A.U.C. under depolarisation conditions relative to basal conditions in 3xTg-AD mouse neurons (Fig 3.6).

These differences in phenotype between the 3xTg-AD mouse and TgF344-AD rat models suggest that Ca^{2+} dysregulation at this early stage of development with respect to amplitude and normalised amplitude is determined by PS1 mutation (*i.e.* $PS1_{\Delta E9}$ *vs* $PS1_{M146V}$; TgF344-AD rat *vs* 3xTg-AD mouse) or the fact that the 3xTg-AD mice also express a mutation in *tau*. Where both mutations could converge in terms of pathogenic effects is with respect to attenuation of I-mGluR-mediated response persistence.

Work by Zhang et al. (2010) suggests that the $PS1_{\Delta E9}$ mutation, expressed by the TgF344-AD rats, resulted in a *gain*-of-leak-function of Ca^{2+} from the ER. Furthermore, at least in MEF cells, transfection with $PS1_{\Delta E9}$ normalised $[Ca^{2+}]_{ER}$ to WT levels despite the fact that in lipid bilayer studies, $PS_{\Delta E9}$ exhibits an approximately 2-fold increase in the rate of Ca^{2+} conductance when compared with WT PS1 (Tu et al., 2011). However, this gain-of leak function is not supported in the current study as the amplitude of I-mGluR-mediated responses under basal conditions (an indirect measurement of resting ER Ca^{2+} levels) was unchanged in TgF344-AD neurons relative to non-Tg controls (data not shown). Indeed, unlike comparisons between non-Tg and 3xTg-AD neurons (Fig 3.7), there were no differences between non-Tg and TgF344-AD neurons with regard to amplitude, duration or A.U.C. of DHPG-mediated responses under basal or depolarisation conditions, or to the depolarisation stimulus itself (data not shown). It may be the case then, that this proposed gain of leak function is

not evident, at least at this early developmental time point in TgF344-AD rat hippocampal neurons, or that it does not operate at a fast-enough rate to minimise the effects of depolarisation-induced ER loading and subsequent stimulation of enhanced responses under depolarisation conditions in TgF344-AD neurons (Fig 3.10).

The fact that there was a significant correlation between the increase in amplitude mediated by the depolarisation stimulus and the amplitude of DHPG responses exhibited by non-Tg mouse, 3xTg-AD mouse, SD rat and non-Tg rat neurons, whereas TgF344-AD rat neurons did not exhibit a significant correlation between these measurements (see 3.4.1 I-mGluR response characteristics), does however suggest a difference in the coupling of depolarisation and/or intracellular Ca^{2+} influx with ER Ca^{2+} release between these models. Interestingly, this is despite the fact that the proportion of TgF344-AD neurons which responded to depolarisation was significantly higher than non-Tg controls, suggesting they were in some way more sensitive to L-type VGCCs activation as a population (Fig 3.3). In circumstances where there is normal cellular calcium homeostasis, an increase in Ca^{2+} influx due to depolarisation and the opening of L-type VGCCs could logically cause larger I-mGluR-mediated Ca^{2+} responses, due to the Ca^{2+} uptake by SERCA into the ER. However, this would not necessarily be expected in 3xTg-AD or TgF344-AD neurons at this age and development *in vitro where PS-dependent ER* Ca^{2+} *dysregulation is likely* (Zhang et al., 2010). Alterations in, for example, L-type VGCC, SERCA, RyR, IP_3R and PS regulation, expression and/or stability could influence whether or not the amount of Ca^{2+} influx due to depolarisation correlates with the amount released from the ER following I-mGluR mediated stimulation. In the context of the Ca^{2+} hypothesis of AD, if the ER was chronically hyper-loaded with Ca^{2+}, one would expect that a further influx of Ca^{2+} would not correlate with an increased I-mGluR elicited Ca^{2+} release relative to basal conditions as this additional calcium could not be taken up by the ER. However, such a correlation *is* observed in data from 3xTg-AD neurons and suggests that the ER may not be loaded *to capacity* in 3xTg-AD neurons under basal conditions. Alternatively, the initial application of DHPG under basal conditions could alleviate the hypothesised chronic increase in ER Ca^{2+} levels (Popugaeva and Bezprozvanny, 2013), such that when DHPG was subsequently applied under depolarisation conditions, this Ca^{2+} influx stimulus is able to increase ER Ca^{2+} levels and, as such, the nature of responses to DHPG. Although there are fundamental differences between TgF344-AD rats and 3xTg-AD mice, including the facts that they are different species, express different PS1 genes (which have opposite effects on ER Ca^{2+} levels; enhanced leak (TgF344-AD) *vs* impaired leak (3xTg-AD); Zhang et al. 2010) and that the 3xTg-AD mice alone express a *tau* mutation, the lack of correlation between the amplitude of depolarisation- and DHPG-

mediated responses observed in TgF344-AD neurons is puzzling given that the profile (at least in terms of amplitude and duration) of I-mGluR-mediated responses is not different in transgenic neurons relative to control. As described previously, if the proposed gain-of-leak $PS_{\Delta E9}$ mutation *were* active at this developmental timepoint the rate of calcium leak may not outcompete the rate of ER loading by SERCA over such an acute time period (Tu et al., 2011, Zhang et al., 2010) and prevent the stimulation of enhanced responses under depolarisation conditions, but its effects may be significant enough to alter the correlation between the amplitude of depolarisation- and I-mGluR-stimulated responses.

It also worth noting, however, that the correlation statistics described above reflect activity only within a subpopulation of neurons which exhibited measurable responses to depolarisation and may not capture the subtleties of store loading following depolarisation. Indeed, previous research has shown that store loading/depolarisation stimuli can enhance I-mGluR-mediated Ca^{2+} responses without any detectable increase in $[Ca^{2+}]_i$ arising from the depolarisation stimulus itself (cultured rat hippocampal neurons, dentate gyrus neurons from *ex vivo* intact hippocampal slices and pancreatic acinar cells; Mogami et al., 1997, Rae et al., 2000, Vaughan et al., 2018)).

Finally, it is worth noting that aside from the aforementioned increase in the proportion of TgF344-AD neurons which responded to the depolarisation stimulus relative to non-Tg controls, there were no differences in a) the proportions of neurons which exhibited detectable responses to DHPG under basal and depolarisation conditions (including those which responded solely under depolarisation conditions) or the depolarisation stimulus itself and b) the percentage of neurons which exhibited spontaneous activity under basal and depolarisation conditions between non-Tg and 3xTg-AD mouse, WT rat and non-Tg rat or non-Tg rat and TgF344-AD rat. This suggests that at the population level, there is nothing inherently different between these murine strains with regards to responsiveness to I-mGluR or L-type VGCC stimulation or spontaneous activity rather it is in the profile and magnitude of the responses themselves where differences between strains occur.

3.5.4 Limitations

Somatic Calcium Responses

The decision to measure somatic calcium responses was, in part, a pragmatic one due to the limitations of our imaging system. Depending on the focal plane, some neuronal processes could be discerned; however, this was not the case for the vast majority of cells we examined. Even if it had

been possible to view dendrites and spines in our hippocampal cultures, the optical resolution of our imaging system was of insufficient quality to accurately measure calcium transients in these microscopic structures. Ideally, it would have been preferable to employ two-photon confocal microscopy for these studies. Unfortunately, significant financial constraints aside, there are no confocal microscopes available at University College Cork that are configured to allow continuous perfusion of living tissue.

Global I-mGluR stimulation

I-mGluRs are prominently expressed in CA1 pyramidal neurons (Conn and Pin, 1997) and indeed, are widely distributed on pyramidal neurons (Lujan et al., 1996). Given that we were 'globally' superfusing an I-mGluR agonist onto neurons, the magnitude of the calcium responses was presumably determined largely by the expression and localisation of the neuronal I-mGluRs. Such global application results in activation of I-mGluRs throughout the neuron, a situation which is unlikely to replicate *in vivo* glutamate-mediated stimulation.

3.5.5 General discussion

Use of young animals

The use of young animals follows the "road map" for the direction of AD research proposed by Selkoe (2002) who, with regard to investigating the aetiology of AD, stated that "The earlier one looks, the better". The findings presented within this thesis support such an assertion as they demonstrate that clear mechanistic changes in calcium signalling occur at early stages of development in AD gene-expressing hippocampal neurons prior to, and apparently independently of, structural changes and or/protein aggregation. These changes, which could be responsible for an early, *subtle* memory loss syndrome, are likely to be underpinned by eventual synaptic deficits and loss at a much earlier stage than other late-stage and commonly investigated AD-related proteins/mechanisms such as Aβ plaques and tangles.

The physiological relevance of I-mGluR evoked hippocampal enhanced $[Ca^{2+}]_i$ signals

Intracellular calcium homeostasis and signalling are universally recognised as being essential to normal neuronal function and health (see *Section 1.3*; *e.g.* Stutzmann, 2007). Given the possibility that dysregulated calcium may also be a primary element in initiating and propagating AD, understanding intracellular Ca^{2+} dynamics in both health and disease states may be key to developing a treatment for the disease (Berridge, 2010). As such, our study not only adds to the current understanding of normal

neuronal calcium handling but also provides important information about how neuronal intracellular Ca^{2+} dynamics can be dramatically altered by specific gene mutations that are associated with FAD.

Specifically, with regard to the enhanced I-mGluR mediated Ca^{2+} signals observed in hippocampal neurons described here, similar types of responses (supralinear responses) may serve as a means of translating changes in neuronal activity (*e.g.* membrane depolarisation) into a physiological response, *via* the loading state of the ER. The Ca^{2+} loading state of the ER could serve as a means of coincidence detection following prior excitatory input to the neuron (*e.g.* which may, under certain circumstances generate back-propagating APs; Nakamura et al., 1999). The fact that these enhanced ER-mediated Ca^{2+} signals can be activated for a relatively long time period following Ca^{2+} loading of the organelle means that they could serve as a memory of recent synaptic activity (*i.e.* a recency detector; Rae et al., 2000). By enhancing the state of ER Ca^{2+} loading, phenomena such as membrane depolarisation and/or NMDAR activation can also increase the frequency and coupling between elementary release sites (Koizumi et al., 1999). This increased coupling could, in turn, lead to the generation of global Ca^{2+} signals which may ultimately convey Ca^{2+} signals from neurites and spines to the nucleus, leading to alterations in gene expression (Berridge, 1998; Nakamura et al., 1999). Indeed, supralinear calcium signalling *via* activation of NMDARs and I-mGluRs may be involved in the modulation of synaptic plasticity in CA1 hippocampal cells during weak stimulation paradigms (Rae et al., 2000), whereas NMDAR activation alone may be sufficient for modulation of synaptic plasticity when stimulation is sufficiently robust (Wilsch et al., 1998). The magnitude of such calcium signals generated by ER calcium release can also be further modulated due to the sensitivity of ER Ca^{2+} release channels to both luminal (Koizumi et al., 1999; Missiaen et al., 1992) and cytosolic $[Ca^{2+}]_i$ (Bezprozvanny et al., 1991; Nakamura et al., 1999). The loss of such physiological function and nuance due to AD-dependent Ca^{2+} dysregulation has the potential to contribute to memory impairments that are characteristic of the disease.

More pertinent to our understanding of the Ca^{2+} hypothesis of AD however, this work adds to the evidence that Ca^{2+} dysregulation is an early-stage event in the pathogenesis of at least certain forms of FAD which are likely caused by neuronal expression of specific PS1 mutations (Guo et al., 1998; Zhang et al., 2010). As discussed, this Ca^{2+} dysregulation takes the form of altered $[Ca^{2+}]_i$ and $[Ca^{2+}]_{ER}$, the former of which is dependent upon the activity of PLC, IP_3R, RyR and/or L-type VGCCs in PC12 and SH-SY5Y cells (Cedazo-Mínguez et al., 2002; Guo et al., 1998, 1997, 1996). In agreement with this, I-mGluR-mediated calcium signalling under basal and depolarisation conditions, likely involving a contribution from, to varying degrees, each of these components, exhibited an altered profile in transgenic

hippocampal neurons (3xTg-AD and TgF344-AD) expressing PS1 mutations relative to non-Tg controls, from a very early age (2 - 5-days-old/2 – 20 DIV; Fig 3.5 – 3.10) and this effect was particularly evident (across all parameters measured) in 3xTg-AD mouse neurons relative to non-Tg control (Fig 3.5 – 3.7).

$[Ca^{2+}]_i$ and $[Ca^{2+}]_{ER}$ are inextricably linked (Bandara et al., 2013; Das et al., 2012; Tu et al., 2006) and in AD, normal homeostatic mechanisms which would return increases in $[Ca^{2+}]_i$ back to baseline are overwhelmed, due in large part to the impaired buffering capacity of the ER. This, in turn, is primarily due to the fact that the ER is pathologically loaded with Ca^{2+} (Berridge, 2010; Mattson, 2002), a statement which the current study supports (see Fig 3.7, 3.11, 3.12 & 3.13). There are numerous lines of evidence that this is a PS1 mutation-dependent effect across a plethora of transgenic cell types (*e.g.* Leissring et al., 2000; see *Section 1.4.4 ER remodelling*) whereas in the context of LOAD, there is a surfeit of evidence for Aβo-mediated Ca^{2+} dysregulation (*e.g.* see Yu et al. 2009; *see Section 1.2.6 Molecular actions of Aβo and related metabolites*). Moreover, the ratio of $[Ca^{2+}]_i$ to $[Ca^{2+}]_{ER}$ in animal models of AD will be determined by which particular PS1 mutation is expressed, *i.e.* whether a mutation increases (including the $PS_{\Delta E9}$) or impairs (including $PS1_{M146V}$) ER Ca^{2+} leak (Zhang et al., 2010), given that 80% of the Ca^{2+} leak from the ER is mediated by PS1 (Tu et al., 2006). In both cases, PS1 mutation could result in chronically increased $[Ca^{2+}]_{cyt}$. In the case of $PS1_{M146V}$, this could occur due to the impaired buffering capacity of a hyper-loaded ER, whereas the $PS1_{\Delta E9}$ mutation could result in a chronically enhanced leak of Ca^{2+} into the cytoplasm. Our experiments in 3xTg-AD neurons which express the proposed impaired leak $PS1_{M146V}$ mutation support these hypotheses as I-mGluR stimulation, the primary consequence of which was to evoke ER Ca^{2+} mobilisation, is enhanced under basal conditions. Furthermore, as described previously, this study suggests an impairment in the passive leak of Ca^{2+} from the ER of 3xTg-AD neurons (Fig 3.13) relative to non-Tg controls, likely in a $PS1_{M146V}$-dependent manner which could lead to a hyper-loaded ER in these cells.

The relative contributions of RyR- and IP_3R- dependent Ca^{2+} signals to I-mGluR-mediated responses aside (see *Chapter 4 &* Kaar and Rae (2015)), this work also supports the extensive evidence that ER Ca^{2+} mobilisation through both IP_3Rs and RyRs is enhanced in AD models in a PS1-dependent manner (see *Section 1.4.4 - Alterations in receptor function*; *e.g.* Stutzman et al. 2007, Zhang et al., 2010).

Basal increases in ER Ca^{2+} levels such as that seen in 3xTg-AD neurons will also have critical implications for SOCE, for which low ER Ca^{2+} levels are a trigger (Venkatachalam et al., 2002). Indeed, Ca^{2+} responses

mediated by SOCE are much larger in non-Tg neurons relative to 3xTg-AD and PS DKO neurons (2-fold increase; cultured hippocampal neurons; 0 - 1-days-old; 12 - 13 DIV) and *in vitro* in cells expressing PS FAD mutations (Akbari et al., 2004; Herms et al., 2003; Leissring et al., 2000; Yoo et al., 2000). In agreement with these studies, we have also found that SOCE stimulation and its inhibition was significantly attenuated in 3xTg-AD cultured hippocampal neurons, relative to non-Tg controls (Fig 3.11 & 3.12). Crucially, in the context of AD pathogenesis, Ca^{2+} dyshomeostasis, including that specifically due to impaired SOCE (Herms et al., 2003; Leissring et al., 2000; Yoo et al., 2000), increases the production of pathological Aβo (Hartigan & Johnson, 1999).

Although I have proposed that I believe that the primary modulator of Ca^{2+} homeostasis observed in transgenic AD neurons used in this study is mutations in PS1, alterations in the levels of APP metabolites, including Aβo, could also contribute to the transgenic phenotype. This, in turn, will likely result in further modulation/dysregulation of the neuronal Ca^{2+} signalling system, including mGluR-mediated signalling, as described in *Section 3.1.4 - I-mGluR signalling and the Ca^{2+} Hypothesis of AD*. Notably, there is conflicting evidence for (Leissring et al., 2002; Lopez et al., 2008; Rojas et al., 2008) and against (Stieren et al., 2010) the ability of APP mutations (independently of PS1 mutations or Aβ production, which have both been definitively determined to cause increased $[Ca^{2+}]_i$; see *Section 1.3.3 Molecular actions of Aβo and related metabolites and Section 1.4 The calcium hypothesis of AD*) to cause neuronal Ca^{2+} dysregulation in animal models of AD. However, the FAD-linked APP mutants such as the Swedish, London, Indiana, Flemish and V717L mutations, had no effect on basal $[Ca^{2+}]_i$, $[Ca^{2+}]_{ER}$ or IP_3R-mediated Ca^{2+} mobilisation in neurosecretory PC12 cells (Stieren et al., 2010). As disparate types of Ca^{2+} dyshomeostasis were induced in our rat and mouse models of AD in spite of the fact that they expressed the same APP_{SWE} mutation, it suggests that this mutation is not the critical factor inducing the early Ca^{2+} dysregulation observed here. Support for this suggestion has been provided by the finding that the 3xTg-AD mutant APP and tau gene products are not expressed in cultured hippocampal neurons before DIV 18 (Zhang et al. 2010). However, that said, the levels of expression of these transgenes was not determined in this particular study so we are unable to state conclusively that they did not play some role in the neuronal Ca^{2+} dyshomeostasis described herein.

3.6. Conclusions

There are numerous differences in the nature of responses to depolarisation and I-mGluR stimulation under basal and depolarisation conditions when comparing cultured transgenic hippocampal neurons to non-transgenic controls. As I-mGluR-elicited calcium responses are mediated primarily by ER Ca^{2+} mobilisation, the differences in the responses observed with the transgenic phenotypes are likely due to alterations in ER Ca^{2+} handling. Under depolarisation conditions, differences in the influx of Ca^{2+} through VGCCs and its uptake by the ER may also influence this transgenic phenotype. Furthermore, the nature of dysregulated I-mGluR-mediated signalling is different when comparing responses from 3xTg-AD mouse or TgF344-AD rat tissue. The most likely candidate underlying Ca^{2+} dysregulation, in general, and also differences in the transgenic phenotype between models are leak-specific mutations in PS1 (*i.e.* γ-secretase and APP processing-independent functions of PS1; Zhang et al., 2010). Together, these data suggest that Ca^{2+} dysregulation is an early-stage phenotype of these particular transgenic models of Alzheimer's disease, *i.e.* PS1-linked FAD could result from chronic Ca^{2+} dysregulation, beginning at very early stages of development.

Moreover, this illustrates the potential effect Ca^{2+} dysregulation could have in the pathogenesis of LOAD. In this case, the cause of Ca^{2+} dysregulation is less clear (see *Chapter 1*) and could arise indirectly from mutations in genes related to APP processing or Aβo removal such as *ApoE* (Coon et al., 2007; Roses et al., 1995), *CLU/APoJ* (Woody and Zhao, 2016), *SORL1* (Rogaeva et al., 2007) and *TREM2* (Colonna and Wang, 2016; Guerreiro et al., 2013; Neumann and Daly, 2013; Yaghmoor et al., 2014) as well as from mutations in genes directly implicated in Ca^{2+} homeostasis such as *CALHM1* (Dreses-Werringloer et al., 2008). That being said, current understanding of AD suggests that subtle Ca^{2+} dysregulation (Khachaturian, 1989), which may precede excessive activation of the amyloidogenic APP processing pathway (Stutzmann, 2007), can induce degenerative pathology involving oxidative stress, mitochondrial impairment, synaptic dysfunction, cognitive deficits and, ultimately, widespread neuronal cell death which characterises the later stages of the disease (Berridge, 2010; Bezprozvanny and Mattson, 2008; Deshpande et al., 2006; Glabe and Kayed, 2006; Kelly and Ferreira, 2006; Stutzmann, 2007; Townsend et al., 2006).

4 ADP-ribosyl cyclase-mediated signalling

4.1 Introduction

Sections of this chapter are taken from a review publication by Kaar and Rae (2015) entitled '*Metabotropic glutamate receptor-mediated cyclic ADP ribose signalling*' which is published in Biochemical Society Transactions (Appendix 2).

In *Chapter 3* I discussed the classical PLC/IP_3R pathway, which is stimulated following I-mGluR activation. However, as mentioned there, several reports have indicated that certain downstream effects of I-mGluR activation, on membrane currents and intracellular Ca^{2+} release, occur independently of either PLC (Chavis et al., 1998; del Río et al., 1999; Ireland et al., 2004, 2002; Sohn et al., 2007; Young et al., 2004) and/or IP_3R activation (Currie et al., 1995; Gafni et al., 1997; Ireland et al., 2002).

These findings led to the suggestion that I-mGluR-mediated calcium signals could, under certain conditions, be mediated by activation of the other main ER calcium release channel, the RyR (Sohn et al., 2011). This was based upon the finding that the plant alkaloid, ryanodine, which can both activate and inhibit RyRs in a concentration-dependent manner, attenuated I-mGluR-evoked responses in rat cerebellar granule neurons and dorsal root ganglion (DRG) neurons (Crawford et al., 1997a; Irving et al., 1992). Furthermore, in dopaminergic neurons of the ventral midbrain, mGluR-mediated Ca^{2+} mobilisation occurs *via* activation of both IP_3R and RyRs (Higashida et al., 2003). Moreover, in "acutely dissociated" (*i.e.* cells which are dissociated and adhered to a substrate for immediate Ca^{2+} imaging (Min et al., 1996), as opposed to the use of cultured cells which are maintained *in vitro* prior to utilisation) rat CA1 hippocampal neurons it is proposed that I-mGluR-mediated Ca^{2+} mobilization was generated in its entirety by activation of the RyRs (Sohn et al., 2011).

The Ca^{2+}-mobilising second messenger cADPR was a prime candidate mediator of I-mGluR-mediated RyR activation as thousands of studies support the model of cADPR mobilisation from a RyR-sensitive ER source (see Morgan et al., 2005) and its activity is established in a plethora of neuronal and neuron-like cells (Currie et al., 1992; Empson and Galione, 1997; Hachisuka et al., 2007; Higashida et al., 2012, 2003; Hua et al., 1994; Jin et al., 2007; Lopatina et al., 2010; Sohn et al., 2011; Yue et al., 2009)(Currie et al., 1992). However, the exact means by which this interaction occurs has yet to be clearly delineated as cADPR does not appear to regulate RyR activity by directly binding to the channel itself (Morgan et al., 2005; Sitsapesan and Williams, 1995). Rather, it is hypothesized that cADPR activates some sort of molecular 'intermediary' which then binds to, and induces the opening of, RyRs (Sitsapesan and

Williams, 1995). As such, several cytosolic proteins including FKPB12.6 (Hashii et al., 2000b; Noguchi et al., 1997; Tang et al., 2002; Y. X. Wang et al., 2004), CaM (Lee et al., 1995; Thomas et al., 2001), CaMKII and PKA (Wehrens et al., 2005b) have been proposed as putative 'missing links' between cADPR generation and RyR activation.

cADPR sensitises RyRs to activation by CICR and increases their open probability, as opposed to a direct ligand-induced gating (Empson and Galione, 1997; Galione et al., 1991; Guo and Becker, 1997; Hachisuka et al., 2007; Lee, 1993). In terms of the modulation of this activity, at submaximal cADPR concentrations, there are synergistic interactions at the same site on RyRs between Ca^{2+}, Sr^{2+}, caffeine and cADPR, which are all known CICR enhancing molecules (Guo and Becker, 1997; Lee, 1993). It is also known that cADPR binding to RyR is unaffected by most CICR modulators (both endogenous and pharmacological), aside from high levels of Ca^{2+} which causes a minor inhibition of cADPR binding (Lee, 1991; Thomas et al., 2001), suggesting that these compounds modulate the CICR response rather than cADPR receptor binding. cADPR can sensitise RyRs to such an extent that they begin to respond to basal $[Ca^{2+}]_i$ and can also potentiate release activated by other signalling processes (Lee et al., 1993). Specifically, cADPR enhances CICR by orthograde signalling, *i.e.* that triggered by calcium influx, in neurons (Empson and Galione, 1997; Hashii et al., 2000b; Pollock et al., 1999). This, in turn, produces a retrograde signal, whereby cADPR-mediated Ca^{2+} mobilisation indirectly primes other RyRs an IP_3Rs (Chavis et al., 1996; Empson and Galione, 1997; Hashii et al., 2000b). Aside from the well-documented ability of cADPR to mobilise Ca^{2+} from intracellular stores, in 3T3 fibroblasts, it can also regulate basal $[Ca^{2+}]_i$(Bruzzone et al., 2003a; Franco et al., 2001a; Zocchi et al., 1998).

cADPR is abundant in the brain (Partida-Sánchez et al., 2001; Walseth et al., 1997) and ARC activity has been detected from 1 week of age in rat hippocampal tissue homogenates (Higashida et al., 2003; Reyes-Harde et al., 1999a). In the brain, cADPR plays a role in numerous calcium-dependent aspects of neuronal and glial signalling (Bruzzone et al., 2004; Lee, 2001) such as neurotransmitter release (Mothet et al., 1998; Verderio et al., 2001), excitability (Budde et al., 2000; Ceni et al., 2006), plasticity (Linden et al., 1995; Morikawa et al., 2003; Pollock et al., 1999; Reyes-Harde et al., 1999a) and neuron-glia signalling (Higashida et al., 2001a). It also plays an important role in regulating inflammation and repair processes in the brain (and other tissues) through the modulation of Ca^{2+} signalling and migration of inflammatory cells (Blacher et al., 2015).

4.1.1 ARC enzymes

cADPR is catalysed from β-nicotinamide adenine dinucleotide (NAD^+) by ADP ribosyl cyclase (ARC; Morgan et al., 2005). Currently, an "*Aplysia* cyclase" (Glick et al., 1991; Mothet et al., 1998) and two mammalian cyclases - CD38 and CD157 are well characterised which are homologous and structurally similar (Liu et al., 2005; Malavasi et al., 2008; Morgan et al., 2005; Prasad et al., 1996; States et al., 1992; Yamamoto-Katayama et al., 2002). Numerous studies suggest that CD157 does not play a critical role in brain ARC activity (Hirata et al., 1994; Hussain et al., 1998; Itoh et al., 1994; Kaisho et al., 1994; Kajimoto et al., 1996; Lopatina et al., 2014) and therefore, it will not be discussed in any further detail. CD38 is widely expressed in vertebrate cells (Zocchi et al., 1999), including neurons (human cerebral and cerebellar cortical lysates and cultured mouse hippocampal neurons; Ceni et al., 2003b; Mizuguchi et al., 1995), astrocytes (Banerjee et al., 2008; Ma et al., 2014) and microglia (Ceni et al., 2003a; Jin et al., 2007; Mayo et al., 2008), where it is known to influence Ca^{2+} homeostasis (Bruzzone et al., 2004; Higashida et al., 2007; Verderio et al., 2001) and cell survival (Ma et al., 2014). In the mouse, ARC activity was primarily mediated by CD38 and was highest in the hypothalamus with activity also detectable in the cerebellum, cerebrum and posterior pituitary (Jin et al., 2007). CD38 exhibits developmental dependent CNS expression with activity detectable from E15 in mouse (Choe et al., 2011; Higashida et al., 2007). CD38 staining is dense in the soma and dendrites of murine and human neurons (Ceni et al., 2003a; Jin et al., 2007; Mizuguchi et al., 1995) and is expressed on synaptosomes (Durnin et al., 2012) supporting a role for cADPR in synaptic transmission and plasticity (Linden et al., 1995; Morikawa et al., 2003; Pollock et al., 1999; Reyes-Harde et al., 1999a). In human neuronal cultures, co-culture of neurons with astrocytes resulted in astrocytic CD38 overexpression (both plasma membrane and intracellularly) in a glutamate-mediated fashion. It is suggested, therefore, that CD38 may also have a role in glutamate-mediated neuronal-glial communication (Bruzzone et al., 2004).

ARC enzymes have three known catalytic activities (Fig 4.1), the products of which stimulate distinct Ca^{2+} signalling pathways (Fig 4.1 & Fig 4.2; see (Berridge, 2014a; Fliegert et al., 2007):

1. Cyclisation of NAD^+ and nicotinamide guanine dinucleotide (NGD) to **cADPR** and cGDPR respectively. CD38 exhibits cyclase activity (Ceni et al., 2003b; Deshpande et al., 2003; Howard et al., 1993; Itoh et al., 1994; Quarona et al., 2013) producing a *relatively* small amount of cADPR (2% of products arising from the application of NAD^+ *vs* 98% ADPR, *in vitro*) regardless of which is still *physiologically* important

(Ceni et al., 2003a; Schuber and Lund, 2004; Takasawa et al., 1993; Ziegler, 2000).

2. Hydrolysation of NAD^+ and cADPR to **ADPR**, an enzymatic activity which is solely exhibited by CD38 and is its predominant mode of action (Hirata et al., 1994; Howard et al., 1993; Snell et al., 1984; Takasawa et al., 1993). ADPR is also involved in Ca^{2+} signalling (Ayub and Hallett, 2004) and homeostasis (Perraud et al., 2001; Sano et al., 2001) and activates RyR1 when micromolar $[Ca^{2+}]_i$ levels are also present (Bastide et al., 2002). The majority of investigations of ADPR-mediated Ca^{2+} signalling are concerned with the stimulation of Ca^{2+} entry into cells through TRPM2, a non-selective cation channel that is expressed in a variety of tissues, with highest levels in the brain and immune cells (for review of ADPR signalling see Ernst et al., 2013). ADPR-mediated activation of TRPM2 is synergised by $[Ca^{2+}]_i$, cADPR, NAADP and ROS (Sumoza-Toledo and Penner, 2011).

3. The production of **nicotinamide** and **$NAADP^+$** by catalysing a base exchange reaction, *i.e.* catalysing the exchange of the $NADP^+$ nicotinamide group with free nicotinic acid (Aarhus et al., 1995; Fliegert et al., 2007). The substrate $NADP^+$ which is required for this reaction is formed from NAD^+ by NAD^+ kinase (Pollak et al., 2007). NAADP is a Ca^{2+} mobiliser (for reviews see Fliegert et al., 2007 and Galione, 2011) which is considered to be critical for the development of global Ca^{2+} signals and the regulation of membrane excitability (Galione, 2011; Schmid et al., 2011). In different cell types it mediates its effects *via* IP_3Rs (Singaravelu and Deitmer, 2006), RyRs (Dammermann and Guse, 2005; Gerasimenko et al., 2006; Hohenegger et al., 2002; Langhorst et al., 2004) and two-pore channels (TPCs; expressed on endolysosomes; for review see Morgan et al., 2015; Patel et al., 2010) and from both ER and endolysosomal stores (Gerasimenko et al., 2003; Kinnear et al., 2004).

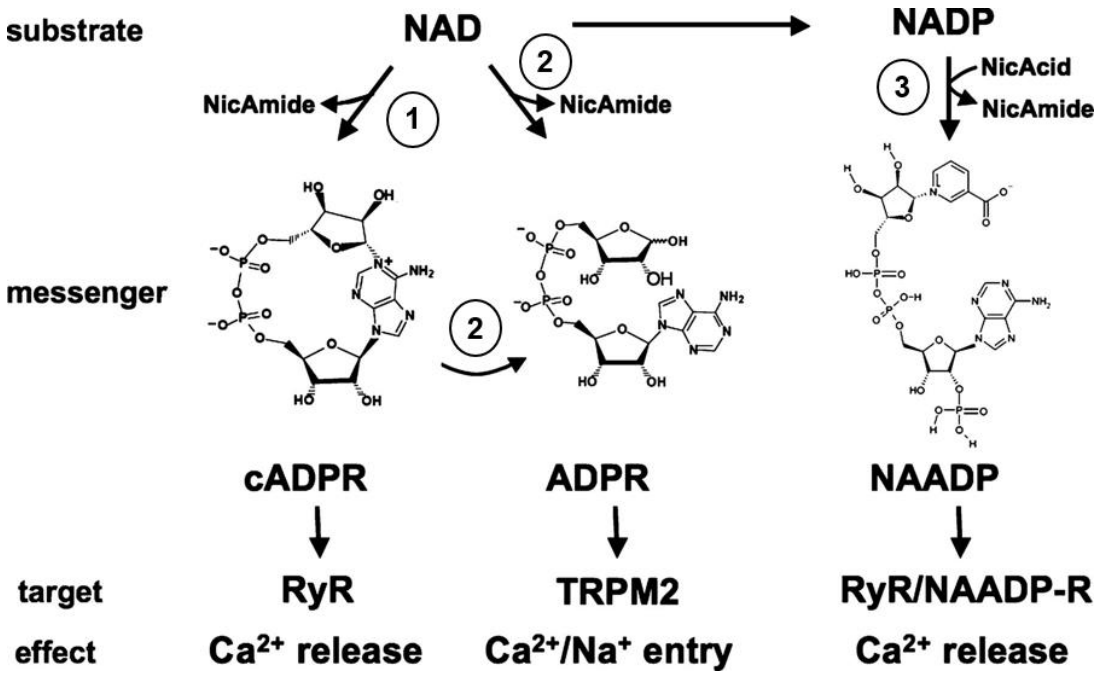

Figure 4.1 Formation of cADPR, ADPR and NAADP

There is a close metabolic relationship between these compounds that are formed from the three main enzymatic functions of ADP-ribosyl cyclases (ARCs):

1) cADPR is primarily formed from the cyclisation of the substrate NAD^+ (also producing nicAmide). cADPR mediates Ca^{2+} mobilisation through RyRs.

2) NAD^+ and cADPR are hydrolysed to ADPR (also producing nicAmide). ADPR activates Ca^{2+} and/or Na^+ entry through TRPM2.

3) NAD^+ is converted to $NADP^+$ by NAD^+ kinase. NADP is then converted by a base-exchange reaction to $NAADP^+$ and nicAmide. $NAADP^+$ activates RyRs and/or a proposed NAADP receptor (NAADP-R; which we now know is either RyRs, IP_3Rs or endolysosomal TPCs, dependent on cell type) resulting in intracellular Ca^{2+} mobilization.

Abbreviations used: ADP-ribose (ADPR), cyclic adenosine 5'-diphosphoribose (cADPR), nicotinamide adenine dinucleotide (NAD), nicotinate adenine dinucleotide phosphate (NAADP), the proposed NAADP receptor (NAADP-R), nicotinamide (NicAmide), nicotinic acid (NicAcid), two pore channel (TPC) and transient receptor potential (TRP) melastatin 2.

Modified with permission from Fliegert et al. (2007).

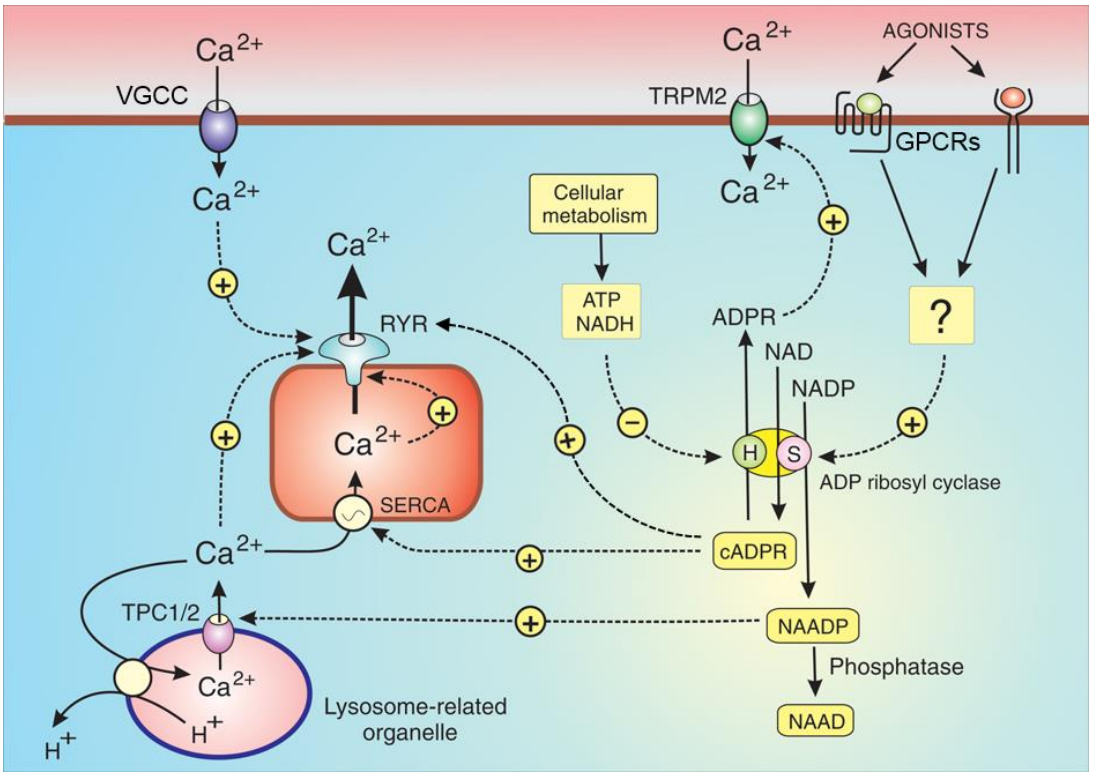

Figure 4.2 ADP ribosyl cyclase activation and associated intracellular signalling

ADP ribosyl cyclase (ARC) is activated by exogenous plasma membrane-bound receptors including GPCRs such as mGluRs. This produces three Ca^{2+} mobilising second messengers cADPR, ADPR and NAADP (from NAD, cADPR and NADP, respectively).

There are multiple proposed mechanism which result in cADPR-mediated Ca^{2+} mobilisation from ER, such as enhancing the activity of SERCA and by activation of RyRs.

ADPR activates TRPM2 channels causing Ca^{2+} influx whereas NAADP activates TPC channels on lysosome related organelles stimulating Ca^{2+} mobilisation resulting in an intracellular Ca^{2+} response, possibly in a co-operative manner with other relevant receptors such as VGCCs.

Note: ARC activity is also influenced by cellular metabolism and the levels of intracellular ATP and NADH.

Abbreviations used: ADP-ribose (ADPR), cyclic adenosine 5'-diphosphoribose (cADPR), G-protein-coupled receptor (GPCR), metabotropic glutamate receptor (mGluR) nicotinamide adenine dinucleotide (NAD), nicotinate adenine dinucleotide phosphate (NADP), nicotinic acid adenine dinucleotide phosphate (NAADP), sarco/endoplasmic reticulum Ca2+-ATPase (SERCA), transient receptor potential (TRP) melastatin 2 and voltage-gated Ca^{2+} channels (VOC)

Modified with permission from Berridge (2014)

Notably, evidence supporting ARC (including CD38) regulation of basal and/or stimulus-induced (Aarhus et al., 1995; Cosker et al., 2010) NAADP levels in a manner that is physiologically relevant is conflicting (Aarhus et al., 1995; Gul et al., 2016; Schmid et al., 2011) and has been shown in non-CNS cells, *in vitro* and in a cell-type specific manner. In fact, there is evidence from non-CNS cells and tissue that CD38 may degrade NAADP(Aarhus et al., 1995; Schmid et al., 2011; Soares et al., 2007). Alternatively, however, the degradation of NAADP to 2′-phospho-ADPR may also occur in these cells *via* nucleotide pyrophosphatases (Graeff et al., 2006).

Importantly, ARC preference for the production of either cADPR or NAADP can be altered with pH (Aarhus et al., 1995; Bacher et al., 2004; Graeff et al., 1998; Howard et al., 1993). When placed in an acidic environment (approximately pH 4.5 - 5) and with excess nicotinic acid, CD38 exhibited a preference for base-exchange activity and NAADP generation which outweighed its hydrolysis (Aarhus et al., 1995). However, when conditions were more neutral (both pH 7 and pH 7.4) with low nicotinic acid concentrations, base-exchange did not occur and degradation to 2′-phospho-ADPR was enhanced. cADPR was also produced at this more neutral pH. Given the importance of pH on ARC function, the location of the enzyme within the cell may be a primary determinant of enzyme activity.

The catalytic domains of membrane-bound ARC, including CD38 which is predominately a transmembrane ectoenzyme (Schuber and Lund, 2004), have been demonstrated as acting extracellularly, as measured by the extracellular production of ADPR, cADPR and NAADP utilising numerous cell types including rat cortical astrocytes (Gelman et al., 1993; Hirata et al., 1994; Hotta et al., 2000; Hussain et al., 1998; Ishihara and Hirano, 2000; Itoh et al., 1994; Kajimoto et al., 1996; Malavasi et al., 2008; Pawlikowska et al., 1996; Yamamoto-Katayama et al., 2002). This leads to the “topological paradox” of cADPR production (De Flora et al., 2004), *i.e.* that extracellular synthesis of cADPR conflicts with intracellular activity. However, there are numerous ways in which this paradox could be satisfied physiologically. Firstly, NAD^+ efflux and availability may be enabled via the gap junction protein connexin 43 (Cx43; Bruzzone et al., 2001a) and connexin 43 (Cx43)-independent transporters, including P2X, ligand-gated ion channel, 7 (P2X7R)-mediated NADH / NAD^+ symport (Lu et al., 2007; Romanello et al., 2002; Salmina et al., 2014). Cx43-mediated NAD^+ efflux is hypothesised to be negatively regulated by Ca^{2+}-dependent (Zocchi et al., 1999) and PKC-mediated phosphorylation of Cx43. This decreases the open probability of Cx43 connexon, preventing NAD^+ delivery to the proposed extracellular active site of CD38, thereby inhibiting CD38-mediated Ca^{2+} increases (Bruzzone et al., 2001). There are also three potential mechanisms for cADPR influx which could also allow cADPR to act as a paracrine Ca^{2+}

signalling molecule (De Flora et al., 2004; Franco et al., 2001). Namely, CD38-mediated concentrative cADPR transport (De Flora et al., 2004; Franco et al., 1998; Jin et al., 2007), co-internalisation with CD38 possibly in a ligand (Zumaquero et al., 2010) and-or NAD^+-induced manner (McCarthy et al., 2003) which may be balanced with lysosomal degradation of CD38 at least during periods of prolonged RyR1 activation (Chidambaram and Chang, 1999; Franco et al., 1998; M.-K. Han et al., 2002; McCarthy et al., 2003; Zocchi et al., 1999) and CD38-independent transport (both concentrative and equilibrative) of cADPR (Bruzzone et al., 2003b; De Flora et al., 2004; Franco et al., 2001; Guida et al., 2002) by nucleoside transporters (Guida et al., 2004, 2002). These discussions centre upon the assumption that CD38 is an ectoenzyme. However, extra-plasma membrane expression of CD38 and the presence of non-CD38 ARC enzymes (see below) may negate the issues surrounding the topological paradox in certain cell types. In more detail, CD38 expression has been detected in the cytosol (Durnin et al., 2012) and in ER, mitochondrial, nuclear and exosome membranes in numerous non-neuronal cell types (Adebanjo et al., 1999; Khoo et al., 2000; Khoo and Chang, 2002, 1999; Matsumura and Tanuma, 1998; Orciani et al., 2008; Sternfeld et al., 2003; Sun et al., 2002; Zumaquero et al., 2010). Furthermore, in addition to the type I conformation, where the CD38 active site is extracellular, CD38 has been observed in type II (intracellular) conformation, allowing for cADPR and ADPR production in the cytosol (Zhao et al., 2012).

Importantly, in the context of this thesis, CD38 and RyRs were colocalised in osteoblastic MC3T3-E1 cells and NIH3T3 cells, suggesting a functional coupling of CD38 to intracellular Ca^{2+} mobilisation (Sun et al., 2002). Furthermore, mitochondrial CD38 expression (Liang et al., 1999) has potential relevance to both the upregulated Ca^{2+} signalling and activation of cell death pathways evident in AD (Celsi et al., 2009). In more detail, mitochondrial impermeability to NAD^+ (Stein and Imai, 2012) is compromised following MPT-opening which, aside from depleting mitochondrial NAD^+, also perturbs cellular levels of NAD^+ and NADH. This culminates in the activation of NAD^+-glycohydrolases, which alters cellular bioenergetics (Kristian et al., 2011). The localisation of Cx43 in the mitochondrial compartment is critical in mPTP-opening (Azarashvili et al., 2011). Given the association of CD38 with Cx43, this provides a mechanism by which NAD^+ released from mitochondria in damaged cells could be rapidly utilised (Salmina et al., 2008), with subsequent metabolite formation and downstream Ca^{2+} signalling.

Other ARC isoforms

Due to the relatively small rates of cADPR production by CD38 discussed previously, and the fact that the cADPR content of certain tissues is largely unaffected by CD38 KO (Partida-Sánchez et al., 2001), the

physiological importance of CD38 in cADPR-mediated signalling has been questioned (Ceni et al., 2003a). The necessity of CD38 for cADPR production seems to be variable across tissues and between studies. For instance, CD38 KO either slightly decreases (Partida-Sánchez et al., 2001), drastically decreases (Ceni et al., 2003a; Jin et al., 2007), or has no effect on, brain cADPR levels relative to controls (Soares et al., 2007). An alternative CNS ARC enzyme, with cyclase (10% of products formed; hypothesised to be able to replenish brain cell cADPR levels within 1 min) and NAD-glycohydrolase activity (1000-fold lower than CD38 activity) activities was detected in a PM and ER-enriched fraction from CD38 KO total brains harvested from either neonate and adult tissue (Ceni et al., 2006). This novel enzyme is membrane localised, but with an intracellular active site regulated by G-proteins. Furthermore, this enzyme was functional at both pH 6 (optimal) and pH 7 and inhibited by Zn^{2+}. Interestingly, this enzyme differentiates itself from other known ARCs as it appears to not possess NGD cyclization activity (Ceni et al., 2006). Such lack of NGD utilisation has been recorded previously for a lymphocyte ARC which was observed to have a physiological role in signalling following T-cell receptor activation (Guse et al., 1999).

Aside from the cyclase identified by Ceni et al. (2006), it is hypothesised that numerous, as yet molecularly unidentified, ARC isoforms exist (Morgan et al., 2005). This suggestion is based upon the detection of ARCs (including in CD38 KO cells) which have characteristics unlike CD157 and CD38, such as different mechanisms of regulation (e.g. sensitivity to inhibition by Cu^{2+}), agonist specificity (e.g. to ACh, cholecystokinin (CCK) and a membrane-permeant analogue of cGMP) and different intracellular localisations (including soluble). Such ARCs have been detected in a plethora of non-CNS cell types (Bacher et al., 2004; Bruzzone et al., 2003b; de Toledo et al., 2000; Graeff et al., 1998; Gul et al., 2008; Guse et al., 1999; B.-J. Kim et al., 2008; Matsumura and Tanuma, 1998; Nam et al., 2006; Park et al., 2011; Soares et al., 2007; Sternfeld et al., 2003; Wilson and Galione, 1998; Xie et al., 2003) and brain homogenates (Matsumura and Tanuma, 1998).

4.1.2 Downstream effects of cADPR

cADPR has numerous molecular targets, but in the context of neuronal signalling, the most interesting of these are RyRs, TRPM ion channels and purinergic P2X7 receptors. The primary effect of cADPR production is Ca^{2+} mobilisation and as such the processes outlined in *Chapter 3,* including SOCE, activation of Ca^{2+}-dependent K^+ currents and

modulation of membrane excitability are also pertinent to the ultimate effects of cADPR on cellular physiology.

RyR

In general, cADPR-mediated activation of RyR1 and RyR3 is quite variable across cell types and preparations, ranging from inactive to robust and potentially allowing for a degree of redundancy in the system (Copello et al., 2001; Fulceri et al., 2001; Kunerth et al., 2004; Mészáros et al., 1993; Morrissette et al., 1993; Murayama and Ogawa, 2002; Sitsapesan and Williams, 1995; Sonnleitner et al., 1998). Conversely, cADPR activates RyR2 across numerous cell types (Barone et al., 2002; Rakovic et al., 1996; Sitsapesan and Williams, 1995; Takasawa et al., 1998; Y. X. Wang et al., 2004).

cADPR-mediated calcium release is generally considered to be independent of IP_3- and NAADP-mediated Ca^{2+} release processes. This is due to the fact that each receptor homologously desensitises, *i.e.* desensitisation of one receptor system does not influence the ability of either of the other systems to be activated (Churchill et al., 2002; Clapper et al., 1987; Galione et al., 1991; Lee and Aarhus, 1997; Masgrau et al., 2003). Furthermore, antagonists of IP_3Rs do not generally affect cADPR-mediated signalling (Cancela et al., 1999; Lee, 1993) with the exception of experiments in bone marrow mesenchymal stem cells (Tao et al., 2011). However, this does not preclude these alternative intracellular Ca^{2+} mobilisation sources from acting in a sequential and/or contributing manner to propagate response to stimuli.

Indeed, T-cell signalling provides an interesting case study of how related signalling pathways, particularly those stimulated by other NAD^+ metabolites, can work in tandem during physiological responses. Thus, TCR/CD3 ligation by an antigenic peptide results in the intracellular formation of NAADP within 10 – 20 seconds (Gasser et al., 2006a). A rapid decrease in NAADP levels occurs within the first minute, although they remain elevated for 5 – 20 minutes. At the same time, a smaller rise in intracellular Ca^{2+} occurs over several minutes (Gasser et al., 2006b). It is hypothesised that NAADP produces a local Ca^{2+} signal, which sensitises IP_3Rs and RyRs, thereby facilitating global amplification of the initial NAADP signal (Ernst et al., 2013). IP_3 is formed soon after the initial NAADP peak (Guse et al., 1995) resulting in IP_3R-mediated Ca^{2+} mobilisation (Guse et al., 1992). Lastly, cADPR levels increase and cause RyR-mediated Ca^{2+} mobilisation (Guse et al., 1999) which is likely facilitated by Ca^{2+} release arising from both NAADP and IP_3 stimulation (Ernst et al., 2013). This continuous Ca^{2+} mobilisation decreases $[Ca^{2+}]_{ER}$ and activates SOCE (Ernst et al., 2013; Guse, 1999). This amplification and propagation of Ca^{2+} signals by cADPR has also been observed during pacemaker signals in T cells (Bruzzone et al., 2003b;

Kunerth et al., 2004). Furthermore, intracellular Ca^{2+} mobilisation and resulting cellular motility following IL-8 application in natural killer cells result from the activities of cGMP, cADPR and PLCβ (Rah et al., 2005). Aside from RyRs, cADPR also interacts with Ca^{2+}-ATPases, IP_3Rs, FKBPs, TRP channels and P2XY7Rs (outlined in subsequent sections). RyR-independent modulatory effects of cADPR may add an even greater degree of complexity to cADPR- mediated signalling, in terms of increasing specificity or redundancy to its processes.

IP_3R

The presence of a regulatory site for cADPR in the ligand-binding domain of IP_3R1 and IP_3R2, but not IP_3R3, has been identified in permeabilised A7r5 smooth-muscle cells (Vanlingen et al., 2001). Furthermore, cADPR increased the binding of IP_3 to IP_3R1 (rabbit cerebellar microsomes), IP_3R2 (RBL-2H3 rat mucosal mast cells) and IP_3R3 (16HBE14o- human bronchial epithelial cells; Vanlingen et al., 1999) However, cADPR can also inhibit IP_3R-mediated calcium signals in 16HBE14o-cells (Missiaen et al., 1998). Aside from direct regulation *via* the aforementioned regulatory site, cADPR could also mediate these effects *via* interaction with the IP_3R regulatory protein FK506 binding protein 12.6 (FKBP12.6; Noguchi et al., 1997).

FKBP12.6

FKBP12.6 acts to stabilize and suppress RyR- and IP_3R-mediated Ca^{2+} release (Ahern et al., 1997; Chelu et al., 2004; Patterson et al., 2004) and is a regulator of hippocampal LTP as well as learning, memory and behaviour (Hoeffer et al., 2008; Yuan et al., 2016). FKBP12.6 disassociation from RyRs is enhanced by PKA phosphorylation (Marx et al., 2000) as well as oxidation and nitrosylation resulting in Ca^{2+} leak which is implicated in numerous pathologies (Shan et al., 2010; Wehrens et al., 2006, 2005b).

cADPR has also been shown to bind to FKBP12.6, resulting in its dissociation from RyRs and IP_3R, priming these channels for activation and/or delaying their inactivation (Hashii et al., 2000b; Noguchi et al., 1997). Furthermore, in airway smooth muscle cells of FKBP12.6 null mice (Y. X. Wang et al., 2004) and arterial preparations functionally or physically stripped of FKBP12.6, cADPR failed to elicit calcium release (Tang et al., 2002). Conversely, cADPR did not modulate the association between recombinant FKBP isoforms and RyR3 (Bultynck et al., 2001), suggesting a RyR subtype specific modulatory role for FKBP12.6 with regard to cADPR signalling.

Additional modulators of cADPR-mediated calcium release include CaM (Lee et al., 1994), CaM-Kinase II and PKA (potentially *via* the aforementioned phosphorylation of RyRs and FKBP12.6 dissociation; Wehrens et al., 2005). In more detail, CaM binds to RyRs (Wagenknecht et al., 1997) and sensitises them to CICR (Fruen et al., 2000; Lee et al., 1995; Tripathy et al., 1995). When a threshold intracellular level of cADPR is reached, CAM dissociates from RyRs, resulting in a refractory period until cADPR levels are decreased, allowing for negative feedback regulation (Thomas et al., 2002).

4.1.3 CD38 regulation

So far, I have discussed how cADPR is formed by ARC, its mechanism of action and its effects at both the cellular and systems level. However, a fundamental question which also remains unanswered some 30 years after the initial discovery of cADPR as a Ca^{2+} signalling molecule is exactly how ARC itself is activated following activation of exogenous plasma membrane-bound receptors? Although, as discussed below, there are numerous lines of evidence to suggest that I-mGluR-elicited ARC activation may be mediated by a cholera toxin (CTx; Gs activator and inhibitor of GTPase activity (Mangmool and Kurose, 2011) sensitive G-protein.

Regulation at the enzyme level includes its ultrastructural organisation where it can exist in either a monomeric (Terhorst et al., 1981) and/or dimeric/multimeric form (Mallone et al., 1998). It is also proposed by Zhao et al. (2012) that CD38 can alter its cell surface positioning to expose an active site either intracellularly or extracellularly. Modulation of the structure of its catalytic centre (Salmina et al., 2014), as well as the targeting of its expression on numerous intracellular organelles, reveals further mechanisms of regulation (Quarona et al., 2013). Indirect regulation includes that dictated by the intracellular levels of substrates and modulators, including NADH, NAD^+, cADPR, NADP, ADPR, ATP and the non-substrate ligand CD31 (Salmina et al., 2014).

The end result of ARC activation is increased $[Ca^{2+}]_i$ which can, at least following cholinergic agonist stimulation in chromaffin cell membranes (Morita et al., 1997) and adult cardiomyocytes (Xie et al., 2003) in turn, activate ARC *via* adenylyl cyclase/ cAMP/ PKA-dependent phosphorylation. Fukushi et al., 2001; Higashida et al., 2007, 1997; Sternfeld et al., 2003; Zhang et al., 2005).

A plethora of physiological mediators regulate ARC expression and activity (including CD38 specific studies) in a variety of cell types including neuronal cells (for review see; Guse, 1999; Higashida et al., 2007). There is

a significant body of evidence in support of G-protein (Gi and Gq) involvement in ARC activation across these different cell types and different molecular pathways (Barisione et al., 2010; Fukushi et al., 2001; Higashida et al., 2007, 2003, 2001b, 2000, 1999, 1997; Hotta et al., 2000; Shi et al., 2007; Sternfeld et al., 2003; Zhang et al., 2005).

Those of which are particularly relevant to neuronal ARC activation include: Angiotensin II (Higashida et al., 2000), non-specific beta-adrenergic receptor stimulation (Barisione et al., 2010; Higashida et al., 2003, 2001b, 1999, 1997; Hotta et al., 2000), endothelin receptors (Barone et al., 2002), mAChRs - M1 & M3 (Fukushi et al., 2001; Higashida et al., 2007, 2001b, 1999, 1997; Sternfeld et al., 2003; Zhang et al., 2005), mGluR1, 3, 5 & 6 (Higashida et al., 2003; Morita et al., 1997; Xie et al., 2003), Nitric oxide (NO) (Clementi et al., 1996; Galione et al., 1993; Reyes-Harde et al., 1999a; Willmott et al., 1996), oxytocin (Kim et al., 2016), VGCCs (possibly *via* NO; Morita et al., 1997; Xie et al., 2003) and inflammatory mediators such as bradykinin, histamine (Deshpande et al., 2005; Higashida et al., 2006), TNF-α, IL-1β, interferon gamma (Deshpande et al., 2003), IL-8 (Rah et al., 2005) and lipopolysaccharide (LPS; implicating ARC activity in LPS-mediated microglial activation; Barone et al., 2002; Higashida et al., 2007; Mayo et al., 2008). Notably, mGluR2, M2, M4 and NMDA receptor stimulation inhibits ARC activity (Higashida, 1997; Higashida et al., 2003, 1997; Salmina et al., 2011). As the focus of this chapter is on I-mGluR mediated ARC activation, this will now be discussed in greater detail.

Activation of ARC by mGluRs is mediated by specific mGluR subtypes in a cell-specific manner. For instance, ARC activation occurs *via* mGluR6 stimulation in crude rat and mouse retinal membranes and *via* I-mGluRs in rat superior cervical ganglion (SCG) membranes. Notably, however, glutamate had little effect on ARC activity in membranes from rat and mouse olfactory bulb, cerebral cortex, hippocampus, and cerebellum (Higashida et al., 2003). Activation of transiently overexpressed mGluR subtypes in NG108-15 cells with glutamate also differentially modulated ARC activity, with cells expressing mGluR1, 3, 5 and 6 increasing ARC activity (CTx sensitive), cells expressing mGluR2 decreasing activity (PTx sensitive) and with no change in activity being observed in mGluR4 and 7 expressing cells (Higashida et al., 2003). Mechanistically, in retinal and SCG membranes and NG108-15 cells (Higashida et al., 1997) cADP-ribose hydrolase activity was barely detectable and unchanged in the presence or absence of glutamate respectively, suggesting glutamate-induced cADPR accumulation was due to increases in production rather than the inhibition of hydrolysis. Notably, I-mGluR agonists can reverse NMDAR-mediated ARC inhibition, suggesting a hierarchy in glutamate-mediated ARC inhibition (Salmina et al., 2011).

This evidence clearly supports a role for mGluRs in the G-protein mediated activation of ARC, in a cell type-dependent manner. Notably, as mentioned previously, RyR-mediated Ca^{2+} mobilisation following I-mGluR stimulation also supports the suggestions of a role for cADPR in this signalling pathway as observed in hippocampal, cerebellar granule, midbrain dopaminergic and DRG neurons (Crawford et al., 1997a; Higashida et al., 2003; Irving et al., 1992; Morikawa et al., 2003; Sohn et al., 2011).

It is clear though that across different tissues, and even within the same tissue, where evidence of I-mGluR – induced RyR - evoked calcium signals have been provided, the contribution, or otherwise, of cADPR to the generation of those signals is highly variable. For example, in studies on whole labyrinth preparations, Hendricson and Guth (2002), demonstrated that although I-mGluR stimulation did activate RyRs, this was induced by calcium-induced calcium release (CICR), initiated by calcium release through IP_3Rs, rather than being due to ARC - mediated cADPR production. Indeed, RyR function was necessary for IP_3R-mediated Ca^{2+} release, at least in rat cerebellar granule cells where RyR antagonism inhibited mAChR/IP_3-mediated Ca^{2+} responses (Irving et al., 1992a). In this scenario, it is proposed that an initial Ca^{2+} release *via* IP_3R triggers a major regenerative Ca^{2+} response component through CICR (Berridge, 1998; Crawford et al., 1997; Irving et al., 1992a, 1992b; Simpson et al., 1995). However, when the contribution of RyR-mediated Ca^{2+} mobilisation to IP_3R-stimulated responses in mouse cortical neurons was quantified by Stutzmann et al. (2007), it was found to be relatively modest (caged IP_3 = 20 ± 7%; AP-evoked = 15 ± 5%; 4 - 6 weeks of age).

In contrast, within cultured rat DRG neurons, I-mGluR activation did evoke cADPR - dependent calcium release *via* RyR activation. However, because the potential contribution of IP_3R - mediated signalling to the overall I-mGluR - evoked calcium signal was not measured, it is unclear what the net relative contributions of the two calcium signalling pathways to the overall calcium response were (Crawford et al., 1997b). Of particular interest in this respect was the study of Sohn et al. (2011) which, using acutely dissociated rat hippocampal neurons, indicated that I-mGluR-mediated Ca^{2+} mobilization was generated in its entirety by activation of the cADPR/RyR pathway. This finding was supported by the fact that I-mGluR-mediated Ca^{2+} signals were evoked in hippocampal neurons derived from PLCβ1 and PLCβ4 knockout mice (Sohn et al., 2011). The nature of this Ca^{2+} mobilisation in cultured hippocampal neurons, in terms of the involvement of IP_3Rs and RyRs and whether or not it is altered in transgenic models of AD, is the focus of this thesis chapter.

4.1.4 Implication of ARCs/cADPR signalling in AD

There is considerable overlap between processes regulated by CD38 and those implicated in AD pathology, including Ca^{2+} signalling and regulation of inflammatory processes such as microglial activation (Franco et al., 2006; Mayo et al., 2008). However, the ARC signalling system has not been investigated in any great depth in the context of AD aside from the observations that, a) the percentage of CD38 positive PBMCs was upregulated in samples from AD patients (Kassner et al., 2008), b) CD38 has been observed to accumulate in NFTs (Otsuka et al., 1994) and, c) intracerebral injection of Aβ increased CD38 and Cx43 expression in the cortex and hippocampus, which could lead to Ca^{2+} dysregulation, but decreased expression in the amygdala (Salmina et al., 2014).

Blacher et al. (2015) conducted the most extensive study with regard to CD38 in the context of AD published to date. When CD38 KO $APP_{SWE}/PS1_{\Delta E9}$ mice were compared with controls (8- and 14-month-old), KO mice displayed significant reductions in both soluble and insoluble Aβ levels and total brain plaque load which correlated with improved spatial learning. Furthermore, the reduction in $Aβ_{42}$ levels observed in mice brain samples was also mirrored in cerebral cortical cultures from CD38 KO mice and in APP/PS cultures treated with a CD38 enzyme inhibitor or a competitive antagonist of cADPR-dependent Ca^{2+} signalling, relative to control. This suggested that the pathological effects of this enzyme were mediated, partly at least, by cADPR. Indeed, cADPR is implicated directly in AD with respect to P2X7 purinergic receptor (P2X7Rs) and TRP activity.

P2X7 in the brain are expressed primarily on microglia and astrocytes (Kamatsuka et al., 2014; Yamamoto et al., 2013) where they transport NAD^+, NADH and ions across the PM in both neuronal and glial cells (Lu et al., 2007; Salmina et al., 2014). Moreover, cADPR is implicated in P2XYR-dependent Ca^{2+} influx, mitochondrial activity and cell death (Bruzzone et al., 2010, 2007). In mice, expression of P2X7R was required for Aβ-mediated microglial activation and neuroinflammation (Sanz et al., 2009) resulting in ROS production and synaptotoxicity in $APP_{SWE}/PS1_{\Delta E9}$ mice (Lee et al., 2011). Furthermore, inhibition of native or overexpressed P2X7R inhibited glycogen synthase kinase 3β (GSK3β)-mediated increases α-secretase activity, in cell lines (Diaz-Hernandez et al., 2012) and reduced Aβ plaque number in $APP_{SWE/V717F(Indiana)}$ mice (Diaz-Hernandez et al., 2012).

TRP ion channels are expressed abundantly in the brain including on neurons (Okada et al., 1998; Tóth et al., 2010), astroglia (Verkhratsky et al., 2013) and microglia (Kraft et al., 2003) where their modulation of Ca^{2+} influx is regulated by cADPR and $[Ca^{2+}]_i$ (Starkus et al., 2007; Tao et al., 2011). TRPM2 dysfunction contributes to Aβ-induced cerebrovascular pathology

and neurotoxicity in AD (Fonfria et al., 2005; L. Park et al., 2014) and is implicated in the development of oxidative stress in brain cells (Bai and Lipski, 2010). Interestingly in T-lymphocytes and neutrophils, although TRPM2 is activated by micromolar concentrations of NAADP, this activation is significantly synergised by cADPR (Beck et al., 2006; Lange et al., 2008). Conversely however, cADPR modulation of TRPM2 signalling was not observed in HEK293 cells overexpressing TRPM2 (Tóth and Csanády, 2010). However, the active molecule at TRPM2 may also be ADPR (Ernst et al., 2013), which is a common contaminant of commercial cADPR preparations (Kirchberger et al., 2009).

It is also possible that the “anti-amyloid” effects of CD38 KO in AD models are mediated by increases in its substrate, NAD^+ (Aksoy et al., 2006b; Blacher et al., 2015). This is supported by the finding that application of NAD^+ to APP_{SWE} mouse neocortical cultures as well as to APP/PS and/or CD38 KO cerebral cortical cultures reduced Aβ levels (Aksoy et al., 2006b; Blacher et al., 2015; Qin et al., 2006). Furthermore, treatment of APP_{SWE} mice with an NAD^+ precursor, attenuated cognitive deficits (Gong et al., 2013). The process underlying these observations likely involves a reduction in Aβ production and/or secretion on the basis that CD38 KO reduced the number but not the size of plaques, reduced both soluble and insoluble Aβ levels, decreased β- secretase and γ-secretase activity and did not alter expression of genes known to be involved in microglia/macrophage-mediated Aβ phagocytosis or degradation (Blacher et al., 2015).

NAD^+ levels decrease with ageing (Imai and Guarente, 2014) which impairs cellular respiration, decreases mitochondrial ATP and contribute to cell death (Yao et al., 2017). As such, NAD^+ depletion and the resulting cellular energy deficits attributed to the effects of neurodegeneration are proposed as a potential therapeutic target (Liu et al., 2008). In order to increase NAD^+ levels, one of four NAD^+ synthesising pathways present in mammals would need to be enhanced. The principal route of NAD^+ production is *via* the salvage pathway where nicotinamide, nicotinic acid, nicotinamide riboside are utilised (Yao et al., 2017). There is also an additional *de novo* NAD^+ synthesis pathway which utilises tryptophan (Yamamoto et al., 2014).

NAD^+ also seems to interact with the JNK family of protein kinases which, in addition to being involved in regulating brain development, repair and memory formation, are also mediators of neuroinflammation and neuronal death, and as such are implicated in neurodegenerative conditions including AD (Mehan et al., 2011; Yarza et al., 2016). Indeed, JNK is abnormally activated in transgenic models of AD and in AD patients (Braithwaite et al., 2010; Sclip et al., 2011; Thakur et al., 2007). Interestingly in this regard, application of the NAD^+ precursor, nicotinamide

mononucleotide (NMN), inhibits JNK and decreases Aβ production, Aβ plaque burden, synaptic loss, inflammatory responses and cognitive impairments in $APP_{SWE}/PS1_{\Delta E9}$ mice. Aside from the effects mediated by the inhibition of JNK activation, NMN also upregulates the non-amyloidogenic processing of APP (Yao et al., 2017).

The aforementioned potential decrease in NAD^+ levels in AD models could subsequently alter metabolic activity, by decreasing glycolysis and glycolysis-associated NAD^+ regeneration (Salmina et al., 2014). Astrocytes are particularly sensitive to NAD^+ depletion compared to neurons (Alano et al., 2010; Ying et al., 2005a) as they are highly dependent on glycolysis (Hertz et al., 2007). Furthermore, astrocytic NAD^+ depletion also decreases astrocytic lactate production which, in turn, impacts upon neuronal metabolism as lactate is a major energy source for neurons (Bouzier-Sore et al., 2003; Wyss et al., 2011) and is shuttled from glia-neurons by Cx (Bennett et al., 2012) for use in oxidative metabolism (Pellerin et al., 1998; Pellerin and Magistretti, 1994).

Aside from ARCs, numerous other enzymes, including poly-ADP-ribose polymerases (PARP), ADP-ribosyltransferases (ART) and SIRTs, use NAD^+ and its metabolites as substrates (Haigis and Sinclair, 2010; Hassa and Hottiger, 2008). PARP and ART activity regulate cell signalling, DNA repair and apoptosis (Haag et al., 2007). It is proposed that ARCs/CD38 (CD38 is the principal mammalian ARC; Bruzzone et al., 2004) regulate NAD^+ homeostasis under normal physiological conditions. Conversely, in pathological conditions, where significant DNA damage has occurred, it is proposed that PARPs principally regulate NAD^+ levels (Ying et al., 2005b). In AD, astrocytic PARP-1 activation by Aβ indirectly mediates neuronal cell death (Abeti and Duchen, 2012). PARP-1 is a DNA repair enzyme which is activated by single strand breaks associated with oxidative stress (de Murcia and de Murcia, 1994). This catalyses the formation of poly ADP-ribose polymers from NAD^+. Pathological activation of PARP-1 by Aβ leads to NAD^+ depletion and cell death (Abeti and Duchen, 2012; Ying et al., 2003). As such, prevention of NAD^+ depletion is a proposed therapeutic approach for AD (Braidy et al., 2008).

NAD^+ also interacts with the NAD-dependent deacetylase, SIRT1, the activity of which is increased in the brains of CD38KO mice (Barbosa et al., 2007; Blacher et al., 2015), likely due to decreased nuclear CD38 expression (Aksoy et al., 2006a). Aside from their role in energy metabolism (Haag et al., 2007; Malavasi et al., 2010), in the brain SIRTs are critical for normal learning, memory, and synaptic plasticity, at least in mice (Michan et al., 2010). They are also implicated in ageing (Haag et al., 2007; Malavasi et al., 2010) and neurodegeneration (Outeiro et al., 2008), including AD (Braidy et al., 2012; Wang et al., 2010). SIRT1 also enhances α-secretase activity and

expression which decreases Aβ levels in APP_{SWE} mice (Qin et al., 2006). The SIRT1/PGC-1a pathway has also been shown to promote BACE1 degradation resulting in a reduction in β-secretase activity (Gong et al., 2013). That being said, in the study by Blacher et al. (2015) utilising APP/PS/CD38KO mice, α-secretase and ADAM10 activity were not increased, nor were BACE1 levels decreased, suggesting that the effect of CD38KO on Aβ dynamics and neuroprotection was not due to SIRT1-mediated reduction in α- secretase and/or β- secretase expression and/or activity (Blacher et al., 2015).

4.2 Aims

Based primarily upon the finding that I-mGluR mediated Ca^{2+} signals were cADPR-dependent (and PLC-independent) in pyramidal neurons from acutely dissociated SD rat CA1 hippocampal tissue (Sohn et al., 2011), the aim of this chapter was to determine the proportion, if any, of I-mGluR-mediated responses which were mediated by the ARC/cADPR/RyR signalling pathway in cultured rat hippocampal neurons. Specifically, to add weight to any determination of the importance of this pathway to I-mGluR-mediated signals, I wished to compare results from the inhibition of both the enzyme which produces cADPR, ARC (utilising nicotinamide and NGD), as well as the primary target of cADPR-mediated Ca^{2+} mobilisation, RyRs (utilising dantrolene).

I also sought to determine if any observed results were reproducible across different murine across species (comparing data from SD rat with that from non-Tg mouse). Moreover, I also wished to determine whether or not the contribution of the ARC/RyR pathway was altered in 3xTg-AD neurons relative to non-Tg controls.

4.3 Materials and Methods

4.3.1 Ca^{2+} imaging

Ca^{2+} imaging experiments and data analysis were carried out as described in *Section 3.3. Materials and methods*. For experiments which compared the percentage increase from baseline between two unpaired nonparametric populations (See Fig 4.3) the Mann Whitney test was utilised. This set of experiments differs from those presented in *Chapter 3* in that application of DHPG under depolarisation conditions served as the control responses which were then compared with DHPG-evoked responses under depolarisation conditions but in the presence of, and subsequent to incubation (4 mins) with, antagonists of either ARC (nicotinamide; 5 mM) and NGD; 100 µM) or RyRs (dantrolene; 10 µM). Negative control experiments for nicotinamide were conducted using an analogue, benzamide (5 mM) (Martino Carpi et al., 2018) but does not inhibit of CD38 (Migaud et al., 1999a).

4.3.2 Applied compounds

- Benzamide (Sigma, cat. no. 135828)
- DMSO (Sigma, cat. no. W387520)
- Nicotinamide (Sigma, cat. no. 72340)
- Nicotinamide guanine dinucleotide (NGD) sodium salt (Sigma, cat. no. N5131)
- Dantrolene (Sigma, cat. no. 1163140) dissolved in DMSO
- U73122 (Tocris, cat. no. 1268)

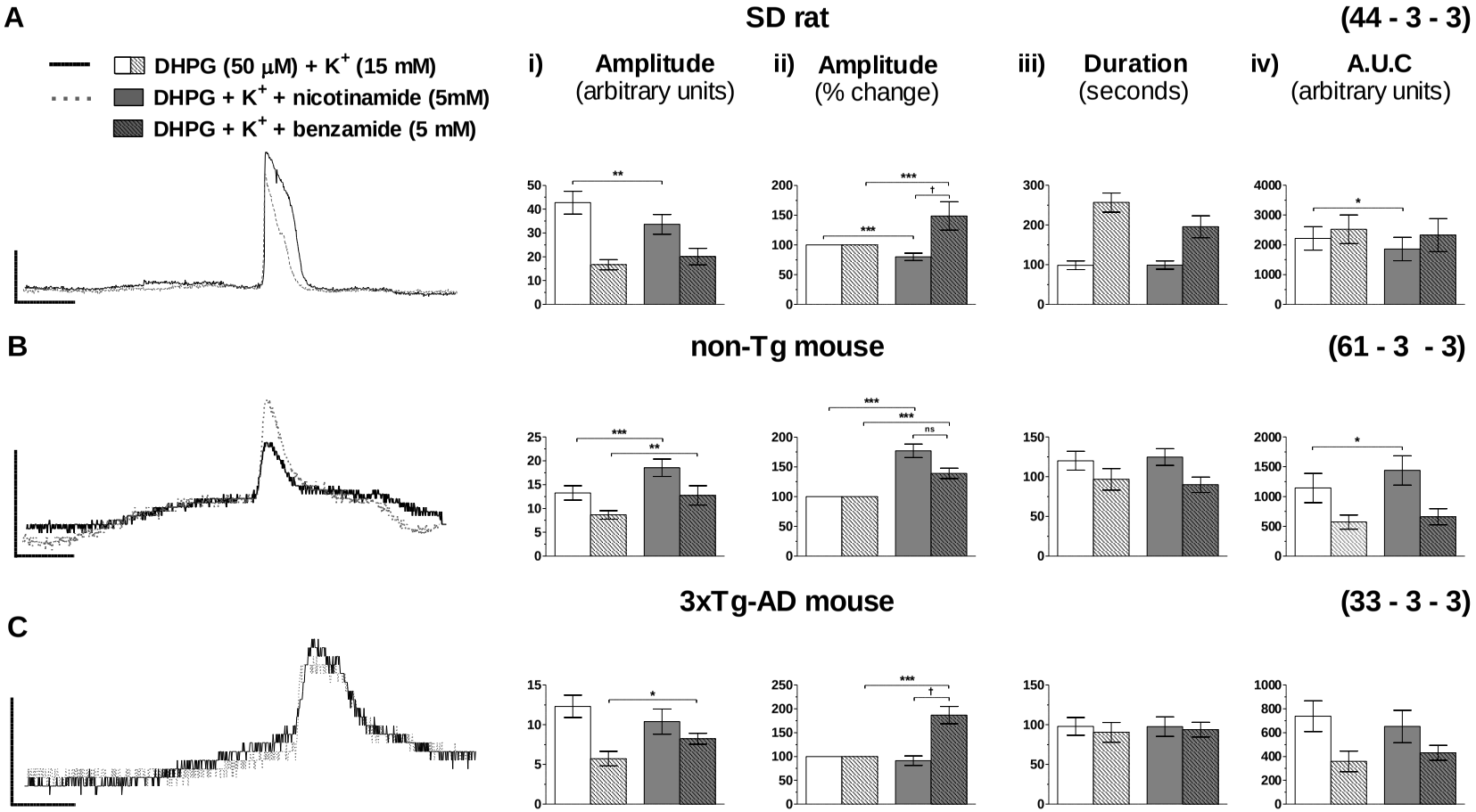

Figure 4.3. Somatic I-mGluR-mediated (DHPG = 50 µM) Ca^{2+} responses of SD rat (A), non-transgenic (non-Tg) mouse (B) and 3xTg-AD mouse (C) cultured hippocampal neurons (3 – 5-days-old) under depolarisation conditions (K^+ = 15 mM) with and without prior incubation with the ARC inhibitor nicotinamide (5 mM) which prevents the formation of cyclic ADP-ribose (cADPR).

Representative traces illustrate somatic intracellular DHPG-mediated Ca^{2+} responses of cultured hippocampal neurons under depolarisation conditions (DHPG = 50 µM; K^+ = 15 mM) with (grey dashed line) and without (control; solid black line) prior incubation with the ARC antagonist nicotinamide (4 mins; 5 mM; a 50-minute agonist washout period separates both experimental phases). **A** SD rat; 3-days-old / 6 - 13 DIV, **B** non-transgenic mouse; 3 - 4-days-old / 2 DIV and **C** = 3xTg-AD mouse; 4 – 5-days-old / 3 - 9 DIV. The horizontal axis represents 120 seconds (s) and the vertical axis represents 25 arbitrary units (a.u.) of fluorescence.

Histograms illustrate the amplitude (a.u.; **i**) , normalised amplitude (% change; **ii**), duration (s; **iii**) and area under the curve (A.U.C.; measured in a.u.; **iv**) of DHPG-mediated calcium responses under depolarisation conditions (control; DHPG = 50 µM; K^+ = 15 mM; white bars) and following prior incubation with the ARC inhibitor nicotinamide (4 mins; 5 mM; grey bars). Negative control experiments replacing nicotinamide with benzamide (5 mM; grey dashed bars) were also carried out (control; white dashed bars) and are displayed paired with the corresponding phase of the nicotinamide experiments for comparison. * and † indicate significant differences between paired and unpaired observations, respectively. Populations used in negativecontrol experiments: SD rat = 4-days-old / 2 – 6 DIV, non-Tg mouse = 3-days-old / 6 – 13 DIV, 3xTg-AD mouse = 2-days-old / 2 DIV.

When DHPG-mediated responses under depolarisation conditions were compared with and without prior incubation with nicotinamide, we found that nicotinamide produced a significant decrease in the amplitude, normalised amplitude and A.U.C. (amplitude = 43 ± 5 *vs* 32 ± 4 a.u., p = 0.003; normalised amplitude = 100 *vs* 80 ± 6%, p = 0.001; A.U.C. = 2216 ± 394 *vs* 1659 ± 348 a.u.; p = 0.01; n = 44; control *vs* nicotinamide) of responses in SD rat neurons (Fig 4.3, A; 3 days-old; 6 – 13 DIV). These results are likely under-represented, given that the off-target effects of the nicotinamide analogue benzamide modified I-mGluR signals in a significantly different manner to nicotinamide, (p = 0.01; n = 44 *vs* 22; nicotinamide *vs* benzamide), namely, benzamide significantly *enhanced* I-mGluR signals, at least in data normalised to the control phase of the experiment (100 *vs* 149 ± 24%; p = 0.0001; n = 22; 4 days old 2 – 6 DIV; Fig 4.3, A, ii, dashed bars). Conversely, the amplitude (raw a.u.) and A.U.C. of I-mGluR signals were unchanged by benzamide (amplitude = 17 ± 2 *vs* 21 ± 3 a.u., p = 0.27; A.U.C. = 2526 ± 479 *vs* 2328 ± 552 a.u.; p = 0.74; n = 22; control *vs* benzamide).

In contrast to the nicotinamide experiments carried out in SD rat neurons, in non-Tg neurons (Fig 4.3, B; 3 - 4 days-old; 2 DIV), prior incubation with nicotinamide increased amplitude, normalised amplitude and A.U.C. of I-mGluR-mediated responses relative to I-mGluR stimulation alone (amplitude = 13 ± 2 *vs* 19 ± 2 a.u., p = <0.0001; normalised amplitude = 100 *vs* 177 ± 11%, p = <0.0001; A.U.C. = 1144 ± 247 *vs* 1439 ± 247 a.u.; p = 0.05; n = 61; control *vs* nicotinamide). These effects are likely due to extra-ARC nicotinamide side effects given that the amplitude and normalised amplitude (but not A.U.C.) of I-mGluR responses was also increased with benzamide co-application (amplitude = 9 ± 1 *vs* 13 ± 2 a.u., p = 0.007; normalised amplitude = 100 *vs* 139 ± 9%, p = 0.0001; A.U.C. = 572 ± 119 *vs* 660 ± 134 a.u., p = 0.35; n = 34; control *vs* benzamide). Furthermore, the effect of nicotinamide and benzamide on I-mGluR signals was statistically similar (p = 0.06; n = 61 *vs* 32; nicotinamide *vs* benzamide)

In 3xTg-AD mouse neurons (Fig 4.3, C; 4 - 5 days-old; 3 - 9 DIV), co-application of nicotinamide and DHPG had no effect on amplitude, normalised amplitude or A.U.C. relative to DHPG application alone (amplitude = 12 ± 1 *vs* 11 ± 2 a.u., p = 0.07; normalised amplitude = 100 *vs* 91 ± 10%, p = 0.29; A.U.C. = 738 ± 130 *vs* 652 ± 136 a.u.; p = 0.40; n = 33; control *vs* nicotinamide). Again, these figures are likely under-represented (p < 0.0001; n = 33 *vs* 41; nicotinamide *vs* benzamide) given that the amplitude and normalised amplitude (but not A.U.C.) of I-mGluR responses were both enhanced in 3xTg-AD neurons with benzamide co-application (amplitude = 6 ± 1 *vs* 8 ± 1 a.u., p = 0.02; normalised amplitude = 100 *vs* 187 ± 18%, p = <

0.0001; A.U.C. = 358 ± 87 *vs* 431 ± 62 a.u., p = 0.33; n = 41; control *vs* benzamide).

Duration was unchanged between these experimental conditions in all animal models used in nicotinamide (SD rat = 98 ± 11 *vs* 96 ± 10 s, p = 0.8; non-Tg mouse = 120 ± 12 *vs* 124 ± 11 s, p = 0.63; 3xTg-AD mouse = 98 ± 11 *vs* 98 ± 12 s, p = 0.98; control *vs* nicotinamide) and benzamide experiments (SD rat = 257 ± 24 *vs* 196 ± 28 s, p = 0.08; non-Tg mouse = 97 ± 14 *vs* 89 ± 10 s, p = 0.28; 3xTg-AD mouse = 90 ± 12 *vs* 94 ± 9 s, p = 0.65; control *vs* benzamide).

4.4.2 Effect of NGD on I-mGluR-evoked neuronal calcium signals

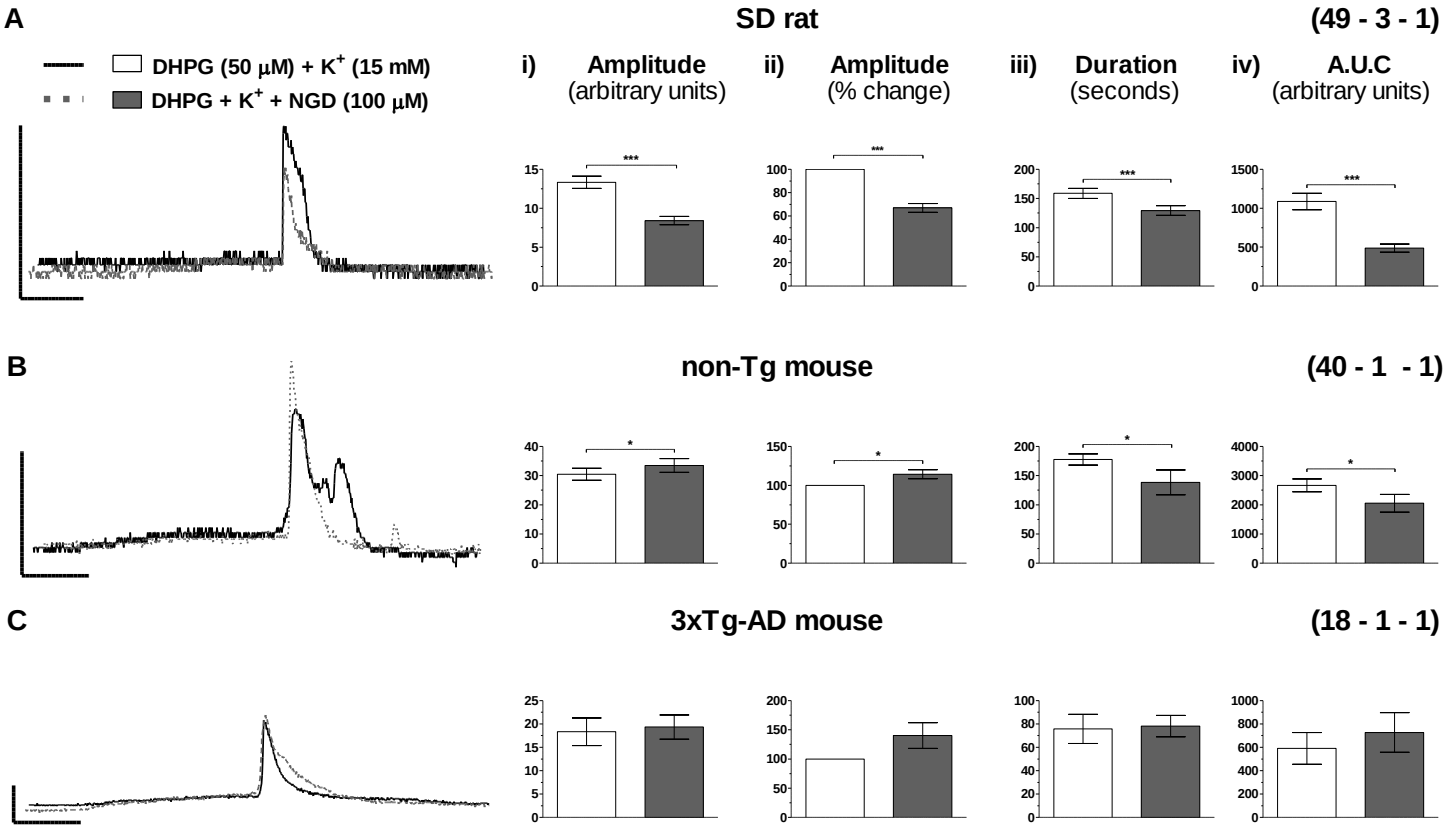

Figure 4.4. Somatic I-mGluR-mediated (DHPG = 50 μM) Ca^{2+} responses of SD rat (A), non-transgenic mouse (B) and 3xTg-AD mouse (C) cultured hippocampal neurons (3 – 5-days-old) under depolarisation conditions (K^+ = 15 mM) with and without prior incubation with the ARC inhibitor nicotinamide guanine dinucleotide (NGD; 100 μM) which prevents the formation of cyclic ADP-ribose (cADPR).

Representative traces illustrate somatic intracellular DHPG-mediated Ca^{2+} responses of cultured hippocampal neurons under depolarisation conditions (DHPG = 50 μM; K^+ = 15 mM) with (grey dashed line) and without (control; solid black line) prior incubation with the ARC antagonist NGD (4 mins; 100 μM; a 50 minute agonist washout period separates both experimental phases). **A** = SD rat; 5-days-old / 2 - 6 DIV, **B** = non-transgenic mouse; 2-days-old / 11 DIV and **C** = 3xTg-AD mouse; 4-days-old / 9 DIV. The horizontal axis represents 120 seconds (s) and the vertical axis represents 25 arbitrary units (a.u.) of fluorescence.

Histograms illustrate the amplitude (a.u.; **i**) , normalised amplitude (% change; **ii**), duration (s; **iii**) and area under the curve (A.U.C.; measured in a.u.; **iv**) of DHPG-mediated calcium responses under depolarisation conditions (control; DHPG = 50 μM; K^+ = 15 mM; white bars) and following prior incubation with the ARC inhibitor NGD (4 mins; 100 μM; grey bars). Data are pooled from the following populations.

Experiments to determine the effect of inhibiting cADPR production on I-mGluR-mediated Ca^{2+} signals were repeated utilising an alternative ARC antagonist, NGD (100 µM). In experiments utilising SD rat neurons, prior incubation with NGD resulted in a significant decrease in all I-mGluR mediated response parameters measured (amplitude = 13 ± 1 vs 8 ± 1 a.u., p = < 0.0001; normalised amplitude = 100 vs 67 ± 4%, p = < 0.0001; duration = 159 ± 9 vs 129 ± 8 s, p = 0.009; A.U.C. = 159 ± 9 vs 129 ± 8 a.u.; p = 0.0009; n = 49; control vs NGD; Fig 4.4, A), relative to I-mGluR application alone.

In contrast, in non-Tg neurons NGD significantly, but slightly, increased the amplitude (amplitude = 30 ± 2 vs 33 ± 2 a.u., p = 0.03; normalised amplitude = 100 vs 114 ± 6%, p = 0.01; control *vs* NGD) of DHPG-mediated Ca^{2+} responses, relative to control (Fig 4.4, B; n = 40), whereas the duration and A.U.C. were decreased with NGD and DHPG co-application (duration = 178 ± 9 vs 138 ± 21 s, p = 0.02; A.U.C. = 2667 ± 221 *vs* 2056 ± 304 a.u.; p = 0.02; control *vs* NGD).

In experiments utilising 3xTg-AD mouse neurons (4 days old; 9 DIV), NGD had no significant effect (albeit in a single experiment) on the amplitude, duration or A.U.C. of DHPG-responses, relative to DHPG application alone (amplitude = 18 ± 3 *vs* 19 ± 3 a.u., p = 0.63; normalised amplitude = 100 *vs* 140 ± 22%, p = 0.22; duration = 76 ± 12 *vs* 78 ± 9 s, p = 0.75; A.U.C. = 591 ± 135 *vs* 727 ± 170 a.u.; p = 0.16; n = 18; control *vs* NGD; Fig 4.4, C).

4.4.3 Effect of dantrolene on I-mGluR-evoked neuronal calcium signals

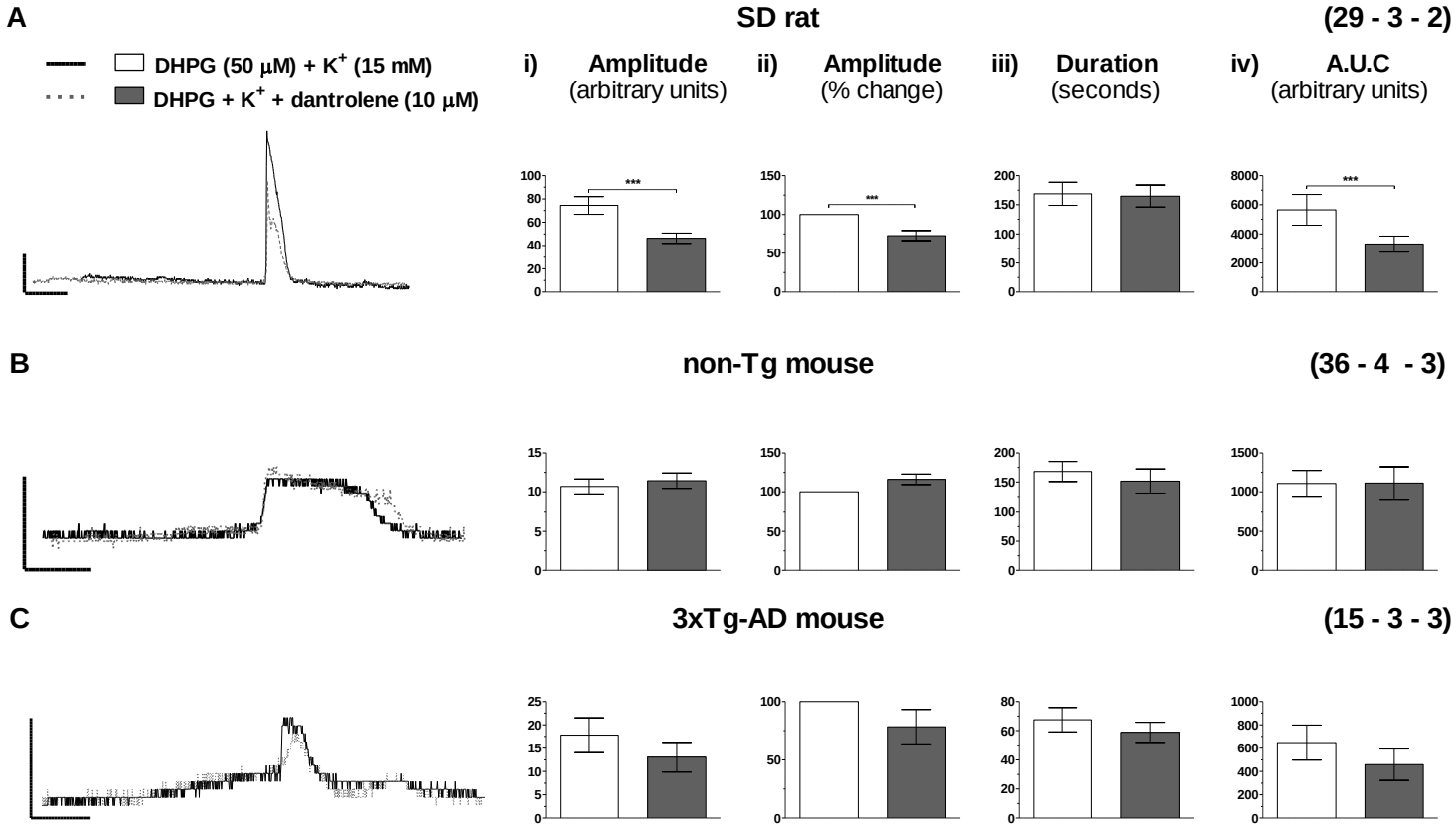

Figure 4.5. Somatic I-mGluR-mediated (DHPG = 50 μM) Ca^{2+} responses of SD rat (A), non-transgenic mouse (B) and 3xTg-AD mouse (C) cultured hippocampal neurons (3 – 4-days-old) under depolarisation conditions (K^+ = 15 mM) with and without prior incubation with the ryanodine receptor (RyR) antagonist dantrolene (10 μM).

Representative traces illustrate somatic intracellular DHPG-mediated Ca^{2+} responses of cultured hippocampal neurons under depolarisation conditions (DHPG = 50 μM; K^+ = 15 mM) with (grey dashed line) and without (control; solid black line) prior incubation with the RyR antagonist dantrolene (4 mins; 10 μM; a 50 minute agonist washout period separates both experimental phases). **A** = SD rat; 3-days-old / 7 - 13 DIV, **B** = non-transgenic mouse; 3 - 4-days-old/3 – 9 DIV and **C** = 3xTg-AD mouse; 3 - 4-days-old / 5 - 14 DIV. The horizontal axis represents 120 seconds (s) and the vertical axis represents 25 arbitrary units (a.u.) of fluorescence.

Histograms illustrate the amplitude (a.u. ; **i**) , normalised amplitude (% change; **ii**), duration (s; **iii**) and area under the curve (A.U.C.; measured in a.u.; **iv**) of DHPG-mediated calcium responses under depolarisation conditions (control; DHPG = 50 μM; K^+ = 15 mM; white bars) and following prior incubation with the RyR antagonist dantrolene (4 mins; 10 μM; grey bars).

The RyR antagonist dantrolene (10 μM) significantly decreased the amplitude and A.U.C. (amplitude = 74 ± 8 *vs* 46 ± 4 a.u., p = < 0.0001; normalised amplitude = 100 *vs* 73 ± 6%, p = 0.0002; A.U.C. = 5658 ± 1052 *vs* 3302 ± 555 a.u.; p = 0.0004), but not duration (76 ± 12 *vs* 78 ± 9 s, p = 0.75; n = 29; control *vs* dantrolene; Fig 4.5, A) of I-mGluR-mediated calcium responses under depolarisation conditions in SD rat neurons.

When these experiments were repeated with non-Tg mouse neurons, the normalised amplitude of I-mGluR responses were significantly enhanced following prior incubation with dantrolene relative to I-mGluR responses alone (100 *vs* 116 ± 7%, p = 0.02; n = 36; control *vs* dantrolene; Fig 4.5, B, ii). Conversely, amplitude (measured in a.u.), duration and A.U.C. of I-mGuR responses were unchanged by dantrolene (amplitude = 11 ± 1 *vs* 11 ± 1 a.u., p = 0.96; duration = 168 ± 17 *vs* 152 ± 21 s, p = 0.19; A.U.C. = 1107 ± 166 *vs* 1111 ± 209 a.u.; p = 0.97; control *vs* dantrolene; Fig 4.5, B).

Dantrolene had no effect on any I-mGluR response parameters measured in neurons from 3xTg-AD mice (albeit from one experiment; amplitude = 18 ± 4 *vs* 13 ± 3 a.u., p = 0.09; normalised amplitude = 100 *vs* 78 ± 15%, p = 0.19; duration = 68 ± 8 *vs* 59 ± 7 s, p = 0.15; A.U.C. = 648 ± 151 *vs* 459 ± 135 a.u.; p = 0.14; n = 15; control *vs* dantrolene; Fig 4.5, C).

Notably, there were no significant differences between the levels of inhibition of the amplitude of the I-mGluR signal between any of the antagonists used (i.e. nicotinamide, NGD or dantrolene) in SD rat neurons (one-way ANOVA with Tukey's multiple comparison test; ns). Conversely, in non-Tg mouse experiments, the level of I-mGluR response agonism was significantly less with NGD co-application relative to nicotinamide (14 ± 6% *vs* 177 ± 11%; n = 40 *vs* 61; p = < 0.0001). In 3xTg-AD experiments (although there was no significant effect of nicotinamide, NGD or dantrolene on DHPG responses relative to DHPG responses alone) NGD application (n = 18) resulted in a significantly different effect on DHPG responses compared with nicotinamide or dantrolene whereas there were no significant differences between co-application of nicotinamide or dantrolene with DHPG (p = 0.48; n = 33 *vs* 15; nicotinamide *vs* dantrolene).

4.5 Discussion

4.5.1 Contribution of ARC/RyR pathway to I-mGluR signalling

The central aim of this study was to add to the limited experimental data investigating whether cADPR is a second messenger downstream of neuronal I-mGluR stimulation. In order to determine if a given drug can be related to its proposed effect, in this case; DHPG / I-mGluR-mediated stimulation of the ARC/cADPR/RyR system, it needs to satisfy the five characteristics of second messengers as proposed by Sutherland and Robison (1966; and expanded upon by others (Gao and Vanhoutte, 2014; Hardman et al., 1971; Schultz and Rosenthal, 1985)).

Two of these characteristics are concerned with established effects downstream of cADPR production, i.e. that the cADPR signal can be terminated and that cADPR can act as a cellular effector (controlling a biological function in cells, organs or tissues), which have been explained previously in both this chapter and in reviews covering the status of cADPR as a *bona fide* second messenger (Guse, 2004; Lee, 2011). Of note, with respect to glutamate signalling, ARC may be regulated in a hierarchical manner (at least in cerebellar granule cells), whereby NMDAR activation inhibits ARC activity which, in turn, can be reversed by I-mGluR and II-mGluR activation (Salmina et al., 2011). The remaining three characteristics are more relevant to the proposed coupling of I-mGluR signalling with ARC/cADPR and will be discussed in more detail below.

Firstly, does ARC respond to I-mGluR-stimulation in broken cell preparations as might be expected in results with intact tissues? I-mGluR-mediated ARC stimulation in broken cell preparations exhibits significant variability across cell types and/or brain regions. For instance, glutamate-stimulated ARC on NG108-15 cell membranes overexpressing mGluR1 and 5 only and I-mGluR stimulation activated ARC in SCG membrane preparations. Conversely, glutamate or DHPG had little effect on ARC activity in membranes from rat and mouse retina, olfactory bulb, cerebral cortex, hippocampus, and cerebellum (Higashida et al., 2003).

Secondly, with regard to regulation, does the concentration of cADPR in intact cells change when I-mGluRs are stimulated and does this generation occur rapidly enough to accompany or precede the known physiological effect? The precise intracellular concentration of cADPR cannot yet be visualised directly in intact cells. However, there are indirect methods of measuring cADPR levels in intact cells including Ca^{2+} imaging following intracellular injection of cADPR, as well as an indirect determination of ARC activity using a fluorogenic substrate nicotinamide guanine dinucleotide (see Morgan et al., 2005). It is known that extracellular stimuli, *generally*, cause a rapid increase in intracellular cADPR (Guse et al., 1999; Leckie et al., 2003;

Yamasaki et al., 2005). Evidence for I-mGluR stimulation, *specifically*, is lacking although ARC activity is increased (rate was not measured) in cerebellar granule cells following I-mGluR stimulation (Salmina et al., 2011). Furthermore, within cultured rat DRG neurons, I-mGluR and II-mGluR co-activation (with a non-specific agonist) evoked calcium release via RyR activation which was mimicked by extracellular application of the cADPR precursor NAD^+. This observation suggests cADPR generation could occur rapidly enough to be involved in I-mGluR-mediated neuronal signalling. However, as mentioned previously, this study contains a major flaw in that the potential contribution of IP_3R - mediated signalling to the overall I-mGluR - evoked calcium signal was not measured (Crawford et al., 1997b).

Thirdly, can the physiological effect of I-mGluR stimulation be mimicked by cADPR (not membrane permeable; Morgan, 2005), a cADPR derivative or a membrane-permeable cADPR analogue? The major downstream physiological effect, at least with respect to this project, of DHPG / I-mGluR stimulation is RyR-(and/or IP_3R-) mediated Ca^{2+} signalling as a potential molecular mechanism for synaptic plasticity (Futagi and Kitano, 2015; Rose and Konnerth, 2001; Sajikumar et al., 2009). Although ARC is implicated in mediating such I-mGluR signals, and cADPR can certainly mimic ER Ca^{2+} release (Crawford et al., 1997a; Higashida et al., 2003; Irving et al., 1992; Morikawa et al., 2003; Sohn et al., 2011), little is known about ARC/cADPR involvement in synaptic plasticity (Reyes-Harde et al., 1999a) or in I-mGluR-mediated enhanced signals proposed to correlate to “learning events” (Nakamura et al., 1999; Rae et al., 2000). It is in this context that the current project sought to determine cADPR involvement, albeit not specifically by utilising cADPR analogues, but instead indirectly by way of ARC inhibition and/or cADPR antagonism.

This approach was utilised previously by Sohn et al. (2011) who proposed that I-mGluR-mediated Ca^{2+} mobilization in acutely dissociated SD rat CA1 pyramidal neurons was generated in its entirety by activation of the cADPR/RyR pathway. Although this finding was supported by the demonstration that I-mGluR-mediated Ca^{2+} signals were still evoked in neurons derived from PLCβ1- and PLCβ4-knockout mice, the investigators failed to either quantify how large these signals were relative to those evoked in control neurons or, indeed, to demonstrate that these calcium signals were blocked by their chosen cADPR antagonists (Sohn et al., 2011). This is a particularly important distinction given the aforementioned canonical coupling of I-mGluRs to IP_3Rs. Furthermore, in whole labyrinth preparations at least, I-mGluR-mediated RyR activation occurred *via* IP_3R-initiated CICR and not due to ARC-mediated cADPR production (Hendricson and Guth, 2002).

When we attempted to replicate the findings of Sohn et al. (2011), using cultured SD rat hippocampal neurons, rather than acutely dissociated

SD rat CA1 pyramidal neurons, we found that the cADPR/RyR calcium signalling pathway was indeed responsible for a significant proportion of the overall I-mGluR-mediated calcium signal (Fig 4.3 - 4.5; Kaar and Rae, 2014). However, this portion comprised a much lower proportion of the total I-mGluR mediated response (ARC inhibition = 20 ± 6% (nicotinamide) and 33 ± 4% (NGD); RyR inhibition = 17 ± 6% (dantrolene); % decrease in amplitude; Fig 4.3 – 4.5, A, ii) in comparison to the entirety of the signal proposed by Sohn et al. (2011). However, as detailed below, the effect of nicotinamide is likely underrepresented given the opposing effects of negative controls used in these experiments (Fig 4.3). Interestingly, our finding of potential redundancy in the IP_3/IP_3R and cADPR/RyR pathways activated by I-mGluR stimulation was mirrored by findings from rat midbrain dopaminergic neurons. Here, both the IP_3/IP_3R and cADPR/RyR pathways were necessary to mediate maximum magnitude intracellular calcium responses to I-mGluR activation, but both 'arms' of the calcium signalling cascade evoked intracellular calcium release independently of one another (Morikawa et al., 2003).

By using dantrolene I was able to determine the role of the putative cADPR target, RyR, in I-mGluR mediated Ca^{2+} signals with the caveat that there are question marks regarding its isoform specificity (see *Section 4.5 - Limitations*). There were no significant differences in the level of I-mGluR-mediated calcium signal reduction following inhibition of the synaptosomal cyclase (with NGD) or RyRs. This suggests that the entirety of the dantrolene- sensitive RyR-evoked signal (potentially through RyR1 and 3 subtypes, solely (F. Zhao et al., 2001)) downstream of I-mGluR activation is stimulated by cADPR derived from this synaptosomal cyclase.

Conversely, when negative control experiments are factored in for nicotinamide inhibition of CD38 (likely meaning that levels of I-mGluR inhibition are much greater in reality with this antagonist; Fig 3.4; A; ii) it suggests that, a) both the synaptosomal cyclase and CD38 are mediators of I-mGluR stimulated ER Ca^{2+} mobilisation and that, b) there is a RyR-accessible Ca^{2+} pool which is not inhibited by dantrolene (possibly through RyR2; F. Zhao et al., 2001) in SD rat hippocampal neurons. Conversely, if dantrolene is an effective pan-RyR inhibitor, it suggests that the effects of the proposed cADPR binding to, and enhancement of, IP_3R1-3 Ca^{2+} mobilisation (Vanlingen et al., 1999) and/or SERCA activation (Bradley et al., 2003; Lukyanenko et al., 2001; Yamasaki-Mann et al., 2009) also contribute to this I-mGluR-elicited signal. Notably, NGD at high concentrations (2 mM) is also considered to be a general ARC (including CD38) inhibitor. However, it is unknown if the 100 µM concentrations used in this study inhibited other ARCs aside from the synaptosomal species (Fritz et al., 2005). Had time and

circumstances permitted them, experiments in which these antagonists were co-applied would have been useful in determining this definitively.

Although ARC-mediated I-mGluR signalling appears under-represented in this study, it is still markedly lower than the entirety of the signal suggested by Sohn et al. (2011). The reason(s) for such a marked difference in results between the two studies is unclear but one obvious suggestion is that the culturing process itself might somehow alter the phenotype of intracellular calcium signals evoked by I-mGluR stimulation, relative to those observed in acutely dissociated cells. A similar discrepancy in IP_3-mediated calcium mobilisation between cultured, compared to acutely dissociated, cells has been noted when utilising rat DRG neurons, although overall responsiveness to I-mGluR stimulation appeared to also be a function of DRG soma size (Pollock et al., 1999; Svichar et al., 1997a). In order to determine, in a relatively definitive manner, if the culturing process did indeed induce a rapid alteration in I-mGluR-activated calcium signalling pathways relative to more 'physiological' preparations, experiments which examined the contribution of the cADPR/RyR pathway to I-mGluR-mediated signals in dentate gyrus neurons within intact hippocampal slices using "bulk-loading" calcium imaging have also been carried out by Dr Rae's lab group. Thus far only the effects of nicotinamide on I-mGluR-mediated Ca^{2+} signals have been investigated. It caused a significant decrease in I-mGluR-mediated Ca^{2+} signals in both non-Tg mouse (11 ± 5%; n = 30 from 5 experiments) and 3xTg-AD mouse neurons (23 ± 6; n = 22 from 3 experiments; Vaughan et al., 2018). Alternatively, hippocampal neurons can exhibit differences in mGluR expression, localisation and activity in a manner dependent on postnatal development (2 – 3 weeks *vs* 6 – 8 weeks; CA1 pyramidal neurons; intact hippocampal slices; Ireland and Abraham, 2002; Mannaioni et al., 2001). This factors may be relevant to differences in phenotype between acutely dissociated neurons in the Sohn et al. (2011) study (7 to 14-days-old) and cultured hippocampal neurons (3 days-old; 6 - 13 DIV) in the present study.

Caution must be taken when making comparisons between the results of Sohn *et al.* (2011) utilising acutely dissociated rat neurons, results from Vaughan et al. (2018) utilising dentate gyrus mouse neurons from intact hippocampal slices and my own research utilising cultured mouse and rat hippocampal neurons, as the role of cADPR signalling in I-mGluR-evoked calcium responses may vary between species and neuronal populations and may even be dependent on I-mGluR localisation within the same cell. For example, dendritic I-mGluR mediated Ca^{2+} signalling within hippocampal neurons appears to be mediated solely by the IP_3R pathway (Nakamura et al., 2000, 1999), whereas, as discussed above, cADPR appears to mediate at least a proportion of the I-mGluR mediated calcium signal evoked within

the somata of both hippocampal (Kaar and Rae, 2014; Sohn et al., 2011) and adult DRG neurons (Svichar et al., 1997b), with or without additional involvement of IP_3-evoked signalling. Importantly, in the current study, species differences were evident between SD rat and non-Tg mouse neurons. Specifically, ARC inhibition with nicotinamide prior to and during I-mGluR stimulation enhanced Ca^{2+} signals (77 ± 11% increase; Fig 4.3, A, ii) in non-Tg mouse neurons. This is in direct contrast to the decrease we saw using nicotinamide in SD rat experiments (reduced amplitude and A.U.C.; duration unchanged). The fact that our benzamide experiments mirrored the results of our nicotinamide experiments in non-Tg mouse neurons (Fig 4.3; B; ii) suggests that the effects we witnessed were due to off-target effects of nicotinamide and (unlike in SD rat, where the effects observed in control conditions and in the presence of nicotinamide were opposed) may suggest that CD38 does not play a role in I-mGluR-evoked signals in these mouse neurons. Potential off-target effects of both the synaptosomal cyclase inhibitor, NGD, and nicotinamide may occur by enhanced ER Ca^{2+} release as cADPR can stimulate SERCAs (Bradley et al., 2003; Lukyanenko et al., 2001; Yamasaki-Mann et al., 2009) and IP_3Rs (Tao et al., 2011; Vanlingen et al., 1999). However, conversely, Missiaen et al. (1998) presented evidence of the exact opposite effect, *i.e.* cADPR-mediated inhibition of SERCA and IP_3Rs.

Similar to our nicotinamide experiments, NGD caused a small but significant increase in the amplitude of I-mGluR-evoked signals in non-Tg mouse experiments (14 ± 6% increase; Fig 4.4, B, ii) which could also be due to off-target effects of this antagonist (although to significantly lower levels than observed with nicotinamide; 14 ± 6% and 77 ± 11% increase respectively). Aside from off-target effects perhaps explaining the enhancement of I-mGluR-mediated signals we observed following ARC inhibition, another possibility is that an I-mGluR-mediated persistent (>20 minutes) suppression of sAHP, similar to that described by Ireland and Abraham (2002) following application of a I- and II-mGluR agonist (Ireland and Abraham, 2002), may result in a greater activation of L-type VGCCs upon the second depolarisation stimulus, potentially allowing greater uptake of Ca^{2+} by the ER and its subsequent mobilisation by DHPG. However, in control experiments (repeated DHPG applications under depolarisation conditions) there was a decrease in the amplitude of I-mGluR-evoked responses in non-Tg mouse neurons over time (16 ± 5%; $p = 0.006$; $n = 58$).

To complicate matters further, however, the duration and A.U.C. of DHPG-mediated responses were decreased in the presence of NGD in both non-Tg mouse and SD rat neurons (Fig 4.4; A & B, iii & iv). This could suggest that potential off-target effects of this antagonist in non-Tg mouse experiments mask its ARC inhibiting effects with respect to calcium signal

amplitude, but not with respect to signal A.U.C. (Fig 4.4; B; I & ii *vs* iii & iv). Furthermore, despite response size differences between non-Tg mouse and SD rat neurons in the *initial* I-mGluR mediated ER Ca^{2+} release following inhibition of the synaptosomal cyclase (amplitude), the *magnitude* (A.U.C.) of the resultant sustained somatic Ca^{2+} signals were not different and decreased in both models when DHPG and NGD were co-applied. Could it be that in non-Tg neurons, inhibition of the synaptosomal cyclase (and a rapid decrease in cADPR) relieves a negative regulation of IP_3Rs, causing an initial increase (amplitude) of the I-mGluR response, whereas a reduction in cADPR ultimately results in less CICR and a decrease in the sustained I-mGluR response? However, if this were the case, quite why it would be a signalling algorithm in non-Tg mouse but not SD rat neurons is unclear. Furthermore, if this was the case one would expect the RyR antagonist dantrolene to have the same effect on the A.U.C. of I-mGluR responses as the ARC inhibitors, which is not the case (Fig 4.5, B, iv). In fact, dantrolene did not alter I-mGluR responses in non-Tg neurons, suggesting a lack of involvement of RyR1 and 3 (and potentially 2) in this signalling system. It is also a possibility that these unique differences between enhanced amplitude but inhibited duration and A.U.C. of I-mGluR responses with NGD co-application (Fig 4.4; B) reflect that this single non-Tg mouse experiment was an outlier.

This large inter-species variability is in contrast to the work of Higashida et al. (2003) which found consensus between mouse (“adult WT”) and Wistar rat (1 – 12 weeks-old) in that mGluR or I-mGluR stimulation did not affect ARC activity in membranes from the retina, olfactory bulb, cerebral cortex, hippocampus, and cerebellum. Aside from species differences, an added layer of variability could also arise from the fact that SD rats are a genetically heterogeneous outbred strain in comparison to our inbred strain of non-Tg mice (C57BL6/129sv).

An added layer of complexity to this story comes from the finding that in NG108-15 cells and rat cerebellar granule neurons, cADPR signalling seems to be dependent upon the excitation state of the cell as well as the loading state of the ER. For example, under resting conditions, intracellularly applied cADPR failed to evoke any form of Ca^{2+} mobilisation, but did amplify both depolarization-induced Ca^{2+} mobilisation (by acting as an agonist of RyRs at the ER) as well as Ca^{2+} influx through L-type VGCCs (De Flora et al., 1996; Empson and Galione, 1997; Hashii et al., 2000b). These findings support previous research which showed that the loading state of the ER had an important bearing on the magnitude of signals evoked by ER stimulation (Rae et al., 2000; Rae and Irving, 2004). Similarly, oxytocin release in hypothalamic neurons in response to depolarization was decreased in CD38 null mice (Higashida et al., 2012; Jin et al., 2007). Therefore, it would be of

interest to investigate whether the contribution of the ARC/RyR pathway to I-mGluR-evoked calcium signals displayed a similar modulation under basal conditions, relative to depolarisation conditions, in our model of cultured hippocampal neurons.

Another consideration that must be borne in mind when interpreting putative cADPR-evoked Ca^{2+} signalling data is the possibility that RyR-mediated CICR can be induced both by cADPR alone (Ayar and Scott, 1999; Crawford et al., 1997b; Empson and Galione, 1997; Hua et al., 1994) and by amplification of local signals following IP_3R activation (Morgan and Cyclic, 2002; Stutzmann et al., 2007). Thus, one may show the sensitivity of one's Ca^{2+} signals to RyR blockade, but it may be that the responses are mediated *via* IP_3R-evoked CICR, rather than cADPR activation of RyRs *per se*. This might explain why I-mGluR evoked responses which can be inhibited by IP_3R and/or PLC antagonists are also sensitive to inhibition by RyR antagonists (Abdul-Ghani et al., 1996). However, in the case of hippocampal neurons at least, I-mGluR mediated calcium signals can still be evoked even following putative IP_3R blockade with heparin in acutely dissociated hippocampal CA1 neurons (Sohn et al., 2011) and cultured SD rat hippocampal neurons (150 μM 2-APB; no effect on DHPG-evoked Ca^{2+} signals; $p = 0.97$; $n = 17$; Kaar and Rae, 2013), although this finding is absolutely contingent upon the antagonists being specific for IP_3Rs, which is less than certain in some cases (Bootman et al., 2002; Chung et al., 2004; Dasso and Taylor, 1991; Lemonnier et al., 2004; Peppiatt et al., 2003; Rae et al., 2012). Indeed, this last point highlights a problem which continues to beset this field of study: the lack of specific antagonists and agonists for IP_3Rs, RyRs and ARC with which to pharmacologically dissect out the relative contributions of IP_3-mediated *versus* cADPR/RyR-mediated I-mGluR-evoked Ca^{2+} signals (as discussed below - *Limitations*). This usually necessitates the requirement for multiple approaches to establish a single datum piece which, in addition to being both costly and time-consuming, may still be regarded with some suspicion by others in the field.

Finally, there is evidence to suggest that both I-mGluR subtypes, mGluR1 and mGluR5, may mediate cADPR/RyR-activated Ca^{2+} signals. For example, Higashida et al. (2003) showed that activation of I-mGluRs stimulated ARC activity and increased cADPR concentration in rat SCG membranes. Interestingly, they also demonstrated that both mGluR1 and mGluR5 were relatively equally effective in stimulating ARC activity when these receptors were overexpressed in NG108-15 cells (Higashida et al., 2003). Conversely, mGluR-mediated cADPR responses in rat DRG neurons and acutely dissociated CA1 hippocampal neurons were proposed to be mediated solely by mGluR5 (Pollock et al., 1999; Sohn et al., 2011). This may suggest some receptor redundancy in cells where both receptor

subtypes are expressed, such as rat CA1 hippocampal neurons, as has been shown in other studies with regard to I-mGluR-evoked Ca^{2+} signals previously ascribed to activation of IP_3Rs (*e.g.* Rae and Irving, 2004).

4.5.2 ARC/RyR-mediated signalling in AD

The final aim of the work detailed in this chapter was to determine whether or not the contribution of the ARC/RyR pathway was altered in 3xTg-AD neurons relative to non-Tg controls. This investigation was predicated upon the results of Stutzmann et al. (2007) who found that the contribution of RyR-mediated Ca^{2+} mobilisation to IP_3R-stimulated responses in non-Tg cortical neurons was relatively modest (caged IP_3 = 20 ± 7%; action potential-evoked = 15 ± 5%). This was replicated in the current study as the RyR antagonist dantrolene had no effect on the amplitude, duration or A.U.C. of I-mGluR mediated responses (Fig 5.5; B). However, as evidenced by the aforementioned apparent enhanced inhibition of I-mGluR signals with nicotinamide, compared with dantrolene there appears to be a dantrolene insensitive RyR pool accessed by I-mGluRs, at least at the concentration used in these experiments.

The contribution of RyRs to caged IP_3 induced signals (i.e. due to CICR) was increased in $PS1_{M146V}$ and 3xTg-AD neurons (which also express $PS1_{M146V}$) to 59 ± 11% and 71 ± 9%, respectively, suggesting an upregulation of RyRs in these models (Stutzmann et al., 2007). This apparent increase in the amplitude of RyR-mediated Ca^{2+} responses in 3xTg-AD neurons, relative to $PS1_{M146V}$ neurons, suggested an additive effect of either APP_{SWE} or Tau_{P301L} to PS1 $_{M146V}$-mediated Ca^{2+} dysregulation. When compared to the experiments contained herein, there was no significant difference in the amplitude, duration or A.U.C. of I-mGluR responses following dantrolene incubation. However, the caveat of a low *n* number (15 cells) used in these experiments should be considered in this case as well as the fact there is a trend towards an inhibitory effect of dantrolene on I-mGluR responses (Fig 4.5; C).

Interestingly however, unlike in non-Tg mouse where the synaptosomal cyclase appears to modify I-mGluR-mediated signals (Fig 4.4; B) in 3xTg-AD mouse neurons NGD did not alter I-mGluR signals (albeit in one experiment; n = 18; Fig 4.4, C), suggesting an alteration in I-mGluR coupling to this enzyme. Furthermore, when negative control experiments are factored in to CD38 inhibition experiments and results are compared between non-Tg and 3xTg-AD mouse experiments (Fig 4.3; B *vs* C) it appears that CD38 does not modulate the amplitude of I-mGluR responses (although off-target effects of nicotinamide do; Fig 4.3, B, ii) in non-Tg neurons, whereas this pathway is utilised in 3xTg-AD neurons. This could

have the effect of upregulating ER Ca^{2+} signals which is a proposed characteristic of a neuron affected by AD pathology (Berridge, 2010).

In summary, these results suggest that FAD mutations, most likely in *PS1*, can alter the dynamics of I-mGluR-mediated ER Ca^{2+} mobilisation in terms of the relative contributions of IP_3Rs and RyRs to overall stimulated Ca^{2+} mobilisation. As discussed previously and investigated in *Chapter 5*, this transgenic phenotype could be underpinned by increased RyR expression in transgenic cultured neurons (Chakroborty et al., 2009; Kelliher et al., 1999; Oules et al., 2012; Stutzmann et al., 2006; see Fig 5.3) and/or a more general increase in ER Ca^{2+} levels due to impaired PS1-mediated Ca^{2+} leak (Zhang et al., 2010). With regard to ARC, there is tentative evidence that its activities are altered between non-Tg and 3xTg-AD cultured hippocampal neurons.

4.5.3 Limitations

Morgan et al. (2005) outline common problems surrounding Ca^{2+} imaging experiments which may influence the results presented herein. These include the "questionable pharmacology" of antagonists targeting proteins relevant to this field and fluorimetry issues (such as an antagonist which absorbs the exciting light or is auto-fluorescent).

To address the first issue, we utilised two ARC antagonists (nicotinamide and NGD) as well as an antagonist of RyRs (the most likely downstream mediator of ARC-dependent Ca^{2+} mobilisation; RyRs) in order to reduce the likelihood that the effects of these compounds on I-mGluR evoked calcium signals was not completely due to non-specific or unwanted modulation of other Ca^{2+} signalling pathways. Evidence for the effectiveness of these compounds as inhibitors of ARC/RyR signalling is as follows:

1. **Nicotinamide** is a cell-membrane permeant (possibly in a non-passive manner; Olsson et al., 1993) **inhibitor of ARC activity**, which prevents the formation of cADPR (Bruzzone et al., 2003a; Geiger et al., 2000; Liang et al., 1999; Migaud et al., 1999b; Sethi et al., 1996). There is also limited evidence that nicotinamide inhibits PARP1 (Namazi, 2003; Woon and Threadgill, 2005). Of particular relevance to this study, it has been utilised in acutely dissociated rat hippocampal neurons to antagonise I-mGluR/ARC-mediated Ca^{2+} responses (5 mM; 5 mins pre-treatment; Sohn et al., 2011).

2. **NGD** is catalysed by CD38, CD157 and *Aplysia* cyclase to produce hydrolysis- resistant cGDPR (Fernàndez et al., 1998; Graeff et al., 1994;

Guse et al., 2001; Lee et al., 1999; Zocchi et al., 2001). cGDPR does not evoke Ca^{2+} mobilisation and as such is often used to measure ARC activity in cell homogenates (Graeff et al., 1996). The use of NGD, in this context, is based upon the assumption that the active ARC enzyme(s) in one's cell(s) of choice can utilise this substrate. However, as mentioned previously, Ceni et al. (2003) have identified a non-CD38 synaptosomal ARC in mouse whole brain tissue enriched in a PM and ER-fraction which can bind NGD but cannot utilise it as a substrate. Indeed, NGD acts as a competitive antagonist of NAD^+ at the cyclase active site (K_i = 24 μM; Ceni et al., 2006, 2003a). Similarly, high concentrations of NGD (2 mM) inhibited ACch-mediated Ca^{2+} responses and the number of oscillatory responses in permeabilised myocytes (resulting from RyR-mediated CICR). Ach-mediated Ca^{2+} responses in these cells are dependent on a signalling cascade involving muscarinic M2 receptors, ARC (likely CD38), FKBP12.6 and RyR2 (Fritz et al., 2005). Therefore, the use of NGD (in excess) as an **ARC inhibitor** can also be extended to non-synaptosomal ARCs such as CD38, which *do* utilise NGD as a substrate. Previous studies have characterised its function mostly in homogenised or permeabilised cells, however its use as an antagonist in this study is dependent upon either the presence of an extracellular active site on the constitutively active ARC(s) in cultured hippocampal neurons or the transport of NGD across the plasma membrane. To the best of our knowledge such transport has not yet been described but may involve similar mechanisms to the transport of cADPR (including that by NTRs or concomitant with CD38 internalisation; Guida et al., 2004, Zumaquero et al., 2010) or its analogue NAD^+ (including that by P2X7Rs; Salmina et al., 2014), as described previously in *Section 4.1 - Transport of NAD+/cADPR*.

3. **Dantrolene** has been characterised as a membrane-permeable **RyR antagonist**. However, there are still numerous questions surrounding its molecular action and binding sites on RyRs (Krause et al., 2004). Although it has been established that dantrolene inhibits RyR1 (in a CaM-dependent manner; native SR vesicles; Zhao et al., 2001) and RyR3 (expressed in HEK-293 cells; Zhao et al., 2001), its activity at RyR2 is less clear. In this particular context, although dantrolene has inhibits RyR2 in CHO cells, a finding which is supported by an abundance of literature on cardiac tissue where RyR2 is predominately expressed (for review see Wehrens and Marks, 2005), it failed to inhibit RyR2 in native cardiac SR vesicles or when they were expressed in HEK-293 and CHO cells (F. Zhao et al., 2001). As all three RyR isoforms are expressed in mouse, rat and human brain (Bennett et al., 1996), it is possible that a component of the I-mGluR-mediated Ca^{2+} signals in hippocampal neurons described here (Fig 4.5) is mediated *via* RyR2 in neurons, which

would not have been blocked by dantrolene (S. Kim et al., 2007). This suggestion is all the more pertinent given that cADPR-mediated activation of RyR1 and RyR3 is variable across cell types (Copello et al., 2001; Fulceri et al., 2001; Kunerth et al., 2004; Morrissette et al., 1993; Murayama and Ogawa, 2002; Sitsapesan and Williams, 1995; Sonnleitner et al., 1998), whereas it universally activates RyR2 (Barone et al., 2002; Rakovic et al., 1996; Sitsapesan and Williams, 1995; Takasawa et al., 1998; Y. X. Wang et al., 2004).

4. **U73122** has been utilised in numerous previous studies as an irreversible cell membrane permeant **inhibitor of PLC** (Bleasdale et al., 1990) and PLC-dependent Ca^{2+} mobilisation. As such, this compound was utilised by Jin et al., (1994) to study PLC function in neuronal NG108-15 cells and rat DRG neurons where they found that it inhibited bradykinin-induced increases in $[Ca^{2+}]_i$ (IC_{50} of 1 μM after 3 mins incubation and 200 nM after a 20-minute incubation). However, U73122 also inhibited VGCCs, preventing depolarisation-induced Ca^{2+} influx in both NG108-15 cells and DRG neurons (Jin et al., 1994). U73122 also stimulated a slight Ca^{2+} mobilisation in NG108-15 cells, DRG neurons and MDCK cells (Jin et al., 1994) and Ca^{2+} influx in MDCK cells (Jan et al., 1998). Furthermore, in myocytes, U73122 (10 μM) inhibited SERCA, increased steady-state $[Ca^{2+}]_{cyto}$ and sensitised IP_3Rs and RyRs to stimulated Ca^{2+} release (Macmillan and McCarron, 2010). Notably, in a cell-free system, human PLCβ was, in fact, *activated* by U73122 (EC_{50} = 13.6 ± 5 μM; (Klein et al., 2011). Therefore, caution clearly needs to be exercised when interpreting experiments utilising this compound. In our hands, U73122 (10 μM; 8 mins) induced widespread death of our cultured hippocampal neurons as evidenced by phenomena such as cell lysis, cell shrinkage or rapidly increasing or decreasing $[Ca^{2+}]_i$ baselines (unpublished observations). These findings are in agreement with other studies which showed that U73122 (10 μM) was pro-apoptotic in cultured human umbilical vein endothelial cells (Miao et al., 1997) and PC12 cells where it resulted in decreased Bcl-2 expression and activation of caspase-2, at least following hydrogen peroxide-induced cell insult mediated by PLC-γ1 (Yuan et al., 2009).

The choice of antagonists and agonists of both the ARC/RyR and PLC/IP_3 systems in this study was limited by the commercial availability of membrane-permeable compounds. To add weight to the proposal that I-mGluR signalling is mediated in part by the ARC/RyR pathway, it would have been useful to have employed several more alternative agonists, antagonists and/or modulators of these signalling systems. Unfortunately, time

constraints did not allow for such experiments to be undertaken in this period of study. These compounds include:

1. Membrane-permeant **cADPR competitive-antagonists** 8-Br-cADPR and 7-deaza-8-Br-cADPR (Barone et al., 2002; Lukyanenko et al., 2001; Sethi et al., 1997; Walseth et al., 1993).
2. **cADPR mimetics (agonists).** A large number of cADPR derivatives have been developed of which N1-cyclic inosine diphosphoribose (N1-cIDPR) has an almost-identical biological activity to cADPR (Wagner et al., 2005) and its derivatives are membrane permeant (Guse et al., 2005; Jianfeng Xu et al., 2006; Xianfeng Gu et al., 2004).
3. **ARC antagonists.** Flavonoids, including luteolinidin, inhibit CD38 (membrane permeant; Kellenberger et al., 2011) and mirror results from CD38 KO mice (Blacher et al., 2015).
4. **IP_3R antagonists.** Heparin (non-cell permeant), xestospongin C and 2-APB are utilised as IP_3Rs blockers but have numerous side-effects (Morgan et al., 2005). For instance, heparin uncouples GPCRs from G-proteins (Dasso and Taylor, 1991), xestospongin C inhibits SERCA (Castonguay and Robitaille, 2002; De Smet et al., 1999; Solovyova et al., 2002), and 2-APB inhibits SERCA, SOCCs, $GABA_A$ and TRPV3 (Bootman et al., 2002; Chung et al., 2004; Lemonnier et al., 2004; Peppiatt et al., 2003; Rae et al., 2012). For this reason, preliminary experiments utilising 2-APB in cultured SD rat neurons, which did not inhibit I-mGluR-mediated signals (described previously; Kaar and Rae, 2013) were not expanded upon further.
5. **RyR antagonists.** Ruthenium red inhibits RyRs but is also a potent blocker of the MCU (Matlib et al., 1998). Although ryanodine is recognised as a concentration-dependent RyR agonist/antagonist, the precise concentration ranges which have to be utilised vary between experimental preparations. Furthermore, it binds to the open-state of RyRs only and therefore its effectiveness is determined by the activation state of the receptor (Morgan et al., 2005).

Lastly, with regard to fluorimetry issues, dantrolene exhibits fluorescent properties with an excitation at 395 nm and emission at 530 nm (Dehpour et al., 1982; Hollifield and Conklin, 1968). However, although this is of concern when utilising fura-2 (excitation = 340/380 nm (high/low Ca^{2+}); emission = 505 nm; Coleman, 2005), given that fluo-2 has markedly different excitation (491 nm) and emission (515 nm) properties to dantrolene, the auto-fluorescent effects of dantrolene were likely to be negligible in our protocol. Indeed, this was tested by recording baseline fluorescence before and after dantrolene application in basal and high K^+ HBSS and was found to be unaltered by dantrolene (data not shown).

4.6 Conclusions

In conclusion, nearly 30 years after its initial discovery, much work still remains to be done to characterise neuronal cADPR /RyR signalling both in terms of its fundamental mechanics and interactions with other calcium signalling systems. Although this work informs the proposal of cADPR acting as a second messenger downstream of I-mGluR stimulation, at least in SD rat neurons, much further characterisation needs to be done. As outlined by Seifert et al. (2015), the harnessing of technologies including high-performance liquid chromatography (HPLC), mass spectrometry (MS), combined LC-MS, dynamic mass redistribution (DMR) and the creation of membrane permeable cADPR-AM dyes may be pivotal in answering this question.

Crucially, the possible role for, or alteration of, cADPR / RyR signalling in human pathology has yet to be investigated to any significant degree. This is surprising given the putative role that dysregulation of normal cellular calcium homeostasis and/or calcium signalling pathways are proposed to play in several major human diseases such as cardiac disease, schizophrenia, bipolar disorder and AD.

Specifically with regard to AD, there is now substantial evidence, gleaned from both human and animal studies, that alterations in neuronal calcium homeostasis, with the knock-on effect that this has on both IP_3 - and RyR - mediated signalling (including that mediated by I-mGluRs), may be the key underlying factor in the disease pathogenesis. In transgenic models of AD, these alterations occur long before any behavioural changes or overt histopathology appears (Berridge, 2014b, 2012; Stutzmann, 2007). Therefore, it is not inconceivable that one may also detect alterations in cADPR - mediated signalling within these animals, and in the process, uncover a hithertofore unrecognised novel therapeutic target. Given that AD is currently one of the greatest public health threats facing mankind in the forthcoming century, this would be no small feat.

5. Bcl-2 Superfamily

5.1.1 Introduction

The superfamily of Bcl-2 proteins are critical regulators of cell death and survival by virtue of the fact that they are primary regulators of apoptosis, the major mode of programmed cell death (for review see: Czabotar et al., 2013; Youle and Strasser, 2008), necrosis (Tsujimoto et al., 1997) and, indeed, the balance between these two forms of cell death (Du et al., 2006; Meilhac et al., 1999).

Bcl-2 family proteins contain blocks of sequence homology called Bcl-2 Homology (BH) domains (Fig 5.1).

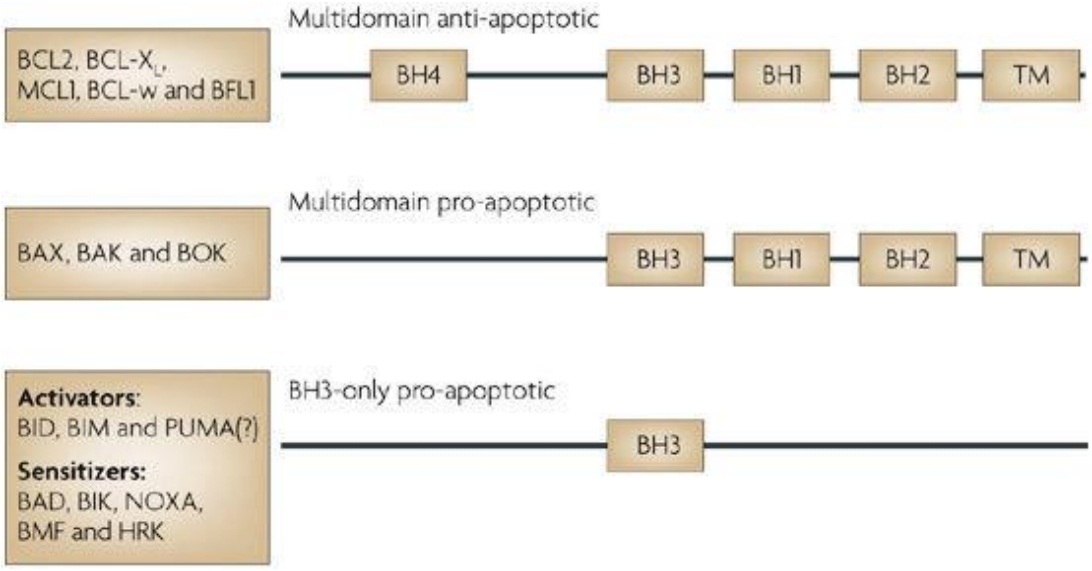

Figure 5.1 Structures of the three main classes of BCl-2 family proteins

Anti-apoptotic Bcl-2 proteins contain four α-helical Bcl-2 homology (BH) domains. BH1 2 and 3 form a hydrophobic cleft which binds to the hydrophobic surface of pro-apoptotic BH3 proteins. These include multi-domain pro-apoptotic proteins and BH3-only pro-apoptotic proteins.

Acronyms used: Bcl-2 antagonist of cell death (BAD), Bcl-2 antagonist of cell death (BAK), Bcl-2-associated X protein (BAX), B-cell lymphoma 2 (BCL2), Bcl-2 homology (BH) domain, BH3-interacting domain death agonist (BID), Bcl-2-interacting killer (BIK), Bcl-2-modifying factor (BMF), Bcl-2-related ovarian killer (BOK), myeloid cell leukaemia sequence 1 (MCL1), transmembrane domain (TM).

The anti-apoptotic Bcl-2, Bcl-X_L, Bcl-w, Mcl-1, A1 (BFL1) and Bcl-B and pro-apoptotic multi-domain effector proteins BAX, BAK and BOK, all share three BH domains (BH 1 – 3; Fig 5.1; Kvansakul et al., 2008) which give these proteins a common structure (Muchmore et al., 1996) including a cleft which allows for interactions with BH3-containing proteins (*i.e.* all known Bcl-2 family proteins; Czabotar et al., 2013; Letai, 2008). Anti-apoptotic Bcl-2 family proteins also have a BH4 domain (Letai, 2008) that is critical for binding to ER Ca^{2+} release channels (Rong et al., 2009).

Of these proteins, the focus of this particular investigation was on the relative expression of Bcl-2 and Bcl-X_L in postnatal hippocampal tissue from 3xTg-AD mice (P5, 15 and 21) in comparison to non-transgenic age-matched controls. These proteins were chosen for investigation as increases in their expression and activity correlate with increased neuronal resistance to apoptotic and oxidative stresses both *in vitro* and *in vivo* (for reviews see Merry and Korsmeyer, 1997; Shacka and Roth, 2006) which, as discussed in *Section 1*, are processes of significant relevance to AD.

Bcl-2 and Bcl-X_L also reversibly inhibit IP_3R and RyR gating. This process is itself anti-apoptotic, at least with regard to IP_3Rs, as it reduces Ca^{2+}-dependent apoptosis, but also has important implications for intracellular Ca^{2+} signalling (Hanson et al., 2008; Rong et al., 2008; Vervliet et al., 2014). Furthermore, these Bcl-2 family proteins are of significant interest in early AD pathology due to the fact that there is a growing body of evidence implicating them in almost all aspects of cell death, intracellular Ca^{2+} homeostasis and signalling, as well as ER organelle remodelling (Vervliet et al., 2016), all of which are affected by AD. In the subsequent sections of this chapter, the physiological functions of various Bcl-2 family members, particularly Bcl-2 and Bcl-X_L, will be discussed, with a specific emphasis on Ca^{2+} homeostasis and signalling.

The expression of the ER Ca^{2+} release channels, IP_3Rs and RyRs, which Bcl-2 family members interact with, will also be assessed in this chapter. As these have been discussed thoroughly in *Section 1.3 Ca^{2+} Signalling and 1.4 Ca^{2+} Hypothesis* the reader is directed to these sections for introductory information relating to these receptors, whereas their relevance to Bcl-2 family members, *specifically*, can be found throughout the following sections and in *Section* 5*.4 Discussion.*

Bcl-2

Bcl-2 is predominately expressed as an integral membrane protein which localises to mitochondria, ER and nuclear membranes (Hockenbery et al., 1990; Krajewski et al., 1993; Monaghan et al., 1992; Shimohama et al., 1998), although cytosolic expression of splice variants has also been observed (Chan et al., 1995; Joensuu et al., 1994; Papadimitriou et al.,

1996). Notably, it is a characteristic of Bcl-2 *family members* to be directed by a C-terminal hydrophobic transmembrane domain to intracellular membranes, resulting in the majority of their interactions occurring at these sites(Czabotar et al., 2013).

In rodents, Bcl-2 expression in the CNS begins at the early prenatal period and peaks during embryonic development, where high levels of *Bcl-2* mRNA and protein are widespread in the developing brain (Abe-Dohmae et al., 1993; Castrén et al., 1994; Ferrer et al., 1994b; González-García et al., 1995; Hockenbery et al., 1991; Krajewska et al., 2002; LeBrun et al., 1993; Martinou et al., 1994b; Merry et al., 1994; Shimohama et al., 1998). Bcl-2 mRNA levels decrease slightly in adult mouse brain (8- to 20-week-old; including hippocampal tissue) relative to embryonic and neonatal samples (Castrén et al., 1994; González-García et al., 1995; Vyas et al., 1997). In the adult human brain, Bcl-2 mRNA remains readily detectable (85 – 89 ± 7 years of age; Castrén et al., 1994). Bcl-2 protein is robustly expressed in adult mouse (including in the hippocampus; Karlnoski et al., 2007) and human brain samples (85 – 89 ± 7 years of age; Vyas et al., 1997). There are however conflicting reports showing that Bcl-2 mRNA and protein expression in the adult human brain occurs solely in neurons (Hockenbery et al., 1991; Vyas et al., 1997) or solely in microglia (Merry et al., 1994).

Bcl-X

Bcl-X mRNA and protein is found almost exclusively within neuronal tissue where it is widely expressed during human, rat and mouse development (González-García et al., 1995), as well as in adult brains. It is localised primarily to the soma, although it has also been detected in axons, dendrites and peripheral nerve fibres (Frankowski et al., 1995; González-García et al., 1995, 1994; Krajewski et al., 1994; Parsadanian et al., 1995).

Bcl-X_L is the major form of Bcl-X expressed in the murine nervous system and its expression (RNA and protein) begins early in neurogenesis and increases postnatally until it peaks either at an early prenatal stage (E14; mice; Krajewska et al., 2002), early postnatal stage (P14; rat; Shimohama et al. 1998) or at adulthood (mouse; Frankowski et al., 1995; González-García et al., 1995; Krajewski et al., 1994). In more detail, Shimohama et al. (1998) found that Bcl-X_L protein levels remained high in embryonic and adult rat cerebral cortex lysates over a wide range of ages from E19 days to 96 weeks but found that Bcl-X_L levels peaked at P14. Another detailed study by Krajewska et al. (2002) found that relative Bcl-X_L immunoreactivity, including in hippocampal CA3 pyramidal neurons, increased from E15.5 – E17.5, where levels were maintained postnatally (P0 to 3-months-old) These findings were supported by immunoblot data which demonstrated that Bcl-X_L protein declined only slightly in adult brain (cerebrum and cerebellum) and increased in the cerebellum and spinal cord at both late embryonic stages

and postnatally when compared to early embryonic stages (defined as <E15.5; Krajewska et al., 2002)

Bcl-X_L is primarily found in the membrane-associated, as opposed to the cytosolic, fraction where the other Bcl-X isoform, Bcl-X_β (also called Bcl-Xs), is primarily detected (rat cerebral cortex; E19 – "adult"; Shimohama et al., 1998). Notably, Bcl-X_L has the highest sequence homology of pro-survival Bcl-2 family members with Bcl-2 (Boise et al., 1993). Krajewska et al. (2002) showed that Bcl-X_β expression begins in the CNS at E8.5 - E11.5 and in subsequent embryonic stages, expression is confined to post-mitotic neurons (which are also Bcl-2 and Bcl-X_L positive) but becomes undetectable by later foetal life (E15.5 - 17.5 mice; Krajewska et al., 2002). Thus, this study questions the relevance of Bcl-X_β expression in the tissue harvested postnatally in these studies. Conversely, Shimohama et al., (1998) showed that Bcl-X_β expression mirrors that of Bcl-X_L postnatally, except that its levels are lower than Bcl-X_L at 4 weeks of age and are maintained at moderately high levels thereafter.

In summary, the documented localisation, expression and activity of Bcl-2 and Bcl-X in mouse and human CNS tissue is such that they can be considered candidate modulators of IP_3R and RyR signalling within the hippocampal tissue utilised in this project and their levels could, therefore, be relevant to interpreting the Ca^{2+} signalling experiments outlined in *Chapter 3 & 4*.

5.1.2 Bcl-2 family members and Ca^{2+} regulation

Aside from the aforementioned neuroprotective interactions of anti-apoptotic Bcl-2 family members such as Bcl-2 and Bcl-X_L with proapoptotic Bcl-2 family members *at the mitochondria*, activity *at the ER* also contributes to their anti-apoptotic effects (Akl et al., 2014; Annis et al., 2001; Thomenius et al., 2003) *via* modulation of ER Ca^{2+} signals and intracellular Ca^{2+} homeostasis (Baffy et al., 1993; Lam et al., 1994; Magnelli et al., 1994). For example, Bcl-2 mediated dampening of ER Ca^{2+} signals prevents excessive Ca^{2+} transfer to the mitochondria and therefore, indirectly, prevents mitochondrial outer membrane permeabilisation (MOMP; (Giorgi et al., 2012; Marchi et al., 2014; Pinton et al., 2008).

There are two proposed mechanisms underlying such Bcl-2 mediated dampening of ER Ca^{2+} signals: either Bcl-2 lowers steady-state $[Ca^{2+}]_{ER}$ (Pinton et al., 2000), or Bcl-2 directly suppresses ER Ca^{2+} mobilisation (He et al., 1997; Thomenius and Distelhorst, 2003). Although, this question remains a provocative one in the field (*e.g.* "Bcl-2 and calcium: controversy beneath the surface"; Distelhorst and Shore, 2004), Vervliet et al. (2016) posit that rather than being an “either/or” scenario, the two proposed mechanisms likely reflect the complex and diverse regulation of Ca^{2+} signalling by Bcl-2 family members. Regardless of which hypothesis is correct, it is worth noting that a decrease in $[Ca^{2+}]_{ER}$ (Scorrano et al., 2003), mediated by either anti-apoptotic Bcl-2 (Pinton et al., 2000) or BAX/BAK KO will, on the one hand, limit pro-apoptotic ER Ca^{2+} transfer to the mitochondria (Pinton and Rizzuto, 2006) but, on the other, also have the potential (perhaps at a certain threshold) to trigger ER stress and ER-mediated apoptosis *via* the unfolded protein response (UPR; (Kiviluoto et al., 2013; Mekahli et al., 2011; Urra et al., 2013).

Importantly, there are also examples of Ca^{2+} regulation by Bcl-2 family members which are independent (at least directly) of cell death regulation, such as the fine-tuning of IP_3R signals (Bonneau et al., 2013; Parys, 2014). Indeed, Bcl-2 family members interact with the majority of the known Ca^{2+} signalling toolkit proteins including IP_3Rs (Bcl-2, Bcl-X_L , Mcl-1), RyRs (Bcl-2, Bcl-X_L), SERCA (Bcl-2), PMCA (Bcl-2), mitochondrial VDAC (Bcl-2, Bcl-X_L , Mcl-1) and mitochondrial Na^+/Ca^{2+} exchanger (Bcl-2; for review see Vervliet et al., 2016) as will be discussed next.

IP_3R

Bcl-2 binds to the central modulatory domain of all IP_3R isoforms to inhibit Ca^{2+} release producing an anti-apoptotic effect (Chen et al., 2004; Hanson et al., 2008; Monaco et al., 2013, 2012b; Rong et al., 2009) Conversely, Bcl-X_L binds to IP_3Rs with significantly lower affinity than that of Bcl-2 and lacks Ca^{2+} inhibition activity (Monaco et al., 2012b)

Bcl-X_L overexpression does, however, produce anti-apoptotic effects *via* negative regulation of the expression of IP_3R1 and 3 (in an interleukin-3-dependent lymphoid cell line FL5.12; Li et al., 2002). In line with this, T cell receptor-stimulated Ca^{2+} signals, which are mediated by IP_3Rs, were suppressed in Bcl-X_L overexpressing cells (Jayaraman et al., 1995).

In addition to binding to the central modulatory domain of IP_3Rs, Bcl-2 and Bcl-X_L can also bind to an alternative IP_3R site at the C-terminal region (Eckenrode et al., 2010; Monaco et al., 2012a; White et al., 2005). Binding at this region sensitises IP_3Rs to low/basal levels of IP_3 and promotes Ca^{2+} oscillations regulating mitochondrial bioenergetics and cell survival (Eckenrode et al., 2010; Monaco et al., 2012a; Palmer et al., 2004; White et al., 2005). Binding of Bcl-X_L at the C-terminal region sensitises all three IP_3R isoforms and, notably, binding to the IP_3R3 isoform *alone* causes a reduction in $[Ca^{2+}]_{ER}$ (C. Li et al., 2007).

Bcl-2 can also act as a docking protein for, a) DARPP-32 (a 32kDa phosphoprotein) which is regulated by dopamine cAMP and PKA, and, b) the Ca^{2+}-activated phosphatase, calcineurin (CN). The combined activities of both proteins dynamically control IP_3R1 phosphorylation and activity (Chang et al., 2014).

RyR

The characterisation of the Bcl-2-IP_3R binding site also revealed a homologous region in the central domain of all three RyR isoforms (Vervliet et al., 2015b, 2014) and subsequent co-immunoprecipitation studies demonstrated that RyR1 and RyR3 form complexes with Bcl-2 (full length) and the BH4 domain of Bcl-2 in both HEK293 cells and 21-day-old rat hippocampal lysates. Furthermore, endogenous Bcl-2 expression or application of its BH4 domain both suppressed RyR-mediated Ca^{2+} release in HEK293 cells. Application of the BH4 domain in hippocampal neurons also decreased RyR-mediated Ca^{2+} release (E18; 14 – 18 DIV; Vervliet et al., 2014).

Bcl-X_L also binds to RyR3 *via* its BH4 domain, although with a lower affinity than Bcl-2. Furthermore, caffeine-induced Ca^{2+} release was inhibited by Bcl-X_L-BH4 domain in both RyR3-overexpressing HEK293 cells and dissociated hippocampal neurons (E18; 14 – 18 DIV; Vervliet et al., 2015a).

5.1.3 Bcl-2 family members and AD

Support for the involvement of Bcl-2 family members in AD pathogenesis comes from research utilising murine models of AD and human AD brain samples. Research into the role of Bcl-2 using animal models of AD

is still in its infancy, where Bcl-2 is, so far, the only anti-apoptotic protein characterised to any great extent. The majority of these studies has indicated that Bcl-2 expression generally decreases from around 3 months of age compared to non-transgenic controls (Table 5.1; Giuliani et al., 2013; Karlnoski et al., 2007; Stein and Johnson, 2002; X. Wang et al., 2009). Furthermore, Bcl-2 expression correlates with a reduction in the formation of APP (Poon et al., 2010) and tau pathology *via* caspase cleavage inhibition (Rohn et al., 2008). Bcl-2 expression also protects cells from Aβ-induced toxicity (Deng et al., 1999; Saillé et al., 1999; Song et al., 2004). Conversely, Aβ peptides generally downregulate Bcl-2 (and Bcl-X_L and Bcl-w (Yao et al., 2005)) expression (Clementi et al., 2006; Lee et al., 2015; Paradis et al., 1996). Later stage pathology Aβ plaques increase Bcl-2 and BAX immunoreactivity in human AD brain samples, including in reactive glia surrounding Aβ plaques (Kitamura et al., 1998; Satou et al., 1995; Tortosa et al., 1998), whereas NFTs either have no effect (Tortosa et al., 1998), or actually decrease Bcl-2 immunoreactivity (Satou et al., 1995; Su et al., 1996).

Finally, Bcl-X_L and Bcl-2 interact with PS1 and PS2, which may modulate the threshold for induction of apoptosis (Passer et al., 1999; Schellenberg et al., 1992). These findings are elaborated upon in the following sections.

Bcl-2 protein family expression

At mRNA and protein level, the expression of Bcl-2 in the CNS is altered in animal models of AD relative to controls (Table 5.1). In a study utilising young 3xTg-AD mice (3 months of age), hippocampal levels of Bcl-2 (lower), BAX (higher) and caspase-3 (higher) protein were altered to a more pro-apoptotic phenotype (Giuliani et al., 2013). Similarly, Bcl-2 expression was decreased in the cerebral cortex of 3 – 6-month-old $APP_{SWE}/PS1_{\Delta E9}$ mice (X. Wang et al., 2009). Interestingly, microRNA (miR)-34a was found to be highly expressed in the cerebral cortex of $APP_{SWE}/PS1_{\Delta E9}$ mice (3 – 6 months of age) when compared with age-matched controls (X. Wang et al., 2009). miR-34a interacts with *Bcl-2* mRNA to inhibit its translation, such that miR-34a expression is inversely correlated with Bcl-2 protein levels (Lin et al., 2014). Conversely, miR-34a knockdown increased Bcl-2 protein levels and decreased active caspase-3 in SH-SY5Y cells (X. Wang et al., 2009). In line with the known mediators of Bcl-2 function, $APP_{SWE}/PS1_{\Delta E9}$ mice and miR-34a transfected cell lines exhibited higher levels of active caspase-3 (X. Wang et al., 2009) which is an important apoptotic mediator involved in DNA fragmentation (Friedlander, 2003). Similarly, *Bcl-2* mRNA is upregulated by approximately 25% in the hippocampus and Bcl-2 expression is increased 2-fold in the cortex and hippocampus of “middle-aged”/16-18-month-old mice $APP_{SWE}/PS1_{M146L}$ mice compared with age-matched controls (Karlnoski et

al., 2007). This increase in Bcl-2 expression is also primarily localised to neuronal cells (Karlnoski et al., 2007). The authors of this study speculate that amyloid *deposition* was a key stimulus for Bcl-2 upregulation based on a correlation between the two in tissue of the posterior cortex and cerebellum from both APP_{SWE} and $APP_{SWE}/PS1_{M146L}$ mice, although transgene effects independent of amyloid deposition are also possible. This lack of an Aβ "deposition stimulus" could explain currently limited observations whereby Bcl-2 levels decrease at early stages of the disease and increase thereafter. That being said, more generally, neuroprotective genes such as IGF-2, Akt, Erk1/2, and TTR are upregulated in AD, as is a protective pathway which results in the phosphorylation of the proapoptotic Bcl-2 antagonist of cell death (BAD) at both pre-plaque (6 months of age) and post-plaque (12 months of age) stages in "Aβ containing" hippocampi and cerebellums of APP_{SWE} mice. This suggests that Aβ plaques may not be the determining stimuli for anti-apoptotic protein regulation (Stein and Johnson, 2002).

Animal Models of AD						
Protein	Mouse model	Region	Age	Measurement	Activity or Expression	Reference
Bcl-2	(3xTg-AD) APP_{SWE} $PS1_{M146L}$ Tau_{P301L}	hippocampus	3 months	protein	↓	(Giuliani et al., 2013)
BAX					↑	
Bcl-2	APP_{SWE} $PS1_{\Delta E9}$	cerebral cortex	3 - 6 months	Protein (Indirectly via ↑ miR-34	↓	(Wang et al., 2009)
BAD	APP_{SWE}	Hippocampus & cerebellum	6 -12 months	phosphorylation	↓	(Stein and Johnson, 2002)
Bcl-2	APP_{SWE} $PS1_{M146L}$	Hippocampus & cortex	16 - 18 months	mRNA	↑	(Karlnoski et al., 2007)
BAD				phosphorylation	-	

Table 5.1 Bcl-2, BAX and BAD expression and activity in animal models of AD from 3 - 18-months-old.
The expression or activity of the anti-apoptotic Bcl-2 and the pro-apoptotic BAX and BAD in mouse models of Alzheimer's disease (AD) are displayed in sequential order based on age (relative to non-transgenic controls).
Abbreviations used: amyloid precursor protein (APP), Bcl-2 antagonist of cell death (BAD), Bcl-2-associated X protein (BAX), B-cell lymphoma 2 (Bcl-2), microRNA (miR), presenilin (PS),

Recorded expression levels of Bcl-2 in adult human AD brain tissue, compared with age-matched controls, is limited and exhibits significant variability (see *Table 5.2).*

Human AD Tissue				
Protein	Region	Measurement	Activity or expression	Reference
Bcl-2	nucleus basalis (basal forebrain)	Protein lysates	-	(Vyas et al., 1997)[1]
	Hippocampus dentate gyrus (DG) entorhinal cortex (EC)	Immunoreactivity of neurons	-	(Tortosa et al., 1998)[2]
	Cerebellum frontal cortex (non-significant increase)	Protein lysates	↑	(Engidawork et al., 2001)[3]
	Neocortex	Protein lysates Immunoreactivity of glia	↑	(O'Barr et al., 1996)[4]
	EC subiculum (SUB) hippocampal regions: CA1, CA2, CA3, hilus and DG	Protein lysates Immunoreactivity of astrocytes and neurons	↑	(Satou et al., 1995)[5]
Bcl-2, Bcl-X_L and Bcl-X_β BAK & BAD	temporal cortex	Membrane fraction	↑	(Kitamura et al., 1998)[6]
Bcl-X_β		Cytosolic fraction	↓	
Bcl-X_L	cortex	Immunoreactivity	-	(Giannakopoulos et al., 1999)[7]

Table 5.2 Expression of pro- and anti-apoptotic Bcl-2 family members in human tissue from Alzheimer's disease patients relative to age-matched controls.

The activity or expression of the anti-apoptotic Bcl-2, Bcl-X_L and Bcl-X_β as well as the pro-apoptotic BAK and BAD in Alzheimer's disease (AD) human brain tissue (from numerous brain regions) is displayed, relative to age-matched controls.

Numbers following references refer to their explanation in the preceding list

Abbreviations used: Bcl-2 antagonist of cell death (BAD), Bcl-2 antagonist of cell death (BAK), Bcl-2-associated X protein (BAX), B-cell lymphoma 2 (Bcl-2).

Taken together, these studies suggest that AD does affect the expression of certain Bcl-2 family members in either membrane or cytosolic fractions of the human brain. Specifically with regard to Bcl-2, it is generally increased in AD, most notably of the membrane, rather than the cytosolic, fraction (Karlnoski et al., 2007). There is a paucity of studies investigating Bcl-2 family members in animal models of AD, particularly at early developmental stages. From the limited number of studies in the field, APP

and/or PS1 mutations appear to suppress Bcl-2 expression relative to non-Tg controls.

Bcl-2 and Aβ

There are now numerous studies which have identified a specific connection between Bcl-2 expression and Aβ pathology. In terms of cell death, which is intertwined with Bcl-2 family member expression and function, I have already discussed how Aβo promote cell death pathways and thereby contribute to neurodegeneration in AD (Section 1.2 Amyloid Cascade Hypothesis; e.g. Demuro et al., 2005; Simakova and Arispe, 2007).

Notably, the expression levels of Bcl-X_L are variably altered in studies, depending upon the profile of Aβ exposure utilised. For instance, exposure of SH-SY5Y neuroblastoma cells to "sub-toxic" levels of $Aβ_{40}$ and $Aβ_{25-35}$ up-regulated Bcl-X_L (Luetjens et al., 2001), whereas toxic Aβ exposure using aggregated $Aβ_{40}$, $Aβ_{42}$ and $Aβ_{25-35}$, dramatically reduced Bcl-X_L (Yao et al., 2005). However, regarding Bcl-2, specifically, according to the current research, Aβo appear to reduce its expression regardless of the severity of the insult.

$Aβ_{25-35}$ and $Aβ_{42}$ application resulted in dissipation of mitochondrial transmembrane potential (MMP), decreased Bcl-2/Bax ratio, increased caspase-3 expression and activation and time-dependent decreases in cell viability in SH-SY5Y cells and human neuroblastoma cells (IMR-32) (Lee et al., 2015). Interestingly, the redox state of the Aβ peptides modulated the expression profiles of the aforementioned proteins, revealing yet another AD disease process which can be affected by ROS (Clementi et al., 2006). Similarly, sub-apoptotic inducing levels of $Aβ_{40}$ and $Aβ_{42}$ peptides downregulated Bcl-2 expression, increased neuronal susceptibility to low levels of oxidative stress and, in the case of $Aβ_{42}$ alone, increased BAX expression after 3 DIV in human foetal (13 – 17 week) cerebrum cultures (Paradis et al., 1996).

Logically, increased levels of *anti-apoptotic* Bcl-2 family members including Bcl-2 (in PC12 cells and cortical neurons; Deng et al., 1999; Saillé et al., 1999; Song et al., 2004), Bcl-X_L (in PC12 cells and SH-SY5Y neuroblastoma cells; Luetjens et al., 2001; Tan et al., 1999) and Bcl-w (in cortical neurons and M17 neuroblastoma cells; Yao et al., 2005; Zhu et al., 2004) protect cells from Aβ-induced toxicity, including apoptosis and necrosis, *in vitro.* Furthermore, in APP_{SWE}/$APP_{V717F(INDIANA)}$ mice, Bcl-2 overexpression decreased plaque pathology and reduced $Aβ_{42}$ levels in the hippocampi of aged mice (Poon et al., 2010). In the most comprehensive study conducted to date investigating the links between AD pathology and Bcl-2 family-related signalling, Rohn et al. (2008) found that Bcl-2 *overexpression* prevented the spectrum of AD pathology in 3xTg-AD mice.

Specifically, Bcl-2 overexpression limited caspase-3 and -9 activations and translocation in the neocortex and hippocampus of these animals at 6-, 12- and 18- months of age, resulting in an attenuation of APP and tau cleavage by caspases relative to untreated animals (Rohn et al., 2008). This factor likely attenuated Aβo- and tau-mediated pathology in these animals (Gamblin et al., 2003; Gervais et al., 1999; Rissman et al., 2004; Rohn et al., 2002). Indeed, these Bcl-2 overexpressing mice exhibited; a) reduced caspase-mediated cleavage of tau (6 – 18 months of age), b) reduced "total pathological tau", c) an absence of NFTs (12 months of age) d) reduced $A\beta_{42}$ and $A\beta_{40}$ levels and accumulation (12-18 months of age) and, e) improved place recognition memory (24 months of age; Rohn et al., 2008).

Oxidative stress

Oxidative stress, which is proposed to be of considerable importance in contributing to AD pathogenesis (Gella and Durany, 2009; Huang et al., 2016; Perry et al., 2002), can also increase the expression of Bcl-2 family members, including Bcl-X_L in PC12 cells (Luetjens et al., 2001) and Bcl-2 in the hippocampus and cerebellum of 3- and 24-month-old rats (Kaufmann et al., 2001). Although outside the remit of this general introduction, the reader should note that the activities of other apoptotic regulators such as pro-apoptotic caspases and neuroprotective NFκB can also be altered by AD-linked genetic mutations, excess Ca^{2+} and ROS (Pahl and Baeuerle, 1996; Rohn, 2010).

5.2 Aims

1) To determine the expression of the anti-apoptotic proteins Bcl-2 and Bcl-X_L in total hippocampal lysates from 3xTg-AD mice (P5, 15 and 21) and to compare these with non-transgenic controls.

2) The expression of IP_3Rs and RyRs, which Bcl-2 and Bcl-X_L are reported to regulate, was also investigated in transgenic and non-transgenic control hippocampal tissue in the same age groups as in aim 1.

The expression profiles of each these Ca^{2+} interacting proteins may elucidate underlying mechanisms responsible for altered Ca^{2+} signalling observed in 3xTg-AD mouse neurons.

5.3 Materials and methods

5.3.1 Statement of collaboration

The majority of work presented in this chapter was undertaken in the lab of Dr Geert Bultynck in K.U. Leuven (Belgium), in collaboration with, and under the supervision and expert guidance of, Dr Tim Vervliet. Specifically, animals were sacrificed and hippocampi harvested in University College Cork (UCC; Ireland), as described in *Chapter 2*. I then travelled to Dr Bultynck's lab in Belgium to conduct the actual western blot experiments outlined herein. The data presented in the results section of this chapter investigating BCL-2, Bcl-X_L, IP_3R and RyR expression arise from work carried out during this period of study (1 biological replicate) combined with data that Dr Vervliet subsequently generated independently using additional samples which were harvested by me in UCC (4 biological replicates). I would like to express mine and my lab's sincere gratitude to both Dr Bultynck and Dr Vervliet for their time, expertise and stimulating discussions during this aspect of my doctoral work.

5.3.2 Chemicals, antibodies, peptides

Unless otherwise stated all chemicals were obtained from Sigma–Aldrich. Antibodies used in this study were: mouse monoclonal anti-Bcl-2 (C2; 1:1000: Santa Cruz Biotechnology cat no. sc-7382, Antibody Registry: AB_626736), mouse monoclonal anti-Bcl-X_L antibody (YTH-2H12; 1:1000; Trevigen, cat no. 2300-MC-100, Antibody Registry: AB_2064868), rabbit polyclonal anti-IP_3R1 (Rbt03; 1:1000; made "in-house" as published previously in Parys et al. (1995)), mouse monoclonal anti-RyR (1-3) antibody (34C; 1:2000; Thermo Scientific, cat no. MA3-925, Antibody Registry: AB_2254138), mouse monoclonal anti-RyR (2) antibody (C3:33; 1:2000; Thermo Scientific, cat no. MA3-916, Antibody Registry: AB_2183054), mouse monoclonal anti-actin antibody (AC-74; 1:2000; Sigma Aldrich, cat. no. A222, Antibody Registry: AB_476697), mouse monoclonal anti-GAPDH antibody (GAPDH-71.1; 1:50000; Sigma Aldrich, cat. no. G8795, Antibody Registry: AB_1078991), mouse monoclonal anti-vinculin (VIN-11-5; 1:1000; Sigma Aldrich, cat. no. V4505, Antibody Registry: AB_477617).

5.3.3 Brain samples

3xTg-AD mice and non-transgenic controls at 5-, 15- and 21-days-old were euthanized in accordance with European Directive 2010/63/EU and experiments approved by the Animal Experimentation Ethics Committee of University College of Cork. Hippocampi were removed as described previously (Beaudoin et al., 2012). For experiments comparing the effect of elevated extracellular potassium concentration on Bcl-2 family member expression utilising 5-day-old mice, whole brains were either dissected in the standard manner or placed in either basal HBSS (5mM K^+) or elevated K^+

HBSS (15mM K^+) while the hippocampus was being removed. Hippocampi were frozen in liquid nitrogen before storage at -80^{o}C.

5.3.4 Immunoblots

Samples were prepared and used as described previously (Monaco et al., 2012b). Briefly, tissue was taken from storage at -80^{o}C and placed in iced extraction buffer (pH7.5; 100mM NaCl, 50mM Tris-HCl, 50mM NaF, 2mM EDTA, 1mM Na_3VO_4, Chaps 1%, 2 x protease inhibitor cocktail tablets (Roche, Basel, Switzerland) for tissue homogenisation. Depending upon the size of hippocampal tissue, an appropriate volume of buffer was added (approximate values of 175ul, 250ul and 500ul were used for 5, 15 and 21 DIV mouse samples, respectively, whereas 375ul and 1ml were used for 5 and 21 DIV rat samples, respectively). The hippocampi were incubated in extraction buffer for 30 mins, vortexing at 10-minute intervals, before being centrifuged (4000 xg; 5 mins; 4^{o}C). The protein concentration of samples was determined by Bradford assay (Sigma-Aldrich) using bovine serum albumin (BSA) as standard. Samples containing protein levels of 300 μg, 50ul Lithium Dodecyl Sulfate (LDS) and the remaining volume H_2O up to 200ul were boiled (95°C; 5 min) immediately prior to running on either NuPAGE 4 - 12% Bis-Tris SDS-polyacrylamide gels (180V; 55min; RT) or NuPAGE 3 - 8% Tris-Acetate gels (180V; 1hr30; 4^{o}C; both from Life Technologies). Transfer (100V; 1hr; 4^{o}C) was carried out onto a polyvinylidene fluoride (PVDF) membrane.

After blocking with Tris-buffered saline (TBS) containing 0.1% Tween and 5% non-fat dry milk powder, the membrane was incubated with the primary antibody overnight (1% non-fat dry milk powder 0.1% Tween/TBS was used for all antibody incubations). After washing (3 x 5 mins in 0.1% Tween/TBS), membranes were incubated for 1 hour with a secondary horseradish peroxidase (HRP)-conjugated antibody (dilution 1: 2000 in 0.1% Tween/TBS). After washing (3 x 5 mins in 0.1% Tween/TBS), detection was performed using Pierce ECL Western Blotting Substrate (Thermo Scientific) and the Chemidoc™ MP system (Bio-Rad, Nazareth Eke, Belgium). Band quantification was performed using Image Lab™ software (Bio-Rad).

5.3.5 Statistical analysis

Two-tailed unpaired Student's t-tests were performed when two conditions were compared. When comparing three conditions, a one-way ANOVA with Tukey's multiple comparison test was utilised. * indicates significantly different results ($p<0.05$). Exact P values are indicated in the figure legends.

5.4 Results

5.4.1 Bcl-2 and Bcl-X_L

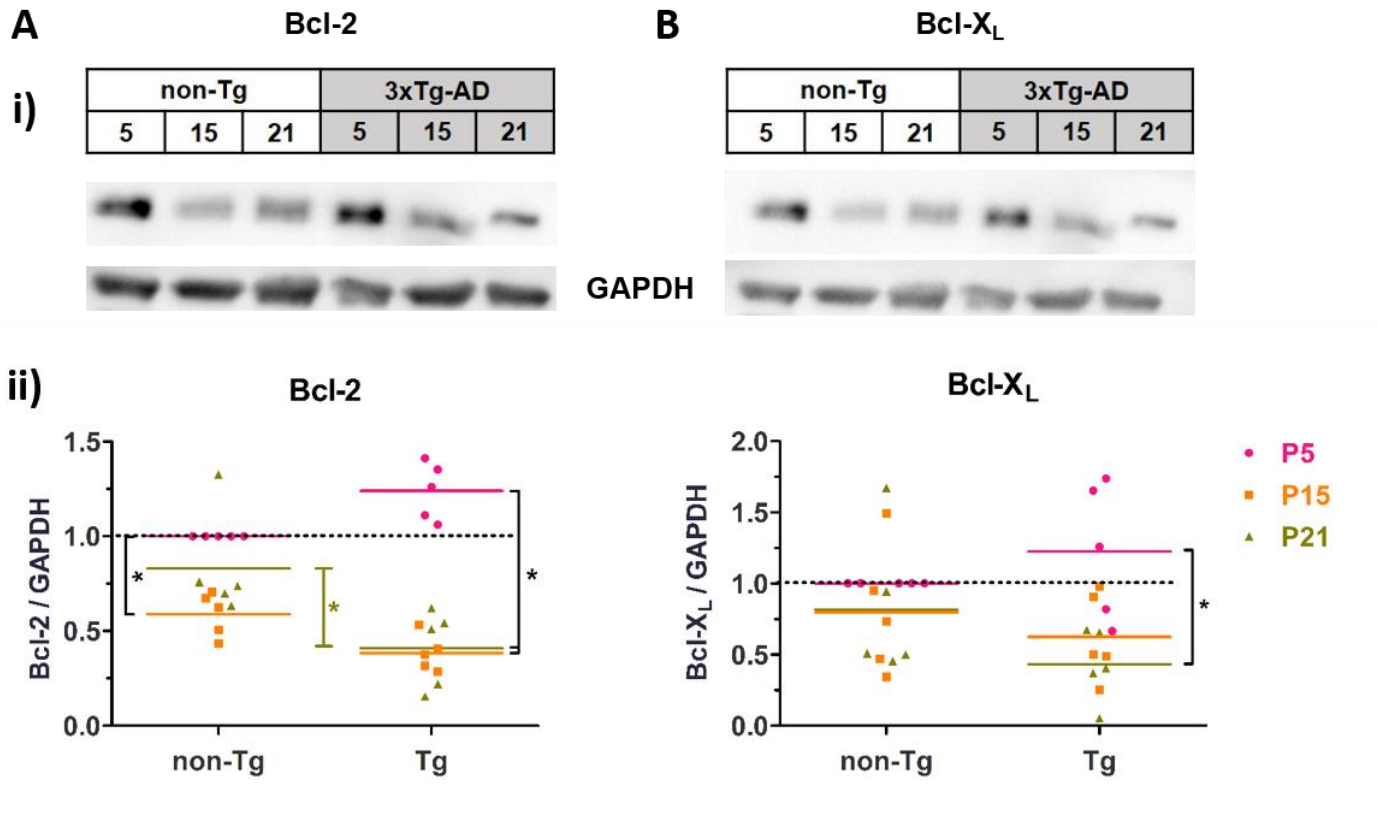

Figure 5.2. Western blot analysis of non-transgenic (non-Tg) and 3xTg-AD (Tg) hippocampal lysates, harvested from animals at 5-, 15- and 21-days-old, with antibodies against Bcl-2 (A) and Bcl-X_L (B).

i) Representative images from five independent experiments (n = 5) are shown. GAPDH was used as a loading control.
ii) Graphical representation of protein expression after densitometric analysis. Data normalised to GAPDH and shown relative to non-Tg P5 expression levels. *$p < 0.05$ (minimum) as determined by Tukey's multiple comparison test.

Western blot analysis of Bcl-2 expression in hippocampal lysates prepared from P5, 15 and 21 non-Tg and 3xTg-AD animals is displayed in Fig 5.2. All data are presented in arbitrary units, normalised to expression of a control protein (either GAPDH, vinculin or actin; see corresponding graphs) and displayed relative to non-Tg P5 expression levels.

Interestingly, and although not significant, there was a trend towards greater Bcl-2 expression in P5 3xTg-AD tissue relative to age-matched controls (1.24 ± 0.07 *vs* 1; Tg P5 *vs* non-Tg P5; p = 0.25, n = 5). It is notable that Bcl-2 expression decreased in *both* control and Tg tissue with increasing age (significantly in controls when comparing P5 to P15 (p = 0.008) and in Tg when comparing P5 with P15 and P21 (p = < 0.0001; n = 5). However, this decrease was even more dramatic in Tg tissue at P21 relative to age-matched controls (0.41 ± 0.09 *vs* 0.83 ± 0.13; p = 0.03; n = 5; Tg P21 *vs* non-Tg P21).

Bcl-X_L expression followed a similar trend to that of Bcl-2 whereby expression appeared to be greater in Tg tissue at P5, relative to non-Tg tissue (although not significantly so; 1.23 ± 0.22 *vs* 1; Tg P5 *vs* non-Tg P5; p = 0.93, n = 5) and decreased thereafter in both non-Tg and Tg tissue although only significantly so in Tg tissue, when comparing P5 with P21 animals; 1.23 ± 0.22 *vs* 0.43 ± 0.11; Tg P5 *vs* Tg P21; p = 0.01, n = 5). There was also a non-significant trend towards a greater decrease in Bcl-X_L levels in Tg tissue with increasing postnatal development, relative to non-Tg tissue (0.79 ± 0.20 *vs* 0.63 ± 0.14, non-Tg P15 *vs* Tg P15, p = 0.5, n = 5; 0.82 ± 0.23 *vs* 0.43 ± 0.11, non-Tg P21 *vs* Tg P21, p = 0.17, n = 5).

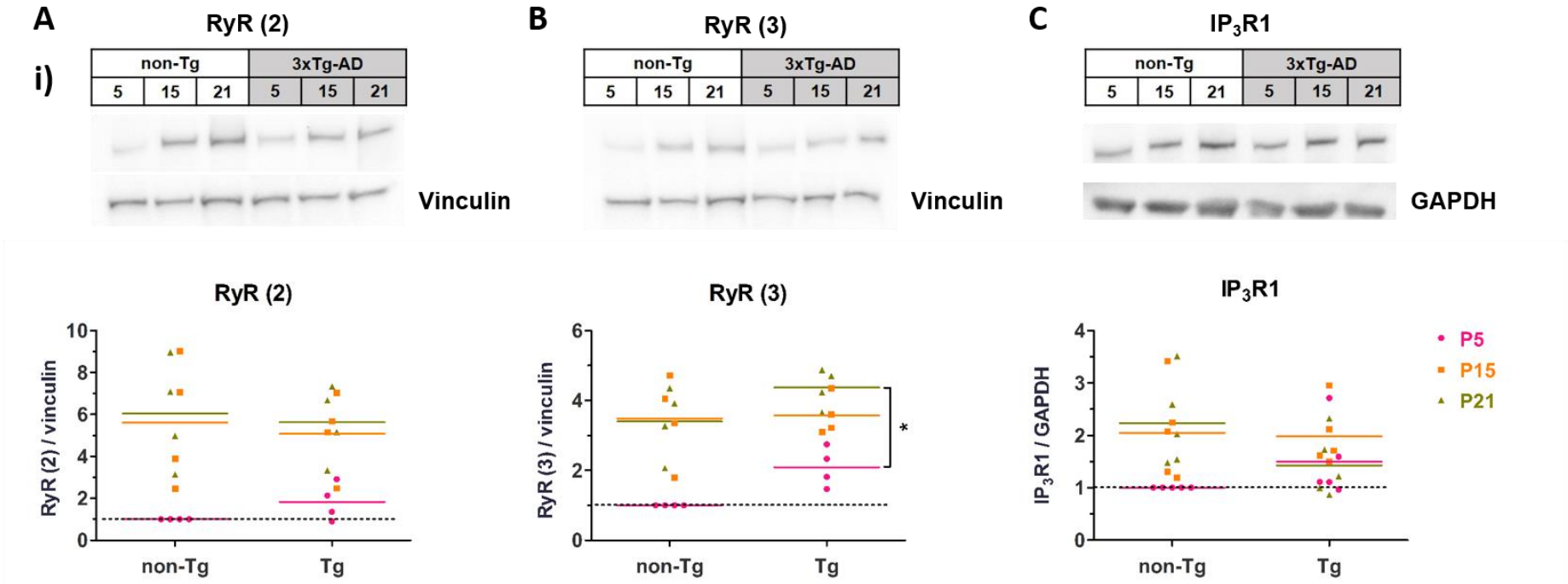

Figure 5.3 Western blot analysis of non-transgenic (non-Tg) and 3xTg-AD (Tg) hippocampal lysates, harvested from animals at 5-, 15- and 21-days-old, with antibodies against RyR (2 – preferentially), RyR (3 - preferentially) and IP_3R1.

i) Representative images of four independent experiments (n = 4) are shown. Vinculin and GAPDH were used as a loading controls.

ii) Graphical representation of protein expression after densitometric analysis. Data normalised to vinculin or GAPDH expression level and shown relative to non-Tg P5 expression levels. *$p < 0.05$ (minimum) as determined by Tukey's multiple comparison test.

We found that there were no *significant* differences in RyR (2), RyR (3) or IP_3R1 expression levels between non-Tg and 3xTg-AD samples at either P5, P15 or P21 (n = 4; Fig 5.3). That being said there were some notable trends. At P5, transgenic tissue had a trend towards increased RyR (2) (2.09 ± 0.28 *vs* 1; p = 0.37; Tg P5 *vs* non-Tg P5), RyR (3) (1.83 ± 0.44 *vs* 1; p = 0.99; Tg P5 *vs* non-Tg P5) and IP_3R1 (2.05 ± 0.39 *vs* 1; p = 0.18; Tg P5 *vs* non-Tg P5), relative to non-Tg controls. At P15 the levels of all three ER release channels were similar between non-Tg and Tg tissue. However, differences between phenotype were observable again at P21, where RyR (3) expression increased in Tg tissue to a greater extent than in controls (4.37 ± 0.27 *vs* 3.4 ± 0.49; p = 0.14; Tg P21 *vs* non-Tg P21), whereas IP_3R1 expression decreased relative to that in non-Tg tissue (5.63 ± 0.9 *vs* 6.04 ± 1.27; p = 0.79; Tg P21 *vs* non-Tg P21).

Both non-Tg and Tg samples followed similar trends of developmental-dependent expression for RyR (2 and 3), which increased with increasing age (although the extent of this increase was quite variable between biological units) and was significant only for the expression of non-Tg RyR (2) (1 *vs* 5.61 ± 1.49 *vs* 6.04 ± 1.27; non-Tg P5 *vs* P15 *vs* P21; p = 0.04 and 0.02, respectively), non-Tg RyR (3) (1 *vs* 3.48 ± 0.63 *vs* 3.4 ± 0.49; non-Tg P5 *vs* P15 *vs* P21; p = 0.003 and 0.004, respectively) and Tg RyR (3) (2.09 ± 0.28 *vs* 4.37 ± 0.27; p = 0.001; Tg P5 *vs* Tg P21).

In immunoblot experiments measuring IP_3R1 expression, there was no significant difference between groups (non-Tg vs Tg) or between ages within groups. In non-Tg tissue, there was a trend towards greater IP_3R1 expression with increasing age, but this was not significant. In Tg tissue, IP_3R1 expression trended towards an increase at P15 but then decreased to near P5 expression levels again in P21 animals.

5.5 Discussion

Bcl-2 and Bcl-X_L expression correlate with resistance to apoptotic and oxidative stresses, two highly relevant processes in AD pathology, *in vitro* and *in vivo* (for reviews see Merry and Korsmeyer, 1997; Shacka and Roth, 2006). However, whether the apparent decreased expression of either Bcl-X_L or Bcl-2 in transgenic tissue relative to controls would have a significant impact upon cell death in these animals at this early time point (P5 – 21) is unknown and was not measured. Instead, the focus of this discussion relates to the ability of Bcl-2 and Bcl-X_L to reversibly inhibit IP_3R- and RyR-gating which, aside from being an important mechanism employed by these proteins to prevent Ca^{2+}-dependent apoptosis (Giorgi et al., 2012; Marchi et al., 2014; Pinton et al., 2008), also has important implications for intracellular Ca^{2+} signalling (Hanson et al., 2008; Rong et al., 2008; Vervliet et al., 2014).

It was our hypothesis that in animal models of AD (such as the 3xTg-AD mouse) which display robust Ca^{2+} dyshomeostasis, including that mediated by ER Ca^{2+}-release channels (see *Chapter 4*), Bcl-2 expression would be increased in a compensatory manner to dampen pathologically increased IP_3R- and RyR- mediated ER signals (Morley et al., 2012). However, the expression levels of Bcl-2 family proteins and/or the activity of their downstream effectors (including caspases) are generally *reduced* in transgenic models of AD and/or following exposure to Aβ proteins *in vitro* (discussed previously). That being said, as is the norm in the field of AD, these investigations were solely concerned with later stages of the disease and comparisons between Tg and non-Tg brain tissue are lacking at earlier disease stages. We were also aware that if murine models of AD displayed upregulation of Bcl-2 relative to controls, the resulting hypothetical Bcl-2 mediated inhibition of IP_3Rs could be counteracted indirectly, by AD-initiated mitochondrial impairment (dependent upon the appearance of mitochondrial impairment in the chronology of the disease). This would induce cytochrome c translocation to the ER where it binds to, and blocks, Ca^{2+}-dependent inhibition of IP_3Rs. This results in sustained, oscillatory increases in $[Ca^{2+}]_i$ levels and amplification of Ca^{2+}-dependent apoptosis (Boehning et al., 2003).

The expression of the anti-apoptotic Bcl-2 and Bcl-X_L as well as two Ca^{2+} release channels with which Bcl-2 and Bcl-X_L interact, IP_3Rs and RyRs, were investigated in whole hippocampal lysates using immunoblot analysis. In summary, although there was a trend towards decreased expression of Bcl-2 and Bcl-$_{XL}$ and a trend towards increased expression of RyR and IP_3R1 with development (P5 *vs* P15 and P5 *vs* P21) regardless of transgenic status, this was only significant in 3xTg-AD tissue only in the case of Bcl-2, Bcl-$_{XL}$ and RyR (2) expression, and generally, solely at the latest stage of development tested, P21.

5.5.1 Characterisation of postnatal Bcl-2 and Bcl-X_L expression

As detailed previously, Bcl-2 expression peaks in the CNS during embryonic development and declines postnatally (Krajewska et al., 2002; Shimohama et al., 1998). In line with these data, we found that Bcl-2 expression decreased with increasing postnatal development (P15 and 21 *vs* P5) in hippocampal lysates from non-Tg and 3xTg-AD mice (19 of 20 samples (regardless of transgenic status) exhibited lower expression when compared to control (non-Tg; P5); group analysis was significant for the following comparisons: non-Tg P5 *vs* P15 and Tg P5 *vs* P15 and P5 *vs* P21; Fig 5.2)

It is worth noting that in agreement with relatively recently observed Bcl-2 protein expression in adult mouse and human brain (Karlnoski et al., 2007, Vyas et al., 1997), as opposed to an absence of Bcl-2 protein expression in older studies (González-García et al., 1995; Merry et al., 1994), Bcl-2 protein was readily detectable in 28 separate postnatal mouse and rat whole hippocampal lysates (data not shown), suggesting that despite a *relative* decline postnatally, Bcl-2 may still be physiologically relevant for both the regulation of Ca^{2+} signalling and neuroprotection. However, whether or not this Bcl-2 signal was derived from neurons or glia, or a combination of both, was not determined in this study. Indeed, there are conflicting reports of Bcl-2 mRNA and protein expression occurring either solely in neurons (Hockenbery et al., 1991; Vyas et al., 1997) or solely in glia (Merry et al., 1994), at least in human CNS tissue.

The physiological process(es) underlying this change in Bcl-2 expression is likely the developmentally-regulated mechanism of naturally occurring cell death (NOCD). NOCD is enhanced during the first postnatal week and decreases thereafter (Ferrer et al., 1994a), in tandem with Bcl-2 expression (Shimohama et al., 1998). Moreover, it is likely that Bcl-2 plays a role in dictating which neurons undergo NOCD, as Bcl-2 overexpression protects neurons from this process (Martinou et al., 1994a). Lower levels of Bcl-2 found in numerous brain regions postnatally (as described previously) may help to protect neurons from more subtle toxic insults such as oxidative stress (Shimohama et al., 1998). Conversely, such low levels may simply indicate that Bcl-X proteins, which are highly expressed postnatally, are the principal anti-apoptotic regulators of neuronal cell death in adult brain (González-García et al., 1995; Shimohama et al., 1998; Yachnis et al., 1998).

Previous research suggests that Bcl-X_L expression (both RNA and protein) begins early in neurogenesis and increases postnatally, peaking either at an early prenatal stage (E14 mouse; Krajewska et al., 2002), early postnatal stage (P14 rat; Shimohama et al. 1998) or at “adulthood” (mouse;

Frankowski et al., 1995; González-García et al., 1995; Krajewski et al., 1994). Conversely, the current research suggests that Bcl-X_L expression actually trended towards a decrease in the early postnatal stages of development in tissue from both non-Tg and 3xTg-AD mice (18 of 20 samples (regardless of transgenic status) exhibited lower expression when compared to control (non-Tg; P5); group analysis was significant only for Tg P5 *vs* P21; Fig 5.2). However, there are some notable differences between our work and that undertaken previously, which may explain this discrepancy. Firstly, Shimohama et al. (1998) showed that Bcl-X_L expression peaked at P14 and remained elevated thereafter (P14 – 96 weeks of age) but this investigation utilised cortical lysates which may have had a different Bcl-X_L expression profile to hippocampal lysates. Secondly, the Krajewska et al. (2002) study also showed that although hippocampal Bcl-X_L immunoreactivity (immunohistochemistry), was maintained at a high level postnatally (mice between P0 – 3 months), this was *predominately* evident only in CA3 hippocampal pyramidal neurons. Although staining may have been strong in this specific region, the overall expression levels may have actually been relatively low when lysates were analysed from whole hippocampi, as utilised in the current study. Furthermore, although protein expression was found to increase postnatally (compared to early embryonic stages; immunoblot) and reduced only slightly in adult tissue in the study by Krajewska et al. (2002), this work was carried out utilising lysates from the cerebrum and cerebellum, not the hippocampus.

Interestingly, two further publications which are often cited as correlating increased Bcl-X_L expression with development, in fact, lack the required evidence to support such a statement. For example, González-García et al. (1995) presented an image of RNA analysis which showed a comparison of Bcl-X_L mRNA levels between E13 – 19, neonatal and adult mouse brain sections (from undefined brain regions) which were not quantified. This lack of quantification was repeated for another image in the same paper which showed that there was elevated Bcl-X_L expression (in comparison to Bcl-2 and Bcl-X_β) in all regions tested in the adult CNS, including the hippocampus. The same study also presented a single western blot showing Bcl-X_L protein expression in lysates from various embryonic (E17; cerebral cortex and cerebellum) and adult (20 weeks-old; cerebral cortex, basal ganglia, cerebellum, spinal cord) brain regions. In said blot, Bcl-X_L protein expression differences are not objectively clear, as no loading control has been used and the blot was not densitometrically analysed (González-García et al., 1995). The study by Krajewski et al., (1994) presented “graded/arbitrary” immunohistochemical staining intensity of Bcl-X_L in the CNS from a range of 4 - 12-week-old mice as well as human biopsy and autopsy samples, but with no analysis of how this changed with development. Based upon the omissions outlined in these papers I would,

therefore, argue that Bcl-X_L expression in the CNS in the early postnatal stages, which I have investigated herein, has not previously been well characterised, particularly in hippocampal tissue. The increase in Bcl-X_L expression established as a trend in the literature may also occur at a later developmental stage than that investigated in this study (post-P21).

5.5.2 Effects on Ca^{2+} signalling

Bcl-2 family members interact with the majority of cellular Ca^{2+} signalling toolkit components such as IP_3Rs, RyRs, SERCAs, PMCAs, mitochondrial VDACs and mitochondrial Na^+/Ca^{2+} exchangers (see *Section 5.*1 and for review see Vervliet et al., 2016). The expression and activity of this family are therefore of great relevance to neuronal mechanisms of Ca^{2+} homeostasis, Ca^{2+} signalling (including I-mGluR-IP_3R/RyR mediated signalling outlined in *Chapter 3 and 4)* and putative 'calciumopathies' such as AD.

Specifically, given our investigations into ER Ca^{2+} dynamics, the mechanisms through which Bcl-2 is proposed to alter Ca^{2+} signalling are particularly relevant. As described previously, these mechanisms include the suppression of ER Ca^{2+} mobilisation through IP_3Rs (binding to all three isoforms; Monaco et al., 2012) and RyRs (He et al., 1997; Thomenius and Distelhorst, 2003), the lowering of steady-state $[Ca^{2+}]_{ER}$ (Pinton et al., 2000) or a combination of all aforementioned forms of regulation (Vervliet et al., 2016). Bcl-X_L also suppresses ER Ca^{2+} release. However, aside from one study which utilised supra-physiological Bcl-X_L concentrations (Yang et al., 2016), this occurs solely *via* RyRs (Monaco et al., 2012b; Vervliet et al., 2015a). Importantly though, Bcl-X_L also indirectly modulates IP_3R-mediated Ca^{2+} release as its expression (at least in overexpression studies) negatively regulates IP_3R1 and 3 expression in an interleukin-3-dependent lymphoid cell line (FL5.12; Li et al., 2002). However, the subtleties of Bcl-X_L expression-mediated regulation of IP_3R expression may be lost amongst the overall developmentally-dependent expression patterns of Bcl-X_L and IP_3R proteins and therefore may not be physiologically relevant during this period of development.

Any changes in the functional activity and/or expression of Bcl-2 and/or Bcl-X_L within neurons will almost certainly modulate I-mGluR mediated signalling. Such modulation could occur by direct regulation of IP_3R- and RyR-mediated Ca^{2+} mobilisation, steady-state $[Ca^{2+}]_{ER}$, IP_3R expression, and/or modulation of the plethora of Ca^{2+} signalosome proteins with which Bcl-2 proteins interact (including FKBPs, SERCA and PMCA; Vervliet et al., 2016).

Our results suggest that in the hippocampi of 3xTg-AD mice (non-significant trend; Fig 5.2) expression of Bcl-2 may be increased (by approximately 25%) at P5 relative to age-matched controls. Hypothetically, an elevation in Tg tissue at such an early postnatal stage could occur as a compensatory response to either increased AD-related susceptibility to cell death or dysregulated intracellular Ca^{2+} homeostasis such as that which has been observed in 3xTg-AD mice at this stage of development (Morley et al., 2012; Zhang et al., 2010). As mentioned previously, in mice, levels of Bcl-2 and Bcl-X_L generally decrease in the hippocampus with increasing postnatal age irrespective of transgenic status. Notably, this decrease in Bcl-2 expression with postnatal developments exaggerated in transgenic hippocampi (significantly *solely* when comparing Bcl-2 expression in hippocampi from 3xTg-AD mice at P21 to non-Tg age-matched controls), a finding which suggests that transgenic neurons are, by an as yet unknown mechanism, unable to maintain protective Bcl-2 protein expression to the same extent as age-matched controls.

Given its roles as a suppressor of ER Ca^{2+} release (Vervliet et al., 2016), lower levels of Bcl- expression in hippocampi from 3xTg-AD mice may contribute to the enhancement of I-mGluR-mediated Ca^{2+} responses in Tg neurons under basal and depolarisation conditions, relative to non-Tg neurons (*see Chapter* 3; Fig 3.7). Furthermore, the fact that RyR (3) expression is significantly increased solely when comparing Tg tissue at P21 v*s* P5 and is unaltered in the same developmental timeline in non-Tg neurons (Fig 5.2) suggests RyR upregulation may further enhance the magnitude of ER Ca^{2+} release in Tg neurons. Indeed, Zhang et al. (2010) showed that RyR expression increased approximately 2-fold in cultured 3xTg-AD hippocampal neurons relative to non-Tg controls at P0-1 (13 DIV). Whether this increase in RyR expression was due to regulation by Bcl-2 family proteins and/or by separate AD-driven process (including, for example, general disruption of normal of ER Ca^{2+} homeostasis, see *Chapter 3*), is not clear.

Interestingly, Bcl-2 expression and activity correlated with a reduction in the formation of APP (Poon et al., 2010), protects cells from Aβ-induced toxicity (Deng et al., 1999; Saillé et al., 1999; Song et al., 2004), and reduces tau-related pathology *via* caspase cleavage inhibition (Rohn et al., 2008). Whether these effects occur in a manner that is dependent upon the previously described modulation of intracellular Ca^{2+} dynamics by Bcl-2 is however currently not clear. The exaggerated decrease of Bcl-2 expression observed in 3xTg-AD hippocampi (Fig 5.2) may leave this region more vulnerable to amyloid- and tau-related pathological insults. Furthermore, Aβo decrease Bcl-2 expression (Clementi et al., 2006; Lee et al., 2015; Paradis et al., 1996) which may, in turn, exacerbate the already decreased Bcl-2

expression in transgenic animal models of AD and enhance ER Ca^{2+} signals further at later stages of the disease (if the appearance of Aβo in these models is subsequent to diminished Bcl-2 expression). Importantly, this work provides entirely novel evidence of altered Bcl-2 expression in the hippocampus of 3xTg-AD mice in early postnatal development (P21). The decrease in Bcl-2 expression that we describe here is in agreement with previous work utilising hippocampi of 3-month-old 3xTg-AD mice (Giuliani et al., 2013) and the cerebral cortex of 3 - 6-month-old APP_{SWE} and $PS1_{\Delta E9}$ mice (Wang et al., 2009). The relevance of this evidence of *decreased* Bcl-2 and Bcl-$_{XL}$ expression collected from animal models to the human condition of AD becomes difficult to determine given that, as discussed previously (see table 5.2), Bcl-2 expression (which is the only Bcl-2 family member studied to any degree in human samples) is generally *increased* in brain samples from AD patients. It could be possible that enhanced Bcl-2 expression in the human brains of AD patients is an end-stage protective mechanism which does not reflect the early response to the disease. Alternatively, the opposite trends in expression profiles of Bcl-2 may simply be due to species differences.

5.6 Conclusions

In summary, the data we present here suggest that in the 3xTg-AD model of AD, the expression profiles of Bcl-2, Bcl-X_L and RyRs, combined with the known regulatory effects of Bcl-2 and Bcl-X_L at these ER Ca^{2+} release channels, could promote dysregulated hippocampal ER Ca^{2+} signalling and disruption of normal Ca^{2+} homeostasis from at 21 days of age.

Appendix

A.1 Kaar et al. (2017)

A.2 Kaar and Rae (2015)

References

Aarhus, R., Graeff, R.M., Dickey, D.M., Walseth, T.F., Lee, H.C., 1995. ADP-ribosyl cyclase and CD38 catalyze the synthesis of a calcium-mobilizing metabolite from NADP. J. Biol. Chem. 270, 30327–30333.

AbdAlla, S., Lother, H., el Missiry, A., Langer, A., Sergeev, P., el Faramawy, Y., Quitterer, U., 2009. Angiotensin II AT2 Receptor Oligomers Mediate G-protein Dysfunction in an Animal Model of Alzheimer Disease. J. Biol. Chem. 284, 6554–6565.

Abdul-Ghani, M.A., Valiante, T.A., Carlen, P.L., Pennefather, P.S., 1996. Metabotropic glutamate receptors coupled to IP3 production mediate inhibition of IAHP in rat dentate granule neurons. J. Neurophysiol. 76, 2691–2700.

Abe-Dohmae, S., Harada, N., Yamada, K., Tanaka, R., 1993. Bcl-2 gene is highly expressed during neurogenesis in the central nervous system. Biochem. Biophys. Res. Commun. 191, 915–21.

Abeti, R., Duchen, M.R., 2012. Activation of PARP by Oxidative Stress Induced by ?-Amyloid: Implications for Alzheimer?s Disease. Neurochem. Res. 37, 2589–2596.

Adebanjo, O.A., Anandatheerthavarada, H.K., Koval, A.P., Moonga, B.S., Biswas, G., Sun, L., Sodam, B.R., Bevis, P.J., Huang, C.L., Epstein, S., Lai, F.A., Avadhani, N.G., Zaidi, M., 1999. A new function for CD38/ADP-ribosyl cyclase in nuclear Ca2+ homeostasis. Nat. Cell Biol. 1, 409–414.

Ahern, G.P., Junankar, P.R., Dulhunty, A.F., 1997. Subconductance states in single-channel activity of skeletal muscle ryanodine receptors after removal of FKBP12. Biophys. J. 72, 146–162.

Ahlemeyer, B., Baumgart-Vogt, E., 2005. Optimized protocols for the simultaneous preparation of primary neuronal cultures of the neocortex, hippocampus and cerebellum from individual newborn (P0.5) C57Bl/6J mice. J. Neurosci. Methods 149, 110–20.

Ahlijanian, M.K., Barrezueta, N.X., Williams, R.D., Jakowski, A., Kowsz, K.P., McCarthy, S., Coskran, T., Carlo, A., Seymour, P.A., Burkhardt, J.E., Nelson, R.B., McNeish, J.D., 2000. Hyperphosphorylated tau and neurofilament and cytoskeletal disruptions in mice overexpressing human p25, an activator of cdk5. Proc. Natl. Acad. Sci. U. S. A. 97.

Ahn, K., Shelton, C.C., Tian, Y., Zhang, X., Gilchrist, M.L., Sisodia, S.S., Li, Y.-M., 2010. Activation and intrinsic gamma-secretase activity of presenilin 1. Proc. Natl. Acad. Sci. U. S. A. 107, 21435–40.

Akbari, Y., Hitt, B.D., Murphy, M.P., Dagher, N.N., Tseng, B.P., Green, K.N., Golde, T.E., LaFerla, F.M., 2004. Presenilin regulates capacitative calcium entry dependently and independently of γ-secretase activity. Biochem. Biophys. Res. Commun. 322, 1145–1152.

Akl, H., Vervloessem, T., Kiviluoto, S., Bittremieux, M., Parys, J.B., De Smedt, H., Bultynck, G., 2014. A dual role for the anti-apoptotic Bcl-2 protein in cancer: Mitochondria versus endoplasmic reticulum. Biochim. Biophys. Acta - Mol. Cell Res. 1843, 2240–2252.

Aksoy, P., Escande, C., White, T.A., Thompson, M., Soares, S., Benech, J.C., Chini, E.N., 2006a. Regulation of SIRT 1 mediated NAD dependent deacetylation: A novel role for the multifunctional enzyme CD38. Biochem. Biophys. Res. Commun. 349, 353–359.

Aksoy, P., White, T.A., Thompson, M., Chini, E.N., 2006b. Regulation of intracellular levels of NAD: a novel role for CD38. Biochem. Biophys. Res. Commun. 345, 1386–92.

Alano, C.C., Garnier, P., Ying, W., Higashi, Y., Kauppinen, T.M., Swanson, R.A., 2010. NAD+ depletion is necessary and sufficient for poly(ADP-ribose) polymerase-1-mediated neuronal death. J. Neurosci. 30, 2967–78.

Albasanz, J.L., Dalfó, E., Ferrer, I., Martín, M., 2005. Impaired metabotropic glutamate receptor/phospholipase C signaling pathway in the cerebral cortex in Alzheimer's disease and dementia with Lewy bodies correlates with stage of Alzheimer's-disease-related changes. Neurobiol. Dis. 20, 685–693.

Allen, N.J., Barres, B.A., 2009. Neuroscience: Glia - more than just brain glue. Nature 457.

Ally, B.A., Hussey, E.P., Ko, P.C., Molitor, R.J., 2013. Pattern separation and pattern completion in Alzheimer's disease: Evidence of rapid forgetting in amnestic mild cognitive impairment. Hippocampus 23, 1246–1258.

Alonso, A. d. C., Li, B., Grundke-Iqbal, I., Iqbal, K., 2006. Polymerization of hyperphosphorylated tau into filaments eliminates its inhibitory activity. Proc. Natl. Acad. Sci. 103, 8864–8869.

Alonso, A.C., Grundke-Iqbal, I., Iqbal, K., 1996. Alzheimer's disease hyperphosphorylated tau sequesters normal tau into tangles of filaments and disassembles microtubules. Nat. Med. 2, 783–7.

Alonso, A.C., Zaidi, T., Grundke-Iqbal, I., Iqbal, K., 1994. Role of abnormally phosphorylated tau in the breakdown of microtubules in Alzheimer disease. Proc. Natl. Acad. Sci. U. S. A. 91, 5562–6.

Alonso, A.D., Grundke-Iqbal, I., Barra, H.S., Iqbal, K., 1997. Abnormal phosphorylation of tau and the mechanism of Alzheimer neurofibrillary degeneration: sequestration of microtubule-associated proteins 1 and 2 and the disassembly of microtubules by the abnormal tau. Proc. Natl. Acad. Sci. U. S. A. 94, 298–303.

Alves da Costa, C., Sunyach, C., Pardossi-Piquard, R., Sevalle, J., Vincent, B., Boyer, N., Kawarai, T., Girardot, N., St. George-Hyslop, P., Checler, F., 2006. Presenilin-Dependent -Secretase-Mediated Control of p53-Associated Cell Death in Alzheimer's Disease. J. Neurosci. 26, 6377–6385.

Alzheimer's Association, 2016. 2016 Alzheimer's disease facts and figures. Alzheimers. Dement. 12, 459–509.

An, W.-L., Cowburn, R.F., Li, L., Braak, H., Alafuzoff, I., Iqbal, K., Iqbal, I.-G., Winblad, B., Pei, J.-J., 2003. Up-Regulation of Phosphorylated/Activated p70 S6 Kinase and Its Relationship to Neurofibrillary Pathology in Alzheimer's Disease. Am. J. Pathol. 163, 591–607.

Andrew, R.J., Kellett, K.A.B., Thinakaran, G., Hooper, N.M., 2016. A Greek Tragedy: The Growing Complexity of Alzheimer Amyloid Precursor Protein Proteolysis. J. Biol. Chem. 291, 19235–19244.

Annaert, W.G., Levesque, L., Craessaerts, K., Dierinck, I., Snellings, G., Westaway, D., St. George-Hyslop, P., Cordell, B., Fraser, P., De Strooper, B., 1999. Presenilin 1 controls γ-secretase processing of amyloid precursor protein in pre-Golgi compartments of hippocampal neurons. J. Cell Biol. 147.

Annis, M.G., Zamzami, N., Zhu, W., Penn, L.Z., Kroemer, G., Leber, B., Andrews, D.W., 2001. Endoplasmic reticulum localized Bcl-2 prevents apoptosis when redistribution of cytochrome c is a late event. Oncogene 20, 1939–1952.

Anwyl, R., 1999. Metabotropic glutamate receptors: electrophysiological properties and role in plasticity. Brain Res. Brain Res. Rev. 29, 83–120.

Araque, A., Navarrete, M., 2010. Glial cells in neuronal network function. Philos. Trans. R. Soc. B Biol. Sci. 365.

Arimura, N., Kaibuchi, K., 2005. Key Regulators in Neuronal Polarity. Neuron 48, 881–884.

Arispe, N., Pollard, H.B., Rojas, E., 1993a. Giant multilevel cation channels formed by Alzheimer disease amyloid beta-protein [A beta P-(1-40)] in bilayer membranes. Proc. Natl. Acad. Sci. U. S. A. 90, 10573–7.

Arispe, N., Rojas, E., Pollard, H.B., 1993b. Alzheimer disease amyloid β protein forms calcium channels in bilayer membranes: Blockade by tromethamine and aluminum. Proc. Natl. Acad. Sci. U. S. A. 90.

Armato, U., Chiarini, A., Chakravarthy, B., Chioffi, F., Pacchiana, R., Colarusso, E., Whitfield, J.F., Dal Prà, I., 2013. Calcium-sensing receptor antagonist (calcilytic) NPS 2143 specifically blocks the increased secretion of endogenous Aβ42 prompted by exogenous fibrillary or soluble Aβ25–35 in human cortical astrocytes and neurons—Therapeutic relevance to Alzheimer's disease. Biochim. Biophys. Acta - Mol. Basis Dis. 1832, 1634–1652.

Arnaudeau, S., Kelley, W.L., Walsh Jr., J.V., Demaurex, N., 2001. Mitochondria Recycle Ca2+ to the Endoplasmic Reticulum and Prevent the Depletion of Neighboring Endoplasmic Reticulum Regions. J. Biol. Chem. 276.

Arnold, S.E., Louneva, N., Cao, K., Wang, L.-S., Han, L.-Y., Wolk, D.A., Negash, S., Leurgans, S.E., Schneider, J.A., Buchman, A.S., Wilson, R.S., Bennett, D.A., 2013. Cellular, synaptic, and biochemical features of resilient cognition in Alzheimer's disease. Neurobiol. Aging 34, 157–168.

Arora, M., 2013. Cell Culture Media: A Review. Mater. Methods 3.

Askarova, S., Yang, X., Lee, J.C.-M., 2011. Impacts of Membrane Biophysics in Alzheimer's Disease: From Amyloid Precursor Protein Processing to A β Peptide-Induced Membrane Changes. Int. J. Alzheimers. Dis. 2011, 1–12.

Atlas, D., 2013. The Voltage-Gated Calcium Channel Functions as the Molecular Switch of Synaptic Transmission. Annu. Rev. Biochem. 82, 607–635.

Auffret, A., Gautheron, V., Mattson, M.P., Mariani, J., Rovira, C., 2010. Progressive age-related impairment of the late long-term potentiation in Alzheimer's disease presenilin-1 mutant knock-in mice. J. Alzheimers. Dis. 19, 1021–33.

Augustine, G.J., Finch, E.A., 1998. Local calcium signalling by inositol-1,4,5-trisphosphate in Purkinje cell dendrites. Nature 396, 753–756.

Auld, D.S., Robitaille, R., 2003. Glial cells and neurotransmission: an inclusive view of synaptic function. Neuron 40, 389–400.

Ayar, A., Scott, R.H., 1999. The actions of ryanodine on Ca2+-activated conductances in rat cultured DRG neurones; evidence for Ca2+-induced Ca2+ release. Naunyn-Schmiedeberg's archives of pharmacology. 359, 81–91.

Ayub, K., Hallett, M.B., 2004. The mitochondrial ADPR link between Ca2+ store release and Ca2+ influx channel opening in immune cells. FASEB J. 18, 1335–1338.

Azarashvili, T., Baburina, Y., Grachev, D., Krestinina, O., Evtodienko, Y., Stricker, R., Reiser, G., 2011. Calcium-induced permeability transition in rat brain mitochondria is promoted by carbenoxolone through targeting connexin43. AJP Cell Physiol. 300, C707–C720.

Ba, F., Pang, P.K.T., Benishin, C.G., 2004. The role of Ca2+ channel modulation in the neuroprotective actions of estrogen in β-amyloid protein and 1-methyl-4-phenyl-1,2,3,6- tetrahydropyridine (MPTP) cytotoxic models. Neurochem. Int. 45.

Baba, A., Yasui, T., Fujisawa, S., Yamada, R.X., Yamada, M.K., Nishiyama, N., Matsuki, N., Ikegaya, Y., 2003. Activity-evoked capacitative Ca2+ entry: implications in synaptic plasticity. J. Neurosci. 23, 7737–41.

Baccaglini, P.I., Spitzer, N.C., 1977. Developmental changes in the inward current of the action potential of Rohon-Beard neurones. J. Physiol. 271, 93–117.

Bacher, I., Zidar, A., Kratzel, M., Hohenegger, M., 2004. Channelling of substrate promiscuity of the skeletal-muscle ADP-ribosyl cyclase isoform. Biochem. J. 381, 147–154.

Backman, L., Small, B.J., Fratiglioni, L., 2001. Stability of the preclinical episodic memory deficit in Alzheimer's disease. Brain 124, 96–102.

Baffy, G., Miyashita, T., Williamson, J.R., Reed, J.C., 1993. Apoptosis induced by withdrawal of interleukin-3 (IL-3) from an IL-3-dependent hematopoietic cell line is associated with repartitioning of intracellular calcium and is blocked by enforced Bcl-2 oncoprotein production. J. Biol. Chem. 268, 6511–9.

Bai, J.-Z., Lipski, J., 2010. Differential expression of TRPM2 and TRPV4 channels and their potential role in oxidative stress-induced cell death in organotypic hippocampal culture. Neurotoxicology 31, 204–214.

Balazs, R., 2006. Trophic effect of glutamate. Curr. Top. Med. Chem. 6, 961–8.

Bales, K.R., Liu, F., Wu, S., Lin, S., Koger, D., DeLong, C., Hansen, J.C., Sullivan, P.M., Paul, S.M., 2009. Human APOE Isoform-Dependent Effects on Brain β-Amyloid Levels in PDAPP Transgenic Mice. J. Neurosci. 29.

Bancher, C., Brunner, C., Lassmann, H., Budka, H., Jellinger, K., Wiche, G., Seitelberger, F., Grundke-Iqbal, I., Iqbal, K., Wisniewski, H.M., 1989. Accumulation of abnormally phosphorylated tau precedes the formation of neurofibrillary tangles in Alzheimer's disease. Brain Res. 477, 90–9.

Bandara, S., Malmersjö, S., Meyer, T., 2013. Regulators of Calcium Homeostasis Identified by Inference of Kinetic Model Parameters from Live Single Cells Perturbed by siRNA. Sci. Signal. 6.

Banerjee, S., Walseth, T.F., Borgmann, K., Wu, L., Bidasee, K.R., Kannan, M.S., Ghorpade, A., 2008. CD38/cyclic ADP-ribose regulates astrocyte calcium signaling: implications for neuroinflammation and HIV-1-associated dementia. J. Neuroimmune Pharmacol. 3, 154–64.

Banker, G. a, Cowan, W.M., 1979. Further observations on hippocampal neurons in dispersed cell culture. J. Comp. Neurol. 187, 469–93.

Banker, G.A., 1980. Trophic interactions between astroglial cells and hippocampal neurons in culture. Science (80-.). 209.

Banker, G.A., Cowan, W.M., 1977. Rat hippocampal neurons in dispersed cell culture. Brain Res. 126, 397–42.

Bannister, N.J., Larkman, A.U., 1995. Dendritic morphology of CA1 pyramidal neurones from the rat hippocampus: II. Spine distributions. J. Comp. Neurol. 360, 161–171.

Barbosa, M.T.P., Soares, S.M., Novak, C.M., Sinclair, D., Levine, J.A., Aksoy, P., Chini, E.N., 2007. The enzyme CD38 (a NAD glycohydrolase, EC 3.2.2.5) is necessary for the development of diet-induced obesity. FASEB J. 21, 3629–39.

Barde, Y.A., 1989. Trophic factors and neuronal survival. Neuron 2, 1525–34.

Barisione, G., Baroffio, M., Crimi, E., Brusasco, V., 2010. Beta-Adrenergic Agonists. Pharmaceuticals (Basel). 3, 1016–1044.

Barker, A.J., Ullian, E.M., 2008. New roles for astrocytes in developing synaptic circuits. Commun. Integr. Biol. 1, 207–11.

Baron, M., 2003. An overview of the Notch signalling pathway. Semin. Cell Dev. Biol. 14, 113–9.

Barone, F., Genazzani, A.A., Conti, A., Churchill, G.C., Palombi, F., Ziparo, E., Sorrentino, V., Galione, A., Filippini, A., 2002. A pivotal role for cADPR-mediated Ca2+ signaling: regulation of endothelin-induced contraction in peritubular smooth muscle cells. FASEB J. 16, 697–705.

Barrow, P.A., Empson, R.M., Gladwell, S.J., Anderson, C.M., Killick, R., Yu, X., Jefferys, J.G.R., Duff, K., 2000. Functional Phenotype in Transgenic Mice Expressing Mutant Human Presenilin-1. Neurobiol. Dis. 7, 119–126.

Barry, A.E., Klyubin, I., McDonald, J.M., Mably, A.J., Farrell, M.A., Scott, M., Walsh, D.M., Rowan, M.J., 2011. Alzheimer's disease brain-derived amyloid-β-mediated inhibition of LTP In Vivo is prevented by immunotargeting cellular prion protein. J. Neurosci. 31.

Barucker, C., Sommer, A., Beckmann, G., Eravci, M., Harmeier, A., Schipke, C.G., Brockschnieder, D., Dyrks, T., Althoff, V., Fraser, P.E., Hazrati, L.-N., George-Hyslop, P.S., Breitner, J.C.S., Peters, O., Multhaup, G., 2015. Alzheimer Amyloid Peptide Aβ42 Regulates Gene

Expression of Transcription and Growth Factors. J. Alzheimer's Dis. 44, 613–624.

Bashir, Z.I., 2003. On long-term depression induced by activation of G-protein coupled receptors. Neurosci. Res. 45, 363–367.

Bastide, B., Snoeckx, K., Mounier, Y., 2002. ADP-ribose stimulates the calcium release channel RyR1 in skeletal muscle of rat. Biochem. Biophys. Res. Commun. 296, 1267–71.

Batchelor, A.M., Garthwaite, J., 1997. Frequency detection and temporally dispersed synaptic signal association through a metabotropic glutamate receptor pathway. Nature 385, 74–77.

Bate, C., Williams, A., 2011. Amyloid-β-induced synapse damage is mediated via cross-linkage of cellular prion proteins. J. Biol. Chem. 286, 37955–63.

Baude, A., Nusser, Z., Roberts, J.D.B., Mulvihill, E., Jeffrey Mcllhinney, R.A., Somogyi, P., 1993. The metabotropic glutamate receptor (mGluRlα) is concentrated at perisynaptic membrane of neuronal subpopulations as detected by immunogold reaction. Neuron 11, 771–787.

Baughman, J.M., Perocchi, F., Girgis, H.S., Plovanich, M., Belcher-Timme, C.A., Sancak, Y., Bao, X.R., Strittmatter, L., Goldberger, O., Bogorad, R.L., Koteliansky, V., Mootha, V.K., 2011. Integrative genomics identifies MCU as an essential component of the mitochondrial calcium uniporter. Nature 476, 341–345.

Bazargani, N., Attwell, D., 2016. Astrocyte calcium signaling: the third wave. Nat. Neurosci. 19, 182–189.

Bear, M.F., Malenka, R.C., 1994. Synaptic plasticity: LTP and LTD. Curr. Opin. Neurobiol. 4, 389–399.

Beaudoin, G.M.J., Lee, S.-H., Singh, D., Yuan, Y., Ng, Y.-G., Reichardt, L.F., Arikkath, J., Beaudoin III, G.M.J., Seung-Hye L, D.S., Yang Y, Y.-G.N., Reichardt L.F, A.J., Beaudoin, G.M.J., Lee, S.-H., Singh, D., Yuan, Y., Ng, Y.-G., Reichardt, L.F., Arikkath, J., 2012. Culturing pyramidal neurons from the early postnatal mouse hippocampus and cortex. Nat. Protoc. 7, 1741–1754.

Becker, J.T., Walker, J.A., Olton, D.S., 1980. Neuroanatomical bases of spatial memory. Brain Res. 200, 307–320.

Beecham, G.W., Schnetz-Boutaud, N., Haines, J.L., Pericak-Vance, M.A., 2009. CALHM1 polymorphism is not associated with late-onset Alzheimer disease. Ann. Hum. Genet. 73, 379–81.

Beffert, U., Stolt, P.C., Herz, J., 2004. Functions of lipoprotein receptors in neurons. J. Lipid Res. 45, 403–9.

Beglopoulos, V., Sun, X., Saura, C.A., Lemere, C.A., Kim, R.D., Shen, J., 2004. Reduced β-amyloid production and increased inflammatory responses in presenilin conditional knock-out mice. J. Biol. Chem. 279.

Bekris, L.M., Yu, C.-E., Bird, T.D., Tsuang, D.W., 2010. Genetics of Alzheimer disease. J. Geriatr. Psychiatry Neurol. 23, 213–27.

Belleville, S., Sylvain-Roy, S., de Boysson, C., Ménard, M.-C., 2008. Chapter 23 Characterizing the memory changes in persons with mild cognitive impairment. In: Progress in Brain Research. pp. 365–375.

Bellone, C., Lüscher, C., Mameli, M., 2008. Mechanisms of synaptic depression triggered by metabotropic glutamate receptors. Cell. Mol. Life Sci. 65, 2913–2923.

Benarroch, E.E., 2008. Metabotropic glutamate receptors: synaptic modulators and therapeutic targets for neurologic disease. Neurology 70, 964–8.

Bennett, D.L., Cheek, T.R., Berridge, M.J., De Smedt, H., Parys, J.B., Missiaen, L., Bootman, M.D., 1996. Expression and function of ryanodine receptors in nonexcitable cells. J. Biol. Chem. 271, 6356–62.

Bennett, M.V.L., Garr?, J.M., Orellana, J.A., Bukauskas, F.F., Nedergaard, M., Giaume, C., S?ez, J.C., 2012. Connexin and pannexin hemichannels in inflammatory responses of glia and neurons. Brain Res. 1487, 3–15.

Benninger, C., Kadis, J., Prince, D.A., 1980. Extracellular calcium and potassium changes in hippocampal slices. Brain Res. 187, 165–82.

Benson, D.L., Watkins, F.H., Steward, O., Banker, G., 1994. Characterization of GABAergic neurons in hippocampal cell cultures. J. Neurocytol. 23, 279–95.

Bentahir, M., Nyabi, O., Verhamme, J., Tolia, A., Horre, K., Wiltfang, J., Esselmann, H., Strooper, B., 2006. Presenilin clinical mutations can affect gamma-secretase activity by different mechanisms. J. Neurochem. 96, 732–742.

Beraldo, F.H., Arantes, C.P., Santos, T.G., Machado, C.F., Roffe, M., Hajj, G.N., Lee, K.S., Magalhães, A.C., Caetano, F.A., Mancini, G.L., Lopes, M.H., Américo, T.A., Magdesian, M.H., Ferguson, S.S.G., Linden, R., Prado, M.A., Martins, V.R., 2011. Metabotropic glutamate receptors transduce signals for neurite outgrowth after binding of the prion protein to laminin $γ$1 chain. FASEB J 25.

Beraldo, F.H., Ostapchenko, V.G., Caetano, F.A., Guimaraes, A.L.S., Ferretti, G.D.S., Daude, N., Bertram, L., Nogueira, K.O.P.C., Silva, J.L., Westaway, D., Cashman, N.R., Martins, V.R., Prado, V.F., Prado, M.A.M., 2016. Regulation of Amyloid β Oligomer Binding to Neurons and Neurotoxicity by the Prion Protein-mGluR5 Complex. J. Biol. Chem. 291, 21945–21955.

Berg, L., McKeel, D.W., Miller, J.P., Storandt, M., Rubin, E.H., Morris, J.C., Baty, J., Coats, M., Norton, J., Goate, A.M., Price, J.L., Gearing, M., Mirra, S.S., Saunders, A.M., 1998. Clinicopathologic studies in cognitively healthy aging and Alzheimer's disease: relation of histologic markers to dementia severity, age, sex, and apolipoprotein E genotype. Arch. Neurol. 55, 326–35.

Bergner, A., Huber, R.M., 2008. Regulation of the endoplasmic reticulum Ca(2+)-store in cancer. Anticancer. Agents Med. Chem. 8.

Berna-Erro, A., Braun, A., Kraft, R., Kleinschnitz, C., Schuhmann, M.K., Stegner, D., Wultsch, T., Eilers, J., Meuth, S.G., Stoll, G., Nieswandt, B., 2009. STIM2 Regulates Capacitive Ca2+ Entry in Neurons and Plays a Key Role in Hypoxic Neuronal Cell Death. Sci. Signal. 2, ra67-ra67.

Bernstein, M., Behnisch, T., Balschun, D., Reymann, K.G., Reiser, G., 1998. Pharmacological characterisation of metabotropic glutamatergic and purinergic receptors linked to Ca2+ signalling in hippocampal astrocytes. Neuropharmacology 37, 169–78.

Berridge, M.J., 1998. Neuronal calcium signaling. Neuron 21, 13–26.

Berridge, M.J., 2002. The endoplasmic reticulum: a multifunctional signaling organelle. Cell Calcium 32, 235–249.

Berridge, M.J., 2006. Calcium microdomains: Organization and function. Cell Calcium 40, 405–412.

Berridge, M.J., 2010. Calcium hypothesis of Alzheimer's disease. Pflügers Arch. - Eur. J. Physiol. 459, 441–449.

Berridge, M.J., 2012. Calcium signalling remodelling and disease. Biochem. Soc. Trans. 40, 297–309.

Berridge, M.J., 2014a. Module 2: Cell Signalling Pathways. Cell Signal. Biol. 6, csb0001002.

Berridge, M.J., 2014b. Calcium regulation of neural rhythms, memory and Alzheimer's disease. J. Physiol. 592, 281–293.

Berridge, M.J., Bootman, M.D., Roderick, H.L., 2003. Calcium: Calcium signalling: dynamics, homeostasis and remodelling. Nat. Rev. Mol. Cell Biol. 4, 517–529.

Berridge, M.J., Lipp, P., Bootman, M.D., 2000. The versatility and universality of calcium signalling. Nat. Rev. Mol. Cell Biol. 1, 11–21.

Berrocal, M., Corbacho, I., Vázquez-Hernández, M., Ávila, J., Sepúlveda, M.R., Mata, A.M., 2015. Inhibition of PMCA activity by tau as a

function of aging and Alzheimer's neuropathology. Biochim. Biophys. Acta - Mol. Basis Dis. 1852, 1465–1476.

Berrocal, M., Sepulveda, M.R., Vazquez-Hernandez, M., Mata, A.M., 2012. Calmodulin antagonizes amyloid-β peptides-mediated inhibition of brain plasma membrane Ca2+-ATPase. Biochim. Biophys. Acta - Mol. Basis Dis. 1822, 961–969.

Bertram, L., McQueen, M.B., Mullin, K., Blacker, D., Tanzi, R.E., 2007. Systematic meta-analyses of Alzheimer disease genetic association studies: the AlzGene database. Nat. Genet. 39, 17–23.

Bertram, L., Schjeide, B.-M.M., Hooli, B., Mullin, K., Hiltunen, M., Soininen, H., Ingelsson, M., Lannfelt, L., Blacker, D., Tanzi, R.E., 2008. No association between CALHM1 and Alzheimer's disease risk. Cell 135, 993-4; author reply 994-6.

Bertram, L., Tanzi, R.E., 2004a. Alzheimer's disease: one disorder, too many genes? Hum. Mol. Genet. 13, 135R–141.

Bertram, L., Tanzi, R.E., 2004b. The current status of Alzheimer?s disease genetics: what do we tell the patients? Pharmacol. Res. 50, 385–396.

Beutner, G., Sharma, V.K., Lin, L., Ryu, S.-Y., Dirksen, R.T., Sheu, S.-S., 2005. Type 1 ryanodine receptor in cardiac mitochondria: Transducer of excitation-metabolism coupling. Biochim. Biophys. Acta - Biomembr. 1717.

Bezprozvanny, llya, Watras, J., Ehrlich, B.E., 1991. Bell-shaped calcium-response curves of lns(l,4,5)P3- and calcium-gated channels from endoplasmic reticulum of cerebellum. Nature 351, 751–754.

Bezprozvanny, I., Hiesinger, P., Andre, V., Cummings, D., Levine, M., Shen, J., Sudhof, T., Shen, J., Xia, W., Tesco, G., Abeliovich, A., 2013. The synaptic maintenance problem: membrane recycling, Ca2+ homeostasis and late onset degeneration. Mol. Neurodegener. 8, 23.

Bezprozvanny, I., Mattson, M.P.M.P., 2008. Neuronal calcium mishandling and the pathogenesis of Alzheimer's disease. Trends Neurosci. 31, 454–463.

Bezprozvanny, I., Supnet, C., Sun, S., Zhang, H., De Strooper, B., 2012. Response to Shilling et al. (10.1074/jbc.M111.300491). J. Biol. Chem. 287, 20469; author reply 20470.

Bianchi, R., Young, S.R., Wong, R.K., 1999. Group I mGluR activation causes voltage-dependent and -independent Ca2+ rises in hippocampal pyramidal cells. J. Neurophysiol. 81, 2903–13.

Biber, K., Laurie, D.J., Berthele, A., Sommer, B., Tölle, T.R., Gebicke-Härter, P.J., van Calker, D., Boddeke, H.W., 1999. Expression and signaling of group I metabotropic glutamate receptors in astrocytes and microglia. J. Neurochem. 72, 1671–80.

Bien-Ly, N., Andrews-Zwilling, Y., Xu, Q., Bernardo, A., Wang, C., Huang, Y., 2011. C-terminal-truncated apolipoprotein (apo) E4 inefficiently clears amyloid-β (Aβ) and acts in concert with Aβ to elicit neuronal and behavioral deficits in mice. Proc. Natl. Acad. Sci. U. S. A. 108.

Billings, L.M., Oddo, S., Green, K.N., McGaugh, J.L., LaFerla, F.M., 2005. Intraneuronal Aβ Causes the Onset of Early Alzheimer's Disease-Related Cognitive Deficits in Transgenic Mice. Neuron 45, 675–688.

Birben, E., Sahiner, U.M., Sackesen, C., Erzurum, S., Kalayci, O., 2012. Oxidative stress and antioxidant defense. World Allergy Organ. J. 5, 9–19.

Blacher, E., Dadali, T., Bespalko, A., Haupenthal, V.J., Grimm, M.O.W., Hartmann, T., Lund, F.E., Stein, R., Levy, A., 2015. Alzheimer's disease pathology is attenuated in a CD38-deficient mouse model. Ann. Neurol. 78, 88–103.

Black, S.A.G., Stys, P.K., Zamponi, G.W., Tsutsui, S., 2014. Cellular prion protein and NMDA receptor modulation: protecting against excitotoxicity. Front. cell Dev. Biol. 2, 45.

Blanchard, B.J., Thomas, V.L., Ingram, V.M., 2002. Mechanism of membrane depolarization caused by the Alzheimer Aβ1–42 peptide. Biochem. Biophys. Res. Commun. 293, 1197–1203.

Bleasdale, J.E., Thakur, N.R., Gremban, R.S., Bundy, G.L., Fitzpatrick, F.A., Smith, R.J., Bunting, S., 1990. Selective inhibition of receptor-coupled phospholipase C-dependent processes in human platelets and polymorphonuclear neutrophils. J. Pharmacol. Exp. Ther. 255, 756–68.

Bliss, T.V.P., Cooke, S.F., 2011. Long-term potentiation and long-term depression: a clinical perspective. Clinics 66, 3–17.

Bloom, G.S., 2014. Amyloid-$β$ and tau: the trigger and bullet in Alzheimer disease pathogenesis. JAMA Neurol 71.

Boada, M., Antúnez, C., López-Arrieta, J., Galán, J.J., Morón, F.J., Hernández, I., Marín, J., Martínez-Lage, P., Alegret, M., Carrasco, J.M., Moreno, C., Real, L.M., González-Pérez, A., Tárraga, L., Ruiz, A., 2010. CALHM1 P86L Polymorphism is Associated with Late-Onset Alzheimer's Disease in a Recessive Model. J. Alzheimer's Dis. 20, 247–251.

Bode, D.C., Baker, M.D., Viles, J.H., 2017. Ion Channel Formation by Amyloid-β42 Oligomers but Not Amyloid-β40 in Cellular Membranes. J. Biol. Chem. 292, 1404–1413.

Boehning, D., Patterson, R.L., Sedaghat, L., Glebova, N.O., Kurosaki, T., Snyder, S.H., 2003. Cytochrome c binds to inositol (1,4,5) trisphosphate receptors, amplifying calcium-dependent apoptosis. Nat. Cell Biol. 5, 1051–1061.

Boise, L.H., González-García, M., Postema, C.E., Ding, L., Lindsten, T., Turka, L.A., Mao, X., Nuñez, G., Thompson, C.B., 1993. bcl-x, a bcl-2-related gene that functions as a dominant regulator of apoptotic cell death. Cell 74, 597–608.

Bojarski, L., Pomorski, P., Szybinska, A., Drab, M., Skibinska-Kijek, A., Gruszczynska-Biegala, J., Kuznicki, J., 2009. Presenilin-dependent expression of STIM proteins and dysregulation of capacitative Ca2+ entry in familial Alzheimer's disease. Biochim. Biophys. Acta - Mol. Cell Res. 1793, 1050–1057.

Bolshakov, V.Y., Carboni, L., Cobb, M.H., Siegelbaum, S.A., Belardetti, F., 2000. Dual MAP kinase pathways mediate opposing forms of long-term plasticity at CA3–CA1 synapses. Nat. Neurosci. 3, 1107–1112.

Bonneau, B., Prudent, J., Popgeorgiev, N., Gillet, G., 2013. Non-apoptotic roles of Bcl-2 family: The calcium connection. Biochim. Biophys. Acta - Mol. Cell Res. 1833, 1755–1765.

Bootman, M.D., Collins, T.J., Mackenzie, L., Roderick, H.L., Berridge, M.J., Peppiatt, C.M., 2002. 2-Aminoethoxydiphenyl borate (2-APB) is a reliable blocker of store-operated Ca2+ entry but an inconsistent inhibitor of InsP3-induced Ca2+ release. FASEB J. 16, 1145–1150.

Boraso, M., Viviani, B., 2011. Glia-neuron sandwich cocultures: An in vitro approach to evaluate cell-to-cell communication in neuroinflammation and neurotoxicity. Methods Mol. Biol. 758, 135–152.

Borchelt, D.R., Thinakaran, G., Eckman, C.B., Lee, M.K., Davenport, F., Ratovitsky, T., Prada, C.M., Kim, G., Seekins, S., Yager, D., Slunt, H.H., Wang, R., Seeger, M., Levey, A.I., Gandy, S.E., Copeland, N.G., Jenkins, N.A., Price, D.L., Younkin, S.G., Sisodia, S.S., 1996. Familial Alzheimer's disease-linked presenilin 1 variants elevate Abeta1-42/1-40 ratio in vitro and in vivo. Neuron 17, 1005–13.

Bortolotto, Z.A., Collingridge, G.L., 1995. On the mechanism of long-term potentiation induced by (1S,3R)-1-aminocyclopentane-1,3-dicarboxylic acid (ACPD) in rat hippocampal slices. Neuropharmacology 34, 1003–14.

Bortolotto, Z.A., Fitzjohn, S.M., Collingridge, G.L., 1999. Roles of metabotropic glutamate receptors in LTP and LTD in the hippocampus. Curr. Opin. Neurobiol. 9, 299–304.

Bouzier-Sore, A.-K., Voisin, P., Canioni, P., Magistretti, P.J., Pellerin, L., 2003. Lactate Is a Preferential Oxidative Energy Substrate Over Glucose for Neurons in Culture. J. Cereb. Blood Flow Metab. 23, 1298–1306.

Boyles, J.K., Zoellner, C.D., Anderson, L.J., Kosik, L.M., Pitas, R.E., Weisgraber, K.H., Hui, D.Y., Mahley, R.W., Gebicke-Haerter, P.J., Ignatius, M.J., 1989. A role for apolipoprotein E, apolipoprotein A-I, and low density lipoprotein receptors in cholesterol transport during regeneration and remyelination of the rat sciatic nerve. J. Clin. Invest. 83, 1015–1031.

Braak, H., Alafuzoff, I., Arzberger, T., Kretzschmar, H., Tredici, K., 2006. Staging of Alzheimer disease-associated neurofibrillary pathology using paraffin sections and immunocytochemistry. Acta Neuropathol. 112, 389–404.

Braak, H., Braak, E., 1991. Neuropathological stageing of Alzheimer-related changes. Acta Neuropathol. 82, 239–59.

Bradley, K.N., Currie, S., MacMillan, D., Muir, T.C., McCarron, J.G., 2003. Cyclic ADP-ribose increases Ca2+ removal in smooth muscle. J. Cell Sci. 116, 4291–306.

Bradley, S.A., Steinert, J.R., 2016. Nitric Oxide-Mediated Posttranslational Modifications: Impacts at the Synapse. Oxid. Med. Cell. Longev. 2016, 1–9.

Braidy, N., Guillemin, G., Grant, R., 2008. Promotion of cellular NAD(+) anabolism: therapeutic potential for oxidative stress in ageing and Alzheimer's disease. Neurotox. Res. 13, 173–84.

Braidy, N., Jayasena, T., Poljak, A., Sachdev, P.S., 2012. Sirtuins in cognitive ageing and Alzheimer?s disease. Curr. Opin. Psychiatry 25, 226–230.

Braithwaite, S.P., Schmid, R.S., He, D.N., Sung, M.L.A., Cho, S., Resnick, L., Monaghan, M.M., Hirst, W.D., Essrich, C., Reinhart, P.H., Lo, D.C., 2010. Inhibition of c-Jun kinase provides neuroprotection in a model of Alzheimer's disease. Neurobiol. Dis. 39.

Bramham, C.R., Alme, M.N., Bittins, M., Kuipers, S.D., Nair, R.R., Pai, B., Panja, D., Schubert, M., Soule, J., Tiron, A., Wibrand, K., 2010. The Arc of synaptic memory. Exp. brain Res. 200, 125–40.

Brandman, O., Liou, J., Park, W.S., Meyer, T., 2007. STIM2 Is a Feedback Regulator that Stabilizes Basal Cytosolic and Endoplasmic Reticulum Ca^{2+} Levels. Cell 131.

Breunig, J.J., Guillot-Sestier, M.-V., Town, T., 2013. Brain injury, neuroinflammation and Alzheimer's disease. Front. Aging Neurosci. 5, 26.

Brewer, G.J., 1997. Isolation and culture of adult rat hippocampal neurons. J. Neurosci. Methods 71, 143–55.

Brewer, G.J., 1998. Age-related toxicity to lactate, glutamate, and beta-amyloid in cultured adult neurons. Neurobiol. Aging 19, 561–568.

Brewer, G.J., Boehler, M.D., Jones, T.T., Wheeler, B.C., 2008. NbActiv4 medium improvement to Neurobasal/B27 increases neuron synapse densities and network spike rates on multielectrode arrays. J. Neurosci. Methods 170, 181–7.

Brewer, G.J., Cotman, C.W., 1989. Survival and growth of hippocampal neurons in defined medium at low density: advantages of a sandwich culture technique or low oxygen. Brain Res. 494, 65–74.

Brewer, G.J., Lim, A., Capps, N.G., Torricelli, J.R., 2005. Age-related calcium changes, oxyradical damage, caspase activation and nuclear condensation in hippocampal neurons in response to glutamate and beta-amyloid. Exp. Gerontol. 40, 426–437.

Brewer, G.J., Reichensperger, J.D., Brinton, R.D., 2006. Prevention of age-related dysregulation of calcium dynamics by estrogen in neurons. Neurobiol. Aging 27, 306–17.

Brewer, G.J., Torricelli, J.R., 2007. Isolation and culture of adult neurons and neurospheres. Nat. Protoc. 2, 1490–8.

Brewer, G.J., Torricelli, J.R., Evege, E.K., Price, P.J., 1993. Optimized survival of hippocampal neurons in B27-supplemented Neurobasal, a new serum-free medium combination. J. Neurosci. Res. 35, 567–76.

Brewster, J.L., Linseman, D.A., Bouchard, R.J., Loucks, F.A., Precht, T.A., Esch, E.A., Heidenreich, K.A., 2006. Endoplasmic reticulum stress and trophic factor withdrawal activate distinct signaling cascades that induce glycogen synthase kinase-3β and a caspase-9-dependent apoptosis in cerebellar granule neurons. Mol. Cell. Neurosci. 32, 242–253.

Brickell, K.L., Steinbart, E.J., Rumbaugh, M., Payami, H., Schellenberg, G.D., Van Deerlin, V., Yuan, W., Bird, T.D., 2006. Early-Onset Alzheimer Disease in Families With Late-Onset Alzheimer Disease. Arch. Neurol. 63, 1307.

Brier, M.R., Gordon, B., Friedrichsen, K., McCarthy, J., Stern, A., Christensen, J., Owen, C., Aldea, P., Su, Y., Hassenstab, J., Cairns, N.J., Holtzman, D.M., Fagan, A.M., Morris, J.C., Benzinger, T.L.S., Ances, B.M., 2016. Tau and Aβ imaging, CSF measures, and cognition in Alzheimer's disease. Sci. Transl. Med. 8.

Briggs, C.A., Chakroborty, S., Stutzmann, G.E., 2017. Emerging pathways driving early synaptic pathology in Alzheimer's disease. Biochem. Biophys. Res. Commun. 483, 988–997.

Briggs, C.A., Schneider, C., Richardson, J.C., Stutzmann, G.E., 2013. Beta amyloid peptide plaques fail to alter evoked neuronal calcium signals in APP/PS1 Alzheimer's disease mice. Neurobiol. Aging 34, 1632–1643.

Brower, M., Grace, M., Kotz, C.M., Koya, V., 2015. Comparative analysis of growth characteristics of Sprague Dawley rats obtained from different sources. Lab. Anim. Res. 31, 166–73.

Brown, J.T., Chin, J., Leiser, S.C., Pangalos, M.N., Randall, A.D., 2011. Altered intrinsic neuronal excitability and reduced Na+ currents in a mouse model of Alzheimer's disease. Neurobiol. Aging 32, 2109.e1-2109.e14.

Bruno, A.M., Huang, J.Y., Bennett, D.A., Marr, R.A., Hastings, M.L., Stutzmann, G.E., 2011. Altered ryanodine receptor expression in mild cognitive impairment and Alzheimer's disease. Neurobiol. Aging 33, 1001.e1-1001.e6.

Bruno, V., Ksiazek, I., Battaglia, G., Lukic, S., Leonhardt, T., Sauer, D., Gasparini, F., Kuhn, R., Nicoletti, F., Flor, P.J., 2000. Selective blockade of metabotropic glutamate receptor subtype 5 is neuroprotective. Neuropharmacology 39, 2223–30.

Bruzzone, S., Basile, G., Chothi, M.P., Nobbio, L., Usai, C., Jacchetti, E., Schenone, A., Guse, A.H., Di Virgilio, F., De Flora, A., Zocchi, E., 2010. Diadenosine homodinucleotide products of ADP-ribosyl cyclases behave as modulators of the purinergic receptor P2X7. J. Biol. Chem. 285, 21165–74.

Bruzzone, S., De Flora, A., Usai, C., Graeff, R., Lee, H.C., 2003a. Cyclic ADP-ribose is a second messenger in the lipopolysaccharide-stimulated proliferation of human peripheral blood mononuclear cells. Biochem. J. 375, 395–403.

Bruzzone, S., Dodoni, G., Kaludercic, N., Basile, G., Millo, E., De Flora, A., Di Lisa, F., Zocchi, E., 2007. Mitochondrial dysfunction induced by a cytotoxic adenine dinucleotide produced by ADP-ribosyl cyclases from cADPR. J. Biol. Chem. 282, 5045–52.

Bruzzone, S., Franco, L., Guida, L., Zocchi, E., Contini, P., Bisso, A., Usai, C., De Flora, A., 2001. A self-restricted CD38-connexin 43 cross-talk affects NAD+ and cyclic ADP-ribose metabolism and regulates intracellular calcium in 3T3 fibroblasts. J. Biol. Chem. 276, 48300–8.

Bruzzone, S., Kunerth, S., Zocchi, E., De Flora, A., Guse, A.H., 2003b. Spatio-temporal propagation of Ca2+ signals by cyclic ADP-ribose in 3T3 cells stimulated via purinergic P2Y receptors. J. Cell Biol. 163, 837–45.

Bruzzone, S., Verderio, C., Schenk, U., Fedele, E., Zocchi, E., Matteoli, M., De Flora, A., 2004. Glutamate-mediated overexpression of CD38 in astrocytes cultured with neurones. J. Neurochem. 89, 264–272.

Bu, G., 2009. Apolipoprotein E and its receptors in Alzheimer's disease: pathways, pathogenesis and therapy. Nat. Rev. Neurosci. 10, 333–344.

Bu, G., 2009. Apolipoprotein e and its receptors in Alzheimer's disease: Pathways, pathogenesis and therapy. Nat. Rev. Neurosci. 10.

Buckmaster, C.A., Eichenbaum, H., Amaral, D.G., Suzuki, W.A., Rapp, P.R., 2004. Entorhinal cortex lesions disrupt the relational organization of memory in monkeys. J. Neurosci. 24, 9811–25.

Budde, T., Sieg, F., Braunewell, K.H., Gundelfinger, E.D., Pape, H.C., 2000. Ca2+-induced Ca2+ release supports the relay mode of activity in thalamocortical cells. Neuron 26, 483–92.

Bultynck, G., Rossi, D., Callewaert, G., Missiaen, L., Sorrentino, V., Parys, J.B., De Smedt, H., 2001. The conserved sites for the FK506-binding proteins in ryanodine receptors and inositol 1,4,5-trisphosphate receptors are structurally and functionally different. J. Biol. Chem. 276, 47715–24.

Burda, J.E., Sofroniew, M. V, 2014. Reactive gliosis and the multicellular response to CNS damage and disease. Neuron 81, 229–48.

Burdakov, D., Petersen, O.H., Verkhratsky, A., 2005. Intraluminal calcium as a primary regulator of endoplasmic reticulum function. Cell Calcium 38.

Burgoyne, T., Patel, S., Eden, E.R., 2015. Calcium signaling at ER membrane contact sites. Biochim. Biophys. Acta - Mol. Cell Res. 1853, 2012–2017.

Busche, M.A., Eichhoff, G., Adelsberger, H., Abramowski, D., Wiederhold, K.-H., Haass, C., Staufenbiel, M., Konnerth, A., Garaschuk, O., 2008. Clusters of Hyperactive Neurons Near Amyloid Plaques in a Mouse Model of Alzheimer's Disease. Science (80-.). 321.

Buxbaum, J.D., Ruefli, A.A., Parker, C.A., Cypess, A.M., Greengard, P., 1994. Calcium regulates processing of the Alzheimer amyloid protein precursor in a protein kinase C-independent manner. Proc. Natl. Acad. Sci. U. S. A. 91.

Cacace, R., Sleegers, K., Van Broeckhoven, C., 2016. Molecular genetics of early-onset Alzheimer's disease revisited. Alzheimer's Dement. 12, 733–748.

Cahalan, M.D., 2009. STIMulating store-operated Ca2+ entry. Nat. Cell Biol. 11, 669–677.

Cai, C., Lin, P., Cheung, K.-H., Li, N., Levchook, C., Pan, Z., Ferrante, C., Boulianne, G.L., Foskett, J.K., Danielpour, D., Ma, J., 2006. The presenilin-2 loop peptide perturbs intracellular Ca2+ homeostasis and accelerates apoptosis. J. Biol. Chem. 281, 16649–55.

Cai, H., Wang, Y., McCarthy, D., Wen, H., Borchelt, D.R., Price, D.L., Wong, P.C., 2001. BACE1 is the major beta-secretase for generation of Abeta peptides by neurons. Nat. Neurosci. 4, 233–234.

Calabrese, V., Mancuso, C., Calvani, M., Rizzarelli, E., Butterfield, D.A., Giuffrida Stella, A.M., 2007. Nitric oxide in the central nervous system: neuroprotection versus neurotoxicity. Nat. Rev. Neurosci. 8, 766–775.

Cameron, A.M., Nucifora, F.C., Fung, E.T., Livingston, D.J., Aldape, R.A., Ross, C.A., Snyder, S.H., 1997. FKBP12 binds the inositol 1,4,5-trisphosphate receptor at leucine-proline (1400-1401) and anchors calcineurin to this FK506-like domain. J. Biol. Chem. 272, 27582–8.

Cameron, A.M., Steiner, J.P., Roskams, A.J., Ali, S.M., Ronnett, G. V, Snyder, S.H., 1995a. Calcineurin associated with the inositol 1,4,5-trisphosphate receptor-FKBP12 complex modulates Ca2+ flux. Cell 83, 463–72.

Cameron, A.M., Steiner, J.P., Sabatini, D.M., Kaplin, A.I., Walensky, L.D., Snyder, S.H., 1995b. Immunophilin FK506 binding protein associated with inositol 1,4,5-trisphosphate receptor modulates calcium flux. Proc. Natl. Acad. Sci. U. S. A. 92, 1784–8.

Cancela, J.M., Churchill, G.C., Galione, A., 1999. Coordination of agonist-induced Ca2+-signalling patterns by NAADP in pancreatic acinar cells. Nature 398, 74–6.

Caporaso, G.L., Takei, K., Gandy, S.E., Matteoli, M., Mundigl, O., Greengard, P., De Camilli, P., 1994. Morphologic and biochemical analysis of the intracellular trafficking of the Alzheimer beta/A4 amyloid precursor protein. J. Neurosci. 14, 3122–38.

Castellani, R.J., Smith, M.A., 2011. Compounding artefacts with uncertainty, and an amyloid cascade hypothesis that is 'too big to fail.' J. Pathol. 224, 147–152.

Castellano, J.M., Kim, J., Stewart, F.R., Jiang, H., DeMattos, R.B., Patterson, B.W., Fagan, A.M., Morris, J.C., Mawuenyega, K.G., Cruchaga, C., Goate, A.M., Bales, K.R., Paul, S.M., Bateman, R.J., Holtzman, D.M., 2011. Human apoE Isoforms Differentially Regulate Brain Amyloid-β Peptide Clearance. Sci. Transl. Med. 3.

Castello, M.A., Jeppson, J.D., Soriano, S., 2014. Moving beyond anti-amyloid therapy for the prevention and treatment of Alzheimer's disease. BMC Neurol. 14, 169.

Castonguay, A., Robitaille, R., 2002. Xestospongin C is a potent inhibitor of SERCA at a vertebrate synapse. Cell Calcium 32, 39–47.

Castrén, E., Ohga, Y., Berzaghi, M.P., Tzimagiorgis, G., Thoenen, H., Lindholm, D., 1994. bcl-2 messenger RNA is localized in neurons of the developing and adult rat brain. Neuroscience 61, 165–77.

Cedazo-Mínguez, A., Popescu, B.O., Ankarcrona, M., Nishimura, T., Cowburn, R.F., 2002. The presenilin 1 ΔE9 mutation gives enhanced basal phospholipase C activity and a resultant increase in intracellular calcium concentrations. J. Biol. Chem. 277.

Celsi, F., Pizzo, P., Brini, M., Leo, S., Fotino, C., Pinton, P., Rizzuto, R., 2009. Mitochondria, calcium and cell death: A deadly triad in neurodegeneration. Biochim. Biophys. Acta - Bioenerg. 1787, 335–344.

Ceni, C., Muller-Steffner, H., Lund, F., Pochon, N., Schweitzer, A., De Waard, M., Schuber, F., Villaz, M., Moutin, M.-J.J., 2003a. Evidence for an intracellular ADP-ribosyl cyclase/NAD+-glycohydrolase in brain from CD38-deficient mice. J. Biol. Chem. 278, 40670–40678.

Ceni, C., Pochon, N., Brun, V., Muller-Steffner, H., Andrieux, A., Grunwald, D., Schuber, F., De Waard, M., Lund, F., Villaz, M., Moutin, M.-J., 2003b. CD38-dependent ADP-ribosyl cyclase activity in developing and adult mouse brain. Biochem. J. 370, 175–83.

Ceni, C., Pochon, N., Villaz, M., Muller-Steffner, H., Schuber, F., Baratier, J., De Waard, M., Ronjat, M., Moutin, M.-J., 2006. The CD38-independent ADP-ribosyl cyclase from mouse brain synaptosomes: a comparative study of neonate and adult brain. Biochem. J. 395, 417–426.

Cerbai, F., Lana, D., Nosi, D., Petkova-Kirova, P., Zecchi, S., Brothers, H.M., Wenk, G.L., Giovannini, M.G., 2012. The Neuron-Astrocyte-Microglia Triad in Normal Brain Ageing and in a Model of Neuroinflammation in the Rat Hippocampus. PLoS One 7, e45250.

Chakroborty, S., Goussakov, I., Miller, M.B., Stutzmann, G.E., 2009. Deviant Ryanodine Receptor-Mediated Calcium Release Resets Synaptic Homeostasis in Presymptomatic 3xTg-AD Mice. J. Neurosci. 29, 9458–9470.

Chakroborty, S., Kim, J., Schneider, C., Jacobson, C., Molgó, J., Stutzmann, G.E., 2012. Early Presynaptic and Postsynaptic Calcium Signaling Abnormalities Mask Underlying Synaptic Depression in Presymptomatic Alzheimer's Disease Mice. J. Neurosci. 32.

Chakroborty, S., Kim, J., Schneider, C., West, A.R., Stutzmann, G.E., 2015. Nitric Oxide Signaling Is Recruited As a Compensatory Mechanism for Sustaining Synaptic Plasticity in Alzheimer's Disease Mice. J. Neurosci. 35.

Chakroborty, S., Stutzmann, G.E., 2014. Calcium channelopathies and Alzheimer's disease: Insight into therapeutic success and failures. Eur. J. Pharmacol. 739, 83–95.

Chan, S.L., Mayne, M., Holden, C.P., Geiger, J.D., Mattson, M.P., 2000. Presenilin-1 mutations increase levels of ryanodine receptors and calcium release in PC12 cells and cortical neurons. J. Biol. Chem. 275, 18195–200.

Chan, W.K., Mole, M.M., Levison, D.A., Ball, R.Y., Lu, Q.-L., Patel, K., Hanby, A.M., 1995. Nuclear and cytoplasmicbcl-2 expression in

endometrial hyperplasia and adenocarcinoma. J. Pathol. 177, 241–246.

Chang, M.-J., Zhong, F., Lavik, A.R., Parys, J.B., Berridge, M.J., Distelhorst, C.W., 2014. Feedback regulation mediated by Bcl-2 and DARPP-32 regulates inositol 1,4,5-trisphosphate receptor phosphorylation and promotes cell survival. Proc. Natl. Acad. Sci. 111, 1186–1191.

Chapman, P.F., White, G.L., Jones, M.W., Cooper-Blacketer, D., Marshall, V.J., Irizarry, M., Younkin, L., Good, M.A., Bliss, T.V.P., Hyman, B.T., Younkin, S.G., Hsiao, K.K., 1999. Impaired synaptic plasticity and learning in aged amyloid precursor protein transgenic mice. Nat. Neurosci. 2, 271–276.

Charpak, S., Gähwiler, B.H., Do, K.Q., Knöpfel, T., 1990. Potassium conductances in hippocampal neurons blocked by excitatory amino-acid transmitters. Nature 347, 765–767.

Chauvet, S., Jarvis, L., Chevallet, M., Shrestha, N., Groschner, K., Bouron, A., 2016. Pharmacological Characterization of the Native Store-Operated Calcium Channels of Cortical Neurons from Embryonic Mouse Brain. Front. Pharmacol. 7, 486.

Chavis, P., Ango, F., Michel, J.M., Bockaert, J., Fagni, L., 1998. Modulation of big K+ channel activity by ryanodine receptors and L-type Ca2+ channels in neurons. Eur. J. Neurosci. 10, 2322–7.

Chavis, P., Fagni, L., Lansman, J.B., Bockaert, J., 1996. Functional coupling between ryanodine receptors and L-type calcium channels in neurons. Nature 382, 719–722.

Chelu, M.G., Danila, C.I., Gilman, C.P., Hamilton, S.L., 2004. Regulation of Ryanodine Receptors by FK506 Binding Proteins. Trends Cardiovasc. Med. 14, 227–234.

Chen, J., Li, Q., Wang, J., 2011. Topology of human apolipoprotein E3 uniquely regulates its diverse biological functions. Proc. Natl. Acad. Sci. 108, 14813–14818.

Chen, Q.-S., Wei, W.-Z., Shimahara, T., Xie, C.-W., 2002. Alzheimer amyloid β-peptide inhibits the late phase of long-term potentiation through calcineurin-dependent mechanisms in the hippocampal dentate gyrus. Neurobiol. Learn. Mem. 77.

Chen, R., Valencia, I., Zhong, F., McColl, K.S., Roderick, H.L., Bootman, M.D., Berridge, M.J., Conway, S.J., Holmes, A.B., Mignery, G.A., Velez, P., Distelhorst, C.W., 2004. Bcl-2 functionally interacts with inositol 1,4,5-trisphosphate receptors to regulate calcium release from the ER in response to inositol 1,4,5-trisphosphate. J. Cell Biol. 166, 193–203.

Chen, S.-H., Oyarzabal, E.A., Hong, J.-S., 2013. Preparation of rodent primary cultures for neuron-glia, mixed glia, enriched microglia, and reconstituted cultures with microglia. Methods Mol. Biol. 1041, 231–40.

Chen, S., Yadav, S.P., Surewicz, W.K., 2010. Interaction between human prion protein and amyloid-β (Aβ) oligomers: Role of N-terminal residues. J. Biol. Chem. 285.

Chen, W.S., Yueh, C.Y., Huang, Y.A., Hwang, E., 2011. An inverted method for culturing dissociated mouse hippocampal neurons. Neurosci. Res. 70, 118–123.

Chen, X., Huang, T., Zhang, J., Song, J., Chen, L., Zhu, Y., 2008. Involvement of calpain and p25 of CDK5 pathway in ginsenoside Rb1's attenuation of β-amyloid peptide25-35-induced tau hyperphosphorylation in cortical neurons. Brain Res. 1200.

Chen, Y., Stevens, B., Chang, J., Milbrandt, J., Barres, B.A., Hell, J.W., 2008. NS21: Re-defined and modified supplement B27 for neuronal cultures. J. Neurosci. Methods 171, 239–247.

Cheng, K.T., Ong, H.L., Liu, X., Ambudkar, I.S., 2013. Contribution and regulation of TRPC channels in store-operated Ca2+ entry. Curr. Top. Membr. 71, 149–79.

Chernecky, C.C., Berger, B.J., 2013. Blood gases, arterial (ABG) - blood. In: Laboratory Tests and Diagnostic Procedures. Elsevier/Saunders, Philadelphia, PA, pp. 208–213.

Cheung, K.-H., Mei, L., Mak, D.-O.D., Hayashi, I., Iwatsubo, T., Kang, D.E., Foskett, J.K., 2010. Gain-of-Function Enhancement of IP3 Receptor Modal Gating by Familial Alzheimer's Disease-Linked Presenilin Mutants in Human Cells and Mouse Neurons. Sci. Signal. 3, ra22-ra22.

Cheung, K.-H., Shineman, D., Müller, M., Cárdenas, C., Mei, L., Yang, J., Tomita, T., Iwatsubo, T., Lee, V.M.-Y.V.M.-Y., Foskett, J.K.K., 2008. Mechanism of Ca2+ Disruption in Alzheimer's Disease by Presenilin Regulation of InsP3 Receptor Channel Gating. Neuron 58, 871–883.

Chidambaram, N., Chang, C.F., 1999. NADP+-Dependent internalization of recombinant CD38 in CHO cells. Arch. Biochem. Biophys. 363, 267–272.

Chin, J., Massaro, C.M., Palop, J.J., Thwin, M.T., Yu, G.-Q., Bien-Ly, N., Bender, A., Mucke, L., 2007. Reelin Depletion in the Entorhinal Cortex of Human Amyloid Precursor Protein Transgenic Mice and Humans with Alzheimer's Disease. J. Neurosci. 27, 2727–2733.

Choe, C., Lardong, K., Gelderblom, M., Ludewig, P., Leypoldt, F., Koch-Nolte, F., Gerloff, C., Magnus, T., 2011. CD38 Exacerbates Focal Cytokine Production, Postischemic Inflammation and Brain Injury after Focal Cerebral Ischemia. PLoS One 6, e19046.

Choi, D.W., Maulucci-Gedde, M., Kriegstein, A.R., 1987. Glutamate Neurotoxicity in Cortical Cell Culture. J. Neurosci. 7, 357–388.

Choi, S., Lovinger, D.M., 1996. Metabotropic glutamate receptor modulation of voltage-gated Ca2+ channels involves multiple receptor subtypes in cortical neurons. J. Neurosci. 16, 36–45.

Chuang, S.-C., Zhao, W., Young, S.R., Conquet, F., Bianchi, R., Wong, R.K.S., 2002. Activation of group I mGluRs elicits different responses in murine CA1 and CA3 pyramidal cells. J. Physiol. 541, 113–21.

Chuang, S.C., Bianchi, R., Kim, D., Shin, H.S., Wong, R.K., Group, I., 2001. metabotropic glutamate receptors elicit epileptiform discharges in the hippocampus through PLCbeta1 signaling. J. Neurosci. Off. J. Soc. Neurosci. 21, 6387–6394.

Chuang, S.C., Bianchi, R., Wong, R.K., 2000. Group I mGluR activation turns on a voltage-gated inward current in hippocampal pyramidal cells. J. Neurophysiol. 83, 2844–53.

Chung, E., Ji, Y., Sun, Y., Kascsak, R.J., Kascsak, R.B., Mehta, P.D., Strittmatter, S.M., Wisniewski, T., 2010. Anti-PrPC monoclonal antibody infusion as a novel treatment for cognitive deficits in an alzheimer's disease model mouse. BMC Neurosci. 11, 130.

Chung, M.-K., Lee, H., Mizuno, A., Suzuki, M., Caterina, M.J., 2004. 2-Aminoethoxydiphenyl Borate Activates and Sensitizes the Heat-Gated Ion Channel TRPV3. J. Neurosci. 24, 5177–5182.

Churchill, G.C., Okada, Y., Thomas, J.M., Genazzani, A.A., Patel, S., Galione, A., 2002. NAADP mobilizes Ca(2+) from reserve granules, lysosome-related organelles, in sea urchin eggs. Cell 111, 703–8.

Cirrito, J.R., Yamada, K.A., Finn, M.B., Sloviter, R.S., Bales, K.R., May, P.C., Schoepp, D.D., Paul, S.M., Mennerick, S., Holtzman, D.M., 2005. Synaptic Activity Regulates Interstitial Fluid Amyloid-β Levels In Vivo. Neuron 48, 913–922.

Clapper, D.L., Walseth, T.F., Dargie, P.J., Lee, H.C., 1987. Pyridine nucleotide metabolites stimulate calcium release from sea urchin egg microsomes desensitized to inositol trisphosphate. J. Biol. Chem. 262, 9561–8.

Clark, J.K., Furgerson, M., Crystal, J.D., Fechheimer, M., Furukawa, R., Wagner, J.J., 2015. Alterations in synaptic plasticity coincide with deficits in spatial working memory in presymptomatic 3xTg-AD mice. Neurobiol. Learn. Mem. 125, 152–162.

Clementi, E., Riccio, M., Sciorati, C., Nisticò, G., Meldolesi, J., 1996. The type 2 ryanodine receptor of neurosecretory PC12 cells is activated by cyclic ADP-ribose - Role of the nitric oxide cGMP pathway. J. Biol. Chem. 271, 17739–17745.

Clementi, M.E., Pezzotti, M., Orsini, F., Sampaolese, B., Mezzogori, D., Grassi, C., Giardina, B., Misiti, F., 2006. Alzheimer's amyloid β-peptide (1–42) induces cell death in human neuroblastoma via bax/bcl-2 ratio increase: An intriguing role for methionine 35. Biochem. Biophys. Res. Commun. 342, 206–213.

Cobb, S.R., Bulters, D.O., Davies, C.H., 2000. Coincident activation of mGluRs and mAChRs imposes theta frequency patterning on synchronised network activity in the hippocampal CA3 region. Neuropharmacology 39, 1933–42.

Cochilla, A.J., Alford, S., 1998. Metabotropic Glutamate Receptor–Mediated Control of Neurotransmitter Release. Neuron 20, 1007–1016.

Cohen, R.M., Rezai-zadeh, K., Weitz, T.M., Rentsendorj, A., Gate, D., Spivak, I., Bholat, Y., Vasilevko, V., Glabe, C.G., Breunig, J.J., Rakic, P., Davtyan, H., Agadjanyan, M.G., Kepe, V., Barrio, J.R., Bannykh, S., Szekely, C.A., Pechnick, R.N., Town, T., 2013. Neurobiology of Disease A Transgenic Alzheimer Rat with Plaques , Tau Pathology , Behavioral Impairment , Oligomeric A □ , and Frank Neuronal Loss. J. Neurosci. 33, 6245–6256.

Cohen, S.I.A., Linse, S., Luheshi, L.M., Hellstrand, E., White, D.A., Rajah, L., Otzen, D.E., Vendruscolo, M., Dobson, C.M., Knowles, T.P.J., 2013. Proliferation of amyloid- 42 aggregates occurs through a secondary nucleation mechanism. Proc. Natl. Acad. Sci. 110, 9758–9763.

Coleman, P.D., Yao, P.J., 2003. Synaptic slaughter in Alzheimer's disease. Neurobiol. Aging 24.

Coleman, R.M. (Robert M., 2005. Trends in neurochemistry research. Nova Science Publishers.

Collie, A., Maruff, P., 2000. The neuropsychology of preclinical Alzheimer's disease and mild cognitive impairment. Neurosci. Biobehav. Rev. 24, 365–74.

Collins, M.O., Husi, H., Yu, L., Brandon, J.M., Anderson, C.N., Blackstock, W.P., Choudhary, J.S., Grant, S.G., 2006. Molecular characterization and comparison of the components and multiprotein complexes in the postsynaptic proteome. J. Neurochem. 97 Suppl 1.

Colonna, M., Wang, Y., 2016. TREM2 variants: new keys to decipher Alzheimer disease pathogenesis. Nat. Rev. Neurosci. 17, 201–207.

Colton, C.A., Vitek, M.P., Wink, D.A., Xu, Q., Cantillana, V., Previti, M.L., Van Nostrand, W.E., Weinberg, J.B., Weinberg, B., Dawson, H., 2006. NO synthase 2 (NOS2) deletion promotes multiple pathologies in a mouse model of Alzheimer's disease. Proc. Natl. Acad. Sci. U. S. A. 103, 12867–72.

Comley, L.H., Fuller, H.R., Wishart, T.M., Mutsaers, C.A., Thomson, D., Wright, A.K., Ribchester, R.R., Morris, G.E., Parson, S.H., Horsburgh, K., Gillingwater, T.H., 2011. ApoE isoform-specific regulation of regeneration in the peripheral nervous system. Hum. Mol. Genet. 20, 2406–2421.

Congar, P., Leinekugel, X., Ben-Ari, Y., Crépel, V., 1997. A Long-Lasting Calcium-Activated Nonselective Cationic Current Is Generated by Synaptic Stimulation or Exogenous Activation of Group I Metabotropic Glutamate Receptors in CA1 Pyramidal Neurons. J. Neurosci. 17.

Conley, Y.P., Mukherjee, A., Kammerer, C., DeKosky, S.T., Kamboh, M.I., Finegold, D.N., Ferrell, R.E., 2009. Evidence supporting a role for the calcium-sensing receptor in Alzheimer disease. Am. J. Med. Genet. Part B Neuropsychiatr. Genet. 150B, 703–709.

Conlon, R.A., Reaume, A.G., Rossant, J., 1995. Notch1 is required for the coordinate segmentation of somites. Development 121, 1533–45.

Conn, P.J., Pin, J.P., 1997. Pharmacology and functions of metabotropic glutamate receptors. Annu. Rev. Pharmacol. Toxicol. 37, 205–237.

Connor, J.A., Petrozzino, J., Pozzo-Miller, L.D., Otani, S., 1999. Calcium signals in long-term potentiation and long-term depression. Can. J. Physiol. Pharmacol. 77, 722–34.

Conquet, F., Bashir, Z.I., Davies, C.H., Daniel, H., Ferraguti, F., Bordi, F., Franz-Bacon, K., Reggiani, A., Matarese, V., Condé, F., Collingridge, G.L., Crépel, F., 1994. Motor deficit and impairment of synaptic plasticity in mice lacking mGluR1. Nature 372, 237–243.

Coon, K.D., Myers, A.J., Craig, D.W., Webster, J.A., Pearson, J. V, Lince, D.H., Zismann, V.L., Beach, T.G., Leung, D., Bryden, L., Halperin, R.F., Marlowe, L., Kaleem, M., Walker, D.G., Ravid, R., Heward, C.B., Rogers, J., Papassotiropoulos, A., Reiman, E.M., Hardy, J., Stephan, D.A., 2007. A high-density whole-genome association study reveals that APOE is the major susceptibility gene for sporadic late-onset Alzheimer's disease. J. Clin. Psychiatry 68, 613–8.

Copello, J.A., Qi, Y., Jeyakumar, L.H., Ogunbunmi, E., Fleischer, S., 2001. Lack of effect of cADP-ribose and NAADP on the activity of skeletal muscle and heart ryanodine receptors. Cell Calcium 30, 269–84.

Copray, J.C., Liem, R.S., 1993. Survival and neurite formation of mesencephalic trigeminal neurones of the rat in vitro. Arch. Oral Biol. 38, 547–57.

Corder, E.H., Saunders, A.M., Strittmatter, W.J., Schmechel, D.E., Gaskell, P.C., Small, G.W., Roses, A.D., Haines, J.L., Pericak-Vance, M.A., 1993. Gene dose of apolipoprotein E type 4 allele and the risk of Alzheimer's disease in late onset families. Science 261, 921–3.

Corradetti, R., Gaïarsa, J.L., Ben-Ari, Y., 1988. D-aminophosphonovaleric acid-sensitive spontaneous giant EPSPs in immature rat hippocampal neurones. Eur. J. Pharmacol. 154, 221–2.

Cosker, F., Cheviron, N., Yamasaki, M., Menteyne, A., Lund, F.E., Moutin, M.J.M.-J.M.J., Galione, A., Cancela, J.M.J.-M., 2010. The ecto-enzyme CD38 is a Nicotinic Acid Adenine Dinucleotide Phosphate (NAADP) synthase that couples receptor activation to Ca2+ mobilization from lysosomes in pancreatic acinar cells. J. Biol. Chem. 285, 38251–38259.

Coutinho, V., Knöpfel, T., 2002. Book Review: Metabotropic Glutamate Receptors: Electrical and Chemical Signaling Properties. Neurosci. 8, 551–561.

Craig, A.M., Banker, G., 1994. Neuronal Polarity. Annu. Rev. Neurosci. 17, 267–310.

Cramer, P.E., Cirrito, J.R., Wesson, D.W., Lee, C.Y.D., Karlo, J.C., Zinn, A.E., Casali, B.T., Restivo, J.L., Goebel, W.D., James, M.J., Brunden, K.R., Wilson, D.A., Landreth, G.E., 2012. ApoE-Directed Therapeutics Rapidly Clear -Amyloid and Reverse Deficits in AD Mouse Models. Science (80-.). 335, 1503–1506.

Crawford, J.H., Wootton, J.F., Seabrook, G.R., Scott, R.H., 1997a. Activation of Ca2+-dependent currents in dorsal root ganglion neurons by metabotropic glutamate receptors and cyclic ADP-ribose precursors. J. Neurophysiol. 77, 2573–2584.

Crawford, J.H., Wootton, J.F., Seabrook, G.R., Scott, R.H., 1997b. Activation of Ca 2+ -dependent currents in dorsal root ganglion neurons by metabotropic glutamate receptors and cyclic ADP- ribose precursors. J. Neurophysiol. 77, 2573–2584.

Crepel, V., Aniksztejn, L., Ben-Ari, Y., Hammond, C., 1994. Glutamate metabotropic receptors increase a Ca(2+)-activated nonspecific cationic current in CA1 hippocampal neurons. J. Neurophysiol. 72.

Csordás, G., Várnai, P., Golenár, T., Roy, S., Purkins, G., Schneider, T.G., Balla, T., Hajnóczky, G., 2010. Imaging Interorganelle Contacts and Local Calcium Dynamics at the ER-Mitochondrial Interface. Mol. Cell 39, 121–132.

Cullen, D.K., Gilroy, M.E., Irons, H.R., LaPlaca, M.C., 2010. Synapse-to-neuron ratio is inversely related to neuronal density in mature neuronal cultures. Brain Res. 1359, 44–55.

Cullen, W.K., Wu, J., Anwyl, R., Rowan, M.J., 1996. beta-Amyloid produces a delayed NMDA receptor-dependent reduction in synaptic

transmission in rat hippocampus. Neuroreport 8, 87–92.

Cummings, J.A., Mulkey, R.M., Nicoll, R.A., Malenka, R.C., 1996. Ca2+ signaling requirements for long-term depression in the hippocampus. Neuron 16.

Cupers, P., Bentahir, M., Craessaerts, K., Orlans, I., Vanderstichele, H., Saftig, P., De Strooper, B., Annaert, W., 2001. The discrepancy between presenilin subcellular localization and γ -secretase processing of amyloid precursor protein. J. Cell Biol. 154, 731–740.

Currie, K.P., Swann, K., Galione, A., Scott, R.H., 1992. Activation of Ca(2+)-dependent currents in cultured rat dorsal root ganglion neurones by a sperm factor and cyclic ADP-ribose. Mol. Biol. Cell 3, 1415–1425.

Currie, K.P., Wootton, J.F., Scott, R.H., 1995. Activation of Ca(2+)-dependent Cl-currents in cultured rat sensory neurones by flash photolysis of DM-nitrophen. J. Physiol. 482 Pt 2 291–307.

Czabotar, P.E., Lessene, G., Strasser, A., Adams, J.M., 2013. Control of apoptosis by the BCL-2 protein family: implications for physiology and therapy. Nat. Rev. Mol. Cell Biol. 15, 49–63.

D'Souza-Li, L., 2006. The calcium-sensing receptor and related diseases. Arq. Bras. Endocrinol. Metabol. 50, 628–39.

Dammermann, W., Guse, A.H., 2005. Functional ryanodine receptor expression is required for NAADP-mediated local Ca2+ signaling in T-lymphocytes. J. Biol. Chem. 280, 21394–21399.

Das, H.K., Tchedre, K., Mueller, B., 2012. Repression of transcription of presenilin-1 inhibits γ-secretase independent ER Ca2+ leak that is impaired by FAD mutations. J. Neurochem. 122, 487–500.

Das, U., Scott, D.A., Ganguly, A., Koo, E.H., Tang, Y., Roy, S., 2013. Activity-Induced Convergence of APP and BACE-1 in Acidic Microdomains via an Endocytosis-Dependent Pathway. Neuron 79, 447–460.

Das, U., Wang, L., Ganguly, A., Saikia, J.M., Wagner, S.L., Koo, E.H., Roy, S., 2015. Visualizing APP and BACE-1 approximation in neurons yields insight into the amyloidogenic pathway. Nat. Neurosci. 19, 55–64.

Dasso, L.L., Taylor, C.W., 1991. Heparin and other polyanions uncouple alpha 1-adrenoceptors from G-proteins. Biochem. J. 280 (Pt 3), 791–5.

Davies, C.H., Clarke, V.R., Jane, D.E., Collingridge, G.L., 1995. Pharmacology of postsynaptic metabotropic glutamate receptors in rat hippocampal CA1 pyramidal neurones. Br. J. Pharmacol. 116, 1859–69.

Davis, K.E., Eacott, M.J., Easton, A., Gigg, J., 2013a. Episodic-like memory is sensitive to both Alzheimer's-like pathological accumulation and normal ageing processes in mice. Behav. Brain Res. 254, 73–82.

Davis, K.E., Easton, A., Eacott, M.J., Gigg, J., 2013b. Episodic-like memory for what-where-which occasion is selectively impaired in the 3xTgAD mouse model of Alzheimer's disease. J. Alzheimers. Dis. 33, 681–98.

Davis, K.E., Fox, S., Gigg, J., Waldvogel, H., Faull, R., 2014. Increased Hippocampal Excitability in the 3xTgAD Mouse Model for Alzheimer's Disease In Vivo. PLoS One 9, e91203.

Dawkins, E., Small, D.H., 2014. Insights into the physiological function of the β-amyloid precursor protein: beyond Alzheimer's disease. J. Neurochem. 129, 756–769.

Dawson, G.R., Seabrook, G.R., Zheng, H., Smith, D.W., Graham, S., O'Dowd, G., Bowery, B.J., Boyce, S., Trumbauer, M.E., Chen, H.Y., Van der Ploeg, L.H., Sirinathsinghji, D.J., 1999. Age-related cognitive deficits, impaired long-term potentiation and reduction in synaptic marker density in mice lacking the beta-amyloid precursor protein. Neuroscience 90, 1–13.

de Calignon, A., Polydoro, M., Suárez-Calvet, M., William, C., Adamowicz, D.H., Kopeikina, K.J., Pitstick, R., Sahara, N., Ashe, K.H., Carlson, G.A., Spires-Jones, T.L., Hyman, B.T., 2012. Propagation of tau pathology in a model of early Alzheimer's disease. Neuron 73, 685–97.

De Felice, F.G., Velasco, P.T., Lambert, M.P., Viola, K., Fernandez, S.J., Ferreira, S.T., Klein, W.L., 2007. Aβ oligomers induce neuronal oxidative stress through an N-methyl-D-aspartate receptor-dependent mechanism that is blocked by the Alzheimer drug memantine. J. Biol. Chem. 282.

De Flora, A., Guida, L., Franco, L., Zocchi, E., Pestarino, M., Usai, C., Marchetti, C., Fedele, E., Fontana, G., Raiteri, M., 1996. Ectocellular in vitro and in vivo metabolism of cADP-ribose in cerebellum. Biochem. J 320, 665–672.

De Flora, A., Zocchi, E., Guida, L., Franco, L., Bruzzone, S., 2004. Autocrine and paracrine calcium signaling by the CD38/NAD+/cyclic ADP-ribose system. Ann. N. Y. Acad. Sci. 1028, 176–91.

de Murcia, G., de Murcia, J.M., 1994. Poly(ADP-ribose) polymerase: a molecular nick-sensor. Trends Biochem. Sci. 19, 172–176.

De Smet, P., Parys, J.B., Callewaert, G., Weidema, A.F., Hill, E., De Smedt, H., Erneux, C., Sorrentino, V., Missiaen, L., 1999. Xestospongin C is an equally potent inhibitor of the inositol 1,4,5-trisphosphate receptor and the endoplasmic-reticulum Ca(2+) pumps. Cell Calcium 26, 9–13.

De Stefani, D., Raffaello, A., Teardo, E., Szabò, I., Rizzuto, R., 2011. A forty-kilodalton protein of the inner membrane is the mitochondrial calcium uniporter. Nature 476, 336–340.

De Strooper, B., Iwatsubo, T., Wolfe, M.S., 2012. Presenilins and γ-secretase: structure, function, and role in Alzheimer Disease. Cold Spring Harb. Perspect. Med. 2, a006304.

de Toledo, F.G., Cheng, J., Liang, M., Chini, E.N., Dousa, T.P., 2000. ADP-Ribosyl cyclase in rat vascular smooth muscle cells: properties and regulation. Circ. Res. 86, 1153–9.

Deane, R., Sagare, A., Hamm, K., Parisi, M., Lane, S., Finn, M.B., Holtzman, D.M., Zlokovic, B. V., 2008. apoE isoform–specific disruption of amyloid β peptide clearance from mouse brain. J. Clin. Invest. 118, 4002–4013.

Decuypere, J.-P., Monaco, G., Bultynck, G., Missiaen, L., De Smedt, H., Parys, J.B., 2011. The IP3 receptor–mitochondria connection in apoptosis and autophagy. Biochim. Biophys. Acta - Mol. Cell Res. 1813, 1003–1013.

Dedkova, E.N., Sigova, A.A., Zinchenko, V.P., 2000. Mechanism of action of calcium ionophores on intact cells: ionophore-resistant cells. Membr. Cell Biol. 13, 357–68.

Degenetais, E., Thierry, A.-M., Glowinski, J., Gioanni, Y., 2003. Synaptic Influence of Hippocampus on Pyramidal Cells of the Rat Prefrontal Cortex: An In Vivo Intracellular Recording Study. Cereb. Cortex 13, 782–792.

Dehmelt, L., Halpain, S., 2005. The MAP2/Tau family of microtubule-associated proteins. Genome Biol. 6, 204.

Dehpour, A.R., Mofakham, S., Mahmoudian, M., 1982. In vitro binding of dantrolene to sarcoplasmic reticulum of rabbit skeletal muscle. Biochem. Pharmacol. 31, 965–8.

DeKosky, S.T., Scheff, S.W., 1990. Synapse loss in frontal cortex biopsies in Alzheimer's disease: Correlation with cognitive severity. Ann. Neurol. 27, 457–464.

Del Prete, D., Checler, F., Chami, M., Kriegstein, A., Nicoll, R., Takao, K., Takeshima, H., Miyakawa, T., Mikoshiba, K., Reed, J., Arancio, O., Bush, A., Nakai, A., Nishida, K., Kurihara, S., Donoviel, D., Bernstein, A., Tomita, T., Iwatsubo, T., Hori, M., Otsu, K., 2014. Ryanodine receptors: physiological function and deregulation in Alzheimer disease. Mol. Neurodegener. 9, 21.

del Río, E., McLaughlin, M., Downes, C.P., Nicholls, D.G., 1999. Differential coupling of G-protein-linked receptors to Ca2+ mobilization through inositol(1,4,5)trisphosphate or ryanodine receptors in cerebellar granule cells in primary culture. Eur. J. Neurosci. 11, 3015–22.

Demuro, A., Mina, E., Kayed, R., Milton, S.C., Parker, I., Glabe, C.G., 2005. Calcium Dysregulation and Membrane Disruption as a Ubiquitous Neurotoxic Mechanism of Soluble Amyloid Oligomers. J. Biol. Chem. 280, 17294–17300.

Demuro, A., Parker, I., 2013. Cytotoxicity of intracellular aβ42 amyloid oligomers involves Ca2+ release from the endoplasmic reticulum by stimulated production of inositol trisphosphate. J. Neurosci. 33, 3824–33.

Demuro, A., Parker, I., Stutzmann, G.E., 2010. Calcium Signaling and Amyloid Toxicity in Alzheimer Disease. J. Biol. Chem. 285, 12463–12468.

Deng, G., Su, J.H., Ivins, K.J., Van Houten, B., Cotman, C.W., 1999. Bcl-2 Facilitates Recovery from DNA Damage after Oxidative Stress. Exp. Neurol. 159, 309–318.

Deniaud, A., Sharaf El Dein, O., Maillier, E., Poncet, D., Kroemer, G., Lemaire, C., Brenner, C., 2008. Endoplasmic reticulum stress induces calcium-dependent permeability transition, mitochondrial outer membrane permeabilization and apoptosis. Oncogene 27.

Desai, M.K., Sudol, K.L., Janelsins, M.C., Mastrangelo, M.A., Frazer, M.E., Bowers, W.J., 2009. Triple-transgenic Alzheimer's disease mice exhibit region-specific abnormalities in brain myelination patterns prior to appearance of amyloid and tau pathology. Glia 57, 54–65.

Deshpande, A., Mina, E., Glabe, C., Busciglio, J., 2006. Different Conformations of Amyloid β Induce Neurotoxicity by Distinct Mechanisms in Human Cortical Neurons. J. Neurosci. 26, 6011–6018.

Deshpande, D.A., Walseth, T.F., Panettieri, R.A., Kannan, M.S., 2003. CD38-cyclic ADP-ribose-mediated Ca2+ signaling contributes to airway smooth muscle hyperresponsiveness. FASEB J. 17, 452–4.

Deshpande, D.A., White, T.A., Dogan, S., Walseth, T.F., Panettieri, R.A., Kannan, M.S., 2005. CD38/cyclic ADP-ribose signaling: role in the regulation of calcium homeostasis in airway smooth muscle. AJP Lung Cell. Mol. Physiol. 288, L773–L788.

Deshpande, L.S., Limbrick, D.D., Sombati, S., DeLorenzo, R.J., 2007. Activation of a Novel Injury-Induced Calcium-Permeable Channel That Plays a Key Role in Causing Extended Neuronal Depolarization and Initiating Neuronal Death in Excitotoxic Neuronal Injury. J. Pharmacol. Exp. Ther. 322, 443–452.

Deshpande, L.S., Sun, D.A., Sombati, S., Baranova, A., Wilson, M.S., Attkisson, E., Hamm, R.J., DeLorenzo, R.J., 2008. Alterations in neuronal calcium levels are associated with cognitive deficits after traumatic brain injury. Neurosci. Lett. 441, 115–119.

Diaz-Hernandez, J.I., Gomez-Villafuertes, R., Le?n-Otegui, M., Hontecillas-Prieto, L., del Puerto, A., Trejo, J.L., Lucas, J.J., Garrido, J.J., Gualix, J., Miras-Portugal, M.T., Diaz-Hernandez, M., 2012. In vivo P2X7 inhibition reduces amyloid plaques in Alzheimer's disease through GSK3? and secretases. Neurobiol. Aging 33, 1816–1828.

Dickson, D.W., Crystal, H.A., Bevona, C., Honer, W., Vincent, I., Davies, P., 1995. Correlations of synaptic and pathological markers with cognition of the elderly. Neurobiol. Aging 16, 285-98; discussion 298-304.

Dineley, K.T., Hogan, D., Zhang, W.-R., Taglialatela, G., 2007. Acute inhibition of calcineurin restores associative learning and memory in Tg2576 APP transgenic mice. Neurobiol. Learn. Mem. 88.

Dings, J., Meixensberger, J., Jäger, A., Roosen, K., 1998. Clinical Experience with 118 Brain Tissue Oxygen Partial Pressure Catheter Probes. Neurosurgery 43, 1082–1094.

Distelhorst, C.W., Shore, G.C., 2004. Bcl-2 and calcium: controversy beneath the surface. Oncogene 23, 2875–2880.

Dotti, C.G., Sullivan, C.A., Banker, G.A., 1988. The establishment of polarity by hippocampal neurons in culture. J. Neurosci. 8, 1454–68.

Dreses-Werringloer, U., Lambert, J.-C., Vingtdeux, V., Zhao, H., Vais, H., Siebert, A., Jain, A., Koppel, J., Rovelet-Lecrux, A., Hannequin, D., Pasquier, F., Galimberti, D., Scarpini, E., Mann, D., Lendon, C., Campion, D., Amouyel, P., Davies, P., Foskett, J.K., Campagne, F., Marambaud, P., 2008. A Polymorphism in CALHM1 Influences Ca^{2+} Homeostasis, Aβ Levels, and Alzheimer's Disease Risk. Cell 133.

Drysdale, A.J., Ryan, D., Pertwee, R.G., Platt, B., 2006. Cannabidiol-induced intracellular Ca2+ elevations in hippocampal cells. Neuropharmacology 50, 621–631.

Du, G.-J., Lin, H.-H., Xu, Q.-T., Wang, M.-W., 2006. Bcl-2 switches the type of demise from apoptosis to necrosis via cyclooxygenase-2 upregulation in HeLa cell induced by hydrogen peroxide. Cancer Lett. 232, 179–188.

Duff, K., Eckman, C., Zehr, C., Yu, X., Prada, C.-M., Perez-Tur, J., Hutton, M., Buee, L., Harigaya, Y., Yager, D., Morgan, D., Gordon, M.N., Holcomb, L., Refolo, L., Zenk, B., Hardy, J., Younkin, S., 1996. Increased amyloid-β42(43) in brains of mice expressing mutant presenilin 1. Nature 383.

Duffy, Á.M., Morales-Corraliza, J., Bermudez-Hernandez, K.M., Schaner, M.J., Magagna-Poveda, A., Mathews, P.M., Scharfman, H.E., 2015. Entorhinal cortical defects in Tg2576 mice are present as early as 2–4 months of age. Neurobiol. Aging 36, 134–148.

Dulin, F., Léveillé, F., Ortega, J.B., Mornon, J.-P., Buisson, A., Callebaut, I., Colloc'h, N., 2008. p3 peptide, a truncated form of Aβ devoid of synaptotoxic effect, does not assemble into soluble oligomers, FEBS Letters.

Dumuis, A., Sebben, M., Fagni, L., Prézeau, L., Manzoni, O., Cragoe, E.J., Bockaert, J., 1993. Stimulation by glutamate receptors of arachidonic acid release depends on the Na+/Ca2+ exchanger in neuronal cells. Mol. Pharmacol. 43, 976–81.

Durell, S.R., Guy, H.R., Arispe, N., Rojas, E., Pollard, H.B., 1994. Theoretical models of the ion channel structure of amyloid beta-protein. Biophys. J. 67, 2137–2145.

Durnin, L., Dai, Y., Aiba, I., Shuttleworth, C.W., Yamboliev, I.A., Mutafova-Yambolieva, V.N., 2012. Release, neuronal effects and removal of extracellular ??-nicotinamide adenine dinucleotide (??-NAD +) in the rat brain. Eur. J. Neurosci. 35, 423–435.

Dursun, E., Gezen-Ak, D., Yilmazer, S., 2011. A novel perspective for Alzheimer's disease: vitamin D receptor suppression by amyloid-β and preventing the amyloid-β induced alterations by vitamin D in cortical neurons. J. Alzheimers. Dis. 23, 207–19.

Eagle, H., Oyama, V.I., Levy, M., Horton, C.L., Fleischman, R., 1956. The growth response of mammalian cells in tissue culture to L-glutamine and L-glutamic acid. J. Biol. Chem. 218, 607–16.

Ebrahimi, M., Yamamoto, Y., Sharifi, K., Kida, H., Kagawa, Y., Yasumoto, Y., Islam, A., Miyazaki, H., Shimamoto, C., Maekawa, M., Mitsushima, D., Yoshikawa, T., Owada, Y., 2016. Astrocyte-expressed FABP7 regulates dendritic morphology and excitatory synaptic function of cortical neurons. Glia 64.

Eckenrode, E.F., Yang, J., Velmurugan, G. V., Foskett, J.K., White, C., 2010. Apoptosis Protection by Mcl-1 and Bcl-2 Modulation of Inositol 1,4,5-Trisphosphate Receptor-dependent Ca^{2+} Signaling. J. Biol. Chem. 285, 13678–13684.

Eckert, A., Schindowski, K., Leutner, S., Luckhaus, C., Touchet, N., Czech, C., Müller, W.E., 2001. Alzheimer's Disease-like Alterations in Peripheral Cells from Presenilin-1 Transgenic Mice. Neurobiol. Dis. 8, 331–342.

Edbauer, D., Winkler, E., Regula, J.T., Pesold, B., Steiner, H., Haass, C., 2003. Reconstitution of γ-secretase activity. Nat. Cell Biol. 5, 486–488.

Edwards, D., Das, M., Molnar, P., Hickman, J.J., 2010. Addition of glutamate to serum-free culture promotes recovery of electrical activity in adult hippocampal neurons in vitro. J. Neurosci. Methods 190, 155–63.

Egorov, A. V, Hamam, B.N., Fransén, E., Hasselmo, M.E., Alonso, A.A., 2002. Graded persistent activity in entorhinal cortex neurons. Nature 420, 173–8.

Ehlers, M.D., Heine, M., Groc, L., Lee, M.-C., Choquet, D., 2007. Diffusional Trapping of GluR1 AMPA Receptors by Input-Specific Synaptic Activity. Neuron 54.

Ehlers, M.D., Zhang, S., Bernhardt, J.P., Huganir, R.L., 1996. Inactivation of NMDA Receptors by Direct Interaction of Calmodulin with the NR1 Subunit. Cell 84, 745–755.

Eide, L., McMurray, C.T., 2005. Culture of adult mouse neurons. Biotechniques 38, 99–104.

Elder, G.A., Cho, J.Y., English, D.F., Franciosi, S., Schmeidler, J., Sosa, M.A.G., Gasperi, R. De, Fisher, E.A., Mathews, P.M., Haroutunian, V., Buxbaum, J.D., 2007. Elevated plasma cholesterol does not affect brain A? in mice lacking the low-density lipoprotein receptor. J. Neurochem. 102, 1220–1231.

Emilsson, L., Saetre, P., Jazin, E., 2006. Alzheimer's disease: mRNA expression profiles of multiple patients show alterations of genes involved with calcium signaling. Neurobiol. Dis. 21, 618–625.

Empson, R.M., Galione, A., 1997. Cyclic ADP-ribose enhances coupling between voltage-gated Ca2+ entry and intracellular Ca2+ release. J. Biol. Chem. 272, 20967–70.

Enokido, Y., Araki, T., Aizawa, S., Hatanaka, H., 1996. p53 involves cytosine arabinoside-induced apoptosis in cultured cerebellar granule neurons. Neurosci. Lett. 203, 1–4.

Erecińska, M., Silver, I.A., 2001. Tissue oxygen tension and brain sensitivity to hypoxia. Respir. Physiol. 128, 263–276.

Ernst, I.M.A., Fliegert, R., Guse, A.H., 2013. Adenine Dinucleotide Second Messengers and T-lymphocyte Calcium Signaling. Front. Immunol. 4, 259.

Etcheberrigaray, R., Hirashima, N., Nee, L., Prince, J., Govoni, S., Racchi, M., Tanzi, R.E., Alkon, D.L., 1998. Calcium responses in fibroblasts from asymptomatic members of Alzheimer's disease families. Neurobiol. Dis. 5.

Faber, E.S.L., Delaney, A.J., Sah, P., 2005. SK channels regulate excitatory synaptic transmission and plasticity in the lateral amygdala. Nat. Neurosci. 8, 635–641.

Fagan, A.M., Murphy, B.A., Patel, S.N., Kilbridge, J.F., Mobley, W.C., Bu, G., Holtzman, D.M., 1998. Evidence for Normal Aging of the Septo-Hippocampal Cholinergic System in apoE (?/?) Mice but Impaired Clearance of Axonal Degeneration Products Following Injury. Exp. Neurol. 151, 314–325.

Fagni, L., Chavis, P., Ango, F., Bockaert, J., 2000. Complex interactions between mGluRs, intracellular Ca2+ stores and ion channels in neurons. Trends Neurosci. 23, 80–8.

Faissner, A., Steindler, D., 1995. Boundaries and inhibitory molecules in developing neural tissues. Glia 13, 233–254.

Fanutza, T., Del Prete, D., Ford, M.J., Castillo, P.E., D'Adamio, L., 2015. APP and APLP2 interact with the synaptic release machinery and facilitate transmitter release at hippocampal synapses. Elife 4, e09743.

Farrer, L.A., Cupples, L.A., Haines, J.L., Hyman, B., Kukull, W.A., Mayeux, R., Myers, R.H., Pericak-Vance, M.A., Risch, N., van Duijn, C.M., 1997. Effects of age, sex, and ethnicity on the association between apolipoprotein E genotype and Alzheimer disease. A meta-analysis. APOE and Alzheimer Disease Meta Analysis Consortium. JAMA 278, 1349–56.

Federovitch, C.M., Ron, D., Hampton, R.Y., 2005. The dynamic ER: Experimental approaches and current questions. Curr. Opin. Cell Biol. 17.

Ferguson, S.S., 2001. Evolving concepts in G protein-coupled receptor endocytosis: the role in receptor desensitization and signaling. Pharmacol. Rev. 53, 1–24.

Fernàndez, J.E., Deaglio, S., Donati, D., Beusan, I.S., Corno, F., Aranega, A., Forni, M., Falini, B., Malavasi, F., 1998. Analysis of the distribution of human CD38 and of its ligand CD31 in normal tissues. J. Biol. Regul. Homeost. Agents 12, 81–91.

Fernandez, M.A., Klutkowski, J.A., Freret, T., Wolfe, M.S., 2014. Alzheimer Presenilin-1 Mutations Dramatically Reduce Trimming of Long Amyloid -Peptides (A) by -Secretase to Increase 42-to-40-Residue A. J. Biol. Chem. 289, 31043–31052.

Ferreiro, E., Oliveira, C.R., Pereira, C.M.F., 2008. The release of calcium from the endoplasmic reticulum induced by amyloid-beta and prion peptides activates the mitochondrial apoptotic pathway. Neurobiol. Dis. 30.

Ferrer, I., Tortosa, A., Blanco, R., Martín, F., Serrano, T., Planas, A., Macaya, A., 1994a. Naturally occurring cell death in the developing cerebral cortex of the rat. Evidence of apoptosis-associated internucleosomal DNA fragmentation. Neurosci. Lett. 182.

Ferrer, I., Tortosa, A., Condom, E., Blanco, R., Macaya, A., Planas, A., 1994b. Increased expression of bcl-2 immunoreactivity in the developing cerebral cortex of the rat. Neurosci. Lett. 179, 13–6.

Finder, V.H., Glockshuber, R., 2007. Amyloid-beta aggregation. Neurodegener. Dis. 4, 13–27.

Finnema, S.J., Nabulsi, N.B., Eid, T., Detyniecki, K., Lin, S. -f., Chen, M.-K., Dhaher, R., Matuskey, D., Baum, E., Holden, D., Spencer, D.D., Mercier, J., Hannestad, J., Huang, Y., Carson, R.E., 2016. Imaging synaptic density in the living human brain. Sci. Transl. Med. 8, 348ra96-348ra96.

Fitz, N.F., Cronican, A.A., Saleem, M., Fauq, A.H., Chapman, R., Lefterov, I., Koldamova, R., 2012. Abca1 Deficiency Affects Alzheimer's Disease-Like Phenotype in Human ApoE4 But Not in ApoE3-Targeted Replacement Mice. J. Neurosci. 32, 13125–13136.

Fitzjohn, S.M., Morton, R.A., Kuenzi, F., Rosahl, T.W., Shearman, M., Lewis, H., Smith, D., Reynolds, D.S., Davies, C.H., Collingridge, G.L., Seabrook, G.R., 2001. Age-Related Impairment of Synaptic Transmission But Normal Long-Term Potentiation in Transgenic Mice that Overexpress the Human APP695SWE Mutant Form of Amyloid Precursor Protein. J. Neurosci. 21.

Flaherty, D.B., Soria, J.P., Tomasiewicz, H.G., Wood, J.G., 2000. Phosphorylation of human tau protein by microtubule-associated kinases: GSK3β and cdk5 are key participants. J. Neurosci. Res. 62.

Fleming, L.M., Johnson, G.V.W., 1995. Modulation of the phosphorylation state of tau in situ: The roles of calcium and cyclic AMP. Biochem. J. 309.

Fletcher, T.L., Banker, G.A., 1989. The establishment of polarity by hippocampal neurons: the relationship between the stage of a cell's development in situ and its subsequent development in culture. Dev. Biol. 136, 446–54.

Fliegert, R., Gasser, A., Guse, A.H., 2007. Regulation of calcium signalling by adenine-based second messengers. Biochem. Soc. Trans. 35, 109–114.

Fonfria, E., Marshall, I.C.B., Boyfield, I., Skaper, S.D., Hughes, J.P., Owen, D.E., Zhang, W., Miller, B.A., Benham, C.D., McNulty, S., 2005. Amyloid beta-peptide(1-42) and hydrogen peroxide-induced toxicity are mediated by TRPM2 in rat primary striatal cultures. J. Neurochem. 95, 715–723.

Foo, L., Allen, N., Bushong, E., Ventura, P., Chung, W.-S., Zhou, L., Cahoy, J., Daneman, R., Zong, H., Ellisman, M., Barres, B., 2011. Development of a method for the purification and culture of rodent astrocytes. Neuron 71.

Foster, T.C.T.C., 2007. Calcium homeostasis and modulation of synaptic plasticity in the aged brain. Aging Cell 6, 319–325.

Franco, L., Bodrato, N., Moreschi, I., Usai, C., Bruzzone, S., Scarf ì, S., Zocchi, E., De Flora, A., 2006. Cyclic ADP-ribose is a second messenger in the lipopolysaccharide-stimulated activation of murine N9 microglial cell line. J. Neurochem. 99, 165–76.

Franco, L., Guida, L., Bruzzone, S., Zocchi, E., Usai, C., De Flora, A., 1998. The transmembrane glycoprotein CD38 is a catalytically active transporter responsible for generation and influx of the second messenger cyclic ADP-ribose across membranes. FASEB J. 12, 1507–20.

Franco, L., Zocchi, E., Usai, C., Guida, L., Bruzzone, S., Costa, A., De Flora, A., 2001. Paracrine Roles of NAD+ and Cyclic ADP-ribose in Increasing Intracellular Calcium and Enhancing Cell Proliferation of 3T3 Fibroblasts. J. Biol. Chem. 276, 21642–21648.

Frankowski, H., Missotten, M., Fernandez, P.A., Martinou, I., Michel, P., Sadoul, R., Martinou, J.C., 1995. Function and expression of the Bcl-x gene in the developing and adult nervous system. Neuroreport 6, 1917–21.

Franzini-Armstrong, C., Protasi, F., 1997. Ryanodine receptors of striated muscles: a complex channel capable of multiple interactions. Physiol. Rev. 77, 699–729.

Frazzini, V., Guarnieri, S., Bomba, M., Navarra, R., Morabito, C., Mariggiò, M.A., Sensi, S.L., 2016. Altered Kv2.1 functioning promotes increased excitability in hippocampal neurons of an Alzheimer's disease mouse model. Cell Death Dis. 7, e2100.

Freir, D.B., Costello, D.A., Herron, C.E., 2003. Aβ25-35-induced depression of long-term potentiation in area CA1 in vivo and in vitro is attenuated by verapamil. J. Neurophysiol. 89.

Freir, D.B., Nicoll, A.J., Klyubin, I., Panico, S., Mc Donald, J.M., Risse, E., Asante, E.A., Farrow, M.A., Sessions, R.B., Saibil, H.R., Clarke, A.R., Rowan, M.J., Walsh, D.M., Collinge, J., 2011. Interaction between prion protein and toxic amyloid β assemblies can be therapeutically targeted at multiple sites. Nat. Commun. 2, 336.

Frieden, C., Garai, K., 2012. Structural differences between apoE3 and apoE4 may be useful in developing therapeutic agents for Alzheimer's disease. Proc. Natl. Acad. Sci. 109, 8913–8918.

Friedlander, R.M., 2003. Apoptosis and Caspases in Neurodegenerative Diseases. N. Engl. J. Med. 348, 1365–1375.

Friedlich, A.L., Lee, J.-Y., van Groen, T., Cherny, R.A., Volitakis, I., Cole, T.B., Palmiter, R.D., Koh, J.-Y., Bush, A.I., 2004. Neuronal Zinc Exchange with the Blood Vessel Wall Promotes Cerebral Amyloid Angiopathy in an Animal Model of Alzheimer's Disease. J. Neurosci. 24, 3453–3459.

Frisoni, G.B., Ganzola, R., Canu, E., Rub, U., Pizzini, F.B., Alessandrini, F., Zoccatelli, G., Beltramello, A., Caltagirone, C., Thompson, P.M., 2008. Mapping local hippocampal changes in Alzheimer's disease and normal ageing with MRI at 3 Tesla. Brain 131, 3266–3276.

Fritz, N., Macrez, N., Mironneau, J., Jeyakumar, L.H., Fleischer, S., Morel, J.-L., 2005. Ryanodine receptor subtype 2 encodes Ca2+ oscillations activated by acetylcholine via the M2 muscarinic receptor/cADP-ribose signalling pathway in duodenum myocytes. J. Cell Sci. 118, 2261–70.

Fruen, B.R., Bardy, J.M., Byrem, T.M., Strasburg, G.M., Louis, C.F., 2000. Differential Ca(2+) sensitivity of skeletal and cardiac muscle ryanodine receptors in the presence of calmodulin. Am. J. Physiol. Cell Physiol. 279, C724-33.

Fryer, J.D., Demattos, R.B., McCormick, L.M., O'Dell, M.A., Spinner, M.L., Bales, K.R., Paul, S.M., Sullivan, P.M., Parsadanian, M., Bu, G., Holtzman, D.M., 2005. The low density lipoprotein receptor regulates the level of central nervous system human and murine apolipoprotein E but does not modify amyloid plaque pathology in PDAPP mice. J. Biol. Chem. 280, 25754–9.

Fujii, S., Matsumoto, M., Igarashi, K., Kato, H., Mikoshiba, K., 2000. Synaptic plasticity in hippocampal CA1 neurons of mice lacking type 1 inositol-1,4,5-trisphosphate receptors. Learn. Mem. 7, 312–20.

Fukumoto, H., Cheung, B.S., Hyman, B.T., Irizarry, M.C., 2002. Beta-secretase protein and activity are increased in the neocortex in Alzheimer disease. Arch. Neurol. 59, 1381–9.

Fukushi, Y., Kato, I., Takasawa, S., Sasaki, T., Ong, B.H., Sato, M., Ohsaga, A., Sato, K., Shirato, K., Okamoto, H., Maruyama, Y., 2001. Identification of cyclic ADP-ribose-dependent mechanisms in pancreatic muscarinic Ca(2+) signaling using CD38 knockout mice. J. Biol. Chem. 276, 649–55.

Fulceri, R., Rossi, R., Bottinelli, R., Conti, A., Intravaia, E., Galione, A., Benedetti, A., Sorrentino, V., Reggiani, C., 2001. Ca2+ release induced by cyclic ADP ribose in mice lacking type 3 ryanodine receptor. Biochem. Biophys. Res. Commun. 288, 697–702.

Furuichi, T., Kohda, K., Miyawaki, A., Mikoshiba, K., 1994. Intracellular channels. Curr. Opin. Neurobiol. 4, 294–303.

Furukawa, K., Wang, Y., Yao, P.J., Fu, W., Mattson, M.P., Itoyama, Y., Onodera, H., D'Souza, I., Poorkaj, P.H., Bird, T.D., Schellenberg, G.D., 2003. Alteration in calcium channel properties is responsible for the neurotoxic action of a familial frontotemporal dementia tau mutation. J. Neurochem. 87.

Futagi, D., Kitano, K., 2015. Ryanodine-receptor-driven intracellular calcium dynamics underlying spatial association of synaptic plasticity. J. Comput. Neurosci. 39, 329–347.

Gabellini, N., Manev, R.M., Candeo, P., Favaron, M., Manev, H., 1993. Carboxyl domain of glutamate receptor directs its coupling to metabolic pathways. Neuroreport 4, 531–4.

Gafni, J., Munsch, J.A., Lam, T.H., Catlin, M.C., Costa, L.G., Molinski, T.F., Pessah, I.N., 1997. Xestospongins: Potent Membrane Permeable Blockers of the Inositol 1,4,5-Trisphosphate Receptor. Neuron 19, 723–733.

Galimberti, D., Scarpini, E., 2011. Behavioral Genetics of Neurodegenerative Disorders. In: Current Topics in Behavioral Neurosciences. pp. 615–631.

Galione, A., 2011. NAADP Receptors. Cold Spring Harb. Perspect. Biol. 3, a004036–a004036.

Galione, A., Lee, H.C., Busa, W.B., 1991. Ca(2+)-induced Ca2+ release in sea urchin egg homogenates: modulation by cyclic ADP-ribose. Science 253, 1143–6.

Galione, A., White, A., Willmott, N., Turner, M., Potter, B.V.L., Watson, S.P., 1993. cGMP mobilizes intracellular Ca2+ in sea urchin eggs by stimulating cyclic ADP-ribose synthesis. Nature 365, 456–459.

Gallego-Sandín, S., Alonso, M.T., García-Sancho, J., 2011. Calcium homoeostasis modulator 1 (CALHM1) reduces the calcium content of the endoplasmic reticulum (ER) and triggers ER stress. Biochem. J. 437.

Galvan, V., Gorostiza, O.F., Banwait, S., Ataie, M., Logvinova, A. V., Sitaraman, S., Carlson, E., Sagi, S.A., Chevallier, N., Jin, K., Greenberg, D.A., Bredesen, D.E., 2006. Reversal of Alzheimer's-like pathology and behavior in human APP transgenic mice by mutation of Asp664. Proc. Natl. Acad. Sci. 103, 7130–7135.

Gamblin, T.C., Chen, F., Zambrano, A., Abraha, A., Lagalwar, S., Guillozet, A.L., Lu, M., Fu, Y., Garcia-Sierra, F., LaPointe, N., Miller, R., Berry, R.W., Binder, L.I., Cryns, V.L., 2003. Caspase cleavage of tau: linking amyloid and neurofibrillary tangles in Alzheimer's disease. Proc. Natl. Acad. Sci. U. S. A. 100, 10032–7.

Gandy, S.E., Caporaso, G.L., Buxbaum, J.D., de Cruz Silva, O., Iverfeldt, K., Nordstedt, C., Suzuki, T., Czernik, A.J., Nairn, A.C., Greengard, P., 1993. Protein phosphorylation regulates relative utilization of processing pathways for Alzheimer beta/A4 amyloid precursor protein.

Ann. N. Y. Acad. Sci. 695, 117–21.

Gant, J.C., Blalock, E.M., Chen, K.-. C., Kadish, I., Porter, N.M., Norris, C.M., Thibault, O., Landfield, P.W., 2014. FK506-binding protein 1b/12.6: A key to aging-related hippocampal Ca2+ dysregulation? Eur. J. Pharmacol. 739, 74–82.

Gao, Y., Vanhoutte, P.M., 2014. Tissues cIMPly do not lie. Naunyn. Schmiedebergs. Arch. Pharmacol. 387, 901–903.

Garaschuk, O., Yaari, Y., Konnerth, A., 1997. Release and sequestration of calcium by ryanodine-sensitive stores in rat hippocampal neurones. J. Physiol. 502 (Pt 1), 13–30.

Gasser, A., Bruhn, S., Guse, A.H., 2006a. Second messenger function of nicotinic acid adenine dinucleotide phosphate revealed by an improved enzymatic cycling assay. J. Biol. Chem. 281, 16906–16913.

Gasser, A., Glassmeier, G., Fliegert, R., Langhorst, M.F., Meinke, S., Hein, D., Krüger, S., Weber, K., Heiner, I., Oppenheimer, N., Schwarz, J.R., Guse, A.H., 2006b. Activation of T Cell Calcium Influx by the Second Messenger ADP-ribose. J. Biol. Chem. 281, 2489–2496.

Gatz, M., Reynolds, C.A., Fratiglioni, L., Johansson, B., Mortimer, J.A., Berg, S., Fiske, A., Pedersen, N.L., 2006. Role of genes and environments for explaining Alzheimer disease. Arch. Gen. Psychiatry 63, 168–74.

Gee, C.E., Benquet, P., Gerber, U., 2003. Group I metabotropic glutamate receptors activate a calcium-sensitive transient receptor potential-like conductance in rat hippocampus. J. Physiol. 546, 655–64.

Geiger, J., Zou, A.P., Campbell, W.B., Li, P.L., 2000. Inhibition of cADP-ribose formation produces vasodilation in bovine coronary arteries. Hypertens. (Dallas, Tex. 1979) 35, 397–402.

Gella, A., Durany, N., 2009. Oxidative stress in Alzheimer disease. Cell Adh. Migr. 3, 88–93.

Gelman, L., Deterre, P., Gouy, H., Boumsell, L., Debré, P., Bismuth, G., 1993. The lymphocyte surface antigen CD38 acts as a nicotinamide adenine dinucleotide glycohydrolase in human T lymphocytes. Eur. J. Immunol. 23, 3361–4.

Genetos, D.C., Cheung, W.K., Decaris, M.L., Leach, J.K., 2010. Oxygen tension modulates neurite outgrowth in PC12 cells through a mechanism involving HIF and VEGF. J. Mol. Neurosci. 40, 360–6.

Gerasimenko, J. V., Maruyama, Y., Yano, K., Dolman, N.J., Tepikin, A. V., Petersen, O.H., Gerasimenko, O. V., 2003. NAADP mobilizes Ca2+ from a thapsigargin-sensitive store in the nuclear envelope by activating ryanodine receptors. J. Cell Biol. 163, 271–282.

Gerasimenko, J. V., Sherwood, M., Tepikin, A. V., Petersen, O.H., Gerasimenko, O. V., 2006. NAADP, cADPR and IP3 all release Ca2+ from the endoplasmic reticulum and an acidic store in the secretory granule area. J. Cell Sci. 119.

Gerrard, J.L., Burke, S.N., McNaughton, B.L., Barnes, C.A., 2008. Sequence reactivation in the hippocampus is impaired in aged rats. J. Neurosci. 28, 7883–90.

Gervais, F.G., Xu, D., Robertson, G.S., Vaillancourt, J.P., Zhu, Y., Huang, J., LeBlanc, A., Smith, D., Rigby, M., Shearman, M.S., Clarke, E.E., Zheng, H., Van Der Ploeg, L.H., Ruffolo, S.C., Thornberry, N.A., Xanthoudakis, S., Zamboni, R.J., Roy, S., Nicholson, D.W., 1999. Involvement of caspases in proteolytic cleavage of Alzheimer's amyloid-beta precursor protein and amyloidogenic A beta peptide formation. Cell 97, 395–406.

Gimbel, D.A., Nygaard, H.B., Coffey, E.E., Gunther, E.C., Laurén, J., Gimbel, Z.A., Strittmatter, S.M., 2010. Memory Impairment in Transgenic Alzheimer Mice Requires Cellular Prion Protein. J. Neurosci. 30.

Giorgi, C., Baldassari, F., Bononi, A., Bonora, M., De Marchi, E., Marchi, S., Missiroli, S., Patergnani, S., Rimessi, A., Suski, J.M., Wieckowski, M.R., Pinton, P., 2012. Mitochondrial Ca2+ and apoptosis. Cell Calcium 52, 36–43.

Giorgi, C., De Stefani, D., Bononi, A., Rizzuto, R., Pinton, P., 2009. Structural and functional link between the mitochondrial network and the endoplasmic reticulum. Int. J. Biochem. Cell Biol. 41.

Giuffrida, M.L., Caraci, F., Pignataro, B., Cataldo, S., De Bona, P., Bruno, V., Molinaro, G., Pappalardo, G., Messina, A., Palmigiano, A., Garozzo, D., Nicoletti, F., Rizzarelli, E., Copani, A., 2009. β-Amyloid Monomers Are Neuroprotective. J. Neurosci. 29.

Giuliani, D., Ottani, A., Zaffe, D., Galantucci, M., Strinati, F., Lodi, R., Guarini, S., 2013. Hydrogen sulfide slows down progression of experimental Alzheimer's disease by targeting multiple pathophysiological mechanisms. Neurobiol. Learn. Mem. 104, 82–91.

Glabe, C.G., 2008. Structural classification of toxic amyloid oligomers. J. Biol. Chem. 283.

Glabe, C.G., Kayed, R., 2006. Common structure and toxic function of amyloid oligomers implies a common mechanism of pathogenesis. Neurology 66, S74–S78.

Glick, D.L., Hellmich, M.R., Beushausen, S., Tempst, P., Bayley, H., Strumwasser, F., 1991. Primary structure of a molluscan egg-specific NADase, a second-messenger enzyme. Cell Regul. 2, 211–8.

Goedert, M., Spillantini, M.G., Jakes, R., Rutherford, D., Crowther, R.A., 1989. Multiple isoforms of human microtubule-associated protein tau: sequences and localization in neurofibrillary tangles of Alzheimer's disease. Neuron 3, 519–26.

Golby, A., Silverberg, G., Race, E., Gabrieli, S., O'Shea, J., Knierim, K., Stebbins, G., Gabrieli, J., 2005. Memory encoding in Alzheimer's disease: an fMRI study of explicit and implicit memory. Brain 128, 773–787.

Gómez-Isla, T., Price, J.L., McKeel, D.W., Morris, J.C., Growdon, J.H., Hyman, B.T., 1996. Profound loss of layer II entorhinal cortex neurons occurs in very mild Alzheimer's disease. J. Neurosci. 16, 4491–500.

Gong, B., Pan, Y., Vempati, P., Zhao, W., Knable, L., Ho, L., Wang, J., Sastre, M., Ono, K., Sauve, A.A., Pasinetti, G.M., 2013. Nicotinamide riboside restores cognition through an upregulation of proliferator-activated receptor-γ coactivator 1α regulated β-secretase 1 degradation and mitochondrial gene expression in Alzheimer's mouse models. Neurobiol. Aging 34, 1581–8.

González-García, M., García, I., Ding, L., O'Shea, S., Boise, L.H., Thompson, C.B., Núñez, G., 1995. bcl-x is expressed in embryonic and postnatal neural tissues and functions to prevent neuronal cell death. Proc. Natl. Acad. Sci. U. S. A. 92, 4304–8.

González-García, M., Pérez-Ballestero, R., Ding, L., Duan, L., Boise, L.H., Thompson, C.B., Núñez, G., 1994. bcl-XL is the major bcl-x mRNA form expressed during murine development and its product localizes to mitochondria. Development 120, 3033–42.

González-Sánchez, P., del Arco, A., Esteban, J.A., Satrústegui, J., 2017. Store-Operated Calcium Entry Is Required for mGluR-Dependent Long Term Depression in Cortical Neurons. Front. Cell. Neurosci. 11, 363.

Gouras, G.K., Tsai, J., Naslund, J., Vincent, B., Edgar, M., Checler, F., Greenfield, J.P., Haroutunian, V., Buxbaum, J.D., Xu, H., Greengard, P., Relkin, N.R., 2000. Intraneuronal Abeta42 accumulation in human brain. Am. J. Pathol. 156, 15–20.

Goussakov, I., Miller, M.B., Stutzmann, G.E., 2010. NMDA-Mediated Ca 2 ∂ Influx Drives Aberrant Ryanodine Receptor Activation in Dendrites of Young Alzheimer ' s Disease Mice. J Neurosci 30, 12128–12137.

Graeff, R., Liu, Q., Kriksunov, I.A., Hao, Q., Lee, H.C., 2006. Acidic Residues at the Active Sites of CD38 and ADP-ribosyl Cyclase Determine Nicotinic Acid Adenine Dinucleotide Phosphate (NAADP) Synthesis and Hydrolysis Activities. J. Biol. Chem. 281, 28951–28957.

Graeff, R.M., Franco, L., De Flora, A., Lee, H.C., 1998. Cyclic GMP-dependent and -independent effects on the synthesis of the calcium messengers cyclic ADP-ribose and nicotinic acid adenine dinucleotide phosphate. J. Biol. Chem. 273, 118–25.

Graeff, R.M., Walseth, T.F., Fryxell, K., Branton, W.D., Lee, H.C., 1994. Enzymatic synthesis and characterizations of cyclic GDP-ribose. A procedure for distinguishing enzymes with ADP-ribosyl cyclase activity. J. Biol. Chem. 269, 30260–7.

Graeff, R.M., Walseth, T.F., Hill, H.K., Lee, H.C., 1996. Fluorescent Analogs of Cyclic ADP-Ribose: Synthesis, Spectral Characterization, and Use †. Biochemistry 35, 379–386.

Graham, D., Darles, G., Langer, S.Z., 1992. The neuroprotective properties of ifenprodil, a novel NMDA receptor antagonist, in neuronal cell culture toxicity studies. Eur. J. Pharmacol. 226, 373–6.

Gralle, M., Ferreira, S.T., 2007. Structure and functions of the human amyloid precursor protein: The whole is more than the sum of its parts. Prog. Neurobiol. 82, 11–32.

Grant, S.G.N., O'Dell, T.J., Karl, K.A., Stein, P.L., Soriano, P., Kandel, E.R., 1992. Impaired long-term potentiation, spatial learning, and hippocampal development in fyn mutant mice. Science (80-.). 258.

Green, K.N., LaFerla, F.M., 2008. Linking Calcium to Aβ and Alzheimer's Disease. Neuron 59, 190–194.

Green, K.N., Smith, I.F., Laferla, F.M., 2007. Role of calcium in the pathogenesis of Alzheimer's disease and transgenic models. Subcell. Biochem. 45.

Green, K.N.K.N., Demuro, A., Akbari, Y., Hitt, B.D.B.D., Smith, I.F.I.F., Parker, I., LaFerla, F.M.F.M., 2008. SERCA pump activity is physiologically regulated by presenilin and regulates amyloid β production 181.

Greenfield, J.P., Tsai, J., Gouras, G.K., Hai, B., Thinakaran, G., Checler, F., Sisodia, S.S., Greengard, P., Xu, H., 1999. Endoplasmic reticulum and trans-Golgi network generate distinct populations of Alzheimer beta-amyloid peptides. Proc. Natl. Acad. Sci. U. S. A. 96, 742–7.

Grehan, S., Tse, E., Taylor, J.M., 2001. Two distal downstream enhancers direct expression of the human apolipoprotein E gene to astrocytes in the brain. J. Neurosci. 21, 812–22.

Griffin, W.S.T., 2006. Inflammation and neurodegenerative diseases 1 – 4. Am. J. Clin. Nutr. 83(suppl), 470S–4S.

Grill, R.J., Pixley, S.K., 1993. 2-Mercaptoethanol is a survival factor for olfactory, cortical and hippocampal neurons in short-term dissociated cell culture. Brain Res. 613, 168–72.

Gruszczynska-Biegala, J., Kuznicki, J., 2013. Native STIM2 and ORAI1 proteins form a calcium-sensitive and thapsigargin-insensitive complex in cortical neurons. J. Neurochem. 126, 727–738.

Gruszczynska-Biegala, J., Pomorski, P., Wisniewska, M.B., Kuznicki, J., Chu, G., 2011. Differential Roles for STIM1 and STIM2 in Store-Operated Calcium Entry in Rat Neurons. PLoS One 6, e19285.

Guerineau, N., Bossu, J., Gahwiler, B., Gerber, U., 1995. Activation of a nonselective cationic conductance by metabotropic glutamatergic and muscarinic agonists in CA3 pyramidal neurons of the rat hippocampus. J. Neurosci. 15.

Guérineau, N.C., Gähwiler, B.H., Gerber, U., 1994. Reduction of resting K+ current by metabotropic glutamate and muscarinic receptors in rat CA3 cells: mediation by G-proteins. J. Physiol. 474, 27–33.

Guerreiro, R., Wojtas, A., Bras, J., Carrasquillo, M., Rogaeva, E., Majounie, E., Cruchaga, C., Sassi, C., Kauwe, J.S.K., Younkin, S., Hazrati, L., Collinge, J., Pocock, J., Lashley, T., Williams, J., Lambert, J.-C., Amouyel, P., Goate, A., Rademakers, R., Morgan, K., Powell, J., St. George-Hyslop, P., Singleton, A., Hardy, J., Alzheimer Genetic Analysis Group, 2013. *TREM2* Variants in Alzheimer's Disease. N. Engl. J. Med. 368, 117–127.

Guida, L., Bruzzone, S., Sturla, L., Franco, L., Zocchi, E., De Flora, A., 2002. Equilibrative and concentrative nucleoside transporters mediate influx of extracellular cyclic ADP-ribose into 3T3 murine fibroblasts. J. Biol. Chem. 277, 47097–105.

Guida, L., Franco, L., Bruzzone, S., Sturla, L., Zocchi, E., Basile, G., Usai, C., De Flora, A., 2004. Concentrative influx of functionally active cyclic ADP-ribose in dimethyl sulfoxide-differentiated HL-60 cells. J. Biol. Chem. 279, 22066–75.

Gul, R., Kim, S.-J.S.-Y.S.-J.S.-Y., Park, K.-H.K.-H., Kim, B.-J.B.-J., Kim, S.-J.S.-Y.S.-J.S.-Y., Im, M.-J.M.-J.M.-J., Kim, U.-H., 2008. A novel signaling pathway of ADP-ribosyl cyclase activation by angiotensin II in adult rat cardiomyocytes. Am. J. Physiol. Heart Circ. Physiol. 295, H77–H88.

Gul, R., Park, D.-R., Shawl, A.I., Im, S.-Y., Nam, T.-S., Lee, S.-H., Ko, J.-K., Jang, K.Y., Kim, D., Kim, U.-H., 2016. Nicotinic Acid Adenine Dinucleotide Phosphate (NAADP) and Cyclic ADP-Ribose (cADPR) Mediate Ca2+ Signaling in Cardiac Hypertrophy Induced by β-Adrenergic Stimulation. PLoS One 11, e0149125.

Guo, Q., Christakos, S., Robinson, N., Mattson, M.P., 1998. Calbindin D28K blocks the proapoptotic actions of mutant presenilin 1: Reduced oxidative stress and preserved mitochondrial function. Proc. Natl. Acad. Sci. U. S. A. 95.

Guo, Q., Fu, W., Sopher, B.L., Miller, M.W., Ware, C.B., Martin, G.M., Mattson, M.P., 1999. Increased vulnerability of hippocampal neurons to excitotoxic necrosis in presenilin-1 mutant knock-in mice. Nat. Med. 5, 101–107.

Guo, Q., Furukawa, K., Sopher, B.L., Pham, D.G., Xie, J., Robinson, N., Martin, G.M., Mattson, M.P., 1996. Alzheimer's PS-1 mutation perturbs calcium homeostasis and sensitizes PC12 cells to death induced by amyloid beta-peptide. Neuroreport 8, 379–83.

Guo, Q., Li, H., Gaddam, S.S.K., Justice, N.J., Robertson, C.S., Zheng, H., 2012. Amyloid Precursor Protein Revisited: Neuron-specific expression and highly stable nature of soluble derivatives. J. Biol. Chem. 287, 2437–2445.

Guo, Q., Sopher, B.L., Furukawa, K., Pham, D.G., Robinson, N., Martin, G.M., Mattson, M.P., 1997. Alzheimer's Presenilin Mutation Sensitizes Neural Cells to Apoptosis Induced by Trophic Factor Withdrawal and Amyloid β-Peptide: Involvement of Calcium and Oxyradicals. J. Neurosci. 17.

Guo, X., Becker, P.L., 1997. Cyclic ADP-ribose-gated Ca2+ release in sea urchin eggs requires an elevated [Ca2+]i. J. Biol. Chem. 272, 16984–9.

Gupta, V.B., Laws, S.M., Villemagne, V.L., Ames, D., Bush, A.I., Ellis, K.A., Lui, J.K., Masters, C., Rowe, C.C., Szoeke, C., Taddei, K., Martins, R.N., AIBL Research Group, 2011. Plasma apolipoprotein E and Alzheimer disease risk: the AIBL study of aging. Neurology 76, 1091–8.

Guse, A.H., 1999. Cyclic ADP-ribose: A Novel Ca2+-Mobilising Second Messenger. Cell. Signal. 11, 309–316.

Guse, A.H., 2004. Regulation of calcium signaling by the second messenger cyclic adenosine diphosphoribose (cADPR). Curr. Mol. Med. 4, 239–48.

Guse, A.H., da Silva, C.P., Berg, I., Skapenko, A.L., Weber, K., Heyer, P., Hohenegger, M., Ashamu, G.A., Schulze-Koops, H., Potter, B. V, Mayr, G.W., 1999. Regulation of calcium signalling in T lymphocytes by the second messenger cyclic ADP-ribose. Nature 398, 70–3.

Guse, A.H., Goldwich, A., Weber, K., Mayr, G.W., 1995. Non-radioactive, isomer-specific inositol phosphate mass determinations: high-performance liquid chromatography-micro-metal-dye detection strongly improves speed and sensitivity of analyses from cells and micro-enzyme assays. J. Chromatogr. B Biomed. Sci. Appl. 672, 189–198.

Guse, A.H., Gu, X., Zhang, L.L., Weber, K., Krämer, E., Yang, Z., Jin, H., Li, Q., Carrier, L., Zhang, L.L., 2005. A minimal structural analogue of cyclic ADP-ribose: synthesis and calcium release activity in mammalian cells. J. Biol. Chem. 280, 15952–15959.

Guse, A.H., Roth, E., Emmrich, F., 1992. d-myo-inositol 1,3,4,5-tetrakisphosphate releases Ca2+ from crude microsomes and enriched vesicular plasma membranes, but not from intracellular stores of permeabilized T-lymphocytes and monocytes. Biochem. J. 288.

Guse, A.H., Tsygankov, A.Y., Weber, K., Mayr, G.W., 2001. Transient tyrosine phosphorylation of human ryanodine receptor upon T cell stimulation. J. Biol. Chem. 276, 34722–7.

Györke, S., Terentyev, D., 2008. Modulation of ryanodine receptor by luminal calcium and accessory proteins in health and cardiac disease. Cardiovasc. Res. 77.

Haag, F., Adriouch, S., Bra?, A., Jung, C., M?ller, S., Scheuplein, F., Bannas, P., Seman, M., Koch-Nolte, F., 2007. Extracellular NAD and ATP: Partners in immune cell modulation. Purinergic Signal. 3, 71–81.

Haas, L.T., Kostylev, M.A., Strittmatter, S.M., 2014. Therapeutic molecules and endogenous ligands regulate the interaction between brain cellular prion protein (PrP^C) and metabotropic glutamate receptor 5 (mGluR5). J. Biol. Chem. 289.

Haas, L.T., Salazar, S. V., Kostylev, M.A., Um, J.W., Kaufman, A.C., Strittmatter, S.M., 2016. Metabotropic glutamate receptor 5 couples cellular prion protein to intracellular signalling in Alzheimer's disease. Brain 139, 526–546.

Haass, C., 2004. Take five—BACE and the γ-secretase quartet conduct Alzheimer's amyloid β-peptide generation. EMBO J. 23, 483–488.

Haass, C., Hung, A.Y., Schlossmacher, M.G., Oltersdorf, T., Teplow, D.B., Selkoe, D.J., 1993a. Normal cellular processing of the beta-amyloid precursor protein results in the secretion of the amyloid beta peptide and related molecules. Ann. N. Y. Acad. Sci. 695, 109–16.

Haass, C., Hung, A.Y., Schlossmacher, M.G., Teplow, D.B., Selkoe, D.J., 1993b. beta-Amyloid peptide and a 3-kDa fragment are derived by distinct cellular mechanisms. J. Biol. Chem. 268, 3021–4.

Habermacher, C., Dunning, K., Chataigneau, T., Grutter, T., 2016. Molecular structure and function of P2X receptors. Neuropharmacology 104, 18–30.

Hachisuka, J., Soga-Sakakibara, S., Kubota, M., Narita, K., Kuba, K., 2007. Enhancement of Ca2+-induced Ca2+ release by cyclic ADP-ribose in frog motor nerve terminals. Neuroscience 146, 123–34.

Haigis, M.C., Sinclair, D.A., 2010. Mammalian Sirtuins: Biological Insights and Disease Relevance. Annu. Rev. Pathol. Mech. Dis. 5, 253–295.

Hall, P.E., Lathia, J.D., Caldwell, M.A., Ffrench-Constant, C., 2008. Laminin enhances the growth of human neural stem cells in defined culture media. BMC Neurosci. 9, 71.

Hamid, R., Kilger, E., Willem, M., Vassallo, N., Kostka, M., Bornhövd, C., Reichert, A.S., Kretzschmar, H.A., Haass, C., Herms, J., 2007. Amyloid precursor protein intracellular domain modulates cellular calcium homeostasis and ATP content. J. Neurochem. 102, 1264–1275.

Hamilton, A., Vasefi, M., Vander Tuin, C., McQuaid, R.J.J., Anisman, H., Ferguson, S.S.G.S.G., Vander Tuin, C., McQuaid, R.J.J., Anisman, H., Ferguson, S.S.G.S.G., 2016. Chronic Pharmacological mGluR5 Inhibition Prevents Cognitive Impairment and Reduces Pathogenesis in an Alzheimer Disease Mouse Model. Cell Rep. 15, 1859–1865.

Hamos, J.E., DeGennaro, L.J., Drachman, D.A., 1989. Synaptic loss in Alzheimer's disease and other dementias. Neurology 39, 355–61.

Han, B.H., Xu, D., Choi, J., Han, Y., Xanthoudakis, S., Roy, S., Tam, J., Vaillancourt, J., Colucci, J., Siman, R., Giroux, A., Robertson, G.S., Zamboni, R., Nicholson, D.W., Holtzman, D.M., 2002. Selective, reversible caspase-3 inhibitor is neuroprotective and reveals distinct pathways of cell death after neonatal hypoxic-ischemic brain injury. J. Biol. Chem. 277, 30128–36.

Han, M.-K., Kim, S.-J., Park, Y.-R., Shin, Y.-M., Park, H.-J., Park, K.-J., Park, K.-H., Kim, H.-K., Jang, S.-I., An, N.-H., Kim, U.-H., 2002. Antidiabetic effect of a prodrug of cysteine, L-2-oxothiazolidine-4-carboxylic acid, through CD38 dimerization and internalization. J. Biol. Chem. 277, 5315–5321.

Hannan, A.J., Blakemore, C., Katsnelson, A., Vitalis, T., Huber, K.M., Bear, M., Roder, J., Kim, D., Shin, H.-S., Kind, P.C., 2001. PLC-β1, activated via mGluRs, mediates activity-dependent differentiation in cerebral cortex. Nat. Neurosci. 4, 282–288.

Hanson, C.J., Bootman, M.D., Distelhorst, C.W., Wojcikiewicz, R.J.H., Roderick, H.L., 2008. Bcl-2 suppresses Ca2+ release through inositol 1,4,5-trisphosphate receptors and inhibits Ca2+ uptake by mitochondria without affecting ER calcium store content. Cell Calcium 44, 324–338.

Harada, J., Sugimoto, M., 1999. Activation of caspase-3 in beta-amyloid-induced apoptosis of cultured rat cortical neurons. Brain Res. 842, 311–23.

Hardman, J.G., Robison, G.A., Sutherland, E.W., 1971. Cyclic Nucleotides. Annu. Rev. Physiol. 33, 311–336.

Hardy, J., Duff, K., Hardy, K.G., Perez-Tur, J., Hutton, M., 1998. Genetic dissection of Alzheimer's disease and related dementias: amyloid and its relationship to tau. Nat. Neurosci. 1, 355–358.

Hardy, J.A., Higgins, G.A., 1992. Alzheimer's disease: the amyloid cascade hypothesis. Science (80-.). 256.

Harold, D., Abraham, R., Hollingworth, P., Sims, R., Hamshere, M., Pahwa, J.S., Moskvina, V., Williams, A., Jones, N., Thomas, C., Stretton, A., Lovestone, S., Powell, J., Proitsi, P., Lupton, M.K., Rubinsztein, D.C., Gill, M., Lawlor, B., Lynch, A., Brown, K., Passmore, P., Craig, D., Mcguinness, B., Todd, S., Holmes, C., Mann, D., Smith, a D., Love, S., Patrick, G., Hardy, J., Mead, S., Fox, N., Rossor, M., Collinge, J., Wichmann, H., Carrasquillo, M.M., Pankratz, V.S., 2009. Genome-Wide Association Study Identifies Variants at CLU and PICALM Associated with Alzheimer's Disease, and Shows Evidence for Additional Susceptibility Genes. Nat. Genet. 41, 1088–1093.

Harris, J., Lee, H., Tu, C.T., Cribbs, D., Cotman, C., Jeon, N.L., 2007. Preparing E18 Cortical Rat Neurons for Compartmentalization in a Microfluidic Device. J. Vis. Exp. e305–e305.

Harris, K.M., Weinberg, R.J., 2012. Ultrastructure of synapses in the mammalian brain. Cold Spring Harb. Perspect. Biol. 4, a005587.

Hartley, D.M., Walsh, D.M., Ye, C.P., Diehl, T., Vasquez, S., Vassilev, P.M., Teplow, D.B., Selkoe, D.J., 1999. Protofibrillar Intermediates of Amyloid β-Protein Induce Acute Electrophysiological Changes and Progressive Neurotoxicity in Cortical Neurons. J. Neurosci. 19.

Hartley, T., Lever, C., Burgess, N., O'Keefe, J., 2013. Space in the brain: how the hippocampal formation supports spatial cognition. Philos. Trans. R. Soc. B Biol. Sci. 369, 20120510–20120510.

Harvey, J., Collingridge, G.L., 1993. Signal transduction pathways involved in the acute potentiation of NMDA responses by 1S,3R-ACPD in rat hippocampal slices. Br. J. Pharmacol. 109, 1085–90.

Hashii, M., Minabe, Y., Higashida, H., 2000a. voltage-activated Ca 2 + channels in NG108-15 neuronal cells. Society 215, 207–215.

Hashii, M., Minabe, Y., Higashida, H., 2000b. cADP-ribose potentiates cytosolic Ca2+ elevation and Ca2+ entry via L-type voltage-activated Ca2+ channels in NG108-15 neuronal cells. Biochem. J. 345 Pt 2, 207–15.

Hass, M.R., Yankner, B.A., 2005. A {gamma}-secretase-independent mechanism of signal transduction by the amyloid precursor protein. J. Biol. Chem. 280, 36895–904.

Hassa, P.O., Hottiger, M.O., 2008. The diverse biological roles of mammalian PARPS, a small but powerful family of poly-ADP-ribose polymerases. Front. Biosci. 13, 3046–82.

Hassanpoor, H., Fallah, A., Raza, M., 2013. Effect of BDNF secretion by astrocyte on learning and memory: A modeling approach. In: 2013 2nd International Conference on Advances in Biomedical Engineering, ICABME 2013.

Hayashi, H., Campenot, R.B., Vance, D.E., Vance, J.E., 2004. Glial lipoproteins stimulate axon growth of central nervous system neurons in compartmented cultures. J. Biol. Chem. 279, 14009–15.

Hayashi, H., Campenot, R.B., Vance, D.E., Vance, J.E., 2007. Apolipoprotein E-Containing Lipoproteins Protect Neurons from Apoptosis via a Signaling Pathway Involving Low-Density Lipoprotein Receptor-Related Protein-1. J. Neurosci. 27.

Hayashi, H., Campenot, R.B., Vance, D.E., Vance, J.E., 2009. Protection of neurons from apoptosis by apolipoprotein E-containing lipoproteins does not require lipoprotein uptake and involves activation of phospholipase Cgamma1 and inhibition of calcineurin. J. Biol. Chem. 284, 29605–13.

Hayashi, Y., Majewska, A.K., 2005. Dendritic Spine Geometry: Functional Implication and Regulation. Neuron 46, 529–532.

Hayrapetyan, V., Rybalchenko, V., Rybalchenko, N., Koulen, P., 2008. The N-terminus of presenilin-2 increases single channel activity of brain ryanodine receptors through direct protein–protein interaction. Cell Calcium 44, 507–518.

He, H., Lam, M., McCormick, T.S., Distelhorst, C.W., 1997. Maintenance of calcium homeostasis in the endoplasmic reticulum by Bcl-2. J. Cell Biol. 138, 1219–28.

Hermans, E., Challiss, R.A., 2001. Structural, signalling and regulatory properties of the group I metabotropic glutamate receptors: prototypic family C G-protein-coupled receptors. Biochem. J. 359, 465–84.

Herms, J., Schneider, I., Dewachter, I., Caluwaerts, N., Kretzschmar, H., Van Leuven, F., 2003. Capacitive Calcium Entry Is Directly Attenuated by Mutant Presenilin-1, Independent of the Expression of the Amyloid Precursor Protein. J. Biol. Chem. 278, 2484–2489.

Herrero, I., Miras-, Portugal, M., 1992. Positive feedback of glutamate exocytosis by metabotropic presynaptic receptor stimulation. J SÃ¡nchez-Prieto Nat. 360.

Herrup, K., 2015. The case for rejecting the amyloid cascade hypothesis. Nat. Neurosci. 18, 794–9.

Hertz, L., Peng, L., Dienel, G.A., 2007. Energy Metabolism in Astrocytes: High Rate of Oxidative Metabolism and Spatiotemporal Dependence on Glycolysis/Glycogenolysis. J. Cereb. Blood Flow Metab. 27, 219–249.

Herz, J., 2001. The LDL receptor gene family: (un)expected signal transducers in the brain. Neuron 29, 571–81.

Heuss, C., Scanziani, M., Gähwiler, B.H., Gerber, U., 1999. G-protein-independent signaling mediated by metabotropic glutamate receptors. Nat. Neurosci. 2, 1070–1077.

Hick, M., Herrmann, U., Weyer, S.W., Mallm, J.-P., Tschäpe, J.-A., Borgers, M., Mercken, M., Roth, F.C., Draguhn, A., Slomianka, L., Wolfer, D.P., Korte, M., Müller, U.C., 2015. Acute function of secreted amyloid precursor protein fragment APPsα in synaptic plasticity. Acta Neuropathol. 129, 21–37.

Higashida, H., 1997. ADP-ribosyl cyclase coupled with receptors via G protiens. FEBS Lett. 418, 355–356.

Higashida, H., Egorova, A., Higashida, C., Zhong, Z.G., Yokoyama, S., Noda, M., Zhang, J.S., 1999. Sympathetic potentiation of cyclic ADP-ribose formation in rat cardiac myocytes. J. Biol. Chem. 274, 33348–54.

Higashida, H., Hashii, M., Yokoyama, S., Hoshi, N., Asai, K., Kato, T., 2001a. Cyclic ADP-ribose as a potential second messenger for neuronal Ca2+ signaling. J. Neurochem. 76, 321–31.

Higashida, H., Salmina, A., Hashii, M., Yokoyama, S., Zhang, J.-S., Noda, M., Zhong, Z.-G., Jin, D., 2006. Bradykinin activates ADP-ribosyl cyclase in neuroblastoma cells: intracellular concentration decrease in NAD and increase in cyclic ADP-ribose. FEBS Lett. 580, 4857–60.

Higashida, H., Salmina, A.B., Olovyannikova, R.Y., Hashii, M., Yokoyama, S., Koizumi, K., Jin, D., Liu, H.-X., Lopatina, O., Amina, S., Islam, M.S., Huang, J.-J., Noda, M., 2007. Cyclic ADP-ribose as a universal calcium signal molecule in the nervous system. Neurochem. Int. 51, 192–199.

Higashida, H., Yokoyama, S., Hashii, M., Taketo, M., Higashida, M., Takayasu, T., Ohshima, T., Takasawa, S., Okamoto, H., Noda, M., 1997. Muscarinic receptor-mediated dual regulation of ADP-ribosyl cyclase in NG108-15 neuronal cell membranes. J. Biol. Chem. 272, 31272–7.

Higashida, H., Yokoyama, S., Hoshi, N., Hashii, M., Egorova, A., Zhong, Z.-G., Noda, M., Shahidullah, M., Taketo, M., Knijnik, R., Kimura, Y., Takahashi, H., Chen, X.-L., Shin, Y., Zhang, J.-S., 2001b. Signal Transduction from Bradykinin, Angiotensin, Adrenergic and Muscarinic Receptors to Effector Enzymes, Including ADP-Ribosyl Cyclase. Biol. Chem. 382, 23–30.

Higashida, H., Yokoyama, S., Kikuchi, M., Munesue, T., 2012. CD38 and its role in oxytocin secretion and social behavior. Horm. Behav. 61, 351–358.

Higashida, H., Zhang, J.-S.S., Mochida, S., Chen, X.-L.L., Shin, Y., Noda, M., Hossain, K.Z., Hoshi, N., Hashii, M., Shigemoto, R., Nakanishi, S., Fukuda, Y., Yokoyama, S., 2003. Subtype-specific coupling with ADP-ribosyl cyclase of metabotropic glutamate receptors in retina, cervical superior ganglion and cells. J. Neurochem. 11481158 85, NG108-15.

Higashida, H., Zhang, J., Hashii, M., Shintaku, M., Higashida, C., Takeda, Y., 2000. Angiotensin II stimulates cyclic ADP-ribose formation in neonatal rat cardiac myocytes. Biochem J Nov 15, 197–202.

Himmler, A., Drechsel, D., Kirschner, M.W., Martin, D.W., 1989. Tau consists of a set of proteins with repeated C-terminal microtubule-binding domains and variable N-terminal domains. Mol. Cell. Biol. 9, 1381–8.

Hirakura, Y., Lin, M.-C., Kagan, B.L., 1999. Alzheimer amyloid Aβ1-42 channels: Effects of solvent, pH, and Congo Red. J. Neurosci. Res. 57.

Hirashima, N., Etcheberrigaray, R., Bergamaschi, S., Racchi, M., Battaini, F., Binetti, G., Govoni, S., Alkon, D.L., 1996. Calcium responses in human fibroblasts: A diagnostic molecular profile for Alzheimer's disease. Neurobiol. Aging 17.

Hirata, Y., Kimura, N., Sato, K., Ohsugi, Y., Takasawa, S., Okamoto, H., Ishikawa, J., Kaisho, T., Ishihara, K., Hirano, T., 1994. ADP ribosyl cyclase activity of a novel bone marrow stromal cell surface molecule, BST-1. FEBS Lett. 356, 244–8.

Hirsch-Reinshagen, V., Wellington, C.L., 2007. Cholesterol metabolism, apolipoprotein E, adenosine triphosphate-binding cassette transporters, and Alzheimer?s disease. Curr. Opin. Lipidol. 18, 325–332.

Hisatsune, C., Nakamura, K., Kuroda, Y., Nakamura, T., Mikoshiba, K., 2005. Amplification of Ca2+ Signaling by Diacylglycerol-mediated Inositol 1,4,5-Trisphosphate Production. J. Biol. Chem. 280, 11723–11730.

Hockenbery, D., Nuñez, G., Milliman, C., Schreiber, R.D., Korsmeyer, S.J., 1990. Bcl-2 is an inner mitochondrial membrane protein that blocks programmed cell death. Nature 348, 334–336.

Hockenbery, D.M., Zutter, M., Hickeyt, W., Korsmeyer, S.J., 1991. BCL2 protein is topographically restricted in tissues characterized by apoptotic cell death. Cell Biol. 88, 6961–6.

Hoe, H.-S., Lee, H.-K., Pak, D.T.S., 2012. The Upside of APP at Synapses. CNS Neurosci. Ther. 18, 47–56.

Hoeffer, C.A., Tang, W., Wong, H., Santillan, A., Patterson, R.J., Martinez, L.A., Tejada-Simon, M. V., Paylor, R., Hamilton, S.L., Klann, E., 2008. Removal of FKBP12 Enhances mTOR-Raptor Interactions, LTP, Memory, and Perseverative/Repetitive Behavior. Neuron 60, 832–845.

Hoey, S.E., Williams, R.J., Perkinton, M.S., 2009. Synaptic NMDA Receptor Activation Stimulates -Secretase Amyloid Precursor Protein Processing and Inhibits Amyloid- Production. J. Neurosci. 29, 4442–4460.

Hogins, J., Crawford, D.C., Zorumski, C.F., Mennerick, S., 2011. Excitotoxicity triggered by Neurobasal culture medium. PLoS One 6, e25633.

Hohenegger, M., Suko, J., Gscheidlinger, R., Drobny, H., Zidar, A., 2002. Nicotinic acid-adenine dinucleotide phosphate activates the skeletal muscle ryanodine receptor. Biochem. J. 367, 423–431.

Hollifield, R.D., Conklin, J.D., 1968. A spectrophotofluorometric procedure for the determination oxidase of dantrolene in blood and urine. Arch. Int. Pharmacod 174, 333–341.

Holtzman, D.M., Morris, J.C., Goate, A.M., 2011. Alzheimer's Disease: The Challenge of the Second Century. Sci. Transl. Med. 3, 77sr1-77sr1.

Honarnejad, K., Jung, C.K.E., Lammich, S., Arzberger, T., Kretzschmar, H., Herms, J., 2013. Involvement of presenilin holoprotein upregulation in calcium dyshomeostasis of Alzheimer's disease. J. Cell. Mol. Med. 17, 293–302.

Hossain, S., Sesath Hewapathirane, D., Haas, K., 2012. Dynamic morphometrics reveals contributions of dendritic growth cones and filopodia to dendritogenesis in the intact and awake embryonic brain. Dev. Neurobiol. 72.

Hotta, T., Asai, K., Fujita, K., Kato, T., Higashida, H., 2000. Membrane-bound form of ADP-ribosyl cyclase in rat cortical astrocytes in culture. J. Neurochem. 74, 669–75.

Hou, L., Klann, E., 2004. Activation of the Phosphoinositide 3-Kinase-Akt-Mammalian Target of Rapamycin Signaling Pathway Is Required for Metabotropic Glutamate Receptor-Dependent Long-Term Depression. J. Neurosci. 24, 6352–6361.

Howard, M., Grimaldi, J.C., Bazan, J.F., Lund, F.E., Santos-Argumedo, L., Parkhouse, R.M., Walseth, T.F., Lee, H.C., 1993. Formation and hydrolysis of cyclic ADP-ribose catalyzed by lymphocyte antigen CD38. Science 262, 1056–1059.

Hsia, A.Y., Masliah, E., McConlogue, L., Yu, G.Q., Tatsuno, G., Hu, K., Kholodenko, D., Malenka, R.C., Nicoll, R.A., Mucke, L., 1999. Plaque-independent disruption of neural circuits in Alzheimer's disease mouse models. Proc. Natl. Acad. Sci. U. S. A. 96, 3228–33.

Hsiao, K.K., Chapman, P.F., White, G.L., Jones, M.W., Cooper-Blacketer, D., Marshall, V.J., Irizarry, M., Younkin, L., Good, M.A., Bliss, T.V.P., Hyman, B.T., Younkin, S.G., 1999. Impaired synaptic plasticity and learning in aged amyloid precursor protein transgenic mice. Nat. Neurosci. 2, 271–276.

Hu, G.-Y., Storm, J.F., 1991. Excitatory amino acids acting on metabotropic glutamate receptors broaden the action potential in hippocampal neurons, Brain Research.

Hu, N.-W., Nicoll, A.J., Zhang, D., Mably, A.J., O'Malley, T., Purro, S.A., Terry, C., Collinge, J., Walsh, D.M., Rowan, M.J., 2014. mGlu5 receptors and cellular prion protein mediate amyloid-β-facilitated synaptic long-term depression in vivo. Nat. Commun. 5, 3374.

Hua, S.Y., Tokimasa, T., Takasawa, S., Furuya, Y., Nohmi, M., Okamoto, H., Kuba, K., Cyclic, A.D.P., 1994. ribose modulates Ca2+ release channels for activation by physiological Ca2+ entry in bullfrog sympathetic neurons. Neuron 12, 1073–1079.

Huang, H., van den Pol, A.N., 2007. Rapid direct excitation and long-lasting enhancement of NMDA response by group I metabotropic glutamate receptor activation of hypothalamic melanin-concentrating hormone neurons. J. Neurosci. 27, 11560–72.

Huang, H.M., Ou, H.C., Hsieh, S.J., 2000. Antioxidants prevent amyloid peptide-induced apoptosis and alteration of calcium homeostasis in cultured cortical neurons. Life Sci. 66, 1879–92.

Huang, W.-J., Zhang, X., Chen, W.-W., 2016. Role of oxidative stress in Alzheimer's disease. Biomed. reports 4, 519–522.

Huang, Y., Mucke, L., 2012. Alzheimer mechanisms and therapeutic strategies. Cell 148, 1204–22.

Hui, L., Geiger, N.H., Bloor-Young, D., Churchill, G.C., Geiger, J.D., Chen, X., 2015. Release of calcium from endolysosomes increases calcium influx through N-type calcium channels: Evidence for acidic store-operated calcium entry in neurons. Cell Calcium 58, 617–27.

Huse, J.T., Pijak, D.S., Leslie, G.J., Lee, V.M.-Y., Doms, R.W., 2000. Maturation and Endosomal Targeting of -Site Amyloid Precursor Protein-cleaving Enzyme: THE ALZHEIMER'S DISEASE -SECRETASE. J. Biol. Chem. 275, 33729–33737.

Hussain, A.M.M., Lee, H.C., Chang, C.F., 1998. Functional Expression of Secreted Mouse BST-1 in Yeast. Protein Expr. Purif. 12, 133–137.

Hyman, B.T., Kromer, L.J., Van Hoesen, G.W., 1988. A direct demonstration of the perforant pathway terminal zone in Alzheimer's disease using the monoclonal antibody Alz-50. Brain Res. 450, 392–7.

Hyman, B.T., Trojanowski, J.Q., 1997. Consensus recommendations for the postmortem diagnosis of Alzheimer disease from the National Institute on Aging and the Reagan Institute Working Group on diagnostic criteria for the neuropathological assessment of Alzheimer disease. J. Neuropathol. Exp. Neurol. 56, 1095–7.

Hyman, B.T., Van Hoesen, G.W., Kromer, L.J., Damasio, A.R., 1986. Perforant pathway changes and the memory impairment of Alzheimer's disease. Ann. Neurol. 20, 472–481.

Ichise, T., Kano, M., Hashimoto, K., Yanagihara, D., Nakao, K., Shigemoto, R., Katsuki, M., Aiba, A., 2000. mGluR1 in cerebellar Purkinje cells essential for long-term depression, synapse elimination, and motor coordination. Science 288, 1832–5.

Igelhorst, B.A., Niederkinkhaus, V., Karus, C., Lange, M.D., Dietzel, I.D., 2015. Regulation of neuronal excitability by release of proteins from glial cells. Philos. Trans. R. Soc. Lond. B. Biol. Sci. 370.

Ignatius, M.J., Gebicke-Härter, P.J., Skene, J.H., Schilling, J.W., Weisgraber, K.H., Mahley, R.W., Shooter, E.M., 1986. Expression of apolipoprotein E during nerve degeneration and regeneration. Proc. Natl. Acad. Sci. U. S. A. 83, 1125–9.

Ikeda, S.R., Lovinger, D.M., McCool, B.A., Lewis, D.L., 1995. Heterologous expression of metabotropic glutamate receptors in adult rat sympathetic neurons: subtype-specific coupling to ion channels. Neuron 14, 1029–38.

Imai, S.-I., Guarente, L., 2014. NAD+ and sirtuins in aging and disease. Trends Cell Biol. 24.

Inoue, S., 2008. *In situ* A **beta** pores in AD brain are cylindrical assembly of A **beta** protofilaments. Amyloid 15, 223–233.

Iqbal, K., Grundke-Iqbal, I., Zaidi, T., Merz, P.A., Wen, G.Y., Shaikh, S.S., Wisniewski, H.M., Alafuzoff, I., Winblad, B., 1986. Defective brain microtubule assembly in Alzheimer's disease. Lancet (London, England) 2, 421–6.

Iqbal, K., Liu, F., Gong, C.X., Grundke-Iqbal, I., 2010. Tau in Alzheimer disease and related tauopathies. Curr. Alzheimer Res. 7.

Ireland, D.R., Abraham, W.C., Group, I., 2002. mGluRs increase excitability of hippocampal CA1 pyramidal neurons by a PLC-independent mechanism. J. Neurophysiol. 88, 107–116.

Ireland, D.R., Guevremont, D., Williams, J.M., Abraham, W.C., 2004. Metabotropic glutamate receptor-mediated depression of the slow afterhyperpolarization is gated by tyrosine phosphatases in hippocampal CA1 pyramidal neurons. J. Neurophysiol. 92, 2811–2819.

Iritani, S., Niizato, K., Emson, P.C., 2001. Relationship of calbindin D28K-immunoreactive cells and neuropathological changes in the

hippocampal formation of Alzheimer's disease. Neuropathology 21, 162–7.

Irving, A.J., Collingridge, G.L., 1998. A characterization of muscarinic receptor-mediated intracellular Ca2+ mobilization in cultured rat hippocampal neurones. J. Physiol. 511 (Pt 3), 747–59.

Irving, A.J., Collingridge, G.L., Schofield, J.G., 1992. Interactions between Ca2+ mobilizing mechanisms in cultured rat cerebellar granule cells. J. Physiol. 456, 667–680.

Irving, A.J., Coutts, A.A., Harvey, J., Rae, M.G., Mackie, K., Bewick, G.S., Pertwee, R.G., 2000. Functional expression of cell surface cannabinoid CB1 receptors on presynaptic inhibitory terminals in cultured rat hippocampal neurons. Neuroscience 98, 253–62.

Ishihara, K., Hirano, T., 2000. BST-1/CD157 Regulates the Humoral Immune Responses in vivo. In: Human CD38 and Related Molecules. KARGER, Basel, pp. 235–255.

Ishii, K., Katayama, M., Hori, K., Yodoi, J., Nakanishi, T., 1993. Effects of 2-mercaptoethanol on survival and differentiation of fetal mouse brain neurons cultured in vitro. Neurosci. Lett. 163, 159–62.

Ito, E., Oka, K., Etcheberrigaray, R., Nelson, T.J., McPhie, D.L., Tofel-Grehl, B., Gibson, G.E., Alkon, D.L., 1994. Internal Ca2+ mobilization is altered in fibroblasts from patients with Alzheimer disease. Proc. Natl. Acad. Sci. U. S. A. 91, 534–8.

Itoh, M., Ishihara, K., Tomizawa, H., Tanaka, H., Kobune, Y., Ishikawa, J., Kaisho, T., Hirano, T., 1994. Molecular cloning of murine BST-1 having homology with CD38 and Aplysia ADP-ribosyl cyclase. Biochem. Biophys. Res. Commun. 203, 1309–17.

Ittner, L.M., Ke, Y.D., Delerue, F., Bi, M., Gladbach, A., van Eersel, J., Wölfing, H., Chieng, B.C., Christie, M.J., Napier, I.A., Eckert, A., Staufenbiel, M., Hardeman, E., Götz, J., 2010. Dendritic function of tau mediates amyloid-β toxicity in alzheimer's disease mouse models. Cell 142.

Ivanova, H., Vervliet, T., Missiaen, L., Parys, J.B., De Smedt, H., Bultynck, G., 2014. Inositol 1,4,5-trisphosphate receptor-isoform diversity in cell death and survival. Biochim. Biophys. Acta - Mol. Cell Res. 1843, 2164–83.

Ivenshitz, M., Segal, M., 2010. Neuronal density determines network connectivity and spontaneous activity in cultured hippocampus. J. Neurophysiol. 104.

Iwatsubo, T., Odaka, A., Suzuki, N., Mizusawa, H., Nukina, N., Ihara, Y., 1994. Visualization of A beta 42(43) and A beta 40 in senile plaques with end-specific A beta monoclonals: evidence that an initially deposited species is A beta 42(43). Neuron 13, 45–53.

Jack, C.R., Knopman, D.S., Jagust, W.J., Shaw, L.M., Aisen, P.S., Weiner, M.W., Petersen, R.C., Trojanowski, J.Q., 2010. Hypothetical model of dynamic biomarkers of the Alzheimer's pathological cascade. Lancet Neurol. 9, 119–128.

Jacobsen, J.S., Wu, C.-C., Redwine, J.M., Comery, T.A., Arias, R., Bowlby, M., Martone, R., Morrison, J.H., Pangalos, M.N., Reinhart, P.H., Bloom, F.E., 2006. Early-onset behavioral and synaptic deficits in a mouse model of Alzheimer's disease. Proc. Natl. Acad. Sci. U. S. A. 103, 5161–6.

Jacobson, C., Schnapp, B., Banker, G.A., 2006. A Change in the Selective Translocation of the Kinesin-1 Motor Domain Marks the Initial Specification of the Axon. Neuron 49, 797–804.

Jaffe, D.B., Brown, T.H., 1997. Calcium dynamics in thorny excrescences of CA3 pyramidal neurons. J. Neurophysiol. 78, 10–18.

Jan, C.R., Ho, C.M., Wu, S.N., Tseng, C.J., 1998. The phospholipase C inhibitor U73122 increases cytosolic calcium in MDCK cells by activating calcium influx and releasing stored calcium. Life Sci. 63, 895–908.

Jang, H., Arce, F.T., Ramachandran, S., Capone, R., Azimova, R., Kagan, B.L., Nussinov, R., Lal, R., 2010. Truncated beta-amyloid peptide channels provide an alternative mechanism for Alzheimer's Disease and Down syndrome. Proc. Natl. Acad. Sci. U. S. A. 107, 6538–43.

Jang, S.-S., Chung, H.J., 2016. Emerging Link between Alzheimer's Disease and Homeostatic Synaptic Plasticity. Neural Plast. 2016, 1–19.

Jarrard, L.E., 1993. On the role of the hippocampus in learning and memory in the rat. Behav. Neural Biol. 60, 9–26.

Jarrett, J.T., Berger, E.P., Lansbury, P.T., 1993. The carboxy terminus of the beta amyloid protein is critical for the seeding of amyloid formation: implications for the pathogenesis of Alzheimer's disease. Biochemistry 32, 4693–7.

Jayaraman, T., Ondriasová, E., Ondrias, K., Harnick, D.J., Marks, A.R., 1995. The inositol 1,4,5-trisphosphate receptor is essential for T-cell receptor signaling. Proc. Natl. Acad. Sci. U. S. A. 92, 6007–11.

Jefferson, T., Causevic, M., auf dem Keller, U., Schilling, O., Isbert, S., Geyer, R., Maier, W., Tschickardt, S., Jumpertz, T., Weggen, S., Bond, J.S., Overall, C.M., Pietrzik, C.U., Becker-Pauly, C., 2011. Metalloprotease Meprin Generates Nontoxic N-terminal Amyloid Precursor Protein Fragments in Vivo. J. Biol. Chem. 286, 27741–27750.

Jensen, V.S., Porsgaard, T., Lykkesfeldt, J., Hvid, H., 2016. Rodent model choice has major impact on variability of standard preclinical readouts associated with diabetes and obesity research. Am. J. Transl. Res. 8, 3574–84.

Jia, Z., Lu, Y., Henderson, J., Taverna, F., Romano, C., Abramow-Newerly, W., Wojtowicz, J.M., Roder, J., 1998. Selective abolition of the NMDA component of long-term potentiation in mice lacking mGluR5. Learn. Mem. 5, 331–43.

Jianfeng Xu, #, Zhenjun Yang, #, Werner Dammermann, †, Liangren Zhang, *,#, Andreas H. Guse, † and, Li-he Zhang*, #, 2006. Synthesis and Agonist Activity of Cyclic ADP-Ribose Analogues with Substitution of the Northern Ribose by Ether or Alkane Chains.

Jiang, D., Xiao, B., Yang, D., Wang, R., Choi, P., Zhang, L., Cheng, H., Chen, S.R.W., 2004. RyR2 mutations linked to ventricular tachycardia and sudden death reduce the threshold for store-overload-induced Ca2+ release (SOICR). Proc. Natl. Acad. Sci. 101, 13062–13067.

Jiang, Q., Lee, C.Y.D., Mandrekar, S., Wilkinson, B., Cramer, P., Zelcer, N., Mann, K., Lamb, B., Willson, T.M., Collins, J.L., Richardson, J.C., Smith, J.D., Comery, T.A., Riddell, D., Holtzman, D.M., Tontonoz, P., Landreth, G.E., 2008. ApoE Promotes the Proteolytic Degradation of A? Neuron 58, 681–693.

Jiang, S., Li, Y., Zhang, X., Bu, G., Xu, H., Zhang, Y., 2014. Trafficking regulation of proteins in Alzheimer's disease. Mol. Neurodegener. 9, 6.

Jin, D., Liu, H.-X., Hirai, H., Torashima, T., Nagai, T., Lopatina, O., Shnayder, N.A., Yamada, K., Noda, M., Seike, T., Fujita, K., Takasawa, S., Yokoyama, S., Koizumi, K., Shiraishi, Y., Tanaka, S., Hashii, M., Yoshihara, T., Higashida, K., Islam, M.S., Yamada, N., Hayashi, K., Noguchi, N., Kato, I., Okamoto, H., Matsushima, A., Salmina, A., Munesue, T., Shimizu, N., Mochida, S., Asano, M., Higashida, H., 2007. CD38 is critical for social behaviour by regulating oxytocin secretion. Nature 446, 41–45.

Jin, W., Lo, T.-M., Loh, H.H., Thayer, S.A., 1994. U73122 inhibits phospholipase C-dependent calcium mobilization in neuronal cells. Brain Res. 642, 237–243.

Joensuu, H., Pylkkänen, L., Toikkanen, S., 1994. Bcl-2 protein expression and long-term survival in breast cancer. Am. J. Pathol. 145, 1191–8.

Johnson, M.W., Chotiner, J.K., Watson, J.B., 1997. Isolation and characterization of synaptoneurosomes from single rat hippocampal slices. J. Neurosci. Methods 77, 151–6.

Johnston, J.M., Burnett, P., Thomas, A.P., Tezapsidis, N., 2006. Calcium oscillations in type-1 astrocytes, the effect of a presenilin 1 (PS1) mutation. Neurosci. Lett. 395.

Jonsson, T., Atwal, J.K., Steinberg, S., Snaedal, J., Jonsson, P.V., Bjornsson, S., Stefansson, H., Sulem, P., Gudbjartsson, D., Maloney, J., Hoyte,

K., Gustafson, A., Liu, Y., Lu, Y., Bhangale, T., Graham, R.R., Huttenlocher, J., Bjornsdottir, G., Andreassen, O.A., Jonsson, E.G., Palotie, A., Behrens, T.W., Magnusson, O.T., Kong, A., Thorsteinsdottir, U., Watts, R.J., Stefansson, K., 2012. A mutation in APP protects against Alzheimer's disease and age-related cognitive decline. Nature 488.

Kaar, A., Morley, S.J., Rae, M.G., 2017. An efficient and cost-effective method of generating postnatal (P2–5) mouse primary hippocampal neuronal cultures. J. Neurosci. Methods 286, 69–77.

Kaar, A., Rae, M.G., 2013. Proceedings of the 8th Neuroscience Ireland Conference; September 12-13; Cork, Ireland. Neuroscience Ireland.

Kaar, A., Rae, M.G., 2014. Investigating the role of the cyclic ADP ribose/RyR pathway in Group I mGluR mediated calcium signalling in cultured rat hippocampal neurones. F1000Research 5, 26625.

Kaar, A., Rae, M.G., 2016. Proceedings of the RAMI Section of Biomedical Sciences Annual Meetings, 2013- 2015, Irish Journal of Medical Science. Springer London.

Kaar, A., Rae, M.G.M.G., 2015. Metabotropic glutamate receptor-mediated cyclic ADP ribose signalling. Biochem. Soc. Trans. 43, 405–409.

Kaech, S., Banker, G., 2006. Culturing hippocampal neurons. Nat. Protoc. 1, 2406–2415.

Kajimoto, Y., Miyagawa, J., Ishihara, K., Okuyama, Y., Fujitani, Y., Itoh, M., Yoshida, H., Kaisho, T., Matsuoka, T., Watada, H., Hanafusa, T., Yamasaki, Y., Kamada, T., Matsuzawa, Y., Hirano, T., 1996. Pancreatic Islet Cells Express BST-1, a CD38-like Surface Molecule Having ADP-Ribosyl Cyclase Activity. Biochem. Biophys. Res. Commun. 219, 941–946.

Kakizawa, S., Takeshima, H., Iino, M., 2012. Nitric Oxide-Induced Calcium Release: A Novel Calcium-Mobilizing Mechanism Mediated by S-nitrosylation-Dependent Modulation of Ryanodine Receptor. Messenger 1, 133–140.

Kamatsuka, Y., Fukagawa, M., Furuta, T., Ohishi, A., Nishida, K., Nagasawa, K., 2014. Astrocytes, but not neurons, exhibit constitutive activation of P2X7 receptors in mouse acute cortical slices under non-stimulated resting conditions. Biol. Pharm. Bull. 37, 1958–62.

Kamboh, M.I., 2004. Molecular Genetics of Late-Onset Alzheimer's Disease. Ann. Hum. Genet. 68, 381–404.

Kammermeier, P.J., Ikeda, S.R., 1999. Expression of RGS2 Alters the Coupling of Metabotropic Glutamate Receptor 1a to M-Type K+ and N-Type Ca2+ Channels. Neuron 22, 819–829.

Kanatsu, K., Morohashi, Y., Suzuki, M., Kuroda, H., Watanabe, T., Tomita, T., Iwatsubo, T., 2014. Decreased CALM expression reduces Aβ42 to total Aβ ratio through clathrin-mediated endocytosis of γ-secretase. Nat. Commun. 5, 3386.

Kaneko, A., Sankai, Y., 2014. Long-Term Culture of Rat Hippocampal Neurons at Low Density in Serum-Free Medium: Combination of the Sandwich Culture Technique with the Three-Dimensional Nanofibrous Hydrogel PuraMatrix. PLoS One 9, e102703.

Kano, M., Garaschuk, O., Verkhratsky, A., Konnerth, A., 1995. Ryanodine receptor-mediated intracellular calcium release in rat cerebellar Purkinje neurones. J. Physiol.

Karlnoski, R., Wilcock, D., Dickey, C., Ronan, V., Gordon, M.N., Zhang, W., Morgan, D., Taglialatela, G., 2007. Up-regulation of Bcl-2 in APP transgenic mice is associated with neuroprotection. Neurobiol. Dis. 25, 179–188.

Karran, E., Mercken, M., Strooper, B. De, 2011. The amyloid cascade hypothesis for Alzheimer's disease: an appraisal for the development of therapeutics. Nat. Rev. Drug Discov. 10, 698–712.

Kass, G.E., Orrenius, S., 1999. Calcium signaling and cytotoxicity. Environ. Health Perspect. 107 Suppl 1, 25–35.

Kassner, S.S., Bonaterra, G.A., Kaiser, E., Hildebrandt, W., Metz, J., Schröder, J., Kinscherf, R., 2008. Novel systemic markers for patients with Alzheimer disease? - a pilot study. Curr. Alzheimer Res. 5, 358–66.

Kaufmann, J.A., Bickford, P.C., Taglialatela, G., 2001. Oxidative-stress-dependent up-regulation of Bcl-2 expression in the central nervous system of aged Fisher-344 rats. J. Neurochem. 76, 1099–108.

Kazim, S.F., Chuang, S.-C., Zhao, W., Wong, R.K.S., Bianchi, R., Iqbal, K., 2017. Early-Onset Network Hyperexcitability in Presymptomatic Alzheimer's Disease Transgenic Mice Is Suppressed by Passive Immunization with Anti-Human APP/Aβ Antibody and by mGluR5 Blockade. Front. Aging Neurosci. 9, 71.

Keele, N.B., Arvanov, V.L., Shinnick-Gallagher, P., 1997. Quisqualate-preferring metabotropic glutamate receptor activates Na(+)-Ca2+ exchange in rat basolateral amygdala neurones. J. Physiol. 499 (Pt 1), 87–104.

Kellenberger, E., Kuhn, I., Schuber, F., Muller-Steffner, H., 2011. Flavonoids as inhibitors of human CD38, Bioorganic & Medicinal Chemistry Letters.

Keller, J.N., Germeyer, A., Begley, J.G., Mattson, M.P., 1997. 17β-Estradiol attenuates oxidative impairment of synaptic Na+/K+- ATPase activity, glucose transport, and glutamate transport induced by amyloid β-peptide and iron. J. Neurosci. Res. 50.

Kelliher, M., Fastbom, J., Cowburn, R.F., Bonkale, W., Ohm, T.G., Ravid, R., Sorrentino, V., O'Neill, C., 1999. Alterations in the ryanodine receptor calcium release channel correlate with Alzheimer's disease neurofibrillary and beta-amyloid pathologies. Neuroscience 92, 499–513.

Kelly, B.L., Ferreira, A., 2006. beta-Amyloid-induced Dynamin 1 Degradation Is Mediated by N-Methyl-D-Aspartate Receptors in Hippocampal Neurons. J. Biol. Chem. 281, 28079–28089.

Kessete Afewerky, H., 2016. Roles of Sodium-Calcium Exchanger Isoform-3 toward Calcium Ion Regulation in Alzheimers Disease.

Kettunen, P., Hess, D., El Manira, A., 2003. mGluR1, But Not mGluR5, Mediates Depolarization of Spinal Cord Neurons by Blocking a Leak Current. J. Neurophysiol. 90, 2341–2348.

Khachaturian, Z.S., 1989. Calcium, membranes, aging, and Alzheimer's disease. Introduction and overview. Ann. N. Y. Acad. Sci. 568, 1–4.

Khatoon, S., Grundke-Iqbal, I., Iqbal, K., 1992. Brain levels of microtubule-associated protein tau are elevated in Alzheimer's disease: a radioimmuno-slot-blot assay for nanograms of the protein. J. Neurochem. 59, 750–3.

Khoo, K.M., Chang, C.F., 1999. Characterization and localization of CD38 in the vertebrate eye. Brain Res. 821, 17–25.

Khoo, K.M., Chang, C.F., 2002. Identification and characterization of nuclear CD38 in the rat spleen. Int. J. Biochem. Cell Biol. 34, 43–54.

Khoo, K.M., Han, M.K., Park, J.B., Chae, S.W., Kim, U.H., Lee, H.C., Bay, B.H., Chang, C.F., 2000. Localization of the cyclic ADP-ribose-dependent calcium signaling pathway in hepatocyte nucleus. J. Biol. Chem. 275, 24807–24817.

Khosravani, H., Zhang, Y., Tsutsui, S., Hameed, S., Altier, C., Hamid, J., Chen, L., Villemaire, M., Ali, Z., Jirik, F.R., Zamponi, G.W., 2008. Prion protein attenuates excitotoxicity by inhibiting NMDA receptors. J. Cell Biol. 181, 551–565.

Kim, B.-J., Park, K.-H., Yim, C.-Y., Takasawa, S., Okamoto, H., Im, M.-J., Kim, U.-H., 2008. Generation of Nicotinic Acid Adenine Dinucleotide Phosphate and Cyclic ADP-Ribose by Glucagon-Like Peptide-1 Evokes Ca2+ Signal That Is Essential for Insulin Secretion in Mouse Pancreatic Islets. Diabetes 57, 868–878.

Kim, I., Xu, W., Reed, J.C., 2008. Cell death and endoplasmic reticulum stress: disease relevance and therapeutic opportunities. Nat. Rev. Drug Discov. 7, 1013–1030.

Kim, J., Basak, J.M., Holtzman, D.M., 2009a. The role of apolipoprotein E in Alzheimer's disease. Neuron 63, 287–303.

Kim, J., Castellano, J.M., Jiang, H., Basak, J.M., Parsadanian, M., Pham, V., Mason, S.M., Paul, S.M., Holtzman, D.M., 2009b. Overexpression of Low-Density Lipoprotein Receptor in the Brain Markedly Inhibits Amyloid Deposition and Increases Extracellular A? Clearance. Neuron 64, 632–644.

Kim, J., Onstead, L., Randle, S., Price, R., Smithson, L., Zwizinski, C., Dickson, D.W., Golde, T., McGowan, E., 2007. Aβ40 Inhibits Amyloid Deposition In Vivo. J. Neurosci. 27.

Kim, S., Yun, H.-M., Baik, J.-H., Chung, K.C., Nah, S.-Y., Rhim, H., 2007. Functional interaction of neuronal Cav1.3 L-type calcium channel with ryanodine receptor type 2 in the rat hippocampus. J. Biol. Chem. 282, 32877–89.

Kim, S.H., Fraser, P.E., Westaway, D., St. George-Hyslop, P.H., Ehrlich, M.E., Gandy, S., 2010. Group II Metabotropic Glutamate Receptor Stimulation Triggers Production and Release of Alzheimer's Amyloid 42 from Isolated Intact Nerve Terminals. J. Neurosci. 30, 3870–3875.

Kim, S.J., Kim, Y.S., Yuan, J.P., Petralia, R.S., Worley, P.F., Linden, D.J., 2003. Activation of the TRPC1 cation channel by metabotropic glutamate receptor mGluR1. Nature 426, 285–291.

Kim, S.S.J.S.S.J.S., Kim, T., Lee, H.-R., Jang, E.-H., Ryu, H.-H., Kang, M., Rah, S.-Y., Yoo, J., Lee, B., Kim, J.-I., Lim, C.S., Kim, S.S.J.S.S.J.S., Kim, U.-H., Lee, Y.-S., Kaang, B.-K., 2016. Impaired learning and memory in CD38 null mutant mice. Mol. Brain 9, 16.

Kimberly, W.T., LaVoie, M.J., Ostaszewski, B.L., Ye, W., Wolfe, M.S., Selkoe, D.J., 2003. -Secretase is a membrane protein complex comprised of presenilin, nicastrin, aph-1, and pen-2. Proc. Natl. Acad. Sci. 100, 6382–6387.

Kinnear, N.P., Boittin, F.-X., Thomas, J.M., Galione, A., Evans, A.M., 2004. Lysosome-sarcoplasmic reticulum junctions. A trigger zone for calcium signaling by nicotinic acid adenine dinucleotide phosphate and endothelin-1. J. Biol. Chem. 279, 54319–26.

Kirazov, L., Löffler, T., Schliebs, R., Bigl, V., 1997. Glutamate-stimulated secretion of amyloid precursor protein from cortical rat brain slices. Neurochem. Int. 30, 557–63.

Kitamura, Y., Shimohama, S., Kamoshima, W., Ota, T., Matsuoka, Y., Nomura, Y., Smith, M.A., Perry, G., Whitehouse, P.J., Taniguchi, T., 1998. Alteration of proteins regulating apoptosis, Bcl-2, Bcl-x, Bax, Bak, Bad, ICH-1 and CPP32, in Alzheimer's disease. Brain Res. 780, 260–9.

Kivell, B.M., McDonald, F.J., Miller, J.H., 2000. Serum-free culture of rat post-natal and fetal brainstem neurons. Dev. Brain Res. 120, 199–210.

Kiviluoto, S., Vervliet, T., Ivanova, H., Decuypere, J.-P., De Smedt, H., Missiaen, L., Bultynck, G., Parys, J.B., 2013. Regulation of inositol 1,4,5-trisphosphate receptors during endoplasmic reticulum stress. Biochim. Biophys. Acta - Mol. Cell Res. 1833, 1612–1624.

Klein, R.R., Bourdon, D.M., Costales, C.L., Wagner, C.D., White, W.L., Williams, J.D., Hicks, S.N., Sondek, J., Thakker, D.R., 2011. Direct activation of human phospholipase C by its well known inhibitor u73122. J. Biol. Chem. 286, 12407–16.

Kloosterman, F., van Haeften, T., Lopes da Silva, F.H., 2004. Two reentrant pathways in the hippocampal-entorhinal system. Hippocampus 14, 1026–39.

Kloosterman, F., Van Haeften, T., Witter, M.P., Lopes Da Silva, F.H., 2003. Electrophysiological characterization of interlaminar entorhinal connections: an essential link for re-entrance in the hippocampal-entorhinal system. Eur. J. Neurosci. 18, 3037–52.

Koester, H.J., Sakmann, B., 1998. Calcium dynamics in single spines during coincident pre- and postsynaptic activity depend on relative timing of back-propagating action potentials and subthreshold excitatory postsynaptic potentials. Proc. Natl. Acad. Sci. U. S. A. 95, 9596–601.

Koffie, R.M., Hyman, B.T., Spires-Jones, T.L., 2011. Alzheimer's disease: synapses gone cold. Mol. Neurodegener. 6, 63.

Koffie, R.M., Meyer-Luehmann, M., Hashimoto, T., Adams, K.W., Mielke, M.L., Garcia-Alloza, M., Micheva, K.D., Smith, S.J., Kim, M.L., Lee, V.M., Hyman, B.T., Spires-Jones, T.L., 2009. Oligomeric amyloid β associates with postsynaptic densities and correlates with excitatory synapse loss near senile plaques. Proc. Natl. Acad. Sci. U. S. A. 106.

Koistinaho, M., Lin, S., Wu, X., Esterman, M., Koger, D., Hanson, J., Higgs, R., Liu, F., Malkani, S., Bales, K.R., Paul, S.M., 2004. Apolipoprotein E promotes astrocyte colocalization and degradation of deposited amyloid-? peptides. Nat. Med. 10, 719–726.

Koistinaho, M., Ort, M., Cimadevilla, J.M., Vondrous, R., Cordell, B., Koistinaho, J., Bures, J., Higgins, L.S., 2001. Specific spatial learning deficits become severe with age in beta -amyloid precursor protein transgenic mice that harbor diffuse beta -amyloid deposits but do not form plaques. Proc. Natl. Acad. Sci. U. S. A. 98, 14675–80.

Koizumi, S., Bootman, M.D., Bobanović, L.K., Schell, M.J., Berridge, M.J., Lipp, P., 1999. Characterization of elementary Ca2+ release signals in NGF-differentiated PC12 cells and hippocampal neurons. Neuron 22, 125–37.

Kong, H., Jones, P.P., Koop, A., Zhang, L., Duff, H.J., Chen, S.R.W., 2008. Caffeine induces Ca2+ release by reducing the threshold for luminal Ca2+ activation of the ryanodine receptor. Biochem. J. 414, 441–52.

König, A., Menzel, T., Lynen, S., Wrazel, L., Rosén, A., Al-Katib, A., Raveche, E., Gabrilove, J.L., 1997. Basic fibroblast growth factor (bFGF) upregulates the expression of bcl-2 in B cell chronic lymphocytic leukemia cell lines resulting in delaying apoptosis. Leukemia 11, 258–65.

Koo, E.H., Kopan, R., 2004. Potential role of presenilin-regulated signaling pathways in sporadic neurodegeneration. Nat. Med. 10.

Kos, C.H., Karaplis, A.C., Peng, J.-B., Hediger, M.A., Goltzman, D., Mohammad, K.S., Guise, T.A., Pollak, M.R., 2003. The calcium-sensing receptor is required for normal calcium homeostasis independent of parathyroid hormone. J. Clin. Invest. 111, 1021–1028.

Kotler, S.A., Walsh, P., Brender, J.R., Ramamoorthy, A., 2014. Differences between amyloid-β aggregation in solution and on the membrane: insights into elucidation of the mechanistic details of Alzheimer's disease. Chem. Soc. Rev. 43, 6692–6700.

Kovacs, D.M., Fausett, H.J., Page, K.J., Kim, T.W., Moir, R.D., Merriam, D.E., Hollister, R.D., Hallmark, O.G., Mancini, R., Felsenstein, K.M., Hyman, B.T., Tanzi, R.E., Wasco, W., 1996. Alzheimer-associated presenilins 1 and 2: neuronal expression in brain and localization to intracellular membranes in mammalian cells. Nat. Med. 2, 224–9.

Kovalchuk, Y., Eilers, J., Lisman, J., Konnerth, A., 2000. NMDA receptor-mediated subthreshold Ca(2+) signals in spines of hippocampal neurons. J. Neurosci. 20, 1791–9.

Kraft, R., Grimm, C., Grosse, K., Hoffmann, A., Sauerbruch, S., Kettenmann, H., Schultz, G., Harteneck, C., 2003. Hydrogen peroxide and ADP-ribose induce TRPM2-mediated calcium influx and cation currents in microglia. Am. J. Physiol. - Cell Physiol. 286.

Krajewska, M., Mai, J.K., Zapata, J.M., Ashwell, K.W., Schendel, S.L., Reed, J.C., Krajewski, S., 2002. Dynamics of expression of apoptosis-regulatory proteins Bid, Bcl-2, Bcl-X, Bax and Bak during development of murine nervous system. Cell Death Differ. 9, 145–157.

Krajewski, S., Krajewska, M., Shabaik, A., Wang, H.G., Irie, S., Fong, L., Reed, J.C., 1994. Immunohistochemical analysis of in vivo patterns of Bcl-X expression. Cancer Res. 54, 5501–7.

Krajewski, S., Tanaka, S., Takayama, S., Schibler, M.J., Fenton, W., Reed, J.C., 1993. Investigation of the subcellular distribution of the bcl-2 oncoprotein: residence in the nuclear envelope, endoplasmic reticulum, and outer mitochondrial membranes. Cancer Res. 53, 4701–14.

Krause, M., Offermanns, S., Stocker, M., Pedarzani, P., 2002. Functional specificity of G alpha q and G alpha 11 in the cholinergic and

glutamatergic modulation of potassium currents and excitability in hippocampal neurons. J. Neurosci. 22, 666–73.

Krause, T., Gerbershagen, M.U., Fiege, M., Weisshorn, R., Wappler, F., 2004. Dantrolene--a review of its pharmacology, therapeutic use and new developments. Anaesthesia 59, 364–73.

Krieger, P., Hellgren-Kotaleski, J., Kettunen, P., El Manira, A.J., 2000. Interaction between metabotropic and ionotropic glutamate receptors regulates neuronal network activity. J. Neurosci. 20, 5382–91.

Kristian, T., Balan, I., Schuh, R., Onken, M., 2011. Mitochondrial dysfunction and nicotinamide dinucleotide catabolism as mechanisms of cell death and promising targets for neuroprotection. J. Neurosci. Res. 89, 1946–1955.

Kubo, Y., Miyashita, T., Murata, Y., 1998. Structural basis for a Ca2+-sensing function of the metabotropic glutamate receptors. Science 279, 1722–5.

Kubokawa, K., Miyashita, T., Nagasawa, H., Kubo, Y., 1996. Cloning and characterization of a bifunctional metabotropic receptor activated by both extracellular calcium and glutamate. FEBS Lett. 392, 71–76.

Kuchibhotla, K. V, Goldman, S.T., Lattarulo, C.R., Wu, H.-Y., Hyman, B.T., Bacskai, B.J., 2008. Abeta plaques lead to aberrant regulation of calcium homeostasis in vivo resulting in structural and functional disruption of neuronal networks. Neuron 59, 214–25.

Kudo, W., Lee, H.-P., Zou, W.-Q., Wang, X., Perry, G., Zhu, X., Smith, M.A., Petersen, R.B., Lee, H. -g., 2012. Cellular prion protein is essential for oligomeric amyloid- -induced neuronal cell death. Hum. Mol. Genet. 21, 1138–1144.

Kullmann, D.M., Lamsa, K., 2008. Roles of distinct glutamate receptors in induction of anti-Hebbian long-term potentiation. J. Physiol. 586, 1481–1486.

Kumar, A., 2011. Long-Term Potentiation at CA3-CA1 Hippocampal Synapses with Special Emphasis on Aging, Disease, and Stress. Front. Aging Neurosci. 3, 7.

Kunerth, S., Langhorst, M.F., Schwarzmann, N., Gu, X., Huang, L., Yang, Z., Zhang, L., Mills, S.J., Zhang, L.-H., Potter, B.V.L., Guse, A.H., 2004. Amplification and propagation of pacemaker Ca2+ signals by cyclic ADP-ribose and the type 3 ryanodine receptor in T cells. J. Cell Sci. 117, 2141–9.

Kurumatani, T., Fastbom, J., Bonkale, W.L., Bogdanovic, N., Winblad, B., Ohm, T.G., Cowburn, R.F., 1998. Loss of inositol 1,4,5-trisphosphate receptor sites and decreased PKC levels correlate with staging of Alzheimer's disease neurofibrillary pathology. Brain Res. 796, 209–21.

Kuwajima, G., Futatsugi, A., Niinobe, M., Nakanishi, S., Mikoshiba, K., 1992. Two types of ryanodine receptors in mouse brain: Skeletal muscle type exclusively in Purkinje cells and cardiac muscle type in various neurons. Neuron 9, 1133–1142.

Kvansakul, M., Yang, H., Fairlie, W.D., Czabotar, P.E., Fischer, S.F., Perugini, M.A., Huang, D.C.S., Colman, P.M., 2008. Vaccinia virus anti-apoptotic F1L is a novel Bcl-2-like domain-swapped dimer that binds a highly selective subset of BH3-containing death ligands. Cell Death Differ. 15, 1564–1571.

Lacor, Buniel, M.C., Chang, L., Fernandez, S.J., Gong, Y., Viola, K.L., Lambert, M.P., Velasco, P.T., Bigio, E.H., Finch, C.E., Krafft, G.A., Klein, W.L., 2004a. Synaptic targeting by Alzheimer's-related amyloid β oligomers. J. Neurosci. 24.

Lacor, Buniel, M.C., Chang, L., Fernandez, S.J., Gong, Y., Viola, K.L., Lambert, M.P., Velasco, P.T., Bigio, E.H., Finch, C.E., Krafft, G.A., Klein, W.L., 2004b. Synaptic Targeting by Alzheimer's-Related Amyloid Oligomers. J. Neurosci. 24, 10191–10200.

Lacor, Buniel, M.C., Furlow, P.W., Clemente, A.S., Velasco, P.T., Wood, M., Viola, K.L., Klein, W.L., 2007. Aβ oligomer-induced aberrations in synapse composition, shape, and density provide a molecular basis for loss of connectivity in Alzheimer's disease. J. Neurosci. 27.

LaDu, M.J., Falduto, M.T., Manelli, A.M., Reardon, C.A., Getz, G.S., Frail, D.E., 1994. Isoform-specific binding of apolipoprotein E to beta-amyloid. J. Biol. Chem. 269, 23403–6.

LaFerla, F.M., 2002. Calcium dyshomeostasis and intracellular signalling in alzheimer's disease. Nat. Rev. Neurosci. 3, 862–872.

LaFerla, F.M., Oddo, S., 2005. Alzheimer's disease: Aβ, tau and synaptic dysfunction. Trends Mol. Med. 11, 170–176.

Lam, M., Dubyakt, G., Chent, L., Nufiez, G., Miesfeldt, R.L., Distelhorst, C.W., 1994. Evidence that BCL-2 represses apoptosis by regulating endoplasmic reticulum-associated Ca2+ fluxes (pogammed cel death/gucocorlcosteroid/mouse lymphoma cell/calcium. Med. Sci. 91, 6569–6573.

Lambert, J.-C., Heath, S., Even, G., Campion, D., Sleegers, K., Hiltunen, M., Combarros, O., Zelenika, D., Bullido, M.J., Tavernier, B., Letenneur, L., Bettens, K., Berr, C., Pasquier, F., Fiévet, N., Barberger-Gateau, P., Engelborghs, S., De Deyn, P., Mateo, I., Franck, A., Helisalmi, S., Porcellini, E., Hanon, O., European Alzheimer's Disease Initiative Investigators, M.M., de Pancorbo, M.M., Lendon, C., Dufouil, C., Jaillard, C., Leveillard, T., Alvarez, V., Bosco, P., Mancuso, M., Panza, F., Nacmias, B., Bossù, P., Piccardi, P., Annoni, G., Seripa, D., Galimberti, D., Hannequin, D., Licastro, F., Soininen, H., Ritchie, K., Blanché, H., Dartigues, J.-F., Tzourio, C., Gut, I., Van Broeckhoven, C., Alpérovitch, A., Lathrop, M., Amouyel, P., 2009. Genome-wide association study identifies variants at CLU and CR1 associated with Alzheimer's disease. Nat. Genet. 41, 1094–9.

Lambert, J.-C., Sleegers, K., González-Pérez, A., Ingelsson, M., Beecham, G.W., Hiltunen, M., Combarros, O., Bullido, M.J., Brouwers, N., Bettens, K., Berr, C., Pasquier, F., Richard, F., DeKosky, S.T., Hannequin, D., Haines, J.L., Tognoni, G., Fiévet, N., Dartigues, J.-F., Tzourio, C., Engelborghs, S., Arosio, B., Coto, E., De Deyn, P., Del Zompo, M., Mateo, I., Boada, M., Antunez, C., Lopez-Arrieta, J., Epelbaum, J., Schjeide, B.-M.M., Frank-Garcia, A., Giedraitis, V., Helisalmi, S., Porcellini, E., Pilotto, A., Forti, P., Ferri, R., Delepine, M., Zelenika, D., Lathrop, M., Scarpini, E., Siciliano, G., Solfrizzi, V., Sorbi, S., Spalletta, G., Ravaglia, G., Valdivieso, F., Vepsäläinen, S., Alvarez, V., Bosco, P., Mancuso, M., Panza, F., Nacmias, B., Bossù, P., Hanon, O., Piccardi, P., Annoni, G., Mann, D., Marambaud, P., Seripa, D., Galimberti, D., Tanzi, R.E., Bertram, L., Lendon, C., Lannfelt, L., Licastro, F., Campion, D., Pericak-Vance, M.A., Soininen, H., Van Broeckhoven, C., Alpérovitch, A., Ruiz, A., Kamboh, M.I., Amouyel, P., 2010. The CALHM1 P86L Polymorphism is a Genetic Modifier of Age at Onset in Alzheimer's Disease: a Meta-Analysis Study. J. Alzheimer's Dis. 22, 247–255.

Lambert, M.P., Barlow, A.K., Chromy, B.A., Edwards, C., Freed, R., Liosatos, M., Morgan, T.E., Rozovsky, I., Trommer, B., Viola, K.L., Wals, P., Zhang, C., Finch, C.E., Krafft, G.A., Klein, W.L., 1998. Diffusible, nonfibrillar ligands derived from Abeta1-42 are potent central nervous system neurotoxins. Proc. Natl. Acad. Sci. U. S. A. 95, 6448–53.

Landfield, P.W., Thibault, O., Mazzanti, M.L., Porter, N.M., Kerr, D.S., 1992. Mechanisms of neuronal death in brain aging and alzheimer's disease: Role of endocrine-mediated calcium dyshomeostasis. J. Neurobiol. 23, 1247–1260.

Landis, D.M.D., Weinstein, L.A., Skordeles, C.J., 1990. Serum influences the differentiation of membrane structure in cultured astrocytes. Glia 3.

Langhorst, M.F., Schwarzmann, N., Guse, A.H., 2004. Ca2+ release via ryanodine receptors and Ca2+ entry: major mechanisms in NAADP-mediated Ca2+ signaling in T-lymphocytes. Cell. Signal. 16, 1283–1289.

Larson, J., Lynch, G., Games, D., Seubert, P., 1999. Alterations in synaptic transmission and long-term potentiation in hippocampal slices from young and aged PDAPP mice. Brain Res. 840, 23–35.

Larson, M., Sherman, M.A., Amar, F., Nuvolone, M., Schneider, J.A., Bennett, D.A., Aguzzi, A., Lesne, S.E., 2012. The Complex PrPc-Fyn Couples Human Oligomeric A with Pathological Tau Changes in Alzheimer's Disease. J. Neurosci. 32, 16857–16871.

Lasky, J.L., Wu, H., 2005. Notch Signaling, Brain Development, and Human Disease. Pediatr. Res. 57, 104R–109R.

Laßek, M., Weingarten, J., Einsfelder, U., Brendel, P., Müller, U., Volknandt, W., 2013. Amyloid precursor proteins are constituents of the presynaptic active zone. J. Neurochem. 127, n/a-n/a.

Lathia, J.D., Mattson, M.P., Cheng, A., 2008. Notch: from neural development to neurological disorders. J. Neurochem. 107, 1471–81.

Laude, A.J., Simpson, A.W.M., 2009. Compartmentalized signalling: Ca2+ compartments, microdomains and the many facets of Ca2+ signalling. FEBS J. 276, 1800–1816.

Laurén, J., 2014. Cellular Prion Protein as a Therapeutic Target in Alzheimer's Disease. J. Alzheimer's Dis. 38, 227–244.

Laurén, J., Gimbel, D.A., Nygaard, H.B., Gilbert, J.W., Strittmatter, S.M., 2009. Cellular prion protein mediates impairment of synaptic plasticity by amyloid-B oligomers. Nature 457.

Lebart, M.-C., Benyamin, Y., 2006. Calpain involvement in the remodeling of cytoskeletal anchorage complexes. FEBS J. 273.

LeBlanc, A.C., Chen, H.Y., Autilio-Gambetti, L., Gambetti, P., 1991. Differential APP gene expression in rat cerebral cortex, meninges, and primary astroglial, microglial and neuronal cultures. FEBS Lett. 292, 171–8.

LeBrun, D.P., Warnke, R.A., Cleary, M.L., 1993. Expression of bcl-2 in fetal tissues suggests a role in morphogenesis. Am. J. Pathol. 142, 743–53.

Leckie, C., Empson, R., Becchetti, A., Thomas, J., Galione, A., Whitaker, M., 2003. The NO pathway acts late during the fertilization response in sea urchin eggs. J. Biol. Chem. 278, 12247–12254.

Lee, C., Park, G.-H., Lee, J.-W., Jang, J.-H., 2015. Protective Effect of Wheat Bran Extract against β-Amyloid-induced Cell Death and Memory Impairment. Kor. J. Herbol. 30, 67–75.

Lee, G., Thangavel, R., Sharma, V.M., Litersky, J.M., Bhaskar, K., Fang, S.M., Do, L.H., Andreadis, A., Van Hoesen, G., Ksiezak-Reding, H., 2004. Phosphorylation of Tau by Fyn: Implications for Alzheimer's Disease. J. Neurosci. 24.

Lee, H.C., 1991. Specific binding of cyclic ADP-ribose to calcium-storing microsomes from sea urchin eggs. J. Biol. Chem. 266, 2276–81.

Lee, H.C., 1993. Potentiation of calcium- and caffeine-induced calcium release by cyclic ADP-ribose. J. Biol. Chem. 268, 293–9.

Lee, H.C., 2001. Physiological functions of cyclic ADP-ribose and NAADP as calcium messengers. Annu. Rev. Pharmacol. Toxicol. 41, 317–45.

Lee, H.C., 2011. Cyclic ADP-ribose and NAADP: fraternal twin messengers for calcium signaling. Sci. China Life Sci. 54, 699–711.

Lee, H.C., Aarhus, R., 1997. Structural determinants of nicotinic acid adenine dinucleotide phosphate important for its calcium-mobilizing activity. J. Biol. Chem. 272, 20378–83.

Lee, H.C., Aarhus, R., Graeff, R., Gurnack, M.E., Walseth, T.F., 1994. Cyclic ADP ribose activation of the ryanodine receptor is mediated by calmodulin. Nature 370, 307–309.

Lee, H.C., Aarhus, R., Graeff, R.M., 1995. Sensitization of calcium-induced calcium release by cyclic ADP-ribose and calmodulin. J. Biol. Chem. 270, 9060–9066.

Lee, H.C., Aarhus, R., Walseth, T.F., 1993. Calcium mobilization by dual receptors during fertilization of sea urchin eggs. Science 261, 352–5.

Lee, H.C., Munshi, C., Graeff, R., 1999. Structures and activities of cyclic ADP-ribose, NAADP and their metabolic enzymes. Mol. Cell. Biochem. 193, 89–98.

Lee, H.G., Won, S.M., Gwag, B.J., Lee, Y.B., 2011. Microglial P2X $_{7}$ receptor expression is accompanied by neuronal damage in the cerebral cortex of the APP $_{swe}$ /PS1dE9 mouse model of Alzheimer's disease. Exp. Mol. Med. 43, 7.

Lee, J.-Y., Cole, T.B., Palmiter, R.D., Suh, S.W., Koh, J.-Y., 2002. Contribution by synaptic zinc to the gender-disparate plaque formation in human Swedish mutant APP transgenic mice. Proc. Natl. Acad. Sci. 99, 7705–7710.

Leighty, R.E., Nilsson, L.N.., Potter, H., Costa, D.A., Low, M.A., Bales, K.R., Paul, S.M., Arendash, G.W., 2004. Use of multimetric statistical analysis to characterize and discriminate between the performance of four Alzheimer's transgenic mouse lines differing in Aβ deposition. Behav. Brain Res. 153, 107–121.

Leissring, M.A., Akbari, Y., Fanger, C.M., Cahalan, M.D., Mattson, M.P., LaFerla, F.M., 2000. Capacitative calcium entry deficits and elevated luminal calcium content in mutant presenilin-1 knockin mice. J. Cell Biol. 149, 793–797.

Leissring, M.A., LaFerla, F.M., Callamaras, N., Parker, I., 2001. Subcellular mechanisms of presenilin-mediated enhancement of calcium signaling. Neurobiol. Dis. 8.

Leissring, M.A., Murphy, M.P., Mead, T.R., Akbari, Y., Sugarman, M.C., Jannatipour, M., Anliker, B., Müller, U., Saftig, P., De Strooper, B., Wolfe, M.S., Golde, T.E., LaFerla, F.M., 2002. A physiologic signaling role for the gamma -secretase-derived intracellular fragment of APP. Proc. Natl. Acad. Sci. U. S. A. 99, 4697–702.

Leissring, M.A., Parker, I., LaFerla, F.M., 1999a. Presenilin-2 mutations modulate amplitude and kinetics of inositol 1, 4,5-trisphosphate-mediated calcium signals. J. Biol. Chem. 274, 32535–8.

Leissring, M.A., Paul, B.A., Parker, I., Cotman, C.W., LaFerla, F.M., 1999b. Alzheimer's presenilin-1 mutation potentiates inositol 1,4,5-trisphosphate-mediated calcium signaling in Xenopus oocytes. J. Neurochem. 72, 1061–8.

Lemonnier, L., Prevarskaya, N., Mazurier, J., Shuba, Y., Skryma, R., 2004. 2-APB inhibits volume-regulated anion channels independently from intracellular calcium signaling modulation. FEBS Lett. 556, 121–6.

Lesné, S.E., Sherman, M.A., Grant, M., Kuskowski, M., Schneider, J.A., Bennett, D.A., Ashe, K.H., 2013. Brain amyloid-β oligomers in ageing and Alzheimer's disease. Brain 136, 1383–98.

Letai, A.G., 2008. Diagnosing and exploiting cancer's addiction to blocks in apoptosis. Nat. Rev. Cancer 8, 121–132.

Leuba, G., Vernay, A., Vu, D., Walzer, C., Belloir, B., Kraftsik, R., Bouras, C., Savioz, A., 2004. Differential expression of LMO4 protein in Alzheimer's disease. Neuropathol. Appl. Neurobiol. 30, 57–69.

Levi-Montalcini, R., 1966. The nerve growth factor: its mode of action on sensory and sympathetic nerve cells. Harvey Lect. 60, 217–59.

Lewis, J., Dickson, D.W., Lin, W.L., Chisholm, L., Corral, A., Jones, G., Yen, S.H., Sahara, N., Skipper, L., Yager, D., Eckman, C., Hardy, J., Hutton, M., McGowan, E., 2001. Enhanced Neurofibrillary Degeneration in Transgenic Mice Expressing Mutant Tau and APP. Science (80-.). 293, 1487–1491.

Li, B., Chohan, M.O., Grundke-Iqbal, I., Iqbal, K., 2007. Disruption of microtubule network by Alzheimer abnormally hyperphosphorylated tau. Acta Neuropathol. 113, 501–511.

Li, C., Wang, X., Vais, H., Thompson, C.B., Foskett, J.K., White, C., 2007. Apoptosis regulation by Bcl-xL modulation of mammalian inositol 1,4,5-trisphosphate receptor channel isoform gating. Proc. Natl. Acad. Sci. 104, 12565–12570.

Li, H., Wetten, S., Li, L., St. Jean, P.L., Upmanyu, R., Surh, L., Hosford, D., Barnes, M.R., Briley, J.D., Borrie, M., Coletta, N., Delisle, R., Dhalla, D., Ehm, M.G., Feldman, H.H., Fornazzari, L., Gauthier, S., Goodgame, N., Guzman, D., Hammond, S., Hollingworth, P., Hsiung, G.-Y., Johnson, J., Kelly, D.D., Keren, R., Kertesz, A., King, K.S., Lovestone, S., Loy-English, I., Matthews, P.M., Owen, M.J.,

Plumpton, M., Pryse-Phillips, W., Prinjha, R.K., Richardson, J.C., Saunders, A., Slater, A.J., St. George-Hyslop, P.H., Stinnett, S.W., Swartz, J.E., Taylor, R.L., Wherrett, J., Williams, J., Yarnall, D.P., Gibson, R.A., Irizarry, M.C., Middleton, L.T., Roses, A.D., 2008. Candidate Single-Nucleotide Polymorphisms From a Genomewide Association Study of Alzheimer Disease. Arch. Neurol. 65, 45–53.

Li, J., Ning, Y., Hedley, W., Saunders, B., Chen, Y., Tindill, N., Hannay, T., Subramaniam, S., 2002. The Molecule Pages database. Nature 420, 716–717.

Li, L., Sengupta, A., Haque, N., Grundke-Iqbal, I., Iqbal, K., 2004. Memantine inhibits and reverses the Alzheimer type abnormal hyperphosphorylation of tau and associated neurodegeneration. FEBS Lett. 566.

Li, S., Hong, S., Shepardson, N.E., Walsh, D.M., Shankar, G.M., Selkoe, D., 2009. Soluble Oligomers of Amyloid β Protein Facilitate Hippocampal Long-Term Depression by Disrupting Neuronal Glutamate Uptake. Neuron 62, 788–801.

Li, S., Jin, M., Koeglsperger, T., Shepardson, N.E., Shankar, G.M., Selkoe, D.J., 2011. Soluble Aβ oligomers inhibit long-term potentiation through a mechanism involving excessive activation of extrasynaptic NR2B-containing NMDA receptors. J. Neurosci. 31, 6627–38.

Li, X.-M., Li, C.-C., Yu, S.-S., Chen, J.-T., Sabapathy, K., Ruan, D.-Y., 2007. JNK1 contributes to metabotropic glutamate receptor-dependent long-term depression and short-term synaptic plasticity in the mice area hippocampal CA1. Eur. J. Neurosci. 25, 391–396.

Li, X., Dang, S., Yan, C., Gong, X., Wang, J., Shi, Y., 2012. Structure of a presenilin family intramembrane aspartate protease. Nature 493, 56–61.

Liang, M., Chini, E.N., Cheng, J., Dousa, T.P., 1999. Synthesis of NAADP and cADPR in Mitochondria. Arch. Biochem. Biophys. 371, 317–325.

Liazoghli, D., Perreault, S., Micheva, K.D., Desjardins, M., Leclerc, N., 2005. Fragmentation of the Golgi Apparatus Induced by the Overexpression of Wild-Type and Mutant Human Tau Forms in Neurons. Am. J. Pathol. 166, 1499–1514.

LIN, H., Bhatia, R., Lal, R., 2001. Amyloid beta protein forms ion channels: implications for Alzheimer's disease pathophysiology. FASEB J. 15, 2433–2444.

Lin, W.-L., Lewis, J., Yen, S.-H., Hutton, M., Dickson, D.W., 2003. Ultrastructural neuronal pathology in transgenic mice expressing mutant (P301L) human tau. J. Neurocytol. 32, 1091–1105.

Lin, X., Guan, H., Huang, Z., Liu, J., Li, H., Wei, G., Cao, X., Li, Y., 2014. Downregulation of Bcl-2 expression by miR-34a mediates palmitate-induced Min6 cells apoptosis. J. Diabetes Res. 2014, 258695.

Linden, D.J., Dawson, T.M., Dawson, V.L., 1995. An evaluation of the nitric oxide/cGMP/cGMP-dependent protein kinase cascade in the induction of cerebellar long-term depression in culture. J. Neurosci. 15, 5098–105.

Linden, D.J., Smeyne, M., Connor, J.A., 1994. Trans-ACPD, a metabotropic receptor agonist, produces calcium mobilization and an inward current in cultured cerebellar Purkinje neurons. J. Neurophysiol. 71, 1992–8.

Liou, J., Fivaz, M., Inoue, T., Meyer, T., 2007. Live-cell imaging reveals sequential oligomerization and local plasma membrane targeting of stromal interaction molecule 1 after Ca2+ store depletion. Proc. Natl. Acad. Sci. U. S. A. 104, 9301–6.

Liou, J., Kim, M.L., Do Heo, W., Jones, J.T., Myers, J.W., Ferrell, J.E., Meyer, T., 2005. STIM Is a Ca2+ Sensor Essential for Ca2+-Store-Depletion-Triggered Ca2+ Influx, Current Biology.

Liu, C.-C., Kanekiyo, T., Xu, H., Bu, G., 2013. Apolipoprotein E and Alzheimer disease: risk, mechanisms and therapy. Nat. Rev. Neurol. 9, 106–118.

Liu, C., Hermann, T.E., 1978. Characterization of ionomycin as a calcium ionophore. J. Biol. Chem. 253, 5892–4.

Liu, D., Pitta, M., Mattson, M.P., 2008. Preventing NAD+ depletion protects neurons against excitotoxicity: Bioenergetic effects of mild mitochondrial uncoupling and caloric restriction, Annals of the New York Academy of Sciences.

Liu, F., Ma, X.H., Ule, J., Bibb, J.A., Nishi, A., DeMaggio, A.J., Yan, Z., Nairn, A.C., Greengard, P., 2001. Regulation of cyclin-dependent kinase 5 and casein kinase 1 by metabotropic glutamate receptors. Proc. Natl. Acad. Sci. U. S. A. 98, 11062–8.

Liu, Q., Kriksunov, I.A., Graeff, R., Munshi, C., Lee, H.C., Hao, Q., 2005. Crystal Structure of Human CD38 Extracellular Domain. Structure 13, 1331–1339.

Liu, S.J., Zhang, A.H., Li, H.L., Wang, Q., Deng, H.M., Netzer, W.J., Xu, H., Wang, J.Z., 2003. Overactivation of glycogen synthase kinase-3 by inhibition of phosphoinositol-3 kinase and protein kinase C leads to hyperphosphorylation of tau and impairment of spatial memory. J. Neurochem. 87, 1333–44.

Lopatina, O., Liu, H.-X., Amina, S., Hashii, M., Higashida, H., 2010. Oxytocin-induced elevation of ADP-ribosyl cyclase activity, cyclic ADP-ribose or Ca(2+) concentrations is involved in autoregulation of oxytocin secretion in the hypothalamus and posterior pituitary in male mice. Neuropharmacology 58, 50–5.

Lopez, J.R., Lyckman, A., Oddo, S., LaFerla, F.M., Querfurth, H.W., Shtifman, A., 2008. Increased intraneuronal resting [Ca2+] in adult Alzheimer's disease mice. J. Neurochem. 105, 262–271.

Lorent, K., Overbergh, L., Moechars, D., De Strooper, B., Van Leuven, F., Van den Berghe, H., 1995. Expression in mouse embryos and in adult mouse brain of three members of the amyloid precursor protein family, of the alpha-2-macroglobulin receptor/low density lipoprotein receptor-related protein and of its ligands apolipoprotein E, lipoprotein lipase, alpha-2-macroglobulin and the 40,000 molecular weight receptor-associated protein. Neuroscience 65, 1009–25.

Lu, D.C., Soriano, S., Bredesen, D.E., Koo, E.H., 2003. Caspase cleavage of the amyloid precursor protein modulates amyloid beta-protein toxicity. J. Neurochem. 87, 733–41.

Lu, H., Burns, D., Garnier, P., Wei, G., Zhu, K., Ying, W., 2007. P2X7 receptors mediate NADH transport across the plasma membranes of astrocytes. Biochem. Biophys. Res. Commun. 362, 946–950.

Lu, Y.M., Jia, Z., Janus, C., Gerlai, R., Wojtowicz, J.M., Roder, J.C., 1997. Mice lacking metabotropic glutamate receptor 5 show impaired learning and reduced CA1 long-term potentiation (LTP) but normal CA3 LTP. J Neurosci 17.

Lucius, R., Mentlein, R., 1995. Development of a culture system for pure rat neurons: advantages of a sandwich technique. Ann. Anat. 177, 447–54.

Lue, L.F., Kuo, Y.M., Roher, A.E., Brachova, L., Shen, Y., Sue, L., Beach, T., Kurth, J.H., Rydel, R.E., Rogers, J., 1999. Soluble amyloid beta peptide concentration as a predictor of synaptic change in Alzheimer's disease. Am. J. Pathol. 155, 853–62.

Luetjens, C.M., Lankiewicz, S., Bui, N.T., Krohn, A.J., Poppe, M., Prehn, J.H., 2001. Up-regulation of Bcl-xL in response to subtoxic beta-amyloid: role in neuronal resistance against apoptotic and oxidative injury. Neuroscience 102, 139–50.

Luik, R.M., Wang, B., Prakriya, M., Wu, M.M., Lewis, R.S., 2008. Oligomerization of STIM1 couples ER calcium depletion to CRAC channel activation. Nature 454, 538–542.

Lujan, R., Nusser, Z., Roberts, J.D., Shigemoto, R., Somogyi, P., 1996. Perisynaptic location of metabotropic glutamate receptors mGluR1 and mGluR5 on dendrites and dendritic spines in the rat hippocampus. Eur. J. Neurosci. 8, 1488–500.

Luján, R., Roberts, J.D.B., Shigemoto, R., Ohishi, H., Somogyi, P., 1997. Differential plasma membrane distribution of metabotropic glutamate receptors mGluR1α, mGluR2 and mGluR5, relative to neurotransmitter release sites. J. Chem. Neuroanat. 13.

Lukyanenko, V., Györke, I., Wiesner, T.F., Györke, S., 2001. Potentiation of Ca(2+) release by cADP-ribose in the heart is mediated by enhanced SR Ca(2+) uptake into the sarcoplasmic reticulum. Circ. Res. 89, 614–22.

Luo, W. -j., Wang, H., Li, H., Kim, B.S., Shah, S., Lee, H.-J., Thinakaran, G., Kim, T.-W., Yu, G., Xu, H., 2003. PEN-2 and APH-1 Coordinately Regulate Proteolytic Processing of Presenilin 1. J. Biol. Chem. 278, 7850–7854.

Luo, Y., Bolon, B., Kahn, S., Bennett, B.D., Babu-Khan, S., Denis, P., Fan, W., Kha, H., Zhang, J., Gong, Y., Martin, L., Louis, J.-C., Yan, Q., Richards, W.G., Citron, M., Vassar, R., 2001. Mice deficient in BACE1, the Alzheimer's beta-secretase, have normal phenotype and abolished beta-amyloid generation. Nat. Neurosci. 4, 231–232.

Lüscher, C., Huber, K.M., 2010. Group 1 mGluR-dependent synaptic long-term depression: mechanisms and implications for circuitry and disease. Neuron 65, 445–59.

Lüthi, A., Gähwiler, B.H., Gerber, U., 1996. A slowly inactivating potassium current in CA3 pyramidal cells of rat hippocampus in vitro. J. Neurosci. 16, 586–94.

Lynch, G., Larson, J., Kelso, S., Barrionuevo, G., Schottler, F., 1983. Intracellular injections of EGTA block induction of hippocampal long-term potentiation. Nature 305, 719–21.

Lytton, J., Westlin, M., Hanley, M.R., 1991. Thapsigargin inhibits the sarcoplasmic or endoplasmic reticulum Ca-ATPase family of calcium pumps. J. Biol. Chem. 266, 17067–71.

Ma, Y., Wu, D., Ding, X., Ying, W., 2014. CD38 plays key roles in both antioxidation and cell survival of H2O2-treated primary rodent astrocytes. Int. J. Physiol. Pathophysiol. Pharmacol. 6, 102–8.

Ma, Z., Siebert, A.P., Cheung, K.-H., Lee, R.J., Johnson, B., Cohen, A.S., Vingtdeux, V., Marambaud, P., Foskett, J.K., 2012. Calcium homeostasis modulator 1 (CALHM1) is the pore-forming subunit of an ion channel that mediates extracellular Ca2+ regulation of neuronal excitability. Proc. Natl. Acad. Sci. 109, E1963–E1971.

Maarouf, C.L., Daugs, I.D., Kokjohn, T.A., Walker, D.G., Hunter, J.M., Kruchowsky, J.C., Woltjer, R., Kaye, J., Castaño, E.M., Sabbagh, M.N., Beach, T.G., Roher, A.E., 2011. Alzheimer's Disease and Non-Demented High Pathology Control Nonagenarians: Comparing and Contrasting the Biochemistry of Cognitively Successful Aging. PLoS One 6, e27291.

Maccioni, R.B., Farías, G., Morales, I., Navarrete, L., 2010. The Revitalized Tau Hypothesis on Alzheimer's Disease. Arch. Med. Res. 41, 226–231.

MacDonald, J.F., Xiong, Z.-G., Jackson, M.F., 2006. Paradox of Ca2+ signaling, cell death and stroke. Trends Neurosci. 29, 75–81.

MacLennan, D.H., Chen, S.R.W., 2009. Store overload-induced Ca2+ release as a triggering mechanism for CPVT and MH episodes caused by mutations in RYR and CASQ genes. J. Physiol. 587, 3113–5.

Macmillan, D., McCarron, J.G., 2010. The phospholipase C inhibitor U-73122 inhibits Ca(2+) release from the intracellular sarcoplasmic reticulum Ca(2+) store by inhibiting Ca(2+) pumps in smooth muscle. Br. J. Pharmacol. 160, 1295–301.

Magee, J.C., Johnston, D., 1997. A Synaptically Controlled, Associative Signal for Hebbian Plasticity in Hippocampal Neurons. Science (80-.). 275.

Magi, S., Castaldo, P., Macrì, M.L., Maiolino, M., Matteucci, A., Bastioli, G., Gratteri, S., Amoroso, S., Lariccia, V., 2016. Intracellular Calcium Dysregulation: Implications for Alzheimer's Disease. Biomed Res. Int. 2016, 1–14.

Magistretti, J., de Curtis, M., Vescovi, A., Galli, R., Gritti, A., 1996. Long-term survival of cortical neurones from adult guinea-pig maintained in low-density cultures. Neuroreport 7, 1559–64.

Magnelli, L., Cinelli, M., Turchetti, A., Chiarugi, V.P., 1994. Bcl-2 Overexpression Abolishes Early Calcium Waving Preceding Apoptosis in NIH-3T3 Murine Fibroblasts. Biochem. Biophys. Res. Commun. 204, 84–90.

Mahley, R.W., Weisgraber, K.H., Huang, Y., 2006. Apolipoprotein E4: A causative factor and therapeutic target in neuropathology, including Alzheimer's disease. Proc. Natl. Acad. Sci. 103, 5644–5651.

Mairet-Coello, G., Courchet, J., Pieraut, S., Courchet, V., Maximov, A., Polleux, F., 2013. The CAMKK2-AMPK Kinase Pathway Mediates the Synaptotoxic Effects of Aβ Oligomers through Tau Phosphorylation. Neuron 78, 94–108.

Malavasi, F., Deaglio, S., Funaro, A., Ferrero, E., Horenstein, A.L., Ortolan, E., Vaisitti, T., Aydin, S., 2008. Evolution and Function of the ADP Ribosyl Cyclase/CD38 Gene Family in Physiology and Pathology. Physiol. Rev. 88.

Malavasi, F., Deaglio, S., Zaccarello, G., Horenstein, A.L., Chillemi, A., Audrito, V., Serra, S., Gandione, M., Zitella, A., Tizzani, A., 2010. The hidden life of NAD+-consuming ectoenzymes in the endocrine system. J. Mol. Endocrinol. 45, 183–91.

Malenka, R.C., Bear, M.F., 2004. LTP and LTD. Neuron 44, 5–21.

Malenka, R.C., Kauer, J.A., Zucker, R.S., Nicoll, R.A., 1988. Postsynaptic calcium is sufficient for potentiation of hippocampal synaptic transmission. Science 242, 81–4.

Mallone, R., Ferrua, S., Morra, M., Zocchi, E., Mehta, K., Notarangelo, L.D., Malavasi, F., 1998. Characterization of a CD38-like 78-kilodalton soluble protein released from B cell lines derived from patients with X-linked agammaglobulinemia. J. Clin. Invest. 101, 2821–2830.

Mangmool, S., Kurose, H., 2011. G(i/o) protein-dependent and -independent actions of Pertussis Toxin (PTX). Toxins (Basel). 3, 884–99.

Mannaioni, G., Marino, M.J., Valenti, O., Traynelis, S.F., Conn, P.J., 2001. Metabotropic glutamate receptors 1 and 5 differentially regulate CA1 pyramidal cell function. J. Neurosci. 21, 5925–34.

Manthorpe, M., Engvall, E., Ruoslahti, E., Longo, F.M., Davis, G.E., Varon, S., 1983. Laminin Promotes Neuritic Regeneration from Cultured Peripheral and Central Neurons. J. Cell Biol. 97, 1882–90.

Mao, L., Wang, J.Q., 2001. Gliogenesis in the striatum of the adult rat: alteration in neural progenitor population after psychostimulant exposure. Brain Res. Dev. Brain Res. 130, 41–51.

Mao, L., Wang, J.Q., 2003. Group I metabotropic glutamate receptor-mediated calcium signalling and immediate early gene expression in cultured rat striatal neurons. Eur. J. Neurosci. 17, 741–50.

Marchetti, C., Marie, H., 2011. Hippocampal synaptic plasticity in Alzheimer's disease: what have we learned so far from transgenic models? Rev. Neurosci. 22, 373–402.

Marchi, S., Patergnani, S., Pinton, P., 2014. The endoplasmic reticulum–mitochondria connection: One touch, multiple functions. Biochim. Biophys. Acta - Bioenerg. 1837, 461–469.

Margallo-Lana, M., Morris, C.M., Gibson, A.M., Tan, A.L., Kay, D.W.K., Tyrer, S.P., Moore, B.P., Ballard, C.G., 2004. Influence of the amyloid precursor protein locus on dementia in Down syndrome. Neurology 62, 1996–8.

Marín, N., Romero, B., Bosch-Morell, F., Llansola, M., Felipo, V., Romá, J., Romero, F.J., 2000. Beta-amyloid-induced activation of caspase-3

in primary cultures of rat neurons. Mech. Ageing Dev. 119, 63–7.

Mark, R.J., Hensley, K., Butterfield, D.A., Mattson, M.P., 1995. Amyloid beta-peptide impairs ion-motive ATPase activities: evidence for a role in loss of neuronal Ca2+ homeostasis and cell death. J. Neurosci. 15, 6239–49.

Markram, H., Lübke, J., Frotscher, M., Sakmann, B., 1997. Regulation of Synaptic Efficacy by Coincidence of Postsynaptic APs and EPSPs. Science (80-.). 275.

Marriott, D.R., Hirst, W.D., Ljunberg, C.M., 1995. Astrocytes. In: Cohen, J., Wilkin (Eds.), Neural Cell Culture. Oxford Univ. Press, NY, pp. 85–96.

Martino Carpi, F., Cortese, M., Orsomando, G., Polzonetti, V., Vincenzetti, S., Moreschini, B., Coleman, M., Magni, G., Pucciarelli, S., 2018. Simultaneous quantification of nicotinamide mononucleotide and related pyridine compounds in mouse tissues by UHPLC-MS/MS. Sep. Sci. Plus 1, 22–30.

Martinou, J.C., Dubois-Dauphin, M., Staple, J.K., Rodriguez, I., Frankowski, H., Missotten, M., Albertini, P., Talabot, D., Catsicas, S., Pietra, C., 1994a. Overexpression of BCL-2 in transgenic mice protects neurons from naturally occurring cell death and experimental ischemia. Neuron 13, 1017–30.

Martinou, J.C., Frankowski, H., Missotten, M., Martinou, I., Potier, L., Dubois-Dauphin, M., 1994b. Bcl-2 and neuronal selection during development of the nervous system. J. Physiol. Paris 88, 209–11.

Marx, S.O., Reiken, S., Hisamatsu, Y., Jayaraman, T., Burkhoff, D., Rosemblit, N., Marks, A.R., 2000. PKA phosphorylation dissociates FKBP12.6 from the calcium release channel (ryanodine receptor): defective regulation in failing hearts. Cell 101, 365–76.

Masgrau, R., Churchill, G.C., Morgan, A.J., Ashcroft, S.J.H., Galione, A., 2003. NAADP: a new second messenger for glucose-induced Ca2+ responses in clonal pancreatic beta cells. Curr. Biol. 13, 247–51.

Masliah, E., Mallory, M., Alford, M., DeTeresa, R., Hansen, L.A., McKeel, D.W., Morris, J.C., 2001. Altered expression of synaptic proteins occurs early during progression of Alzheimer's disease. Neurology 56, 127–9.

Masliah, E., Mallory, M., Ge, N., Alford, M., Veinbergs, I., Roses, A.D., 1995. Neurodegeneration in the Central Nervous System of apoE-Deficient Mice. Exp. Neurol. 136, 107–122.

Mastrangelo, M.A., Bowers, W.J., 2008. Detailed immunohistochemical characterization of temporal and spatial progression of Alzheimer's disease-related pathologies in male triple-transgenic mice. BMC Neurosci. 9, 81.

Mata, A.M., Berrocal, M., Sepúlveda, M.R., 2011. Impairment of the activity of the plasma membrane Ca $^{2+}$ -ATPase in Alzheimer's disease. Biochem. Soc. Trans. 39, 819–822.

Matlib, M.A., Zhou, Z., Knight, S., Ahmed, S., Choi, K.M., Krause-Bauer, J., Phillips, R., Altschuld, R., Katsube, Y., Sperelakis, N., Bers, D.M., 1998. Oxygen-bridged dinuclear ruthenium amine complex specifically inhibits Ca2+ uptake into mitochondria in vitro and in situ in single cardiac myocytes. J. Biol. Chem. 273, 10223–31.

Matsumura, N., Tanuma, S., 1998. Involvement of cytosolic NAD+ glycohydrolase in cyclic ADP-ribose metabolism. Biochem. Biophys. Res. Commun. 253, 246–252.

Mattson, M.P., 2002. Oxidative Stress, Perturbed Calcium Homeostasis, and Immune Dysfunction in Alzheimer's Disease. J. Neurovirol. 8, 539–550.

Mattson, M.P., 2004. Pathwyas Towards and Away from Alzheimer's Disease. Nature 430, 631–639.

Mattson, M.P., 2007. Calcium and neurodegeneration. Aging Cell 6, 337–350.

Mattson, M.P., Cheng, B., Davis, D., Bryant, K., Lieberburg, I., Rydel, R.E., 1992. beta-Amyloid peptides destabilize calcium homeostasis and render human cortical neurons vulnerable to excitotoxicity. J. Neurosci. 12, 376–89.

Mattson, M.P., LaFerla, F.M., Chan, S.L., Leissring, M.A., Shepel, P.N., Geiger, J.D., 2000. Calcium signaling in the ER: its role in neuronal plasticity and neurodegenerative disorders. Trends Neurosci. 23, 222–229.

Mauch, D.H.H., Nägier, K., Schumacher, S., Göritz, C., Müller, E.-C.C., Otto, A., Pfrieger, F.W.W., Nägler, K., Schumacher, S., Göritz, C., Müller, E.-C.C., Otto, A., Pfrieger, F.W.W., 2001. CNS synaptogenesis promoted by glia-derived cholesterol. Science 294, 1354–7.

Mayford, M., Siegelbaum, S.A., Kandel, E.R., 2012. Synapses and memory storage. Cold Spring Harb. Perspect. Biol. 4, a005751.

Mayo, L., Jacob-Hirsch, J., Amariglio, N., Rechavi, G., Moutin, M.-J., Lund, F.E., Stein, R., 2008. Dual role of CD38 in microglial activation and activation-induced cell death. J. Immunol. 181, 92–103.

McCarthy, T. V, Datar, S., Mackrill, J.J., 2003. Activation of ryanodine receptor/Ca2+ release channels downregulates CD38 in the Namalwa B lymphoma. FEBS Lett. 554, 133–7.

McCombs, J.E., Palmer, A.E., 2008. Measuring calcium dynamics in living cells with genetically encodable calcium indicators. Methods 46, 152–159.

McCool, B.A., Pin, J.P., Harpold, M.M., Brust, P.F., Stauderman, K.A., Lovinger, D.M., 1998. Rat group I metabotropic glutamate receptors inhibit neuronal Ca2+ channels via multiple signal transduction pathways in HEK 293 cells. J. Neurophysiol. 79, 379–91.

McDonough, M.J., Allen, C.E., Ng-Sui-Hing, N.-K.-L.A., Rabe, B.A., Lewis, B.B., Saha, M.S., 2012. Dissection, culture, and analysis of Xenopus laevis embryonic retinal tissue. J. Vis. Exp.

McGuinness, N., Anwyl, R., Rowan, M., 1991. Trans-ACPD enhances long-term potentiation in the hippocampus. Eur. J. Pharmacol. 197, 231–232.

McKhann, G., Drachman, D., Folstein, M., Katzman, R., Price, D., Stadlan, E.M., 1984. Clinical diagnosis of Alzheimer's disease: report of the NINCDS-ADRDA Work Group under the auspices of Department of Health and Human Services Task Force on Alzheimer's Disease. Neurology 34, 939–44.

Mehan, S., Meena, H., Sharma, D., Sankhla, R., 2011. JNK: A stress-activated protein kinase therapeutic strategies and involvement in Alzheimer's and various neurodegenerative abnormalities. J. Mol. Neurosci. 43.

Mehta, B., Begum, G., Joshi, N.B., Joshi, P.G., 2008. Nitric oxide-mediated modulation of synaptic activity by astrocytic P2Y receptors. J. Gen. Physiol. 132, 339–49.

Meilhac, O., Escargueil-Blanc, I., Thiers, J.C., Salvayre, R., Négre-Salvayre, A., 1999. Bcl-2 alters the balance between apoptosis and necrosis, but does not prevent cell death induced by oxidized low density lipoproteins. FASEB J. 13, 485–94.

Mekahli, D., Bultynck, G., Parys, J.B., De Smedt, H., Missiaen, L., 2011. Endoplasmic-Reticulum Calcium Depletion and Disease. Cold Spring Harb. Perspect. Biol. 3, a004317–a004317.

Menéndez, M., 2005. Down syndrome, Alzheimer's disease and seizures. Brain Dev. 27, 246–252.

Merry, D.E., Veis, D.J., Hickey, W.F., Korsmeyer, S.J., 1994. bcl-2 protein expression is widespread in the developing nervous system and retained in the adult PNS. Development 120, 301–11.

Mészáros, L.G., Bak, J., Chu, A., 1993. Cyclic ADP-ribose as an endogenous regulator of the non-skeletal type ryanodine receptor Ca2+ channel. Nature 364, 76–9.

Miao, J.Y., Kaji, K., Hayashi, H., Araki, S., 1997. Inhibitors of phospholipase promote apoptosis of human endothelial cells. J. Biochem. 121, 612–8.

Michan, S., Li, Y., Chou, M.M.-H., Parrella, E., Ge, H., Long, J.M., Allard, J.S., Lewis, K., Miller, M., Xu, W., Mervis, R.F., Chen, J., Guerin, K.I., Smith, L.E.H., McBurney, M.W., Sinclair, D.A., Baudry, M., de Cabo, R., Longo, V.D., 2010. SIRT1 Is Essential for Normal Cognitive Function and Synaptic Plasticity. J. Neurosci. 30, 9695–9707.

Michelangeli, F., Ogunbayo, O.A., Wootton, L.L., 2005. A plethora of interacting organellar Ca2+ stores. Curr. Opin. Cell Biol. 17.

Michikawa, M., Fan, Q.W., Isobe, I., Yanagisawa, K., 2000. Apolipoprotein E exhibits isoform-specific promotion of lipid efflux from astrocytes and neurons in culture. J. Neurochem. 74, 1008–16.

Migaud, M.E., Pederick, R.L., Bailey, V.C., Potter, B.V.L., 1999a. Probing Aplysia californica Adenosine 5'-Diphosphate Ribosyl Cyclase for Substrate Binding Requirements: Design of Potent Inhibitors. Biochemistry 38, 9105–9114.

Migaud, M.E., Pederick, R.L., Bailey, V.C., Potter, B.V.L., 1999b. Probing Aplysia californica Adenosine 5'-Diphosphate Ribosyl Cyclase for Substrate Binding Requirements: Design of Potent Inhibitors. Biochemistry 38, 9105–9114.

Migliore, M., Ferrante, M., Ascoli, G.A., 2005. Signal propagation in oblique dendrites of CA1 pyramidal cells. J. Neurophysiol. 94, 4145–55.

Miho, Y., Kouroku, Y., Fujita, E., Mukasa, T., Urase, K., Kasahara, T., Isoai, A., Momoi, M.Y., Momoi, T., 1999. bFGF inhibits the activation of caspase-3 and apoptosis of P19 embryonal carcinoma cells during neuronal differentiation. doi.org 6, 463–470.

Miller, J.H., Azmitia, E.C., 1999. Growth inhibitory effects of a mu opioid on cultured cholinergic neurons from fetal rat ventral forebrain, brainstem, and spinal cord. Brain Res. Dev. Brain Res. 114, 69–77.

Miller, M.L., Johnson, G.V.W., 1995. Transglutaminase Cross-Linking of the τ Protein. J. Neurochem. 65.

Min, B. Il, Kim, C.J., Rhee, J.S., Akaike, N., 1996. Modulation of glycine-induced chloride current in acutely dissociated rat periaqueductal gray neurons by μ-opioid agonist, DAGO. Brain Res. 734, 72–78.

Minster, R.L., Demirci, F.Y., DeKosky, S.T., Kamboh, M.I., 2009. No association between *CALHM1* variation and risk of Alzheimer disease. Hum. Mutat. 30, E566–E569.

Mirzabekov, T.A., Lin, M.-C., Kagan, B.L., 1996. Pore formation by the cytotoxic islet amyloid peptide amylin. J. Biol. Chem. 271.

Missiaen, L., De Smedt, H., Droogmans, G., Casteels, R., 1992. Ca2+ release induced by inositol 1,4,5-trisphosphate is a steady-state phenomenon controlled by luminal Ca2+ in permeabilized cells. Nature 357, 599–602.

Missiaen, L., De Smedt, H., Parys, J.B., Casteels, R., 1994. Co-activation of inositol trisphosphate-induced Ca^{2+} release by cytosolic Ca^{2+} is loading-dependent. J. Biol. Chem. 269.

Missiaen, L., Parys, J.B., De Smedt, H., Sienaert, I., Sipma, H., Vanlingen, S., Maes, K., Kunzelmann, K., Casteels, R., 1998. Inhibition of inositol trisphosphate-induced calcium release by cyclic ADP-ribose in A7r5 smooth-muscle cells and in 16HBE14o- bronchial mucosal cells. Biochem. J. 489–95.

Miyoshi, K., Ohyagi, Y., Sakae, N., Motomura, K., Ma, L., Taniwaki, T., Furuya, H., Tabira, T., Kira, J., 2009. Enhancement of Activation of Caspases by Presenilin 1 Gene Mutations and its Inhibition by Secretase Inhibitors. J. Alzheimer's Dis. 16, 551–564.

Mizuguchi, M., Otsuka, N., Sato, M., Ishii, Y., Kon, S., Yamada, M., Nishina, H., Katada, T., Ikeda, K., 1995. Neuronal localization of CD38 antigen in the human brain. Brain Res. 697, 235–40.

Moccia, F., Zuccolo, E., Soda, T., Tanzi, F., Guerra, G., Mapelli, L., Lodola, F., D'Angelo, E., 2015. Stim and Orai proteins in neuronal Ca2+ signaling and excitability. Front. Cell. Neurosci. 9, 153.

Moechars, D., Dewachter, I., Lorent, K., Reversé, D., Baekelandt, V., Naidu, A., Tesseur, I., Spittaels, K., Haute, C. V, Checler, F., Godaux, E., Cordell, B., Van Leuven, F., 1999. Early phenotypic changes in transgenic mice that overexpress different mutants of amyloid precursor protein in brain. J. Biol. Chem. 274, 6483–92.

Mogami, H., Nakano, K., Tepikin, A. V, Petersen, O.H., 1997. Ca2+ flow via tunnels in polarized cells: recharging of apical Ca2+ stores by focal Ca2+ entry through basal membrane patch. Cell 88, 49–55.

Momeni, H.R., 2011. Role of calpain in apoptosis. Cell J. 13, 65–72.

Monaco, G., Beckers, M., Ivanova, H., Missiaen, L., Parys, J.B., De Smedt, H., Bultynck, G., 2012a. Profiling of the Bcl-2/Bcl-XL-binding sites on type 1 IP3 receptor. Biochem. Biophys. Res. Commun. 428, 31–35.

Monaco, G., Decrock, E., Akl, H., Ponsaerts, R., Vervliet, T., Luyten, T., De Maeyer, M., Missiaen, L., Distelhorst, C.W., De Smedt, H., Parys, J.B., Leybaert, L., Bultynck, G., 2012b. Selective regulation of IP3-receptor-mediated Ca2+ signaling and apoptosis by the BH4 domain of Bcl-2 versus Bcl-Xl. Cell Death Differ. 19, 295–309.

Monaco, G., Decrock, E., Nuyts, K., Wagner II, L.E., Luyten, T., Strelkov, S. V., Missiaen, L., De Borggraeve, W.M., Leybaert, L., Yule, D.I., De Smedt, H., Parys, J.B., Bultynck, G., 2013. Alpha-Helical Destabilization of the Bcl-2-BH4-Domain Peptide Abolishes Its Ability to Inhibit the IP3 Receptor. PLoS One 8, e73386.

Monaghan, P., Robertson, D., Amos, T.A., Dyer, M.J., Mason, D.Y., Greaves, M.F., 1992. Ultrastructural localization of bcl-2 protein. J. Histochem. Cytochem. 40, 1819–1825.

Moreno-López, B., González-Forero, D., 2006. Nitric oxide and synaptic dynamics in the adult brain: physiopathological aspects. Rev. Neurosci. 17, 309–57.

Moreno-Ortega, A.J., Buendia, I., Mouhid, L., Egea, J., Lucea, S., Ruiz-Nuño, A., López, M.G., Cano-Abad, M.F., 2015. CALHM1 and its polymorphism P86L differentially control Ca^{2+}homeostasis, mitogen-activated protein kinase signaling, and cell vulnerability upon exposure to amyloid β. Aging Cell 14, 1094–102.

Moreno-Ortega, A.J., Garcia, A., Ruiz-Nuño, A., Cano-Abad, M., 2011. The mutation P86L-CALHM1, linked to Alzheimer's disease, alters the nuclear calcium signalling. Alzheimer's Dement. 7, S581.

Moreno, H., Morfini, G., Buitrago, L., Ujlaki, G., Choi, S., Yu, E., Moreira, J.E., Avila, J., Brady, S.T., Pant, H., Sugimori, M., Llinás, R.R., 2016. Tau pathology-mediated presynaptic dysfunction. Neuroscience 325, 30–38.

Morgan, A., Churchill, G., Masgrau, R., Ruas, M., Davis, L., Billington, R., Patel, S., Yamasaki, M., Thomas, J., Genazzani, A., Galione, A., 2005. Methods in Cyclic ADP-Ribose and NAADP Research. In: Putney, J.W. (Ed.), Calcium Signaling, Second Edition. CRC Press, pp. 265–334.

Morgan, A.J.G., Cyclic, A.D.P., 2002. A. Sensitizing Calcium-Induced Calcium Relase, Role of cADPR as an Endogenous Modulator. ribose NAADP Struct. Metab. Funct. pp Dordr. Kluwer 167–197.

Morgan, D., Diamond, D.M., Gottschall, P.E., Ugen, K.E., Dickey, C., Hardy, J., Duff, K., Jantzen, P., DiCarlo, G., Wilcock, D., Connor, K., Hatcher, J., Hope, C., Gordon, M., Arendash, G.W., 2000. A β peptide vaccination prevents memory loss in an animal model of

Alzheimer's disease. Nature 408.

Morikawa, H., Khodakhah, K., Williams, J.T., 2003. Two intracellular pathways mediate metabotropic glutamate receptor-induced Ca2+ mobilization in dopamine neurons. J. Neurosci. 23, 149–57.

Morita, K., Kitayama, S., Dohi, T., 1997. Stimulation of cyclic ADP-ribose synthesis by acetylcholine and its role in catecholamine release in bovine adrenal chromaffin cells. J. Biol. Chem. 272, 21002–9.

Morley, S., Kaar, A., Rae, M., 2012. Evoked hippocampal supralinear intracellular calcium responses are absent in 3xTg Alzheimer's mice. Alzheimer's Dement. 8, P409.

Morley, S.J., Keogh, M.K., Rae, M.G., 2011. Evidence of altered intracellular calcium handling in week old cultured hippocampal neurones of a murine model of Alzheimer's disease (3xTg AD). Irish J. Med. Sci. 180, S303–S304.

Morrissette, J., Heisermann, G., Cleary, J., Ruoho, A., Coronado, R., 1993. Cyclic ADP-ribose induced Ca2+ release in rabbit skeletal muscle sarcoplasmic reticulum. FEBS Lett. 330, 270–4.

Mothet, J.P., Fossier, P., Meunier, F.M., Stinnakre, J., Tauc, L., Baux, G., 1998. Cyclic ADP-ribose and calcium-induced calcium release regulate neurotransmitter release at a cholinergic synapse of Aplysia. J. Physiol. 507 (Pt 2, 405–414.

Muchmore, S.W., Sattler, M., Liang, H., Meadows, R.P., Harlan, J.E., Yoon, H.S., Nettesheim, D., Chang, B.S., Thompson, C.B., Wong, S.-L., Ng, S.-C., Fesik, S.W., 1996. X-ray and NMR structure of human Bcl-xL, an inhibitor of programmed cell death. Nature 381, 335–341.

Mucke, L., Masliah, E., Yu, G.-Q., Mallory, M., Rockenstein, E.M., Tatsuno, G., Hu, K., Kholodenko, D., Johnson-Wood, K., McConlogue, L., 2000. High-Level Neuronal Expression of Aβ1–42 in Wild-Type Human Amyloid Protein Precursor Transgenic Mice: Synaptotoxicity without Plaque Formation. J. Neurosci. 20.

Mulkey, R.M., Malenka, R.C., 1992. Mechanisms underlying induction of homosynaptic long-term depression in area CA1 of the hippocampus. Neuron 9, 967–75.

Müller, M., Cheung, K.-H., Foskett, J.K., 2011. Enhanced ROS Generation Mediated by Alzheimer's Disease Presenilin Regulation of $InsP_3R$ Ca^{2+} Signaling. Antioxid. Redox Signal. 14, 1225–1235.

Muller, U.C., Deller, T., Korte, M., 2017. Not just amyloid: physiological functions of the amyloid precursor protein family. Nat Rev Neurosci 18, 281–298.

Müller, U.C., Zheng, H., 2012. Physiological functions of APP family proteins. Cold Spring Harb. Perspect. Med. 2, a006288.

Murayama, T., Ogawa, Y., 2002. Roles of two ryanodine receptor isoforms coexisting in skeletal muscle. Trends Cardiovasc. Med. 12, 305–11.

Murphy, M.P., 2009. How mitochondria produce reactive oxygen species. Biochem. J. 417, 1–13.

Murphy, M.P., LeVine, H., 2010. Alzheimer's Disease and the Amyloid-β Peptide. J. Alzheimer's Dis. 19, 311–323.

Murphy, S.N., Miller, R.J., 1988. A glutamate receptor regulates Ca2+ mobilization in hippocampal neurons. Proc. Natl. Acad. Sci. U. S. A. 85, 8737–8741.

Murphy, S.N., Miller, R.J., 1989. Two distinct quisqualate receptors regulate Ca2+ homeostasis in hippocampal neurons in vitro. Mol. Pharmacol. 35, 671–80.

Mutel, V., Ellis, G.J., Adam, G., Chaboz, S., Nilly, A., Messer, J., Bleuel, Z., Metzler, V., Malherbe, P., Schlaeger, E.-J., Roughley, B.S., Faull, R.L.M., Richards, J.G., 2008. Characterization of [3H]Quisqualate Binding to Recombinant Rat Metabotropic Glutamate 1a and 5a Receptors and to Rat and Human Brain Sections. J. Neurochem. 75, 2590–2601.

Mynlieff, M., 1997. Dissociation of postnatal hippocampal neurons for short term culture. J. Neurosci. Methods 73, 35–44.

Naber, P.A., Witter, M.P., Lopes Silva, F.H., 2000. Networks of the hippocampal memory system of the rat. The pivotal role of the subiculum. Ann. N. Y. Acad. Sci. 911, 392–403.

Nakamura, T., Barbara, J.G., Nakamura, K., Ross, W.N., 1999. Synergistic release of Ca2+ from IP3-sensitive stores evoked by synaptic activation of mGluRs paired with backpropagating action potentials. Neuron 24, 727–737.

Nakamura, T., Lasser-Ross, N., Nakamura, K., Ross, W.N., 2002. Spatial Segregation and Interaction of Calcium Signalling Mechanisms in Rat Hippocampal CA1 Pyramidal Neurons. J. Physiol. 543, 465–480.

Nakamura, T., Lipton, S.A., 2011. Redox modulation by S-nitrosylation contributes to protein misfolding, mitochondrial dynamics, and neuronal synaptic damage in neurodegenerative diseases. Cell Death Differ. 18, 1478–1486.

Nakamura, T., Nakamura, K., Lasser-Ross, N., Barbara, J.G., Sandler, V.M., Ross, W.N., 2000. Inositol 4,5-trisphosphate (IP3)-mediated Ca2+ release evoked by metabotropic agonists and backpropagating action potentials in hippocampal CA1 pyramidal neurons. J. Neurosci. Off. J. Soc. Neurosci. 20 1, 8365–8376.

Nakamura, Y., Fukami, K., 2017. Regulation and physiological functions of mammalian phospholipase C. J. Biochem. 161, mvw094.

Nakamura, Y., Harada, H., Kamasawa, N., Matsui, K., Rothman, J.S., Shigemoto, R., Silver, R.A., DiGregorio, D.A., Takahashi, T., 2015. Nanoscale distribution of presynaptic Ca(2+) channels and its impact on vesicular release during development. Neuron 85, 145–58.

Nakanishi, S., 1992. Molecular diversity of glutamate receptors and implications for brain function. Science 258, 597–603.

Nam, T.-S., Choi, S.H., Rah, S.-Y., Kim, S.-Y., Jang, W., Im, M.-J., Kwon, H.J., Kim, U.-H., 2006. Discovery of a small-molecule inhibitor for kidney ADP-ribosyl cyclase: Implication for intracellular calcium signal mediated by cyclic ADP-ribose. Exp. Mol. Med. 38, 718–26.

Namazi, M.R., 2003. Nicotinamide: a potential addition to the anti-psoriatic weaponry. FASEB J. 17, 1377–1379.

Nash, M.S., Saunders, R., Young, K.W., Challiss, R.A., Nahorski, S.R., 2001. Reassessment of the Ca2+ sensing property of a type I metabotropic glutamate receptor by simultaneous measurement of inositol 1,4,5-trisphosphate and Ca2+ in single cells. J. Biol. Chem. 276, 19286–93.

Näslund, J., Haroutunian, V., Mohs, R., Davis, K.L., Davies, P., Greengard, P., Buxbaum, J.D., 2000. Correlation Between Elevated Levels of Amyloid β-Peptide in the Brain and Cognitive Decline. JAMA 283, 1571.

Nedergaard, M., Ransom, B., Goldman, S.A., 2003. New roles for astrocytes: Redefining the functional architecture of the brain. Trends Neurosci. 26.

Nelson, O., Supnet, C., Liu, H., Bezprozvanny, I., 2010. Familial Alzheimer's Disease Mutations in Presenilins: Effects on Endoplasmic Reticulum Calcium Homeostasis and Correlation with Clinical Phenotypes. J. Alzheimer's Dis. 21, 781–793.

Nelson, O., Supnet, C., Tolia, A., Horre, K., De Strooper, B., Bezprozvanny, I., 2011. Mutagenesis Mapping of the Presenilin 1 Calcium Leak Conductance Pore. J. Biol. Chem. 286, 22339–22347.

Nelson, O., Tu, H., Lei, T., Bentahir, M., de Strooper, B., Bezprozvanny, I., 2007. Familial Alzheimer disease–linked mutations specifically disrupt Ca2+ leak function of presenilin 1. J. Clin. Invest. 117, 1230–1239.

Nerbonne, J., Gurney, A., 1989. Development of excitable membrane properties in mammalian sympathetic neurons. J. Neurosci. 9.

Neumann, H., Daly, M.J., 2013. Variant *TREM2* as Risk Factor for Alzheimer's Disease. N. Engl. J. Med. 368, 182–184.

Nhan, H.S., Chiang, K., Koo, E.H., 2015. The multifaceted nature of amyloid precursor protein and its proteolytic fragments: friends and foes. Acta Neuropathol. 129, 1–19.

Niswender, C.M., Conn, P.J., 2010. Metabotropic glutamate receptors: physiology, pharmacology, and disease. Annu. Rev. Pharmacol. Toxicol. 50, 295–322.

Nitsch, R.M., Deng, A., Wurtman, R.J., Growdon, J.H., 2002. Metabotropic Glutamate Receptor Subtype mGluR1α Stimulates the Secretion of the Amyloid β-Protein Precursor Ectodomain. J. Neurochem. 69, 704–712.

Niu, Y., Su, Z., Zhao, C., Song, B., Zhang, X., Zhao, N., Shen, X., Gong, Y., 2009. Effect of amyloid β on capacitive calcium entry in neural 2a cells. Brain Res. Bull. 78, 152–157.

Noble, W., Hanger, D.P., Miller, C.C.J., Lovestone, S., 2013. The importance of tau phosphorylation for neurodegenerative diseases. Front. Neurol. 4, 83.

Noguchi, N., Takasawa, S., Nata, K., Tohgo, A., Kato, I., Ikehata, F., Yonekura, H., Okamoto, H., 1997. Cyclic ADP-ribose binds to FK506-binding protein 12.6 to release Ca2+ from islet microsomes. J. Biol. Chem. 272, 3133–6.

Nomura, A., Shigemoto, R., Nakamura, Y., Okamoto, N., Mizuno, N., Nakanishi, S., 1994. Developmentally regulated postsynaptic localization of a metabotropic glutamate receptor in rat rod bipolar cells. Cell 77, 361–369.

Nordstedt, C., Caporaso, G.L., Thyberg, J., Gandy, S.E., Greengard, P., 1993. Identification of the Alzheimer beta/A4 amyloid precursor protein in clathrin-coated vesicles purified from PC12 cells. J. Biol. Chem. 268, 608–12.

Nunan, J., Small, D.H., 2000. Regulation of APP cleavage by α-, β- and γ-secretases. FEBS Lett. 483.

Nunez, J., 2008. Primary Culture of Hippocampal Neurons from P0 Newborn Rats. J. Vis. Exp. 3–4.

Nusser, Z., Mulvihill, E., Streit, P., Somogyi, P., 1994. Subsynaptic segregation of metabotropic and ionotropic glutamate receptors as revealed by immunogold localization. Neuroscience 61, 421–427.

Oddo, S., Caccamo, A., Kitazawa, M., Tseng, B.P., LaFerla, F.M., 2003a. Amyloid deposition precedes tangle formation in a triple transgenic model of Alzheimer's disease. Neurobiol. Aging 24, 1063–70.

Oddo, S., Caccamo, A., Shepherd, J.D., Murphy, M.P., Golde, T.E., Kayed, R., Metherate, R., Mattson, M.P., Akbari, Y., LaFerla, F.M., 2003b. Triple-Transgenic Model of Alzheimer's Disease with Plaques and TanglesIntracellular Aβ and Synaptic Dysfunction. Neuron 39, 409–421.

Ogihara, T., Miya, K., Morimoto, S., 1990. Possible participation of calcium-regulating factors in senile dementia in elderly female subjects. Gerontology 36 Suppl 1, 25–30.

Oh, K.-J., Perez, S.E., Lagalwar, S., Vana, L., Binder, L., Mufson, E.J., 2010. Staging of Alzheimer's pathology in triple transgenic mice: a light and electron microscopic analysis. Int. J. Alzheimers. Dis. 2010.

Ohno, M., Cole, S.L., Yasvoina, M., Zhao, J., Citron, M., Berry, R., Disterhoft, J.F., Vassar, R., 2007. BACE1 gene deletion prevents neuron loss and memory deficits in 5XFAD APP/PS1 transgenic mice. Neurobiol. Dis. 26, 134–145.

Ohno, M., Sametsky, E.A., Younkin, L.H., Oakley, H., Younkin, S.G., Citron, M., Vassar, R., Disterhoft, J.F., 2004. BACE1 deficiency rescues memory deficits and cholinergic dysfunction in a mouse model of Alzheimer's disease. Neuron 41, 27–33.

Okada, T., Shimizu, S., Wakamori, M., Maeda, A., Kurosaki, T., Takada, N., Imoto, K., Mori, Y., 1998. Molecular cloning and functional characterization of a novel receptor-activated TRP Ca2+ channel from mouse brain. J. Biol. Chem. 273, 10279–87.

Olsson, A., Olofsson, T., Pero, R.W., 1993. Specific binding and uptake of extracellular nicotinamide in human leukemic K-562 cells. Biochem. Pharmacol. 45, 1191–200.

Olton, D.S., Papas, B.C., 1979. Spatial memory and hippocampal function. Neuropsychologia 17, 669–82.

Oorschot, D.E., 1989. Effect of fluorodeoxyuridine on neurons and non-neuronal cells in cerebral explants. Exp. brain Res. 78, 132–8.

Orciani, M., Trubiani, O., Guarnieri, S., Ferrero, E., Di Primio, R., 2008. CD38 is constitutively expressed in the nucleus of human hematopoietic cells. J. Cell. Biochem. 105, 905–912.

Osenkowski, P., Ye, W., Wang, R., Wolfe, M.S., Selkoe, D.J., 2008. Direct and Potent Regulation of ?-Secretase by Its Lipid Microenvironment. J. Biol. Chem. 283, 22529–22540.

Ostapchenko, V.G., Beraldo, F.H., Guimarães, A.L.S., Mishra, S., Guzman, M., Fan, J., Martins, V.R., Prado, V.F., Prado, M.A.M., Guimaraes, A.L., Mishra, S., Guzman, M., Fan, J., Martins, J.R., Prado, V.F., Prado, M.A.M., 2013. Increased prion protein processing and expression of metabotropic glutamate receptor 1 in a mouse model of Alzheimer's disease. J Neurochem 127, 415–425.

Otani, S., Ben-Ari, Y., 1991. Metabotropic receptor-mediated long-term potentiation in rat hippocampal slices. Eur. J. Pharmacol. 205, 325–326.

Otsuka, K., Mizuguchi, M., Aizawa, T., Haga, S., Sato, M., Inoya, H., Namba, Y., Hofbauer, J., Marberger, M., 1994. Immunoreactivity in Alzheimer's neurofibrillary tangles. Brain Pathol 4, 558.

Ott, M.O., Bullock, S.L., 2001. A gene trap insertion reveals that amyloid precursor protein expression is a very early event in murine embryogenesis. Dev. Genes Evol. 211, 355–7.

Ottersen, O.P., Landsend, A.S., 1997. Organization of glutamate receptors at the synapse. Eur. J. Neurosci. 9, 2219–2224.

Oules, B., Del Prete, D., Greco, B., Zhang, X., Lauritzen, I., Sevalle, J., Moreno, S., Paterlini-Brechot, P., Trebak, M., Checler, F., Benfenati, F., Chami, M., Oulès, B., Del Prete, D., Greco, B., Zhang, X., Lauritzen, I., Sevalle, J., Moreno, S., Paterlini-Bréchot, P., Trebak, M., Checler, F., Benfenati, F., Chami, M., Oules, B., Del Prete, D., Greco, B., Zhang, X., Lauritzen, I., Sevalle, J., Moreno, S., Paterlini-Brechot, P., Trebak, M., Checler, F., Benfenati, F., Chami, M., 2012. Ryanodine Receptor Blockade Reduces Amyloid- Load and Memory Impairments in Tg2576 Mouse Model of Alzheimer Disease. J. Neurosci. 32, 11820–11834.

Outeiro, T.F., Marques, O., Kazantsev, A., 2008. Therapeutic role of sirtuins in neurodegenerative disease. Biochim. Biophys. Acta - Mol. Basis Dis. 1782, 363–369.

Page, G., Khidir, F.A.L., Pain, S., Barrier, L., Fauconneau, B., Guillard, O., Piriou, A., Hugon, J., 2006. Group I metabotropic glutamate receptors activate the p70S6 kinase via both mammalian target of rapamycin (mTOR) and extracellular signal-regulated kinase (ERK 1/2) signaling pathways in rat striatal and hippocampal synaptoneurosomes. Neurochem. Int. 49, 413–421.

Pahl, H.L., Baeuerle, P.A., 1996. Activation of NF-kappa B by ER stress requires both Ca2+ and reactive oxygen intermediates as messengers. FEBS Lett. 392, 129–36.

Palmer, A.E., Jin, C., Reed, J.C., Tsien, R.Y., 2004. Bcl-2-mediated alterations in endoplasmic reticulum Ca2+ analyzed with an improved genetically encoded fluorescent sensor. Proc. Natl. Acad. Sci. 101, 17404–17409.

Palop, J.J., Chin, J., Roberson, E.D., Wang, J., Thwin, M.T., Bien-Ly, N., Yoo, J., Ho, K.O., Yu, G.-Q., Kreitzer, A., Finkbeiner, S., Noebels, J.L., Mucke, L., 2007. Aberrant Excitatory Neuronal Activity and Compensatory Remodeling of Inhibitory Hippocampal Circuits in

Mouse Models of Alzheimer's Disease. Neuron 55, 697–711.

Palop, J.J., Jones, B., Kekonius, L., Chin, J., Yu, G.-Q., Raber, J., Masliah, E., Mucke, L., 2003. Neuronal depletion of calcium-dependent proteins in the dentate gyrus is tightly linked to Alzheimer's disease-related cognitive deficits. Proc. Natl. Acad. Sci. 100, 9572–9577.

Palty, R., Hershfinkel, M., Sekler, I., 2012. Molecular Identity and Functional Properties of the Mitochondrial Na^+/Ca^{2+} Exchanger. J. Biol. Chem. 287, 31650–31657.

Papadimitriou, J.C., Ioffe, O.R., Castellani, R.J., Simons, J., Drachenberg, C.B., 1996. Shifting of cytoplasmic pattern of bcl-2 expression in reactive and preneoplastic lesions to nuclear pattern in their malignant counterparts. Cancer Detect. Prev. 20.

Paradis, E., Douillard, H., Koutroumanis, M., Goodyer, C., LeBlanc, A., 1996. Amyloid beta peptide of Alzheimer's disease downregulates Bcl-2 and upregulates bax expression in human neurons. J. Neurosci. 16, 7533–9.

Pardossi-Piquard, R., Petit, A., Kawarai, T., Sunyach, C., Alves da Costa, C., Vincent, B., Ring, S., D'Adamio, L., Shen, J., Müller, U., Hyslop, P.S.G., Checler, F., 2005. Presenilin-Dependent Transcriptional Control of the Aβ-Degrading Enzyme Neprilysin by Intracellular Domains of βAPP and APLP. Neuron 46, 541–554.

Parekh, A.B., Putney, J.W., 2005. Store-Operated Calcium Channels. Physiol. Rev. 85, 757–810.

Parihar, M.S., Brewer, G.J., 2007. Simultaneous age-related depolarization of mitochondrial membrane potential and increased mitochondrial reactive oxygen species production correlate with age-related glutamate excitotoxicity in rat hippocampal neurons. J. Neurosci. Res. 85, 1018–32.

Park, K.-H., Kim, B.-J., Kang, J., Nam, T.-S., Lim, J.M., Kim, H.T., Park, J.K., Kim, Y.G., Chae, S.-W., Kim, U.-H., 2011. Ca2+ Signaling Tools Acquired from Prostasomes Are Required for Progesterone-Induced Sperm Motility. Sci. Signal. 4, ra31-ra31.

Park, L., Wang, G., Moore, J., Girouard, H., Zhou, P., Anrather, J., Iadecola, C., 2014. The key role of transient receptor potential melastatin-2 channels in amyloid-?-induced neurovascular dysfunction. Nat. Commun. 5, 5318.

Park, S.A., Shaked, G.M., Bredesen, D.E., Koo, E.H., 2009. Mechanism of cytotoxicity mediated by the C31 fragment of the amyloid precursor protein. Biochem. Biophys. Res. Commun. 388, 450–455.

Park, Y.J., Woo, M., Kieffer, T.J., Hakem, R., Safikhan, N., Yang, F., Ao, Z., Warnock, G.L., Marzban, L., 2014. The role of caspase-8 in amyloid-induced beta cell death in human and mouse islets. Diabetologia 57, 765–775.

Parsadanian, A.S., Elliott, J.L., Snider, W.D., 1995. Multiple Ced-3 and Ced-9 homologues are expressed in the murine nervous system. Soc Neurosci Abstr 21.

Partida-Sánchez, S., Cockayne, D.A., Monard, S., Jacobson, E.L., Oppenheimer, N., Garvy, B., Kusser, K., Goodrich, S., Howard, M., Harmsen, a, Randall, T.D., Lund, F.E., 2001. Cyclic ADP-ribose production by CD38 regulates intracellular calcium release, extracellular calcium influx and chemotaxis in neutrophils and is required for bacterial clearance in vivo. Nat. Med. 7, 1209–1216.

Partridge, L.D., Müller, T.H., Swandulla, D., 1994. Calcium-activated non-selective channels in the nervous system. Brain Res. Brain Res. Rev. 19, 319–25.

Parys, J.B., 2014. The IP3 Receptor as a Hub for Bcl-2 Family Proteins in Cell Death Control and Beyond. Sci. Signal. 7, pe4-pe4.

Parys, J.B., de Smedt, H., Missiaen, L., Bootman, M.D., Sienaert, I., Casteels, R., 1995. Rat basophilic leukemia cells as model system for inositol 1,4,5-trisphosphate receptor IV, a receptor of the type II family: functional comparison and immunological detection. Cell Calcium 17, 239–49.

Passer, B.J., Pellegrini, L., Vito, P., Ganjei, J.K., D'Adamio, L., 1999. Interaction of Alzheimer's presenilin-1 and presenilin-2 with Bcl-X(L). A potential role in modulating the threshold of cell death. J. Biol. Chem. 274, 24007–13.

Patterson, R.L., Boehning, D., Snyder, S.H., 2004. Inositol 1,4,5-Trisphosphate Receptors as Signal Integrators. Annu. Rev. Biochem. 73, 437–465.

Paula-Lima, A.C., Adasme, T., SanMartín, C., Sebollela, A., Hetz, C., Carrasco, M.A., Ferreira, S.T., Hidalgo, C., 2011. Amyloid β-Peptide Oligomers Stimulate RyR-Mediated Ca^{2+} Release Inducing Mitochondrial Fragmentation in Hippocampal Neurons and Prevent RyR-Mediated Dendritic Spine Remodeling Produced by BDNF. Antioxid. Redox Signal. 14, 1209–1223.

Pawlikowska, L., Cottrell, S.E., Harms, M.B., Li, Y., Rosenberg, P.A., 1996. Extracellular synthesis of cADP-ribose from nicotinamide-adenine dinucleotide by rat cortical astrocytes in culture. J. Neurosci. 16, 5372–81.

Payne, A.J., Kaja, S., Koulen, P., 2015. Regulation of ryanodine receptor-mediated calcium signaling by presenilins. Recept. Clin. Investig. 2, e449.

Pearson, H.A., Peers, C., 2006. Physiological roles for amyloid beta peptides. J. Physiol. 575, 5–10.

Pekny, M., Pekna, M., 2016. Reactive gliosis in the pathogenesis of CNS diseases. Biochim. Biophys. Acta - Mol. Basis Dis. 1862, 483–491.

Pellerin, L., Magistretti, P.J., 1994. Glutamate uptake into astrocytes stimulates aerobic glycolysis: a mechanism coupling neuronal activity to glucose utilization. Proc. Natl. Acad. Sci. U. S. A. 91, 10625–9.

Pellerin, L., Pellegri, G., Bittar, P.G., Charnay, Y., Bouras, C., Martin, J.L., Stella, N., Magistretti, P.J., 1998. Evidence supporting the existence of an activity-dependent astrocyte-neuron lactate shuttle. Dev. Neurosci. 20, 291–9.

Peppiatt, C.M., Collins, T.J., Mackenzie, L., Conway, S.J., Holmes, A.B., Bootman, M.D., Berridge, M.J., Seo, J.T., Roderick, H.L., 2003. 2-Aminoethoxydiphenyl borate (2-APB) antagonises inositol 1,4,5-trisphosphate-induced calcium release, inhibits calcium pumps and has a use-dependent and slowly reversible action on store-operated calcium entry channels. Cell Calcium 34, 97–108.

Perraud, A.-L., Fleig, A., Dunn, C.A., Bagley, L.A., Launay, P., Schmitz, C., Stokes, A.J., Zhu, Q., Bessman, M.J., Penner, R., Kinet, J.-P., Scharenberg, A.M., 2001. No Title. Nature 411, 595–599.

Perroy, J., Raynaud, F., Homburger, V., Rousset, M.-C., Telley, L., Bockaert, J., Fagni, L., 2008a. Direct Interaction Enables Cross-talk between Ionotropic and Group I Metabotropic Glutamate Receptors. J. Biol. Chem. 283, 6799–6805.

Perroy, J., Raynaud, F., Homburger, V., Rousset, M.-C., Telley, L., Bockaert, J., Fagni, L., 2008b. Direct interaction enables cross-talk between ionotropic and group I metabotropic glutamate receptors. J. Biol. Chem. 283.

Perry, G., Cash, A.D., Smith, M.A., 2002. Alzheimer Disease and Oxidative Stress. J. Biomed. Biotechnol. 2, 120–123.

Perry, G., Nunomura, A., Raina, A.K., Smith, M.A., 2000. Amyloid-β junkies. Lancet 355, 757.

Petralia, R.S., Wang, Y.-X., Singh, S., Wu, C., Shi, L., Wei, J., Wenthold, R.J., 1997. A monoclonal antibody shows discrete cellular and subcellular localizations of mGluR1α metabotropic glutamate receptors. J. Chem. Neuroanat. 13, 77–93.

Pfrieger, F.W., 2003. Cholesterol homeostasis and function in neurons of the central nervous system. Cell. Mol. Life Sci. 60, 1158–1171.

Pfrieger, F.W., Barres, B.A., 1997. Synaptic efficacy enhanced by glial cells in vitro. Science 277, 1684–7.

Pierce, K.L., Premont, R.T., Lefkowitz, R.J., 2002. Signalling: Seven-transmembrane receptors. Nat. Rev. Mol. Cell Biol. 3, 639–650.

Pierrot, N., Ferrao Santos, S., Feyt, C., Morel, M., Brion, J.-P., Octave, J.-N., 2006. Calcium-mediated transient phosphorylation of tau and amyloid precursor protein followed by intraneuronal amyloid-β accumulation. J. Biol. Chem. 281.

Pierrot, N., Ghisdal, P., Caumont, A.-S., Octave, J.-N., 2004. Intraneuronal amyloid-β1-42 production triggered by sustained increase of cytosolic calcium concentration induces neuronal death. J. Neurochem. 88, 1140–1150.

Pinheiro, P.S., Mulle, C., 2008. Presynaptic glutamate receptors: physiological functions and mechanisms of action. Nat. Rev. Neurosci. 9, 423–436.

Pinton, P., Ferrari, D., Magalhães, P., Schulze-Osthoff, K., Di Virgilio, F., Pozzan, T., Rizzuto, R., 2000. Reduced loading of intracellular Ca(2+) stores and downregulation of capacitative Ca(2+) influx in Bcl-2-overexpressing cells. J. Cell Biol. 148, 857–62.

Pinton, P., Giorgi, C., Siviero, R., Zecchini, E., Rizzuto, R., 2008. Calcium and apoptosis: ER-mitochondria Ca2+ transfer in the control of apoptosis. Oncogene 27, 6407–6418.

Pinton, P., Rizzuto, R., 2006. Bcl-2 and Ca2+ homeostasis in the endoplasmic reticulum. Cell Death Differ. 13, 1409–1418.

Pisani, A., Calabresi, P., Centonze, D., Bernardi, G., 1997. Enhancement of NMDA responses by group I metabotropic glutamate receptor activation in striatal neurones. Br. J. Pharmacol. 120, 1007–14.

Pitas, R.E., Boyles, J.K., Lee, S.H., Hui, D., Weisgraber, K.H., 1987. Lipoproteins and their receptors in the central nervous system. Characterization of the lipoproteins in cerebrospinal fluid and identification of apolipoprotein B,E(LDL) receptors in the brain. J. Biol. Chem. 262, 14352–60.

Pollak, N., Niere, M., Ziegler, M., 2007. NAD Kinase Levels Control the NADPH Concentration in Human Cells. J. Biol. Chem. 282, 33562–33571.

Pollock, J., Crawford, J.H., Wootton, J.F., Seabrook, G.R., Scott, R.H., 1999. Metabotropic glutamate receptor activation and intracellular cyclic ADP-ribose release Ca2+ from the same store in cultured DRG neurones. Cell Calcium 26, 139–148.

Polvikoski, T., Sulkava, R., Haltia, M., Kainulainen, K., Vuorio, A., Verkkoniemi, A., Niinistö, L., Halonen, P., Kontula, K., 1995. Apolipoprotein E, Dementia, and Cortical Deposition of β-Amyloid Protein. N. Engl. J. Med. 333, 1242–1248.

Poon, W.W., Carlos, A.J., Cotman, C.W., Rohn, T.T., 2010. Overexpression of Bcl-2 in APP transgenic mice reduces amyloid pathology. Alzheimer's Dement. 6, S376.

Poppek, D., Keck, S., Ermak, G., Jung, T., Stolzing, A., Ullrich, O., Davies, K.J.A., Grune, T., 2006. Phosphorylation inhibits turnover of the tau protein by the proteasome: influence of *RCAN1* and oxidative stress. Biochem. J. 400, 511–520.

Popugaeva, E., Bezprozvanny, I., 2013. Role of endoplasmic reticulum Ca2+ signaling in the pathogenesis of Alzheimer disease. Front. Mol. Neurosci. 6, 29.

Popugaeva, E., Supnet, C., Bezprozvanny, I., 2012. Presenilins, Deranged Calcium Homeostasis, Synaptic Loss and Dysfunction in Alzheimer's Disease. Messenger 1, 53–62.

Posse De Chaves, E.I., Vance, D.E., Campenot, R.B., Kiss, R.S., Vance, J.E., 2000. Uptake of lipoproteins for axonal growth of sympathetic neurons. J. Biol. Chem. 275, 19883–90.

Pozzi, D., Ban, J., Iseppon, F., Torre, V., 2017. An improved method for growing neurons: Comparison with standard protocols. J. Neurosci. Methods 280, 1–10.

Prasad, G.S., McRee, D.E., Stura, E.A., Levitt, D.G., Lee, H.C., Stout, C.D., 1996. Crystal structure of Aplysia ADP ribosyl cyclase, a homologue of the bifunctional ectozyme CD38. Nat. Struct. Biol. 3, 957–64.

Price, P.J., Brewer, G.J., 2001. Serum-Free Media for Neural Cell Cultures: Adult and Embryonic. In: Protocols for Neural Cell Culture. Humana Press, New Jersey, pp. 255–264.

Priller, C., Dewachter, I., Vassallo, N., Paluch, S., Pace, C., Kretzschmar, H.A., Van Leuven, F., Herms, J., 2007. Mutant presenilin 1 alters synaptic transmission in cultured hippocampal neurons. J. Biol. Chem. 282, 1119–27.

Prins, D., Michalak, M., 2011. Organellar Calcium Buffers. Cold Spring Harb. Perspect. Biol. 3, a004069–a004069.

Prybylowski, K., Chang, K., Sans, N., Kan, L., Vicini, S., Wenthold, R.J., 2005. The synaptic localization of NR2B-containing NMDA receptors is controlled by interactions with PDZ proteins and AP-2. Neuron 47.

Puschmann, T.B., Zandén, C., De Pablo, Y., Kirchhoff, F., Pekna, M., Liu, J., Pekny, M., 2013. Bioactive 3D cell culture system minimizes cellular stress and maintains the in vivo-like morphological complexity of astroglial cells. Glia 61.

Putney, J.W., 2003. Capacitative calcium entry in the nervous system. Cell Calcium 34, 339–344.

Qin, W., Yang, T., Ho, L., Zhao, Z., Wang, J., Chen, L., Zhao, W., Thiyagarajan, M., MacGrogan, D., Rodgers, J.T., Puigserver, P., Sadoshima, J., Deng, H., Pedrini, S., Gandy, S., Sauve, A.A., Pasinetti, G.M., 2006. Neuronal SIRT1 activation as a novel mechanism underlying the prevention of Alzheimer disease amyloid neuropathology by calorie restriction. J. Biol. Chem. 281, 21745–54.

Qin, Z., Zhou, X., Gomez-Smith, M., Pandey, N.R., Lee, K.F.H., Lagace, D.C., Béïque, J.-C., Chen, H.-H., 2012. LIM Domain Only 4 (LMO4) Regulates Calcium-Induced Calcium Release and Synaptic Plasticity in the Hippocampus. J. Neurosci. 32.

Qiu, A., Fennema-Notestine, C., Dale, A.M., Miller, M.I., 2009. Regional shape abnormalities in mild cognitive impairment and Alzheimer's disease. Neuroimage 45, 656–661.

Quarona, V., Zaccarello, G., Chillemi, A., Brunetti, E., Singh, V.K., Ferrero, E., Funaro, A., Horenstein, A.L., Malavasi, F., 2013. CD38 and CD157: A long journey from activation markers to multifunctional molecules. Cytom. Part B - Clin. Cytom. 84, 207–217.

Querfurth, H.W., Jiang, J., Geiger, J.D., Selkoe, D.J., 1997. Caffeine stimulates amyloid beta-peptide release from beta-amyloid precursor protein-transfected HEK293 cells. J. Neurochem. 69, 1580–91.

Querfurth, H.W., LaFerla, F.M., 2010. Alzheimer's Disease. N. Engl. J. Med. 362, 329–344.

Querfurth, H.W., Selkoe, D.J., 1994. Calcium ionophore increases amyloid beta peptide production by cultured cells. Biochemistry 33, 4550–61.

Rae, M.., Irving, A.J., 2003. Metabotropic glutamate receptors (mGluRs) and dynamic endoplasmic reticulum (ER) loading in CA1 pyramidal neurons. In: Soc. Neuroscience Abs. (801.6).

Rae, M.G., Hilton, J., Sharkey, J., 2012. Putative TRP channel antagonists, SKF 96365, flufenamic acid and 2-APB, are non-competitive antagonists at recombinant human α1β2γ2 GABAA receptors. Neurochem. Int. 60, 543–554.

Rae, M.G., Irving, A.J., 2004. Both mGluR1 and mGluR5 mediate Ca2+ release and inward currents in hippocampal CA1 pyramidal neurons. Neuropharmacology 46, 1057–1069.

Rae, M.G., Martin, D.J., Collingridge, G.L., Irving, a J., 2000. Role of Ca2+ stores in metabotropic L-glutamate receptor-mediated supralinear Ca2+ signaling in rat hippocampal neurons. J. Neurosci. 20, 8628–8636.

Raff, M.C., Fields, K.L., Hakomori, S.I., Mirsky, R., Pruss, R.M., Winter, J., 1979. Cell-type-specific markers for distinguishing and studying neurons and the major classes of glial cells in culture. Brain Res. 174, 283–308.

Rah, S.-Y., Park, K.-H., Han, M.-K., Im, M.-J., Kim, U.-H., 2005. Activation of CD38 by Interleukin-8 Signaling Regulates Intracellular Ca2+ Level and Motility of Lymphokine-activated Killer Cells. J. Biol. Chem. 280, 2888–2895.

Rakovic, S., Galione, A., Ashamu, G.A., Potter, B. V, Terrar, D.A., 1996. A specific cyclic ADP-ribose antagonist inhibits cardiac excitation-contraction coupling. Curr. Biol. 6, 989–96.

Rammes, G., Hasenjäger, A., Sroka-Saidi, K., Deussing, J.M., Parsons, C.G., 2011. Therapeutic significance of NR2B-containing NMDA receptors and mGluR5 metabotropic glutamate receptors in mediating the synaptotoxic effects of β-amyloid oligomers on long-term potentiation (LTP) in murine hippocampal slices. Neuropharmacology 60.

Rao, S.P., Sikdar, S.K., 2004. Estradiol-induced changes in the activity of hippocampal neurons in network culture are suppressed by co-incubation with gabapentin. Brain Res. 1022, 126–36.

Reed, J.M., Squire, L.R., 1997. Impaired recognition memory in patients with lesions limited to the hippocampal formation. Behav. Neurosci. 111, 667–75.

Reitz, C., Brickman, A.M., Brown, T.R., Manly, J., DeCarli, C., Small, S.A., Mayeux, R., 2009. Linking Hippocampal Structure and Function to Memory Performance in an Aging Population. Arch. Neurol. 66, 1385–92.

Renner, M., Lacor, P.N.N., Velasco, P.T.T., Xu, J., Contractor, A., Klein, W.L.L., Triller, A., 2010. Deleterious effects of amyloid beta oligomers acting as an extracellular scaffold for mGluR5. Neuron 66.

Renner, M., Specht, C.G., Triller, A., 2008. Molecular dynamics of postsynaptic receptors and scaffold proteins. Curr. Opin. Neurobiol. 18.

Rensen, P.C., Jong, M.C., van Vark, L.C., van der Boom, H., Hendriks, W.L., van Berkel, T.J., Biessen, E.A., Havekes, L.M., 2000. Apolipoprotein E is resistant to intracellular degradation in vitro and in vivo. Evidence for retroendocytosis. J. Biol. Chem. 275, 8564–71.

Resende, R., Ferreiro, E., Pereira, C., Resende de Oliveira, C., 2008. Neurotoxic effect of oligomeric and fibrillar species of amyloid-beta peptide 1-42: Involvement of endoplasmic reticulum calcium release in oligomer-induced cell death. Neuroscience 155, 725–737.

Resh, M.D., 1998. Fyn, a Src family tyrosine kinase. Int. J. Biochem. Cell Biol. 30, 1159–62.

Reyes-Harde, M., Empson, R., Potter, B.V.L., Galione, A., Stanton, P.K., 1999a. Evidence of a role for cyclic ADP-ribose in long-term synaptic depression in hippocampus. Proc. Natl. Acad. Sci. U. S. A. 96, 4061–6.

Reyes-Harde, M., Potter, B. V, Galione, A., Stanton, P.K., 1999b. Induction of hippocampal LTD requires nitric-oxide-stimulated PKG activity and Ca2+ release from cyclic ADP-ribose-sensitive stores. J. Neurophysiol. 82, 1569–76.

Ribeiro, S., Gervasoni, D., Soares, E.S., Zhou, Y., Lin, S.-C., Pantoja, J., Lavine, M., Nicolelis, M.A.L., 2004. Long-lasting novelty-induced neuronal reverberation during slow-wave sleep in multiple forebrain areas. PLoS Biol. 2, E24.

Ring, S., Weyer, S.W., Kilian, S.B., Waldron, E., Pietrzik, C.U., Filippov, M.A., Herms, J., Buchholz, C., Eckman, C.B., Korte, M., Wolfer, D.P., Muller, U.C., 2007. The Secreted -Amyloid Precursor Protein Ectodomain APPs Is Sufficient to Rescue the Anatomical, Behavioral, and Electrophysiological Abnormalities of APP-Deficient Mice. J. Neurosci. 27, 7817–7826.

Rissman, R.A., Poon, W.W., Blurton-Jones, M., Oddo, S., Torp, R., Vitek, M.P., LaFerla, F.M., Rohn, T.T., Cotman, C.W., 2004. Caspase-cleavage of tau is an early event in Alzheimer disease tangle pathology. J. Clin. Invest. 114, 121–130.

Rizzuto, R., Brini, M., Murgia, M., Pozzan, T., 1993. Microdomains with high Ca2+ close to IP3-sensitive channels that are sensed by neighboring mitochondria. Science 262, 744–7.

Rizzuto, R., De Stefani, D., Raffaello, A., Mammucari, C., 2012. Mitochondria as sensors and regulators of calcium signalling. Nat. Rev. Mol. Cell Biol. 13, 566–578.

Rizzuto, R., Marchi, S., Bonora, M., Aguiari, P., Bononi, A., De Stefani, D., Giorgi, C., Leo, S., Rimessi, A., Siviero, R., Zecchini, E., Pinton, P., 2009. Ca^{2+} transfer from the ER to mitochondria: When, how and why. Biochim. Biophys. Acta - Bioenerg. 1787.

Roberson, E.D., Halabisky, B., Yoo, J.W., Yao, J., Chin, J., Yan, F., Wu, T., Hamto, P., Devidze, N., Yu, G.-Q., Palop, J.J., Noebels, J.L., Mucke, L., 2011. Amyloid-β/fyn-induced synaptic, network, and cognitive impairments depend on tau levels in multiple mouse models of alzheimer's disease. J. Neurosci. 31.

Roberts, G.W., Gentleman, S.M., Lynch, A., Murray, L., Landon, M., Graham, D.I., 1994. Beta amyloid protein deposition in the brain after severe head injury: implications for the pathogenesis of Alzheimer's disease. J. Neurol. Neurosurg. Psychiatry 57, 419–25.

Robinson, J.L., Molina-Porcel, L., Corrada, M.M., Raible, K., Lee, E.B., Lee, V.M.-Y., Kawas, C.H., Trojanowski, J.Q., 2014. Perforant path synaptic loss correlates with cognitive impairment and Alzheimer's disease in the oldest-old. Brain 137, 2578–2587.

Roderick, H.L., Cook, S.J., 2008. Ca2+ signalling checkpoints in cancer: Remodelling Ca 2+ for cancer cell proliferation and survival. Nat. Rev. Cancer 8.

Rogaeva, E., Meng, Y., Lee, J.H., Gu, Y., Kawarai, T., Zou, F., Katayama, T., Baldwin, C.T., Cheng, R., Hasegawa, H., Chen, F., Shibata, N., Lunetta, K.L., Pardossi-Piquard, R., Bohm, C., Wakutani, Y., Cupples, L.A., Cuenco, K.T., Green, R.C., Pinessi, L., Rainero, I., Sorbi, S., Bruni, A., Duara, R., Friedland, R.P., Inzelberg, R., Hampe, W., Bujo, H., Song, Y.-Q., Andersen, O.M., Willnow, T.E., Graff-Radford, N., Petersen, R.C., Dickson, D., Der, S.D., Fraser, P.E., Schmitt-Ulms, G., Younkin, S., Mayeux, R., Farrer, L.A., St George-Hyslop, P., 2007. The neuronal sortilin-related receptor SORL1 is genetically associated with Alzheimer disease. Nat. Genet. 39, 168–177.

Rohn, T.T., 2010. The role of caspases in Alzheimer's disease; potential novel therapeutic opportunities. Apoptosis 15, 1403–1409.

Rohn, T.T., Rissman, R.A., Davis, M.C., Kim, Y.E., Cotman, C.W., Head, E., 2002. Caspase-9 activation and caspase cleavage of tau in the Alzheimer's disease brain. Neurobiol. Dis. 11, 341–54.

Rohn, T.T., Vyas, V., Hernandez-Estrada, T., Nichol, K.E., Christie, L.-A., Head, E., 2008. Lack of Pathology in a Triple Transgenic Mouse Model of Alzheimer's Disease after Overexpression of the Anti-Apoptotic Protein Bcl-2. J. Neurosci. 28.

Rojas, G., Cárdenas, A.M., Fernández-Olivares, P., Shimahara, T., Segura-Aguilar, J., Caviedes, R., Caviedes, P., 2008. Effect of the knockdown of amyloid precursor protein on intracellular calcium increases in a neuronal cell line derived from the cerebral cortex of a trisomy 16 mouse. Exp. Neurol. 209, 234–242.

Romanello, M., Bicego, M., Pirulli, D., Crovella, S., Moro, L., D'Andrea, P., 2002. Extracellular NAD+: a novel autocrine/paracrine signal in osteoblast physiology. Biochem. Biophys. Res. Commun. 299, 424–31.

Rong, Y.-P., Aromolaran, A.S., Bultynck, G., Zhong, F., Li, X., McColl, K., Matsuyama, S., Herlitze, S., Roderick, H.L., Bootman, M.D., Mignery, G.A., Parys, J.B., De Smedt, H., Distelhorst, C.W., 2008. Targeting Bcl-2-IP3 receptor interaction to reverse Bcl-2's inhibition of apoptotic calcium signals. Mol. Cell 31, 255–65.

Rong, Y.-P., Bultynck, G., Aromolaran, A.S., Zhong, F., Parys, J.B., De Smedt, H., Mignery, G.A., Roderick, H.L., Bootman, M.D., Distelhorst, C.W., 2009. The BH4 domain of Bcl-2 inhibits ER calcium release and apoptosis by binding the regulatory and coupling domain of the IP3 receptor. Proc. Natl. Acad. Sci. U. S. A. 106, 14397–402.

Roos, J., DiGregorio, P.J., Yeromin, A. V., Ohlsen, K., Lioudyno, M., Zhang, S., Safrina, O., Kozak, J.A., Wagner, S.L., Cahalan, M.D.,

Veliçelebi, G., Stauderman, K.A., 2005. STIM1, an essential and conserved component of store-operated Ca2+ channel function. J. Cell Biol. 169.

Rose, C.R., Konnerth, A., 2001. Stores Not Just for Storage: Intracellular Calcium Release and Synaptic Plasticity. Neuron 31, 519–522.

Roses, A.D., 1996. Apolipoprotein e alleles as risk factors in Alzheimer's disease. Annu. Rev. Med. 47, 387–400.

Roses, A.D., 2006. On the discovery of the genetic association of Apolipoprotein E genotypes and common late-onset Alzheimer disease. J. Alzheimers. Dis. 9, 361–6.

Roses, A.D., Saunders, A.M., Alberts, M.A., Strittmatter, W.J., Schmechel, D., Gorder, E., Pericak-Vance, M.A., 1995. Apolipoprotein E E4 allele and risk of dementia. JAMA 273, 374-5; author reply 375-6.

Rossi, B., Maton, G., Collin, T., 2008. Calcium-permeable presynaptic AMPA receptors in cerebellar molecular layer interneurones. J. Physiol. 586, 5129–5145.

Rubio-Moscardo, F., Setó-Salvia, N., Pera, M., Bosch-Morató, M., Plata, C., Belbin, O., Gené, G., Dols-Icardo, O., Ingelsson, M., Helisalmi, S., Soininen, H., Hiltunen, M., Giedraitis, V., Lannfelt, L., Frank, A., Bullido, M.J., Combarros, O., Sánchez-Juan, P., Boada, M., Tárraga, L., Pastor, P., Pérez-Tur, J., Baquero, M., Molinuevo, J.L., Sánchez-Valle, R., Fuentes-Prior, P., Fortea, J., Blesa, R., Muñoz, F.J., Lleó, A., Valverde, M.A., Clarimón, J., 2013. Rare variants in calcium homeostasis modulator 1 (CALHM1) found in early onset Alzheimer's disease patients alter calcium homeostasis. PLoS One 8, e74203.

Rumble, B., Retallack, R., Hilbich, C., Simms, G., Multhaup, G., Martins, R., Hockey, A., Montgomery, P., Beyreuther, K., Masters, C.L., 1989. Amyloid A4 Protein and Its Precursor in Down's Syndrome and Alzheimer's Disease. N. Engl. J. Med. 320, 1446–1452.

Rush, A.M., Wu, J., Rowan, M.J., Anwyl, R., 2002. Group I metabotropic glutamate receptor (mGluR)-dependent long-term depression mediated via p38 mitogen-activated protein kinase is inhibited by previous high-frequency stimulation and activation of mGluRs and protein kinase C in the rat dentate gyrus in vitro. J. Neurosci. 22, 6121–8.

Rybalchenko, V., Hwang, S.-Y., Rybalchenko, N., Koulen, P., 2008. The cytosolic N-terminus of presenilin-1 potentiates mouse ryanodine receptor single channel activity. Int. J. Biochem. Cell Biol. 40, 84–97.

Sáez-Valero, J., Angeretti, N., Forloni, G., 2000. Caspase-3 activation by beta-amyloid and prion protein peptides is independent from their neurotoxic effect. Neurosci. Lett. 293, 207–10.

Saido, T.C., Iwata, N., Tsubuki, S., Takaki, Y., Watanabe, K., Sekiguchi, M., Hosoki, E., Kawashima-Morishima, M., Lee, H.-J., Hama, E., Sekine-Aizawa, Y., 2000. Identification of the major Abeta1-42-degrading catabolic pathway in brain parenchyma: suppression leads to biochemical and pathological deposition. Nat. Med. 6, 143–150.

Saillé, C., Marin, P., Martinou, J.C., Nicole, A., London, J., Ceballos-Picot, I., 1999. Transgenic murine cortical neurons expressing human Bcl-2 exhibit increased resistance to amyloid beta-peptide neurotoxicity. Neuroscience 92, 1455–63.

Sajikumar, S., Li, Q., Abraham, W.C., Xiao, Z.C., 2009. Priming of short-term potentiation and synaptic tagging/capture mechanisms by ryanodine receptor activation in rat hippocampal CA1. Learn. Mem. 16, 178–86.

Salido, G.M., Sage, S.O., Rosado, J.A., 2009. Biochemical and functional properties of the store-operated Ca2+ channels. Cell. Signal. 21, 457–461.

Salmina, A.B., Komleva, Y.K., Lopatina, O.L., Gorina, Y. V., Malinovskaya, N.A., Pozhilenkova, E.A., Panina, Y.A., Zhukov, E.L., Medvedeva, N.N., 2014. CD38 and CD157 Expression: Glial Control of Neurodegeneration and Neuroinflammation. Messenger 3, 78–85.

Salmina, A.B., Okuneva, O.S., Malinovskaya, N.A., Taranushenko, T.E., Morgun, A. V., Mantorova, N.S., Mikhutkina, S. V., 2008. NAD+-dependent mechanisms of disturbances of viability of brain cells during the acute period of hypoxic-ischemic perinatal injury. Neurochem. J. 2, 215–221.

Salmina, A.B., Okuneva, O.S., Mikhutkina, S. V., Malinovskaya, N.A., Morgun, A. V., Zykova, L.D., Yudin, G. V., Laletin, D. V., Fursov, M.A., Frolova, O. V., Tagaeva, G.A., Bolshakova, E. V., 2011. Perinatal Hypoxic-Ischemic Brain Injury Affects the Glutamatergic Signal Transduction Coupled with Neuronal ADP-Ribosyl Cyclase Activity. Bull. Exp. Biol. Med. 150, 583–586.

Sammels, E., Parys, J.B., Missiaen, L., De Smedt, H., Bultynck, G., 2010. Intracellular Ca2+ storage in health and disease: A dynamic equilibrium. Cell Calcium 47, 297–314.

Sanan, D.A., Weisgraber, K.H., Russell, S.J., Mahley, R.W., Huang, D., Saunders, A., Schmechel, D., Wisniewski, T., Frangione, B., Roses, A.D., 1994. Apolipoprotein E associates with beta amyloid peptide of Alzheimer's disease to form novel monofibrils. Isoform apoE4 associates more efficiently than apoE3. J. Clin. Invest. 94, 860–869.

Sandbrink, R., Masters, C.L., Beyreuther, K., 1996. APP gene family. Alternative splicing generates functionally related isoforms. Ann. N. Y. Acad. Sci. 777, 281–7.

Sanderson, K.L., Butler, L., Ingram, V.M., 1997. Aggregates of a beta-amyloid peptide are required to induce calcium currents in neuron-like human teratocarcinoma cells: relation to Alzheimer's disease. Brain Res. 744, 7–14.

Sannerud, R., Declerck, I., Peric, A., Raemaekers, T., Menendez, G., Zhou, L., Veerle, B., Coen, K., Munck, S., De Strooper, B., Schiavo, G., Annaert, W., 2011. ADP ribosylation factor 6 (ARF6) controls amyloid precursor protein (APP) processing by mediating the endosomal sorting of BACE1. Proc. Natl. Acad. Sci. 108, E559–E568.

Sano, Y., Inamura, K., Miyake, A., Mochizuki, S., Yokoi, H., Matsushime, H., Furuichi, K., 2001. Immunocyte Ca2+ influx system mediated by LTRPC2 293, 1327–30.

SantaCruz, K., Lewis, J., Spires, T., Paulson, J., Kotilinek, L., Ingelsson, M., Guimaraes, A., DeTure, M., Ramsden, M., McGowan, E., Forster, C., Yue, M., Orne, J., Janus, C., Mariash, A., Kuskowski, M., Hyman, B., Hutton, M., Ashe, K.H., 2005. Tau Suppression in a Neurodegenerative Mouse Model Improves Memory Function. Science (80-.). 309, 476–481.

Sanz, J.M., Chiozzi, P., Ferrari, D., Colaianna, M., Idzko, M., Falzoni, S., Fellin, R., Trabace, L., Di Virgilio, F., 2009. Activation of Microglia by Amyloid ? Requires P2X7 Receptor Expression. J. Immunol. 182, 4378–4385.

Sastre, M., Steiner, H., Fuchs, K., Capell, A., Multhaup, G., Condron, M.M., Teplow, D.B., Haass, C., 2001. Presenilin-dependent γ-secretase processing of β-amyloid precursor protein at a site corresponding to the S3 cleavage of Notch. EMBO Rep. 2, 835–841.

Satou, T., Cummings, B.J., Cotman, C.W., 1995. Immunoreactivity for Bcl-2 protein within neurons in the Alzheimer's disease brain increases with disease severity. Brain Res. 697, 35–43.

Saura, C.A., Choi, S.-Y., Beglopoulos, V., Malkani, S., Zhang, D., Rao, B.S.S., Chattarji, S., Kelleher III, R.J., Kandel, E.R., Duff, K., Kirkwood, A., Shen, J., 2004. Loss of presenilin function causes impairments of memory and synaptic plasticity followed by age-dependent neurodegeneration. Neuron 42.

Scanlon, J.M., Brocard, J.B., Stout, A.K., Reynolds, I.J., 2000. Pharmacological investigation of mitochondrial Ca^{2+} transport in central neurons: Studies with CGP-37157, an inhibitor of the mitochondrial Na^{+} -Ca^{2+} exchanger. Cell Calcium 28.

Scemes, E., Giaume, C., 2006. Astrocyte calcium waves: What they are and what they do. Glia 54, 716–725.

Scheff, S.W., DeKosky, S.T., Price, D.A., 1990. Quantitative assessment of cortical synaptic density in Alzheimer's disease. Neurobiol. Aging

11, 29–37.

Schellenberg, G., Bird, T., Wijsman, E., Orr, H., Anderson, L., Nemens, E., White, J., Bonnycastle, L., Weber, J., Alonso, M., et, al., 1992. Genetic linkage evidence for a familial Alzheimer's disease locus on chromosome 14. Science (80-.). 258, 668–671.

Scheuner, D., Eckman, C., Jensen, M., Song, X., Citron, M., Suzuki, N., Bird, T.D., Hardy, J., Hutton, M., Kukull, W., Larson, E., Levy-Lahad, E., Viitanen, M., Peskind, E., Poorkaj, P., Schellenberg, G., Tanzi, R., Wasco, W., Lannfelt, L., Selkoe, D., Younkin, S., 1996. Secreted amyloid beta-protein similar to that in the senile plaques of Alzheimer's disease is increased in vivo by the presenilin 1 and 2 and APP mutations linked to familial Alzheimer's disease. Nat. Med. 2, 864–70.

Schiller, J., Schiller, Y., Clapham, D.E., 1998. NMDA receptors amplify calcium influx into dendritic spines during associative pre- and postsynaptic activation. Nat. Neurosci. 1, 114–8.

Schmid, F., Bruhn, S., Weber, K., Mittrücker, H.-W.W., Guse, A.H., 2011. CD38: A NAADP degrading enzyme. FEBS Lett. 585, 3544–3548.

Schmitt, H., Gozes, I., Littauer, U.Z., 1977. Decrease in levels and rates of synthesis of tubulin and actin in developing rat brain. Brain Res. 121, 327–42.

Schneider, I., Reverse, D., Dewachter, I., Ris, L., Caluwaerts, N., Kuiperi, C., Gilis, M., Geerts, H., Kretzschmar, H., Godaux, E., Moechars, D., Van Leuven, F., Herms, J., 2001. Mutant presenilins disturb neuronal calcium homeostasis in the brain of transgenic mice, decreasing the threshold for excitotoxicity and facilitating long-term potentiation. J. Biol. Chem. 276, 11539–44.

Schrader, L.A., Tasker, J.G., 1997. Modulation of multiple potassium currents by metabotropic glutamate receptors in neurons of the hypothalamic supraoptic nucleus. J. Neurophysiol. 78, 3428–37.

Schram, M.T., Trompet, S., Kamper, A.M., De Craen, A.J.M., Hofman, A., Euser, S.M., Breteler, M.M.B., Westendorp, R.G.J., 2007. Serum Calcium and Cognitive Function in Old Age. J. Am. Geriatr. Soc. 55, 1786–1792.

Schuber, F., Lund, F.E., 2004. Structure and enzymology of ADP-ribosyl cyclases: conserved enzymes that produce multiple calcium mobilizing metabolites. Curr. Mol. Med. 4, 249–261.

Schultz, G., Rosenthal, W., 1985. Principles of transmembranous signal transduction in the action of hormones and neurotransmitters. Arzneimittelforschung. 35, 1879–85.

Sclip, A., Antoniou, X., Colombo, A., Camici, G.G., Pozzi, L., Cardinetti, D., Feligioni, M., Veglianese, P., Bahlmann, F.H., Cervo, L., Balducci, C., Costa, C., Tozzi, A., Calabresi, P., Forloni, G., Borsello, T., 2011. c-Jun N-terminal kinase regulates soluble Aβ oligomers and cognitive impairment in AD mouse model. J. Biol. Chem. 286.

Scorrano, L., Oakes, S.A., Opferman, J.T., Cheng, E.H., Sorcinelli, M.D., Pozzan, T., Korsmeyer, S.J., 2003. BAX and BAK Regulation of Endoplasmic Reticulum Ca2+: A Control Point for Apoptosis. Science (80-.). 300, 135–139.

Segal, M.M., Baughman, R.W., Jones, K.A., Huettner, J.E., 1998. Mass cultures and microislands of neurons from postnatal rat brain. In: Banker, G. & Goslin, K. (Ed.), Culturing Nerve Cells. The MIT Press, Cambridge, Massachusetts, USA, pp. 339–370.

Seibenhener, M.L., Wooten, M.W., 2012. Isolation and Culture of Hippocampal Neurons from Prenatal Mice. J. Vis. Exp. 4–9.

Selkoe, D.J., 2002. Alzheimer's Disease Is a Synaptic Failure. Science (80-.). 298, 789–791.

Selkoe, D.J., Hardy, J., 2016. The amyloid hypothesis of Alzheimer's disease at 25 years. EMBO Mol. Med. 8, 595–608.

Selkoe, D.J., Schenk, D., 2003. Alzheimer's Disease: Molecular Understanding Predicts Amyloid-Based Therapeutics, Annual Review of Pharmacology and Toxicology.

Sepulveda, F.J., Parodi, J., Peoples, R.W., Opazo, C., Aguayo, L.G., 2010. Synaptotoxicity of Alzheimer Beta Amyloid Can Be Explained by Its Membrane Perforating Property. PLoS One 5, e11820.

Sergé, A., Fourgeaud, L., Hémar, A., Choquet, D., 2002. Receptor Activation and Homer Differentially Control the Lateral Mobility of Metabotropic Glutamate Receptor 5 in the Neuronal Membrane. J. Neurosci. 22.

Serretti, A., Artioli, P., Quartesan, R., De Ronchi, D., 2005. Genes involved in Alzheimer's disease, a survey of possible candidates. J. Alzheimers. Dis. 7, 331–53.

Sethi, J.K., Empson, R.M., Bailey, V.C., Potter, B. V, Galione, A., 1997. 7-Deaza-8-bromo-cyclic ADP-ribose, the first membrane-permeant, hydrolysis-resistant cyclic ADP-ribose antagonist. J. Biol. Chem. 272, 16358–63.

Sethi, J.K., Empson, R.M., Galione, A., 1996. Nicotinamide inhibits cyclic ADP-ribose-mediated calcium signalling in sea urchin eggs. Biochem. J. 319 (Pt 2, 613–617.

Sevigny, J., Chiao, P., Bussière, T., Weinreb, P.H., Williams, L., Maier, M., Dunstan, R., Salloway, S., Chen, T., Ling, Y., O'Gorman, J., Qian, F., Arastu, M., Li, M., Chollate, S., Brennan, M.S., Quintero-Monzon, O., Scannevin, R.H., Arnold, H.M., Engber, T., Rhodes, K., Ferrero, J., Hang, Y., Mikulskis, A., Grimm, J., Hock, C., Nitsch, R.M., Sandrock, A., 2016. The antibody aducanumab reduces Aβ plaques in Alzheimer's disease. Nature 537, 50–56.

Seymour-Laurent, K.J., Barish, M.E., 1995. Inositol 1,4,5-trisphosphate and ryanodine receptor distributions and patterns of acetylcholine- and caffeine-induced calcium release in cultured mouse hippocampal neurons. J. Neurosci. 15, 2592–608.

Shaham, S., 2005. Glia–Neuron Interactions in Nervous System Function and Development. In: Current Topics in Developmental Biology. pp. 39–66.

Shan, J., Betzenhauser, M.J., Kushnir, A., Reiken, S., Meli, A.C., Wronska, A., Dura, M., Chen, B.-X., Marks, A.R., 2010. Role of chronic ryanodine receptor phosphorylation in heart failure and ?-adrenergic receptor blockade in mice. J. Clin. Invest. 120, 4375–4387.

Shankar, G.M., Bloodgood, B.L., Townsend, M., Walsh, D.M., Selkoe, D.J., Sabatini, B.L., 2007. Natural Oligomers of the Alzheimer Amyloid- Protein Induce Reversible Synapse Loss by Modulating an NMDA-Type Glutamate Receptor-Dependent Signaling Pathway. J. Neurosci. 27, 2866–2875.

Shankar, G.M., Li, S., Mehta, T.H., Garcia-Munoz, A., Shepardson, N.E., Smith, I., Brett, F.M., Farrell, M.A., Rowan, M.J., Lemere, C.A., Regan, C.M., Walsh, D.M., Sabatini, B.L., Selkoe, D.J., 2008. Amyloid-β protein dimers isolated directly from Alzheimer's brains impair synaptic plasticity and memory. Nat. Med. 14, 837–842.

Sharp, A.H., McPherson, P.S., Dawson, T.M., Aoki, C., Campbell, K.P., Snyder, S.H., 1993. Differential immunohistochemical localization of inositol 1,4,5-trisphosphate- and ryanodine-sensitive Ca2+ release channels in rat brain. J. Neurosci. 13, 3051–63.

Shea, T.B., Ekinci, F.J., 1999. Biphasic effect of calcium influx on tau phosphorylation: Involvement of calcium-dependent phosphatase and kinase activities. J. Alzheimer's Dis. 1.

Shen, J., Kelleher, R.J., III, 2007. The presenilin hypothesis of Alzheimer's disease: evidence for a loss-of-function pathogenic mechanism. Proc. Natl. Acad. Sci. U. S. A. 104, 403–9.

Shen, W., Slaughter, M.M., 1998. Metabotropic and ionotropic glutamate receptors regulate calcium channel currents in salamander retinal ganglion cells. J. Physiol. 510, 815–828.

Sheng, M., Sabatini, B.L., Südhof, T.C., 2012. Synapses and Alzheimer's disease. Cold Spring Harb. Perspect. Biol. 4.

Shi, G., Partida-Sánchez, S., Misra, R.S., Tighe, M., Borchers, M.T., Lee, J.J., Simon, M.I., Lund, F.E., 2007. Identification of an alternative Gα $_q$ -dependent chemokine receptor signal transduction pathway in dendritic cells and granulocytes. J. Exp. Med. 204, 2705–2718.

Shideman, C.R., Reinardy, J.L., Thayer, S.A., 2009. γ-Secretase activity modulates store-operated Ca2+ entry into rat sensory neurons. Neurosci. Lett. 451, 124–128.

Shigemoto, R., Kinoshita, A., Wada, E., Nomura, S., Ohishi, H., Takada, M., Flor, P.J., Neki, A., Abe, T., Nakanishi, S., Mizuno, N., 1997. Differential presynaptic localization of metabotropic glutamate receptor subtypes in the rat hippocampus. J. Neurosci. Off. J. Soc. Neurosci. 17, 7503–7522.

Shilling, D., Mak, D.-O.D., Kang, D.E., Foskett, J.K., 2012. Lack of evidence for presenilins as endoplasmic reticulum Ca2+ leak channels. J. Biol. Chem. 287, 10933–44.

Shilling, D., Mu, M., Takano, H., Mak, D.D., Abel, T., Coulter, D.A., Foskett, J.K., 2014. Suppression of InsP 3 Receptor-Mediated Ca 2 ⁄ Signaling Alleviates Mutant Presenilin-Linked Familial Alzheimer ' s Disease Pathogenesis 34, 6910–6923.

Shimizu, S., Abt, A., Meucci, O., 2011. Bilaminar co-culture of primary rat cortical neurons and glia. J. Vis. Exp. 2–6.

Shimohama, S., Fujimoto, S., Sumida, Y., Tanino, H., 1998. Differential Expression of Rat Brain Bcl-2 Family Proteins in Development and Aging. Biochem. Biophys. Res. Commun. 252, 92–96.

Shirasaki, T., Harata, N., Akaike, N., 1994. Metabotropic glutamate response in acutely dissociated hippocampal CAI pyramidal neurones of the rat. J. Physiol. 475.

Shirwany, N.A., Payette, D., Xie, J., Guo, Q., 2007. The amyloid beta ion channel hypothesis of Alzheimer's disease. Neuropsychiatr. Dis. Treat. 3, 597–612.

Shmigol, A., Svichar, N., Kostyuk, P., Verkhratsky, A., 1996. Gradual caffeine-induced Ca2+ release in mouse dorsal root ganglion neurons is controlled by cytoplasmic and luminal Ca2+. Neuroscience 73, 1061–7.

Simakova, O., Arispe, N., 2007. The Cell-Selective Neurotoxicity of the Alzheimer's A Peptide Is Determined by Surface Phosphatidylserine and Cytosolic ATP Levels. Membrane Binding Is Required for A Toxicity. J. Neurosci. 27, 13719–13729.

Šimić, G., Babić Leko, M., Wray, S., Harrington, C., Delalle, I., Jovanov-Milošević, N., Bažadona, D., Buée, L., de Silva, R., Di Giovanni, G., Wischik, C., Hof, P.R., 2016. Tau Protein Hyperphosphorylation and Aggregation in Alzheimer's Disease and Other Tauopathies, and Possible Neuroprotective Strategies. Biomolecules 6, 6.

Simpson, P.B., John Challiss, R.A., Nahorski, S.R., 1995. Neuronal Ca2+ stores: activation and function. Trends Neurosci. 18, 299–306.

Simpson, P.B., Nahorski, S.R., Challiss, R.A., 1996. Agonist-evoked Ca2+ mobilization from stores expressing inositol 1,4,5-trisphosphate receptors and ryanodine receptors in cerebellar granule neurones. J. Neurochem. 67, 364–73.

Singaravelu, K., Deitmer, J.W., 2006. Calcium mobilization by nicotinic acid adenine dinucleotide phosphate (NAADP) in rat astrocytes. Cell Calcium 39, 143–153.

Sisodia, S.S., 1992. Beta-amyloid precursor protein cleavage by a membrane-bound protease. Proc. Natl. Acad. Sci. U. S. A. 89, 6075–9.

Sitsapesan, R., Williams, A.J., 1995. Cyclic ADP-ribose and related compounds activate sheep skeletal sarcoplasmic reticulum Ca2+ release channel. Am. J. Physiol. 268, C1235-40.

Sleegers, K., Brouwers, N., Bettens, K., Engelborghs, S., van Miegroet, H., De Deyn, P.P., Van Broeckhoven, C., 2009. No association between *CALHM1* and risk for Alzheimer dementia in a Belgian population. Hum. Mutat. 30, E570–E574.

Slunt, H.H., Thinakaran, G., Von Koch, C., Lo, A.C., Tanzi, R.E., Sisodia, S.S., 1994. Expression of a ubiquitous, cross-reactive homologue of the mouse beta-amyloid precursor protein (APP). J. Biol. Chem. 269, 2637–44.

Small, S.A., Schobel, S.A., Buxton, R.B., Witter, M.P., Barnes, C.A., 2011. A pathophysiological framework of hippocampal dysfunction in ageing and disease. Nat. Rev. Neurosci. 12, 585–601.

Smith, I.F., Hitt, B., Green, K.N., Oddo, S., LaFerla, F.M., 2005. Enhanced caffeine-induced Ca2+ release in the 3xTg-AD mouse model of Alzheimer's disease. J. Neurochem. 94, 1711–1718.

Snell, C.R., Snell, P.H., Richards, C.D., 1984. Degradation of NAD by synaptosomes and its inhibition by nicotinamide mononucleotide: implications for the role of NAD as a synaptic modulator. J. Neurochem. 43, 1610–5.

Snowdon, D.A., 1997. Aging and Alzheimer's disease: lessons from the Nun Study. Gerontologist 37, 150–6.

Snyder, E.M., Nong, Y., Almeida, C.G., Paul, S., Moran, T., Choi, E.Y., Nairn, A.C., Salter, M.W., Lombroso, P.J., Gouras, G.K., Greengard, P., 2005. Regulation of NMDA receptor trafficking by amyloid-β. Nat. Neurosci. 8, 1051–1058.

Soares, S., Thompson, M., White, T., Isbell, A., Yamasaki, M., Prakash, Y., Lund, F.E., Galione, A., Chini, E.N., 2007. NAADP as a second messenger: neither CD38 nor base-exchange reaction are necessary for in vivo generation of NAADP in myometrial cells. Am. J. Physiol. Cell Physiol. 292, C227–C239.

Sohn, J.-W., Yu, W.-J., Lee, D., Shin, H.-S., Lee, S.-H., Ho, W.-K., 2011. Cyclic ADP Ribose-Dependent Ca2+ Release by Group I Metabotropic Glutamate Receptors in Acutely Dissociated Rat Hippocampal Neurons. PLoS One 6, e26625.

Sohn, J.-W.W., Lee, D., Cho, H., Lim, W., Shin, H.-S.S., Lee, S.-H.H., Ho, W.-K.K., 2007. Receptor-specific inhibition of GABAB-activated K+ currents by muscarinic and metabotropic glutamate receptors in immature rat hippocampus. J. Physiol. 580, 411–422.

Sokol, D.K.K., Maloney, B., Long, J.M.M., Ray, B., Lahiri, D.K.K., 2011. Autism, Alzheimer disease, and fragile X: APP, FMRP, and mGluR5 are molecular links. Neurology 76, 1344–1352.

Sokolov, Y., Kozak, J.A., Kayed, R., Chanturiya, A., Glabe, C., Hall, J.E., 2006. Soluble Amyloid Oligomers Increase Bilayer Conductance by Altering Dielectric Structure. J. Gen. Physiol. 128, 637–647.

Solovyova, N., Fernyhough, P., Glazner, G., Verkhratsky, A., 2002. Xestospongin C empties the ER calcium store but does not inhibit InsP3-induced Ca2+ release in cultured dorsal root ganglia neurones. Cell Calcium 32, 49–52.

Sommer, B., Seeburg, P.H., 1992. Glutamate receptor channels: novel properties and new clones. Trends Pharmacol. Sci. 13, 291–296.

Song, Y.S., Park, H.J., Kim, S.Y., Lee, S.H., Yoo, H.S., Lee, H.S., Lee, M.K., Oh, K.W., Kang, S.-K., Lee, S.E., Hong, J.T., 2004. Protective role of Bcl-2 on β-amyloid-induced cell death of differentiated PC12 cells: reduction of NF-κB and p38 MAP kinase activation. Neurosci. Res. 49, 69–80.

Sonnleitner, A., Conti, A., Bertocchini, F., Schindler, H., Sorrentino, V., 1998. Functional properties of the ryanodine receptor type3 (RyR3) Ca2+ release channel. EMBO J. 17, 2790–2798.

Soriano, S., Lu, D.C., Chandra, S., Pietrzik, C.U., Koo, E.H., 2001. The Amyloidogenic Pathway of Amyloid Precursor Protein (APP) Is Independent of Its Cleavage by Caspases. J. Biol. Chem. 276, 29045–29050.

Sorrentino, G., Singh, I.N., Massarelli, R., Kanfer, J.N., 1996. Stimulation of phospholipase C activity by norepinephrine, t-ACPD and bombesin in LA-N-2 cells. Eur. J. Pharmacol. 308, 81–86.

Sparagna, G.C., Gunter, K.K., Sheu, S.-S., Gunter, T.E., 1995. Mitochondrial calcium uptake from physiological-type pulses of calcium: A description of the rapid uptake mode. J. Biol. Chem. 270.

Spasic, D., Tolia, A., Dillen, K., Baert, V., De Strooper, B., Vrijens, S., Annaert, W., 2006. Presenilin-1 Maintains a Nine-Transmembrane Topology throughout the Secretory Pathway. J. Biol. Chem. 281, 26569–26577.

Stahl, W.L., 1984. (Na+ + K+)-ATPase: Function, structure, and conformations. Ann. Neurol. 16, S121–S127.

Standaert, D., 1999. NMDA receptors and nitric oxide synthase. Mol. Psychiatry 4, 13–14.

Starkus, J., Beck, A., Fleig, A., Penner, R., 2007. Regulation of TRPM2 by Extra- and Intracellular Calcium. J. Gen. Physiol. 130, 427–440.

States, D.J., Walseth, T.F., Lee, H.C., 1992. Similarities in amino acid sequences of Aplysia ADP-ribosyl cyclase and human lymphocyte antigen CD38. Trends Biochem. Sci. 17, 495.

Staub, C., Vranesic, I., Knöpfel, T., 1992. Responses to Metabotropic Glutamate Receptor Activation in Cerebellar Purkinje Cells: Induction of an Inward Current. Eur. J. Neurosci. 4, 832–839.

Stein, L.R., Imai, S., 2012. The dynamic regulation of NAD metabolism in mitochondria. Trends Endocrinol. Metab. 23, 420–428.

Stein, T.D., Johnson, J.A., 2002. Lack of neurodegeneration in transgenic mice overexpressing mutant amyloid precursor protein is associated with increased levels of transthyretin and the activation of cell survival pathways. J. Neurosci. 22, 7380–8.

Stéphan, A., Laroche, S., Davis, S., 2001. Generation of Aggregated β-Amyloid in the Rat Hippocampus Impairs Synaptic Transmission and Plasticity and Causes Memory Deficits. J. Neurosci. 21.

Sternfeld, L., Krause, E., Guse, A.H., Schulz, I., 2003. Hormonal control of ADP-ribosyl cyclase activity in pancreatic acinar cells from rats. J. Biol. Chem. 278, 33629–33636.

Sterniczuk, R., Antle, M.C., LaFerla, F.M., Dyck, R.H., 2010a. Characterization of the 3xTg-AD mouse model of Alzheimer's disease: Part 2. Behavioral and cognitive changes. Brain Res. 1348, 149–155.

Sterniczuk, R., Dyck, R.H., LaFerla, F.M., Antle, M.C., 2010b. Characterization of the 3xTg-AD mouse model of Alzheimer's disease: Part 1. Circadian changes. Brain Res. 1348, 139–148.

Stevens, L.M., Brown, R.E., 2015. Reference and working memory deficits in the 3xTg-AD mouse between 2 and 15-months of age: A cross-sectional study. Behav. Brain Res. 278, 496–505.

Stieren, E., Werchan, W.P., El Ayadi, A., Li, F., Boehning, D., 2010. FAD Mutations in Amyloid Precursor Protein Do Not Directly Perturb Intracellular Calcium Homeostasis. PLoS One 5, e11992.

Stiller, I., Lizak, B., Banhegyi, G., 2014. Physiological Functions of Presenilins; Beyond γ-Secretase. Curr. Pharm. Biotechnol. 15, 1019–1025.

Stoppelkamp, S., Riedel, G., Platt, B., 2010. Culturing conditions determine neuronal and glial excitability. J. Neurosci. Methods 194, 132–138.

Stover, K.R., Campbell, M.A., Van Winssen, C.M., Brown, R.E., 2015. Early detection of cognitive deficits in the 3xTg-AD mouse model of Alzheimer's disease. Behav. Brain Res. 289, 29–38.

Strittmatter, W.J., Saunders, A.M., Schmechel, D., Pericak-Vance, M., Enghild, J., Salvesen, G.S., Roses, A.D., 1993. Apolipoprotein E: high-avidity binding to beta-amyloid and increased frequency of type 4 allele in late-onset familial Alzheimer disease. Proc. Natl. Acad. Sci. U. S. A. 90, 1977–81.

Stutzmann, G.E., 2007. The pathogenesis of Alzheimers disease is it a lifelong "calciumopathy"? Neuroscientist 13, 546–559.

Stutzmann, G.E., Caccamo, A., LaFerla, F.M., Parker, I., 2004. Dysregulated IP3 Signaling in Cortical Neurons of Knock-In Mice Expressing an Alzheimer's-Linked Mutation in Presenilin1 Results in Exaggerated Ca2+ Signals and Altered Membrane Excitability. J. Neurosci. 24, 508–513.

Stutzmann, G.E., Mattson, M.P., 2011. Endoplasmic Reticulum Ca2+ Handling in Excitable Cells in Health and Disease. Pharmacol. Rev. 63.

Stutzmann, G.E., Smith, I., Caccamo, A., Oddo, S., Laferla, F.M., Parker, I., 2006. Enhanced ryanodine receptor recruitment contributes to Ca2+ disruptions in young, adult, and aged Alzheimer's disease mice. J. Neurosci. 26, 5180–9.

Stutzmann, G.E., Smith, I., Caccamo, A., Oddo, S., Parker, I., Laferla, F., 2007. Enhanced Ryanodine-Mediated Calcium Release in Mutant PS1-Expressing Alzheimer's Mouse Models. Ann. N. Y. Acad. Sci. 1097, 265–277.

Su, J.H., Satou, T., Anderson, A.J., Cotman, C.W., 1996. Up-regulation of Bcl-2 is associated with neuronal DNA damage in Alzheimer's disease. Neuroreport 7, 437–40.

Suh, P.-G., Park, J.-I., Manzoli, L., Cocco, L., Peak, J.C., Katan, M., Fukami, K., Kataoka, T., Yun, S., Ryu, S.H., 2008. Multiple roles of phosphoinositide-specific phospholipase C isozymes. BMB Rep. 41, 415–34.

Sulger, J., Dumais-Huber, C., Zerfass, R., Henn, F.A., Aldenhoff, J.B., 1999. The calcium response of human T lymphocytes is decreased in aging but increased in Alzheimer's dementia. Biol. Psychiatry 45, 737–42.

Sumoza-Toledo, A., Penner, R., 2011. TRPM2: a multifunctional ion channel for calcium signalling. J. Physiol. 589, 1515–25.

Sun, D., Bullock, M.R., McGinn, M.J., Zhou, Z., Altememi, N., Hagood, S., Hamm, R., Colello, R.J., 2009. Basic fibroblast growth factor-enhanced neurogenesis contributes to cognitive recovery in rats following traumatic brain injury. Exp. Neurol. 216, 56–65.

Sun, L., Adebanjo, O.A., Koval, A., Anandatheerthavarada, H.K., Iqbal, J., Wu, X.Y., Moonga, B.S., Wu, X.B., Biswas, G., Bevis, P.J.R., Kumegawa, M., Epstein, S., Huang, C.L.-H., Avadhani, N.G., Abe, E., Zaidi, M., 2002. A novel mechanism for coupling cellular intermediary metabolism to cytosolic Ca2+ signaling via CD38/ADP-ribosyl cyclase, a putative intracellular NAD+ sensor. FASEB J. 16, 302–14.

Sun, S., Zhang, H., Liu, J., Popugaeva, E., Xu, N.-J., Feske, S., White, C.L.C., Bezprozvanny, I., Xia, W., Tesco, G., al., et, 2014. Reduced Synaptic STIM2 Expression and Impaired Store-Operated Calcium Entry Cause Destabilization of Mature Spines in Mutant Presenilin Mice. Neuron 82, 79–93.

Supnet, C., Bezprozvanny, I., 2010. The dysregulation of intracellular calcium in Alzheimer disease. Cell Calcium 47, 183–189.

Supnet, C., Grant, J., Kong, H., Westaway, D., Mayne, M., 2006. Amyloid-beta-(1-42) Increases Ryanodine Receptor-3 Expression and Function in Neurons of TgCRND8 Mice. J. Biol. Chem. 281, 38440–38447.

Supnet, C., Noonan, C., Richard, K., Bradley, J., Mayne, M., 2010. Up-regulation of the type 3 ryanodine receptor is neuroprotective in the TgCRND8 mouse model of Alzheimerâ€™s disease. J. Neurochem. 112, 356–365.

Suzuki, M., Nagai, Y., Wada, K., Koike, T., 2012. Calcium leak through ryanodine receptor is involved in neuronal death induced by mutant huntingtin. Biochem. Biophys. Res. Commun. 429, 18–23.

Svendsen, C.N., Fawcett, J.W., Bentlage, C., Dunnett, S.B., 1995. Increased survival of rat EGF-generated CNS precursor cells using B27 supplemented medium. Exp. brain Res. 102, 407–14.

Svichar, N., Shmigol, A., Verkhratsky, A., Kostyuk, P., 1997a. InsP 3 -induced Ca 2 + release in dorsal root ganglion neurones. Neurosci. Lett.

227, 107–110.

Svichar, N., Shmigol, A., Verkhratsky, A., Kostyuk, P., 1997b. InsP3-induced Ca2+ release in dorsal root ganglion neurones. Neurosci. Lett. 227, 107–110.

Swann, J.W., Brady, R.J., Martin, D.L., 1989. Postnatal development of GABA-mediated synaptic inhibition in rat hippocampus. Neuroscience 28, 551–61.

Swiatek, P.J., Lindsell, C.E., del Amo, F.F., Weinmaster, G., Gridley, T., 1994. Notch1 is essential for postimplantation development in mice. Genes Dev. 8, 707–19.

Sze, C.I., Troncoso, J.C., Kawas, C., Mouton, P., Price, D.L., Martin, L.J., 1997. Loss of the presynaptic vesicle protein synaptophysin in hippocampus correlates with cognitive decline in Alzheimer disease. J. Neuropathol. Exp. Neurol. 56, 933–44.

Szegedi, V., Juhász, G., Budai, D., Penke, B., 2005. Divergent effects of Aβ1-42 on ionotropic glutamate receptor-mediated responses in CA1 neurons in vivo. Brain Res. 1062.

Szlufcik, K., Missiaen, L., Parys, J.B., Callewaert, G., De Smedt, H., 2006. Uncoupled IP<inf>3</inf> receptor can function as a Ca^{2+}-leak channel: Cell biological and pathological consequences. Biol. Cell 98.

Takahashi, R.H., Milner, T.A., Li, F., Nam, E.E., Edgar, M.A., Yamaguchi, H., Beal, M.F., Xu, H., Greengard, P., Gouras, G.K., 2002. Intraneuronal Alzheimer abeta42 accumulates in multivesicular bodies and is associated with synaptic pathology. Am. J. Pathol. 161, 1869–79.

Takasawa, S., Akiyama, T., Nata, K., Kuroki, M., Tohgo, A., Noguchi, N., Kobayashi, S., Kato, I., Katada, T., Okamoto, H., 1998. Cyclic ADP-ribose and inositol 1,4,5-trisphosphate as alternate second messengers for intracellular Ca2+ mobilization in normal and diabetic beta-cells. J. Biol. Chem. 273, 2497–500.

Takasawa, S., Tohgo, A., Noguchi, N., Koguma, T., Nata, K., Sugimoto, T., Yonekura, H., Okamoto, H., 1993. Synthesis and hydrolysis of cyclic ADP-ribose by human leukocyte antigen CD38 and inhibition of the hydrolysis by ATP. J. Biol. Chem. 268, 26052–4.

Takasugi, N., Tomita, T., Hayashi, I., Tsuruoka, M., Niimura, M., Takahashi, Y., Thinakaran, G., Iwatsubo, T., 2003. The role of presenilin cofactors in the γ-secretase complex. Nature 422, 438–441.

Takechi, H., Eilers, J., Konnerth, A., 1998. A new class of synaptic response involving calcium release in dendritic spines. Nature 396, 757–60.

Tamaru, Y., Nomura, S., Mizuno, N., Shigemoto, R., 2001. Distribution of metabotropic glutamate receptor mGluR3 in the mouse CNS: differential location relative to pre-and postsynaptic sites. Neuroscience 106, 481–503.

Tang, W.-X., Chen, Y.-F., Zou, A.-P., Campbell, W.B., Li, P.-L., 2002. Role of FKBP12.6 in cADPR-induced activation of reconstituted ryanodine receptors from arterial smooth muscle. Am. J. Physiol. Heart Circ. Physiol. 282, H1304-10.

Tanzi, R.E., Bertram, L., 2005. Twenty Years of the Alzheimer's Disease Amyloid Hypothesis: A Genetic Perspective. Cell 120, 545–555.

Tao, R., Sun, H.-Y., Lau, C.-P., Tse, H.-F., Lee, H.-C., Li, G.-R., 2011. Cyclic ADP ribose is a novel regulator of intracellular Ca2+ oscillations in human bone marrow mesenchymal stem cells. J. Cell. Mol. Med. 15, 2684–2696.

Tao, Y., Black, I.B., DiCicco-Bloom, E., 1996. Neurogenesis in neonatal rat brain is regulated by peripheral injection of basic fibroblast growth factor (bFGF). J. Comp. Neurol. 376, 653–63.

Tarasoff-Conway, J.M., Carare, R.O., Osorio, R.S., Glodzik, L., Butler, T., Fieremans, E., Axel, L., Rusinek, H., Nicholson, C., Zlokovic, B. V., Frangione, B., Blennow, K., Ménard, J., Zetterberg, H., Wisniewski, T., de Leon, M.J., 2015. Clearance systems in the brain—implications for Alzheimer disease. Nat. Rev. Neurol. 11, 457–470.

Tarassishin, L., Yin, Y.I., Bassit, B., Li, Y.-M., 2004. Processing of Notch and amyloid precursor protein by -secretase is spatially distinct. Proc. Natl. Acad. Sci. 101, 17050–17055.

Terhorst, C., van Agthoven, A., LeClair, K., Snow, P., Reinherz, E., Schlossman, S., 1981. Biochemical studies of the human thymocyte cell-surface antigens T6, T9 and T10. Cell 23, 771–80.

Ternaux, J.P., Portalier, P., 1993. Culture of hypoglossal cells, dissociated from foetal and new-born rats. J. Neurosci. Methods 49, 33–47.

Terry, R.D., 2000. Cell death or synaptic loss in Alzheimer disease. J. Neuropathol. Exp. Neurol. 59.

Terry, R.D., Masliah, E., Salmon, D.P., Butters, N., DeTeresa, R., Hill, R., Hansen, L.A., Katzman, R., 1991. Physical basis of cognitive alterations in alzheimer's disease: Synapse loss is the major correlate of cognitive impairment. Ann. Neurol. 30, 572–580.

Thakur, A., Wang, X., Siedlak, S.L., Perry, G., Smith, M.A., Zhu, X., 2007. c-Jun phosphorylation in Alzheimer disease. J. Neurosci. Res. 85.

Thayer, S.A., Perney, T.M., Miller, R.J., 1988. Regulation of calcium homeostasis in sensory neurons by bradykinin. J. Neurosci. 8, 4089–97.

Thibault, O., Gant, J.C., Landfield, P.W., 2007. Expansion of the calcium hypothesis of brain aging and Alzheimer's disease: minding the store. Aging Cell 6, 307–17.

Thomas, J.M., Masgrau, R., Churchill, G.C., Galione, A., 2001. Pharmacological characterization of the putative cADP-ribose receptor. Biochem. J. 359, 451–7.

Thomas, J.M., Summerhill, R.J., Fruen, B.R., Churchill, G.C., Galione, A., 2002. Calmodulin dissociation mediates desensitization of the cADPR-induced Ca2+ release mechanism. Curr. Biol. 12, 2018–22.

Thomenius, M.J., Distelhorst, C.W., 2003. Bcl-2 on the endoplasmic reticulum: protecting the mitochondria from a distance. J. Cell Sci. 116, 4493–4499.

Thomenius, M.J., Wang, N.S., Reineks, E.Z., Wang, Z., Distelhorst, C.W., 2003. Bcl-2 on the Endoplasmic Reticulum Regulates Bax Activity by Binding to BH3-only Proteins. J. Biol. Chem. 278, 6243–6250.

Thomsen, C., Mulvihill, E.R., Haldeman, B., Pickering, D.S., Hampson, D.R., Suzdak, P.D., 1993. A pharmacological characterization of the mGluR1 alpha subtype of the metabotropic glutamate receptor expressed in a cloned baby hamster kidney cell line. Brain Res. 619, 22–8.

Todd, G.K., Boosalis, C.A., Burzycki, A.A., Steinman, M.Q., Hester, L.D., Shuster, P.W., Patterson, R.L., 2013. Towards Neuronal Organoids: A Method for Long-Term Culturing of High-Density Hippocampal Neurons. PLoS One 8, e58996.

Tomita, T., 2014. Molecular mechanism of intramembrane proteolysis by γ-secretase. J. Biochem. 156, 195–201.

Tong, B.C.-K., Lee, C.S.-K., Cheng, W.-H., Lai, K.-O., Foskett, J.K., Cheung, K.-H., 2016. Familial Alzheimer's disease-associated presenilin 1 mutants promote γ-secretase cleavage of STIM1 to impair store-operated Ca2+ entry. Sci. Signal. 9, ra89.

Topolnik, L., Chamberland, S., Pelletier, J.-G., Ran, I., Lacaille, J.-C., 2009. Activity-Dependent Compartmentalized Regulation of Dendritic Ca2+ Signaling in Hippocampal Interneurons. J. Neurosci. 29, 4658–4663.

Tortosa, A., López, E., Ferrer, I., 1998. Bcl-2 and Bax protein expression in Alzheimer's disease. Acta Neuropathol. 95, 407–12.

Tóth, B., Csanády, L., Toth, B., Csanady, L., 2010. Identification of Direct and Indirect Effectors of the Transient Receptor Potential Melastatin 2 (TRPM2) Cation Channel. J. Biol. Chem. 285, 30091–30102.

Townsend, M., Shankar, G.M., Mehta, T., Walsh, D.M., Selkoe, D.J., 2006. Effects of secreted oligomers of amyloid beta-protein on hippocampal synaptic plasticity: a potent role for trimers. J. Physiol. 572, 477–92.

Tozzi, A., Bengtson, C.P., Longone, P., Carignani, C., Fusco, F.R., Bernardi, G., Mercuri, N.B., 2003. Involvement of transient receptor potential-like channels in responses to mGluR-I activation in midbrain dopamine neurons. Eur. J. Neurosci. 18, 2133–45.

Tozzi, A., Sclip, A., Tantucci, M., de Iure, A., Ghiglieri, V., Costa, C., Di Filippo, M., Borsello, T., Calabresi, P., 2015. Region- and age-dependent reductions of hippocampal long-term potentiation and NMDA to AMPA ratio in a genetic model of Alzheimer's disease. Neurobiol. Aging 36, 123–133.

Tracy, T.E., Gan, L., 2017. Acetylated tau in Alzheimer's disease: An instigator of synaptic dysfunction underlying memory loss. BioEssays 39, 1600224.

Trenkner, E., 1992. Cerebellar cells in culture. In: Banker, G. Goslin, L. (Ed.), Culturing Nerve Cells. Massachusetts Institute of Technology, USA, pp. 283–330.

Triller, A., Choquet, D., 2008. New Concepts in Synaptic Biology Derived from Single-Molecule Imaging. Neuron 59.

Trinchese, F., Fa', M., Liu, S., Zhang, H., Hidalgo, A., Schmidt, S.D., Yamaguchi, H., Yoshii, N., Mathews, P.M., Nixon, R.A., Arancio, O., 2008. Inhibition of calpains improves memory and synaptic transmission in a mouse model of Alzheimer disease. J. Clin. Invest. 118.

Tripathi, A., Schenker, E., Spedding, M., Jay, T.M., 2016. The hippocampal to prefrontal cortex circuit in mice: a promising electrophysiological signature in models for psychiatric disorders. Brain Struct. Funct. 221, 2385–2391.

Tripathy, A., Xu, L., Mann, G., Meissner, G., 1995. Calmodulin activation and inhibition of skeletal muscle Ca2+ release channel (ryanodine receptor). Biophys. J. 69, 106–19.

Trulock, E.P., 1990. Arterial Blood Gases, Clinical Methods: The History, Physical, and Laboratory Examinations. Butterworths.

Tsai, J.-Y., Wolfe, M.S., Xia, W., 2002. The search for γ-secretase and development of inhibitors. Curr. Med. Chem. 9.

Tsujimoto, Y., Shimizu, S., Eguchi, Y., Kamiike, W., Matsuda, H., 1997. Bcl-2 and Bcl-xL block apoptosis as well as necrosis: possible involvement of common mediators in apoptotic and necrotic signal transduction pathways. Leukemia 11 Suppl 3, 380–2.

Tu, H., Nelson, O., Bezprozvanny, A., Wang, Z., Lee, S.-F., Hao, Y.-H., Serneels, L., De Strooper, B., Yu, G., Bezprozvanny, I., 2006. Presenilins Form ER Ca2+ Leak Channels, a Function Disrupted by Familial Alzheimer's Disease-Linked Mutations. Cell 126, 981–993.

Tu, J.C., Xiao, B., Naisbitt, S., Yuan, J.P., Petralia, R.S., Brakeman, P., Doan, A., Aakalu, V.K., Lanahan, A.A., Sheng, M., Worley, P.F., 1999. Coupling of mGluR/Homer and PSD-95 complexes by the Shank family of postsynaptic density proteins. Neuron 23.

Tyler, S.J., Dawbarn, D., Wilcock, G.K., Allen, S.J., 2002. alpha- and beta-secretase: profound changes in Alzheimer's disease. Biochem. Biophys. Res. Commun. 299, 373–6.

Tyszkiewicz, J.P., Yan, Z., 2005. β-Amyloid Peptides Impair PKC-Dependent Functions of Metabotropic Glutamate Receptors in Prefrontal Cortical Neurons. J. Neurophysiol. 93.

Ullian, E.M., Sapperstein, S.K., Christopherson, K.S., Barres, B.A., 2001. Control of synapse number by glia. Science 291, 657–61.

Um, J.W., Kaufman, A.C., Kostylev, M., Heiss, J.K., Stagi, M., Takahashi, H., Kerrisk, M.E., Vortmeyer, A., Wisniewski, T., Koleske, A.J., Gunther, E.C., Nygaard, H.B., Strittmatter, S.M., 2013. Metabotropic Glutamate Receptor 5 Is a Coreceptor for Alzheimer Aβ Oligomer Bound to Cellular Prion Protein. Neuron 79, 887–902.

Um, J.W., Nygaard, H.B., Heiss, J.K., Kostylev, M.A., Stagi, M., Vortmeyer, A., Wisniewski, T., Gunther, E.C., Strittmatter, S.M., 2012. Alzheimer amyloid-Î 2 oligomer bound to postsynaptic prion protein activates Fyn to impair neurons. Nat. Neurosci. 15.

Um, J.W., Strittmatter, S.M., 2013. Amyloid-β induced signaling by cellular prion protein and Fyn kinase in Alzheimer disease. Prion 7, 37–41.

Unni, V.K., Zakharenko, S.S., Zablow, L., DeCostanzo, A.J., Siegelbaum, S.A., 2004. Calcium Release from Presynaptic Ryanodine-Sensitive Stores Is Required for Long-Term Depression at Hippocampal CA3-CA3 Pyramidal Neuron Synapses. J. Neurosci. 24.

Urra, H., Dufey, E., Lisbona, F., Rojas-Rivera, D., Hetz, C., 2013. When ER stress reaches a dead end. Biochim. Biophys. Acta - Mol. Cell Res. 1833, 3507–3517.

Vale, C., Alonso, E., Rubiolo, J.A., Vieytes, M.R., LaFerla, F.M., Giménez-Llort, L., Botana, L.M., 2010. Profile for Amyloid-β and Tau Expression in Primary Cortical Cultures from 3xTg-AD Mice. Cell. Mol. Neurobiol. 30, 577–590.

Valenti, O., Conn, P.J., Marino, M.J., 2002. Distinct physiological roles of the Gq-coupled metabotropic glutamate receptors co-expressed in the same neuronal populations. J. Cell. Physiol. 191, 125–137.

van den Eijnde, S.M., Boshart, L., Baehrecke, E.H., De Zeeuw, C.I., Reutelingsperger, C.P., Vermeij-Keers, C., 1998. Cell surface exposure of phosphatidylserine during apoptosis is phylogenetically conserved. Apoptosis 3, 9–16.

van Groen, T., Miettinen, P., Kadish, I., 2003. The entorhinal cortex of the mouse: organization of the projection to the hippocampal formation. Hippocampus 13, 133–49.

Van Hoesen, G., Pandya, D.N., 1975. Some connections of the entorhinal (area 28) and perirhinal (area 35) cortices of the rhesus monkey. I. Temporal lobe afferents. Brain Res. 95, 1–24.

Van Hoesen, G.W., Hyman, B.T., 1990. Hippocampal formation: anatomy and the patterns of pathology in Alzheimer's disease. Prog. Brain Res. 83, 445–57.

Vance, J.E., 2010. Transfer of Cholesterol by the NPC Team. Cell Metab. 12, 105–106.

Vance, J.E., 2012. Dysregulation of cholesterol balance in the brain: contribution to neurodegenerative diseases. Dis. Model. Mech. 5.

Vanlingen, S., Sipma, H., De Smet, P., Callewaert, G., Missiaen, L., De Smedt, H., Parys, J.B., 2001. Modulation of inositol 1,4,5-trisphosphate binding to the various inositol 1,4,5-trisphosphate receptor isoforms by thimerosal and cyclic ADP-ribose. Biochem. Pharmacol. 61, 803–809.

Vanlingen, S., Sipma, H., Missiaen, L., Smedt, H.D., Smet, P.D., Casteels, R., Parys, J.B., 1999. Modulation of type 1, 2 and 3 inositol 1,4,5-trisphosphate receptors by cyclic ADP-ribose and thimerosal. Cell Calcium 25, 107–114.

Varon, S., Adler, R., 1980. Nerve growth factors and control of nerve growth. Curr. Top. Dev. Biol. 16, 207–52.

Vassar, R., Bennett, B.D., Babu-Khan, S., Kahn, S., Mendiaz, E.A., Denis, P., Teplow, D.B., Ross, S., Amarante, P., Loeloff, R., Luo, Y., Fisher, S., Fuller, J., Edenson, S., Lile, J., Jarosinski, M.A., Biere, A.L., Curran, E., Burgess, T., Louis, J.C., Collins, F., Treanor, J., Rogers, G., Citron, M., 1999. Beta-secretase cleavage of Alzheimer's amyloid precursor protein by the transmembrane aspartic protease BACE. Science 286, 735–41.

Vassilev, P.M., Mitchel, J., Vassilev, M., Kanazirska, M., Brown, E.M., 1997. Assessment of frequency-dependent alterations in the level of extracellular Ca2+ in the synaptic cleft. Biophys. J. 72, 2103–2116.

Vaughan, M.B., Kaar, A., Mauleon, G., Eddington, D.., Rae, M.G., 2018. Calcium homeostasis is significantly disrupted in dentate gyrus neurons of acute, ex vivo hippocampal slices of a mouse model of Alzheimer's disease. In: Europhysiology, Proc. Physiol. Soc. London, U.K.,

pp. 41, C086.

Veinbergs, I., Jung, M.W., Young, S.J., Van Uden, E., Groves, P.M., Masliah, E., 1998. Altered long-term potentiation in the hippocampus of apolipoprotein E-deficient mice. Neurosci. Lett. 249, 71–4.

Venkatachalam, K., van Rossum, D.B., Patterson, R.L., Ma, H.-T., Gill, D.L., 2002. The cellular and molecular basis of store-operated calcium entry. Nat. Cell Biol. 4, E263–E272.

Verderio, C., Bruzzone, S., Zocchi, E., Fedele, E., Schenk, U., De Flora, A., Matteoli, M., 2001. Evidence of a role for cyclic ADP-ribose in calcium signalling and neurotransmitter release in cultured astrocytes. J. Neurochem. 78, 646–57.

Verderio, C., Coco, S., Pravettoni, E., Bacci, A., Matteoli, M., 1999. Synaptogenesis in hippocampal cultures. Cell. Mol. Life Sci. C. 55, 1448–1462.

Verkhratsky, A., Reyes, R.C., Parpura, V., 2013. TRP Channels Coordinate Ion Signalling in Astroglia. In: Reviews of Physiology, Biochemistry and Pharmacology. pp. 1–22.

Verkhratsky, A., Toescu, E.C., 2003. Endoplasmic reticulum Ca^{2+} homeostasis and neuronal death. J. Cell. Mol. Med. 7, 351–361.

Verma, M., Vats, A., Taneja, V., 2015. Toxic species in amyloid disorders: Oligomers or mature fibrils. Ann. Indian Acad. Neurol. 18, 138–45.

Vervliet, T., Decrock, E., Molgo, J., Sorrentino, V., Missiaen, L., Leybaert, L., De Smedt, H., Kasri, N.N., Parys, J.B., Bultynck, G., 2014. Bcl-2 binds to and inhibits ryanodine receptors. J. Cell Sci. 127, 2782–2792.

Vervliet, T., Lemmens, I., Vandermarliere, E., Decrock, E., Ivanova, H., Monaco, G., Sorrentino, V., Nadif Kasri, N., Missiaen, L., Martens, L., De Smedt, H., Leybaert, L., Parys, J.B., Tavernier, J., Bultynck, G., 2015a. Ryanodine receptors are targeted by anti-apoptotic Bcl-XL involving its BH4 domain and Lys87 from its BH3 domain. Sci. Rep. 5, 9641.

Vervliet, T., Parys, J.B., Bultynck, G., 2015b. Bcl-2 and FKBP12 bind to IP3 and ryanodine receptors at overlapping sites: the complexity of protein-protein interactions for channel regulation. Biochem. Soc. Trans. 43, 396–404.

Vervliet, T., Parys, J.B., Bultynck, G., 2016. Bcl-2 proteins and calcium signaling: complexity beneath the surface. Oncogene 35, 5079–5092.

Vezzani, A., Ravizza, T., Balosso, S., Aronica, E., 2008. Glia as a source of cytokines: Implications for neuronal excitability and survival. Epilepsia 49, 24–32.

Vosler, P.S., Brennan, C.S., Chen, J., 2008. Calpain-mediated signaling mechanisms in neuronal injury and neurodegeneration. Mol. Neurobiol. 38, 78–100.

Vyas, S., Javoy-Agid, F., Herrero, M.T., Strada, O., Boissiere, F., Hibner, U., Agid, Y., 1997. Expression of Bcl-2 in adult human brain regions with special reference to neurodegenerative disorders. J. Neurochem. 69, 223–31.

Wagenknecht, T., Radermacher, M., Grassucci, R., Berkowitz, J., Xin, H.-B., Fleischer, S., 1997. Locations of Calmodulin and FK506-binding Protein on the Three-dimensional Architecture of the Skeletal Muscle Ryanodine Receptor. J. Biol. Chem. 272, 32463–32471.

Wagner, G.K., Guse, A.H., Potter, B.V.L., 2005. Rapid Synthetic Route toward Structurally Modified Derivatives of Cyclic Adenosine 5‘-Diphosphate Ribose.

Wahrle, S.E., Jiang, H., Parsadanian, M., Hartman, R.E., Bales, K.R., Paul, S.M., Holtzman, D.M., 2005. Deletion of Abca1 increases Abeta deposition in the PDAPP transgenic mouse model of Alzheimer disease. J. Biol. Chem. 280, 43236–42.

Wahrle, S.E., Jiang, H., Parsadanian, M., Kim, J., Li, A., Knoten, A., Jain, S., Hirsch-Reinshagen, V., Wellington, C.L., Bales, K.R., Paul, S.M., Holtzman, D.M., 2008. Overexpression of ABCA1 reduces amyloid deposition in the PDAPP mouse model of Alzheimer disease. J. Clin. Invest. 118, 671–82.

Wahrle, S.E., Jiang, H., Parsadanian, M., Legleiter, J., Han, X., Fryer, J.D., Kowalewski, T., Holtzman, D.M., 2004. ABCA1 is required for normal central nervous system ApoE levels and for lipidation of astrocyte-secreted apoE. J. Biol. Chem. 279, 40987–93.

Wallace, T.L., Johnson, E.M., 1989. Cytosine arabinoside kills postmitotic neurons: evidence that deoxycytidine may have a role in neuronal survival that is independent of DNA synthesis. J. Neurosci. 9, 115–24.

Walseth, T.F., Aarhus, R., Kerr, J.A., Lee, H.C., 1993. Identification of cyclic ADP-ribose-binding proteins by photoaffinity labeling. J. Biol. Chem. 268, 26686–91.

Walseth, T.F., Wong, L., Graeff, R.M., Lee, H.C., 1997. Bioassay for determining endogenous levels of cyclic ADP-ribose. Methods Enzymol. 280, 287–94.

Walsh, D.M., Klyubin, I., Fadeeva, J. V, Cullen, W.K., Anwyl, R., Wolfe, M.S., Rowan, M.J., Selkoe, D.J., 2002. Naturally secreted oligomers of amyloid beta protein potently inhibit hippocampal long-term potentiation in vivo. Nature 416.

Walter, J., Fluhrer, R., Hartung, B., Willem, M., Kaether, C., Capell, A., Lammich, S., Multhaup, G., Haass, C., 2001. Phosphorylation Regulates Intracellular Trafficking of -Secretase. J. Biol. Chem. 276, 14634–14641.

Wang, B., Wang, Z., Sun, L., Yang, L., Li, H., Cole, A.L., Rodriguez-Rivera, J., Lu, H.-C., Zheng, H., 2014. The Amyloid Precursor Protein Controls Adult Hippocampal Neurogenesis through GABAergic Interneurons. J. Neurosci. 34, 13314–13325.

Wang, D.-S., Iwata, N., Hama, E., Saido, T.C., Dickson, D.W., 2003. Oxidized neprilysin in aging and Alzheimer’s disease brains. Biochem. Biophys. Res. Commun. 310, 236–41.

Wang, J., Fivecoat, H., Ho, L., Pan, Y., Ling, E., Pasinetti, G.M., 2010. The role of Sirt1: At the crossroad between promotion of longevity and protection against Alzheimer’s disease neuropathology. Biochim. Biophys. Acta - Proteins Proteomics 1804, 1690–1694.

Wang, J.Z., Grundke-Iqbal, I., Iqbal, K., 1996. Restoration of biological activity of Alzheimer abnormally phosphorylated tau by dephosphorylation with protein phosphatase-2A, -2B and -1. Brain Res. Mol. Brain Res. 38, 200–8.

Wang, Q., Walsh, D.M., Rowan, M.J., Selkoe, D.J., Anwyl, R., 2004. Block of Long-Term Potentiation by Naturally Secreted and Synthetic Amyloid β-Peptide in Hippocampal Slices Is Mediated via Activation of the Kinases c-Jun N-Terminal Kinase, Cyclin-Dependent Kinase 5, and p38 Mitogen-Activated Protein Kinase as well as …. J. Neurosci. 24.

Wang, X., Liu, P., Zhu, H., Xu, Y., Ma, C., Dai, X., Huang, L., Liu, Y., Zhang, L., Qin, C., 2009. miR-34a, a microRNA up-regulated in a double transgenic mouse model of Alzheimer’s disease, inhibits bcl2 translation. Brain Res. Bull. 80, 268–273.

Wang, Y., Greig, N.H., Yu, Q., Mattson, M.P., 2009. Presenilin-1 mutation impairs cholinergic modulation of synaptic plasticity and suppresses NMDA currents in hippocampus slices. Neurobiol. Aging 30, 1061–1068.

Wang, Y., Wu, J., Rowan, M.J., Anwyl, R., 1996. Ryanodine produces a low frequency stimulation-induced NMDA receptor-independent long-term potentiation in the rat dentate gyrus in vitro. J. Physiol. 495, 755–767.

Wang, Y.X., Zheng, Y.M., Mei, Q.B., Wang, Q.S., Collier, M.L., Fleischer, S., Xin, H.B., Kotlikoff, M.I., 2004. FKBP12.6 and cADPR regulation of Ca2+ release in smooth muscle cells. Am. J. Physiol. Cell Physiol. 286, C538-546.

Waung, M.W., Pfeiffer, B.E., Nosyreva, E.D., Ronesi, J.A., Huber, K.M., 2008. Rapid Translation of Arc/Arg3.1 Selectively Mediates mGluR-Dependent LTD through Persistent Increases in AMPAR Endocytosis Rate. Neuron 59.

Webster, N.J., Ramsden, M., Boyle, J.P., Pearson, H.A., Peers, C., 2006. Amyloid peptides mediate hypoxic increase of L-type Ca2+ channels in central neurones. Neurobiol. Aging 27, 439–445.

Wehrens, X.H.T., Lehnart, S.E., Marks, A.R., 2005a. Intracellular calcium release and cardiac disease. Annu. Rev. Physiol. 67, 69–98.

Wehrens, X.H.T., Lehnart, S.E., Reiken, S., van der Nagel, R., Morales, R., Sun, J., Cheng, Z., Deng, S.-X., de Windt, L.J., Landry, D.W., Marks, A.R., 2005b. Enhancing calstabin binding to ryanodine receptors improves cardiac and skeletal muscle function in heart failure. Proc. Natl. Acad. Sci. 102, 9607–9612.

Wehrens, X.H.T., Lehnart, S.E., Reiken, S., Vest, J.A., Wronska, A., Marks, A.R., 2006. Ryanodine receptor/calcium release channel PKA phosphorylation: A critical mediator of heart failure progression. Proc. Natl. Acad. Sci. 103, 511–518.

Wehrens, X.H.T., Marks, A.R., 2005. Ryanodine receptors : structure, function and dysfunction in clinical disease. Springer.

Weidemann, A., Eggert, S., Reinhard, F.B.M., Vogel, M., Paliga, K., Baier, G., Masters, C.L., Beyreuther, K., Evin, G., 2002. A novel ε-cleavage within the transmembrane domain of the Alzheimer amyloid precursor protein demonstrates homology with notch processing. Biochemistry 41.

Weinberger, S.E., Cockrill, B.A., Mandel, J., Weinberger, S.E., Cockrill, B.A., Mandel, J., 2014. 1 – Pulmonary Anatomy and Physiology: The Basics. In: Principles of Pulmonary Medicine. pp. 1–19.

Weingarten, M.D., Lockwood, A.H., Hwo, S.Y., Kirschner, M.W., 1975. A protein factor essential for microtubule assembly. Proc. Natl. Acad. Sci. U. S. A. 72, 1858–62.

Westmark, C.J., 2013. What's hAPPening at synapses? The role of amyloid β-protein precursor and β-amyloid in neurological disorders. Mol. Psychiatry 18, 425–434.

Westmark, C.J., Malter, J.S., 2007. FMRP Mediates mGluR5-Dependent Translation of Amyloid Precursor Protein. PLoS Biol. 5, e52.

Westmark, P.R., Westmark, C.J., Jeevananthan, A., Malter, J.S., 2011. Preparation of synaptoneurosomes from mouse cortex using a discontinuous percoll-sucrose density gradient. J. Vis. Exp.

White, C., Li, C., Yang, J., Petrenko, N.B., Madesh, M., Thompson, C.B., Foskett, J.K., 2005. The endoplasmic reticulum gateway to apoptosis by Bcl-XL modulation of the InsP3R. Nat. Cell Biol. 7, 1021–1028.

Wiggin, G.R., Fawcett, J.P., Pawson, T., 2005. Polarity Proteins in Axon Specification and Synaptogenesis. Dev. Cell 8, 803–816.

Willem, M., Tahirovic, S., Busche, M.A., Ovsepian, S. V., Chafai, M., Kootar, S., Hornburg, D., Evans, L.D.B., Moore, S., Daria, A., Hampel, H., Müller, V., Giudici, C., Nuscher, B., Wenninger-Weinzierl, A., Kremmer, E., Heneka, M.T., Thal, D.R., Giedraitis, V., Lannfelt, L., Müller, U., Livesey, F.J., Meissner, F., Herms, J., Konnerth, A., Marie, H., Haass, C., 2015. η-Secretase processing of APP inhibits neuronal activity in the hippocampus. Nature 526, 443–447.

Williams, T.L., Serpell, L.C., 2011. Membrane and surface interactions of Alzheimer's Aβ peptide - insights into the mechanism of cytotoxicity. FEBS J. 278, 3905–3917.

Willmott, N., Sethi, J.K., Walseth, T.F., Lee, H.C., White, A.M., Galione, A., 1996. Nitric oxide-induced mobilization of intracellular calcium via the cyclic ADP-ribose signaling pathway. J. Biol. Chem. 271, 3699–3705.

Wilsch, V.W., Behnisch, T., Jäger, T., Reymann, K.G., Balschun, D., 1998. When are class I metabotropic glutamate receptors necessary for long-term potentiation? J. Neurosci. 18, 6071–80.

Wilson, C.A., Doms, R.W., Lee, V.M.-Y., 2003. Distinct Presenilin-Dependent and Presenilin-Independent γ-Secretases Are Responsible for Total Cellular Aβ Production. J. Neurosci. Res. 74.

Wilson, H.L., Galione, A., 1998. Differential regulation of nicotinic acid-adenine dinucleotide phosphate and cADP-ribose production by cAMP and cGMP. Biochem. J. 331 (Pt 3, 837–843.

Wiltgen, B.J., Royle, G.A., Gray, E.E., Abdipranoto, A., Thangthaeng, N., Jacobs, N., Saab, F., Tonegawa, S., Heinemann, S.F., O'Dell, T.J., Fanselow, M.S., Vissel, B., 2010. A Role for Calcium-Permeable AMPA Receptors in Synaptic Plasticity and Learning. PLoS One 5, e12818.

Wisniewski, K.E., Wisniewski, H.M., Wen, G.Y., 1985. Occurrence of neuropathological changes and dementia of Alzheimer's disease in Down's syndrome. Ann. Neurol. 17, 278–282.

Wolfe, M.S., 2010. Structure, mechanism and inhibition of gamma-secretase and presenilin-like proteases. Biol. Chem. 391, 839–47.

Wong, G.T., Manfra, D., Poulet, F.M., Zhang, Q., Josien, H., Bara, T., Engstrom, L., Pinzon-Ortiz, M., Fine, J.S., Lee, H.-J.J., Zhang, L., Higgins, G.A., Parker, E.M., 2004. Chronic Treatment with the γ-Secretase Inhibitor LY-411,575 Inhibits γ-Amyloid Peptide Production and Alters Lymphopoiesis and Intestinal Cell Differentiation. J. Biol. Chem. 279.

Wong, H.-K., Sakurai, T., Oyama, F., Kaneko, K., Wada, K., Miyazaki, H., Kurosawa, M., De Strooper, B., Saftig, P., Nukina, N., 2005. β subunits of voltage-gated sodium channels are novel substrates of β-site amyloid precursor protein-cleaving enzyme (BACE1) and γ-secretase. J. Biol. Chem. 280.

Woodhall, G., Gee, C.E., Robitaille, R., Lacaille, J.-C., 1999. Membrane Potential and Intracellular Ca 2/ Oscillations Activated by mGluRs in Hippocampal Stratum Oriens/Alveus Interneurons.

Woody, S.K., Zhao, L., 2016. Clusterin (APOJ) in Alzheimer's Disease: An Old Molecule with a New Role. In: Update on Dementia. InTech.

Woon, E.C.Y., Threadgill, M.D., 2005. Poly(ADP-ribose)polymerase inhibition - where now? Curr. Med. Chem. 12, 2373–92.

Wu, J., Petralia, R.S., Kurushima, H., Patel, H., Jung, M.-Y., Volk, L., Chowdhury, S., Shepherd, J.D., Dehoff, M., Li, Y., Kuhl, D., Huganir, R.L., Price, D.L., Scannevin, R., Troncoso, J.C., Wong, P.C., Worley, P.F., 2011. Arc/Arg3.1 Regulates an Endosomal Pathway Essential for Activity-Dependent β-Amyloid Generation. Cell 147.

Wu, M.M., Buchanan, J., Luik, R.M., Lewis, R.S., 2006. Ca $^{2+}$ store depletion causes STIM1 to accumulate in ER regions closely associated with the plasma membrane. J. Cell Biol. 174, 803–813.

Wu, R.L., Barish, M.E., 1999. Modulation of a slowly inactivating potassium current, I(D), by metabotropic glutamate receptor activation in cultured hippocampal pyramidal neurons. J. Neurosci. 19, 6825–37.

Wyss, J.M., van Groen, T., 1989. Development of the hippocampal formation. In: Chan-Palay, V., Köhler, C. (Eds.), Neurology and Neurobiology. Alan R. Liss, New York, pp. 1–16.

Wyss, M.T., Jolivet, R., Buck, A., Magistretti, P.J., Weber, B., 2011. In Vivo Evidence for Lactate as a Neuronal Energy Source. J. Neurosci. 31.

Xia, D., Watanabe, H., Wu, B., Lee, S.H., Li, Y., Tsvetkov, E., Bolshakov, V.Y., Shen, J., Kelleher, R.J., 2015a. Presenilin-1 Knockin Mice Reveal Loss-of-Function Mechanism for Familial Alzheimer's Disease. Neuron 85, 967–981.

Xia, D., Watanabe, H., Wu, B., Lee, S.H., Li, Y., Tsvetkov, E., Bolshakov, V.Y., Shen, J., Kelleher, R.J., III, 2015b. Presenilin-1 knockin mice reveal loss-of-function mechanism for familial Alzheimer's disease. Neuron 85, 967–81.

Xianfeng Gu, †, Zhenjun Yang, †, Liangren Zhang, †, Svenja Kunerth, ‡, Ralf Fliegert, ‡, Karin Weber, ‡, Andreas H. Guse, ‡ and, Lihe Zhang*,

†, 2004. Synthesis and Biological Evaluation of Novel Membrane-Permeant Cyclic ADP-Ribose Mimics: N1-[(5‘ ‘-O-Phosphorylethoxy)methyl]-5‘-O-phosphorylinosine 5‘,5‘ ‘-Cyclicpyrophosphate (cIDPRE) and 8-Substituted Derivatives.

Xiao, Q., Gil, S.-C., Yan, P., Wang, Y., Han, S., Gonzales, E., Perez, R., Cirrito, J.R., Lee, J.-M., 2012. Role of Phosphatidylinositol Clathrin Assembly Lymphoid-Myeloid Leukemia (PICALM) in Intracellular Amyloid Precursor Protein (APP) Processing and Amyloid Plaque Pathogenesis. J. Biol. Chem. 287, 21279–21289.

Xie, C., Markesbery, W.R., Lovell, M. a., 2000. Survival of hippocampal and cortical neurons in a mixture of MEM+ and B27-supplemented neurobasal medium. Free Radic. Biol. Med. 28, 665–672.

Xie, G.-H., Rah, S.-Y., Yi, K.S., Han, M.K., Chae, S.W., Im, M.-J., Kim, U.-H., 2003. Increase of intracellular Ca(2+) during ischemia/reperfusion injury of heart is mediated by cyclic ADP-ribose. Biochem. Biophys. Res. Commun. 307, 713–8.

Xie, Z., Romano, D.M., Tanzi, R.E., 2005. Effects of RNAi-Mediated Silencing of PEN-2, APH-1a, and Nicastrin on Wild-Type vs FAD Mutant Forms of Presenilin 1. J. Mol. Neurosci. 25, 067–078.

Xu, Q., Bernardo, A., Walker, D., Kanegawa, T., Mahley, R.W., Huang, Y., 2006. Profile and Regulation of Apolipoprotein E (ApoE) Expression in the CNS in Mice with Targeting of Green Fluorescent Protein Gene to the ApoE Locus. J. Neurosci. 26, 4985–4994.

Xu, X., Zeng, W., Popov, S., Berman, D.M., Davignon, I., Yu, K., Yowe, D., Offermanns, S., Muallem, S., Wilkie, T.M., 1999. RGS proteins determine signaling specificity of Gq-coupled receptors. J. Biol. Chem. 274, 3549–56.

Xue, Y., Lee, S., Ha, Y., 2011. Crystal structure of amyloid precursor-like protein 1 and heparin complex suggests a dual role of heparin in E2 dimerization. Proc. Natl. Acad. Sci. U. S. A. 108, 16229–34.

Yachnis, A.T., Giovanini, M.A., Eskin, T.A., Reier, P.J., Anderson, D.K., 1998. Developmental Patterns of BCL-2 and BCL-X Polypeptide Expression in the Human Spinal Cord. Exp. Neurol. 150, 82–97.

Yaghmoor, F., Noorsaeed, A., Alsaggaf, S., Aljohani, W., Scholtzova, H., Boutajangout, A., Wisniewski, T., 2014. The Role of TREM2 in Alzheimer’s Disease and Other Neurological Disorders. J. Alzheimer’s Dis. Park. 4.

Yamamoto-Katayama, S., Ariyoshi, M., Ishihara, K., Hirano, T., Jingami, H., Morikawa, K., 2002. Crystallographic studies on human BST-1/CD157 with ADP-ribosyl cyclase and NAD glycohydrolase activities. J. Mol. Biol. 316, 711–723.

Yamamoto, M., Kamatsuka, Y., Ohishi, A., Nishida, K., Nagasawa, K., 2013. P2X7 receptors regulate engulfing activity of non-stimulated resting astrocytes. Biochem. Biophys. Res. Commun. 439, 90–95.

Yamamoto, T., Byun, J., Zhai, P., Ikeda, Y., Oka, S., Sadoshima, J., 2014. Nicotinamide Mononucleotide, an Intermediate of NAD+ Synthesis, Protects the Heart from Ischemia and Reperfusion. PLoS One 9, e98972.

Yamasaki-Mann, M., Demuro, A., Parker, I., 2009. cADPR stimulates SERCA activity in Xenopus oocytes. Cell Calcium 45, 293–9.

Yamasaki, M., Thomas, J.M., Churchill, G.C., Garnham, C., Lewis, A.M., Cancela, J.-M., Patel, S., Galione, A., 2005. Role of NAADP and cADPR in the induction and maintenance of agonist-evoked Ca2+ spiking in mouse pancreatic acinar cells. Curr. Biol. 15, 874–878.

Yamashita, N., Nishiyama, N., Abe, K., Saito, H., Fukuda, J., 1992. Primary culture of postnatal rat hypothalamic neurons in astrocyte-conditioned medium. Brain Res. 594.

Yang, J., Vais, H., Gu, W., Foskett, J.K., 2016. Biphasic regulation of $InsP_3$ receptor gating by dual Ca^{2+} release channel BH3-like domains mediates Bcl-x_L control of cell viability. Proc. Natl. Acad. Sci. 113, E1953–E1962.

Yang, L.-B., Lindholm, K., Yan, R., Citron, M., Xia, W., Yang, X.-L., Beach, T., Sue, L., Wong, P., Price, D., Li, R., Shen, Y., 2003. Elevated β-secretase expression and enzymatic activity detected in sporadic Alzheimer disease. Nat. Med. 9, 3–4.

Yang, Y., Cook, D.., 2004. Presenilin-1 deficiency impairs glutamate-evoked intracellular calcium responses in neurons. Neuroscience 124, 501–505.

Yao, M., Nguyen, T.-V. V, Pike, C.J., 2005. -Amyloid-Induced Neuronal Apoptosis Involves c-Jun N-Terminal Kinase-Dependent Downregulation of Bcl-w. J. Neurosci. 25, 1149–1158.

Yao, Z., Yang, W., Gao, Z., Jia, P., 2017. Nicotinamide mononucleotide inhibits JNK activation to reverse Alzheimer disease. Neurosci. Lett. 647, 133–140.

Yarza, R., Vela, S., Solas, M., Ramirez, M.J., 2016. c-Jun N-terminal Kinase (JNK) Signaling as a Therapeutic Target for Alzheimer?s Disease. Front. Pharmacol. 6, 321.

Yasojima, K., McGeer, E.G., McGeer, P.L., 2001. Relationship between beta amyloid peptide generating molecules and neprilysin in Alzheimer disease and normal brain. Brain Res. 919, 115–21.

Ye, C., Ho-Pao, C.L., Kanazirska, M., Quinn, S., Rogers, K., Seidman, C.E., Seidman, J.G., Brown, E.M., Vassilev, P.M., 1997. Amyloid-beta proteins activate Ca(2+)-permeable channels through calcium-sensing receptors. J. Neurosci. Res. 47, 547–54.

Yeckel, M.F., Berger, T.W., 1990. Feedforward excitation of the hippocampus by afferents from the entorhinal cortex: redefinition of the role of the trisynaptic pathway. Proc. Natl. Acad. Sci. U. S. A. 87, 5832–6.

Yeromin, A. V, Roos, J., Stauderman, K.A., Cahalan, M.D., 2004. A store-operated calcium channel in Drosophila S2 cells. J. Gen. Physiol. 123, 167–82.

Yin, R.-H., Yu, J.-T., Tan, L., 2015. The Role of SORL1 in Alzheimer’s Disease. Mol. Neurobiol. 51, 909–918.

Ying, W., Alano, C.C., Garnier, P., Swanson, R.A., 2005a. NAD+ as a Metabolic Link Between DNA Damage and Cell Death. J. Neurosci. Res. 79, 216 –223.

Ying, W., Alano, C.C., Garnier, P., Swanson, R.A., 2005b. NAD+ as a metabolic link between DNA damage and cell death. J. Neurosci. Res. 79, 216–223.

Ying, W., Garnier, P., Swanson, R.A., 2003. NAD+ repletion prevents PARP-1-induced glycolytic blockade and cell death in cultured mouse astrocytes. Biochem. Biophys. Res. Commun. 308, 809–13.

Yoo, A.S., Cheng, I., Chung, S., Grenfell, T.Z., Lee, H., Pack-Chung, E., Handler, M., Shen, J., Xia, W., Tesco, G., Saunders, a J., Ding, K., Frosch, M.P., Tanzi, R.E., Kim, T.W., 2000. Presenilin-mediated modulation of capacitative calcium entry. Neuron 27, 561–572.

Yoshimura, S., Takagi, Y., Harada, J., Teramoto, T., Thomas, S.S., Waeber, C., Bakowska, J.C., Breakefield, X.O., Moskowitz, M.A., 2001. FGF-2 regulation of neurogenesis in adult hippocampus after brain injury. Proc. Natl. Acad. Sci. U. S. A. 98, 5874–9.

Yoshimura, Y., Ichinose, T., Yamauchi, T., 2003. Phosphorylation of tau protein to sites found in Alzheimer’s disease brain is catalyzed by Ca2+/calmodulin-dependent protein kinase II as demonstrated tandem mass spectrometry. Neurosci. Lett. 353.

Yoshiyama, Y., Higuchi, M., Zhang, B., Huang, S.-M., Iwata, N., Saido, T.C., Maeda, J., Suhara, T., Trojanowski, J.Q., Lee, V.M.-Y., 2007. Synapse Loss and Microglial Activation Precede Tangles in a P301S Tauopathy Mouse Model. Neuron 53, 337–351.

Youle, R.J., Strasser, A., 2008. The BCL-2 protein family: opposing activities that mediate cell death. Nat. Rev. Mol. Cell Biol. 9, 47–59.

Young, S.R., Chuang, S.-C.C., Wong, R.K.S., 2004. Modulation of afterpotentials and firing pattern in guinea pig CA3 neurones by group I

metabotropic glutamate receptors. J. Physiol. 554, 371–385.

Yu, J.-T., Chang, R.C.-C., Tan, L., 2009. Calcium dysregulation in Alzheimer's disease: from mechanisms to therapeutic opportunities. Prog. Neurobiol. 89, 240–255.

Yu, S.P., Sensi, S.L., Canzoniero, L.M., Buisson, A., Choi, D.W., 1997. Membrane-delimited modulation of NMDA currents by metabotropic glutamate receptor subtypes 1/5 in cultured mouse cortical neurons. J. Physiol. 499 (Pt 3), 721–32.

Yuan, Q., Deng, K.-Y., Sun, L., Chi, S., Yang, Z., Wang, J., Xin, H.-B., Wang, X., Ji, G., 2016. Calstabin 2: An important regulator for learning and memory in mice. Sci. Rep. 6, 21087.

Yuan, W., Guo, J., Li, X., Zou, Z., Chen, G., Sun, J., Wang, T., Lu, D., 2009. Hydrogen peroxide induces the activation of the phospholipase C-gamma1 survival pathway in PC12 cells: protective role in apoptosis. Acta Biochim. Biophys. Sin. (Shanghai). 41, 625–30.

Yue, J., Wei, W., Lam, C.M.C., Zhao, Y.-J., Dong, M., Zhang, L.-R., Zhang, L.-H., Lee, H.-C., 2009. CD38/cADPR/Ca2+ Pathway Promotes Cell Proliferation and Delays Nerve Growth Factor-induced Differentiation in PC12 Cells. J. Biol. Chem. 284, 29335–29342.

Yuste, J.E., Tarragon, E., Campuzano, C.M., Ros-Bernal, F., 2015. Implications of glial nitric oxide in neurodegenerative diseases. Front. Cell. Neurosci. 9, 322.

Yuste, R., Denk, W., 1995. Dendritic spines as basic functional units of neuronal integration. Nature 375, 682–684.

Zalk, R., Lehnart, S.E., Marks, A.R., 2007. Modulation of the ryanodine receptor and intracellular calcium, Annual Review of Biochemistry.

Zhang, C., Wu, B., Beglopoulos, V., Wines-Samuelson, M., Zhang, D., Dragatsis, I., Südhof, T.C., Shen, J., 2009. Presenilins are essential for regulating neurotransmitter release. Nature 460, 632–636.

Zhang, D., Zhang, C., Ho, A., Kirkwood, A., Südhof, T.C., Shen, J., 2010. Inactivation of presenilins causes pre-synaptic impairment prior to post-synaptic dysfunction. J. Neurochem. 115, 1215–1221.

Zhang, H., Liu, J., Sun, S., Pchitskaya, E., Popugaeva, E., Bezprozvanny, I., 2015a. Calcium Signaling, Excitability, and Synaptic Plasticity Defects in a Mouse Model of Alzheimer's Disease. J. Alzheimer's Dis. 45, 561–580.

Zhang, H., Wu, L., Pchitskaya, E., Zakharova, O., Saito, T., Saido, T., Bezprozvanny, I., 2015b. Neuronal Store-Operated Calcium Entry and Mushroom Spine Loss in Amyloid Precursor Protein Knock-In Mouse Model of Alzheimer's Disease. J. Neurosci. 35, 13275–13286.

Zhang, J.-S., Jin, D., Higashida, H., 2005. Acetylcholine stimulates cyclic ADP-ribose formation via M1 muscarinic receptors in rat superior cervical ganglion. Biochem. Biophys. Res. Commun. 335, 920–4.

Zhang, Sun, S., Herreman, A., De Strooper, B., Bezprozvanny, I., 2010. Role of presenilins in neuronal calcium homeostasis. J. Neurosci. 30, 8566–80.

Zhang, W., Hu, Y., Newman, E.A., Mulholland, M.W., 2006. Serum-free culture of rat postnatal neurons derived from the dorsal motor nucleus of the vagus. J. Neurosci. Methods 150, 1–7.

Zhang, Y. -w., Wang, R., Liu, Q., Zhang, H., Liao, F.-F., Xu, H., 2007. Presenilin/ -secretase-dependent processing of beta-amyloid precursor protein regulates EGF receptor expression. Proc. Natl. Acad. Sci. 104, 10613–10618.

Zhang, Y., Bhavnani, B.R., 2005. Glutamate-induced apoptosis in primary cortical neurons is inhibited by equine estrogens via down-regulation of caspase-3 and prevention of mitochondrial cytochrome c release. BMC Neurosci. 6, 13.

Zhang, Y., Thompson, R., Zhang, H., Xu, H., 2011. APP processing in Alzheimer's disease. Mol. Brain 4, 3.

Zhang, Z., Nadeau, P., Song, W., Donoviel, D., Yuan, M., Bernstein, A., Yankner, B.A., 2000. Presenilins are required for γ-secretase cleavage of β-APP and transmembrane cleavage of Notch-1. Nat. Cell Biol. 2.

Zhao, D., Watson, J.B., Xie, C.-W., 2004. Amyloid β prevents activation of calcium/calmodulin-dependent protein kinase II and AMPA receptor phosphorylation during hippocampal long-term potentiation. J. Neurophysiol. 92.

Zhao, F., Li, P., Chen, S.R.W., Louis, C.F., Fruen, B.R., 2001. Dantrolene inhibition of ryanodine receptor Ca2+ release channels. Molecular mechanism and isoform selectivity. J. Biol. Chem. 276, 13810–13816.

Zhao, W., Bianchi, R., Wong, R., 2001. Ca2+ store-dependent and -independent population activity induced by the activation of group I mGluRs in the hippocampus. Soc. Neurosci. Abstr. 27, 599.

Zhao, X.-L., Wang, W.-A., Tan, J.-X., Huang, J.-K., Zhang, X., Zhang, B.-Z., Wang, Y.-H., YangCheng, H.-Y., Zhu, H.-L., Sun, X.-J., Huang, F.-D., 2010. Expression of -Amyloid Induced Age-Dependent Presynaptic and Axonal Changes in Drosophila. J. Neurosci. 30, 1512–1522.

Zhao, Y.J., Lam, C.M.C., Lee, H.C., 2012. The Membrane-Bound Enzyme CD38 Exists in Two Opposing Orientations. Sci. Signal. 5, ra67-ra67.

Zheng, H., Jiang, M., Trumbauer, M.E., Sirinathsinghji, D.J., Hopkins, R., Smith, D.W., Heavens, R.P., Dawson, G.R., Boyce, S., Conner, M.W., Stevens, K.A., Slunt, H.H., Sisoda, S.S., Chen, H.Y., Van der Ploeg, L.H., 1995. beta-Amyloid precursor protein-deficient mice show reactive gliosis and decreased locomotor activity. Cell 81, 525–31.

Zheng, L., Cedazo-Minguez, A., Hallbeck, M., Jerhammar, F., Marcusson, J., Terman, A., 2012. Intracellular distribution of amyloid beta peptide and its relationship to the lysosomal system. Transl. Neurodegener. 1, 19.

Zhong, N., Weisgraber, K.H., 2009. Understanding the Association of Apolipoprotein E4 with Alzheimer Disease: Clues from Its Structure. J. Biol. Chem. 284, 6027–6031.

Ziegler, M., 2000. New functions of a long-known molecule. Emerging roles of NAD in cellular signaling. Eur. J. Biochem. 267, 1550–1564.

Zimmerman, A.N., Hülsmann, W.C., 1966. Paradoxical influence of calcium ions on the permeability of the cell membranes of the isolated rat heart. Nature 211, 646–7.

Zingarelli, B., Cuzzocrea, S., Zsengellér, Z., Salzman, A.L., Szabó, C., 1997. Protection against myocardial ischemia and reperfusion injury by 3-aminobenzamide, an inhibitor of poly (ADP-ribose) synthetase. Cardiovasc. Res. 36, 205–215.

Zocchi, E., Carpaneto, A., Cerrano, C., Bavestrello, G., Giovine, M., Bruzzone, S., Guida, L., Franco, L., Usai, C., 2001. The temperature-signaling cascade in sponges involves a heat-gated cation channel, abscisic acid, and cyclic ADP-ribose. Proc. Natl. Acad. Sci. U. S. A. 98, 14859–64.

Zocchi, E., Usai, C., Guida, L., Franco, L., Bruzzone, S., Passalacqua, M., De Flora, A., 1999. Ligand-induced internalization of CD38 results in intracellular Ca2+ mobilization: role of NAD+ transport across cell membranes. FASEB J. 13, 273–83.

Zola-Morgan, S., Squire, L.R., Amaral, D.G., 1986. Human amnesia and the medial temporal region: enduring memory impairment following a bilateral lesion limited to field CA1 of the hippocampus. J. Neurosci. 6, 2950–67.

Zou, W.-Q., Xiao, X., Yuan, J., Puoti, G., Fujioka, H., Wang, X., Richardson, S., Zhou, X., Zou, R., Li, S., Zhu, X., McGeer, P.L., McGeehan, J., Kneale, G., Rincon-Limas, D.E., Fernandez-Funez, P., Lee, H.-G., Smith, M.A., Petersen, R.B., Guo, J.-P., 2011. Amyloid-β42 interacts mainly with insoluble prion protein in the Alzheimer brain. J. Biol. Chem. 286.

Zumaquero, E., Mu?oz, P., Cobo, M., Lucena, G., Pav?n, E.J., Mart?n, A., Navarro, P., Garc?a-P?rez, A., Ariza-Veguillas, A., Malavasi, F.,

Sancho, J., Zubiaur, M., 2010. Exosomes from human lymphoblastoid B cells express enzymatically active CD38 that is associated with signaling complexes containing CD81, Hsc-70 and Lyn. Exp. Cell Res. 316, 2692–2706.